Facile Preparation of Glycomimetics from Uronic Acids

By

Craig Richard Smith

Submitted in Partial Fulfillment of the Requirements

for the Degree of

Master of Science

in the Chemistry Program

YOUNGSTOWN STATE UNIVERSITY

August 2005

Facile Preparation of Glycomimetics from Uronic Acids

Craig Richard Smith

I hereby release this thesis to the public. I understand that this thesis will be made available from the OhioLINK ETD Center and the Maag Library Circulation Desk for public access. I also authorize the University or other individuals to make copies of this thesis as needed for scholarly research.

Signature:

Craig Richard Smith Date

Approvals:

Dr. Peter Norris Date
Thesis Advisor

Dr. John Jackson Date
Committee Member

Dr. Sherri Lovelace-Cameron Date
Committee Member

Dr. Peter J. Kasvinsky Date
Dean of Graduate Studies and Research

Thesis Abstract

The following work describes facile methods for the preparation of amino sugar analogs of *N*-acetyl-2-amino-2-deoxy-D-mannopyranose uronic acid (D-ManAcA). Two main approaches were investigated in the synthesis of *N*-glycosides. Staudinger and aza-Wittig approaches were used to synthesize glucosyl amides and imines. Another approach to the synthesis of *N*-glycosides involved the application of 1,3-dipolar cycloadditions of azides and alkynes in the presence of a Cu(I) catalyst. The synthesis of *O*-glycosides and *C*-glycosides of the methyl ester of glucuronic acid were studied in regard to the development of high yielding, stereospecific mimetic syntheses.

Acknowledgements

I would like to thank the Youngstown State University Department of Chemistry and the School of Graduate Studies for allowing me to pursue my Master's of Science degree, as well as Dr. John Jackson and Dr. Sherri Lovelace-Cameron for being members of my thesis committee and for giving me time and advice when I needed them. I would like to thank Ray Hoff, Dr. Roland Riesen, and Dr. Matthias Zeller for providing assistance with instrumentation. Thanks to all of the people in the Norris Research Group for making a long day of work in the lab much more tolerable.

Most of my gratitude goes to Dr. Peter Norris for giving me a chance to grow as a chemist and also as an individual. I also want to thank him for believing in me. I cannot thank you enough for all of the help and things that you have done for me over the past two years. You have given me not only the knowledge that I need as a chemist but also for your support when I was in need. The chemist that I am now is largely because of you and I will always be indebted to you for that fact.

I would also like to thank my parents and immediate family for their support and understanding. Finally, I would like to thank my fiancée for her support, understanding, and patience with all of my eccentricities.

Table of Contents

List of Tables

List of Schemes

List of Equations

List of Figures

Introduction

Glycobiology

Glycobiology deals with the nature and role of carbohydrates in biological recognition events, as well as in the influence that carbohydrates have upon the protein to which they are attached. The chemical study of the biological functions of carbohydrates sounds relatively simple due to the fact that there are a limited number of naturally occurring carbohydrates, but in all actuality, carbohydrates differ from nucleic acids and peptides by two important characteristics: carbohydrates are highly branched molecules, and their monomeric units may be connected to one another *via* many different linkage types.[1] This complexity allows carbohydrates to provide an almost unlimited number of variations in their structures.

Glycobiology has proven that there is no single unifying function for oligosaccharides, and it is known that oligosaccharides play important functions in binding, recognition, intercellular interactions, and cellular control and signaling. Any of these functions can be drastically modified by simple alterations of glycosylation due to the fact that glycosylation processes are highly selective and sensitive to modulations. Alterations of glycosylations, which are specific to glycoconjugates, are now believed to act in a manner similar to a point mutation in DNA or RNA, altering the structure and possibly the function of the protein to which the oligosaccharide moiety is attached.[2]

Glycan biosynthesis is mediated via multiple factors such as amino acid sequences, and available carbohydrates and transferases, which contribute to the specific site and connectivity of glycosidation.[1] The primary amino acid sequence determines the number of possible glycosylation sites via enzymatically mediated processes. The three major classes of glycans found in Nature are N-linked, O-linked, and

glycophosphatidylinostitol (GPI) anchored carbohydrate units. Of these three units, only the N-linked glycans contain a specific pentasaccharide core that acts as the basis of structure for the carbohydrate residues to be attached.[3] The elegant biosynthetic glycan-processing pathway in cells allows the same oligosaccharide to be attached to quite different proteins without having to code the information into the DNA that codes for individual proteins.

It has become clear that in addition to simple mono- and polysaccharides, naturally occurring carbohydrates are commonly conjugated to proteins and lipids. Protein glycosylation is influenced by the overall protein conformation, the effect of local conformation, and the available gamut of glycosylation-processing enzymes for the particular cell type of interest.[1] The recognition of oligosaccharides by lectins is influenced by their accessibility, the number of copies of the oligosaccharides, and their precise geometry of presentation.[4] The fact that one set of structures on different proteins can result in quite dramatic variations in the properties of glycoproteins, emphasizes the fact that carbohydrates are a great source of variation and uniqueness of functionality in Nature.

Staphylococcus aureus and Antibiotic Resistance

Staphylococci are spherical Gram-positive bacteria that are commonly found in the mucous membranes and on the skin of humans. Most of these bacteria are harmless under normal conditions but can be classified as opportunistic pathogens. *Staphylococcus aureus* (*S. aureus*) is ranked as the number one cause of hospital-borne infections each year in the United States.[5] They are responsible for food poisoning, blood stream infections, and septic shock syndrome.[5] The frequency of fatal cases among

children due to *S. aureus* has increased over the past decade in the United States.[6] *S. aureus* is the most significant microbe isolated from skin and soft tissue in hospitals throughout the United States,[7] are *S. aureus* may be responsible for as high as 45% of secondary infections in third world countries.[6] As the aforementioned studies demonstrate, microbial infections caused by *S. aureus* are a major threat to the welfare of people worldwide.

Multiple forms of bacteria are adapting and altering their genetic makeup to resist many of the currently available antibiotics. Both the World Health Organization and the Center for Disease Control and Prevention estimate that roughly fifty thousand people die each day throughout the world due to infectious diseases.[8] Antibiotic resistant pathogens are also becoming a serious problem in medicine. It has been estimated that as many as 90% of *S. aureus* contain antibiotic resistance genes as part of their genetic information.[9]

Penicillin was introduced in 1944 to help combat the rise of sulphonamide resistant *S. aureus*, and by 1950, approximately one-half of all clinical isolates of *S. aureus* contained plasmids that carried penicillinase resistance genes.[10] Fortunately, other natural antibiotics were developed shortly after the introduction of penicillin. These antibiotics included chloramphenicol, erythromycin, streptomycin, and tetracycline. At first, all were active against *S. aureus* but resistance emerged rapidly, often mediated by the transduction, transformation, and conjugation of plasmids between bacteria and viruses.[11] The nature of this resistance then required the introduction of stronger, more effective antibiotics to combat the more virulent isolates.

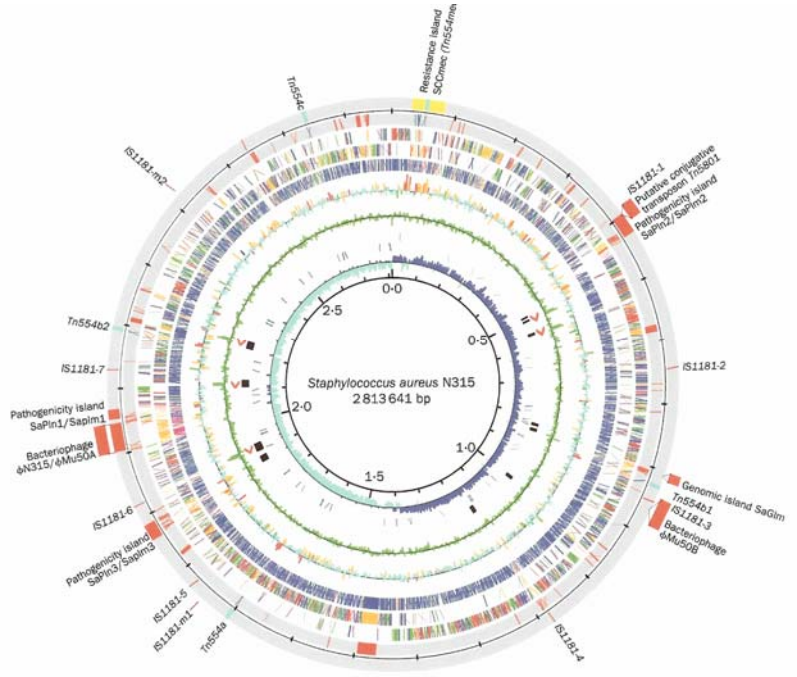

Figure 1: Antibiotic resistant genome map of *S. aureus* where antibiotic resistance genes are represented by the outermost layer of the map.[12]

The 1960's saw the introduction of methicillin, gentamicin, and vancomycin, which had better anti-*staphylococcal* activity and less toxicity than earlier aminoglycosides.[13] The first methicillin-resistant *S. aureus* (MRSA) were discovered in 1961, the same year that methicillin reached the market.[10] The first MRSA with reduced susceptibility to vancomycin were isolated in Japan in 1997.[14] The most serious recent development came in the form of vancomycin resistant *enterococci* (VRE), which has now become an established nosocomial pathogen contributing significantly to hospital-acquired infection worldwide. In the past two years, a transfer of vancomycin resistance has been noted between *Enterococci faecalis* and *S. aureus* via a plasmid to produce vancomycin-resistant *S. aureus* (VRSA),[15] which have only been found to be susceptible to teicoplanin and a combination of rifampicin and fusidic acid.[16]

As a result of the appearance of antibiotic resistant bacterial isolates, new methods have been developed to combat the dissemination of infection and virulence of the new VRSA. Due to this emergence of these antibiotic resistant microbes, compounds that target the inhibition of cell wall synthesis have become a widely studied methodology to produce antimicrobial drug candidates.

Biosynthesis of the *S. aureus* Capsular Polysaccharide

S. aureus organisms have been found to cause a diverse continuum of infectious diseases in hospitals as well as in communities at large. The most virulent factors among *S. aureus* strains are Serotypes five and eight. The capsule that protects *S. aureus* is composed of trisaccharide repeating units and is called the capsular polysaccharide of the bacterium.[17] The capsular polysaccharide (CP) of *S. aureus* is composed of repeat units (Figure 2) that are made up from three monomer amino sugars: *N*-acetyl-2-amino-2-deoxy-D-mannopyranose uronic acid (D-ManAcA), *N*-acetyl-2-amino-2-deoxy-D-fucopyranose (D-FucNAc), and *N*-acetyl-2-amino-2-deoxy-L-fucopyranose (L-FucNAc) (Figure 3).

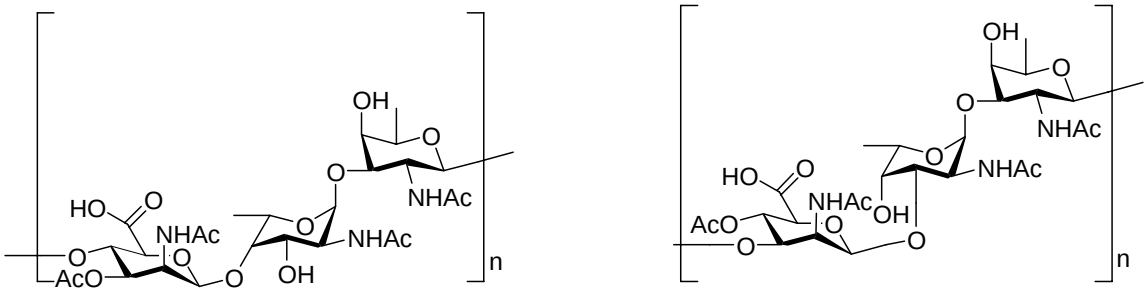

Serotype 5 Serotype 8

Figure 2: The repeating amino sugar units contained within the Type 5 and 8 capsular polysaccharides of *S. aureus.*

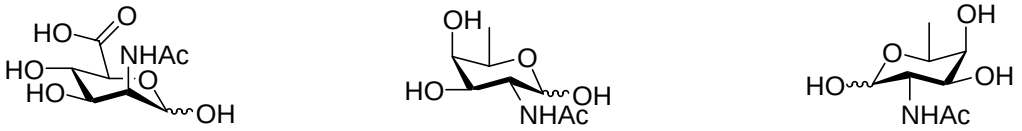

D-ManAcA D-FucNAc L-FucNAc

Figure 3: Amino sugar components of the *S. aureus* capsular polysaccharide.

The biosynthesis of the CP of *S. aureus* depends on a series of specific enzymatic reactions. The study of these enzymes at the molecular and functional levels has become an important approach to the inhibition of capsular polysaccharide formation. Studies of multiple pathogenic strains have revealed that the enzymes D-GlcNAc epimerase and D-ManAc dehydrogenase arbitrate the formation of the D-ManAcA portion of the CP.[18] D-GlcNAc epimerase is responsible for the synthesis of the precursor compound, which is linked to an accepting sugar by a glycosyl transferase enzyme via a glycosidic bond. Pathogenic strains of bacteria such as *E. faecalis* reveal that enzymes similar to UDP-GlcNAc 2-epimerase are involved in an initial *anti*-elimination of UDP to generate a glycal, followed by a *syn*-addition to generate the UDP-ManNAc product (Scheme 1).[19]

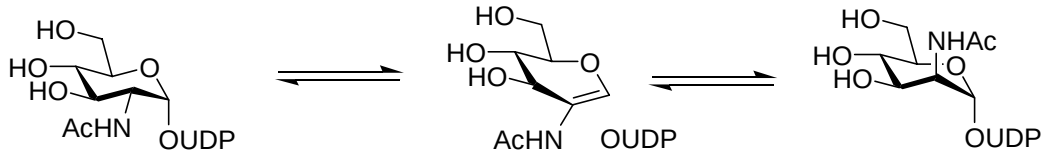

UDP-GlcNAc UDP-ManNAc

Scheme 1: Epimerization of UDP-GlcNAc to UDP-ManNAc.

UDP-ManNAc is then oxidized by a UDP-dehydrogenase to give UDP-D-ManNAcA. In the presence of a transferase, the UDP-D-ManNAcA is then linked to another amino sugar as part of the biochemical synthesis of the CP (Scheme 2).[20]

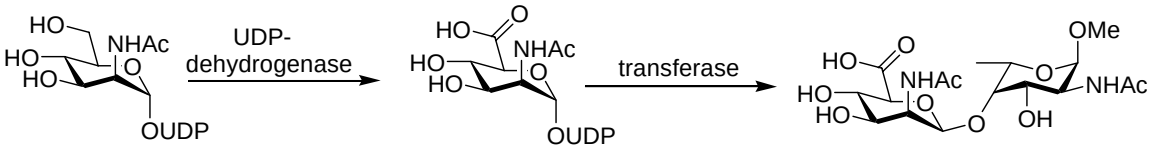

Scheme 2: Glycosyl linkage formation catalyzed by a transferase enzyme.

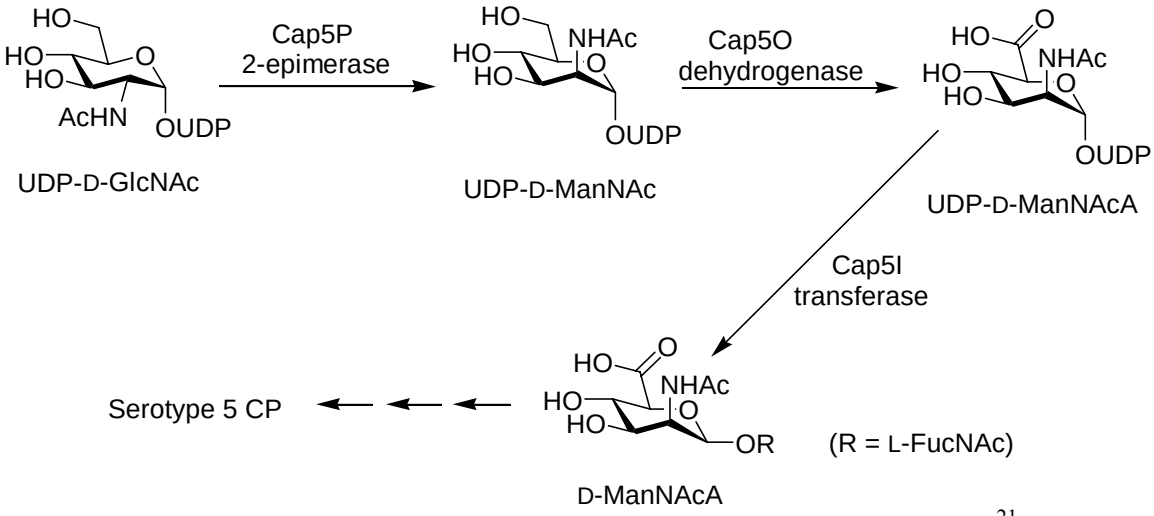

Figure 4: Proposed pathway for the biosynthesis of *S. aureus* CP5.[21]

Due to the fact that each enzyme in the sequence catalyses a specific modification of carbohydrate substrates, the synthesis of glycomimetics that follow a pathway similar to those found in Nature may have significant potential to produce inhibitors of CP synthesis at multiple stages along the biosynthetic pathway. Glycomimetics have the ability to compete for binding sites with the natural substrates or resemble the structures formed in an intermediate or transition state of an enzymatic process.[19] By the aforementioned means, these glycomimetic compounds could possibly act as competitive inhibitors by binding to the enzyme of interest to inhibit a biological process. Other mimetics could act as replacement sugars attached to a UDP complex, which would inhibit the formation of the required glycosidic bond during enzymatic catalysis.[22]

Carbohydrate Structure

Carbohydrates are essential biopolymers of life that are responsible for a number of molecular processes including sources of biological energy, as well as catalysis and molecular recognition processes for cells. Saccharides are also important biological mediators in more complex processes such as cell-cell recognition and interaction, fertilization, embryogenesis, hormone activities, cellular proliferation, apoptosis, and bacterial infections.[23] Apart from roles in energy and structure, saccharides also comprise the major blood group antigens, protective cell walls, and some antibiotics of microorganisms which are a major source of branched-chain sugars.

Carbohydrates are the most abundant class of biomolecules, and they allow for an almost limitless number of structural variations due to their chiral diversity, numerous functional groups, and multiplicity of linkage possibilities.[24] An increased appreciation of the roles of carbohydrates in biological and pharmaceutical processes has developed as a result of the glycobiological movement to understand the influence that carbohydrates have upon natural processes. The advancement of studies geared toward carbohydrates lagged far behind that of other important biological molecules due to the structural diversity and complexity of polysaccharide systems. Initial investigations of carbohydrate structure began in the late 1800's with the work of Emil Fischer.

In 1884, Fischer began his work on sugars; he studied the development of synthetic strategies directed toward known carbohydrates. Fischer discovered D-L isomerization in sugars, he studied the fermentation of sugars and the enzymes that controlled the process of fermentation, and he established the stereochemical nature and isomerization of sugars.[25] Later, he worked out the stereochemical configurations of all of

the aldohexoses. In 1890, he developed a complete synthesis of glucose, fructose, and mannose from glycerol. In 1902, Fischer was awarded the Nobel Prize in Chemistry for his work on carbohydrate synthesis. His studies developed a strong foundation for future work and biochemical studies of carbohydrates and enzyme-mediated processes.

Carbohydrate is a general name referring to monosaccharides, disaccharides, trisaccharides, oligosaccharides, and polysaccharides. The simplest members of the carbohydrate family are generally referred to as "saccharides" due to their characteristically sweet flavor. Carbohydrate literally means, "hydrates of carbon," and although this name applies to a large number of carbohydrates such as glucose and sucrose, it does not accurately describe all known carbohydrate molecules. Carbohydrates generally have the empirical formula of CH_2O, or more specifically, a molecular formula of $C_6H_{12}O_6$ for hexoses.[26] A more accurate description of carbohydrates comes in the form of polyhydroxyaldehydes or polyhydroxyketones. The chemistry of simple carbohydrates can be considered to be that of alcohols and aldehydes or ketones, or hydroxyl groups and the carbonyl group, respectively. Monosaccharides are the building blocks of more structurally complex saccharide molecules. Monosaccharides generally have from three to eight carbon atoms as denoted by the prefix tri-, tetra-, penta-, etc. and the name of the sugar ends in the suffix "-ose." Carbohydrates derived from ketones are referred to as ketoses and aldehyde -based sugars are known as aldoses.

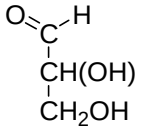

glyceraldehydes

(an aldotriose)

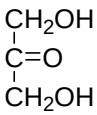

dihydroxyacetone

(a ketotriose)

Figure 5: Structure of simple aldose and ketose sugars.

Most carbohydrates have at least one stereocenter, such as glyceraldehyde which has only a single stereocenter, and therefore has two possible enantiomers. The stereochemistry of carbohydrates is usually denoted as "D" and "L" as opposed to either "*R*" or "*S*."

(*R*)-glyceraldehyde (*S*)-glyceraldehyde D-glyceraldehyde L-glyceraldehyde

Figure 6: Structure of enantiomers of glyceraldehyde.

In a Fischer projection "D" is used when the hydroxyl group on the first carbon from the bottom is on the right side, and "L" is used when the hydroxyl group on the first chiral carbon is on the left side.[27]

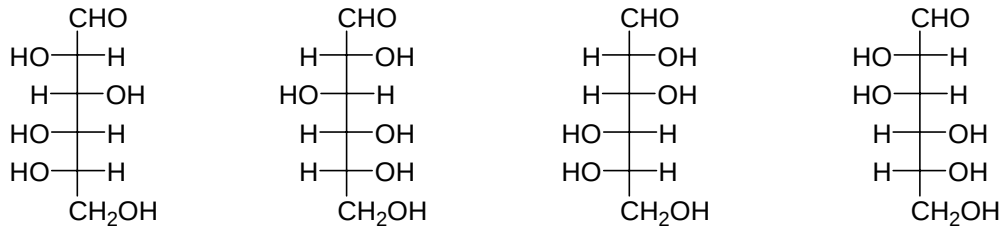

L-Glucose D-Glucose L-Mannose D-Mannose

Figure 7: Structures of the D and L isomers of glucose and mannose.

Monosaccharides exist as acyclic, furanose (five-membered ring), and pyranose (six-membered ring) forms in solution. In Figure 7, **1a** is the acyclic form of the sugar, **1b** is an alpha-pyranose sugar, **1c** is a beta-pyranose sugar, **1d** is an alpha-furanose sugar, and **1e** is a beta-furanose sugar.

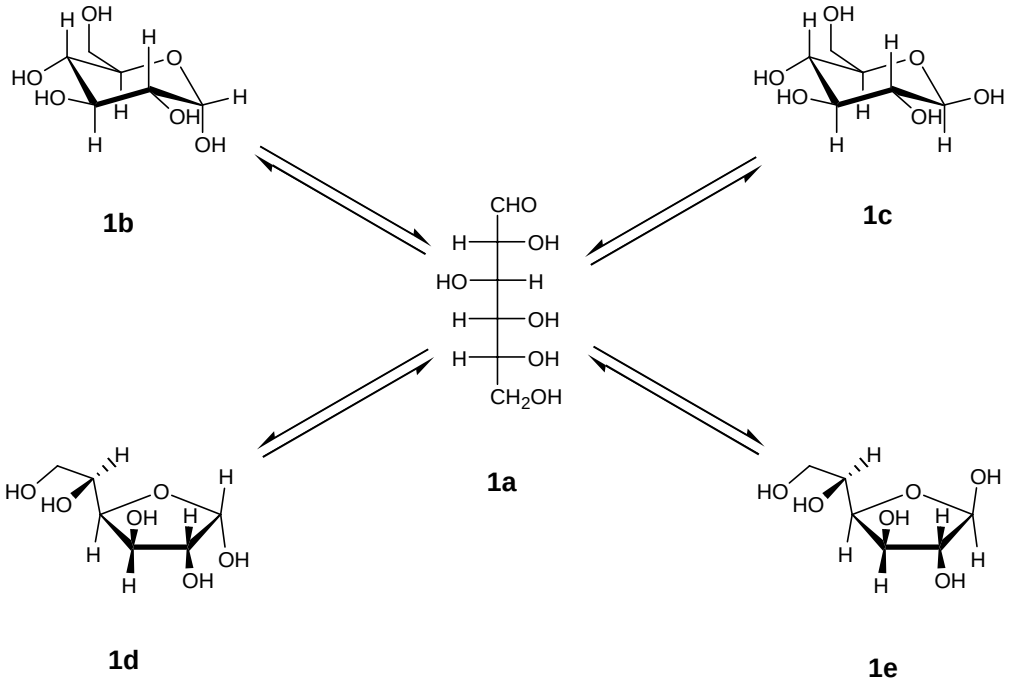

Figure 8: Configurations of D-glucose in solution.

The formation of a ring in glucose results from the nucleophilic attack of an oxygen atom attached to C-4 or C-5 upon the electrophilic carbon of the aldehyde. Upon closure of the ring two different structures can be drawn, one with the hydroxyl group in the down position (α), and the second with the hydroxyl group in the up position (β).[28] The α and β designations are used specifically to refer to the orientation of the hydroxyl group at C-1 (the anomeric carbon) relative to the functionality at C-5.

Carbohydrate Synthesis

Based upon biological significance, carbohydrates can be divided into three major categories, which are aminosugars, glycols, and glycosides. Aminosugars are a class of carbohydrates in which one or more of the hydroxyl groups has been changed to an amino group commonly, but not necessarily at the anomeric position. The synthesis of

aminosugars has been investigated in great detail due to the fact that they are an important component of naturally occurring polysaccharides. Some naturally occurring aminosugars are D-glucosamine, D-galactosamine, and *N*-acetyl-D-galactosamine (e.g. Figure 9).

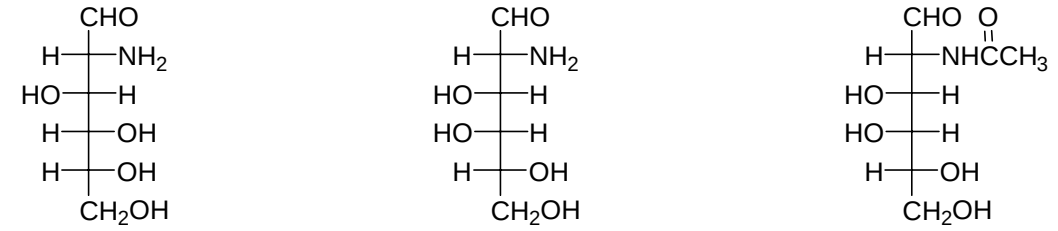

D-Glucosamine D-Galactosamine *N*-Acetyl-D-galactosamine

Figure 9: Structures of common naturally occurring amino sugars.

Glycals are carbohydrate derivatives that contain a highly reactive double bond between carbon atoms 1 and 2, and glycals have proved to be useful starting points in the stereoselective synthesis of *O*-glycosides. Glycals are usually synthesized in one of two manners; (1) zinc-catalyzed reductive elimination on an acetobromo moiety, or (2) via a standard E2 mechanism (i.e. Scheme 5). The reductive elimination may be carried out with zinc/acetic acid solutions, reactions with or without platinic chloride have been commonly used, but higher yields have been reported with a titanium (III) reagents.[29] These conditions are applicable where further functionalization is going to be carried out in either neutral or basic conditions, but reactions involving acid-catalysis are incompatible due to the presence of the acid-sensitive enol ether generated during the course of the reaction. E2 reactions to produce a glycal are carried out with a stoichiometric amount of diethylamine to create basic conditions in which a halogen and

hydrogen leave to produce the double bond and neutralize the liquid medium as the reaction completes.[30]

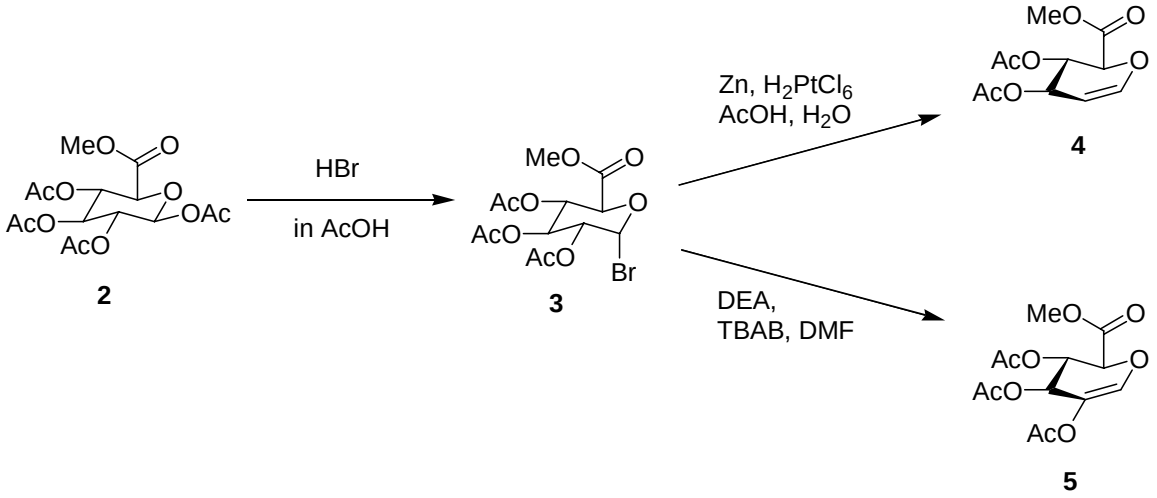

Scheme 3: Possible glycal synthetic strategies.

Finally, glycosides comprise the last major naturally occurring class of carbohydrate synthetic targets. A glycoside is a sugar in which the hydroxyl group at the anomeric position has been exchanged with another functionality like -*O*R, -*C*R, -*N*R, or –*S*R, resulting in *O*-glycosides, *C*-glycosides, *N*-glycosides, and *S*-glycosides respectively. Although the history of some glycosides is more than one hundred years old, glycosides have only come to the forefront of scientific investigation in the past half century. The formation of glycosides usually involves the formation of a linkage between the hydroxyl group of an aglycone and the anomeric center of another sugar moiety.[31]

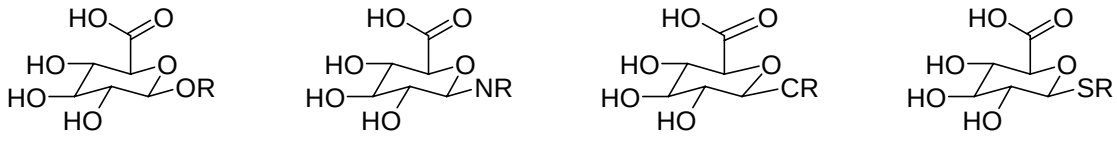

6a *O*-glycoside | **6b** *N*-glycoside | **6c** *C*-glycoside | **6d** *S*-glycoside

Figure 10: Representation of common glycoside classes.

Iminosugars

One of the approaches used to synthesize immunosuppressive agents, enzyme inhibitors, and antimicrobial compounds is in the production of iminosugars. Iminosugars are carbohydrates in which a nitrogen atom replaces the endocyclic ring oxygen of the carbohydrate and are known specifically to inhibit glycosidases, which are enzymes that catalyze the hydrolysis of glycosidic bonds in oligosaccharides and polysaccharides.[32] In the context of *S. aureus*, such alterations to typical function could block the expression or alter the structure of the capsular polysaccharide, increasing the bacteria's susceptibility to antibiotic agents.[33] As a result of studies on the mechanistic transition states of reactions, many inhibitor analogs, such as iminocyclitols and nojirimycins have been developed.[34,35]

Iminocyclitols can be synthesized via a hydrogenation of azido-sugars.[36] Azide **7** is reduced via a hydrogenation reaction to yield amine **8a**. The amine intermediate can then undergo isomerization to yield a cyclic imine (**8b**). Imine **8b** may then further undergo reduction to produce a disubstituted cyclic amine (**9**), which is a biologically active iminocyclitol. The cyclic imine sugar may mimic the reducing sugar in the transition state of a glycosyl transferase and inhibit the transfer to an accepting sugar (e.g. Figure 11).[37]

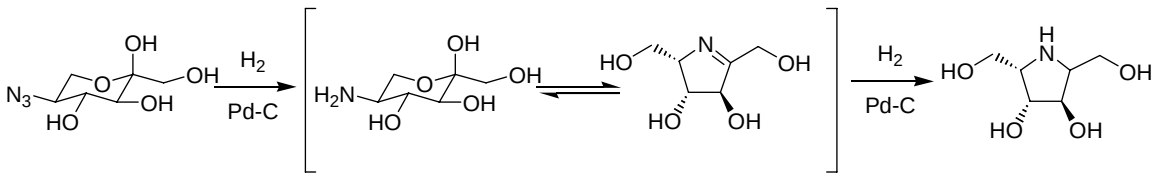

7 **8a** **8b** **9**

Scheme 4: The hydrogenation of an azidosugar to an iminocyclitol.

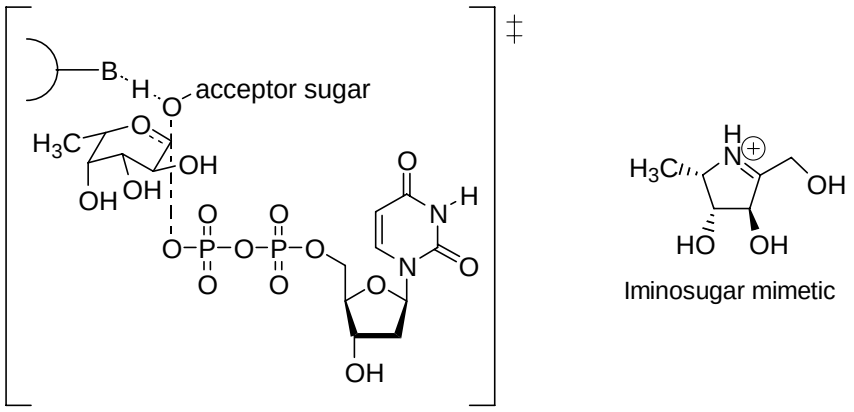

Figure 11: Transition state of a transferase and a possible mimetic.

Iminosugars can also be synthesized in other manners beyond that of a hydrogenation of an azido-sugar. Nojirimycin derivatives are often synthesized via three major routes: (1) selective Fowler reductions,[38] (2) from chiral nonracemic bicyclic lactams,[39] and (3) via standard protections and functional group manipulations.[40] This class of iminosugars are of great interest due to the fact that isofagomine and other compounds are anomer-selective inhibitors. Selective Fowler reductions use combinations of borohydrides and methyl and ethyl chloroformates to produce the 1,2-, 1,4-, and 1,6- reduction products of a pyridine-based starting material (e.g. Scheme 7).[38]

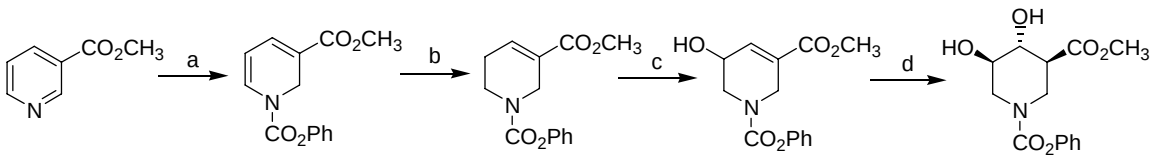

10 **11** **12** **13** **14**

(a) $NaBH_4$, PhOC(O)Cl, CH_3OH, -78 °C; (b) $NaBH_4$-TFAA, PhH, 5 °C; (c) i. *m*CPBA, CH_2Cl_2, -70 to 0 °C, ii. TMSOTf, BH_3-THF, -70 to 0 °C; (d) BH_3-THF, H_2O_2, NaOAc.

Scheme 5: Selective Fowler reduction to produce isofagomine.

Examination of the total synthesis of isofagamine includes a series of selective Fowler reductions beginning with the treatment of methyl ester (**10**) with phenyl cloroformate to reduce **10** from an aromatic pyridine derivative to a multiply substituted nitrogen-linked ester **11**. The combination of sodium borohydride and trifluoroacetic acid then further reduces **11** to the tetrahydropyridine **12**. Hydroboration of **12** yielded the hydroxyl containing iminosugar derivative **13** in high yield. The final step in the synthesis of **14** included the hydrolysis of the double bond in compound **13**.

Several iminosugars have been prepared in a rapid and efficient way by employing the appropriate bicyclic lactam template.[39] It has also been proven that these iminosugar analogs can be produced in a stereo-controlled manner that allows for the retention of multiple functional groups including esters, amines, and alcohols (e.g. Scheme 6).[40]

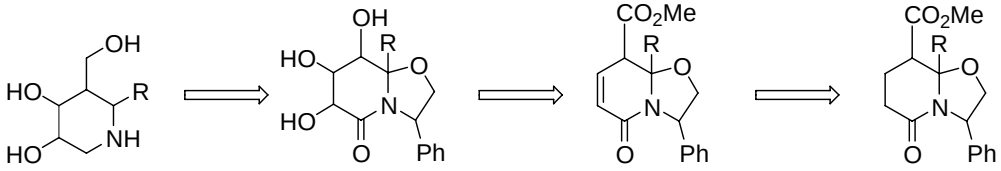

Scheme 6: Retrosynthesis of iminosugars *via* bicyclic lactam template opening.

Other methodologies for the production of iminosugars generally include the selective protection and manipulation of selected carbohydrate precursors. Kim and Sawada use a series of protections and functionalizations via hydride bases and hydride donors to obtain the proper functionalization of the carbohydrate of interest before using triphenyl phosphine to close the nitrogen-containing carbohydrate ring of the iminosugar.[41, 42]

The search to find better antibiotic agents has been stimulated by the fact that most microbes isolated contain antibiotic resistance genes and the fact that the toxicity of many of the current agents have been reduced. Iminosugars are potent inhibitors of many carbohydrate-processing enzymes involved in important biological systems.[43] These unique molecules promise a new generation of iminosugar based medicines that may help to combat viral and bacterial infections.

_N_-Glycoside Chemistry

Of importance in many biological systems are *N*-glycosides.[44] Of notable importance are the *N*-glycosides formed via reactions of D-ribose and 2-deoxy-D-ribose with purine and pyrimidine bases in the construction of nucleosides and analogs thereof in DNA and RNA production. The new bond that is formed during this type of reaction between the nitrogen of the base and the anomeric carbon of the carbohydrate moiety is referred to as an *N*-glycosidic bond. The formation of this glycosidic bond can be represented in a reaction between cytosine (**16**) and 2-deoxy-D-ribofuranose (**15**) which yields the deoxyribonucleoside **17** (Equation 1).

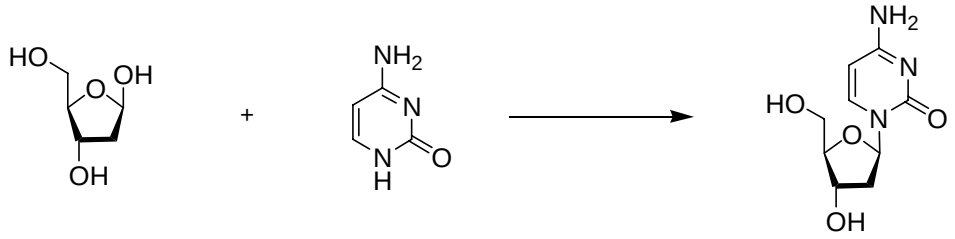

15 **16** **17**

D-deoxyribofuranose cytosine deoxyribonucleoside

Equation 1: Synthesis of deoxyribonucleoside from deoxyribose sugar.

A growing interest in the synthesis of glycosylamides and glycosylamines as *N*-glycosides has been driven by the knowledge that similar types of compounds are found in naturally occurring macromolecules such as nucleic acids and glycoproteins. Glycosylamides have been suggested as potential glycomimetics for the inhibition of glycosyl hydrolases and as useful precursors in the synthesis of peptide containing antimicrobial agents such as bacitracin.[45] Amphiphilic glycosylamides constitute a valuable class of non-ionic biosurfactants.[45]

Boullanger et al. presented a versatile synthesis of amphiphilic glycosylamides without the transient reduction of the azide to an amine. The synthesis of amides from azides via a modified Staudinger reaction proceeds in a high-yielding, stereospecific manner in which a reactive nitrogen atom attacks a carboxylic acid, acid halide, anhydride, or carboxylic acid ester to form the expected product. The modified Staudinger reaction proceeds via the loss of nitrogen gas to provide a reactive sugar ylide intermediate. This reaction proceeds through a series of intermediates which include an ylide phosphazene, an oxychloridate, and finally, an imidoyl chloride (Scheme 9).[45]

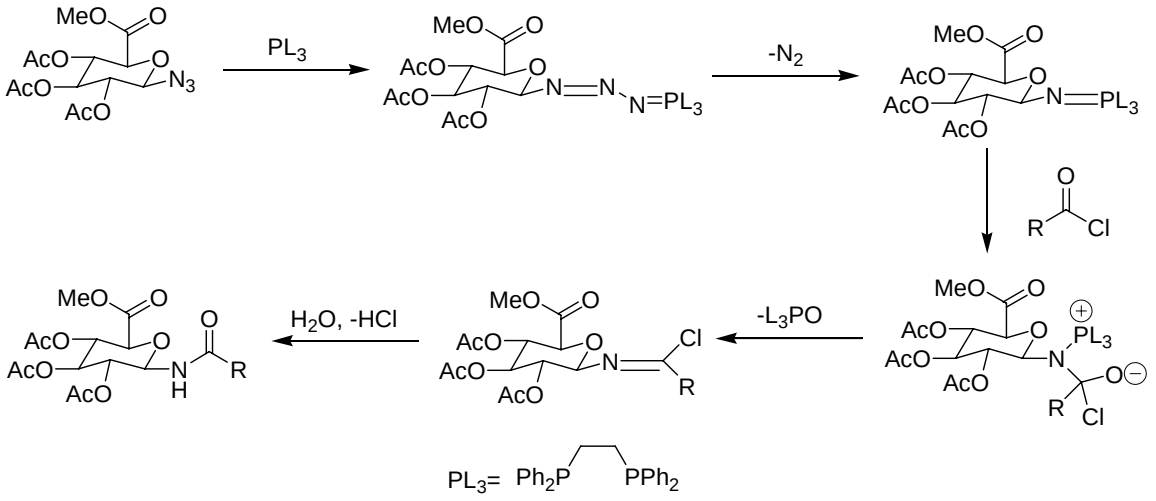

Scheme 7: The Modified Staudinger intermediate reaction pathway.

The design and synthesis of novel scaffolds possessing unique structural and biological properties such as amines and imines is of particular interest due to the fact that they may act as peptidomimetic compounds or pharmaceutics.[46] The modified Staudinger reaction with an aldehyde or ketone produces an intermediate in the synthesis of the amine product known as an imine. The imine then may undergo a process known as a reductive amination in which either a borohydride reducing reagent or a metal hydrogenation agent is used to reduce the carbon-nitrogen double bond to a single bond.[47] The process of reductive amination is believed to proceed via a hydride attack from a borohydride reagent at the partially positive carbonyl carbon (e.g. on **18**) followed by the addition of a proton to the nucleophilic nitrogen atom (e.g. **19**, Scheme 8), to afford the amine (**20**).

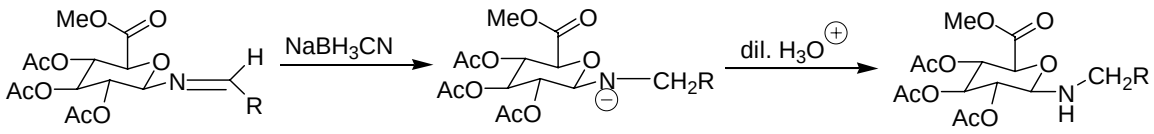

18 **19** **20**

Scheme 8: A representative scheme of the important intermediate of reductive amination with sodium cyanoborohydride.

Other methods of reductive amination include reactions of activated metal complexes such as hydrogen adsorbed onto palladium or ruthenium metals, and reactions with Raney Nickel, which has an oxidation state of zero. The mechanisms of metal complex amination reactions are not fully known or understood, but it is hypothesized that the reductive processes occur at the surface interface of the activated metal.

Azide Chemistry

Click chemistry is a modular approach that focuses upon only the most practical and reliable chemical transformations from high energy starting materials. Click chemistry simplifies compound synthesis, through the use of selective chemical transformations, thus providing the means for the rapid and selective synthesis of synthetically desired target molecules. A reaction can be termed a "click reaction" when the reaction is wide in scope, gives high yields consistently, the reaction is easy to perform, is insensitive to water and oxygen, and the purification is simple due to the production of few inoffensive by-products.[48]

Triazoles are important synthetic products because they can be found as agrochemical and pharmaceutical intermediates in the synthesis of heterocyclic systems. Triazoles have characteristically been synthesized in three ways. The first manner, which is not regiospecific and creates mixtures of the 1,4- and 1,5-triazole products requires a suitable azide and an alkyne to be stirred under reflux for extended periods and has been characterized by low yields, side reactions, and difficult purification.[46] The second method requires the use of a Grignard reaction to afford 1,5-triazoles in moderate yields.[49] The third method was reported by Sharpless, and affords pure 1,4-triazole (e.g. **23**) product in excess of 90% when the azide (**21**) and an alkyne (**22**) are brought together in the presence of an ascorbic acid-copper sulfate catalyst system (Equation 2).[50]

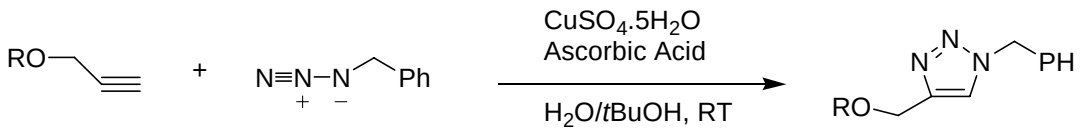

21 **22** **23**

Equation 2: Huisgen 1,3-dipolar cycloaddition scheme.

Azides serve as one of the most reliable manners by which nitrogen can be introduced via a substitution reaction and, moreover, azides are unique for click chemistry purposes due to their extraordinary stability toward water, oxygen, and a majority of reaction conditions and pre-existing molecular functionalities. Meldal and co-workers have reported the copper(I)-catalyzed 1,3-dipolar cycloaddition of alkynes and azides on solid phase.[51] The resin bound copper-acetylide was reacted with an assortment of azides and azido sugars at ambient temperature, producing 1,4-disubstituted 1*H*-[1,2,3]-triazoles regiospecifically with high yields and high purity.

_O_-Glycoside Chemistry

In addition to the synthesis of *N*-glycosidic mimetic compounds, the synthesis of *O*-glycosidic oligomers is of great interest due to their potential ability to inhibit cell wall biosynthesis.[53] These oligo-mimetic molecules often tend to be combinations of *O*- and *N*-saccharide linkages. As nitrogen linkages have previously been explored, the formation of oxygen-linked sugar systems will now be summarized.

In the synthesis of *O*-glycosides, a glycosyl donor is reacted with a free hydroxyl group of a glycosyl acceptor in the presence of a promoter to produce a linked glycoside. In the formation of an *O*-glycoside, the glycosyl donors that are often used appear as an intermediate with heteroatom-stabilized cationic character that is located at the anomeric center. The stabilized carbocation is then attacked by the nucleophilic group of the acceptor to produce the aforementioned glycosyl linkage.

Koenigs and Knorr described the use of silver (I) salts as promoters for glycosidation reactions in the presence of an alcohol. It can be deduced that the use of insoluble silver (I) salts such as silver oxide and silver carbonate would lead to the formation of water during the glycosylation reaction, which would lead to the hydrolysis of the starting material.[54] Although some chemists have attempted to overcome this problem via the use of drying agents, the idea of soluble mercury promoters came to the forefront. Later, soluble mercury (II) salts were explored as promoters due to the fact that mercury (II) salts often do not liberate water throughout the course of a reaction.

The first method ([1], Scheme 9) of *O*-glycoside production, is known as the Koenigs-Knorr method,[55] which employs a mercury (II) salt such as mercuric bromide as the halogen atom binding species to draw the halogen away from the anomeric carbon, creating a heteroatom stabilized carbocation that can then undergo an S_N1-like process with a weak nucleophile such as an alcohol (Scheme 9).

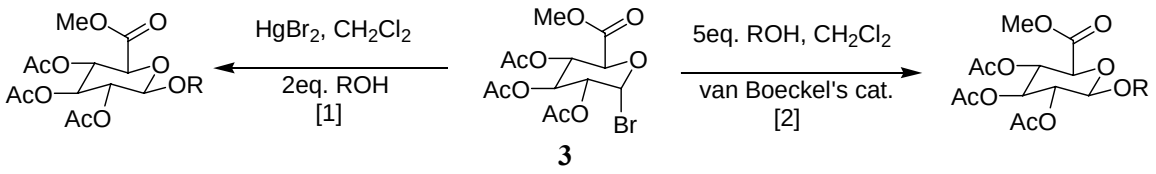

Scheme 9: *O*-Glycoside synthetic methodology.

Recently, the use of insoluble silver (I) salts has been advocated for the synthesis of β-glycosidic bonds. The insoluble silver salts are believed to act as promoters, forming an oxocarbonium ion which rapidly collapses to produce the product with dissociation of the glycosyl donor's tight-ion pair.[54] The aforementioned method ([2], Scheme 9), is that which employs the use of insoluble silver (I) salts in stoichiometric quantities to draw a

bromide atom off of the anomeric carbon allowing for either an S_N1 or an S_N2 process to occur depending upon the time of attack of the nucleophile throughout the spectrum of the substitution reaction. The method that is of particular interest employs the use of silver aluminosilicate,[30,54] which is commonly referred to as the van Boeckel catalyst.

The presence of either a participating group or a group that produces a strong electron-withdrawing effect via the carbon atom adjacent to the site of glycosylation appears to decisively influence the stereochemical outcome of the glycosylation process. The high β-selectivity of these glycosidations may be deduced from van Boeckel's rationalization,[54] that electron-withdrawing substituents at C-2 and C-4 facilitate an S_N2-like attack of the alcohol component in a type one insoluble silver salt-mediated glycosidation.

_C_-Glycoside Chemistry

Synthetically prepared *C*-glycosides have been shown to prevent bacterial and viral infections by inhibiting glycosidase enzymes, which are involved in the growth and development of certain bacteria and viruses. There are several common methods used to synthesize *C*-glycosides which include the following; organolithium or Grignard reactions, the dithiane approach, hypervalent silicate chemistry, and the use of Lewis acid-mediated processes.

Organometallic approaches to *C*-glycoside synthesis are usually limited to carbohydrates that are protected with ethereal protecting groups, such as benzyl or isopropylidene groups.[56] Drawbacks to organometallic methods include formation of by-products via elimination reactions can be prevalent within the reaction mixture, and mixtures at the anomeric position are often observed due to reduced specificity of attack.

Dithiane chemistry requires the presence of a primary hydroxyl group on the carbohydrate starting material of interest, and the reaction is often described in a manner similar to that to a Wittig reaction in which a dipole inversion or an inversion of reactivity occurs.[57] 1,3-Dithianes are often important molecules in the overall synthetic strategies of natural and unnatural product synthesis due to the fact that the dithiane anion is highly reactive and the dithiane product acts as a good protecting group for carbonyl moieties. Dithianes are removed in the same manner in which acetals or ketals are removed from other synthetic targets.[58]

Another popular strategy in the formation of *C*-glycosides is through the use of hypervalent silicate chemistry,[59] where TMS-CN would be reacted with a halosugar and a fluoride donating species to elicit the formation of the silicon-fluorine bond, which will release the fully anionic cyanide species into solution (e.g. conversion of **3** to **25**, Scheme 10).

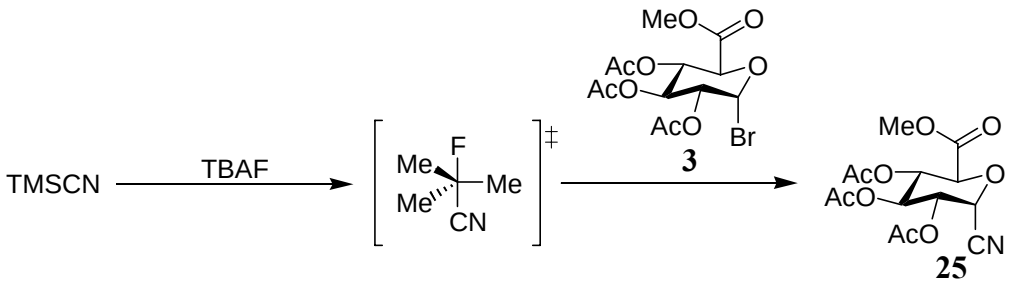

Scheme 10: Proposed route of hypervalent *C*-glycosylation reaction.

This method has been applied with great success to non-carbohydrate systems with TMS-N_3 and TBAF, but has not been fully explored with cyanide, or with carbohydrates.[60] The hypervalent silicate chemistry of interest is an improvement upon an older method in which "naked" cyanide ions were reacted in solutions of dimethylsulfoxide or dimethylformamide at elevated temperatures for extended periods

of time.[60] Metal impurities such as the counter cation were often removed using toxic crown ethers as trapping molecules to form crystalline complexes which could be filtered from the reaction mixture. This is often a synthetically useful purification method.[61]

The last method of *C*-glycoside synthesis that will be discussed revolves around one-carbon extensions best achieved by a cyanation reaction with TMSCN under Lewis acidic conditions to introduce a cyano group into the anomeric position of the sugar. This reaction produces the desired nitrile in a *beta* configuration, which acts as a useful handle for further synthetic manipulation. Unfortunately, standard acidic or basic hydrolysis conditions can lead to alterations of the nitrile functionality. This method provides an expedient route to *C*-glycosides that may contain interesting pharmacological properties, or potential drug candidates in the fight against *Staphylococcus aureus*.[62]

As is now apparent, it is necessary to produce new drugs that are effective in the treatment of diseases caused by drug resistant bacteria. Due to the concern that arose from the increased antibiotic resistance of *S. aureus*, derivatives of uronic acids were investigated. Multiple synthetic methods were explored to produce a large number of compounds that mat eventually lead to the development of new antimicrobial agents.

Statement of Problem

With the appearance of multiple new antibiotic resistant strains of *Staphylococcus aureus*, there is a growing need for new and more effective pharmaceutical methods for treatment. *S. aureus* is one of these bacteria that are continuing to develop greater resistance to current antibiotics, and is responsible for infectious diseases found in communities and hospitals. Many strains of this microbe have a protective coat called the capsular polysaccharide, which provides protection against phagocytosis. The goal of this research is to develop glycomimetics that possess structural similarities to an aminosugar found in the capsular polysaccharide of *S. aureus*.

The following work describes new synthetic pathways toward *N*-, *O*-, and *C*-glycosidic monosaccharide units, and the analogs thereof, of *Staphylococcus aureus* Type 5 and Type 8 capsular polysaccharide. The main approaches for the synthesis of *N*-glycosidic monosaccharides include the synthesis of a glucopyranuronosyl azide derivative followed by functionalization via either triazole synthesis, which is a [3+2] cycloaddition, or an aza-Wittig reaction to produce nitrogen-linked amides and imines.

The main approach for the synthesis of the *O*-glycoside derivatives is through the use of an insoluble silver salt-mediated, stereoselective substitution reaction, which produces primarily the β-anomer. The final synthetic procedure is directed toward the synthesis of *C*-glycoside compounds through the use of hypervalent silicate chemistry to install either a nitrile or other carbon-based functionality at C-1 in a stereoselective manner to allow for further functionalization.

Results and Discussion

1. Synthesis of precursor compounds for D-ManAcA glycomimetics

Lichtenthaler, et al. developed an excellent method for the synthesis of the precursor compounds of D-ManAcA that provided the advantage of obtaining most of the pathway intermediates in crystalline form.[30] Each step of the synthesis of intermediates is discussed in detail below.

The initial step of the synthesis (Scheme 11) involves the treatment of D-glucurono-6,3-lactone (**26**), which can be obtained inexpensively from Aldrich, with a catalytic amount of sodium hydroxide in methanol for one hour to produce the methyl D-glucopyranuronates (**27**). After the evaporation of the mixture of **27**, it was acetylated with acetic anhydride in pyridine to protect all of the hydroxyl groups. The mixture was reacted for three hours and reaction was confirmed with by disappearance of starting material and appearance of a new spot with a higher R_f value on the TLC plate. The crude material was purified via a simple aqueous workup using methylene chloride for extraction to provide a mixture of isomers (**2 α/β**). The major product, methyl 1,2,3,4-tetra-*O*-acetyl-β-D-glucopyranuronate (**2β**) was isolated through recrystallization by dissolving the mixture in hot isopropyl alcohol, which afforded 67% of **2β** as clear crystals. Single crystal X-ray data (Figure 12) was obtained for the α-anomer of the tetraacetate to confirm that the isomers were being separated during recrystallization and then properly characterized. The X-ray structure of the β-anomer of **2** had been reported previously.[63]

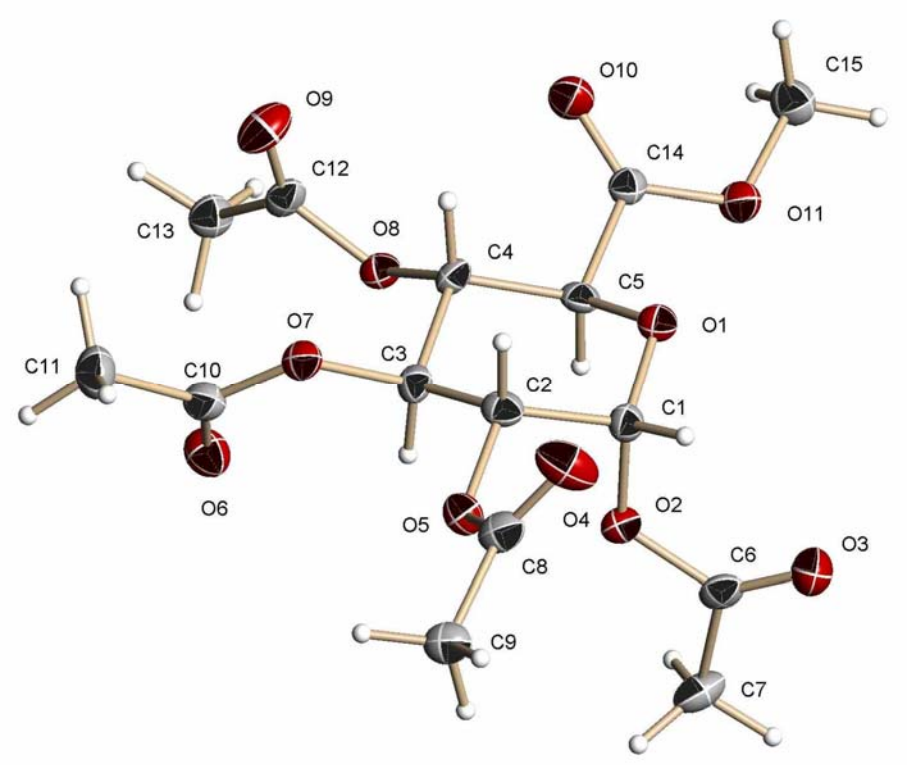

Figure 12: X-ray structure of D-glucopyranuronate **2α**.

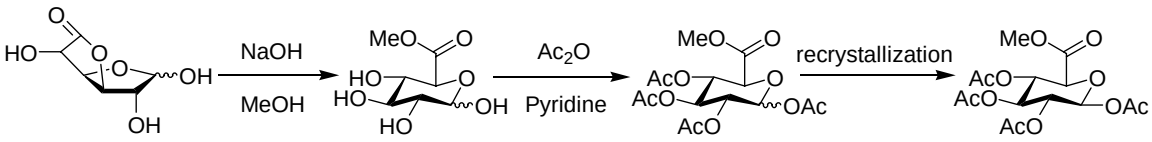

26 **27** **2 α/β** **2β**

Scheme 11: Preparation of methyl 1,2,3,4-tetra-*O*-acetyl-β-D-glucopyranuronate (**2β**).

The ^{1}H NMR spectrum of **2β** showed three signals at 2.04, 2.05, and 2.13 ppm (one double intensity) that correspond to the acetyl protecting groups. Also, a singlet was observed at 3.75 ppm for the methyl group of the ester at C-6. The coupling constant of H-1 and H-2, 9.15 Hz, shows that the positions of these two hydrogen atoms are axial, which aided in the identification of the compound as **2β**. Analysis of the ^{13}C NMR spectrum showed the signals of the carbonyl carbons of the acetyl protecting groups, and

also the ester group, which had shifts between 167.7-170.7 ppm. Electrospray Ionization (ESI) mass spectrometry shows an M^+ of 399.1 for both **2α** and **2β**, which corresponds to the addition of sodium to the molecular weight of 376.31.

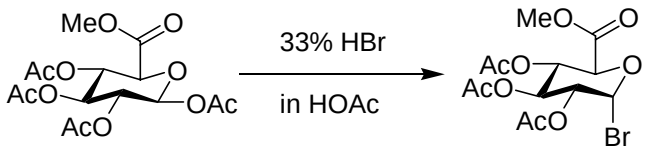

2β **3**

Equation 3: Synthesis of methyl 2,3,4-tri-*O*-acetyl-α-D-glucopyranuronosyl bromide (**3**).

Bromide **3** was readily synthesized by treatment of **2β** with 33% hydrobromic acid in acetic acid for four hours to give a single stereoisomer in 98% yield (Equation 3). There is a preference for the bromine atom to be in the axial position due to the anomeric effect, in which the anti-bonding σ*-orbital overlaps with the sp^3-orbital of the valence electrons of the oxygen atom in the carbohydrate ring. TLC indicated a UV-active spot with a lower R_f value than that of the starting material, and the ^{1}H NMR spectrum showed the loss of the C-1 acetyl protecting group signal and a downfield shift for the anomeric proton to 6.47 ppm. The remaining acetyl protecting group signals were observed at 1.84 and 1.89 ppm. (one double intensity). The ^{13}C NMR spectrum provided evidence for the presence of four carbonyl carbons, three of which were for acetyl protecting groups and the final carbonyl carbon was representative of the carbonyl carbon of the methyl ester appearing between 167.3 and 170.3 ppm. Also evident are the signals around 21 ppm illustrating the methyl groups associated with the acetyl protecting groups. The signal for the methyl group associated with the ester at C-6 was further downfield due to the neighboring oxygen atom and it was seen at 54.1 ppm. Mass

spectral data shows an M^+ at 399.1 that corresponds to the calculated molecular weight of 397.17 with the addition of a proton.

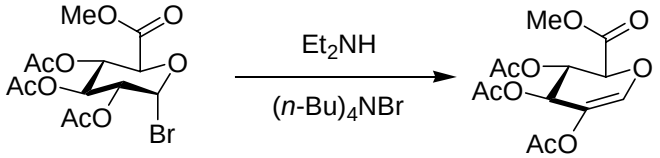

3 **5**

Equation 4: The synthesis of glycal **5** *via* elimination reaction.

Because Br is such a good leaving group, reaction with diethylamine and tetrabutylammonium bromide in DMF gave glycal **5** via an elimination reaction (Equation 4). TLC showed a UV-active spot that burned at a slightly lower R_f value than that of bromide **3**. The product was purified by elution from a silica gel column to afford **5** in 73% yield. The ^{1}H NMR spectrum showed the change of the H-1 proton signal of the starting material at 6.47 ppm, which now appears as a singlet at 6.83 ppm. This was due to the absence of a neighboring hydrogen atom as well as the introduction of a π bond between the C-1 and C-2 carbon atoms. Again, the signals for the methyl groups of the acetyl protecting groups appear at 2.02, 2.11, and 2.15 ppm. Also, there was a change in the shape of the signal for H-3 from a doublet of doublets to a doublet with a coupling constant of J = 2.38 Hz.

Analysis of the ^{13}C NMR spectrum showed the carbonyl carbons of the protecting groups as well as the carbonyl carbon of C-6 between 168.9 and 170.8 ppm. The signal for the anomeric carbon was shifted downfield from 89.0 to 139.2 ppm due to the presence of the π-bond between C-1 and C-2. A similar result was also seen for C-2, which was shifted from 70.1 to 127.2 ppm. The rest of the signals showed very little

change when they were compared to the spectrum of the starting material. Mass spectrometry provided an M^+ of 317.0, which corresponds to the addition of a proton to the calculated molecular weight of 316.26.

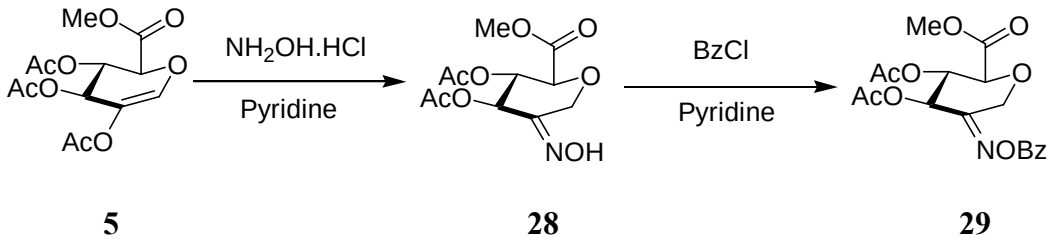

5 **28** **29**

Scheme 12: *O*-Benzoyloxime of methyl 3,4-di-*O*-acetyl-1,5-anhydro-D-fructouronate.

The reaction of glycal **5** with hydroxylamine hydrochloride in pyridine afforded a 66% yield of oxime **28** as a pale orange solid (Scheme 12). The TLC showed a spot that was UV-active and burned at a lower R_f than that of the starting material. Based upon the ^{1}H NMR spectrum analysis, the disappearance of a signal for the methyl group associated with an acetyl protecting group indicates the loss of one -$COCH_3$ group. Also shown in the spectrum is a change for the H-1 signal for the starting material, which was shifted upfield and shows as a doublet of doublets between 4.68 and 4.88 ppm, with a coupling constant of J = 15.75 Hz. The ^{13}C NMR provided more evidence for the reaction of enol acetate **5** by showing the upfield shift of the C-1 signal from 139.2 to 60.3 ppm, but the C-2 signal remained downfield, due to the loss of the double bond at C-1 and the formation of a new double bond between C-2 and the N atom to form the oxy-imine. The signals that appeared at 21.9 and 22.1 ppm correspond to the methyl group of the acetyl protecting groups and the signal at 53.8 ppm for the methyl group of the ester at C-6. The rest of the signals appeared between 60.3 and 75.4 ppm, which correspond to the

remaining carbons of **28**. A signal for the NOH proton did not appear in the ^{1}H NMR spectrum.

An X-ray crystal structure was obtained for oxime **28** supporting the stereochemistry as determined from the NMR spectra and it revealed that the oxime hydrogen bonds to itself via the hydrogen of the oxyimine and the ethereal oxygen and the acyl oxygen of the methyl ester of an associated sugar molecule (Figure 13). ESI mass spectrometry shows an M^{+} of 312.1, which is in agreement with the addition of sodium to the calculated molecular mass of 289.20.

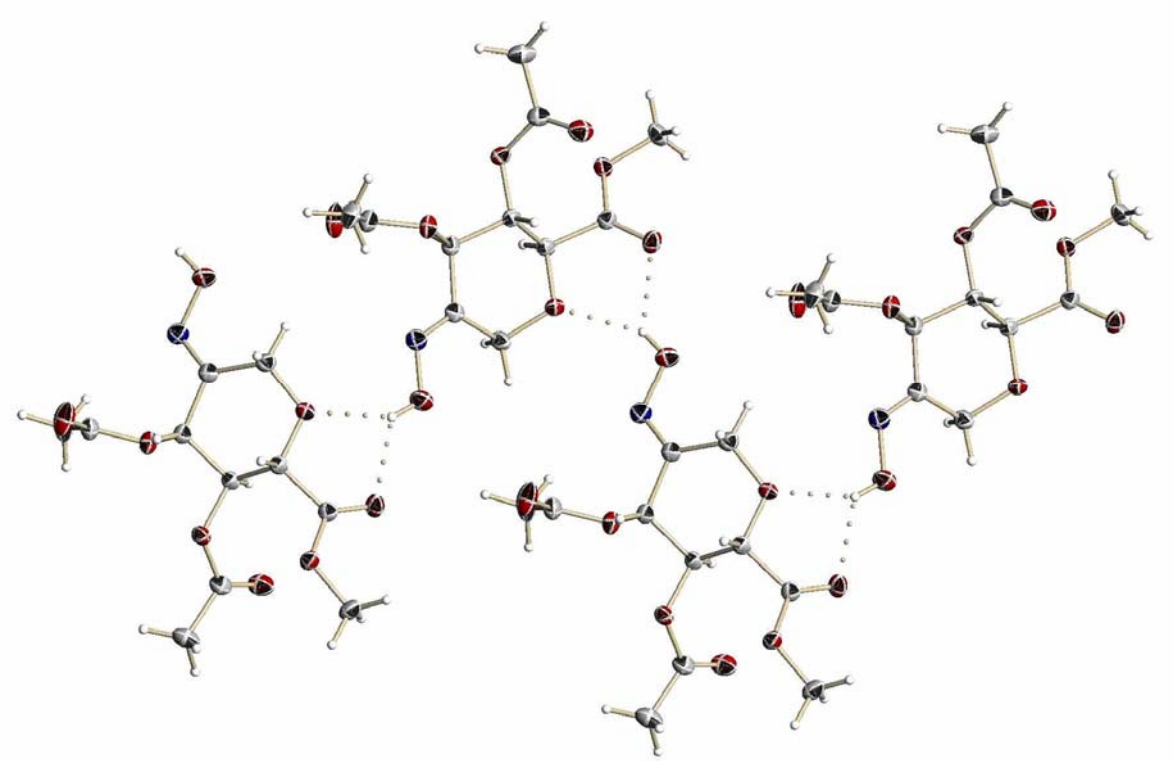

Figure 13: X-ray structure of oxime **28**.

The benzoylation of **28** with benzoyl chloride in pyridine afforded *O*-benzoyloxime **29** in 28% yield as a yellow solid (Scheme 12). The TLC of the reaction mixture showed a spot that was UV-active and an R_f value that showed a slight difference

in the polarity between the starting material and the product. Investigation of the ^{1}H NMR spectrum showed the appearance of signals that correspond to the benzoyl protecting group at 7.49 (*m*-Ar-H), 7.64 (*p*-Ar-H), and 8.04 (*o*-Ar-H). The C-1 proton signals were shown between 4.95 and 5.03 ppm as a doublet of doublets with a coupling constant of J = 15.84 Hz. The signals for both H-3 and H-5 were shown as doublets at 5.70 and 4.46 ppm respectively due to the presence of a neighboring hydrogen atom for each (H-4). The ^{13}C NMR spectrum also provided evidence for the formation of the product by new signals for the carbon atoms of the benzene ring between 128.9 and 134.9 ppm, as well as a corresponding carbonyl signal at 158.5 ppm.

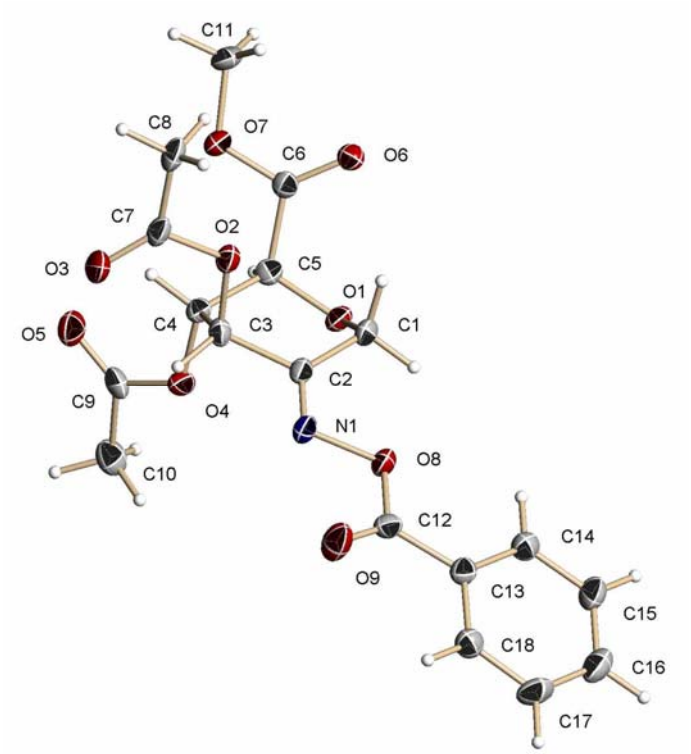

Figure 14: X-ray structure of benzoyloxime **29**.

X-ray crystallography shows a structure that contains all functional groups in axial positions, which appears to be due to the fact that the oxyimine locks the

conformation of the sugar. This locking of conformation is supported by proton NMR data due to the fact that the coupling constants for H-3, H-4, and H-5 are between approximately 3.5 and 4.5 Hz, which means that the protons are in a pseudo-equatorial orientation. Electrospray Ionization (ESI) mass spectrometry shows an M^+ of 416.1, which corresponds to the calculated molecular mass of 393.30.

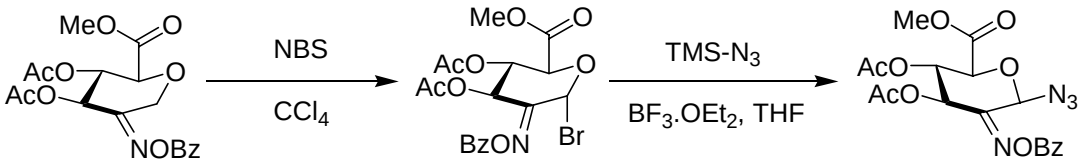

29 **30** **31**

Scheme 13: Formation of azide **31**.

The first step involved in the synthesis of methyl 3,4-di-*O*-acetyl-2-(benzoyloximino)-1-bromo-2-deoxyl-α-D-*arabino*-hexopyranuronate (**30**) was the introduction of bromide via radical substitution of **29** (Scheme 13). The gentle reflux of a mixture of **29** and NBS in CCl_4 was achieved using a 250 W lamp as a heat source. A UV-active spot that was slightly lower than the starting material on a TLC plate was observed. Two singlets observed on the ^{1}H NMR at approximately 2.0 ppm correspond to the methyl portions of the acetyl protecting groups of the sugar at C-3 and C-4. The signal for the methyl group of the methyl ester appears at 3.80 ppm, which is a slight shift upfield from that of the starting material. The proton signals at 4.95 and 5.03 ppm for H-1 and H-1' had disappeared and a new singlet appeared further downfield due to the electronegativity of the bromine atom (at 7.42 ppm), which supports formation of the product. The ^{13}C NMR data also supported the fact that the bromination took place at C-1 with the change of the signal from 60.6 to 73.2 ppm.

The formation of benzoyloxime azide **31** was achieved by reacting **30** with trimethylsilyl azide in the presence of boron trifluoride diethyl etherate in tetrahydrofuran. After three hours, the TLC plate indicated the consumption of the starting material. The product was found to be UV-active and also with a higher R_f than that of the starting material. The crude ^{1}H NMR spectrum provided signals corresponding to the product. The disappearance of the C-1 proton signal at approximately 7.4 ppm and the appearance of a new singlet at ~6.6 ppm indicated the loss of the Br atom at C-1. The remaining proton signals of **31** showed a slight upfield shift in comparison to those of starting material **30**.

2. Synthesis of D-glucopyranosyl azide and nitrile

Preparation of glucuronosyl azide **32** was achieved by substitution on 2,3,4-tri-*O*-acetyl-α-D-glucopyranosyl bromide (**3**) itself formed from acetylated **2α** (Scheme 14). The first step in the synthetic strategy was the bromination of **2α** with HBr, which gave the thermodynamically favored compound **3** in 97% yield. The material shown on the TLC gave a UV-active spot that burned at a slightly lower R_f value than that of the starting material. The absence of one of the acetyl protecting group signals between 1.84-1.89 ppm in the ^{1}H NMR spectrum and the appearance of a doublet, which corresponds to the C-1 proton at 6.47 ppm, indicates the bromination of **2α** at C-1. The ^{13}C NMR also supported the bromination of **3** with the disappearance of a carbonyl signal that was observed between 164 and 170 ppm on the ^{13}C NMR spectrum of the starting material.

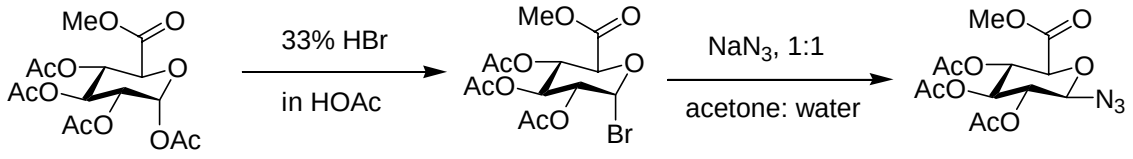

2α **3** **32**

Scheme 14: Synthesis of glucopyranosyl azide **32**.

2,3,4-Tri-*O*-acetyl-α-D-glucopyranosyl bromide (**3**) reacts readily with NaN_3 to afford glucuronate azide **32** (Scheme 14) as a yellow syrup. TLC showed a UV-active spot burning at a higher R_f value than that of the starting material. The ^1H NMR spectrum showed the signal shift from 6.47 ppm to 4.72 ppm due to shielding from the N_3 group with the coupling constant of 8.79 Hz. All of the acetyl protecting group signals were observed with the same intensity at approximately 2.00 ppm. The carboxylic acid methyl ester at C-6 was seen again at approximately 3.80 ppm. Comparing the ^{13}C NMR spectrum with that of the starting material, there was a slight shift observed for the anomeric carbon as well as for one of the carbonyl carbons, but the rest of the signals were virtually identical to the shifts observed in the carbon spectrum of the starting material.

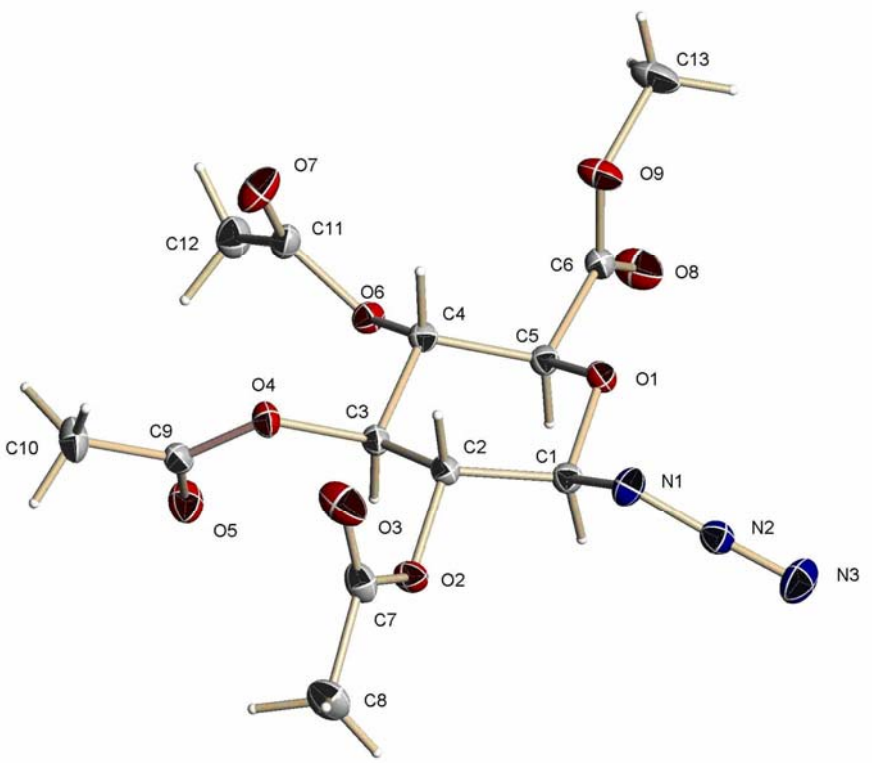

Figure 15: X-ray structure of glucuronosyl azide **32**.

Crystallography data supports the exclusive formation of β-azide (Figure 15). Mass spectrometry data supports the formation of product due to an M+ of 382.1, which corresponds to the calculated molecular mass and the presence of sodium.

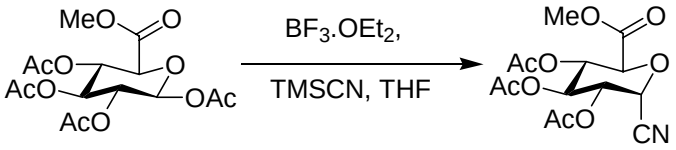

2β **25**

Equation 5: Preparation of glucopyranosyl nitrile **25**.

Preparation of glucuronosyl nitrile **25** was achieved via the reaction of methyl 1,2,3,4-tetra-*O*-acetyl-β-D-glucopyranuronate (**2β**) with trimethylsilyl cyanide in the

presence of a stoichiometric amount of boron trifluoride etherate. TLC showed a UV-active spot burning at a higher R_f value than that of the starting material. Three singlets observed on the ^{1}H NMR at approximately 2.0 ppm correspond to the methyl portions of the acetyl protecting groups of the sugar at C-2, C-3 and C-4. The disappearance of one of the methyl signals for an acetyl protecting group signifies the loss of one of these groups via a substitution reaction. The signal for the methyl group of the methyl ester appears at 3.75 ppm, which is a slight shift downfield from that of the starting material.

A shift of the C-1 peak of the starting material occurred from 5.77 Hz to 5.90 Hz with a coupling constant of J = 4.76 Hz suggesting that the alpha anomer was formed preferentially. Examination of the ^{13}C NMR spectrum also provided evidence for the formation of the nitrile via the appearance of a new signal at 117.3 Hz, which is representative of a triple bond between a carbon and a nitrogen atom. There was a slight shift observed for the anomeric carbon as well as for one of the carbonyl carbons, but the rest of the signals were virtually identical to the shifts observed in the carbon spectrum of the starting material. Electrospray ionization (ESI) mass spectrometry shows an M^+ of 366.2 which corresponds to the calculated molecular mass.

3. Conversion of glycosyl azide into amides

Formation of the amide from the azide was achieved using the modified Staudinger reaction with bis(diphenylphosphino)ethane.[45] The reaction sequence includes the formation of a triazaphosphadiene intermediate first, followed by the loss of nitrogen to afford a phosphinimine ylide (Scheme 15).

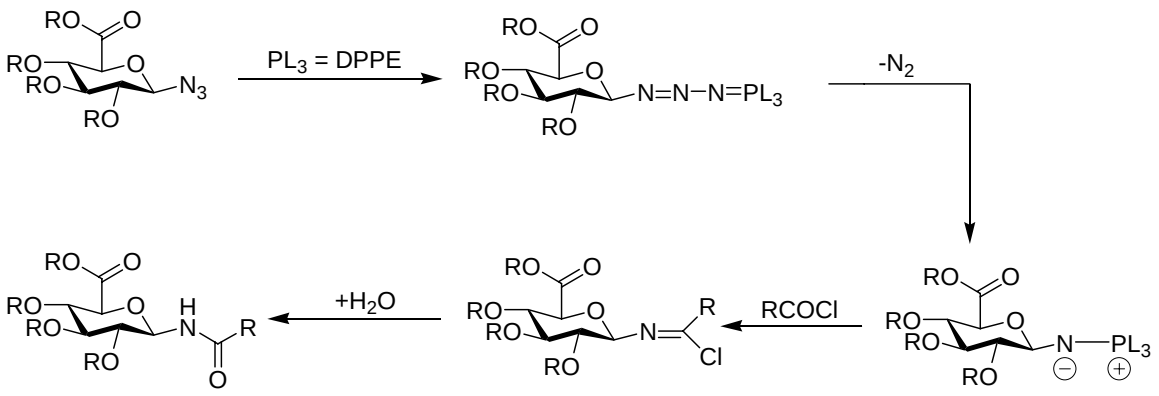

Scheme 15: Amide synthesis *via* Staudinger reactions.

The phosphinimine ylide was then reacted with an acid chloride to yield *N*-linked glycosyl amides. Because of the ready availability of glycosyl azides, the introduction of different substituents at C-1 to provide a stereoselective synthesis of β-glycosyl amides was investigated. The use of DPPE allowed for easy purification and high yields of products. Mechanistically, the first step involves the formation of an ylide, which then attacks the electrophilic carbonyl carbon of the acid chloride to afford an imidoyl chloride intermediate, followed by hydrolysis to yield the amide product (Scheme 15).

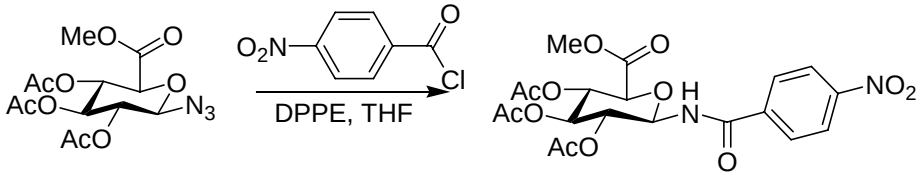

32 **33**

Equation 6: *p*-Nitrobenzoic acid-(β-D-glucopyranuronosyl)-amide (**33**).

The reaction of azide **32** with DPPE and *p*-nitrobenzoyl chloride (Equation 6) afforded a high yield (72%) of **33** as a yellow crystalline solid (Table 1). Study of the TLC plate showed a UV-active spot that burned at a lower R_f value than that of the

starting material. Investigation of the ^{1}H NMR spectrum indicated that the signal at 5.42 ppm is actually the overlap of two doublets of doublets, and the integration value provided the evidence of this signal as two hydrogen atoms (shown as a "quintet" signal shape). One of the signals had a coupling constant of 8.97 Hz, which is the same value as for the NH doublet signal which appeared at 7.39 ppm, thus it was determined to be that of the H-1 proton. Aryl ring resonances indicated two types of protons that appeared at 7.93 and 8.30 ppm as doublets. COSY experiments support the proper assignment of carbohydrate ring protons.

Analysis of the ^{13}C NMR spectrum provided evidence for the formation of **33** by presenting five signals in the region of 166.5-171.8 ppm, which indicates the carbonyl groups of the acetyl protecting groups, the carbonyl carbon of the methyl ester at C-6, and the carbonyl carbon of the newly formed amide. The aryl ring carbon signals also appear between 124.7 and 150.8 ppm, and the signal at 54.0 ppm represents the methyl group of the carboxylic acid ester. The signal for the methyl group of the acid ester appeared farther downfield than that of the acetyl protecting groups at approximately 22 ppm due to the direct attachment of the carbon atom to a highly electronegative oxygen atom. ESI mass spectrometric analysis provides an M+ of 505.0, which corresponds to the calculated molecular mass with the addition of a sodium atom. X-ray crystallography data supports the exclusive formation of the β-anomer of compound **33** (Figure 16).

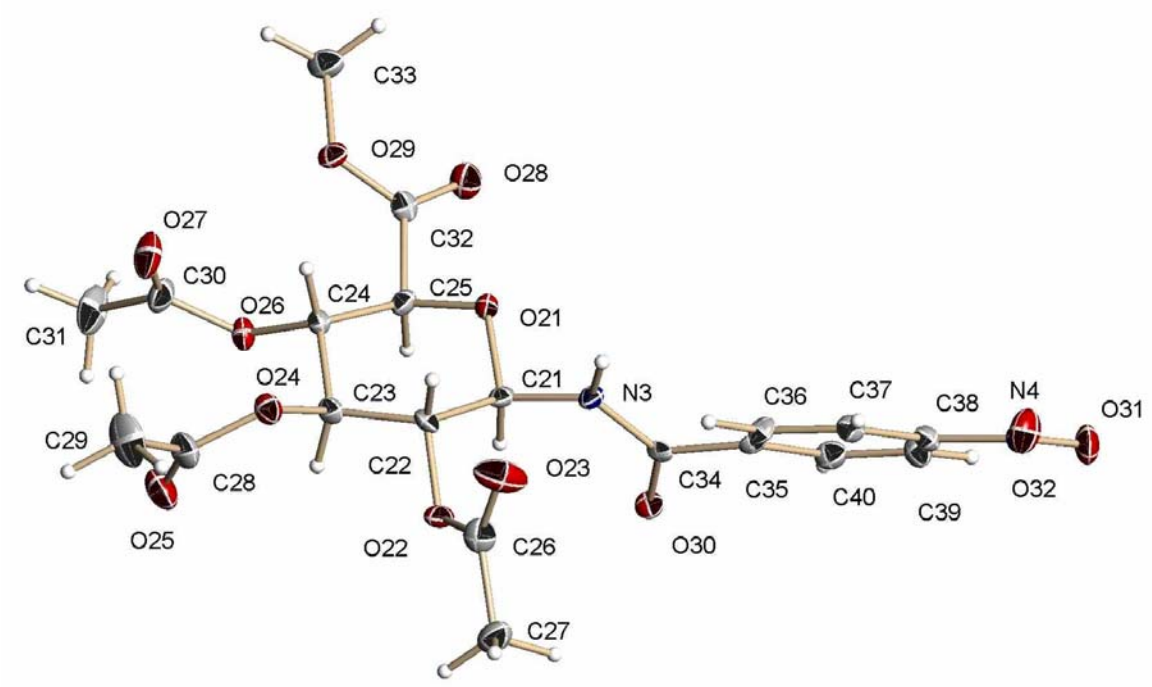

Figure 16: X-ray structure of amide **33**.

Starting Material	Acid Chloride	Product	% Yield	R_f value*
32	*p*-Nitrobenzoyl Chloride	**33**	72	0.24
	p-Fluorobenzoyl Chloride	**34**	80	0.29
	Butyryl Chloride	**35**	70	0.20
	Benzoyl Chloride	**36**	98	0.37
	Pentafluorobenzoyl Chloride	**37**	86	0.43
	Isovaleryl Chloride	**38**	56	0.23
	2-Furoyl Chloride	**39**	60	0.27
	2-Naphthoyl Chloride	**40**	63	0.35

* Solvent System- 1:1 hexanes: ethyl acetate

Table 1: Synthesis of amides *via* Staudinger reaction (Glucuronosyl azide **32**).

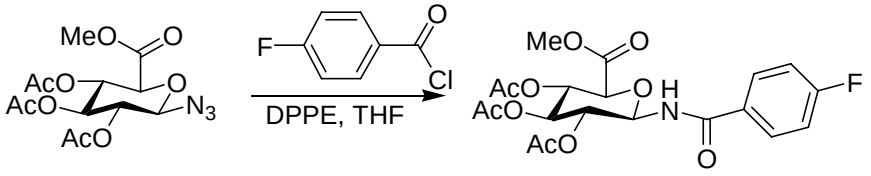

32 **34**

Equation 7: *p*-Fluorobenzoic acid-(β-D-glucopyranuronosyl)-amide (**34**).

The reaction between azide **32**, DPPE, and *p*-fluorobenzoyl chloride afforded a high yield (80%) of amide **34** as a colorless syrup (Table 1). Examination of the TLC plate showed a UV-active spot that burned at a lower R_f value than that of the starting material. Investigation of the ^{1}H NMR spectrum indicated the presence of the H-1 triplet at 7.06 ppm, which had a coupling constant of 8.51 Hz. A short, broad doublet also appeared at approximately 7.4 ppm to indicate the presence of the N-H proton of the amide. Further investigation of the proton NMR spectrum provided two aryl ring resonances as doublets of doublets at 7.06 and 7.77 ppm due to H-F coupling.

Analysis of the ^{13}C NMR spectrum provided evidence for the formation of **34** by presenting five signals in the region of 164.8-172.6 ppm, which indicates the carbonyl groups of the acetyl protecting groups, ester and amide. The aryl ring carbon signals also appear between 116.6 and 166.1 ppm and also show C-F coupling. The signal at 54.0 ppm represents the methyl group of the carboxylic acid ester. The carbon signal at 166.1 has a coupling constant of J = 252.5 Hz due to the fact that carbon-13 and fluorine-19 couple. Also evident are the signals around 21 ppm illustrating the methyl groups associated with the acetyl protecting groups. ESI mass spectral data provides evidence that the experimental M^+ is in agreement with the calculated molecular ion (plus sodium) of 478.1.

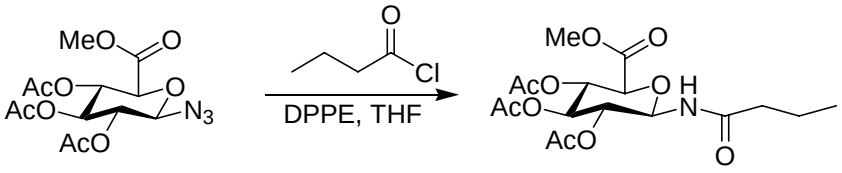

32 **35**

Equation 8: Butyric acid-(β-D-glucopyranuronosyl)-amide (**35**).

In the reaction of **32** with butyryl chloride, TLC showed a UV-active spot that burned at a slightly lower R_f value than that of azide **32**. The product was purified by elution from a silica gel column to afford **35** in 70% yield as white solid (Equation 8). The ^{1}H NMR spectrum showed the downfield shift of the C-1 doublet from the starting material (4.72 ppm), which now appears as a triplet at 5.34 ppm, and which possesses a coupling constant of 9.52 Hz. This shift is due to the greater deshielding of the amide nitrogen in relation to that of the azide precursor. All of the acetyl protecting group signals were observed with the same intensity at approximately 2.00 ppm. The carboxylic acid methyl ester at C-6 was seen again at approximately 3.70 ppm.

Analysis of the ^{13}C NMR spectrum provided evidence for the formation of **35** by the appearance of five signals in the region of 168.1-174.4 ppm, which indicates the carbonyl groups of the acetyl protecting groups, the carboxylic acid ester at C-6, and the newly formed amide carbonyl. Comparing the ^{13}C NMR with that of the starting material, there was a shift observed for the anomeric carbon from 89.0 to 77.9 Hz as well as a minor shift for one of the carbonyl carbons, but the rest of the signals were virtually identical to the shifts observed in the carbon spectrum of the starting material. Mass spectral data shows an M^+ at 426.1 that corresponds to the calculated molecular weight of 403.38 along with the addition of sodium.

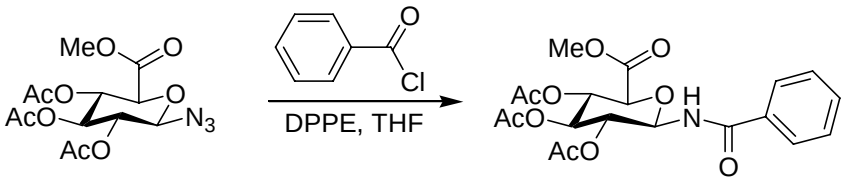

32 **36**

Equation 9: Benzoic acid-(β-D-glucopyranuronosyl)-amide (**36**).

The reaction of **32** with DPPE and benzoyl chloride afforded a high yield (98%) of **36** as a colorless solid (Table 1). Study of the TLC plate showed a UV-active spot that burned at a lower R_f value than that of the starting material. Investigation of the ^{1}H NMR spectrum indicated that the signal at 5.47 ppm is actually the overlap of one doublet of doublets and a triplet, and the integration value provided the evidence of this signal as two protons (shown as a "quintet" signal shape). One of the signals had a coupling constant close to 9.15 Hz, which is the same value as the NH doublet which appeared at 7.15 ppm, thus it was determined to be that of the H-1 proton. Aryl ring resonances indicated two types of protons that appeared at 7.53 and 7.75 ppm as doublets. Examination of the ^{13}C NMR spectrum provided evidence for the formation of **36** by presenting five signals in the region of 168.1-172.1 ppm, which indicates the carbonyl groups of the acetyl protecting groups, the carbonyl carbon of the methyl ester at C-6, and the amide. The aryl ring carbon signals also appear between 128.3 and 133.7 ppm, and the signal at 54.0 ppm represents the methyl group of the carboxylic acid ester. The signal for the methyl group of the acid ester appeared farther downfield than that of the acetyl protecting groups at approximately 22 ppm due to the direct attachment of the carbon atom to a highly electronegative oxygen atom. Mass spectrometry data

determined that the calculated molecular ion of 437.40 was in agreement with the M^+ found.

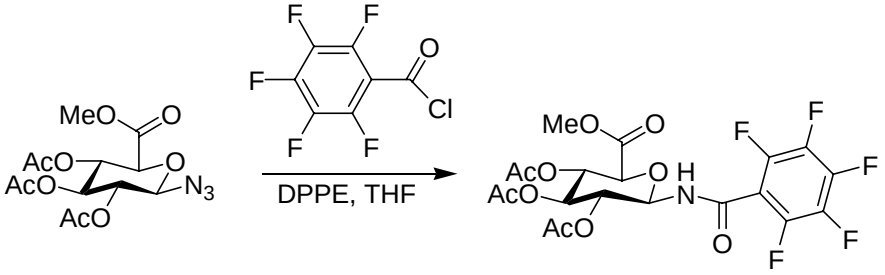

32 **37**

Equation 10: Pentafluorobenzoic acid-(β-D-glucopyranuronosyl)-amide (**37**).

The reaction with pentafluorobenzoyl chloride (Equation 10) afforded a high yield (86%) of **37** as a white syrup (Table 1). Examination of the TLC plate showed a UV-active spot that burned at a lower R_f value than that of the starting material. Investigation of the ^{1}H NMR spectrum indicated the presence of the H-1 triplet at 5.46 ppm, which had a coupling constant of 9.34 Hz. A short, broad doublet also appeared at approximately 7.3 ppm with a coupling constant of approximately 9.2 Hz, to indicate the presence of the N-H proton of the amide. With further analysis of the ^{1}H NMR spectrum, it was noted that there are no peaks in the typical aromatic region of the spectrum due to the fact that the aryl protons have been replaced by fluorine atoms.

Analysis of the ^{13}C NMR spectrum provided evidence for the formation of **37** by the appearance of five signals in the region of 158.6-170.8 ppm, which indicates the carbonyl groups of the acetyl protecting groups, the ester and the amide. The aryl ring carbon signals appeared as doublets with coupling constants of approximately 250 Hz. The carbon of the methyl ester appeared at 54.1 ppm, which is farther downfield than that of the methyl carbons of the acetyl protecting groups, which appeared at approximately

22 ppm. Electrospray Ionization mass spectrometry proved that the M+ found, 550.0, was in agreement with the calculated molecular mass plus sodium.

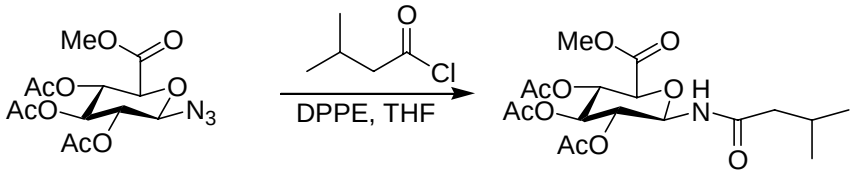

32 **38**

Equation 11: Isovaleric acid-(β-D-glucopyranuronosyl)-amide (**38**).

In the reaction with isovaleryl chloride, TLC showed a UV-active spot that burned at a slightly lower R_f value than that of azide **32**. The product was purified by elution from a silica gel column to afford **38** in moderate yield (56%) as bright yellow foam (Equation 11). The ^{1}H NMR spectrum showed a downfield shift of the H-1 triplet of the starting material at 4.72 ppm, due to the increased deshielding that the amide provides for the anomeric proton. All of the acetyl protecting groups remained throughout the course of the reaction as indicated by the three signals at ~2.0 ppm. The signal for the methyl ester was also maintained from azide **32** with very little alteration of position. Investigation of the ^{13}C NMR spectrum provided evidence for the formation of **38** due to the appearance of a peak at 23.4 ppm that represents the symmetric methyl groups of the *i*-amyl portion of the glycomimetic compound. In addition to the peak at 23.4 ppm, five signals appeared between 168.1 and 173.9 ppm as a representation of the acetyl protecting group, ester and amide carbonyl carbon atoms. Analysis of high resolution mass spectrometry data determines that the M^+ calculated is in agreement with the M^+ found, 440.1.

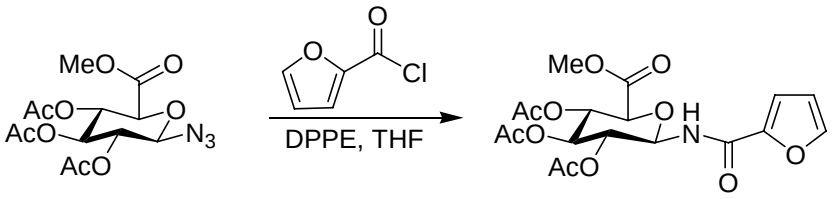

32 **39**

Equation 12: Furan-2-carboxylic acid-(β-D-glucopyranuronosyl)-amide (**39**).

When 2-furoyl chloride was used, TLC showed a UV-active spot that burned at a slightly lower R_f value than that of azide **32**. The product was purified by elution from a silica gel column to afford **39** in moderate yield (61%) as a foam (Equation 12). The ^{1}H NMR spectrum shows a 2H multiplet at 5.43 ppm corresponding to H-1 and H-2. The ^{1}H NMR spectrum also shows a group of multiplets downfield from 6.46 ppm to 7.66 ppm representing the amide proton as well as the three furan protons in product **39**. Investigation of the ^{13}C NMR spectrum provided evidence for the formation of **39** due to the appearance a group of signals from 113.3-159.1 ppm representing the carbon atoms in the amide functionality as well as the furan ring. All other signals in the ^{13}C NMR spectrum appear to be altered only a minor amount compared to the azide precursor. Mass spectrometry data provided evidence that the calculated molecular mass plus a proton agreed with the experimental M^+ of 428.1.

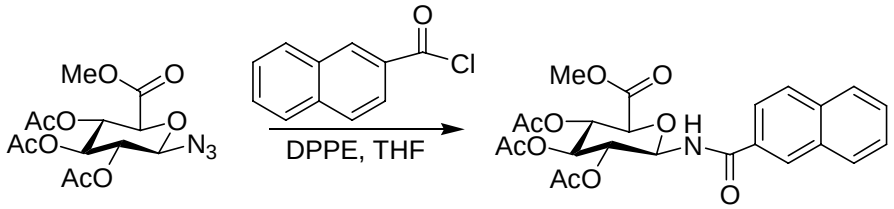

32 **40**

Equation 13: Naphthanoic acid-(β-D-glucopyranuronosyl)-amide (**40**).

The reaction with 2-naphthoyl chloride afforded a modest yield (63%) of **40** as white powder (Equation 13, Table 1). Examination of the TLC plate showed a UV-active spot that burned at a lower R_f value than that of the starting material. Investigation of the ^{1}H NMR spectrum indicated the presence of the H-1 triplet at 5.58 ppm, which had a coupling constant of 9.62 Hz. The spectrum also showed a large grouping of signals in the aromatic region supporting the fact that the naphthoyl ring is attached as a portion of molecule **40**. All of the acetyl protecting groups remained intact throughout the course of the reaction as indicated by the three signals at ~2.0 ppm. The signal for the methyl ester was also maintained from azide **32** with very little alteration of position. Analysis of the ^{13}C NMR spectrum provided evidence for the formation of **40** due to the appearance a group of signals from 124.4-136.1 ppm corresponding to the presence of the naphthoyl moiety. The ^{13}C NMR spectrum also contained a fifth carbonyl signal, representing the amide carbonyl carbon, which was not present in the azide precursor. The analysis of ESI mass spectrometry data provided evidence for the correct molecular mass (with the addition of a proton) from an ion with an *m*/*z* ratio of 488.2.

4. Conversion of glycosyl azide to glycosyl imines

Formation of the amine from the azide was achieved using a modified Staudinger reaction with DPPE. The reaction sequence includes the formation of a triazaphosphadiene intermediate (Scheme 16) first, followed by the loss of nitrogen to afford a phosphinimine ylide.

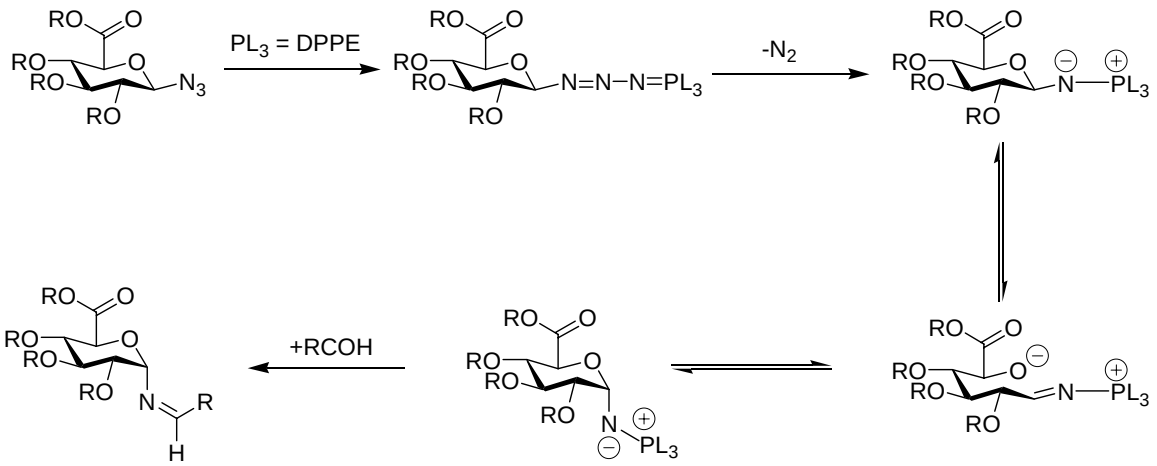

Scheme 16: Imine synthesis *via* Staudinger reactions.

The phosphinimine ylide then undergoes isomerization at equilibrium to produce the alpha ylide, possibly favored due to the anomeric affect, which then readily reacted with an aldehyde to yield *N*-linked glycosyl imines. Due to the ready availability of glycosyl azide **32**, the introduction and study of different substituents at C-1 to provide a stereoselective synthesis of α-glycosyl imines was investigated. Mechanistically, the most interesting portion of the mechanism is the isomerization that occurs around C-1 due to the influence of the free electrons of the nitrogen atom of the phosphinimine ylide.

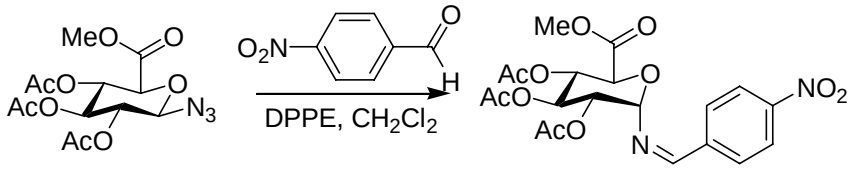

32 **41**

Equation 14: *p*-Nitrobenzoic acid-(α-D-glucopyranuronosyl)-imine (**41**).

The reaction of azide **32** with DPPE and *p*-nitrobenzaldehyde (Equation 14) afforded a moderate yield (42%) of **41** as a colorless crystalline solid. Study of the TLC

plate revealed a UV-active spot that burned at a lower R_f than that of the starting material. Investigation of the ^1H NMR spectrum indicated the presence of a doublet at 5.38 Hz with a coupling constant of 4.22 Hz, corresponding to the proton associated with H-1. Aryl ring resonances indicated the presence of two types of protons that appeared at 7.99 and 8.31 ppm as doublets. Upon further analysis, a singlet corresponding to the imine proton was found at 8.38 ppm.

Analysis of the ^{13}C NMR spectrum provided evidence for the formation of **41** by presenting five carbonyl signals in the region of 162.8-170.6 ppm, which indicates carbonyl groups of the acetyl protecting groups, the methyl ester, and the carbonyl carbon of the newly formed imine. Aryl ring carbon signals also appeared between 125.0 and 150.8 ppm. The signals for the methyl group of the acid ester and the methyl portions of the acetyl protecting groups are still present, exhibiting little alteration from that of the azide precursor. X-ray crystallography data supports the isolation of only the α-anomer of compound **41** (Figure 17). Mass spectral analysis provided evidence that the experimental M^+ is in agreement with the calculated molecular mass.

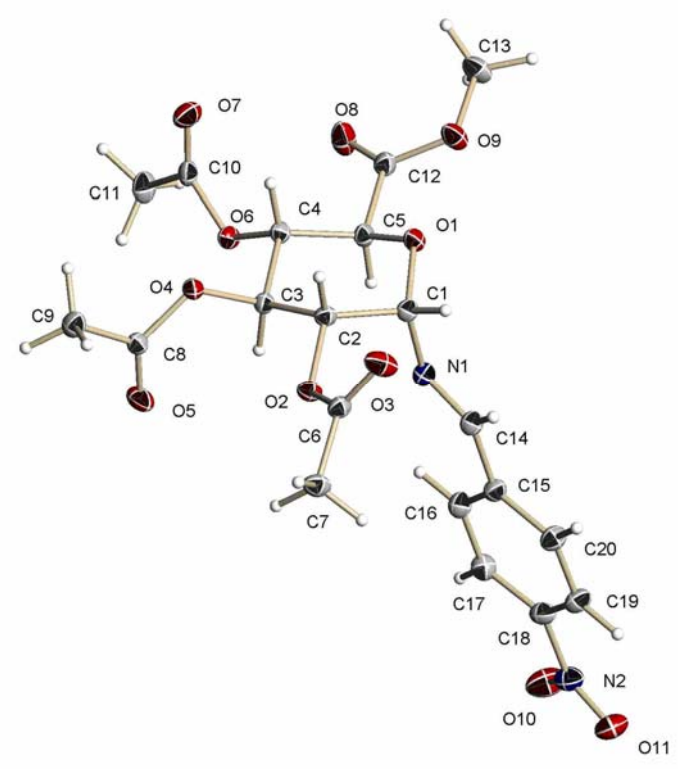

Figure 17: X-ray crystal structure of imine **41**.

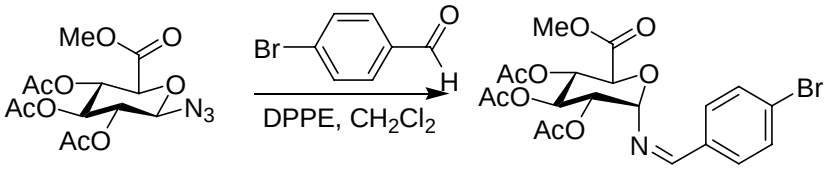

32 **42**

Equation 15: *p*-Bromobenzoic acid-(α-D-glucopyranuronosyl)-imine (**42**).

The reaction of azide **32** with DPPE and *p*-bromobenzaldehyde (Equation 15) afforded a moderate yield (45%) of **42** as a yellow solid. Study of the TLC plate revealed a UV-active spot that burned at a lower R_f than that of the starting material. Investigation of the ^{1}H NMR spectrum indicated the presence of a doublet representing H-1 at 5.27 ppm with a coupling constant of 4.21 Hz, once again suggesting formation of the α-

anomer. Further analysis of the ^{1}H NMR spectrum showed a singlet corresponding to the imine proton at 8.20 ppm. Analysis of the ^{13}C NMR spectrum provided evidence for the formation of **42** by presenting five carbonyl signals in the region of 169.5-171.1 ppm, which indicates carbonyl groups of the acetyl protecting groups, the methyl ester, and the carbonyl carbon of the newly formed imine. Aryl ring carbon signals also appeared between 132.0 and 133.4 ppm. ESI mass spectrometry provided evidence that the calculated molecular mass was in agreement with the experimental M^{+} of 502.1.

5. Conversion of glycosyl azide into glycopyranosyl-[1,2,3]-triazoles

Formation of the triazole was achieved by reacting the azide with a terminal alkyne in the presence of a copper (II) salt and ascorbic acid. The mechanism is similar to that of a Huisgen 1,3-dipolar cycloaddition and a modified organo-cuprate intermediate helps to mediate the addition process by altering the electronic properties of the alkyne.

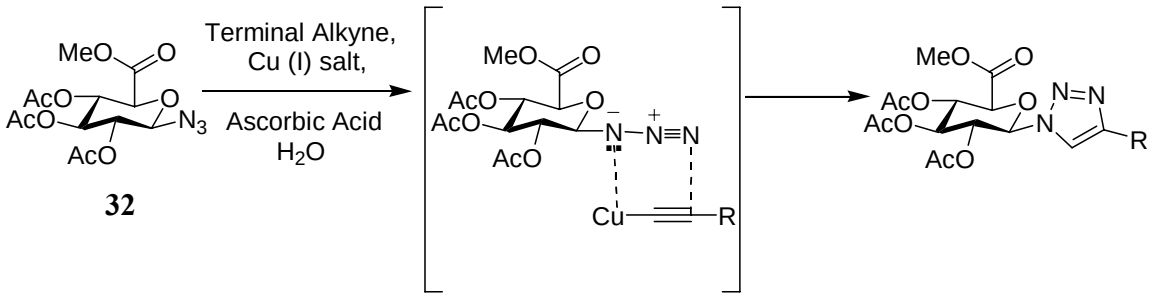

Scheme 17: Synthesis of triazoles *via* the Huisgen reaction.

The partially negatively charged nitrogen of the azide acts as a nucleophile, attacking the terminal carbon of the alkyne, driving π-electrons from the triple bond to attack the azide nitrogen closest to the sugar moiety. This cyclic addition forms two new

bonds during the closing of the heterocyclic aromatic system, producing the 1,4-triazole. The fact that the triazole product is not soluble at reduced temperatures is of great interest due to the ease of isolation via filtration. This method leads to easy product isolation, high yields, and few offensive by-products.

Sharpless has reported that a catalytic amount of Cu(I) salts considerably increases the rate of reaction through a catalytic cycle (Scheme 18), and also increases the regioselectivity of addition to afford 1,4-disubstituted products.[48]

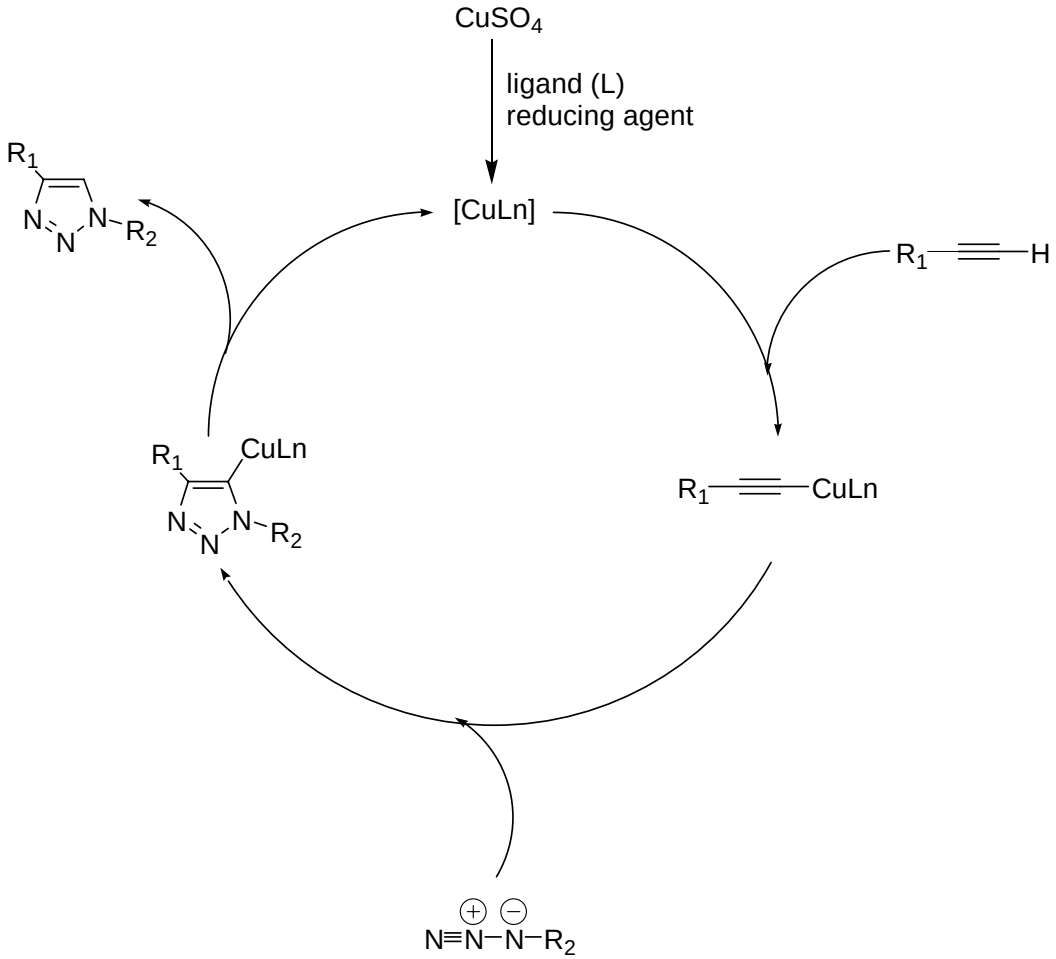

Scheme 18: Catalytic cycle for Cu(I)-catalyzed azide-alkyne coupling.

Glucuronosyl azide (**32**) was reacted with fourteen different alkynes to afford a variety of products (Figure 18), however no triazole products were isolated from reactions with trimethylsilyl acetylene and propiolic acid. Reactions with these two alkynes were monitored by TLC, which showed consumption of the starting material but analysis of the ^{1}H NMR spectra did not reveal formation of the triazole product.

Starting Material	Terminal Alkyne Reagent	Product	% Yield	R_f value*
32	Phenylacetylene	**43**	58	0.31
	3-Cyclopentyl-1-propyne	**44**	90	0.30
	1-Ethynyl-3-fluorobenzene	**45**	81	0.24
	4-Ethynyl Toluene	**46**	87	0.29
	Ethyl Propiolate	**47**	98	0.36
	1-Hexyne	**48**	88	0.49
	Trimethylsilyl Acetylene	N/R	-	-
	4-Ethynylanisole	**49**	64	0.18
	1-Heptyne	**50**	64	0.31
	1-Nonyne	**51**	96	0.36
	Propiolic Acid	N/R	-	-
	1-Decyne	**52**	79	0.58
	1-Dodecyne	**53**	97	0.71
	1-Octyne	**54**	73	0.28

* Solvent System- ethyl acetate

Table 2: Cycloaddition reactions with glucuronosyl azide **32**.

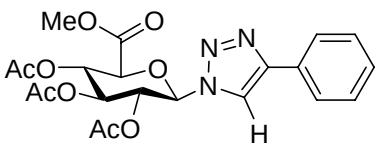

43

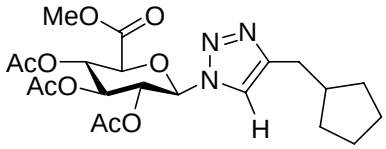

44

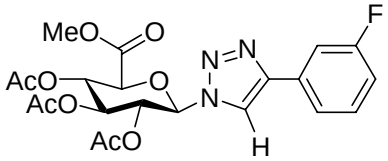

45

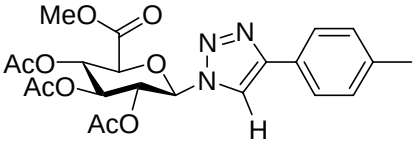

46

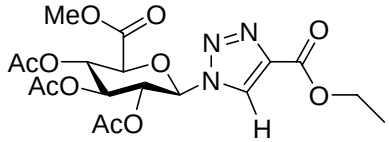

47

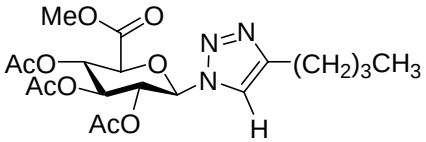

48

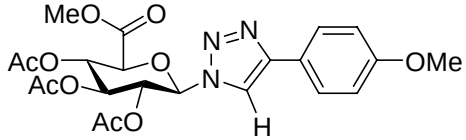

49

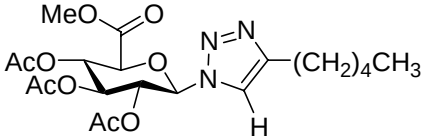

50

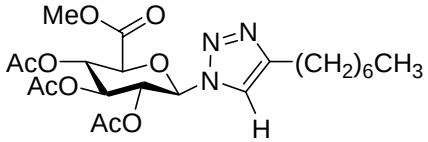

51

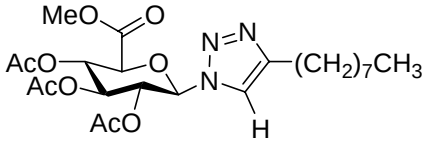

52

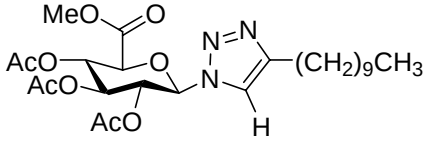

53

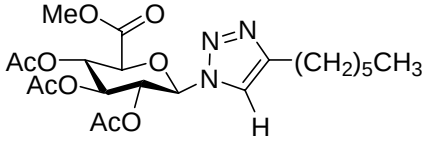

54

Figure 18: Glucuronosyl triazole products.

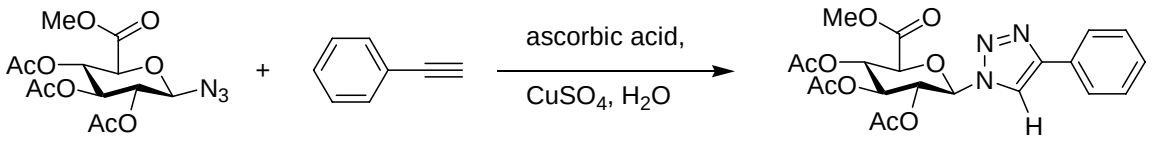

32 **43**

Equation 16: Synthesis of triazole **43** from azide **32**.

Some of the typical results from experiments are presented here. The first alkyne to be reacted with azide **32** was phenyl acetylene (Equation 16). This reaction was heated to 70 °C for sixteen hours and progression of the reaction was monitored via TLC, which showed total consumption of starting material and the formation of a new UV-active spot with an R_f value lower than that of azide **32**. The reaction mixture was then cooled and filtered through a glass frit. The crude product was then recrystallized from warm 95% ethanol to afford 0.74 g of white fluffy solid (58%). The ^{1}H NMR spectrum of product **43** revealed a new singlet at 8.07 ppm that corresponds to the triazole proton and the signals that correspond to the protons of the aromatic ring appeared between 7.36 and 7.84 ppm. The ^{1}H NMR spectrum also revealed a downfield shift for the anomeric proton from 4.72 ppm in the starting material to approximately 5.98 ppm in the 1,4-disubstituted triazole product. COSY NMR experiments assured the proper assignment of carbohydrate ring protons in the ^{1}H NMR spectrum. The ^{13}C NMR spectrum provided evidence for formation of the product through the appearance of aryl ring signals from 126.9-130.8 ppm as well as signals for the carbon-carbon double bond formed as part of the triazole ring at 118.9 and 149.5 ppm. All other signals in the ^{13}C NMR spectrum demonstrated very little alteration from that of the starting material. Mass spectrometry shows a peak

with an M^+ of 462.0, which corresponds to the addition of a proton to the calculated molecular mass of 461.14.

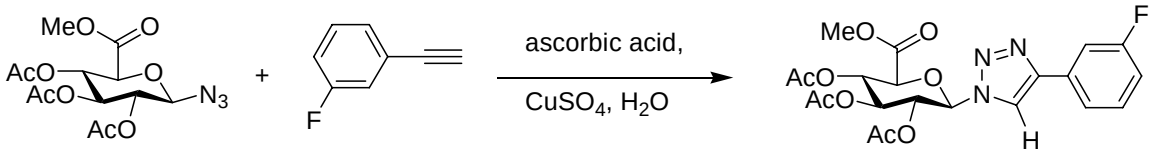

32 **45**

Equation 17: Synthesis of triazole **45** from azide **32**.

The reaction of azide **32** with 1-ethynyl-3-fluorobenzene afforded the triazole product (**45**, Equation 17) in good yield (1.08 g, 81%) as a pale yellow solid upon recrystallization. The reaction progress was monitored by TLC, which showed a UV-active spot that burned at a lower R_f than that of the starting material after a twelve hour reaction time. The ^{1}H NMR spectrum showed evidence of the product by indicating a singlet signal at 8.10 ppm corresponding to the triazole proton. Also shown on the ^{1}H NMR spectrum was a doublet of doublets of doublets at 7.05 ppm due to vicinal, *meta*, and H-F coupling of the aromatic protons of compound **45**. A doublet of doublets was also apparent at 7.40 ppm representing the *para* proton of the phenyl ring, exhibiting both a vicinal and H-F coupling with coupling constants of J = 8.24 and 2.20 Hz. Analysis of the ^{13}C NMR spectrum also provided evidence for the formation of product by indicating Ar-C signals from 115.0-162.0 ppm, and the appearance of signals at 119.4 ppm and 148.5 ppm representing the triazole ring carbon atoms. The signals for the three acetyl protecting groups are still present at approximately 21 ppm. ESI mass spectrometry provided evidence for an M^+ of 480.0, which corresponds to the calculated molecular mass.

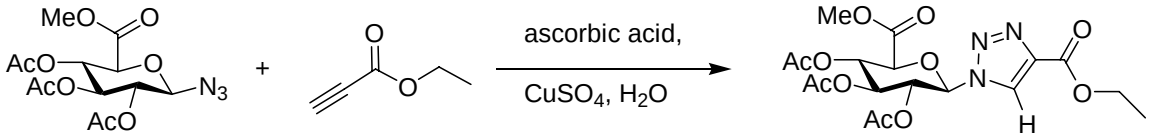

32 **47**

Equation 18: Synthesis of triazole **47** from azide **32**.

Reaction of sugar azide **32** with ethyl propiolate produced triazole **47** in 98% yield upon recrystallization of the filtered, crude product (Equation 18). Examination of the TLC plate revealed that a new UV-active spot had formed at a lower R_f value than that of the associated starting material, which had been consumed throughout the course of the reaction. Analysis of the ^{1}H NMR spectrum revealed a similar downfield shift to that of product **43**, due to an increase in the deshielding of the proton at C-1 along with the presence of the newly formed heteroaromatic system. Further examination of the ^{1}H NMR spectrum revealed the presence of a triplet at 1.42 ppm that corresponds to the methyl group of the ethyl ester, as well as the appearance of a quartet representing the methylene group of the ethyl ester at 4.43 ppm. Inspection of the ^{13}C NMR spectrum showed the presence of five carbonyl signals between 161.03-170.64 ppm, supporting the fact that the ethyl ester has successfully been incorporated into the product. The ^{13}C NMR spectrum contained signals at 127.3 ppm and 142.0 ppm that correspond to the triazole carbons and the signal at 15.6 ppm that corresponds to the methyl group carbon ($CO_2CH_2\underline{C}H_3$). Electrospray Ionization mass spectrometry provides evidence for an M^+ of 480.2, which corresponds to the addition of sodium to the expected molecular mass.

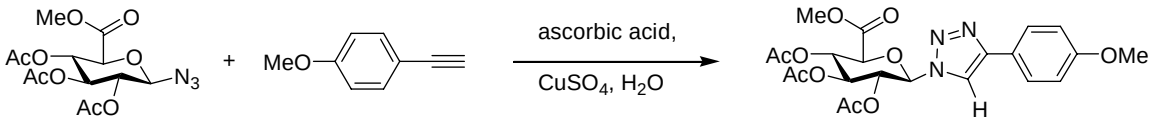

32 **49**

Equation 19: Synthesis of triazole **49** from azide **32**.

Compound **32** was reacted with 1-ethynyl-4-anisole to afford triazole **49** in 64% yield (Equation 19). The investigation of TLC showed a UV-active spot that burned at a slightly lower R_f value than that of the sugar azide precursor. The ^{1}H NMR spectrum showed the presence of a second methoxy group, which corresponds to the methoxy group of the anisole moiety at 3.83 ppm. The ^{1}H NMR spectrum also revealed a typical splitting pattern for the *para*-disubstituted aromatic ring appearing between 6.95 ppm and 7.95 ppm. A downfield shift of the anomeric proton was also observed, while all other signals remained relatively unchanged compared to the starting material. Scrutiny of the ^{13}C NMR spectrum revealed the presence of an aromatic system between 115.3-160.8 ppm, a peak at 56.5 ppm in relation to the aromatic methoxy group, and finally, peaks at 118.0 ppm and 149.4 ppm for the triazole ring carbon atoms. Mass spectral data provides evidence for an M^+ of 492.2, which corresponds directly to the calculated molecular mass.

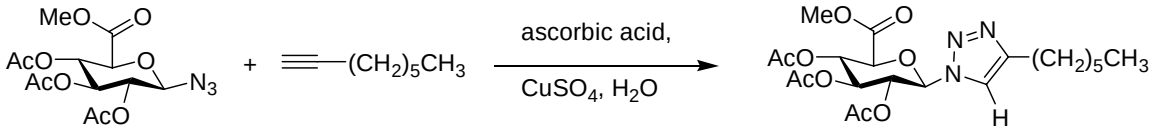

32 **55**

Equation 20: Synthesis of triazole **55** from azide **32**.

The reaction of glucuronosyl azide **32** with 1-octyne afforded triazole product **54** in moderate yield (73%), but high purity after recrystallization (Equation 20). Reaction progress was monitored by TLC until the starting material was consumed. Upon consumption of the starting material, a UV-active spot appeared at a higher R_f value than that of the starting material. The ^{1}H NMR spectrum showed evidence of product by indicating a singlet signal at 7.55 ppm corresponding to the triazole proton. Also shown in the ^{1}H NMR spectrum is a triplet signal at 0.86 ppm with a coupling constant of 6.22 Hz that corresponds to the terminal methyl group of the octyne chain. Analysis of the ^{13}C NMR spectrum also provided evidence for the formation of product **54** by indicating the presence of four carbonyl carbon signals from 167.2-170.6 ppm. The alkyl carbon chain signals can be found between 15.3-30.7 ppm, and the signal at 15.3 ppm represents the methyl group of the alkyl carbon chain. Finally, the ^{13}C NMR spectrum provided evidence of the triazole ring with two signals between 120.0 and 150.2 ppm. Analysis of mass spectral data provided evidence that the M^+ corresponds to the calculated molecular mass along with the addition of sodium.

For the reaction products **43**-**54**, yields of the products in the 58-98% range were obtained. All products afforded clean ^{1}H and ^{13}C NMR spectra that were easy to interpret. The ^{1}H NMR spectra of the products showed similar patterns, the important one being the triazole proton, which was observed as a singlet in the region of 7.55-8.43 ppm. In summary, the presence of $CuSO_4$ and ascorbic acid as a catalytic system not only increased the reaction rates, but also improved product yields and the ease of isolation.

6. Saponification of [1,2,3]-triazoles with lithium hydroxide

Biologically active carbohydrate mimetics are of great interest in glycobiology as well as pharmacology due to the increasing need for new antibiotic compounds.[1] It has been shown that most carbohydrate moieties in antibiotic compounds have no protecting groups, but rather contain multiple hydroxyl, amine, or ether functionalities. A common procedure for eliminating acetyl protecting group as well as esters is via a base-catalyzed saponification reaction. Saponification reactions can be thought of as a nucleophilic acyl substitution at the acyl oxygen of the ester (Scheme 19).

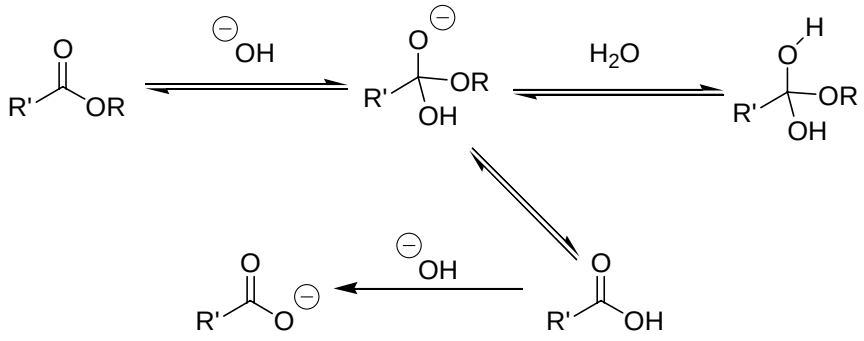

Scheme 19: General mechanism for a saponification reaction.

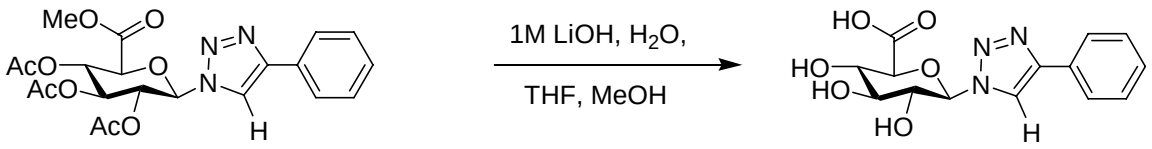

43 **55**

Equation 21: 1-(β-D-glucuronosyl)-4-phenyl-1*H*-[1,2,3]-triazole (**55**).

Some of the typical results from experiments are presented here. The first triazole reacted with a solution of LiOH was triazole **43** (Equation 21). The reaction was run at

room temperature for a period of approximately eighteen hours and progression of the reaction was monitored via TLC, which showed consumption of the starting material and the appearance of a new UV-active spot at an R_f lower than that of the starting material. After acidification, the reaction mixture was evaporated to yield pure product with no need for further purification to afford **55** as a pale brown solid (92%). The ^{13}C NMR spectrum of product **55** revealed the loss of three carbonyl carbon signals compared to the starting material as well as all three methyl groups of the acetyl protecting groups which were apparent at approximately 21 ppm in the ^{13}C NMR spectrum of product **43**. All other shifts in the ^{13}C NMR spectrum demonstrated little alteration from that of the starting material. ESI MS data supports the formation of **55** via an M^+ of 344.0, which corresponds to the addition of sodium to the calculated molecular mass.

Triazole Starting Material	Product	% Yield	R_f value*
43	**55**	92	0.20
44	**56**	72	0.64
45	**57**	64	0.21
46	**58**	93	0.22
52	**59**	99	0.47
49	**60**	99	0.17

* Solvent System- 3:1 ethyl acetate: methanol

Table 3: Respective deprotected 1,2,3-triazole products.

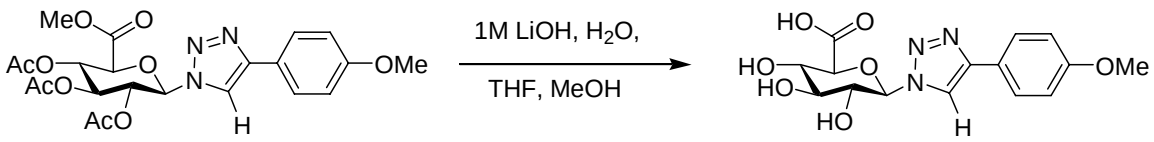

49 **60**

Equation 22: 1-(β-D-glucuronosyl)-4-(4-methoxyphenyl)-1*H*-[1,2,3]-triazole (**60**).

The reaction of triazole **49** with LiOH in a solution of water, methanol, and tetrahydrofuran afforded deprotected product **60** in 99% yield as a yellow powder (Equation 22). Reaction progress was monitored by TLC to illustrate the disappearance of the starting material as well as a UV-active spot at a lower R_f value than that of triazole **49**. The ^{1}H NMR spectrum showed the disappearance of methyl signals, with little alteration of other signals as compared to starting material. No splitting patterns were altered from the NMR of the starting material to that of the product. The ^{13}C NMR spectrum of the product showed loss of three carbonyl signals in the region of approximately 170 ppm from that of the starting material. Mass spectral data shows an M^+ peak at 352.1, which is representative of the calculated molecular mass.

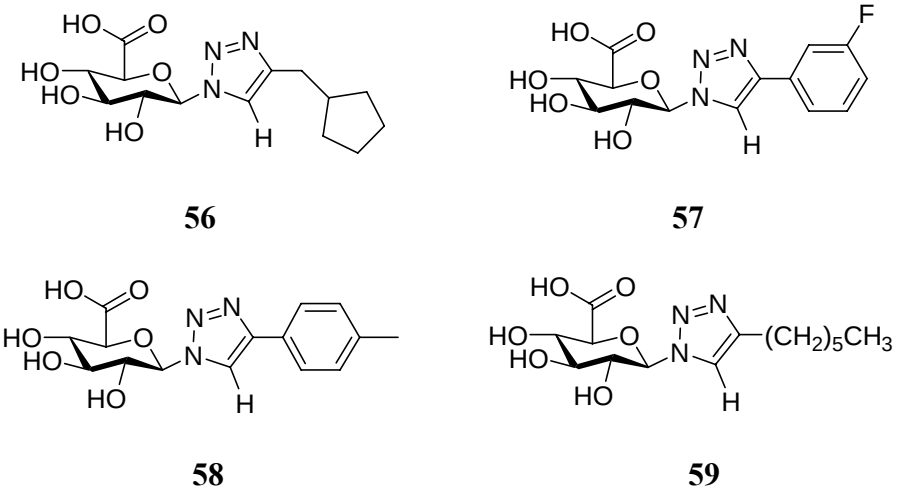

56 **57**

58 **59**

Figure 19: Saponification reaction products for [1,2,3]-disubstituted triazoles.

For the reaction products **55-60**, yields of the products in the 64-98% range were obtained. All products afforded clean ^{1}H and ^{13}C NMR spectra that were easy to interpret. The ^{1}H NMR spectra of the products showed similar patterns, the important change being the loss of carbonyl as well as methyl signals corresponding to the acetyl protecting groups. In summary, the use of LiOH is a rapid and efficient manner in which to deprotect the glycosyl [1,2,3]-disubstituted triazoles of interest with little purification necessary.

7. Formation of divalent [1,2,3]-triazoles

Formation of the divalent triazoles was achieved by reacting two equivalents of azide with a terminal diyne in the presence of a copper(II) salt and ascorbic acid. The mechanism is similar to that of a Huisgen 1,3-dipolar cycloaddition and a modified organo-cuprate intermediate helps to mediate the addition process by altering the electronic properties of the alkyne (Scheme 17). Glucuronosyl azide **32** was reacted with both 1,3- and 1,4-diethynylbenzene to afford the two expected disubstituted triazole products. (Figure 20).

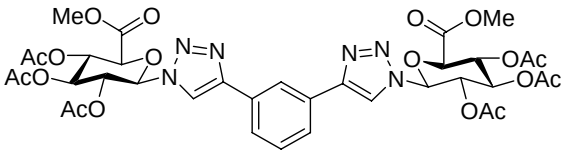

61

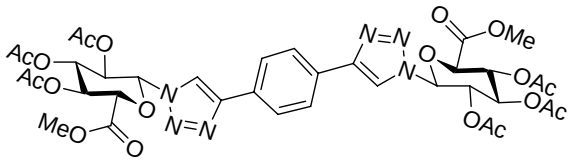

62

Figure 20: Divalent glucuronosyl triazole products.

The first alkyne to be reacted with azide **32** was 1,3-diethynylbenzene. This reaction was heated to 75 °C for eighteen hours and progression of the reaction was

monitored by TLC, which showed total consumption of starting material and the formation of a new UV-active spot with an R_f value lower than that of azide **32**. The reaction mixture was then cooled and filtered through a glass frit. The crude product was then recrystallized from warm isopropyl alcohol to afford 4.65 g of a fine beige powder (66%).

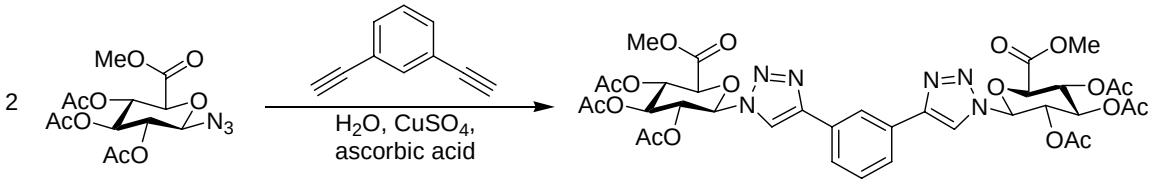

32 **61**

Equation 23: Synthesis of triazole **61**.

Reaction of 1,3-diethynylbenzene with glucuronosyl azide **32** afforded the divalent product in moderate yield (66%) as a beige powder (Equation 23). The ^{1}H NMR spectrum of product **61** revealed a new singlet at 9.15 ppm that corresponds to the triazole proton and the signals that correspond to the protons of the aromatic ring appeared between 7.57 and 8.39 ppm. Signals for the acetyl protecting groups appeared at approximately 2.0 ppm. Mass spectrometry shows a peak that with an M^+ of 785.3, which corresponds to the loss of an acetyl group from the calculated molecular mass of 844.73.

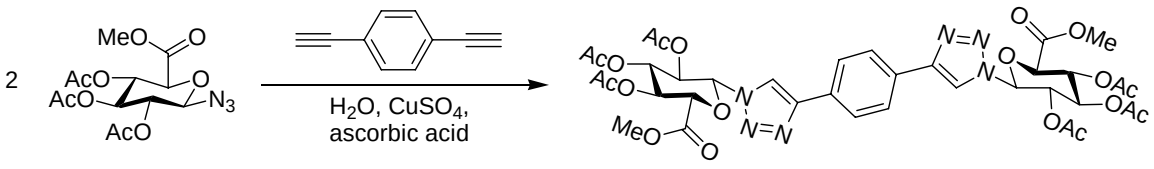

32 **62**

Equation 24: Synthesis of triazole **62**.

Reaction of 1,4-diethynylbenzene with glucuronosyl azide **32** afforded the divalent product in good yield (74%) as a pale orange powder (Equation 24). The ^{1}H NMR spectrum of product **62** revealed a new singlet at 9.09 ppm that corresponds to the triazole proton and the signal that corresponds to the protons of the aromatic ring appeared at 7.94 ppm. Mass spectrometry shows a peak that with an M^+ of 816.3, which corresponds to the loss of a methoxy group from the calculated molecular mass of 844.73.

8. Conversion of glycosyl azide into glycopyranosyl-[1,2,3,5]-tetrazole

Reacting the glucuronosyl azide with a nitrile in the presence of a zinc (II) salt affected a [3+2] cycloaddition to afford the expected tetrazole product. It is probable that an organo-zinc intermediate forms, in a manner that is similar to the formation of an organo-cuprate intermediate to mediate the additive coupling process.

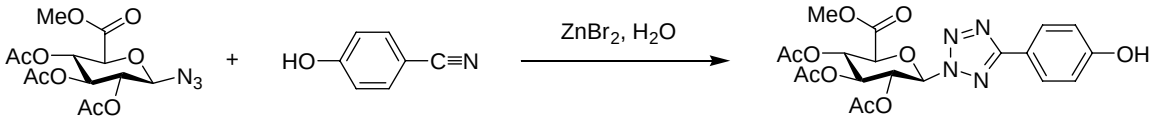

32 **63**

Equation 25: 1-(Methyl 2,3,4-tri-*O*-acetyl-β-D-glucuronosyl)-4-(4-hydroxyphenyl)-1*H*-[1,2,3,5]-tetrazole (**63**).

The reaction of azide **32** and 4-cyanophenol in the presence of zinc bromide monohydrate afforded the tetrazole product **63** in 66% yield (Equation 25) as a white solid upon crystallization from methanol. The reaction progress was monitored by TLC, which showed a UV-active spot that burned at a higher R_f than that of the starting

material after a twelve hour reaction time. The ^{1}H NMR spectrum showed evidence of the product by indicating the presence of one methoxy group corresponding to the methyl ester of the sugar. Two doublets corresponding to the aryl ring protons also appeared between 6.91 ppm and 7.54 ppm. The ^{1}H NMR spectrum indicated the presence of three singlets at approximately 2.0 ppm corresponding to the methyl portion of the acetyl protecting groups. Analysis of the ^{13}C NMR spectrum also provided evidence for the formation of product by indicating aromatic group signals from 103.9-135.2 ppm, and the appearance of a signal at 161.4 ppm representing the tetrazole ring carbon atom. The ^{13}C NMR spectrum also contained three signals at ~21 ppm indicating the presence of the acetyl protecting groups. ESI mass spectrometry shows the presence of a peak corresponding to the calculated molecular mass of tetrazole **63**.

9. Conversion of glycosyl bromide into *O*-glycosides

Formation of the *O*-glycoside from the glycosyl bromide occurs via competing S_N1 and S_N2 processes that are mediated by tight-ion pair overlaps. The reaction proceeds first by complexation of the bromine atom with the silver atom of the silver aluminosilicate catalyst forming a sugar-catalyst complex. The orientation of the -OR group at C-1 then is determined by the time of substitution of the alcohol for the bromide leaving group since the silver complex is drawing the bromine away from C-1. This process allows for competition between S_N1 and S_N2 reactions, which in this case leads to the inversion of configuration at C-1 (Scheme 20).

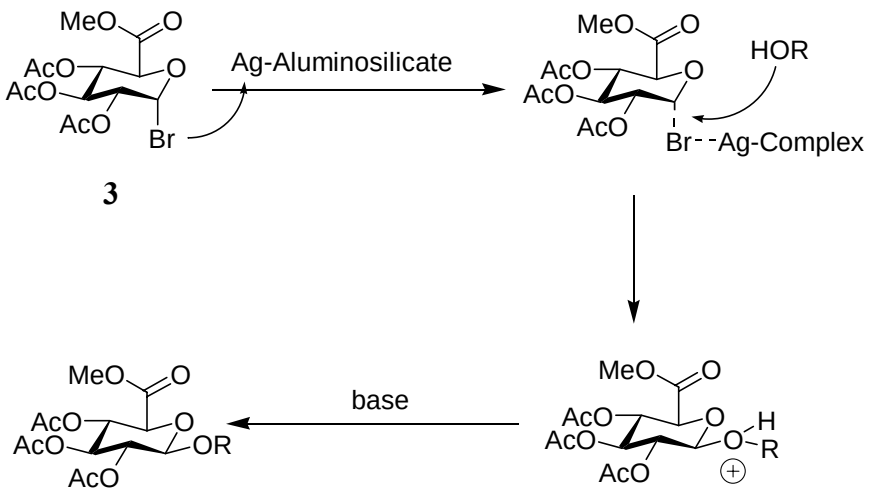

3

Scheme 20: Mechanistic possibility for *O*-glycoside formation.

Typical reactions were carried out upon 0.5 g of glycosyl bromide **3** in a solution of methylene chloride containing two equivalents of van Boeckel's catalyst and five equivalents of the respective alcohol for a period of 12-24 hours at room temperature in the dark (to prevent photodecomposition of the silver catalyst). Reaction at higher temperatures accelerated the decomposition of the catalyst.

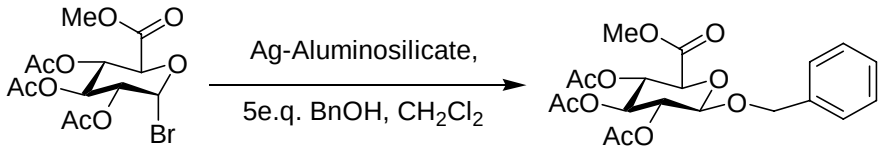

3 **64**

Equation 26: Benzyl (2,3,4-tri-*O*-acetyl-α-D-glucopyranosyl methyl uronate) (**64**).

The reaction of bromide **3** with benzyl alcohol afforded a high yield (78%) of **64** as a fine white solid (Equation 26). Study of the TLC plate showed a UV-active spot that burned at a lower R_f value than that of the starting material. Investigation of the ^{1}H NMR spectrum indicated that the shift of the signal for the anomeric proton did not change

much due to the presence of the -OBn group at C-1 compared to bromide **3**, and the coupling constant increased slightly to 4.48 Hz supporting the fact that the product is the α-anomer. Formation of the product is also supported by the appearance of a 5-H multiplet at approximately 7.3 ppm as well as a singlet signal at 4.66 ppm that corresponds to the two benzyl protons in the product. The other signals in the proton NMR spectrum show little alteration compared to the starting material. Analysis of the ^{13}C NMR spectrum provided evidence for the formation of **64**. The aryl ring carbon signals appear between 128.0 and 141.9 ppm, and the signal at 54.3 ppm represents the methyl group of the carboxylic acid ester. The signal for the benzylic carbon appeared at approximately 66 ppm, and the presence of signals at ~21 ppm indicates that the acetyl protecting groups are still present in *O*-glycoside **64**. Mass spectrometry provided evidence of a peak at 365.1, which most probably corresponds to the loss of an acetyl group.

Starting Material	Alcohol Reagent	Product	% Yield	R_f value*
3	Benzyl Alcohol	**64**	78	0.42
	n-Butanol	**65**	71	0.48
	t-Amyl Alcohol	**66**	65	0.50
	Cyclohexanol	**67**	98	0.50
	n-Propanol	**68**	69	0.50
	Ethanol	**69**	90	0.42

* Solvent System- 1:1 hexanes: ethyl acetate

Table 4: Synthesis of *O*-glycosides using silver catalysis.

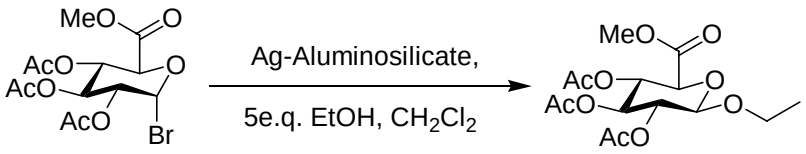

3 **69**

Equation 27: Ethyl (2,3,4-tri-*O*-acetyl-β-D-glucopyranosyl methyl uronate) (**69**).

The reaction of bromide **3** with ethanol afforded a high yield (90%) of **69** as colorless crystals (Equation 27). Examination of the TLC showed a UV-active spot that burned at a lower R_f value than that of the starting material. Investigation of the ^{1}H NMR spectrum indicated the presence of a doublet corresponding to the anomeric proton at ~4.5 ppm. A triplet corresponding to the methyl group of the ethyl glycoside appeared at 1.13 ppm, and the methylene group was represented by two multiplets that appeared from 3.52-3.88 ppm in the ^{1}H NMR spectrum.

Analysis of the ^{13}C NMR spectrum provided evidence for the formation of **69** with the appearance of two new carbon signals at 16.2 ppm ad 66.9 ppm corresponding to the methyl and methylene groups of the ethyl glycoside respectively. The anomeric carbon signal shifted from approximately 87 ppm in bromide **3** to 101.5 ppm in *O*-glycoside **69** due to the presence of two oxygen atoms directly attached to C-1. ESI mass spectrometry provided an M^+ of 385.1, which corresponds to the calculated molecular mass of product **69**. The coupling constant in the ^{1}H NMR spectrum as well as X-ray crystallography data (Figure 21) lend proof that **69** is in fact the β-anomer.

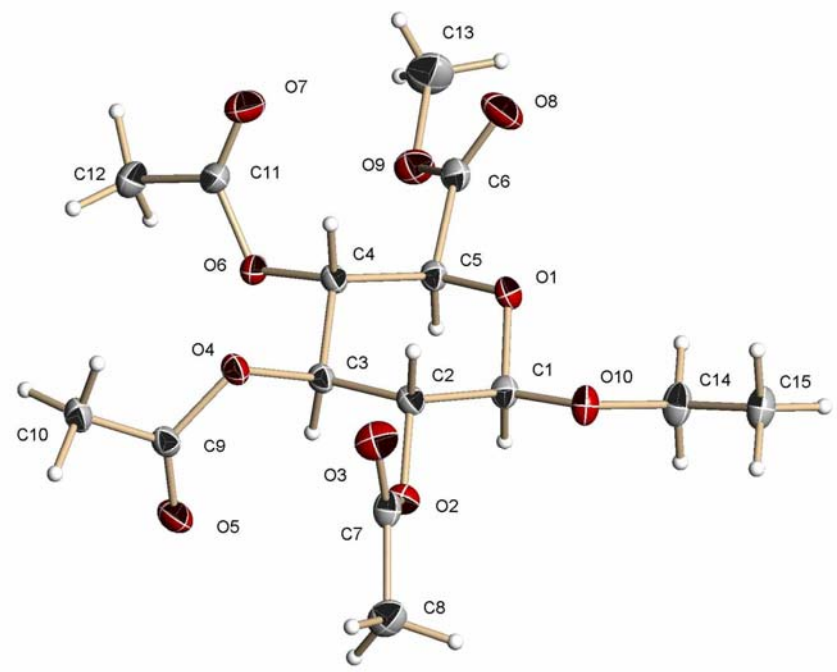

Figure 21: X-ray structure of glycoside **69**.

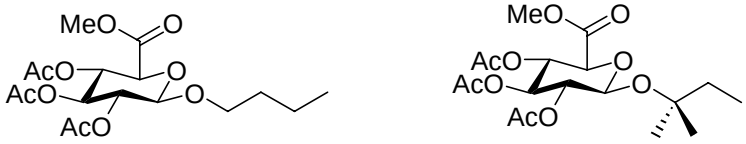

65

66

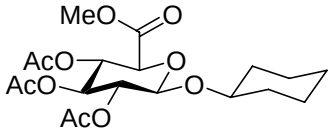

67

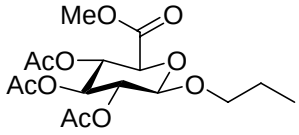

68

Figure 22: *O*-Glycoside products from use of the van Boeckel's catalyst.

For the *O*-glycoside reaction products **64-69**, yields of the products in the 65-98% range were obtained. All products afforded clean ^{1}H and ^{13}C NMR spectra that were easy

to interpret. The ^{1}H NMR spectra of the products showed similar patterns, the important one being the upfield shift for the signal correlating to the anomeric proton, as well as the appearance of new signals for the aglycone substituents. In conclusion, the van Boeckel catalyst provides high yields and stereoselectivity of addition, which are both important considerations in natural or unnatural product synthesis.

10. Production of a D-ManAcA derivative

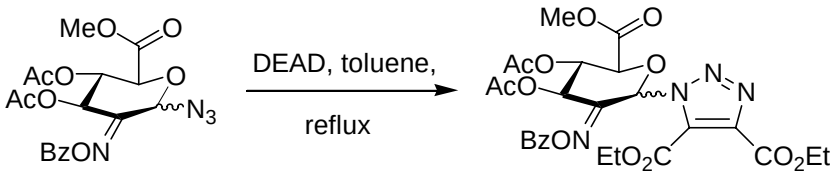

32 **70**

Equation 28: Synthesis of D-ManAcA triazole derivative **70**.

The reaction of azide **32** with DEAD afforded a high yield (82%) of **70** as an orange syrup (Equation 28). Examination of the TLC showed a UV-active spot that burned at a lower R_f value than that of the starting material. Investigation of the ^{1}H NMR spectrum indicated the presence of two triplets corresponding to the methyl groups of the ethyl groups at approximately 1.4 ppm. A set of quartets corresponding to the methylene groups of the ethyl groups appeared at ~4.4 ppm. Investigation of the ^{1}H NMR spectrum indicated the presence of a singlet corresponding to the anomeric proton at approximately 7.5 ppm. ESI mass spectrometry provided an M^+ of 602.5, which corresponds to the calculated molecular mass of product **70**.

The synthesis of **70** again illustrates the importance of the facile preparation of a β-D-ManAcA donor in the study of serotypes 5 and 8 of *S. aureus*. Compound **70** is a key

component in the future production of uronic acid based glycomimetic compounds of *Staphylococcus aureus*.

Experimental

General Procedures

Reaction progress was monitored by thin layer chromatography (TLC) with ultraviolet light detection since most of the reaction materials are UV-active. The TLC plates were treated with a solution of 5% sulfuric acid/ methanol solution to burn the reaction material to provide the indication of a carbohydrate product. Isolation of the product was completed by either recrystallization or flash chromatography performed with 32-63 μm, 60-Å silica gel. A Bruker Esquire-HP 1100 mass spectrometer was used for low-resolution MS. A Varian Gemini 2000 NMR system was used for ^{1}H and ^{13}C spectroscopy at 400 MHz and 100 MHz respectively, using $CDCl_3$ or D_6-DMSO as solvents. Proton and carbon chemical shifts (δ) are recorded in parts per million (ppm). Splitting patterns of multiplets are labeled in the following manner: s (singlet), d (doublet), dd (doublet of doublets), ddd (doublet of doublet of doublets), t (triplet), q (quartet), m (multiplet) with coupling constants measured in Hertz (Hz). X-Ray diffraction was also used to determine the solid-state crystal structure of some the compounds used herein.

Preparation of methyl D-glucopyranuronate (27) from D-glucurono-6,3-lactone (26).

In a 1000 mL round-bottom flask equipped with a septum and magnetic stir bar, NaOH (0.04 g, 1.0 mmol) was dissolved in methanol (300 mL) at room temperature. D-Glucurono-6,3-lactone (**26**) (10.0 g, 56.75 mmol) was added in 0.5 g portions to the mixture and allowed to stir at room temperature for 2.5 hours to convert the furanose into the pyranose.

Preparation of methyl 1,2,3,4-tetra-*O*-acetyl-β-D-glucopyranuronate (2) from D-glucuronolactone pyranose (27) via acetylation and recrystallization of methyl 2,3,4,5-tetra-*O*-acetyl-α/β-D-glucopyranuronate (2 α/β).

After concentration of the mixture from the previous experiment under reduced pressure, the residue (4.90 g, 27.8 mmol) (**27**) was dissolved in 10 mL of dry pyridine and then cooled to 0 °C. Acetic anhydride (10 mL) was added slowly to the mixture, and the solution was allowed to stir at room temperature for 6 hours or until TLC (1:1 hexanes: ethyl acetate, product R_f = 0.61) showed consumption of the starting material. The reaction mixture was then poured over ice water (400 mL) and the organic product was extracted with dichloromethane (3 x 100 mL). The combined organic extracts were washed with 5% sulfuric acid (3 x 50 mL), followed by washing with deionized water (2 x 100 mL). The organic extract was dried over anhydrous magnesium sulfate, filtered, and reduced. In a 500 mL round-bottom flask, the α/β anomers (**2 α/β**) (10.34 g, mixture of α/β) were dissolved in boiling isopropyl alcohol (250 mL). The solution was poured into a 500 mL Erlenmeyer flask to encourage the growth of crystals at room temperature to afford 6.93 g of **2β** (67%). The concentration of the mother liquor gave 3.38 g of syrup that was mainly **2α** (32%).

For the β-isomer:

^{1}H NMR ($CDCl_3$): δ 2.04, 2.05, 2.13 (3s one with double intensity, 12H total, 4 x $COCH_3$), 3.75 (s, 3H, OCH_3), 4.18 (d, 1H, H-5, *J* = 9.52 Hz), 5.15 (t, 1H, H-2, *J* = 8.47 Hz), 5.24 (t, 1H, H-4, *J* = 9.52 Hz), 5.32 (t, 1H, H-3, *J* = 9.15 Hz), 5.77 (d, 1H, H-1, *J* = 7.87 Hz).

^{13}C NMR ($CDCl_3$): δ 21.6, 21.7, 21.9, 54.1, 70.0, 71.2, 72.8, 74.0, 92.3, 167.7, 169.6, 170.0, 170.2, 170.7.

m/z calculated: 376.31 *m/z* found (ESI): 399.1 (+Na)

M.P. = 176-178 °C

R_f = 0.61 (1:1 hexanes: ethyl acetate)

$[\alpha]_D$ = +26.6 (*c* = 1.0, CH_2Cl_2)

For the α-isomer:

^{1}H NMR ($CDCl_3$): δ 2.06, 2.08, 2.17 (3s one with double intensity, 12H total, 4 x $COCH_3$), 3.72 (s, 3H, OCH_3), 4.39 (d, 1H, H-5, *J* = 10.25 Hz), 5.09 (t, 1H, H-2, *J* = 6.25 Hz), 5.19 (t, 1H, H-3, *J* = 9.89 Hz), 5.49 (t, 1H, H-4, *J* = 9.89 Hz), 6.37 (d, 1H, H-1, *J* = 3.66 Hz).

^{13}C NMR ($CDCl_3$): δ 20.5, 20.5, 20.7, 20.9, 53.0, 68.7, 68.8, 69.0, 70.3, 88.6, 164.9, 166.9, 168.2, 169.2, 169.7.

m/z calculated: 376.31 *m/z* found (ESI): 399.1 (+Na)

M.P. = N/A (syrup)

R_f = 0.61 (1:1 hexanes: ethyl acetate)

$[\alpha]_D$ = +134.5 (*c* = 1.0, CH_2Cl_2)

Preparation of methyl 2,3,4-tri-*O*-acetyl-α-D-glucopyranosyl bromide (3) from methyl 1,2,3,4-tetra-*O*-acetyl-β-D-glucopyranuronate (2β).

In a 100 mL round-bottom flask equipped with a septum, vent, a magnetic stir bar, methyl 2,3,4,5-tetra-*O*-acetyl-β-D-glucopyranuronate (**2β**) (4.12 g, 8.0 mmol) was dissolved in 33% HBr in acetic acid (15 mL). The mixture was stirred at room temperature for 4 hours or until the TLC (1:1 hexanes: ethyl acetate, R_f = 0.58) showed consumption of the starting material. After neutralization with 30 mL of 10% NaOH, the mixture was then extracted with chloroform (3 x 25 mL). The organic extracts were then combined and washed with water (3 x 50 mL). The organic extracts were dried over anhydrous magnesium sulfate. The extracts were then filtered and reduced to afford 4.27 g (10.8 mmol) of **3** as a pale yellow syrup (98%).

^{1}H NMR ($CDCl_3$): 1.84, 1.89 (2s one with double intensity, 9H total, 3 x $COCH_3$), 3.54 (s, 3H, OCH_3), 4.34 (d, 1H, H-5, *J* = 10.25 Hz), 4.69 (dd, 1H, H-2, *J* = 4.05, 4.18 Hz), 5.03 (t, 1H, H-4, *J* = 10.25 Hz), 5.37 (t, 1H, H-3, *J* = 9.70 Hz), 6.47 (d, 1H, H-1, *J* = 4.03 Hz).

^{13}C NMR ($CDCl_3$): δ 21.5, 21.6 (2 x C), 54.1, 69.3, 70.2, 71.1, 73.0, 86.8, 167.3, 170.1, 170.25, 170.28.

m/z calculated: 397.17 *m/z* found (ESI): 399.1 ($+H^+$)

M.P. = N/A (syrup)

R_f = 0.58 (1:1 hexanes: ethyl acetate)

$[\alpha]_D$ = +95.1 (*c* = 1.0, CH_2Cl_2)

Formation of methyl 2,3,4-tri-*O*-acetyl-2,6-anhydro-D-*lyxo*-hex-5-enoate (5) from methyl 2,3,4-tri-*O*-acetyl-α-D-glucopyranosyl bromide (3).

To an ice-cooled stirred solution of methyl 3,4,5-tri-*O*-acetyl-α-D-glucopyranosyl bromide (**3**, 6.2 g, 19.6 mmol) and tetrabutylammonium bromide (5.02 g, 19.6 mmol) in DMF (80 mL) in a 250 mL round-bottom flask equipped with septa and magnetic stir bar, was added diethylamine (2.5 mL, 23.9 mmol) dropwise under an atmosphere of nitrogen. The mixture was stirred at room temperature until TLC (1:1 hexanes: ethyl acetate, R_f = 0.44) showed consumption of starting material (~24 hours) and then neutralized with 50-200 Dowex strongly acidic resin. The reaction was filtered to remove the Dowex resin and then partitioned between ice water (30 mL) and methylene chloride (30 mL). The organic phase was washed with 1 M HCl (40 mL), saturated sodium bicarbonate (40 mL), and water (2 x 40 mL). The aqueous extracts were combined and washed with 50 mL of methylene chloride. The organic extracts were then combined and dried with anhydrous magnesium sulfate. Evaporation of solvent gave a residue (4.78 g), which was purified *via* elution from a column of silica gel (2:1 hexane: ethyl acetate). The major fraction was concentrated to yield 3.62 g (73%) of glycal **5** as a light brown syrup.

^{1}H NMR ($CDCl_3$): δ 2.02, 2.11, 2.15 (3s, 9H, 3 x $COCH_3$), 3.81 (s, 3H, OCH_3), 4.84 (d, 1H, H-5, J = 2.30 Hz), 5.39 (d, 1H, H-3, J = 2.47 Hz), 5.47 (dd, 1H, H-4, J = 2.38, 2.41 Hz), 6.83 (s, 1H, H-1).

^{13}C NMR ($CDCl_3$): δ 20.6, 20.8, 21.0, 52.5, 63.4, 67.8, 72.2, 127.2, 139.2, 168.9, 169.1, 169.2, 170.8.

m/z calculated: 316.26 *m/z* found (ESI): 317.0 ($+H^+$)

M.P. = 105-108 °C

R_f = 0.64 (1:1 hexanes: ethyl acetate)

$[\alpha]_D$ = -60.6 (*c* = 1.0, CH_2Cl_2)

Preparation of the oxime of methyl 3,4-di-*O*-acetyl-1,5-anhydro-D-fructuronate (28) from methyl 2,3,4-tri-*O*-acetyl-2,6-anhydro-D-*lyxo*-hex-5-enoate (5).

Methyl 3,4,5-tri-*O*-acetyl-2,6-anhydro-D-*lyxo*-hex-5-enoate (**5**) (3.0 g, 10.4 mmol) was dissolved in dry pyridine (60 mL) containing hydroxylamine hydrochloride (5.2 g, 71 mmol) and placed in a 250 mL round-bottom flask equipped with a septum and magnetic stir bar. The solution was stirred at room temperature for 20 hours when TLC (100% ethyl acetate, R_f = 0.70) showed consumption of starting material. After concentration of the mixture, the residue was diluted with 250 mL of dichloromethane. The solution was then washed with 1 M HCl (200 mL), saturated sodium sulfate (200 mL), and water (3 x 200 mL). The combined organic extracts were dried over anhydrous magnesium sulfate, filtered, and reduced to provide 1.81 g of **28** as a yellow solid (66%).

^{1}H NMR ($CDCl_3$): δ 2.08, 2.12 (2s, 6H, 2 x $COCH_3$), 3.81 (s, 3H, OCH_3), 4.39 (d, 1H, H-5, *J* = 4.58 Hz), 4.68 (d, 1H, H-1, *J* = 15.75 Hz), 4.88 (dd, 1H, H-1', *J* = 15.75 Hz), 5.44 (t, 1H, H-4, *J* = 4.40 Hz), 5.49 (d, 1H, H-3, *J* = 5.13 Hz).

^{13}C NMR ($CDCl_3$): δ 21.9, 22.0, 53.8, 60.3, 69.3, 70.9, 75.4, 150.4, 169.5, 170.0, 170.5.

m/z calculated: 289.20 *m/z* found (ESI): 312.1 (+Na)

M.P. = 141-145 °C

R_f = 0.70 (1:1 hexanes: ethyl acetate)

$[\alpha]_D$ = -5.5 (*c* = 1.0, CH_2Cl_2)

Formation of the *O*-benzoyloxime of methyl 3,4-di-*O*-acetyl-1,5-anhydro-D-fructuronate (29) by reaction of benzoyl chloride with methyl 3,4-di-*O*-acetyl-1,5-anhydro-D-fructuronate oxime (28).

A 50 mL round-bottom flask containing methyl 3,4-di-*O*-acetyl-1,5-anhydro-D-fructuronate oxime (**28**) (1.93 g, 6.7 mmol) dissolved in dry pyridine (40 mL) was equipped with a septum and magnetic stir bar. The solution was then cooled to -10 °C using a 1:1 acetone: ice bath. Benzoyl chloride (1.0 mL, 7.0 mmol) was added dropwise via syringe. The reaction mixture was allowed to stir for 4 hours or until TLC (1:1 hexanes: ethyl acetate, R_f = 0.41) showed consumption of the starting material. The solution was then poured over ice-water (40 mL) and extracted with methylene chloride (3 x 20 mL). The organic layers were then combined, washed with 5% sulfuric acid, 5% aqueous sodium bicarbonate (20 mL), and water (2 x 40 mL), dried over magnesium sulfate, and evaporated to yield 0.71 g of crude product as a yellow solid. The crude product was the eluted across a column of silica gel in 2:1 hexanes: ethyl acetate. The major fraction was collected and then recrystallized from diethyl ether to afford 0.54 g of **29** as a white solid (28%).

^{1}H NMR ($CDCl_3$): δ 2.11, 2.14 (2s, 6H, 2 x $COCH_3$), 3.84 (s, 3H, OCH_3), 4.46 (d, 1H, H-5, *J* = 3.66 Hz), 4.95 (d, 1H, H-1, *J* = 15.84 Hz), 5.03 (d, 1H, H-1', *J* = 15.84 Hz), 5.58 (t, 1H, H-4, *J* = 4.12 Hz), 5.70 (d, 1H, H-3, *J* = 4.58 Hz), 7.49 (t, 2H, *m*-Ar-H, *J* = 7.87 Hz), 7.64 (t, 1H, *p*-Ar-H, *J* = 7.41 Hz), 8.04 (d, 2H, *o*-Ar-H, *J* = 7.87 Hz).

^{13}C NMR ($CDCl_3$): δ 21.8, 22.0 (2 x C), 53.8, 60.6, 68.8, 70.2, 74.9, 128.9, 129.7 (2 x C), 130.7 (2 x C), 134.9, 158.5, 163.6, 169.1, 169.2, 170.1.

m/z calculated: 393.30 *m/z* found (ESI): 416.1 (+Na)

M.P. = 118-120 °C

R_f = 0.41 (1:1 hexanes: ethyl acetate)

$[\alpha]_D$ = -65.1 (*c* = 1.0, CH_2Cl_2)

Formation of methyl 3,4-di-*O*-acetyl-1-α-bromo-5-anhydro-D-fructuronate-*O*-benzoyloxime (30) by irradiation of *N*-bromosuccinimide and the *O*-benzoyloxime of methyl 3,4-di-*O*-acetyl-1,5-anhydro-D-fructuronate (29).

In a nitrogen-charged round-bottom flask containing a magnetic stir bar, (0.33 g, 0.85 mmol) of the *O*-benzoyloxime of methyl 3,4-di-*O*-acetyl-1,5-anhydro-D-fructuronate (**29**) and *N*-bromosuccinimide (0.30 g, 1.70 mmol) was dissolved in carbon tetrachloride (10 mL). The resulting mixture was then irradiated with a 250 W lamp for thirty minutes or until the resulting TLC plate exhibited consumption of starting material and complete product formation (1:1 hexanes: ethyl acetate, R_f = 0.50). The resulting mixture was then cooled in an ice bath to allow excess NBS as well as any insoluble succinimide to precipitate from solution. The cool solution was filtered and then reduced *in vacuo*. The resulting residue was dissolved in methylene chloride (25 mL) and washed with three 20 mL portions of water. The combined aqueous fractions were then washed with dichloromethane (2 x 10 mL). The combined organic layers were dried over anhydrous magnesium sulfate, filtered, and reduced to afford 0.45 g of crude yellow

syrup. The crude reaction product was then recrystallized from hot diethyl ether to afford 0.37 g of **30** as a fine white solid (93%).

^{1}H NMR ($CDCl_3$): δ 2.12, 2.20 (2s, 6H, 2 x $COCH_3$), 3.79 (s, 3H, OCH_3), 4.66 (d, 1H, H-5, *J* = 9.34 Hz), 5.48 (t, 1H, H-4, *J* = 9.52 Hz), 6.23 (d, 1H, H-3, *J* = 9.52 Hz), 7.42 (s, 1H, H-1), 7.50 (t, 2H, *m*-Ar-H, *J* = 8.06 Hz), 7.64 (t, 1H, *p*-Ar-H, *J* = 7.67 Hz), 8.04 (d, 2H, *o*-Ar-H, *J* = 8.61 Hz).

^{13}C NMR ($CDCl_3$): δ 21.75, 21.78, 54.5, 68.0, 69.5, 73.2, 73.6, 128.5, 129.9 (2 x C), 130.8 (2 x C), 135.1, 155.5, 162.7, 167.0, 170.1, 170.4.

m/z calculated: 472.19 *m/z* found (ESI): 392.1 (-Br)

M.P. = 90-93 °C

R_f = 0.50 (1:1 hexanes: ethyl acetate)

$[\alpha]_D$ = +246.3 (*c* = 1.0, CH_2Cl_2)

Preparation of methyl 3,4,5-tri-*O*-acetyl-β-D-glucopyranosyl azide (32) from methyl 2,3,4-tri-*O*-acetyl-α-D-glucopyranosyl bromide (3).

In a 250 mL round-bottom flask equipped with a reflux condenser and a magnetic stir bar, methyl 3,4,5-tetra-*O*-acetyl-α-D-glucopyranosyl bromide (**3**) (18 g, 45.3 mmol) and sodium azide (5.89 g, 2.0 equivalents) were dissolved in 5:1 acetone: water (120 mL). The mixture was then heated to a gentle reflux for 3 hours or until the starting material was consumed as shown by TLC (1:1 hexanes: ethyl acetate, R_f = 0.41). The mixture was then cooled to room temperature and extracted with methylene chloride (3 x 100 mL), the combined organic layers where washed with 10% NaOH (2 x 75 mL), and

then with water (3 x 100 mL). The organic layer was then dried over anhydrous magnesium sulfate, filtered, and reduced *in vacuo* to afford 22.3 g of crude solid. In a 500 mL round-bottom flask the solid was dissolved in methanol (180 mL) at 64 °C. The solution was poured into a 500 mL Erlenmeyer flask to encourage the growth of crystals at room temperature to afford 15.83 g of **31** (97%).

^{1}H NMR ($CDCl_3$): 2.02, 2.04, 2.08 (3s, 9H, 3 x $COCH_3$), 3.78 (s, 3H, OCH_3), 4.13 (d, 1H, H-5, J = 9.70 Hz), 4.72 (d, 1H, H-1, J = 8.79 Hz), 4.96 (t, 1H, H-2, J = 8.97 Hz), 5.26 (m, 2H, H-3, H-4).

^{13}C NMR ($CDCl_3$): δ 21.6, 21.7 (2 x C), 54.1, 70.1, 71.5, 72.9, 75.2, 89.0, 167.4, 170.0, 170.1, 170.7.

m/z calculated: 359.29 *m/z* found (ESI): 382.1 (+Na)

M.P. = 141-143 °C

R_f = 0.41 (1:1 hexanes: ethyl acetate)

$[\alpha]_D$ = -70.4 (c = 1.0, CH_2Cl_2)

Preparation of methyl 2,3,4-tri-*O*-acetyl-α-D-glucopyranosyl nitrile (25) from methyl 1,2,3,4-tetra-*O*-acetyl-β-D-glucopyranuronate (2β).

In a nitrogen-charged round-bottom flask containing a magnetic stir bar, 0.50 g (1.33 mmol) of the methyl 1,2,3,4-tetra-*O*-acetyl-β-D-glucopyranuronate (**2β)** and trimethylsilyl cyanide (0.42 mL, 6.00 mmol) were dissolved in methylene chloride (10 mL). Boron trifluoride etherate (0.12 mL, 1.33 mmol) was added to the reaction mixture dropwise over a period of three minutes. The reaction was then allowed to stir for one

hour or until the reaction was complete by TLC (1:1 ethyl acetate: hexanes, R_f = 0.69). The mixture was then cooled to 0 °C, and extracted with methylene chloride (3 x 5 mL), saturated sodium bicarbonate (2 x 5 mL), and washed with water (3 x 10 mL). The organic layer was then dried over anhydrous magnesium sulfate, filtered, and reduced *in vacuo* to afford 0.78 g of crude solid. The crude reaction mixture was then eluted over a column of silica gel (1:1 ethyl acetate: hexanes) to yield 0.38 g of **25** as yellow syrup (83%).

^{1}H NMR ($CDCl_3$): 1.93, 2.10, 2.11 (3s, 9H, 3 x $COCH_3$), 3.77 (s, 3H, OCH_3), 4.21 (d, 1H, H-5, *J* = 8.24 Hz), 4.39 (t, 1H, H-2, *J* = 6.29 Hz), 5.15 (t, 1H, H-4, *J* = 8.97 Hz), 5.26 (t, 1H, H-3, *J* = 8.97 Hz), 5.90 (d, 1H, H-1, *J* = 4.76 Hz).

^{13}C NMR ($CDCl_3$): δ 21.8, 21.9, 25.8, 54.0, 68.8, 68.9, 69.9, 74.9, 97.4, 117.3, 169.1, 169.59, 169.62, 170.1.

m/z calculated: 343.90 *m/z* found (ESI): 366.1 (+Na)

M.P. = N/A (syrup)

R_f = 0.69 (1:1 hexanes: ethyl acetate)

$[\alpha]_D$ = -8.1 (*c* = 1.0, CH_2Cl_2)

Synthesis of amides: Staudinger reactions

In a flame-dried, nitrogen-flushed 100 mL round-bottom flask, a solution of azide **32** (1.0 g, 2.8 mmol), two equivalents of a selected acid chloride, and 0.65 equivalents of bis(diphenylphosphino)ethylene in tetrahydrofuran (20 mL) was agitated for six hours at room temperature under an atmosphere of nitrogen. Upon consumption of starting

material as determined by TLC (1:1 hexanes: ethyl acetate) the reaction mixture was then hydrolyzed with water (3 mL) overnight. After concentration of the mixture the residue was diluted with chloroform (40 mL). The solution was washed with cold saturated $NaHCO_3$ (20 mL) and water (2 x 25 mL). The combined organic extracts were dried over anhydrous magnesium sulfate, filtered and reduced to provide solid products, which were further purified by flash column chromatography.

Acid chloride	
4-nitrobenzoyl chloride	4-fluorobenzoyl chloride
butyryl chloride	benzoyl chloride
pentafluorobenzoyl chloride	isovaleryl chloride
2-furoyl chloride	2-naphthoyl chloride

Table 5: Acid chloride reagents used.

***p*-Nitrobenzoic acid-(methyl 2,3,4-tri-*O*-acetyl-β-D-glucopyranuronosyl)-amide (33).**

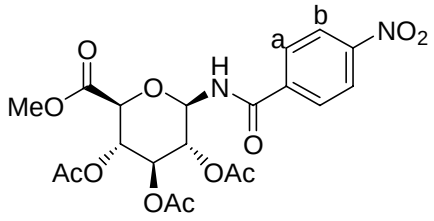

^{1}H NMR ($CDCl_3$): δ 2.05, 2.06 (2s with one double intensity, 9H total, 3 x $COCH_3$), 3.72 (s, 3H, OCH_3), 4.25 (d, 1H, H-5, J = 9.89 Hz), 5.05 (t, 1H, H-4, J = 9.61 Hz), 5.16 (t, 1H, H-2 J = 9.70 Hz), 5.37 (t, 1H, H-3, J = 9.78 Hz), 5.47 (t,

1H, H-1, *J* = 9.05 Hz), 7.39 (d, 1H, NH, *J* = 8.97 Hz), 7.93 (d, 2H, Ar-Ha, *J* = 8.61 Hz), 8.30 (d, 2H, Ar-Hb, *J* = 8.42 Hz).

^{13}C NMR ($CDCl_3$): δ 21.6, 21.7, 21.8, 54.0, 70.5, 71.6, 72.9, 74.5, 79.4, 124.7 (2 x C), 129.8 (2 x C), 139.1, 150.8, 166.6, 168.1, 170.5, 170.7, 171.8.

m/z calculated: 482.40 *m/z* found (ESI): 505.0 (+Na)

High Resolution TOF MS Electrospray: 505.1056 (+Na)

M.P. = 105-107 °C

R_f = 0.24 (1:1 hexanes: ethyl acetate)

$[\alpha]_D$ = -49.7 (*c* = 1.0, CH_2Cl_2)

_p_-Fluorobenzoic acid-(methyl 2,3,4-tri-_O_-acetyl-β-D-glucopyranuronosyl)-amide (34).

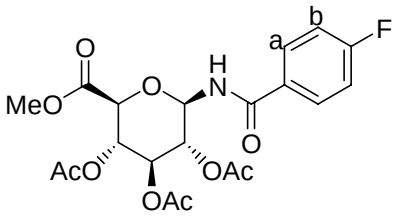

^{1}H NMR ($CDCl_3$): δ 2.00, 2.03 (2s with one double intensity, 9H total, 3 x $COCH_3$), 3.66 (s, 3H, OCH_3), 4.24 (d, 1H, H-5, *J* = 10.07 Hz), 5.09 (t, 1H, H-4, *J* = 9.52 Hz), 5.12 (t, 1H, H-3, *J* = 9.52 Hz), 5.46 (t, 1H, H-2, *J* = 9.52 Hz), 5.50 (t, 1H, H-1, *J* = 9.15 Hz), 7.06 (dd, 2H, Ar-Hb, *J* = 8.51, 8.51 Hz), 7.40 (d, 1H, NH, *J* = 9.15 Hz), 7.76 (dd, 2H, Ar-Ha, *J* = 8.53, 4.67 Hz).

^{13}C NMR ($CDCl_3$): δ 21.7, 21.8, 21.9, 54.0, 70.8, 71.7, 73.0, 74.8, 79.6, 116.6 (d, 2C, Ar-Cb-F, *J* = 22.1 Hz), 129.9, 130.9 (d, 2C, Ar-Ca-F, *J* = 9.2 Hz), 164.8, 166.1 (d, C-F, *J* = 252.5 Hz), 167.3, 168.2, 170.9, 172.6.

m/z calculated: 455.39 *m/z* found (ESI): 478.1 (+Na)

High Resolution TOF MS Electrospray: 478.1133 (+Na)

M.P. = 116-119 °C

R_f = 0.29 (1:1 hexanes: ethyl acetate)

$[\alpha]_D$ = -31.3 (*c* = 1.0, CH_2Cl_2)

Butyric acid-(methyl 2,3,4-tri-*O*-acetyl-β-D-glucopyranuronosyl)-amide (35).

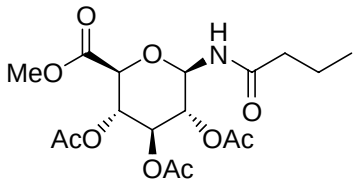

^{1}H NMR ($CDCl_3$): δ 0.84 (t, 3H, Hγ, *J* = 7.32 Hz), 1.56 (sextet, 2H, Hβ, *J* = 3.65 Hz), 1.97, 1.98 (2s with one double intensity, 9H total, 3 x $COCH_3$), 2.10 (t, 2H, Hα, *J* = 7.96 Hz), 3.66 (s, 3H, OCH_3), 4.14 (d, 1H, H-5, *J* = 10.07 Hz), 4.92 (t, 1H, H-4, *J* = 9.61 Hz), 5.08 (t, 1H, H-2, *J* = 9.76 Hz), 5.29 (t, 1H, H-3, *J* = 8.51 Hz), 5.34 (t, 1H, H-1, *J* = 9.52 Hz), 6.59 (d, 1H, NH, *J* = 9.52 Hz).

^{13}C NMR ($CDCl_3$): δ 14.8, 19.8, 21.7, 21.8, 21.9, 39.6, 54.1, 70.7, 71.4, 73.0, 74.8, 77.9, 168.1, 170.4, 170.6, 171.6, 174.4.

m/z calculated: 403.38 *m/z* found (ESI): 426.1 (+Na)

High Resolution TOF MS Electrospray: 426.1365 (+Na)

M.P. = 81-83 °C

R_f = 0.20 (1:1 hexanes: ethyl acetate)

$[\alpha]_D$ = +24.1 (*c* = 1.0, CH_2Cl_2)

Benzoic acid-(methyl 2,3,4-tri-*O*-acetyl-β-D-glucopyranuronosyl)-amide (36).

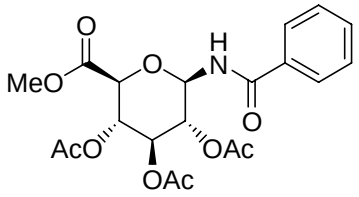

^{1}H NMR ($CDCl_3$): δ 2.04, 2.05, 2.06 (3s, 9H, 3 x $COCH_3$), 3.72 (s, 3H, OCH_3), 4.24 (d, 1H, H-5, *J* = 10.07 Hz), 5.10 (t, 1H, H-4, *J* = 9.61 Hz), 5.18 (t, 1H, H-2, *J* = 10.07 Hz), 5.47 (t, 1H, H-3, *J* = 9.61 Hz), 5.48 (t, 1H, H-1, *J* = 9.23 Hz), 7.15 (d, 1H, NH, *J* = 9.15 Hz), 7.44 (t, 2H, *m*-Ar-H, *J* = 6.61 Hz), 7.53 (t, 1H, *p*-Ar-H, *J* = 7.14 Hz), 7.75 (d, 2H, *o*-Ar-H, *J* = 6.77 Hz).

^{13}C NMR ($CDCl_3$): δ 21.7, 21.8, 21.9, 54.0, 70.8, 71.7, 73.0, 74.9, 79.6, 128.3 (2 x C), 129.7 (2 x C), 133.4, 133.7, 168.1, 168.2, 170.4, 170.7, 172.1.

m/z calculated: 437.40 *m/z* found (ESI): 460.1 (+Na)

High Resolution TOF MS Electrospray: 460.1221 (+Na)

M.P. = 193-195 °C

R_f = 0.37 (1:1 hexanes: ethyl acetate)

$[\alpha]_D$ = -19.1 (*c* = 1.0, CH_2Cl_2)

Pentafluorobenzoic acid-(methyl 2,3,4-tri-*O*-acetyl-β-D-glucopyranuronosyl)-amide (37).

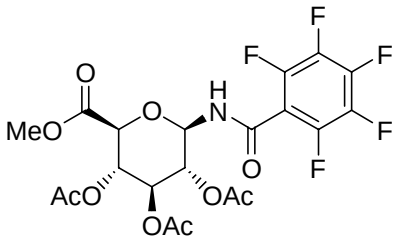

^{1}H NMR ($CDCl_3$): δ 2.02, 2.03, 2.05 (3s, 9H, 3 x $COCH_3$), 3.71 (s, 3H, OCH_3), 4.21 (d, 1H, H-5, *J* = 10.07 Hz), 5.06 (t, 1H, H-4, *J* = 9.52 Hz), 5.13 (t, 1H, H-2, *J* = 9.79 Hz), 5.41 (t, 1H, H-3, *J* = 9.52 Hz), 5.46 (t, 1H, H-1, *J* = 9.34 Hz), 7.26 (d, 1H, NH, *J* = 9.15 Hz).

^{13}C NMR ($CDCl_3$): δ 21.7, 21.8, 21.9, 54.1, 70.6, 71.8, 73.3, 74.1, 78.3, 113.0, 138.4 (d, 2 x C, *J* = 251 Hz), 143.1 (d, 1 x C, *J* = 251 Hz), 144.5 (d, 2 x C, *J* = 251 Hz), 158.6, 168.6, 170.2, 170.7, 170.8.

m/z calculated: 527.35 *m/z* found (ESI): 550.0 (+Na)

High Resolution TOF MS Electrospray: 550.0737 (+Na)

M.P. = 175-178 °C

R_f = 0.43 (1:1 hexanes: ethyl acetate)

$[\alpha]_D$ = +42.6 (*c* = 1.0, CH_2Cl_2)

Isovaleric acid-(2,3,4-tri-*O*-acetyl-β-D-glucopyranuronosyl)-amide (38).

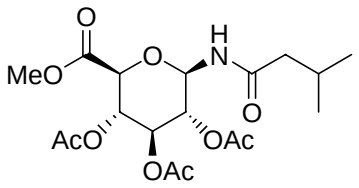

^{1}H NMR ($CDCl_3$): δ 0.90 (d, 6H, Hγ, *J* = 11.17 Hz), 0.97 (d, 2H, Hα, *J* = 6.59 Hz), 2.02 (s, 9H, 3 x $COCH_3$), 2.08 (m, 1H, Hβ), 3.71 (s, 3H, OCH_3), 4.15 (d, 1H, H-5, *J* = 9.80 Hz), 4.94 (t, 1H, H-4, *J* = 9.61 Hz), 5.12 (t, 1H, H-2, *J* = 10.07 Hz), 5.31 (t, 1H, H-3, *J* = 9.52 Hz), 5.37 (t, 1H, H-1, *J* = 9.52 Hz), 6.34 (d, 1H, NH, *J* = 9.34 Hz).

^{13}C NMR ($CDCl_3$): δ 21.7, 21.77, 21.81, 23.4 (2 x C), 27.1, 47.0, 54.1, 70.8, 71.3, 73.1, 74.9, 78.8, 168.1, 170.4, 170.6, 171.7, 173.9.

m/z calculated: 417.41 *m/z* found (ESI): 440.1 (+Na)

High Resolution TOF MS Electrospray: 440.1545 (+Na)

M.P. = 67-70 °C

R_f = 0.23 (1:1 hexanes: ethyl acetate)

$[\alpha]_D$ = +6.0 (*c* = 1.0, CH_2Cl_2)

Furan-2-carboxylic acid-(2,3,4-tri-*O*-acetyl-β-D-glucopyranuronosyl)-amide (39).

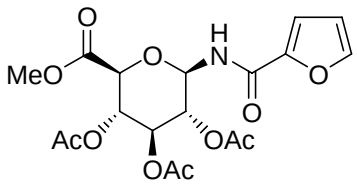

^{1}H NMR ($CDCl_3$): δ 1.99, 2.00, 2.02 (3s, 9H, 3 x $COCH_3$), 3.69 (s, 3H, OCH_3), 4.20 (d, 1H, H-5, *J* = 10.07 Hz), 5.09 (t, 1H, H-4, *J* = 9.70 Hz), 5.14 (t, 1H, H-3, *J* = 9.70 Hz), 5.43 (m, 2H, H-1, H-2), 7.26 (d, 1H, NH, *J* = 10.35 Hz), 7.43 (m, 1H, Ar-H_3), 7.52 (m, 1H, Ar-H_4), 7.63 (m, 1H, Ar-H_5).

^{13}C NMR ($CDCl_3$): δ 21.7, 21.8, 22.0, 54.2, 71.1, 72.9, 74.9, 75.1, 78.8, 113.3, 129.5, 133.0, 146.5, 159.1, 168.1, 170.5, 170.6, 171.7.

m/z calculated: 427.11 *m/z* found (ESI): 428.1 ($+H^+$)

M.P. = 137-140 °C

R_f = 0.27 (1:1 hexanes: ethyl acetate)

$[\alpha]_D$ = +36.0 (*c* = 1.0, CH_2Cl_2)

2-Naphthanoic acid-(2,3,4-tri-*O*-acetyl-β-D-glucopyranuronosyl)-amide (40).

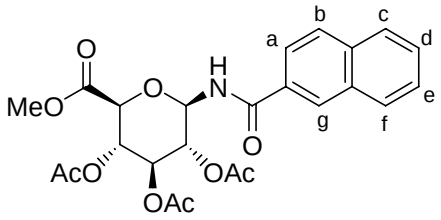

^{1}H NMR ($CDCl_3$): δ 2.02, 2.03, 2.06 (3s, 9H, 3 x $COCH_3$), 3.69 (s, 3H, OCH_3), 4.25 (d, 1H, H-5, *J* = 10.07 Hz), 5.16 (t, 1H, H-4, *J* = 9.02 Hz), 5.19 (t, 1H, H-2, *J* = 9.38 Hz), 5.49 (t, 1H, H-3, *J* = 9.52 Hz), 5.58 (t, 1H, H-1, *J* = 9.62 Hz), 7.48-8.29 (m, 7H, Ar-H).

^{13}C NMR ($CDCl_3$): δ 21.7, 21.9, 22.5, 54.1, 72.9, 73.0, 75.0, 75.1, 79.8, 124.4, 127.8, 128.0, 128.9, 129.3, 129.5, 129.8, 130.0, 130.3, 136.1, 168.2, 168.3, 170.5, 170.7, 172.3.

m/z calculated: 487.15 *m/z* found (ESI): 488.2 ($+H^+$)

M.P. = 198-201 °C

R_f = 0.35 (1:1 hexanes: ethyl acetate)

$[\alpha]_D$ = -29.7 (*c* = 1.0, CH_2Cl_2)

Synthesis of imines: Aza-Wittig Reactions

In a flame-dried, nitrogen-flushed 100 mL round-bottom flask, a solution of azide **32** (1.0 g, 2.8 mmol), 1.2 equivalents of a selected aldehyde or ketone, and 0.55 equivalents of bis(diphenylphosphino)ethylene in methylene chloride (10 mL) was agitated for six hours at room temperature under an atmosphere of nitrogen. Upon consumption of starting material as determined by TLC (1:1 hexanes: ethyl acetate) the reaction mixture was reduced to a syrup. After concentration of the mixture the residue was diluted with chloroform (40 mL). The solution was washed with cold saturated $NaHCO_3$ (20 mL) and water (2 x 25 mL). The combined organic extracts were dried over anhydrous magnesium sulfate, filtered and reduced to provide solid products after completion of flash column chromatography.

_p_-Nitrobenzoic acid-(2,3,4-tri-_O_-acetyl-α-D-glucopyranuronosyl)-imine (41).

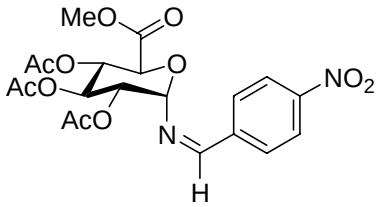

^{1}H NMR ($CDCl_3$): δ 1.97, 2.04, 2.09 (3s, 9H total, 3 x $COCH_3$), 3.72 (s, 3H, -OCH_3), 4.98 (d, 1H, H-5, *J* = 8.97 Hz), 5.19 (t, 1H, H-2, *J* = 9.15 Hz), 5.33 (t, 1H, H-4, *J* = 8.79 Hz), 5.38 (d, 1H, H-1, *J* = 4.22 Hz), 5.58 (t, 1H, H-3, *J* = 8.79 Hz), 7.98 (s, 2H, *o*-Ar-H, *J* = 8.79 Hz), 8.31 (s, 2H, *m*-Ar-H, *J* = 8.79 Hz), 8.38 (s, 1H, R-N=C-H-R').

^{13}C NMR ($CDCl_3$): δ 21.8, 21.9, 22.0, 54.1, 70.5, 70.7, 71.6, 71.7, 91.1, 125.1 (2 x C), 130.8 (2 x C), 140.9, 150.8, 162.8, 169.2, 170.47, 170.53, 170.6.

m/z calculated: 444.23 *m/z* found (ESI): 467.1 (+Na)

M.P. = 129-132 °C

R_f = 0.32 (1:1 hexanes: ethyl acetate)

$[\alpha]_D$ = -54.7 (*c* = 1.0, CH_2Cl_2)

_p_-Bromobenzoic acid-(2,3,4-tri-_O_-acetyl-α-D-glucopyranuronosyl)-imine (42).

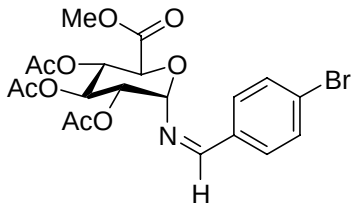

^{1}H NMR ($CDCl_3$): δ 1.95, 2.02, 2.07 (3s, 9H total, 3 x $COCH_3$), 3.72 (s, 3H, -OCH_3), 4.98 (d, 1H, H-5, *J* = 9.70 Hz), 5.14 (t, 1H, H-2, *J* = 9.52 Hz), 5.27 (d, 1H, H-1, *J* = 4.21 Hz), 5.30 (t, 1H, H-4, *J* = 9.52 Hz), 5.60 (t, 1H, H-3, *J* = 9.34 Hz), 7.58 (s, 2H, *o*-Ar-H, *J* = 8.42 Hz), 7.67 (s, 2H, *m*-Ar-H, *J* = 8.42 Hz), 8.20 (s, 1H, R-N=C-H-R').

^{13}C NMR ($CDCl_3$): δ 21.7, 21.8 (2 x C), 54.0, 69.0, 70.3, 70.7, 72.0, 91.2, 132.0 (2 x C), 133.4 (2 x C), 133.4, 168.1, 169.5, 169.6, 170.6, 171.0, 171.1.

m/z calculated: 479.14 *m/z* found (ESI): 502.1 (+Na)

M.P. = N/A (syrup)

R_f = (1:1 hexanes: ethyl acetate)

$[\alpha]_D$ = +45.9 (*c* = 1.0, CH_2Cl_2)

Synthesis of Triazoles: 1,3-dipolar cycloadditions

In a 50 mL two-neck round-bottom flask equipped with a magnetic stir bar and reflux condenser, a solution of azide **32** (1.0 g, 2.8 mmol), one equivalent of a selected terminal alkyne (Table 6), ascorbic acid (0.1 g, 0.06 mmol), and copper sulfate (0.02 g, 0.01 mmol) was stirred in 15 mL of deionized water. The reaction was allowed to progress for 48 hours or until TLC (100% ethyl acetate) showed consumption of starting material. Upon completion, the mixture was allowed to cool to room temperature and then was placed in an ice bath for 30 minutes. After cooling, the mixture was filtered over a glass frit and washed with two 20 mL portions of cold methanol. The crude solids were recrystallized from warm ethanol to afford clean products.

Terminal Alkyne	
Phenylacetylene	3-Cyclopentyl -1-propyne
1-Ethynyl-3-fluorobenzene	4-Ethynyltoluene
Ethyl Propiolate	1-Hexyne
4-Ethynylanisole	1-Heptyne
1-Nonyne	1-Decyne
1-Dodecyne	1-Octyne

Table 6: Alkyne reagents used.

1-(Methyl 2,3,4-tri-*O*-acetyl-β-D-glucopyranuronosyl)-4-phenyl-1*H*-[1,2,3]-triazole (43).

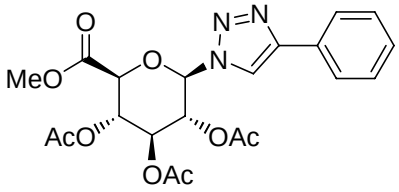

^{1}H NMR ($CDCl_3$): δ 1.89, 2.07, 2.09 (3s, 9H, 3 x $COCH_3$), 3.77 (s, 3H, OCH_3), 4.36 (d, 1H, H-5, *J* = 9.89 Hz), 5.40 (t, 1H, H-4, *J* = 9.52 Hz), 5.51 (t, 1H, H-3, *J* = 9.25 Hz), 5.55 (t, 1H, H-2, *J* = 9.25 Hz), 5.98 (d, 1H, H-1, *J* = 9.15 Hz), 7.36 (t, 2H, *m*-Ar-H, *J* = 7.32 Hz), 7.44 (t, 1H, *p*-Ar-H, *J* = 7.41 Hz), 7.84 (d, 2H, *o*-Ar-H, *J* = 7.14 Hz), 8.07 (s, 1H, triazole-H).

^{13}C NMR ($CDCl_3$): δ 21.5, 21.81, 21.84, 54.4, 70.1, 71.0, 73.1, 76.0, 86.6, 118.9, 126.9 (2 x C), 129.6, 129.9 (2 x C), 130.8, 149.5, 167.2, 169.9, 170.3, 170.7.

m/z calculated: 461.14 *m/z* found (ESI): 462.0 ($+H^+$)

M.P. = 247-250 °C

R_f = 0.31 (1:1 hexanes: ethyl acetate)

$[\alpha]_D$ = -7.0 (*c* = 1.0, CH_2Cl_2)

1-(Methyl 2,3,4-tri-*O*-acetyl-β-D-glucopyranuronosyl)-4-(methylcyclopentyl)-1*H*-[1,2,3]-triazole (44).

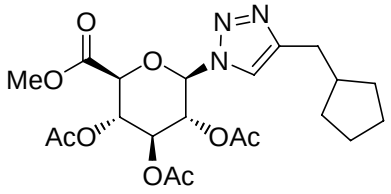

^{1}H NMR ($CDCl_3$): δ 1.20 (m, 2H, δ-H), 1.54 (m, 2H, δ-H), 1.63 (m, 2H, γ-H), 1.75 (m, 2H, γ-H), 1.87, 2.05, 2.07 (3s, 9H, 3 x $COCH_3$), 2.17 (quintet, 1H, β-H *J* = 7.69 Hz), 2.72 (t, 2H, α-H, *J* = 7.23 Hz), 3.76 (s, 3H, OCH_3), 4.31 (d, 1H, H-5, *J* = 9.89 Hz), 5.34 (t, 1H, H-4, *J* = 9.12 Hz), 5.38 (t, 1H, H-3, *J* = 9.01 Hz), 5.47 (t, 1H, H-2, *J* = 9.52 Hz), 5.90 (d, 1H, H-1, *J* = 7.87 Hz), 7.57 (s, 1H, triazole-H).

^{13}C NMR ($CDCl_3$): δ 21.4, 21.7, 21.8, 26.3, 32.8, 33.5, 40.9, 54.4, 70.2, 71.0, 73.0, 75.9, 86.4, 120.2, 149.8, 167.2, 169.7, 170.3, 170.7.

m/z calculated: 467.20 *m/z* found (ESI): 468.1 ($+H^+$)

M.P. = 165-168 °C

R_f = 0.30 (1:1 hexanes: ethyl acetate)

$[\alpha]_D$ = -20.2 (*c* = 1.0, CH_2Cl_2)

1-(Methyl 2,3,4-tri-*O*-acetyl-β-D-glucopyranuronosyl)- 4-(3-fluorophenyl)-1*H*-[1,2,3]-triazole (45).

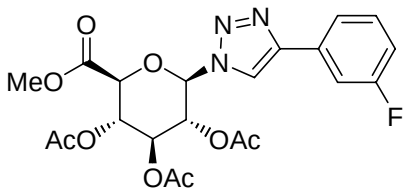

^{1}H NMR ($CDCl_3$): δ 1.90, 2.07, 2.09 (3s, 9H, 3 x $COCH_3$), 3.77 (s, 3H, OCH_3), 4.36 (d, 1H, H-5, *J* = 9.89 Hz), 5.39 (t, 1H, H-4, *J* = 9.76 Hz), 5.54 (t, 1H, H-3, *J* = 6.96 Hz), 5.53 (t, 1H, H-2, *J* = 6.58 Hz), 5.99 (d, 1H, H-1, *J* = 9.15 Hz), 7.05 (ddd, 1H, *o*-Ar-H, *J* = 8.42, 8.42, 1.65 Hz), 7.40 (dd, 1H, *p*-Ar-H, *J* = 8.24, 2.20 Hz), 7.58 (m, 2H), 8.10 (s, 1H, triazole-H).

^{13}C NMR ($CDCl_3$): δ 21.4, 21.7, 21.8, 54.4, 70.1, 71.1, 73.0, 76.0, 86.6, 113.9 (d, *o*-Ar-C, *J* = 22.1 Hz), 116.4 (d, *p*-Ar-C, *J* = 22.3 Hz), 119.4, 122.6 (d, *o*-Ar-C, *J* = 4.6 Hz), 131.5 (d, *m*-Ar-C, *J* = 7.6 Hz), 134.6, 148.5, 163.9 (d, C-F, *J* = 264.7 Hz), 167.1, 169.9, 170.3, 170.6.

m/z calculated: 479.13 *m/z* found (ESI): 480.0 ($+H^+$)

M.P. = 240-241 °C

R_f = 0.24 (1:1 hexanes: ethyl acetate)

$[\alpha]_D$ = -28.2 (*c* = 1.0, CH_2Cl_2)

1-(Methyl 2,3,4-tri-*O*-acetyl-β-D-glucopyranuronosyl)-4-(4-methylphenyl)-1*H*-[1,2,3]-triazole (46).

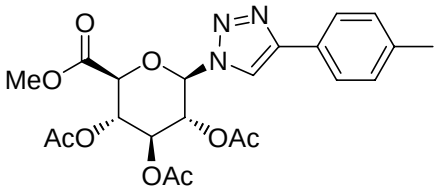

^{1}H NMR ($CDCl_3$): δ 1.88, 2.06, 2.08 (3s, 9H, 3 x $COCH_3$), 2.38 (s, 3H, Ar-CH_3), 3.76 (s, 3H, OCH_3), 4.35 (d, 1H, H-5, *J* = 9.89 Hz), 5.40 (t, 1H, H-4, *J* = 9.43 Hz), 5.50 (t, 1H, H-3, *J* = 8.97 Hz), 5.55 (t, 1H, H-2, *J* = 9.06 Hz), 5.98 (d, 1H, H-1, *J* = 8.97 Hz), 7.24 (d, 2H, *m*-Ar-H, *J* = 7.87 Hz), 7.73 (d, 2H, *o*-Ar-H, *J* = 8.06 Hz), 8.03 (s, 1H, triazole-H).

^{13}C NMR ($CDCl_3$): δ 20.3, 20.6, 21.4, 53.2, 69.0, 69.9, 72.0, 74.9, 85.4, 117.3, 125.7 (2 x C), 126.8, 129.4 (2 x C), 138.3, 166.0, 168.7, 169.1, 169.5.

m/z calculated: 475.16 *m/z* found (ESI): 498.2 (+Na)

M.P. = 232-233 °C

R_f = 0.29 (1:1 hexanes: ethyl acetate)

$[\alpha]_D$ = -15.8 (*c* = 1.0, CH_2Cl_2)

1-(Methyl 2,3,4-tri-*O*-acetyl-β-D-glucopyranuronosyl)-4-(carboxylic acid ethyl ester)-1*H*-[1,2,3]-triazole (47).

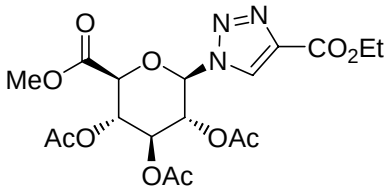

^{1}H NMR ($CDCl_3$): δ 1.42 (t, 3H, -CH_3, *J* = 7.05 Hz), 1.90, 2.06, 2.08 (3s, 9H, 3 x $COCH_3$), 3.77 (s, 3H, OCH_3), 4.34 (d, 1H, H-5, *J* = 9.70 Hz), 4.43 (q, 2H, -CH_2-, *J* = 2.65 Hz), 5.38 (t, 1H, H-4, *J* = 9.52 Hz), 5.44 (t, 1H, H-3, *J* = 9.15 Hz), 5.51 (t, 1H, H-2, *J* = 9.15 Hz), 5.99 (d, 1H, H-1, *J* = 9.15 Hz), 8.43 (s, 1H, triazole-H).

^{13}C NMR ($CDCl_3$): δ 15.6, 21.4, 21.7, 21.8, 54.5, 62.8, 70.0, 71.3, 72.7, 76.0, 86.7, 127.3, 142.0, 161.0, 166.9, 169.8, 170.3, 170.6.

m/z calculated: 457.13 *m/z* found (ESI): 480.2 (+Na)

M.P. = 182-184 °C

R_f = 0.36 (1:1 hexanes: ethyl acetate)

$[\alpha]_D$ = -6.1 (*c* = 1.0, CH_2Cl_2)

1-(Methyl 2,3,4-tri-*O*-acetyl-β-D-glucopyranuronosyl)-4-butyl-1*H*-[1,2,3]-triazole (48).

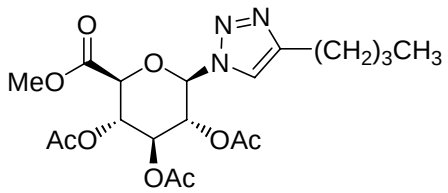

^{1}H NMR ($CDCl_3$): δ 0.93 (t, 3H, δ-H J = 7.32 Hz), 1.37 (sextet, 2H, γ-H, J = 7.38 Hz), 1.65 (quintet, 2H, β-H, J = 7.60 Hz), 1.87, 2.05, 2.08 (3s, 9H, 3 x $COCH_3$), 2.72 (t, 2H, α-H, J = 7.52 Hz), 3.76 (s, 3H, OCH_3), 4.32 (d, 1H, H-5, J = 9.89 Hz), 5.35 (t, 1H, H-4, J = 8.06 Hz), 5.38 (t, 1H, H-3, J = 9.70 Hz), 5.47 (t, 1H, H-2, J = 8.79 Hz), 5.91 (d, 1H, H-1, J = 7.87 Hz), 7.58 (s, 1H, triazole-H).

^{13}C NMR ($CDCl_3$): δ 15.0, 21.3, 21.7 (2 x C), 23.4, 26.4, 32.3, 54.2, 70.1, 71.0, 73.0, 75.8, 86.3, 120.0, 150.1, 167.2, 169.7, 170.2, 170.6.

m/z calculated: 441.17 *m/z* found (ESI): 464.2 (+Na)

M.P. = 179-180 °C

R_f = 0.49 (1:1 hexanes: ethyl acetate)

$[\alpha]_D$ = -13.0 (c = 1.0, CH_2Cl_2)

1-(Methyl 2,3,4-tri-*O*-acetyl-β-D-glucopyranuronosyl)-4-(4-methoxyphenyl)-1*H*-[1,2,3]-triazole (49).

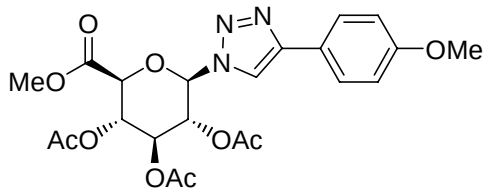

^{1}H NMR ($CDCl_3$): δ 1.87, 2.02, 2.03 (3s, 9H, 3 x $COCH_3$), 3.74 (s, 3H, OCH_3), 3.83 (s, 3H, Ar-OCH_3), 4.34 (d, 1H, H-5, J = 9.89 Hz), 5.38 (t, 1H, H-4, J = 9.61 Hz), 5.49 (t, 1H, H-3, J = 9.52 Hz), 5.52 (t, 1H, H-2, J = 9.34 Hz), 5.96 (d, 1H, H-

1, *J* = 8.97 Hz), 6.95 (t, 2H, *o*-Ar-H, *J* = 6.87 Hz), 7.75 (d, 2H, *m*-Ar-H, *J* = 6.87 Hz), 7.97 (s, 1H, triazole-H).

^{13}C NMR ($CDCl_3$): δ 21.5, 21.78, 21.84, 54.4, 56.5, 70.1, 71.0, 73.1, 76.0, 86.6, 115.3 (2 x C), 118.0, 123.5, 128.2 (2 x C), 149.4, 160.8, 167.1, 169.8, 170.3, 170.7.

m/z calculated: 491.15 *m/z* found (ESI): 492.2 ($+H^+$)

M.P. = 188-190 °C

R_f = 0.18 (1:1 hexanes: ethyl acetate)

$[\alpha]_D$ = -13.1 (*c* = 1.0, CH_2Cl_2)

1-(Methyl 2,3,4-tri-*O*-acetyl-β-D-glucopyranuronosyl)-4-pentyl-1*H*-[1,2,3]triazole (50).

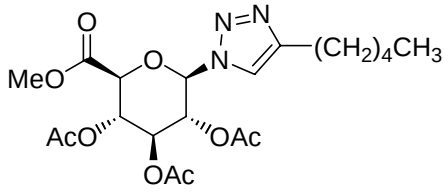

^{1}H NMR ($CDCl_3$): δ 0.90 (t, 3H, $-CH_3$, *J* = 6.77 Hz), 1.33 (m, 4H, $-(CH_2)_2-$), 1.68 (quintet, 2H, β-H, *J* = 7.32 Hz), 1.87, 2.05, 2.07 (3s, 9H, 3 x $COCH_3$), 2.71 (t, 2H, α-H, *J* = 7.69 Hz), 3.76 (s, 3H, OCH_3), 4.31 (d, 1H, H-5, *J* = 9.89 Hz), 5.37 (t, 1H, H-4, *J* = 9.70 Hz), 5.46 (t, 1H, H-3, *J* = 9.52 Hz), 5.48 (t, 1H, H-2, *J* = 9.52 Hz), 5.93 (d, 1H, H-1, *J* = 9.15 Hz), 7.57 (s, 1H, triazole-H).

^{13}C NMR ($CDCl_3$): δ 15.2, 21.3, 21.6, 21.7, 23.5, 26.7, 29.9, 32.4, 54.2, 70.1, 71.0, 71.5, 72.9, 73.0, 75.2, 75.8, 86.2, 120.0, 150.2, 167.2, 169.7, 170.2, 170.6.

m/z calculated: 455.19 *m/z* found (ESI): 478.2 (+Na)

M.P. = 174-176 °C

R_f = 0.31 (1:1 hexanes: ethyl acetate)

$[\alpha]_D$ = -29.0 (*c* = 1.0, CH_2Cl_2)

1-(Methyl 2,3,4-tri-*O*-acetyl-β-D-glucopyranuronosyl)-4-heptyl-1*H*-[1,2,3]-triazole (51).

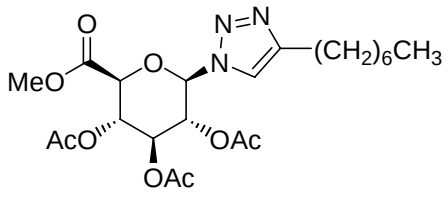

^{1}H NMR ($CDCl_3$): δ 0.88 (t, 3H, -CH_3, *J* = 6.77 Hz), 1.26 (m, 8H, -$(CH_2)_4$-), 1.68 (m, 2H, β-H), 1.87, 2.05, 2.07 (3s, 9H, 3 x $COCH_3$), 2.71 (t, 2H, α-H, *J* = 7.60 Hz), 3.76 (s, 3H, OCH_3), 4.31 (d, 1H, H-5, *J* = 9.89 Hz), 5.37 (t, 1H, H-4, *J* = 9.61 Hz), 5.46 (t, 1H, H-3, *J* = 8.61 Hz), 5.48 (t, 1H, H-2, *J* = 8.61 Hz), 5.91 (d, 1H, H-1, *J* = 8.60 Hz), 7.57 (s, 1H, triazole-H).

^{13}C NMR ($CDCl_3$): δ 15.3, 21.3, 21.7 (2 x C), 23.8, 26.7, 30.2 (3 x C), 32.9, 54.2, 70.2, 71.1, 73.0, 75.7, 86.2, 120.0, 150.1, 167.3, 169.7, 170.2, 170.6.

m/z calculated: 483.22 *m/z* found (ESI): 506.3 (+Na)

M.P. = 152-154 °C

R_f = 0.36 (1:1 hexanes: ethyl acetate)

$[\alpha]_D$ = -12.3 (*c* = 1.0, CH_2Cl_2)

1-(Methyl 2,3,4-tri-*O*-acetyl-β-D-glucopyranuronosyl)-4-octyl-1*H*-[1,2,3]-triazole (52).

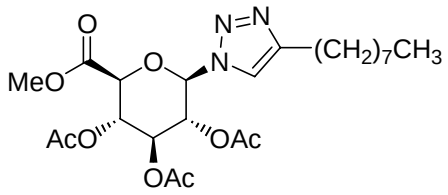

^{1}H NMR ($CDCl_3$): δ 0.88 (t, 3H, -CH_3, *J* = 6.50 Hz), 1.27 (m, 4H, -$(CH_2)_2$-), 1.31 (m, 4H, -$(CH_2)_2$-), 1.67 (m, 2H, β-H), 1.87, 2.05, 2.07 (3s, 9H, 3 x $COCH_3$), 2.71 (t, 2H, α-H, *J* = 7.69 Hz), 3.76 (s, 3H, OCH_3), 4.31 (d, 1H, H-5, *J* = 9.89 Hz), 5.37 (t, 1H, H-4, *J* = 9.34 Hz), 5.46 (t, 1H, H-3, *J* = 8.42 Hz), 5.48 (t, 1H, H-2, *J* = 8.42 Hz), 5.90 (d, 1H, H-1, *J* = 8.24 Hz), 7.56 (s, 1H, triazole-H).

^{13}C NMR ($CDCl_3$): δ 15.3, 21.3, 21.7, 21.8, 23.9, 26.8, 30.3 (2 x C), 30.4, 30.5, 33.0, 54.3, 70.2, 71.0, 73.0, 75.8, 86.3, 120.0, 150.2, 167.2, 169.7, 170.2, 170.6.

m/z calculated: 497.24 *m/z* found (ESI): 520.3 (+Na)

M.P. = 149-151 °C

R_f = 0.58 (1:1 hexanes: ethyl acetate)

$[\alpha]_D$ = -21.2 (*c* = 1.0, CH_2Cl_2)

1-(Methyl 2,3,4-tri-*O*-acetyl-β-D-glucopyranuronosyl)-4-decyl-1*H*-[1,2,3]-triazole (53).

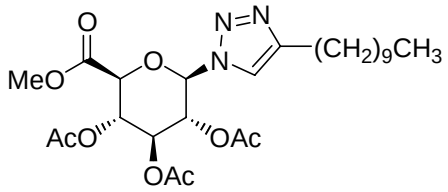

^{1}H NMR ($CDCl_3$): δ 0.88 (t, 3H, -CH_3, *J* = 6.22 Hz), 1.26 (m, 10H, -$(CH_2)_5$-), 1.30 (m, 4H, -$(CH_2)_2$-), 1.65 (m, 2H, β-H), 1.87, 2.05, 2.07 (3s, 9H, 3 x $COCH_3$), 2.70 (t, 2H, α-H, *J* = 7.51 Hz), 3.76 (s, 3H, OCH_3), 4.31 (d, 1H, H-5, *J* = 9.70 Hz), 5.37 (t, 1H, H-4, *J* = 9.15 Hz), 5.46 (t, 1H, H-3, *J* = 8.24 Hz), 5.48 (t, 1H, H-2, *J* = 8.24 Hz), 5.90 (d, 1H, H-1, *J* = 8.61 Hz), 7.56 (s, 1H, triazole-H).

^{13}C NMR ($CDCl_3$): δ 15.4, 21.3, 21.7, 21.8, 23.9, 26.8, 30.3 (2 x C), 30.5 (2 x C), 30.8 (2 x C), 33.1, 54.3, 70.1, 71.0, 73.0, 75.8, 86.3, 120.0, 150.2, 167.2, 169.7, 170.2, 170.6.

m/z calculated: 525.59 *m/z* found (ESI): 548.4 (+Na)

M.P. = 131-135 °C

R_f = 0.71 (1:1 hexanes: ethyl acetate)

$[\alpha]_D$ = -6.5 (*c* = 1.0, CH_2Cl_2)

1-(Methyl 2,3,4-tri-*O*-acetyl-β-D-glucopyranuronosyl)-4-hexyl-1*H*-[1,2,3]-triazole (54).

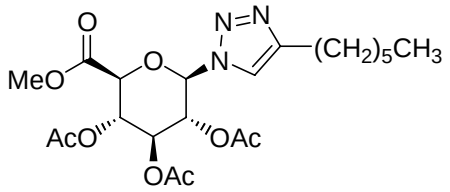

^{1}H NMR ($CDCl_3$): δ 0.86 (t, 3H, -CH_3, *J* = 6.22 Hz), 1.30 (m, 6H, -$(CH_2)_3$-), 1.65 (quintet, 2H, β-H, *J* = 7.32 Hz), 1.85, 2.03, 2.05 (3s, 9H, 3 x $COCH_3$), 2.67 (t, 2H, α-H, *J* = 7.69 Hz), 3.74 (s, 3H, OCH_3), 4.29 (d, 1H, H-5, *J* = 9.89 Hz), 5.38 (t, 1H, H-4, *J* = 9.70 Hz), 5.41 (t, 1H, H-3, *J* = 8.61 Hz), 5.45 (t, 1H, H-2, *J* = 8.60 Hz), 5.89 (d, 1H, H-1, *J* = 9.15 Hz), 7.55 (s, 1H, triazole-H).

^{13}C NMR ($CDCl_3$): δ 15.3, 21.3, 21.6, 21.7, 23.8, 26.8, 30.0, 30.2, 32.7, 54.3, 70.1, 71.0, 73.0, 75.8, 86.3, 120.0, 150.2, 167.2, 169.7, 170.2, 170.6.

m/z calculated: 469.21 *m/z* found (ESI): 492.2 (+Na)

M.P. = 163-165 °C

R_f = 0.28 (1:1 hexanes: ethyl acetate)

$[\alpha]_D$ = -15.5 (*c* = 1.0, CH_2Cl_2)

Synthesis of deprotected triazoles: Lithium hydroxide hydrolysis reactions

In a 50 mL round-bottomed flask were placed 0.40 g of a selected triazole, 30 mL of a 0.2 M solution of LiOH in methanol, tetrahydrofuran, and water (1:2:1), and a magnetic stir bar. The solution was then agitated for 54 hours or until completion by TLC

was observed. Once completed, 2.0 g of 50-200 Dowex strongly acidic resin was added to acidify the solution and trap any lithium salts that had formed throughout the course of reaction. After a period of three hours, the Dowex resin was filtered off and solvent was removed under reduced pressure. The solid products were then maintained under reduced pressure to remove any excess water that had not been previously removed.

Triazoles		
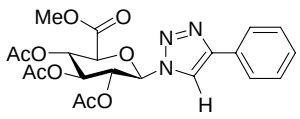 **43**	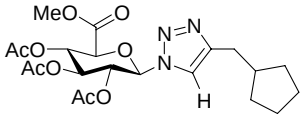 **44**	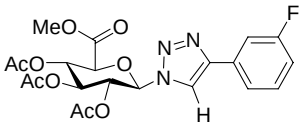 **45**
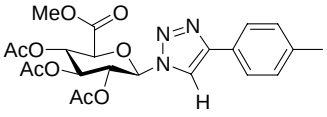 **46**	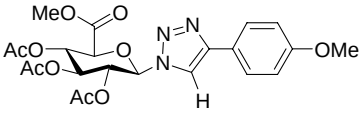 **49**	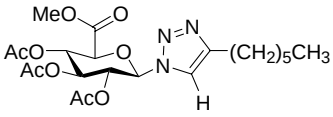 **52**

Table 7: Triazoles used for hydrolysis.

1-(2,3,4-Tri-*O*-hydroxy-β-D-glucuronosyl)-4-phenyl-1*H*-[1,2,3]-triazole (55).

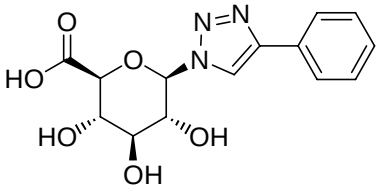

^{1}H NMR (D_6-DMSO): δ 3.45 (td, 1H, H-4, *J* = 8.88 Hz), 3.49 (t, 1H, H-3, *J* = 9.15 Hz), 3.85 (t, 1H, H-2, *J* = 8.90 Hz), 4.03 (d, 1H, H-5, *J* = 9.52 Hz), 4.72 (d, 1H, H-1, *J* = 9.34 Hz), 7.42 (t, 1H, *p*-Ar-H, *J* = 7.87 Hz), 7.45 (t, 2H, *m*-Ar-H, *J* = 7.51 Hz), 7.89 (d, 2H, *o*-Ar-H, *J* = 7.32 Hz), 8.86 (s, 1H, triazole-H).

^{13}C NMR (D_6-DMSO): δ 72.8, 73.4, 77.8, 79.3, 88.9, 122.1, 126.7 (2 x C), 129.6, 130.4 (2 x C), 131.9, 147.9, 171.1.

m/z calculated: 321.29 *m/z* found (ESI): 344.0 (+Na)

M.P. = 178-180 °C

R_f = 0.20 (3:1 ethyl acetate: methanol)

$[\alpha]_D$ = -35.1 (*c* = 1.0, CH_2Cl_2)

1-(2,3,4-Tri-*O*-hydroxy-β-D-glucuronosyl)-4-(methylcyclopentyl)-1*H*-[1,2,3]-triazole (56).

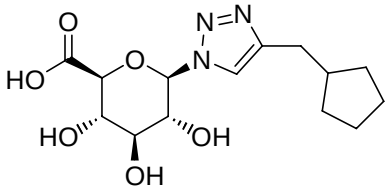

^{1}H NMR (D_6-DMSO): δ 1.15 (quintet, 2H, δ-H, *J* = 6.41 Hz), 1.19 (quintet, 2H, δ-H, *J* = 6.97 Hz), 1.49 (quintet, 2H, γ-H, *J* = 7.32 Hz), 1.64 (quintet, 2H, γ-H, *J* = 6.22 Hz), 2.09 (quintet, 1H, β-H, *J* = 7.41 Hz), 2.59 (d, 2H, α-H, *J* = 7.32 Hz), 3.39 (t, 1H, H-4, *J* = 8.79 Hz), 3.46 (t, 1H, H-3, *J* = 9.34 Hz), 3.80 (t, 1H, H-2, *J* = 9.15 Hz), 3.95 (d, 1H, H-5, *J* = 9.52 Hz), 5.58 (d, 1H, H-1, *J* = 9.15 Hz), 8.04 (s, 1H, triazole-H).

^{13}C NMR (D_6-DMSO): δ 26.3 (3 x C), 32.6, 33.6 (2 x C), 72.8, 73.2, 77.9, 79.3, 88.6, 123.0, 147.8, 171.0.

m/z calculated: 327.33 *m/z* found (ESI): 328.1 ($+H^+$)

M.P. = 98-101 °C

R_f = 0.64 (3:1 ethyl acetate: methanol)

$[\alpha]_D$ = -35.6 (*c* = 1.0, CH_2Cl_2)

1-(2,3,4-Tri-*O*-hydroxy-β-D-glucuronosyl)-4-(3-fluorophenyl)-1*H*-[1,2,3]-triazole (57).

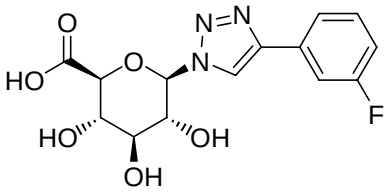

^{1}H NMR (D_6-DMSO): δ 3.46 (t, 1H, H-4, *J* = 8.79 Hz), 3.52 (t, 1H, H-3, *J* = 9.15 Hz), 3.84 (t, 1H, H-2, *J* = 8.80 Hz), 4.05 (d, 1H, H-5, *J* = 9.34 Hz), 5.74 (d, 1H, H-1, *J* = 9.34 Hz), 7.17 (ddd, 1H, *o*-Ar-H, *J* = 8.51, 8.51, 2.67 Hz), 7.51 (dd, 1H, *p*-Ar-H, *J* = 6.04, 1.95 Hz), 7.69 (d, 1H, *o*-Ar-H, *J* = 7.87 Hz), 7.74 (d, 1H, *m*-Ar-H, *J* = 6.96 Hz), 8.95 (s, 1H, triazole-H).

^{13}C NMR (D_6-DMSO): δ 72.8, 73.5, 77.7, 79.3, 88.9, 113.3 (d, *o*-Ar-C, *J* = 22.1 Hz), 116.2 (d, *p*-Ar-C, *J* = 20.6 Hz), 122.7, 122.8, 132.6 (d, *o*-Ar-C, *J* = 4.1 Hz), 134.3(d, *m*-Ar-C, *J* = 8.4 Hz), 146.3, 164.0 (d, C-F, *J* = 249.3 Hz), 171.0.

m/z calculated: 339.28 *m/z* found (ESI): 362.1 (+Na)

M.P. = 102-105 °C

R_f = 0.21 (3:1 ethyl acetate: methanol)

$[\alpha]_D$ = -38.5 (*c* = 1.0, CH_2Cl_2)

1-(2,3,4-Tri-*O*-hydroxy-β-D-glucuronosyl)-4-(4-methylphenyl)-1*H*-[1,2,3]-triazole (58).

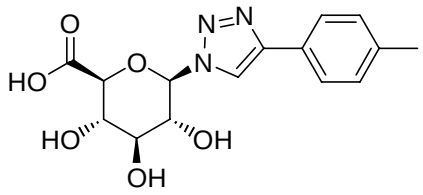

^{1}H NMR (D_6-DMSO): δ 2.48 (s, 3H, Ar-CH_3), 3.46 (t, 1H, H-4, *J* = 8.79 Hz), 3.49 (t, 1H, H-3, *J* = 9.34 Hz), 3.86 (t, 1H, H-2, *J* = 8.97 Hz), 4.03 (d, 1H, H-5, *J* = 9.52 Hz), 5.70 (d, 1H, H-1, *J* = 9.34 Hz), 7.25 (d, 2H, *o*-Ar-H, *J* = 8.06 Hz), 7.76 (d, 2H, *m*-Ar-H, *J* = 8.06 Hz), 8.79 (s, 1H, triazole-H).

^{13}C NMR (D_6-DMSO): δ 22.6, 72.8, 73.4, 77.8, 79.3, 88.9, 121.7, 126.6 (2 x C), 129.1, 131.0 (2 x C), 138.8, 148.0, 171.1.

m/z calculated: 335.31 *m/z* found (ESI): 357.0 (+Na)

M.P. = 88-90 °C

R_f = 0.22 (3:1 ethyl acetate: methanol)

$[\alpha]_D$ = -42.9 (*c* = 1.0, CH_2Cl_2)

1-(2,3,4-Tri-*O*-hydroxy-β-D-glucuronosyl)-4-hexyl-1*H*-[1,2,3]triazole (59).

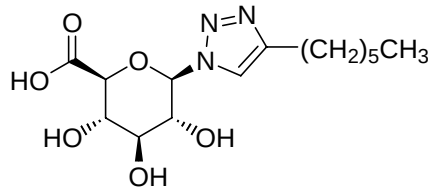

^{1}H NMR (D_6-DMSO): δ 0.84 (m, 3H, -CH_3), 1.26 (m, 6H, -$(CH_2)_3$-), 1.57 (quintet, 2H, -CH_2-, *J* = 6.87 Hz), 2.58 (t, 2H, -CH_2-, *J* = 7.60 Hz), 3.41 (t, 1H, H-4, *J* = 9.70 Hz), 3.46 (t, 1H, H-3, *J* = 9.25 Hz), 3.79 (t, 1H, H-2, *J* = 8.97 Hz), 3.95 (d, 1H, H-5, *J* = 9.52 Hz), 5.58 (d, 1H, H-1, *J* = 9.34 Hz), 8.04 (s, 1H, triazole-H).

^{13}C NMR (D_6-DMSO): δ 15.7, 23.8, 26.7, 30.0, 30.5, 32.7, 72.7, 73.2, 77.9, 79.3, 88.6, 122.5, 148.4, 171.1.

m/z calculated: 329.35 *m/z* found (ESI): 330.1 ($+H^+$)

M.P. = 125-127 °C

R_f = 0.47 (3:1 ethyl acetate: methanol)

$[\alpha]_D$ = -47.8 (*c* = 1.0, CH_2Cl_2)

1-(2,3,4-Tri-*O*-hydroxy-β-D-glucuronosyl)-4-(4-methoxyphenyl)-1*H*-[1,2,3]-triazole (60).

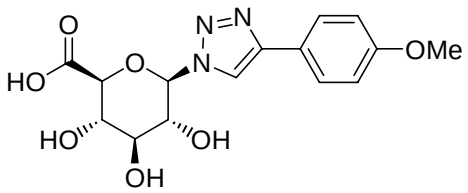

^{1}H NMR (D_6-DMSO): δ 3.47 (t, 1H, H-4, *J* = 8.88 Hz), 3.53 (t, 1H, H-3, *J* = 9.15 Hz), 3.79 (s, 3H, Ar-OCH_3), 3.87 (t, 1H, H-2, *J* = 9.15 Hz), 4.04 (d, 1H, H-5, *J* = 9.34 Hz), 5.71 (d, 1H, H-1, *J* = 9.15 Hz), 7.03 (d, 2H, *o*-Ar-H, *J* = 8.79 Hz), 7.82 (d, 2H, *m*-Ar-H, *J* = 8.61 Hz), 8.76 (s, 1H, triazole-H).

^{13}C NMR (D_6-DMSO): δ 56.8, 72.8, 73.4, 77.8, 79.3, 88.9, 115.8 (2 x C), 121.1, 124.5, 128.1 (2 x C), 147.8, 160.5, 171.1.

m/z calculated: 351.31 *m/z* found (ESI): 352.1 ($+H^+$)

M.P. = 184-186 °C

R_f = 0.17 (3:1 ethyl acetate: methanol)

$[\alpha]_D$ = -39.4 (*c* = 1.0, CH_2Cl_2)

Synthesis of divalent-ethynylbenzene glucuronosyl triazole derivatives

To a flame-dried 500 mL round-bottomed flask, a solution of azide **32** (6.0 g, 25.0 mmol), a selected diethynyl benzene derivative (1.05 g, 12.5 mmol), ascorbic acid (0.25 g, 0.16 mmol), and copper sulfate (0.10 g, 0.10 mmol) was stirred in 250 mL of deionized water. The resulting mixture was heated to a constant temperature of 75 °C for 18 hours or until the TLC plate showed consumption of the starting materials. The reaction mixture was then cooled in an ice bath for forty minutes. At the end of this period of time, the reaction mixture was filtered through a glass frit and washed with water (2 x 100 mL) and methanol (4 x 75 mL). The crude solids were then recrystallized from isopropyl alcohol to give fine beige powders is excess of 65%.

Phenyl 1,3-Bis[methyl 2,3,4-tri-*O*-acetyl-β-D-glucuronosyl-1H-[1,2,3]-triazole] (61).

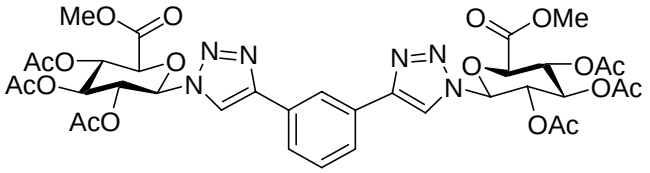

^{1}H NMR (D_6-DMSO): δ 1.81, 1.99, 2.02 (3s, 18H, 6 x $COCH_3$), 3.63 (s, 6H, OCH_3), 4.86 (d, 2H, H-5, *J* = 10.07 Hz), 5.24 (t, 2H, H-2, *J* = 9.70 Hz), 5.65 (t, 2H, H-4, *J* = 9.25 Hz), 5.72 (t, 2H, H-3, *J* = 9.25 Hz), 6.47 (d, 2H, H-1, *J* = 8.97 Hz), 7.57 (t, 1H, *m*-Ar-H, *J* = 7.69 Hz), 7.82 (d, 2H, *o*-Ar-H, *J* = 7.69 Hz), 8.39 (s, 1H, *o*-Ar-H), 9.15 (s, 2H, triazole-H).

m/z calculated: 844.73 *m/z* found (ESI): 785.3 ($-CO_2CH_3$)

M.P. = 260-262 °C

R_f = 0.11 (100% ethyl acetate)

$[\alpha]_D$ = +7.4 (*c* = 1.0, CH_2Cl_2)

Phenyl 1,4-Bis[methyl 2,3,4-tri-*O*-acetyl-β-D-glucuronosyl-1H-[1,2,3]-triazole] (62).

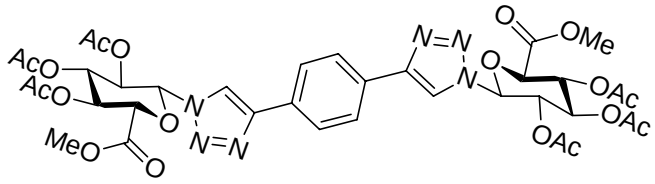

^{1}H NMR (D_6-DMSO): δ 1.81, 1.99, 2.02 (3s, 18H, 6 x $COCH_3$), 3.63 (s, 6H, OCH_3), 4.85 (d, 2H, H-5, *J* = 10.07 Hz), 5.23 (t, 2H, H-2, *J* = 9.79 Hz), 5.66 (t,

2H, H-4, *J* = 9.45 Hz), 5.75 (t, 2H, H-3, *J* = 9.45 Hz), 6.46 (d, 2H, H-1, *J* = 8.97 Hz), 7.94 (s, 4H, *o*-Ar-H), 9.09 (s, 2H, triazole-H).

m/z calculated: 844.73 *m/z* found (ESI): 816.3 ($-OCH_3$)

M.P. = 266-268 °C

R_f = 0.12 (100% ethyl acetate)

$[\alpha]_D$ = +7.6 (*c* = 1.0, CH_2Cl_2)

N-linked Tetrazole Preparation

In a 100 mL two-neck round-bottom flask equipped with a magnetic stir bar and reflux condenser, a solution of **32** (1.0 g, 2.8 mmol), one equivalent of 4-cyanophenol, and one half of an equivalent of zinc bromide (0.31 g, 1.4 mmol) was stirred in 30 mL of 2:1 deionized water: isopropyl alcohol at reflux for 12 hours. Upon completion of reaction, which was established via TLC plate, the reaction mixture was then cooled in an ice bath. Upon completion of cooling, 10 mL of 3 N HCl and 20 mL of methylene chloride were added to the stirring solution. The stirring was allowed to continue for a period of two hours. At the end of this period of time, the solution was separated and the aqueous layer was extracted with dichloromethane (2 x 10 mL). The combined organic layers were dried, filtered, and reduced to afford pure tetrazole product in excess of 85% yield.

1-(Methyl 2,3,4-tri-*O*-acetyl-β-D-glucuronosyl)-4-(4-hydroxyphenyl)-1*H*-[1,2,3,5]-tetrazole (63).

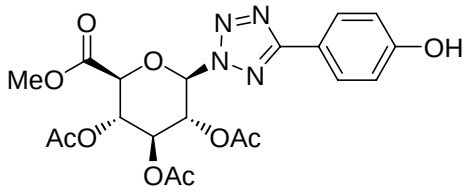

^{1}H NMR ($CDCl_3$): δ 2.02, 2.03, 2.07 (3s, 9H, 3 x -$COCH_3$), 3.77 (s, 3H, -OCH_3), 4.43 (d, 1H, H-5, *J* = 9.52 Hz), 4.72 (d, 1H, H-1, *J* = 8.79 Hz), 4.95 (t, 1H, H-2, *J* = 8.79 Hz), 5.22 (t, 1H, H-4, *J* = 9.43 Hz), 5.27 (t, 1H, H-3, *J* = 9.15 Hz), 6.91 (d, 2H, *o*-Ar-H, *J* = 8.60 Hz), 7.54 (d, 2H, *m*-Ar-H, *J* = 8.42 Hz).

^{13}C NMR ($CDCl_3$): δ 21.7, 21.78, 21.82, 54.4, 70.2, 71.6, 73.0, 75.1, 89.1, 103.9, 117.5 (2 x C), 120.4, 135.2 (2 x C), 161.4, 167.8, 170.5, 170.6, 171.2.

m/z calculated: 478.41 *m/z* found (ESI): 501.4 (+Na)

M.P. = 86-90 °C

R_f = 0.47 (1:1 hexanes: ethyl acetate)

$[\alpha]_D$ = -55.6 (*c* = 1.0, CH_2Cl_2)

Synthesis of *O*-glycosides

A suspension of benzyl alcohol (0.68 mL, 6.30 mmol), silver aluminosilicate (1.00 g, 4.11 mmol), and 0.50 g of powdered acid-washed molecular sieves in dichloromethane (25 mL), was stirred at room temperature for 1 h with exclusion of moisture. A solution of glucopyranuronosyl bromide **3** (0.50 g, 1.26 mmol) in 10 mL of

dichloromethane was then added and the mixture was allowed to stir for approximately 72 hours. The mixture was then filtered through Celite, followed by the removal of solvent *in vacuo* to afford 0.86 g of yellow syrup. The crude material was then passed over a column of silica gel (1:1 hexanes: ethyl acetate) to afford 0.42 g of clear syrup (77.8%).

Silver Aluminosilicate Preparation

A slurry of silica alumina SHPV catalyst (activated porous surface, FLUKA Chemical, 10 g) in NaOH (1 M, 175 mL) was stirred at 100 °C for 2 h. The powdered material was then filtered, washed with water (5 x 50 mL), and stirred with an aqueous solution of $AgNO_3$ (0.2 M, 300 mL) in the dark for a period of 16 h at room temperature. Filtration and washing of the residue with water (2 x 100 mL) and acetone (5 x 50 mL), followed by drying *in vacuo* for 3 days and drying at 110 °C for 2 days, gave the activated catalyst.

Alcohol	
benzyl alcohol	*n*-butanol
t-amyl alcohol	cyclohexanol
n-propanol	ethanol

Table 8: Selected alcohol reagent.

Benzyl (2,3,4-tri-*O*-acetyl-α-D-glucopyranosyl methyl uronate) (64).

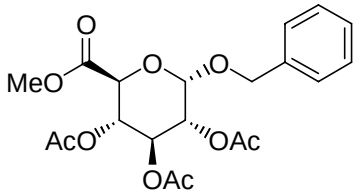

^{1}H NMR ($CDCl_3$): δ 2.03, 2.07 (2s with one double intensity, 9H total, 3 x $COCH_3$), 3.74 (s, 3H, -OCH_3), 4.56 (d, 1H, H-5, *J* = 10.26 Hz), 4.66 (s, 2H, -CH_2-), 4.82 (dd, 1H, H-2, *J* = 4.58, 10.07 Hz), 5.21 (t, 1H, H-4, *J* = 9.52 Hz), 5.59 (t, 1H, H-3, *J* = 9.70 Hz), 6.62 (d, 1H, H-1, *J* = 5.48 Hz), 7.27 (m, 5H, Ar).

^{13}C NMR ($CDCl_3$): δ 21.7, 21.9 (2 x C), 54.3, 66.4, 69.6, 70.4, 71.4, 73.2, 86.5, 128.0 (2 x C), 128.6, 129.5 (2 x C), 141.9, 167.6, 170.4, 170.60, 170.64.

m/z calculated: 424.14 *m/z* found (ESI): 365.1 (-CO_2CH_3)

M.P. = 126-129 °C

R_f = 0.42 (1:1 hexanes: ethyl acetate)

$[\alpha]_D$ = +9.5 (*c* = 1.0, CH_2Cl_2)

_n_-Butyl (2,3,4-tri-_O_-acetyl-β-D-glucopyranosyl methyl uronate) (65).

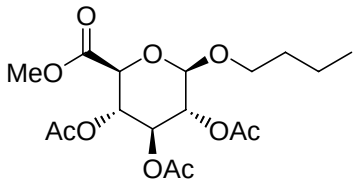

^{1}H NMR ($CDCl_3$): δ 0.87 (t, 3H, -CH_3, *J* = 7.14 Hz), 1.33 (m, 2H, γ-H), 1.52 (m, 2H, β-H), 2.00, 2.01 (2s with one double intensity, 9H total, 3 x $COCH_3$), 3.46 (m, 2H, α-H), 3.74 (s, 3H, -OCH_3), 4.01 (d, 1H, H-5, *J* = 9.52 Hz), 4.51 (d, 1H, H-1, *J* = 7.69 Hz), 4.98 (t, 1H, H-2, *J* = 8.42 Hz), 5.19 (t, 1H, H-4, *J* = 8.58 Hz), 5.21 (t, 1H, H-3, *J* = 8.58 Hz).

^{13}C NMR ($CDCl_3$): δ 15.0, 20.2, 21.8, 21.88, 21.93, 32.5, 54.1, 70.6, 71.2, 72.4, 73.2, 73.7, 101.9, 168.2, 170.1, 170.3, 171.1.

m/z calculated: 390.15 *m/z* found (ESI): 413.3 (+Na)

M.P. = 84-86 °C

R_f = 0.48 (1:1 hexanes: ethyl acetate)

$[\alpha]_D$ = -28.5 (*c* = 1.0, CH_2Cl_2)

_t_-Amyl (2,3,4-tri-_O_-acetyl-β-D-glucopyranosyl methyl uronate) (66).

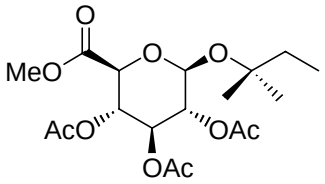

^{1}H NMR ($CDCl_3$): δ 0.81 (t, 3H, -CH_3, γ-H, *J* = 7.14 Hz), 1.12 (s, 3H, β-H_a), 1.15 (s, 3H, β-H_b), 1.49 (m, 2H, β-H_c), 1.97, 1.98 (2s with one double intensity, 9H total, 3 x $COCH_3$), 3.70 (s, 3H, -OCH_3), 3.97 (d, 1H, H-5, *J* = 9.70 Hz), 4.66 (d, 1H, H-1, *J* = 7.87 Hz), 4.92 (t, 1H, H-2, *J* = 7.87 Hz), 5.15 (t, 1H, H-4, *J* = 9.54 Hz), 5.21 (t, 1H, H-3, *J* = 9.52 Hz).

^{13}C NMR ($CDCl_3$): δ 21.8, 21.9, 21.9 (2 x C), 26.3, 27.5, 35.5, 54.0, 70.7, 72.47, 73.51, 73.5, 80.2, 96.5, 168.2, 170.0, 170.3, 171.2.

m/z calculated: 404.17 *m/z* found (ESI): 427.2 (+Na)

M.P. = 100-102 °C

R_f = 0.50 (1:1 hexanes: ethyl acetate)

$[\alpha]_D$ = +100.7 (*c* = 1.0, CH_2Cl_2)

Cyclohexyl (2,3,4-tri-*O*-acetyl-β-D-glucopyranosyl methyl uronate) (67).

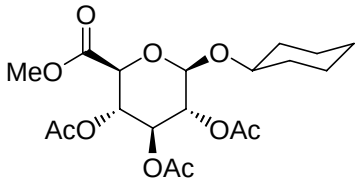

^{1}H NMR ($CDCl_3$): δ 0.83 (m, 2H, δ-H), 1.16 (m, 4H, γ-H), 1.61 (m, 4H, β-H), 1.95, 1.96 (2s with one double intensity, 9H total, 3 x $COCH_3$), 3.20 (m, 1H, α-H), 3.69 (s, 3H, -OCH_3), 3.96 (d, 1H, H-5, *J* = 9.15 Hz), 4.46 (d, 1H, H-1, *J* = 7.69 Hz), 4.93 (t, 1H, H-2, *J* = 8.06 Hz), 5.14 (t, 1H, H-4, *J* = 8.97 Hz), 5.18 (t, 1H, H-3, *J* = 9.15 Hz).

^{13}C NMR ($CDCl_3$): δ 21.7, 21.8, 26.9, 27.7, 30.7 (2 x C), 38.8 (2 x C), 54.0, 70.6, 72.3, 73.2, 73.7, 77.1, 102.1, 168.2, 170.1, 170.3, 171.0.

m/z calculated: 416.17 *m/z* found (ESI): 414.3 (-2H^+)

M.P. = 87-90 °C

R_f = 0.50 (1:1 hexanes: ethyl acetate)

$[\alpha]_D$ = -93.8 (*c* = 1.0, CH_2Cl_2)

_n_-Propyl (2,3,4-tri-_O_-acetyl-β-D-glucopyranosyl methyl uronate) (68).

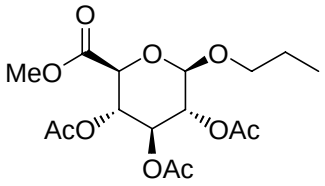

^{1}H NMR ($CDCl_3$): δ 0.82 (t, 3H, -CH_3, *J* = 7.32 Hz), 1.51 (m, 2H, β-H), 1.94, 1.95, 1.96 (3s, 9H total, 3 x $COCH_3$), 3.37 (m, 1H, α-H), 3.68 (s, 3H, -OCH_3), 3.79 (m, 1H, α'-H), 3.98 (d, 1H, H-5, *J* = 9.34 Hz), 4.49 (d, 1H, H-1, *J* = 7.69 Hz), 4.93 (t, 1H, H-2, *J* = 7.87 Hz), 5.14 (t, 1H, H-4, *J* = 9.54 Hz), 5.19 (t, 1H, H-3, *J* = 9.52 Hz).

^{13}C NMR ($CDCl_3$): δ 11.5, 21.7, 21.8 (2 x C), 23.8, 54.0, 70.6, 72.3, 73.0, 73.2, 83.6, 101.8, 168.2, 170.1, 170.2, 171.0.

m/z calculated: 376.36 *m/z* found (ESI): 399.2 (+Na)

M.P. = 91-94 °C

R_f = 0.49 (1:1 hexanes: ethyl acetate)

$[\alpha]_D$ = -8.5 (*c* = 1.0, CH_2Cl_2)

Ethyl (2,3,4-tri-_O_-acetyl-β-D-glucopyranosyl methyl uronate) (69).

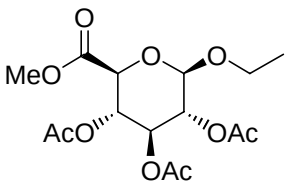

^{1}H NMR ($CDCl_3$): δ 1.13 (t, 3H, -CH_3, *J* = 6.04 Hz), 1.96, 1.99 (2s with one double intensity, 9H total, 3 x $COCH_3$), 3.52 (m, 1H, α-H), 3.70 (s, 3H, -OCH_3), 3.88 (m, 1H, α'-H), 3.99 (d, 1H, H-5, *J* = 9.52 Hz), 4.51 (d, 1H, H-1, *J* = 7.69 Hz), 4.93 (t, 1H, H-2, *J* = 8.24 Hz), 5.17 (t, 1H, H-4 *J* = 9.41 Hz), 5.23 (t, 1H, H-3, *J* = 9.41 Hz).

^{13}C NMR ($CDCl_3$): δ 16.2, 21.7, 21.8, 21.9, 54.0, 66.9, 70.6, 72.4, 73.2, 73.7, 101.5, 168.2, 170.1, 170.2, 171.0.

m/z calculated: 362.33 *m/z* found (ESI): 385.1 (+Na)

M.P. = 99-103 °C

R_f = 0.44 (1:1 hexanes: ethyl acetate)

$[\alpha]_D$ = +36.0 (*c* = 1.0, CH_2Cl_2)

Methyl 3,4-di-*O*-acetyl-1-([1,2,3]-4,5-dicarboxylic acid ethyl ester)-5-anhydro-D-fructuronate-*O*-benzoyloxime triazole (70).

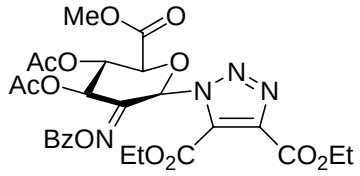

^{1}H NMR ($CDCl_3$): δ 1.30 (t, 3H, -CH_3, *J* = 7.14 Hz), 1.40 (t, 3H, -CH_3, *J* = 7.14 Hz), 2.13 (1s with double intensity, 6H total, 2 x $COCH_3$), 3.54 (s, 3H, -OCH_3), 4.27 (q, 2H, -CH_2-, *J* = 7.14 Hz), 4.43 (q, 2H, -CH_2-, *J* = 7.14 Hz), 4.49 (d, 1H, *J* = 9.52 Hz), 4.64 (d, 1H, *J* = 6.02 Hz), 5.85 (t, 1H, *J* = 6.42 Hz), 5.98 (s, 1H), 7.35

(t, 2H, *m*-Ar-H, *J* = 7.69 Hz), 7.53 (t, 1H, *p*-Ar-H, *J* = 7.68 Hz), 7.67 (d, *o*-Ar-H, *J* = 6.98 Hz).

m/z calculated: 604.70 *m/z* found (ESI): 602.5 ($-H^+$)

M.P. = N/A (syrup)

R_f = 0.13 (1:1 hexanes: ethyl acetate)

$[\alpha]_D$ = -16.3 (*c* = 1.0, CH_2Cl_2)

References

1. Dwek, R.A. "Glycobiology: Toward Understanding the Function of Sugars," *Chem. Rev.* **1996**, *96*, 683-720.
2. Schachter, H. "The Clinical Relevance of Glycobiology," *J. Clin. Invest*. **2001**, *108*, 1579-1582.
3. Lee, Y.C.; Lee, R.T. "Carbohydrate-Protein Interactions: Basis of Glycobiology," *Acc. Chem. Res*. **1995**, *28*, 321-327.
4. Bertozzi, C.R.; Kiessling, L.L. "Chemical Glycobiology," *Science*, **2001**, *291*, 2357-2363.
5. EurekAlert Home Page. http://www.eurekalert.org/pub_releases/2002-03/ru-sdc030102.php (accessed Nov **2004**).
6. Quan, L.; Zhu, B.; Ishida, K.; Taniguchi, M.; Oritani, S.; Kamikodai, Y.; Fujita, M.; Masaki, Q.; Maeda, H. "Sudden Infant Death Attributed to Peracute Pulmonary Infection: Two Autopsy Cases," *Legal Medicine,* **2000**, *2*, 79-83.
7. CDC Home Page. http://www.cdc.gov/epo/mmwr/preview/mmrwhtml/mm4832a2.htm (accessed Nov **2004**).
8. Yoshikawa, T. "Antimicrobial Resistance and Aging: Beginning of the End of the Antibiotic Era?" *J. Am. Geriatrics. Soc.* **2002**, *50*, 226-229.
9. Morgan, P. M.; Sala, R. F.; Tanner, E. "Eliminations in the Reaction Catalyzed by UDP-*N*-Acetylglucosamine 2-Epimerase," *J. Am. Chem. Soc.* **1997**, *119*, 10269-10277.
10. Livermore, D.M. "Antibiotic Resistance in *Staphylococci*," *Int. J. Antimicrobial Agents*, **2000**, *16*, S3-S10.

11. Chambers, H.F. "The Changing Epidemiology of *Staphylococcus aureus*?," *Emerging Infectious Disease*, **2001**, *7*, 202-207.

12. Kuroda, M. *et al.* "Whole Genome Sequencing of Methicillin-resistant *Staphylococcus aureus*," *Lancet*, **2001**, *357*, 1225-1240.

13. Yoshida, J.; Nagata, T.; Nishioka, Y.; Nose, Y.; Tanaka, M. "Outbreak of Multi-Drug Resistant *Staphylococcus aureus*: A Cluster Analysis," *J. Clin. Epidemiol*. **1996**, *49*, 1447-1452.

14. Howe, R.A.; Monk, A.; Wootton, M.; Walsh, T.R.; Enright, M.C. "Vancomycin Susceptibility within Methicillin-resistant *Staphylococcus aureus* Lineages," *Emerging Infectious Disease*, **2004**, *10*, 855-857.

15. Gemmell, C.G. "Glycopeptide Resistance in *Staphylococcus aureus*: Is it a Real Threat?," *J. Infect. Chemother*. **2004**, *10*, 69-75.

16. Cuny, C.; Werner, G.; Braulke, C.; Klare, I.; Witte, W. "Diagnostics of *Staphylococci* with Special Reference to MRSA," *J. Lab. Med*. **2002**, *26*, 165-173.

17. Stick, R.V. "Carbohydrates: The Sweet Molecules of Life" Academic Press: San Diego, California, **2001**, 220-227.

18. Field, R.A.; Naismith, J.H. "Structural and Mechanistic Basis of Bacterial Sugar Nucleotide-Modifying Enzymes," *Biochemistry*, **2003**, *42*, 7637-7647.

19. Kiser, K.B.; Bhasin, N.; Deng, L.; Lee, J.C. "*Staphylococcus aureus cap5P* Encodes a UDP-*N*-Acetylglucosamine 2-Epimerase with Functional Redundancy," *J. Bacteriol.* **1999**, *181*, 4818-4824.

20. Chou, W.C.; Hinderlich, S.; Reutter, W.; Tanner, M.E. "Sialic Acid Biosynthesis: Stereochemistry and Mechanism of the Reaction Catalyzed by Mammalian UDP-*N*-Acetylglucosamine 2-Epimerase," *J. Am. Chem. Soc*. **2003**, *125*, 2455-2461.

21. O'Riordan, K.; Lee, J.C. "*Staphylococcus aureus* Capsular Polysaccharides," *Clin. Microbiol. Rev.* **2004**, *17*, 218-234.

22. Davey, M.W.; Gilot, C.; Perisau, G.; Ostergaard, J.; Ha, Y.; Bauw, G.C.; van Montagu, M.C. "Ascorbate Biosynthesis in Arabidopsis Cell Suspension Culture," *Plant Physiol.* **1999**, *121*, 535-543.

23. Boons, G-J. "Carbohydrate Chemistry," Blackie Academic & Professional: London, England, **1998**, 430-442.

24. El Khadem, H.S. "Carbohydrate Chemistry: Monosaccharides and Their Oligomers," Academic Press, Inc.: San Diego, California, **1988**, 1-8, 191-202.

25. Guthrie, R.D.; Honeyman, J. "An Introduction to the Chemistry of Carbohydrates," Clarendon Press: Oxford, England, **1968**, 9-25, 34-39.

26. Bols, M. "Carbohydrate Building Blocks," Wiley: New York, New York, **1996**, 1-18.

27. Kennedy, J.F. "Carbohydrate Chemistry," Clarendon Press: Oxford, England, **1988**, 3-40, 73-114.

28. Collins, P.M.: Ferrier, R.J. "Monosaccharides: Their Chemistry and Their Roles in Natural Products," Wiley: New York, New York, **1995**, 1-38.

29. Osborn, H.M.I., "Carbohydrates," Academic Press: Boston, Massachusetts, **2003**, 109-118.

30. Lichtenthaler, F. W.; Kaji, E.; Osa, Y.; Takahashi, K.; Hirooka, M.; Zen, S. "Facile Preparation and Utilization of a Novel β-D-ManNAcA-Donor: Methyl 2-

Benzoyl-oxyimino-1-bromo-2-deoxy-α-D-*arabino*-hexopyranuronate," *Bull. Chem. Soc. Jpn.* **1994**, *67*, 1130-1140.

31. Ikan, R., "Naturally Occurring Glycosides," John Wiley & Sons: New York, New York, **1999**, 2-21.

32. Zechel, D.L.; Boraston, A.B.; Gloster, T.; Boraston, C.M.; MacDonald, J.M.; Tilbrook, M.G.; Stick, R.V.; Davies, G.J. "Iminosugar Glycosidase Inhibitors: Structural and Thermodynamic Dissection of the Binding of Isofagomine and 1-Deoxynojirimycin to β-Glucosidases," *J. Am. Chem Soc.* **2003**, *125*, 14313-14323.

33. Williams, S.J.; Hoos, R.; Withers, S.G. "Nanomolar versus Millimolar Inhibition by Xylobiose-derived Azasugars: Significant Differences Between Two Structurally Distinct Xyloses," *J. Am. Chem. Soc.* **2000**, *122*, 2223-2235.

34. Wong, H.C.; Halcomb R.L.; Ichikawa, Y.; Kajimoto, T. "Enzymes in Organic Synthesis: Application to the Problems of Carbohydrate Recognition. Part 2," *Angew. Chem. Int. Ed. Engl.* **1995**, *34*, 521.

35. Nishimura, Y.; Shitara, E.; Adachi, H.; Toyoshima, M.; Nakajima, M.; Okami, Y.; Takeuchi, T. "Flexible Synthesis and Biological Activity of Uronic Acid-type *gem*-Diamine 1-*N*-Iminosugars: A New Family of Glycosidase Inhibitors," *J. Org. Chem.* **2000**, *65*, 2-11.

36. Jensen, H.H.; Jensen, A.; Hazell, R.; Bols, M. "Synthesis and Investigation of L-Fuco- and D-Glucurono-azafagomine," *J. Chem. Soc., Perkin Trans. 1*, **2002**, 1190-1198.

37. Takayama, S.; Martin, R.; Wu, J.; Laslo, K.; Siuzdak, G.; Wong, C-H. "Chemoenzymatic Preparation of Novel Cyclic Imino Sugars and Rapid

Biological Activity Evaluation Using Electrospray Mass Spectrometry and Kinetic Analysis," *J. Am. Chem. Soc.* **1997**, *119*, 8146-8151.

38. Zhao, G.; Deo, U.C.; Ganem, B. "Selective Fowler Reductions: Asymmetric Total Syntheses of Isofagomine and Other 1-Azasugars from Methyl Nicotinate," *Org. Lett*. **2001**, *3*, 201-203.

39. Nishimura, Y.; Satoh, T.; Adachi, H.; Kondo, S.; Takeuchi, T.; Azetaka, M.; Fukuyasu, H.; Iizuka, Y. "Synthesis of Antimetastatic Activity of L-Iduronic Acid-type 1-*N*-Iminosugars," *J. Med. Chem.* **1997**, *40*, 2626-2633.

40. Xie J.; Gueveli, T.; Hebbe, S.; Dechoux, L. "Synthesis of Novel 1-*N*-Iminosugars from Chiral Nonracemic Bicyclic Lactams," *Tetrahedron Lett*. **2004**, *45*, 4903-4906.

41. Kim, J.Y.; Ichikawa, M.; Ichakawa, Y. "Highly Selective Synthesis of 1-*N*-Iminosugars of the D-Glucose and D-Glucuronic Acid Types," *J. Org. Chem.* **2000**, *65*, 2599-2602.

42. Sawada, D.; Takahashi, H.; Ikegami, S. "Efficient Synthesis of 1-Deoxy-Azasugars as Useful Synthetic Tools," *Tetrahedron Lett*. **2003**, *44*, 3085-3088.

43. Ye, X-S.; Sun, F.; Liu, M.; Li, Q.; Wang, Y.; Zhang, G.; Zhang, L-H.; Zhang, X-L. "Synthetic Iminosugar Derivatives as New Potential Immunosuppressive Agents," *J. Med. Chem., Letters,* **2005**, *48*, 3688-3691.

44. Kren, V.; Martinkova, L. "Glycosides in Medicine: The Role of Glycosidic Residue in Biological Activity," *Curr. Med. Chem.* **2001**, *8*, 1303-1328.

45. Boullanger, P.; Maunier, V.; Lafont, D. "Syntheses of Amphiphilic Glycosylamides from Glycosyl Azides without Transient Reduction to Glycosylamines," *Carbohydr. Res.* **2000**, *324*, 97-106.

46. Ying, L.; Gervay-Hague, J. "General Methods for the Synthesis of Glycopyranosyluronic Acid Azides," *Carbohydr. Res.* **2003**, *338*, 835-841.

47. O'Neil, I.A.; Thompson, S.; Murray, C.L.; Kalindjian, S.B. "DPPE: A Convenient Replacement for Triphenylphosphine in the Staudinger and Mitsunobu Reactions," *Tetrahedron Lett*. **1998**, *39*, 7787-7790.

48. Kolb, H.C.; Sharpless, K.B. "The Growing Impact of Click Chemistry on Drug Discovery," *Drug Discovery Today*, **2003**, *8*, 1128-1137.

49. Krasinski, A.; Fokin, V.V.; Sharpless, K.B. "Direct Synthesis of 1,5-Disubstituted-4-magnesio-1,2,3-triazoles, Revisited," *Org. Lett.* **2004**, *6*, 1237-1240.

50. Li, Z.; Seo, T.S.; Ju, J. "1,3-Dipolar Cycloadditions of Azide with Electron-deficient Alkynes Under Mild Condition in Water," *Tetrahedron Lett*. **2004**, *45*, 3143-3146.

51. Tornøe, C.W.; Christensen, C.; Meldal, M. "Peptidotriazoles on Solid Phase: [1,2,3]-Triazoles by Regiospecific Copper(I)-catalyzed 1,3-Dipolar Cycloadditions of Terminal Alkynes to Azides," *J. Org. Chem.* **2002**, *67*, 3057-3064.

52. Bagga, K.; Dua, G.; Williams, G.; Simmonds, R. J. "Synthesis of Glycosides in which the Aglycon is an *N*-(Hydroxymethyl)-amino-1,3,5-triazine Derivative," *Glycoconjugate J.* **1997**, *14*, 519-521.

53. Yin, H.; Lowary, T.L. "Synthesis of Arabinofuranosides *via* Low-temperature Activation of Thioglycosides," *Tetrahedron Lett*. **2001**, *42*, 5829-5832.

54. van Boeckel, C.A.A.; Beetz T.; van Aelst, S.F. "Substituent Effects on Carbohydrate Coupling Reactions Promoted by Insoluble Silver Salts" *Tetrahedron*, **1984**, *40*, 4097-4107.

55. Stazi, F.; Palmisano, G.; Turconi, M.; Clini, S.; Santagostino, M. "Accelerated Koenigs-Knorr Glucuronidation of a Deactivated Nitrophenol: Unveiling the Role of Polyamine Additive 1,1,4,7,10,10-Hexamethyltriethylenetetramine through Design of Experiments," *J. Org. Chem*. **2004**, *69*, 1097-1103.

56. McCartney, J.L.; Meta, C.T.; Cicchillo, R.M.; Bernardina, M.D.; Wagner, T.R.; Norris, P. "Addition of Lithiated *C*-Nucleophiles to 2,3-*O*-Isopropylidene-D-erythronolactone: Stereoselective Formation of a Furanose *C*-Disaccharide," *J. Org. Chem.* **2003**, *68*, 10152-10155.

57. Seebach, D.; Corey, E.J. "Generation and Synthetic Applications of 2-Lithio-1,3-dithianes," *J. Org. Chem.* **1975**, *40*, 231-237.

58. Smith III, A.B.; Adams, C.M. "Evolution of Dithiane-based Strategies for the Construction of Architecturally Complex Natural Products," *Acc. Chem. Res.* **2004**, *37*, 365-377.

59. Soli, E.D.; Manoso, A.S.; Patterson, M.C.; DeShong, P.; Favor, D.A.; Hirschmann, R.; Smith III, A.B. "Azide and Cyanide Displacements *via* Hypervalent Silicate Intermediates," *J. Org. Chem.* **1999**, *64*, 3171-3177.

60. Friedman, L.; Shechter, H. "Preparation of Nitriles from Halides and Sodium Cyanide. An Advantageous Nucleophilic Displacement in Dimethyl Sulfoxide," *J. Org. Chem.* **1960**, *25*, 877-879.

61. Cook, F.L.; Bowers, C.L.; Liotta, C.L. “Chemistry of “Naked” Anions III. Reactions of the 18-Crown-6 Complex of Potassium Cyanide with Organic Substrates in Aprotic Organic Solvents,” *J. Org. Chem.* **1974**, *39*, 3416-3418.

62. Khan, S.H.; O’Neill, R.A. “Modern Methods in Carbohydrate Synthesis,” Harwood Academic Publications: Newark, New Jersey, **1996**, 316-351.

63. Root, Y.Y.; Wagner, T.R.; Norris, P. “Crystal Structure of Methyl 1,2,3,4-tetra-*O*-acetyl-β-D-glucopyranuronate,”*Carbohydr. Res*. **2002**, *337*, 2343-2346.

Appendix A

NMR and Mass Spectra

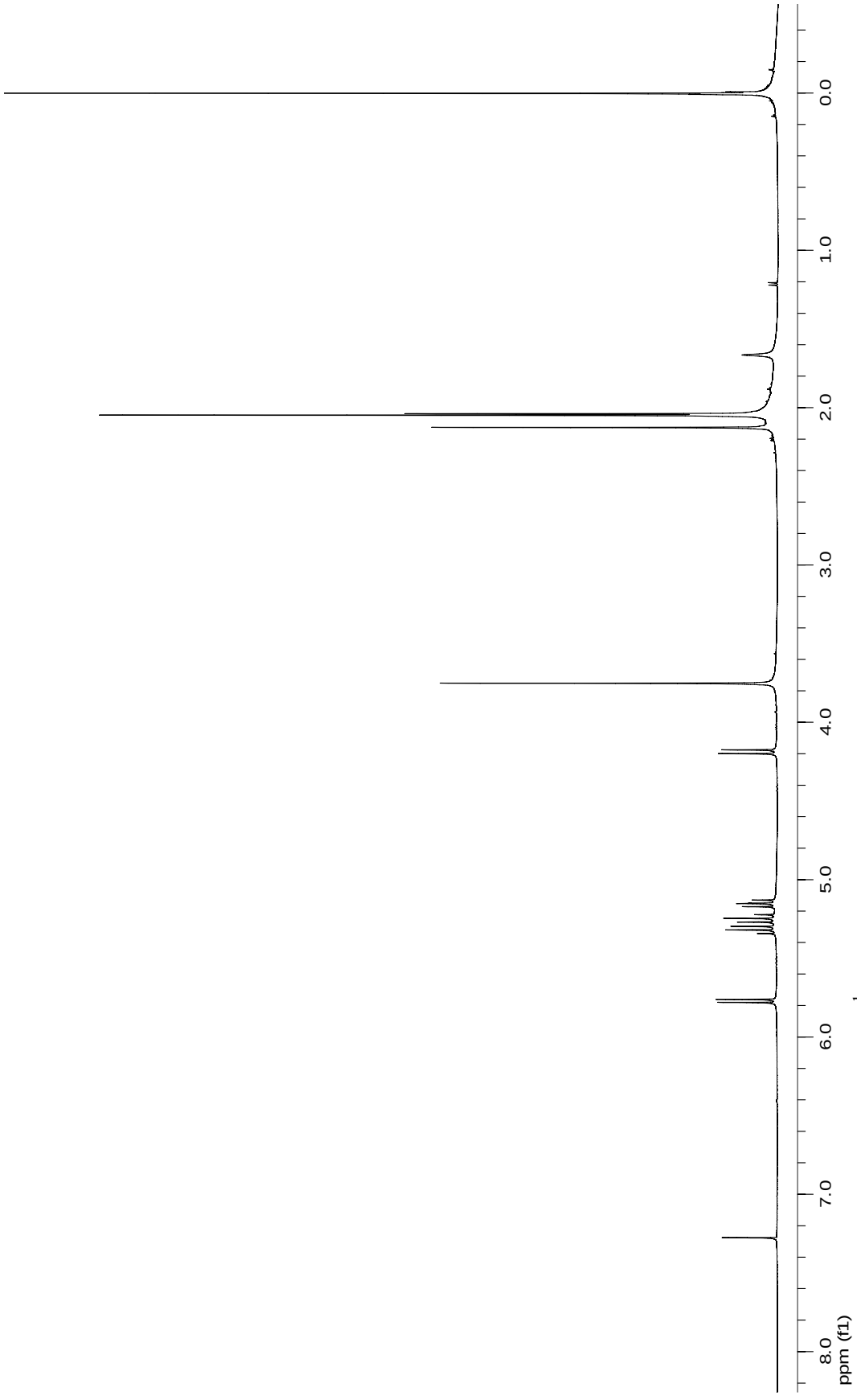

Figure 23: 400 MHz ^{1}H NMR spectrum of methyl 1,2,3,4-tetra-*O*-acetyl-β-D-glucopyranuronate (**2β**).

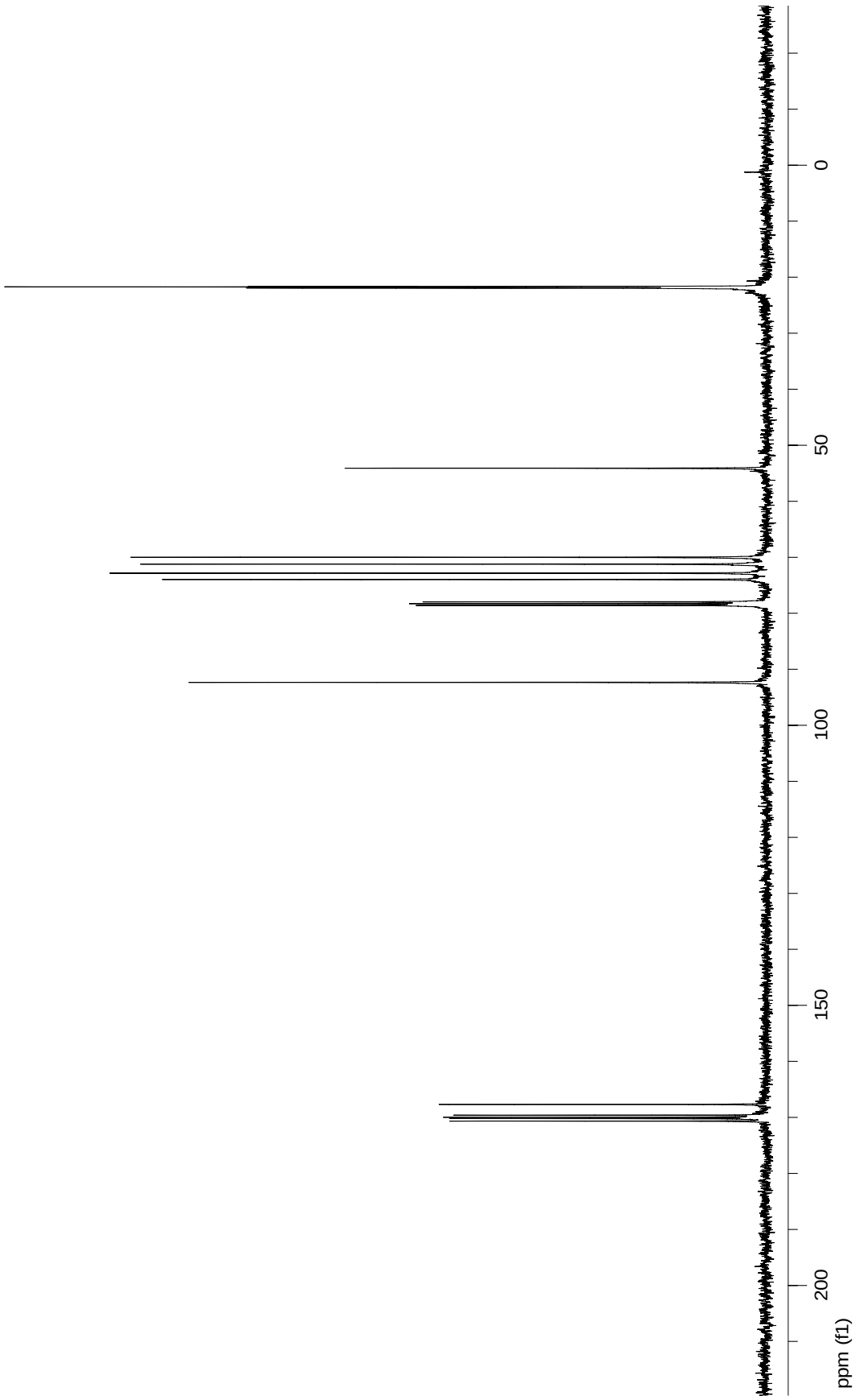

Figure 24: 100 MHz ^{13}C NMR spectrum of methyl 1,2,3,4-tetra-*O*-acetyl-β-D-glucopyranuronate (**2β**).

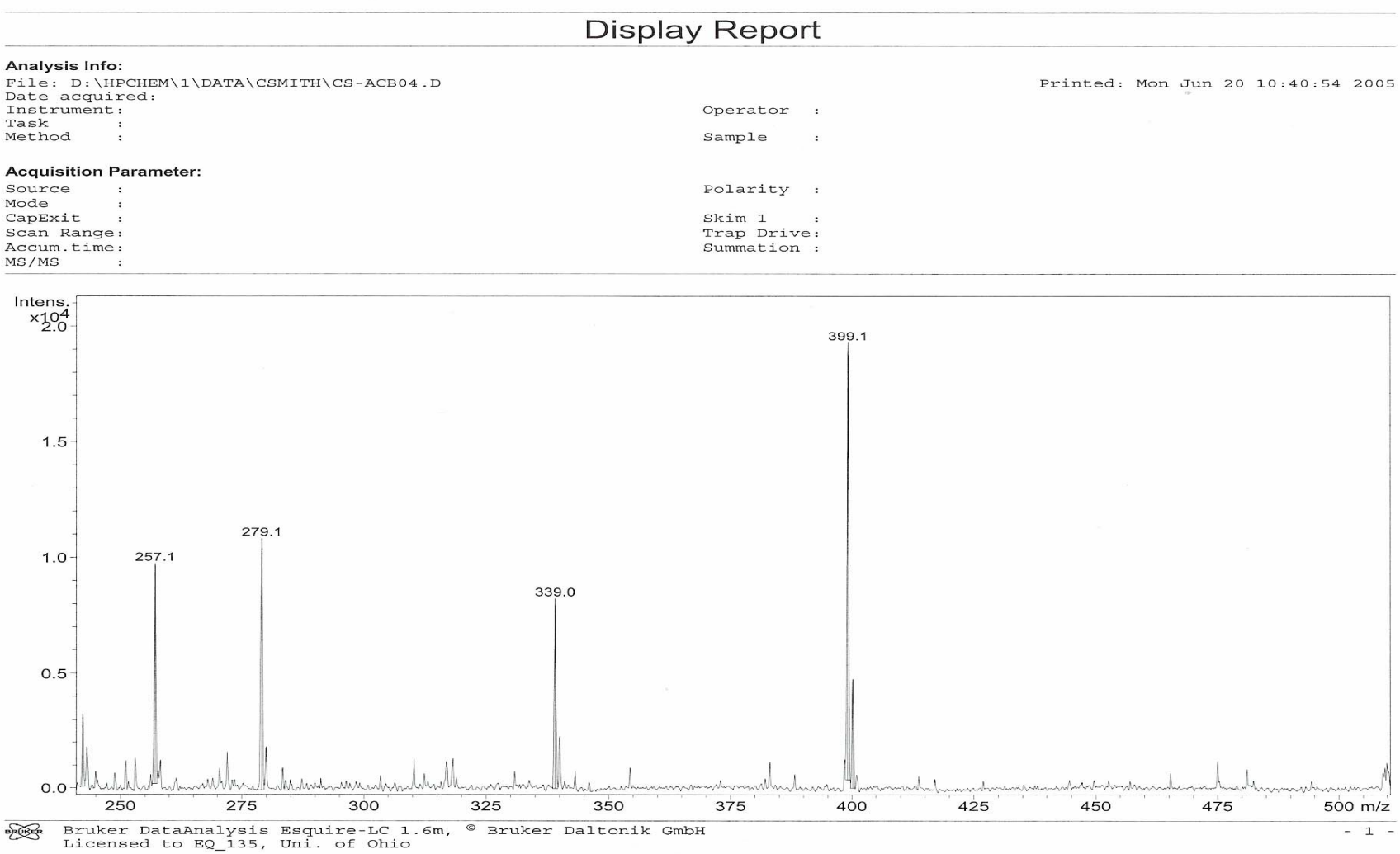

Figure 25: Mass spectrum of methyl 1,2,3,4-tetra-*O*-acetyl-β-D-glucopyranuronate (**2β**).

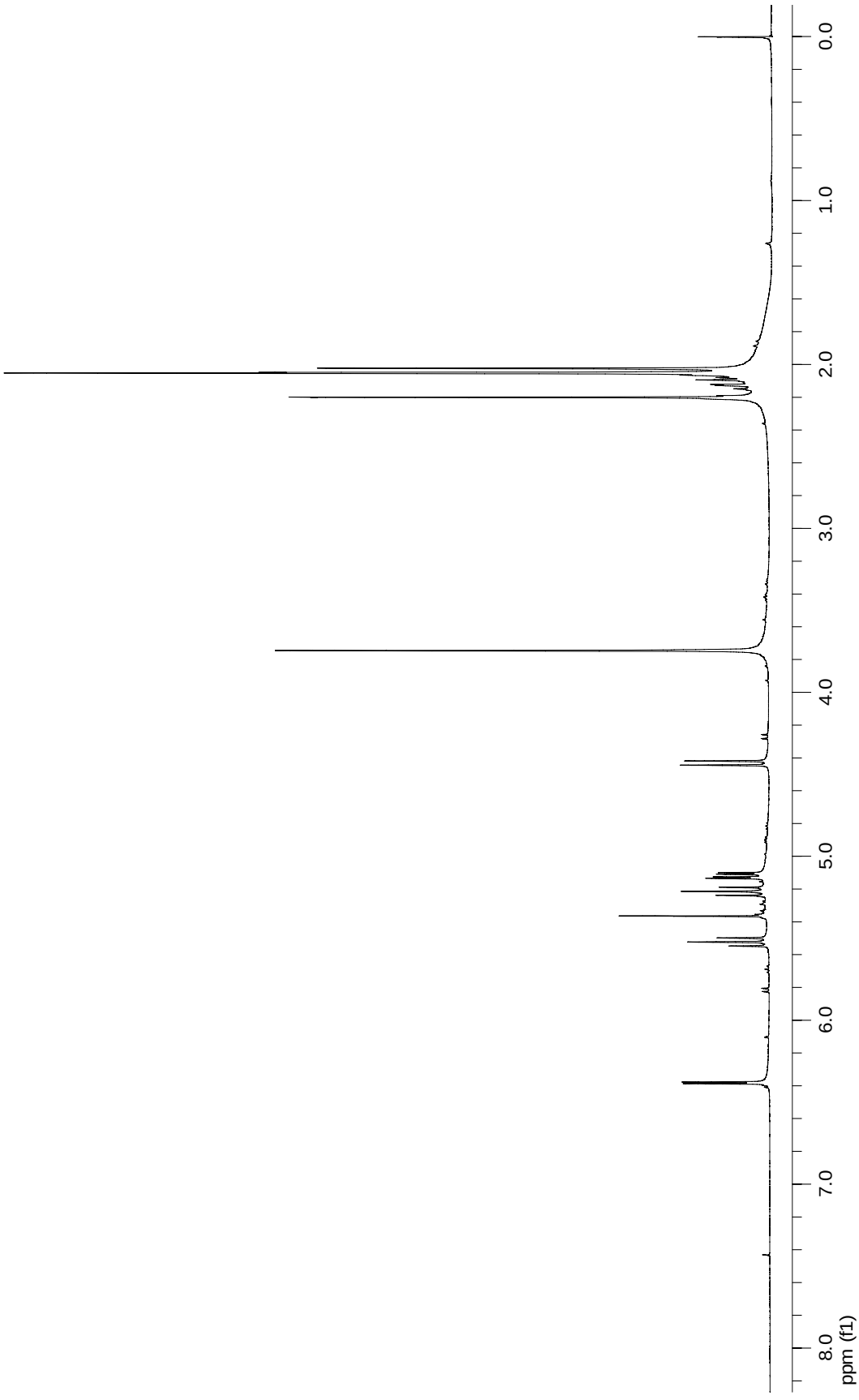

Figure 26: 400 MHz ^{1}H NMR spectrum of methyl 1,2,3,4-tetra-*O*-acetyl-α-D-glucopyranuronate (**2*α***).

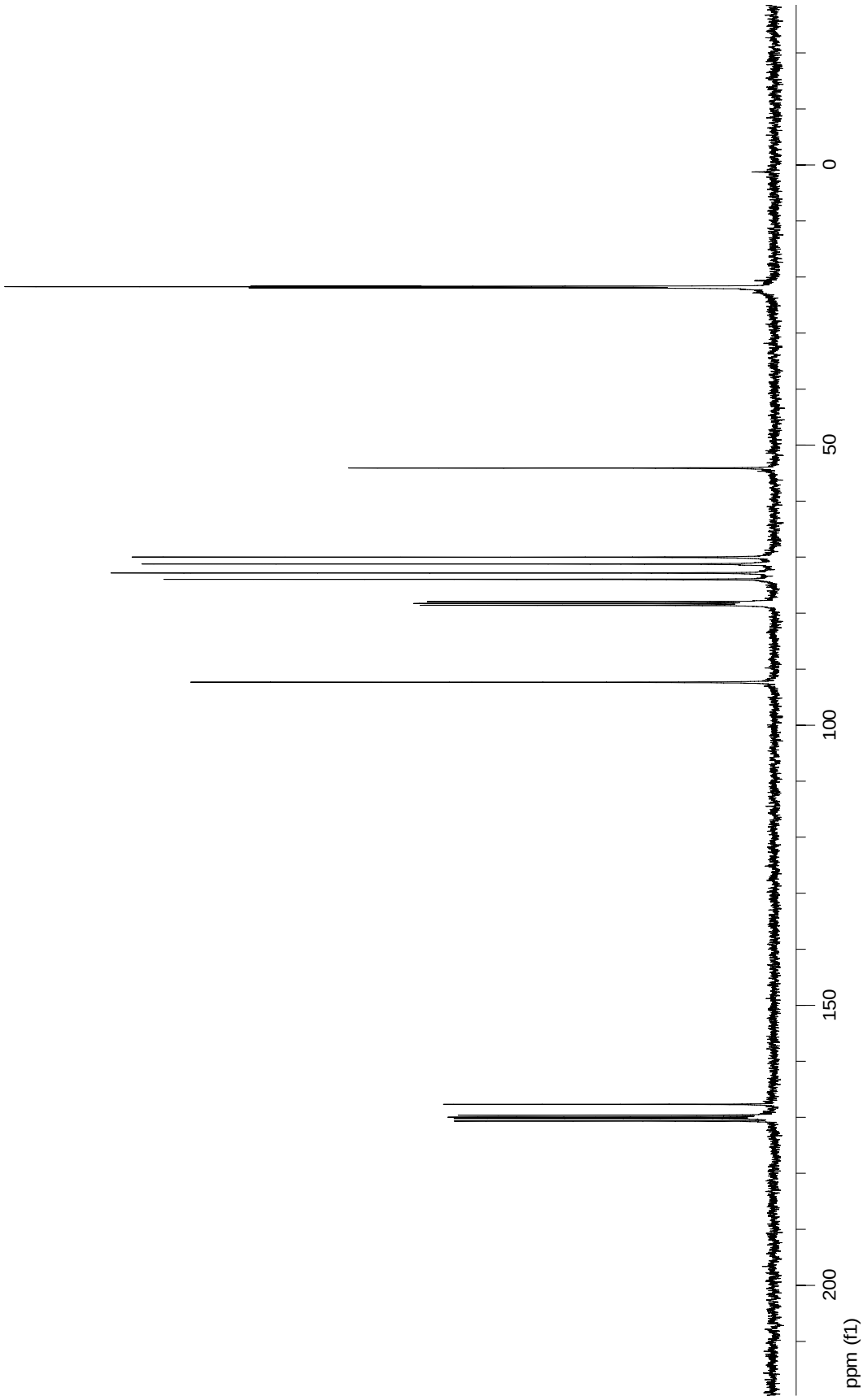

Figure 27: 100 MHz ^{13}C NMR spectrum of methyl 1,2,3,4-tetra-*O*-acetyl-α-D-glucopyranuronate (**2*α***).

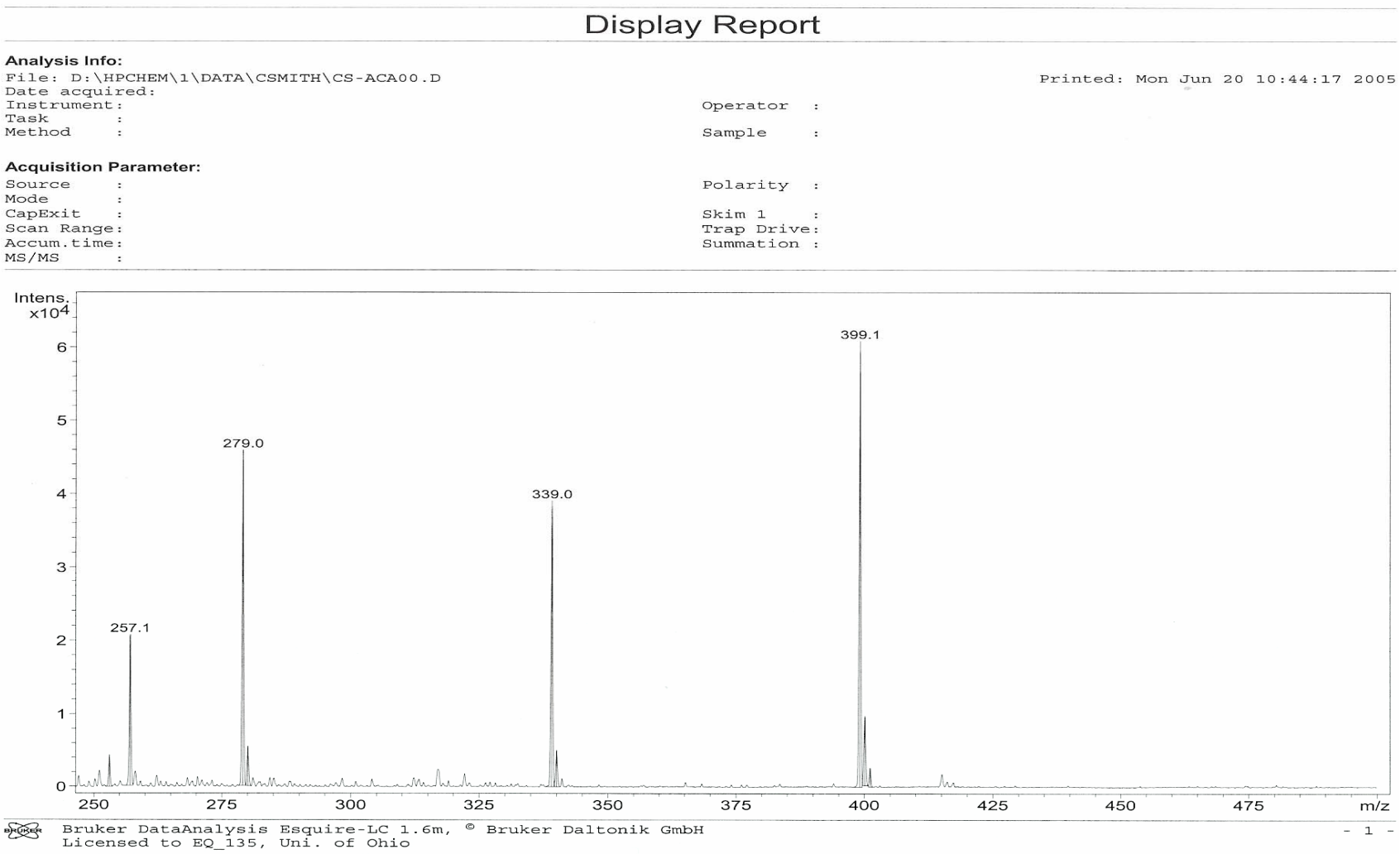

Figure 28: Mass spectrum of methyl 1,2,3,4-tetra-*O*-acetyl-α-D-glucopyranuronate (**2α**).

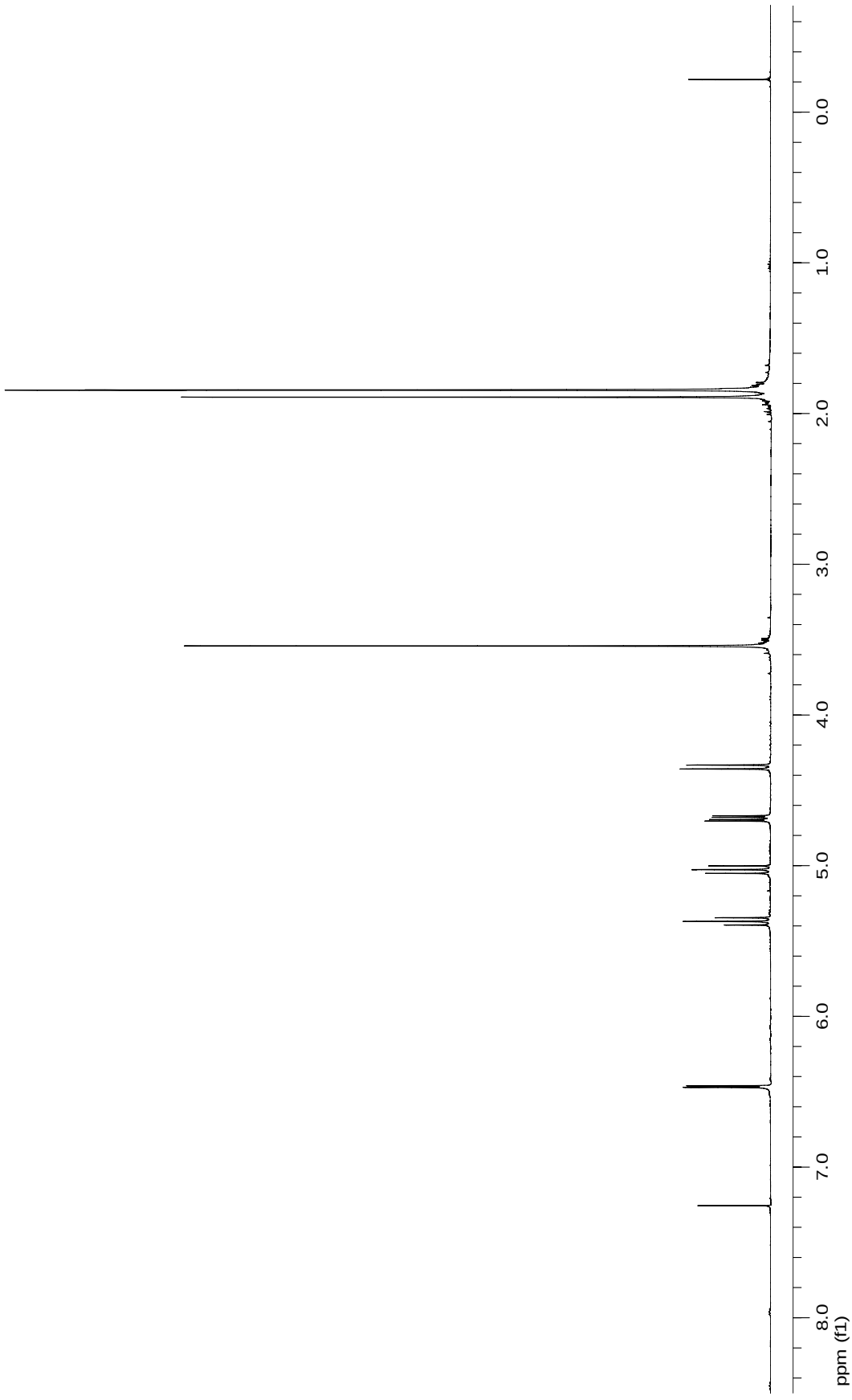

Figure 29: 400 MHz ^{1}H NMR spectrum of methyl 2,3,4-tri-*O*-acetyl-α-D-glucopyranosyl bromide (**3**).

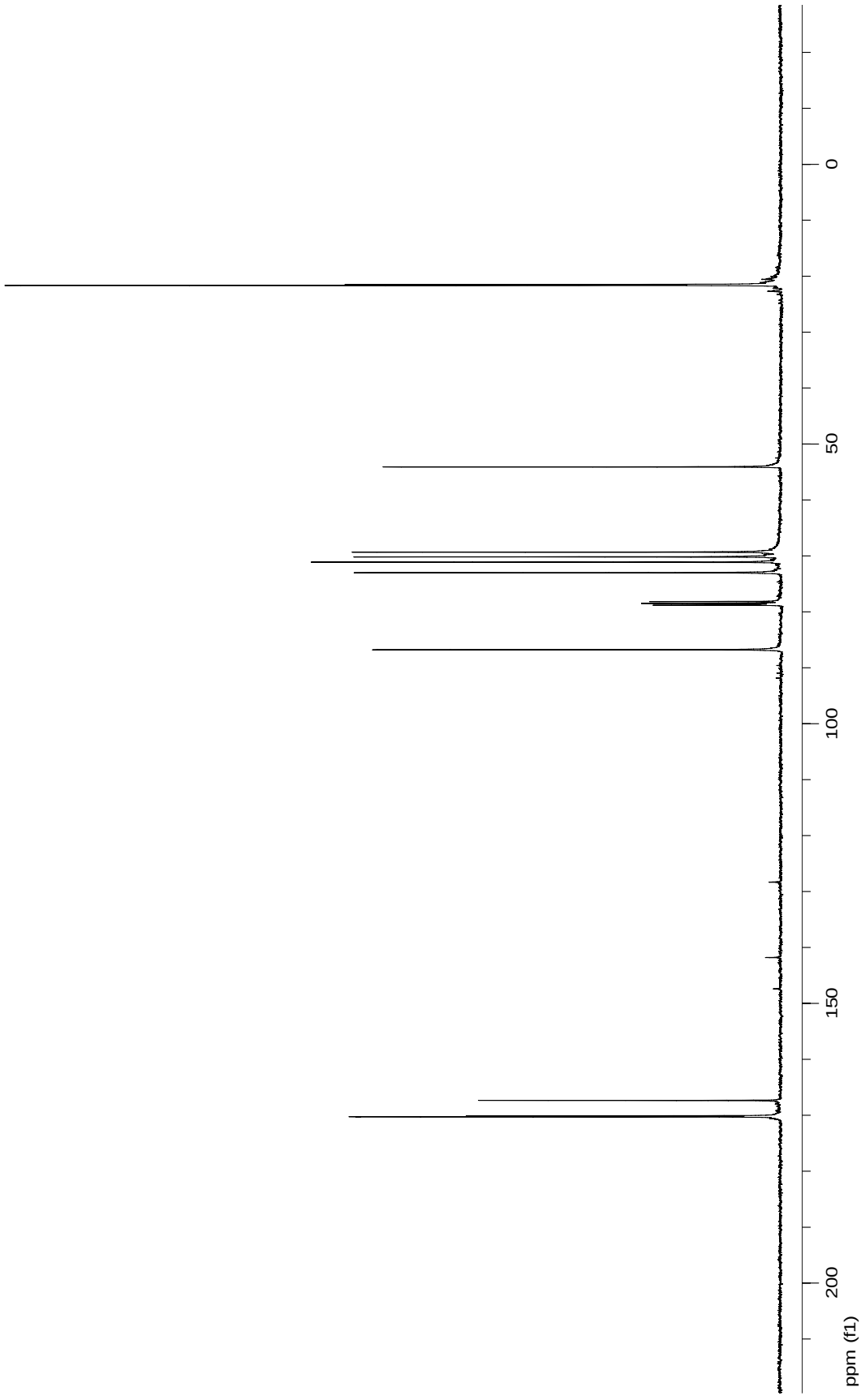

Figure 30: 100 MHz ^{13}C NMR spectrum of methyl 2,3,4-tri-*O*-acetyl-α-D-glucopyranosyl bromide (**3**).

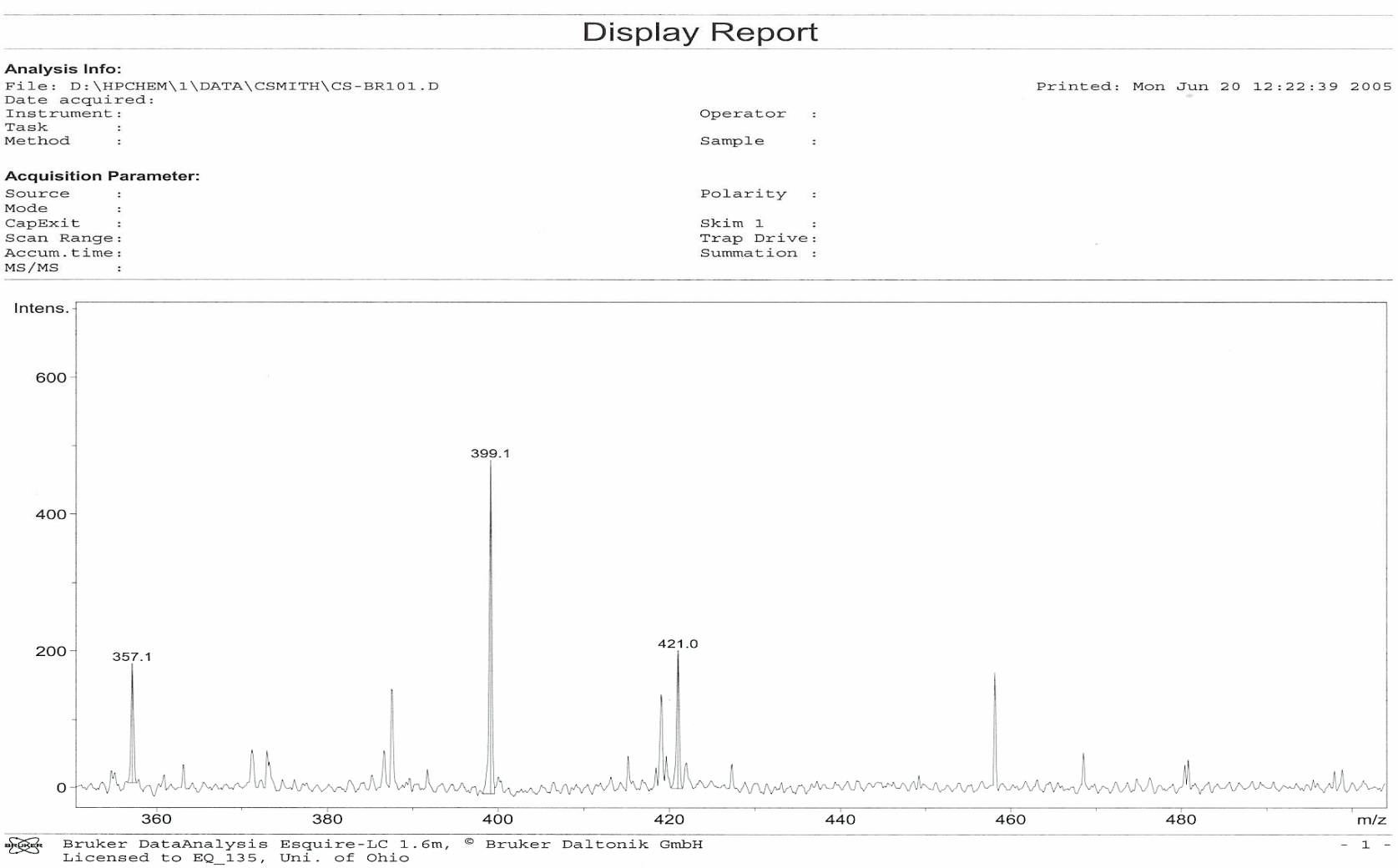

Figure 31: Mass spectrum of methyl 2,3,4-tri-*O*-acetyl-α-D-glucopyranosyl bromide (**3**).

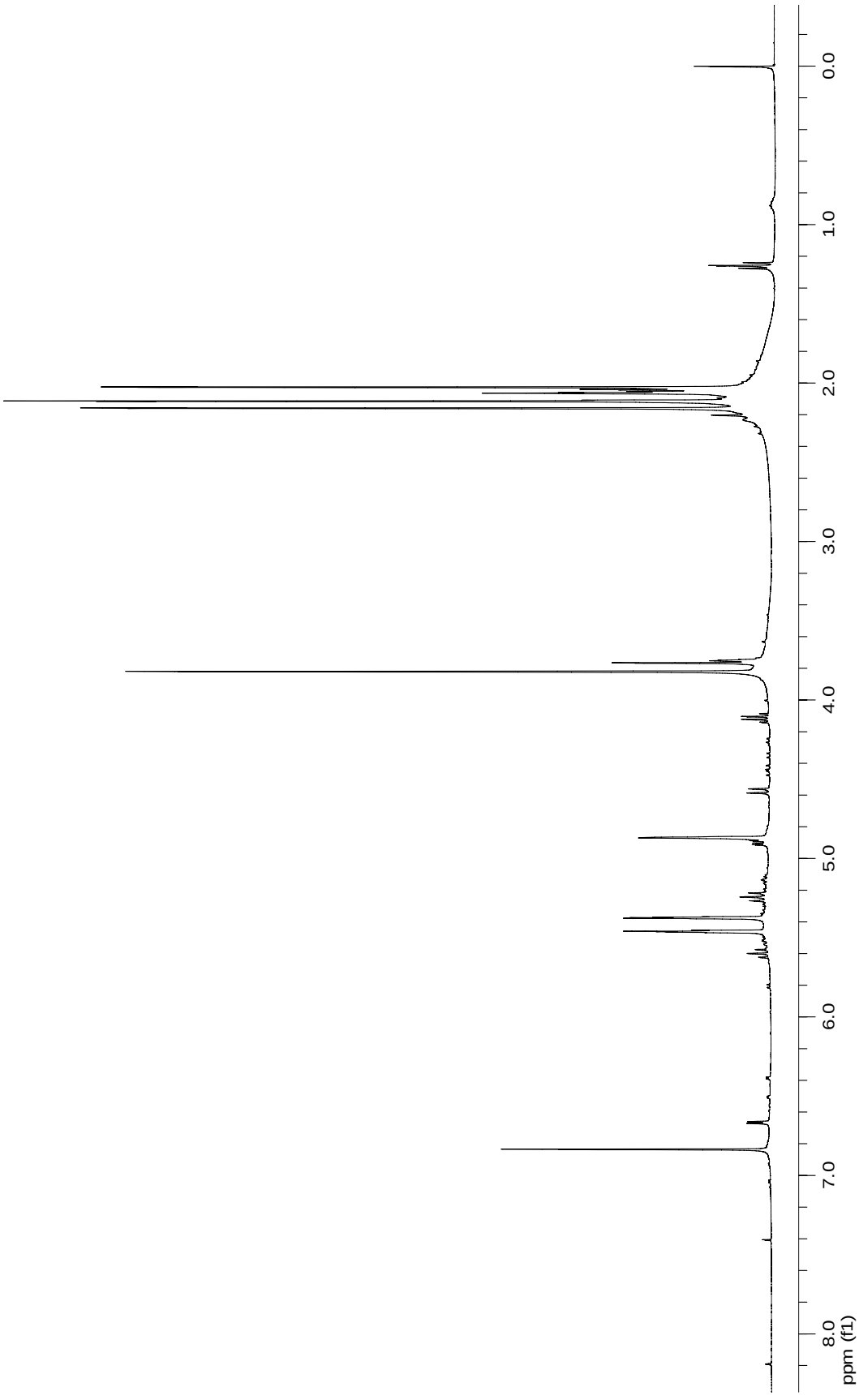

Figure 32: 400 MHz ^{1}H NMR spectrum of methyl 2,3,4-tri-*O*-acetyl-2,6-anhydro-D-*lyxo*-hex-5-enoate (**5**).

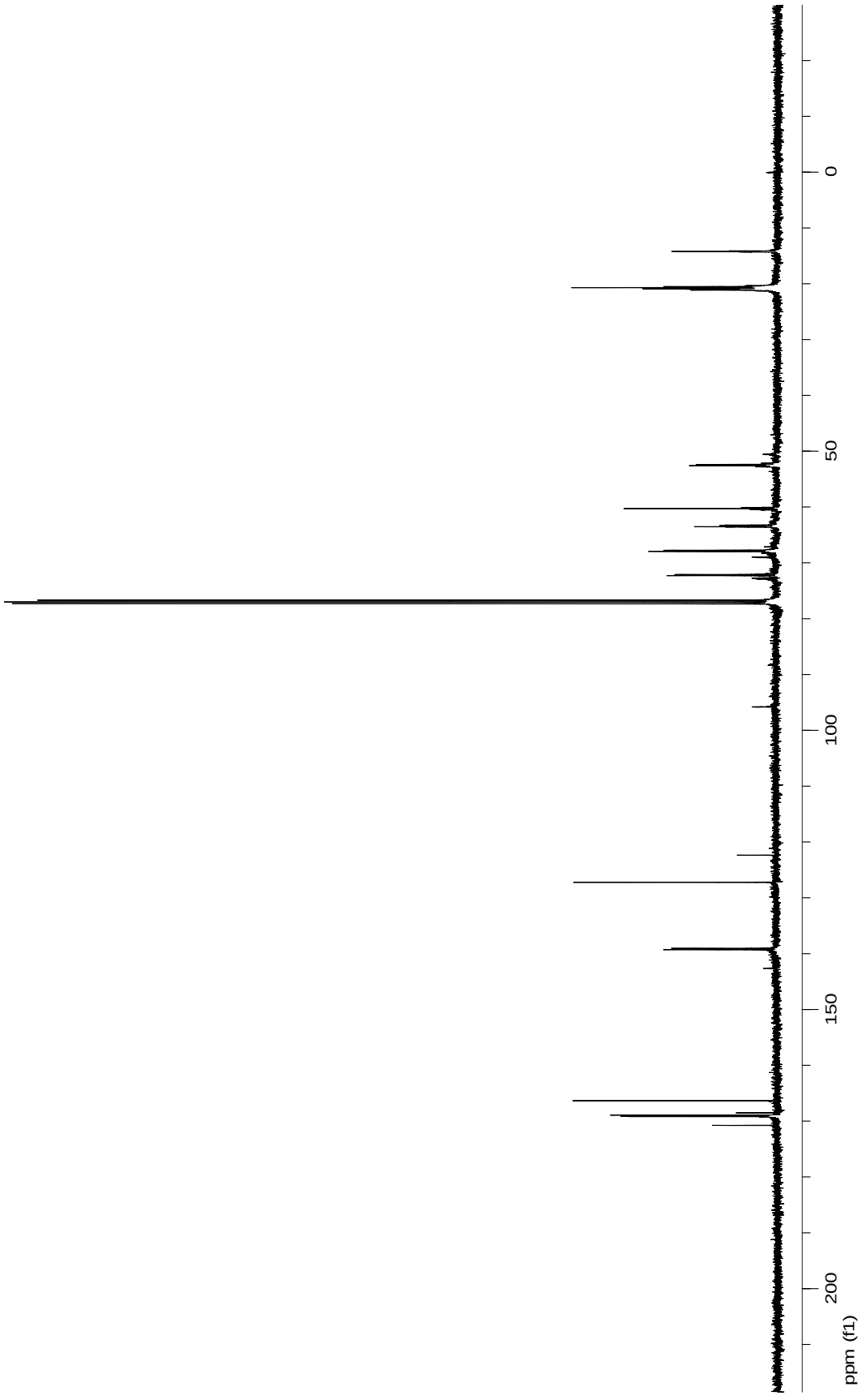

Figure 33: 100 MHz ^{13}C NMR spectrum of methyl 2,3,4-tri-*O*-acetyl-2,6-anhydro-D-*lyxo*-hex-5-enoate (**5**).

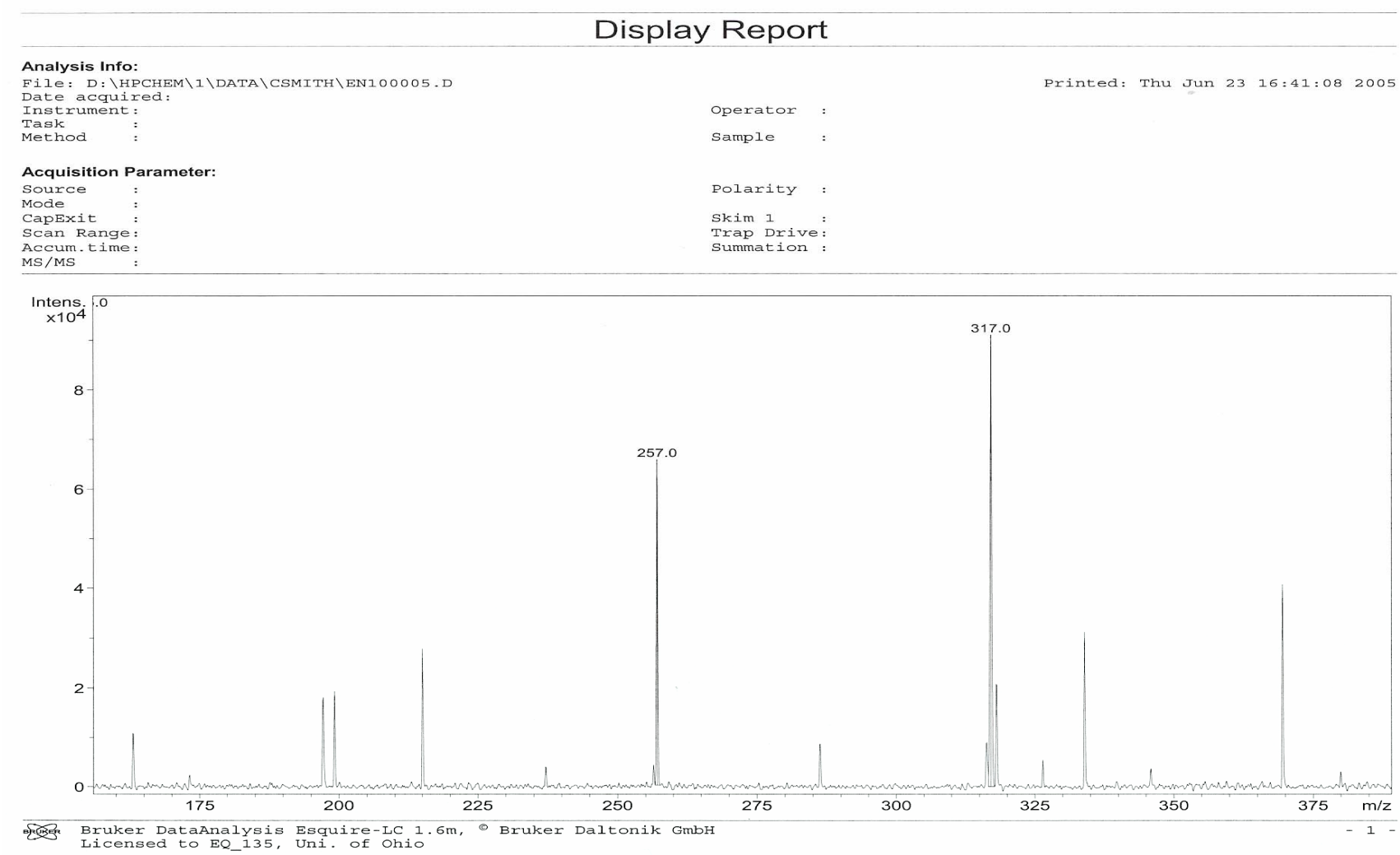

Figure 34: Mass spectrum of methyl 2,3,4-tri-*O*-acetyl-2,6-anhydro-D-*lyxo*-hex-5-enoate (**5**).

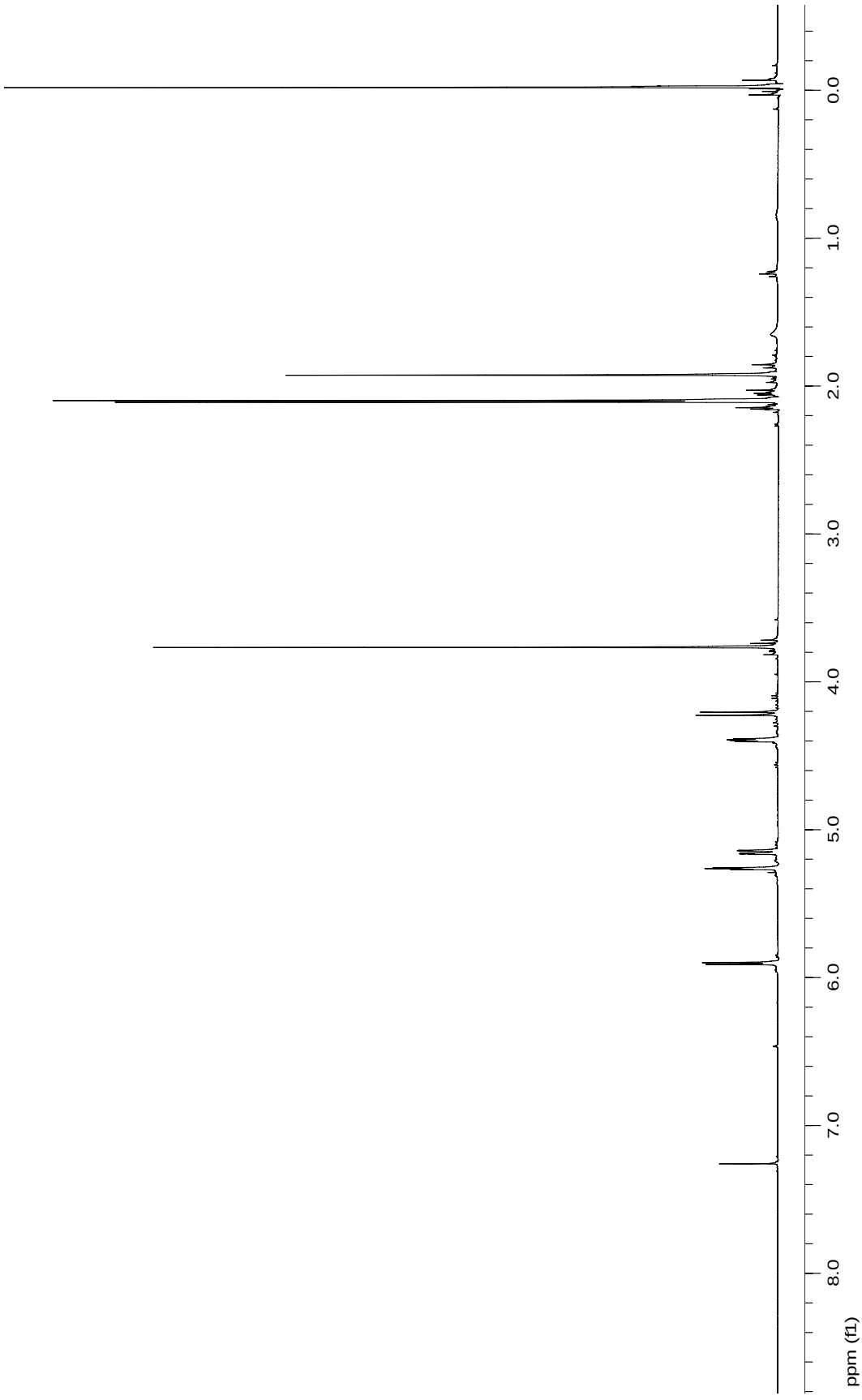

Figure 35: 400 MHz ^{1}H NMR of methyl 2,3,4-tri-*O*-acetyl-α-D-glucopyranosyl nitrile (**25**).

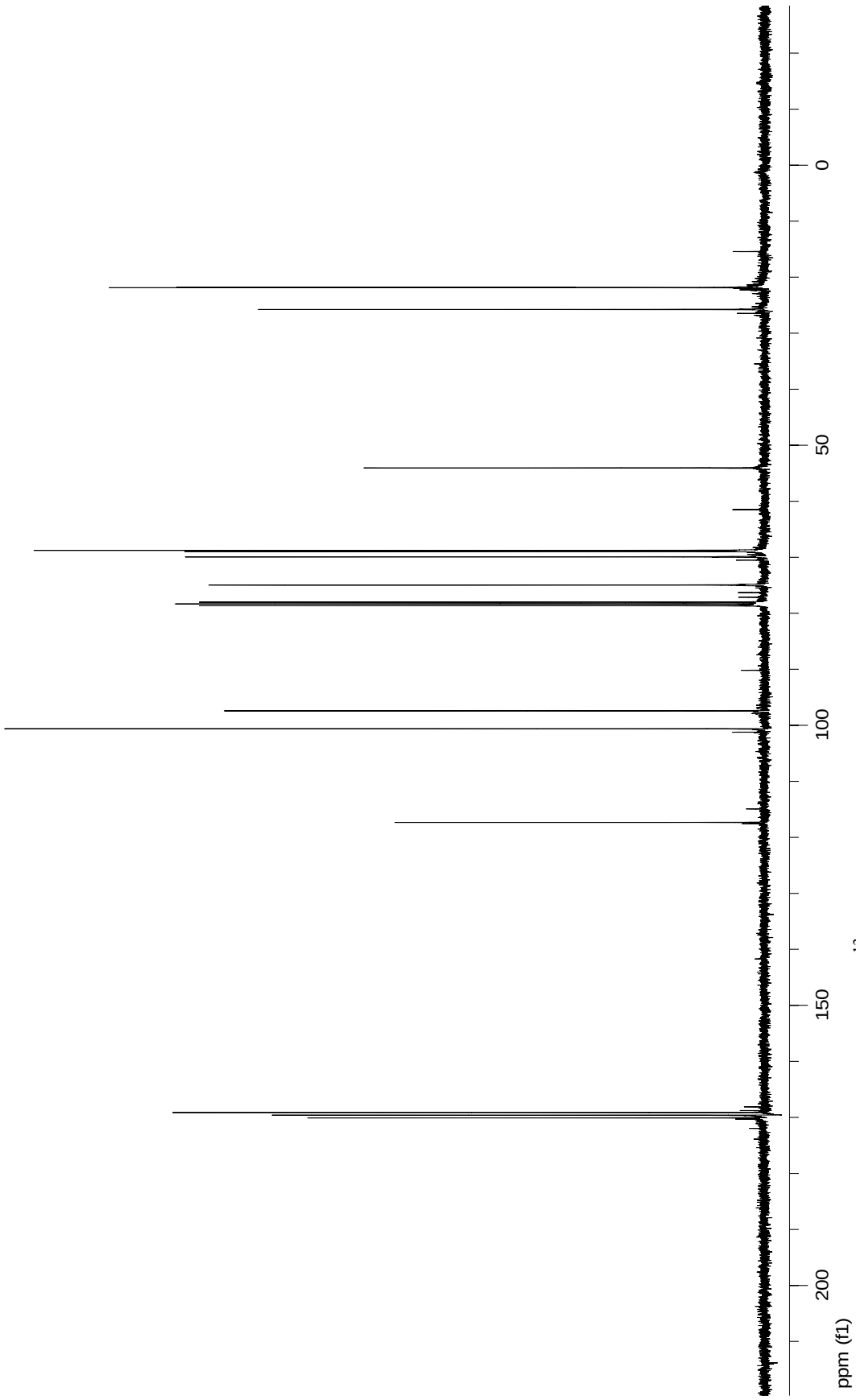

Figure 36: 100 MHz ^{13}C NMR of methyl 2,3,4-tri-*O*-acetyl-α-D-glucopyranosyl nitrile (**25**).

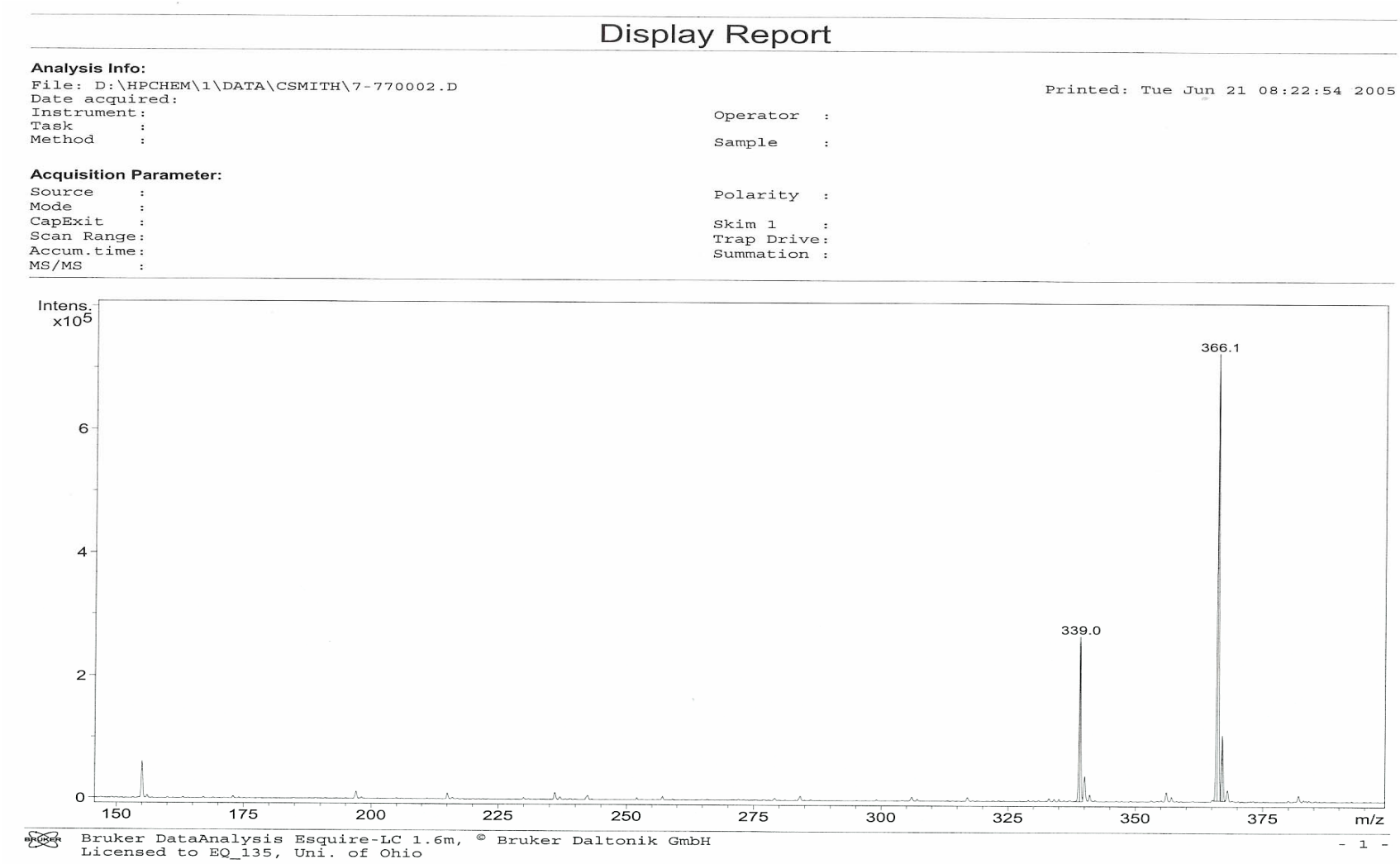

Figure 37: Mass spectrum of methyl 2,3,4-tri-*O*-acetyl-α-D-glucopyranosyl nitrile (**25**).

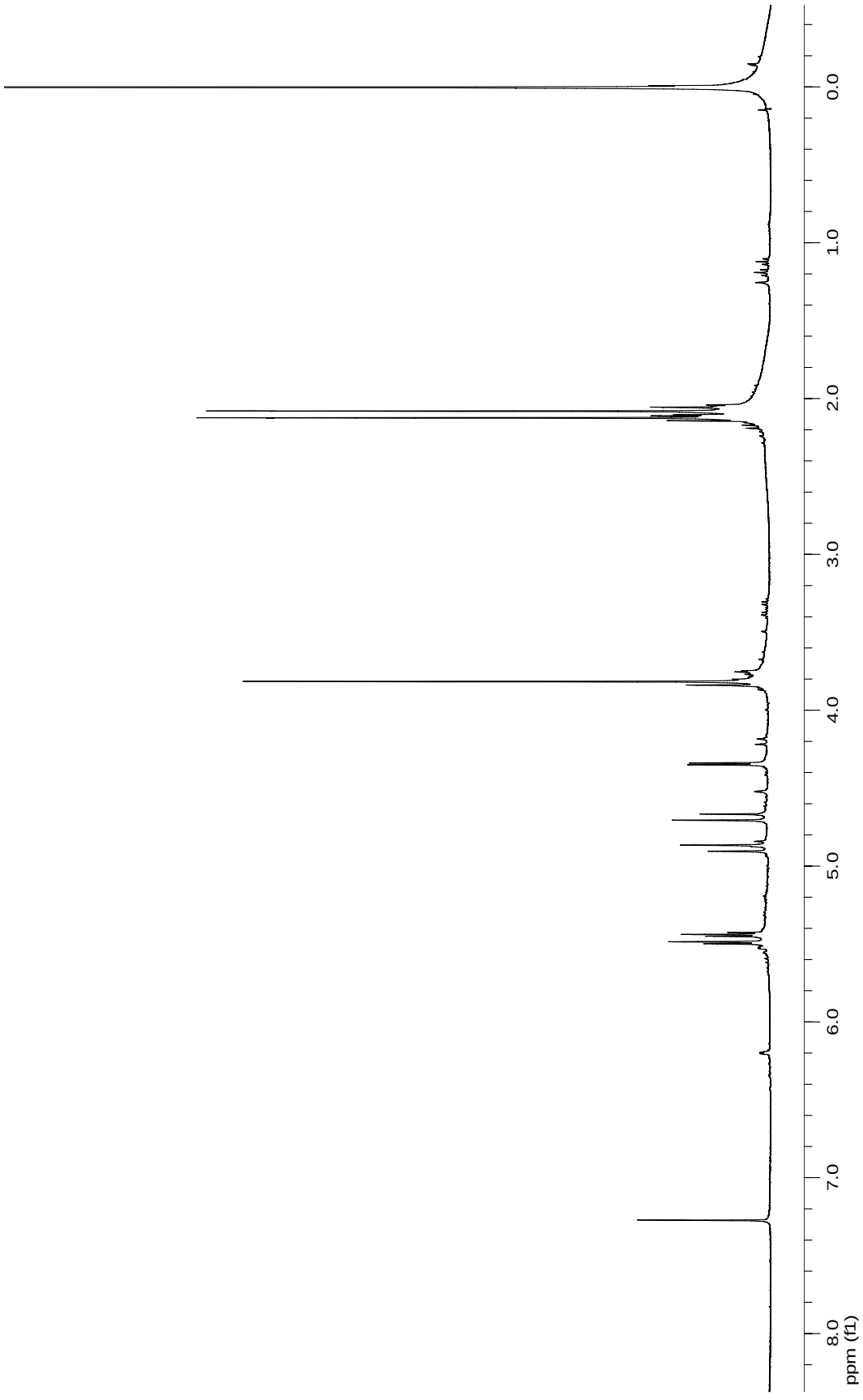

Figure 38: 400 MHz ^{1}H NMR spectrum of the oxime of methyl 3,4-di-*O*-acetyl-1,5-anhydro-D-fructuronate (**28**).

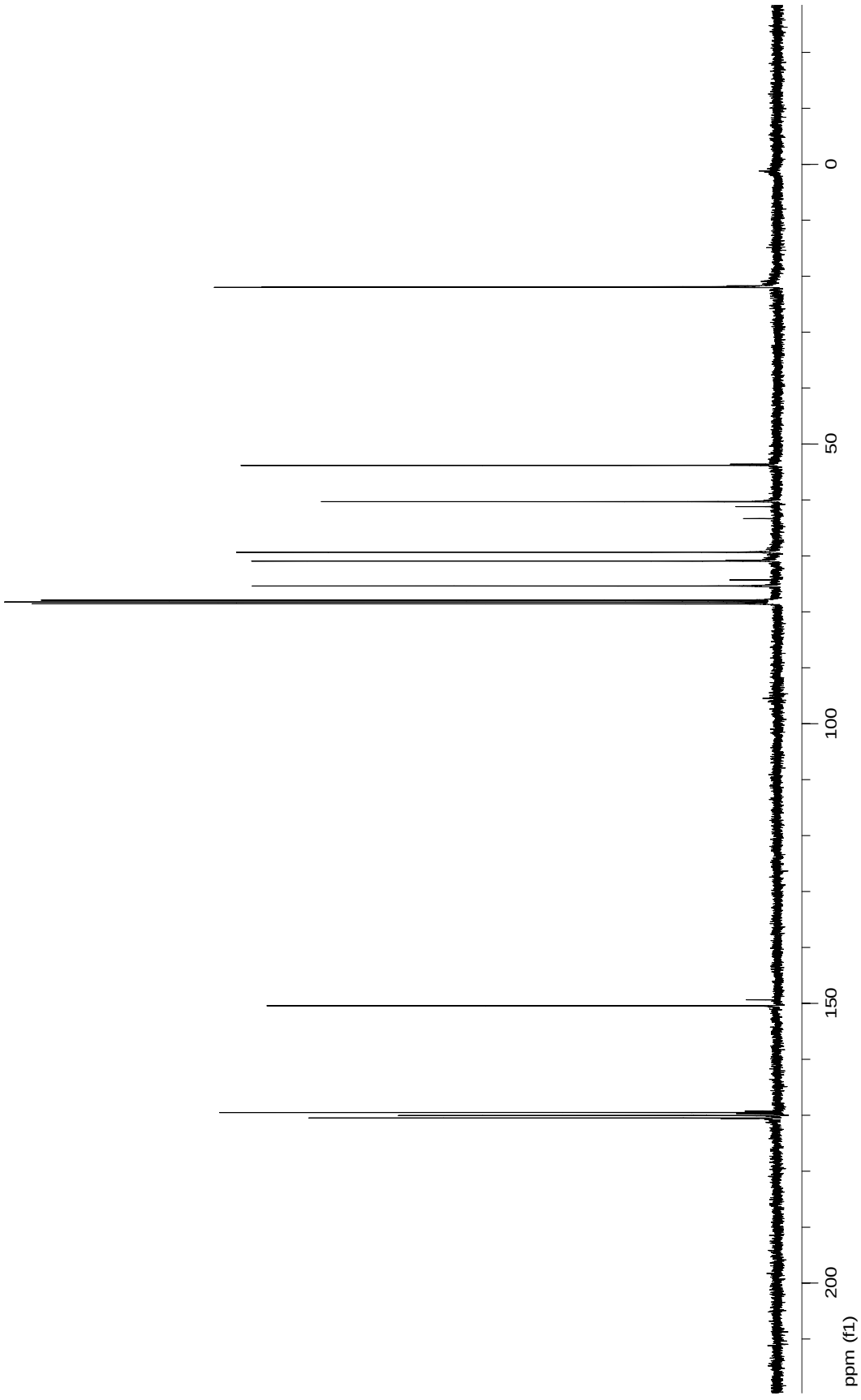

Figure 39: 100 MHz ^{13}C NMR spectrum of the oxime of methyl 3,4-di-*O*-acetyl-1,5-anhydro-D-fructuronate (**28**).

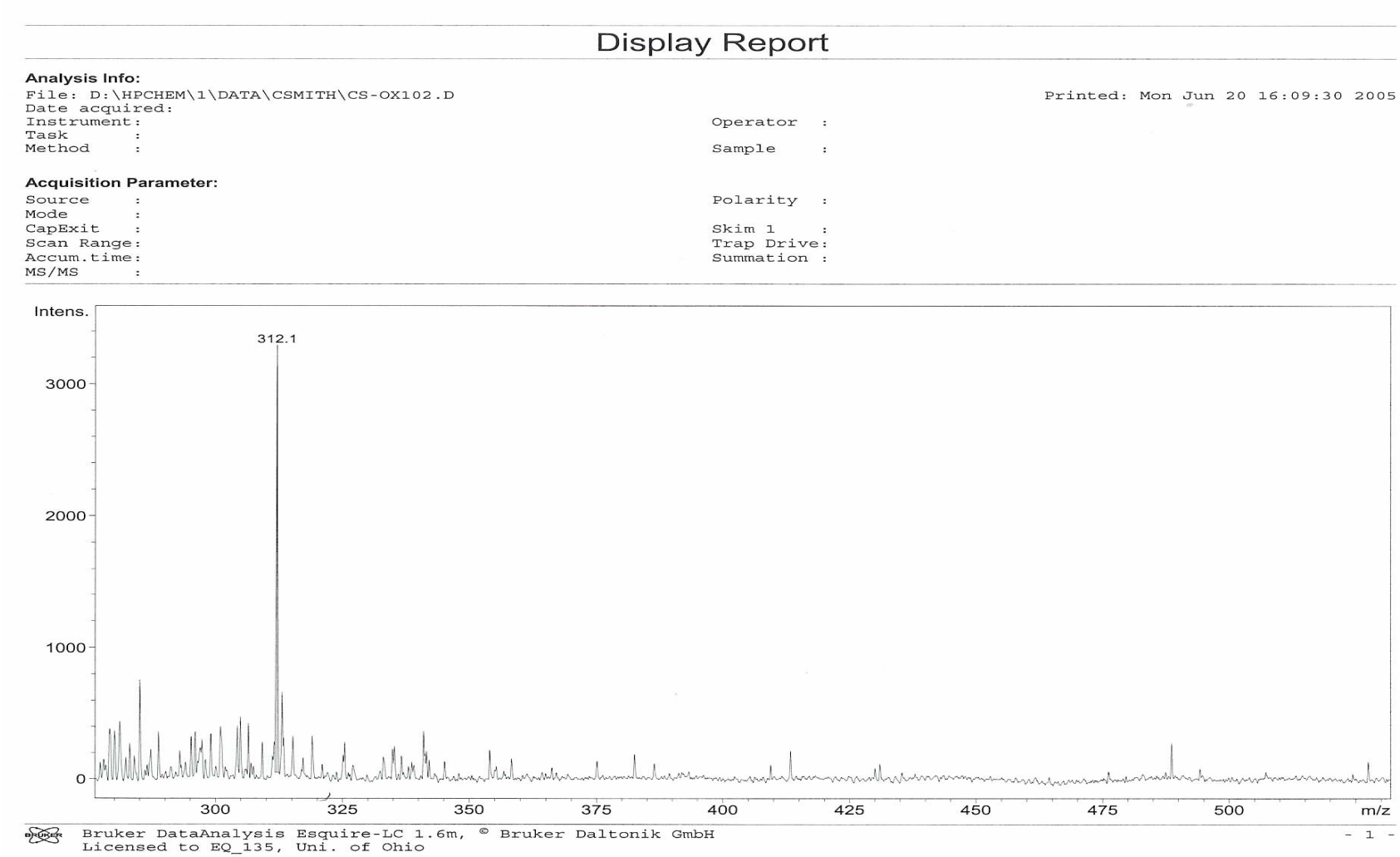

Figure 40: Mass spectrum of the oxime of methyl 3,4-di-*O*-acetyl-1,5-anhydro-D-fructuronate (**28**).

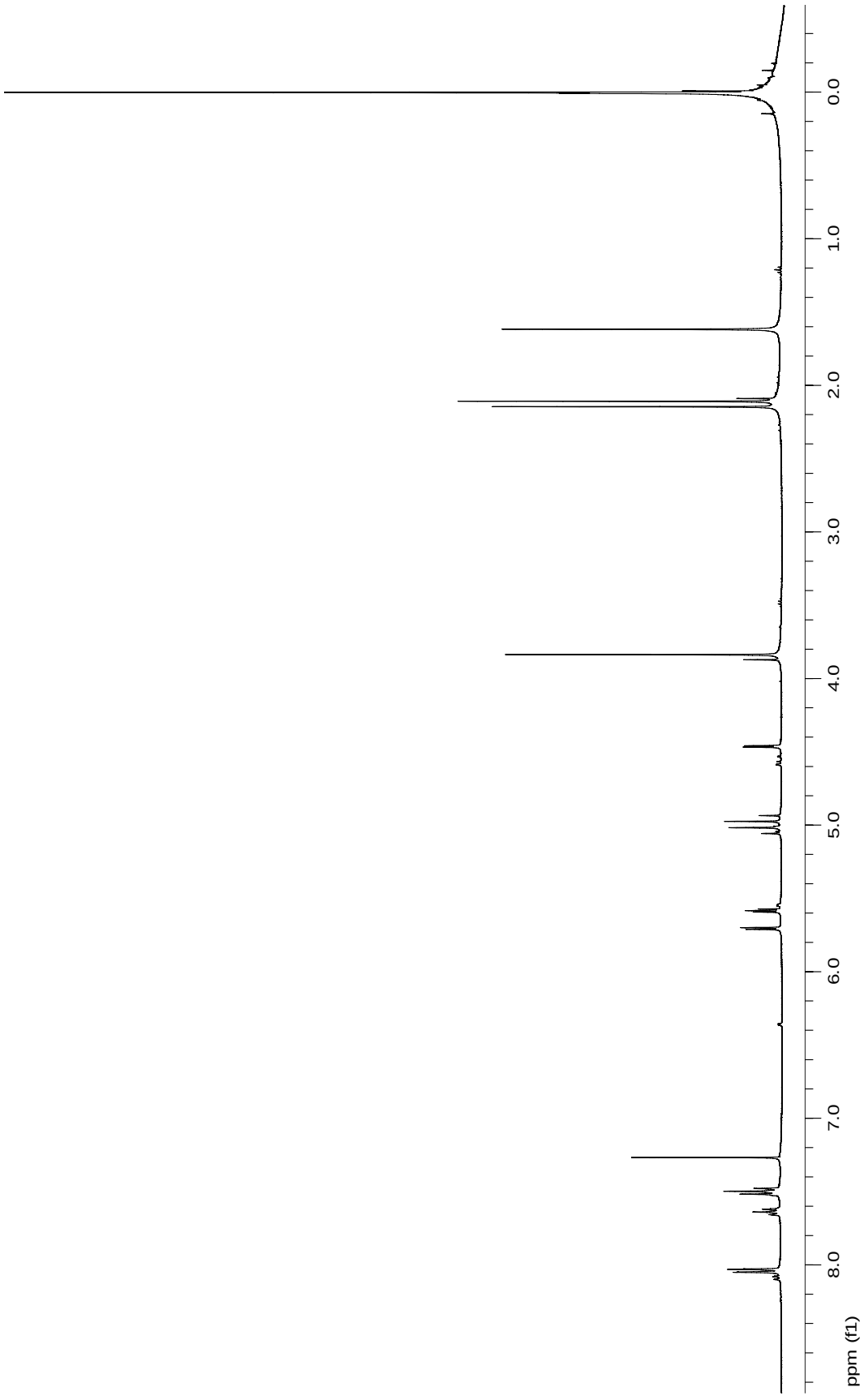

Figure 41: 400 MHz ^{1}H NMR spectrum of *O*-benzoyloxime of methyl 3,4-di-*O*-acetyl-1,5-anhydro-D-fructuronate (**29**).

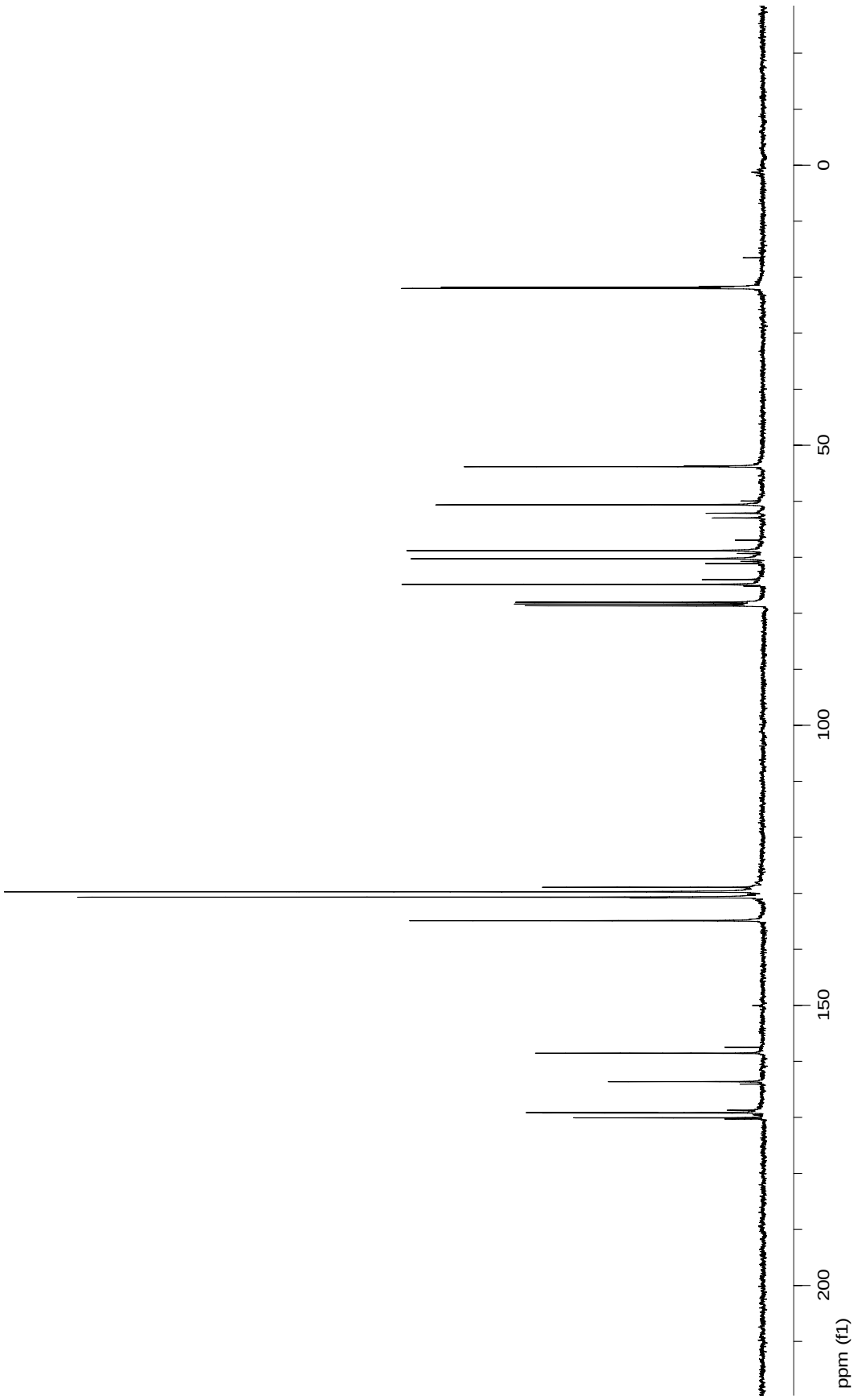

Figure 42: 100 MHz ^{13}C NMR spectrum of *O*-benzoyloxime of methyl 3,4-di-*O*-acetyl-1,5-anhydro-D-fructuronate (**29**).

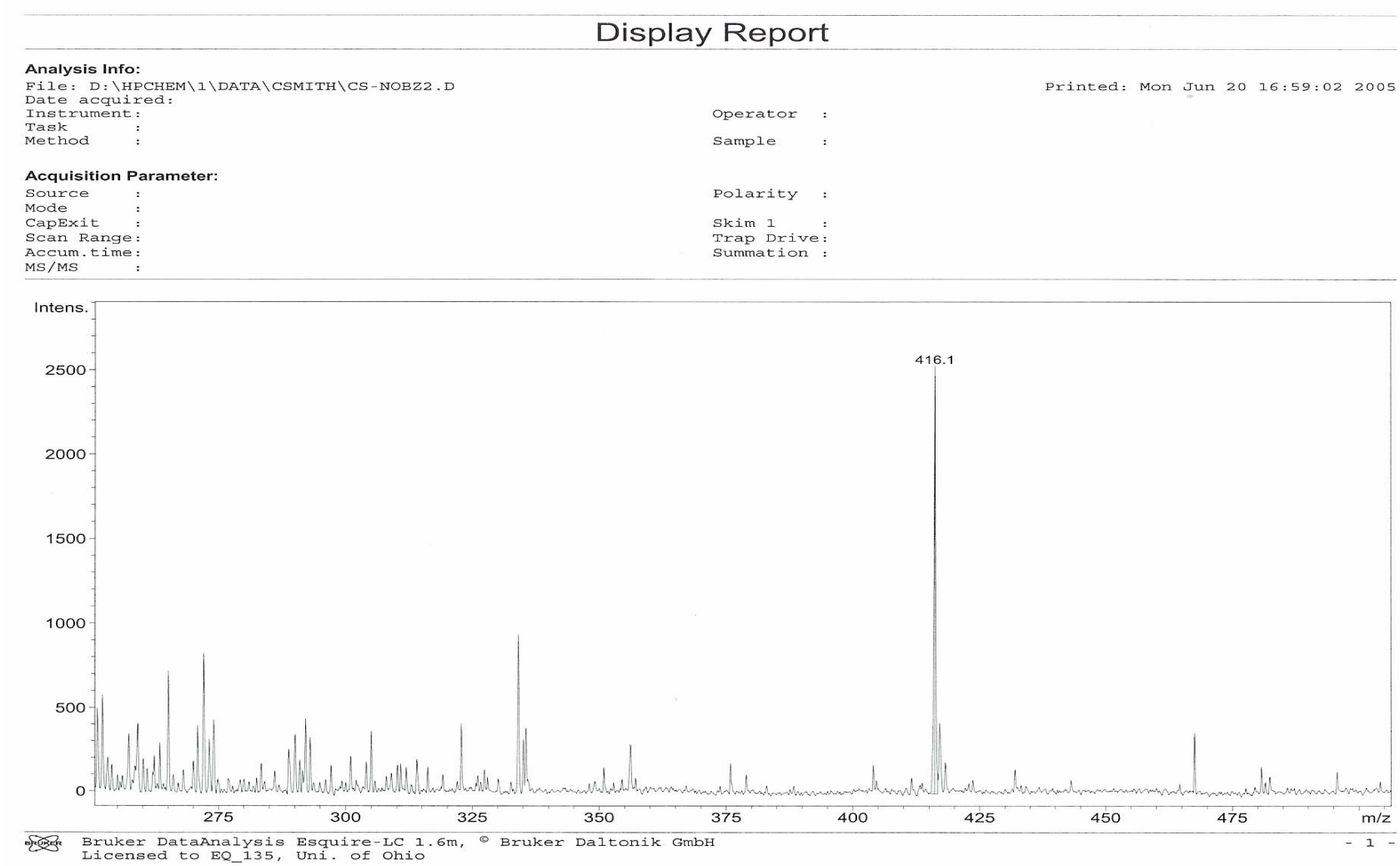

Figure 43: Mass spectrum of *O*-benzoyloxime of methyl 3,4-di-*O*-acetyl-1,5-anhydro-D-fructuronate (**29**).

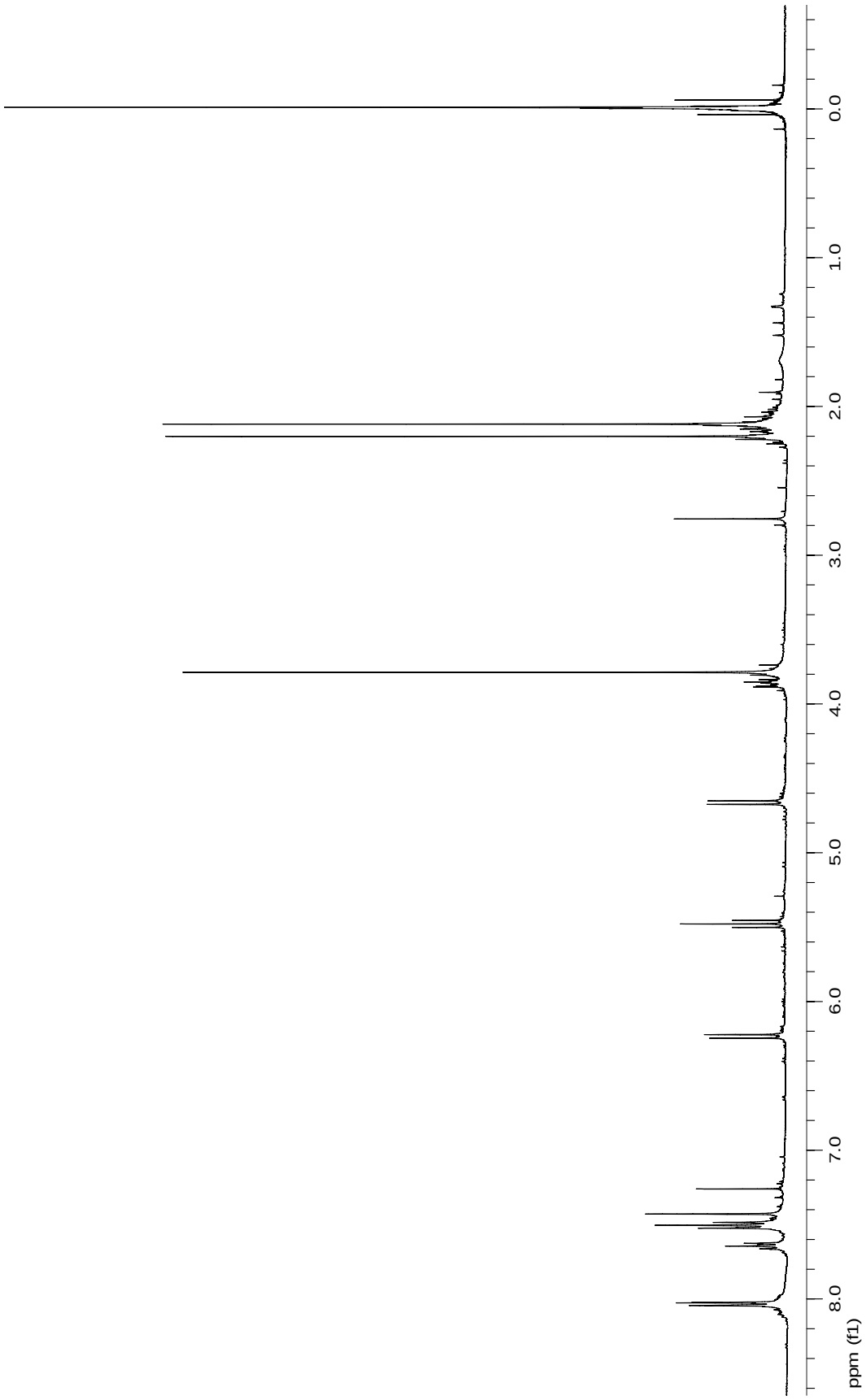

Figure 44: 400 MHz ^{1}H NMR spectrum of 1-bromo-2-*O*-benzoyloxime of methyl 3,4-*O*-acetyl-5-anhydro-D-fructuronate (**30**).

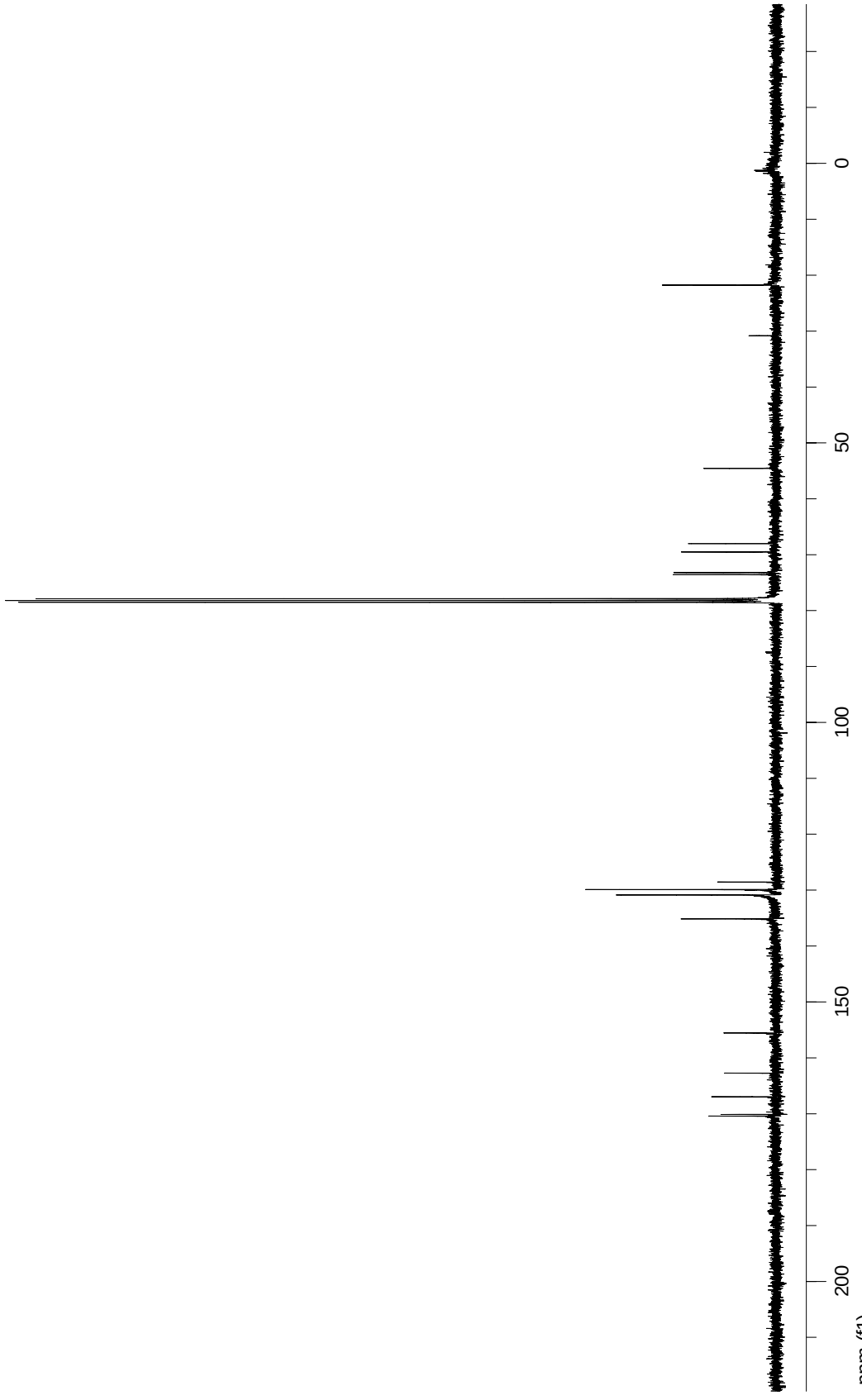

Figure 45: 100 MHz ^{13}C NMR spectrum of 1-bromo-2-*O*-benzoyloxime of methyl 3,4-*O*-acetyl-5-anhydro-D-fructuronate (**30**).

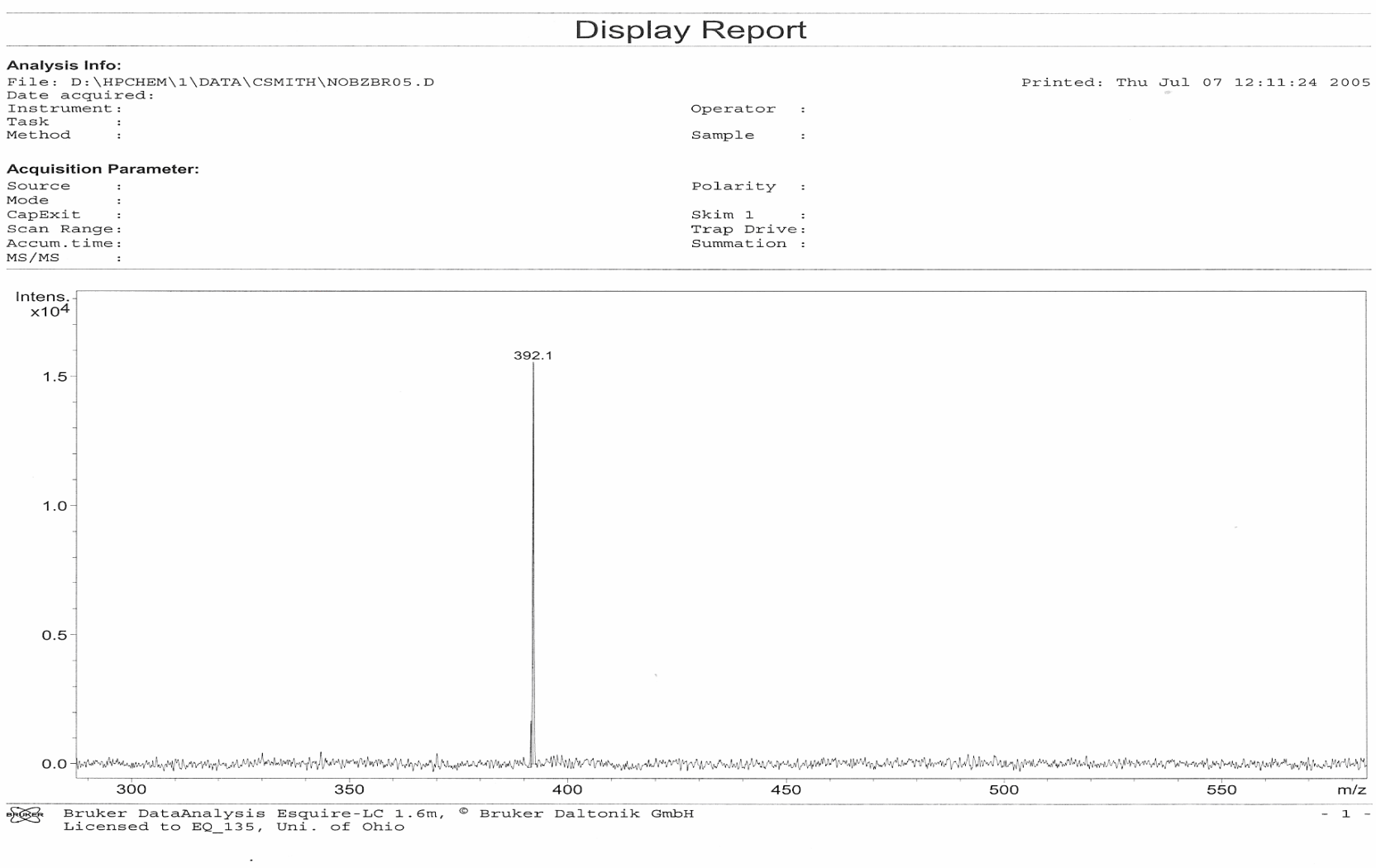

Figure 46: Mass spectrum of 1-bromo-2-*O*-benzoyloxime of methyl 3,4-*O*-acetyl-5-anhydro-D-fructuronate (**30**).

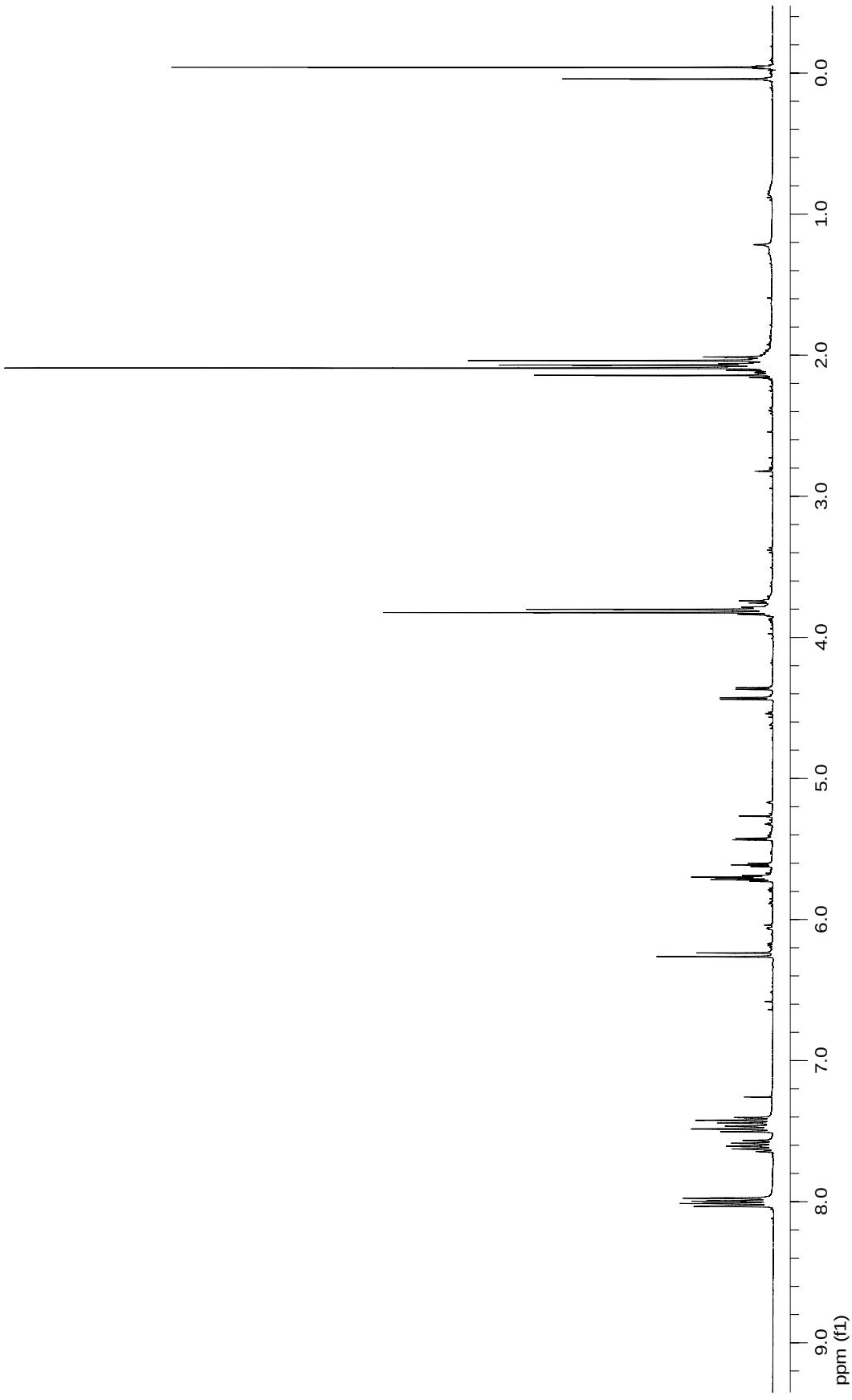

Figure 47: 400 MHz ^{1}H NMR spectrum of benzoyloxime azide **31**.

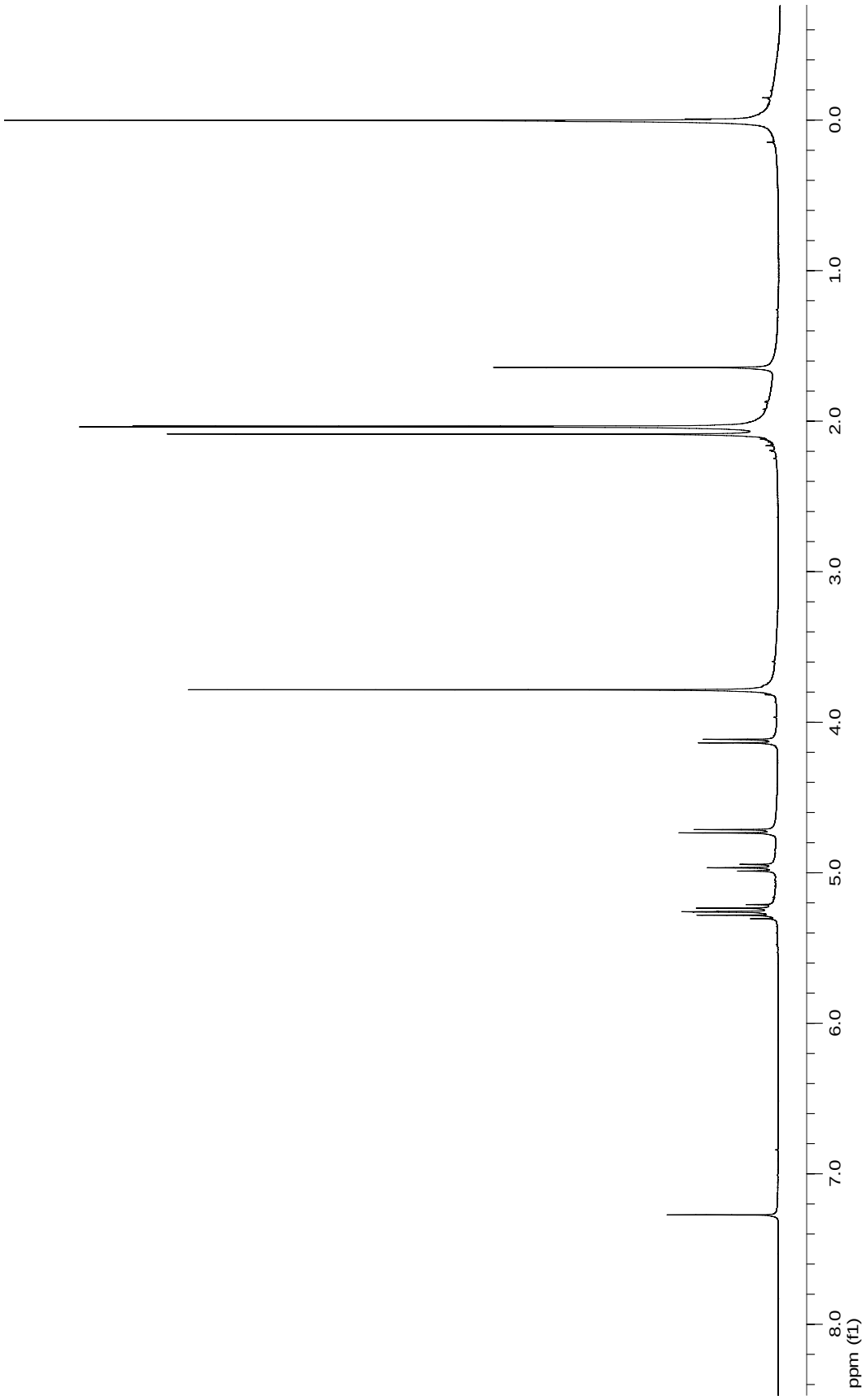

Figure 48: 400 MHz ^{1}H NMR spectrum of methyl 2,3,4-tri-*O*-acetyl-β-D-glucopyranosyl azide (**32**).

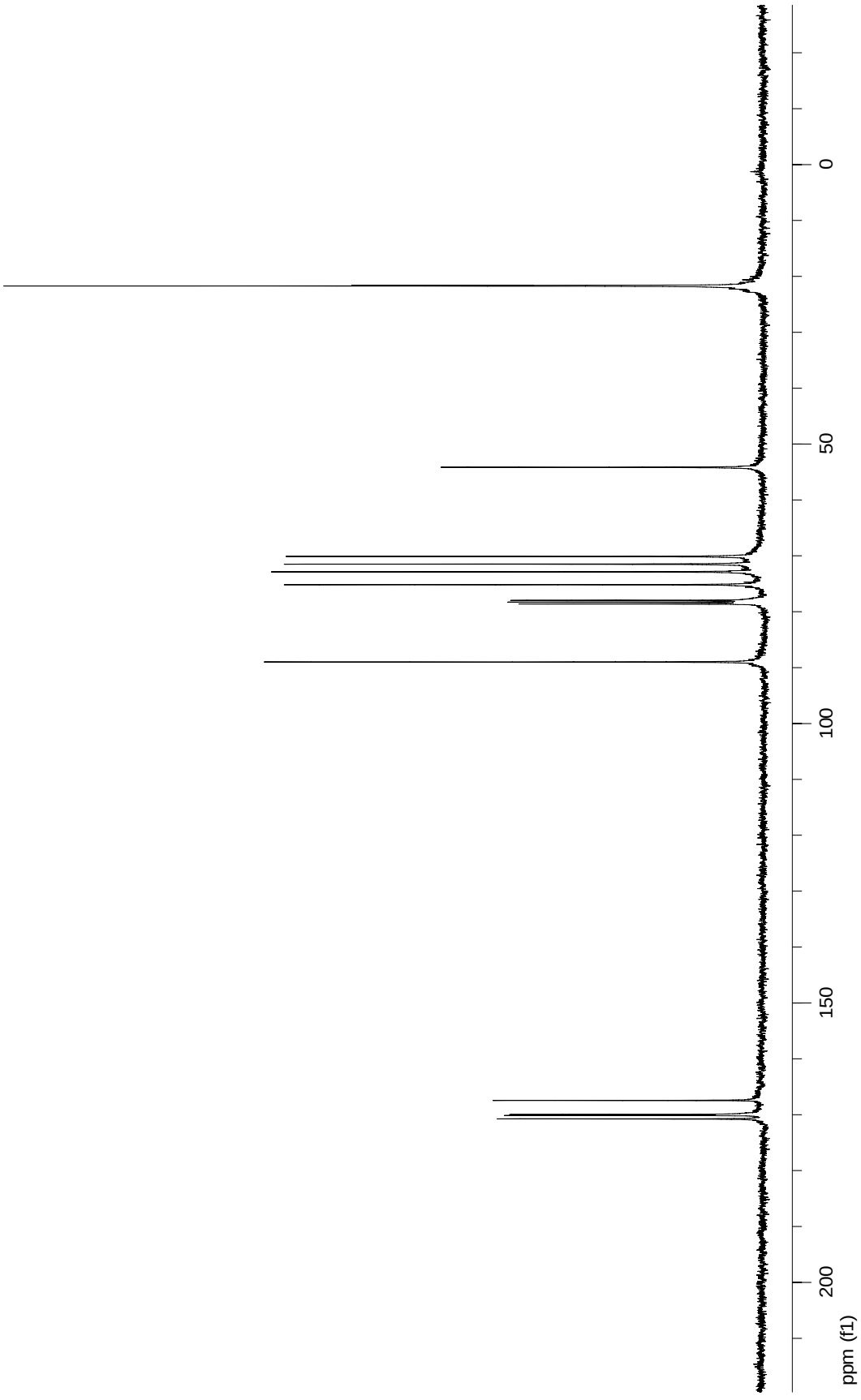

Figure 49: 100 MHz ^{13}C NMR spectrum of methyl 2,3,4-tri-*O*-acetyl-β-D-glucopyranosyl azide (**32**).

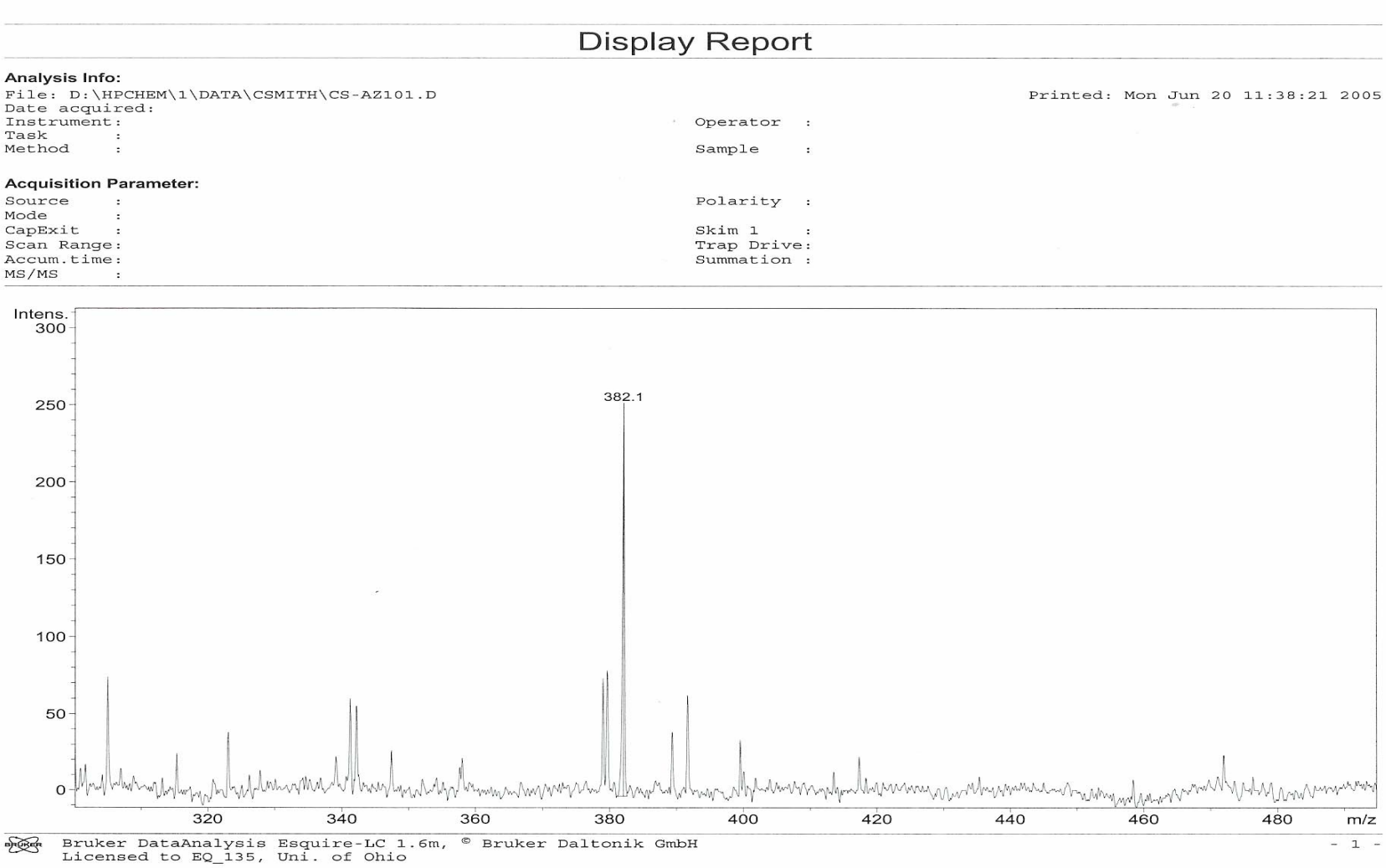

Figure 50: Mass spectrum of methyl 2,3,4-tri-*O*-acetyl-β-D-glucopyranosyl azide (**32**).

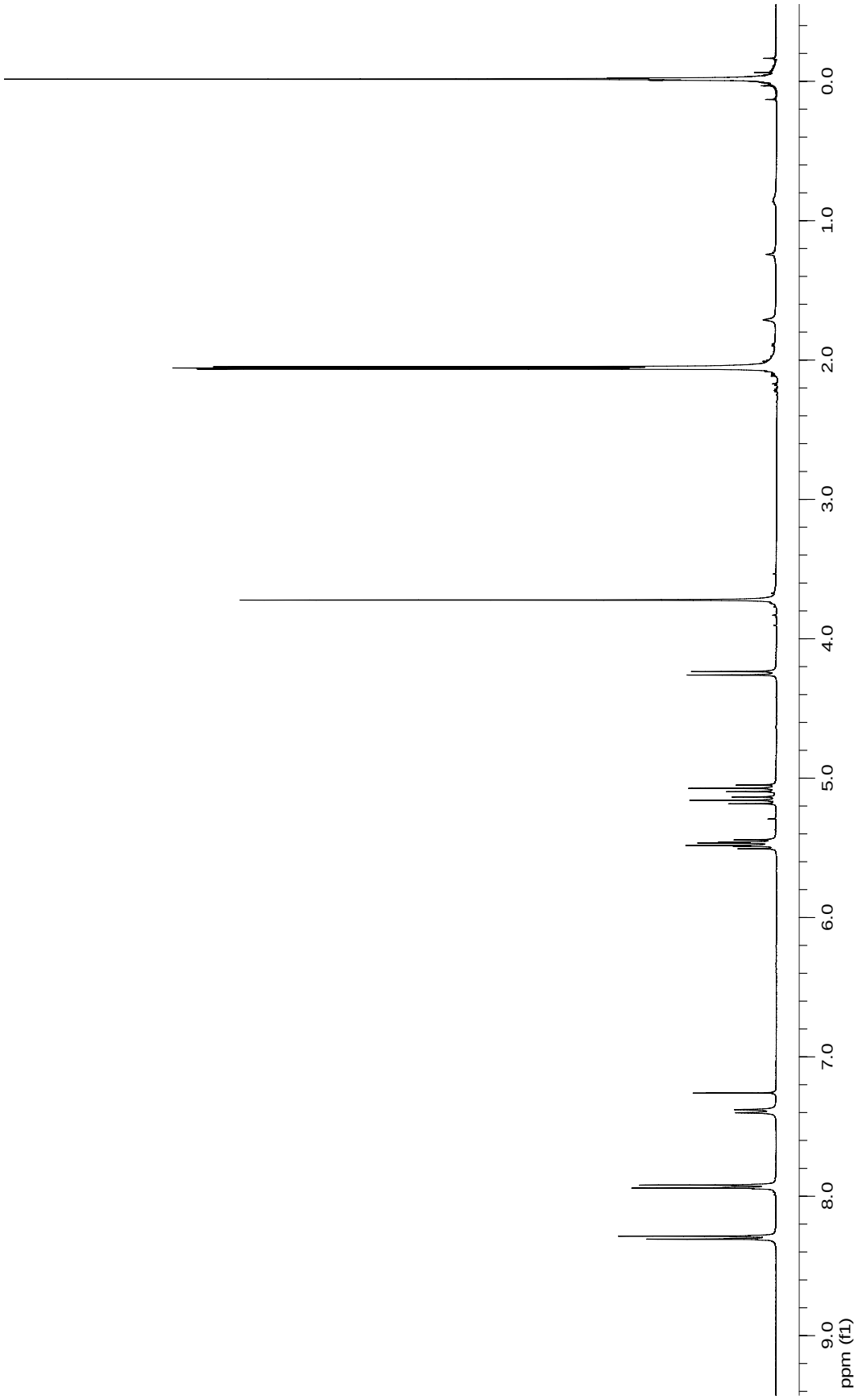

Figure 51: 400 MHz ^{1}H NMR spectrum of *p*-nitrobenzoic acid-(β-D-glucopyranuronosyl)-amide (**33**).

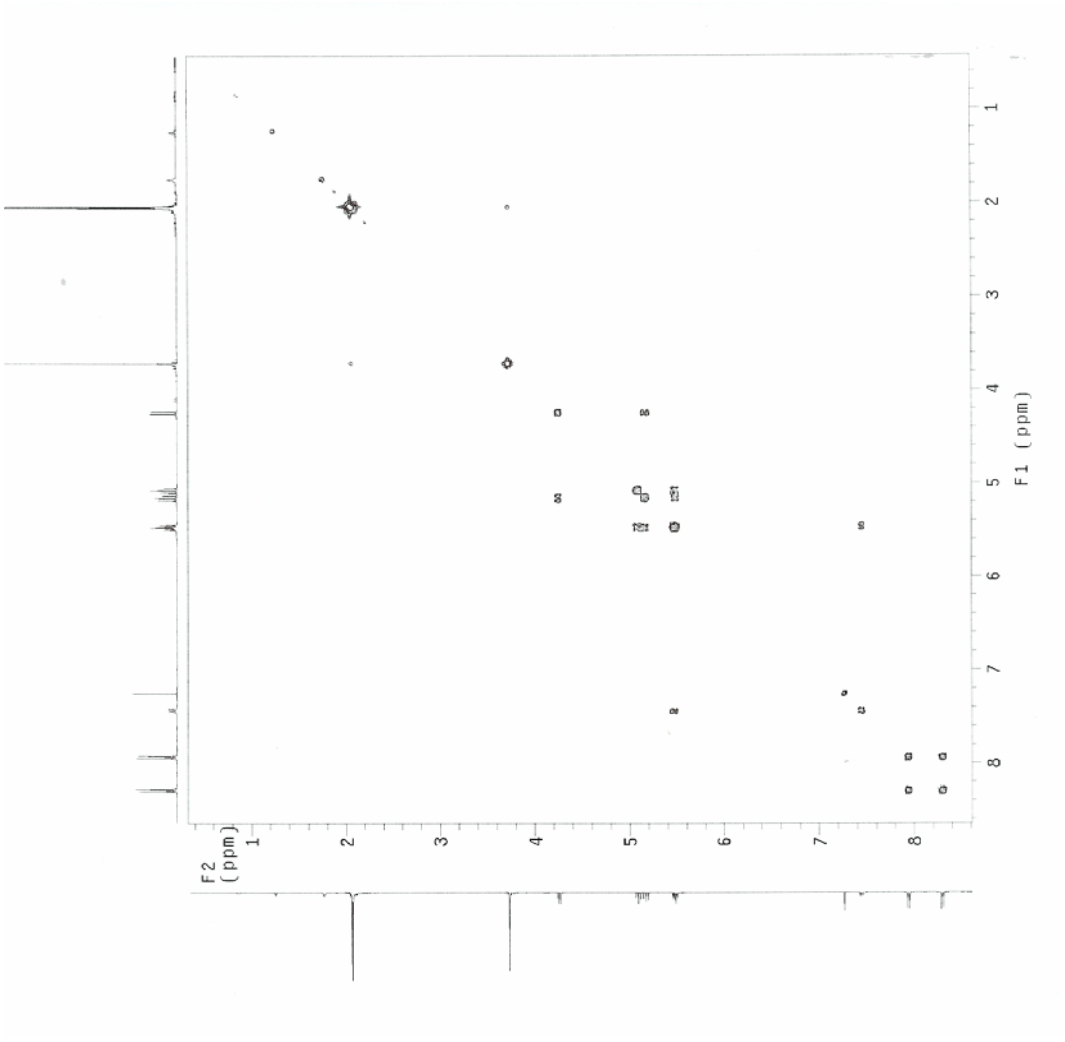

Figure 52: 400 MHz ^{1}H COSY NMR spectrum of *p*-nitrobenzoic acid-(β-D-glucopyranuronosyl)-amide (**33**).

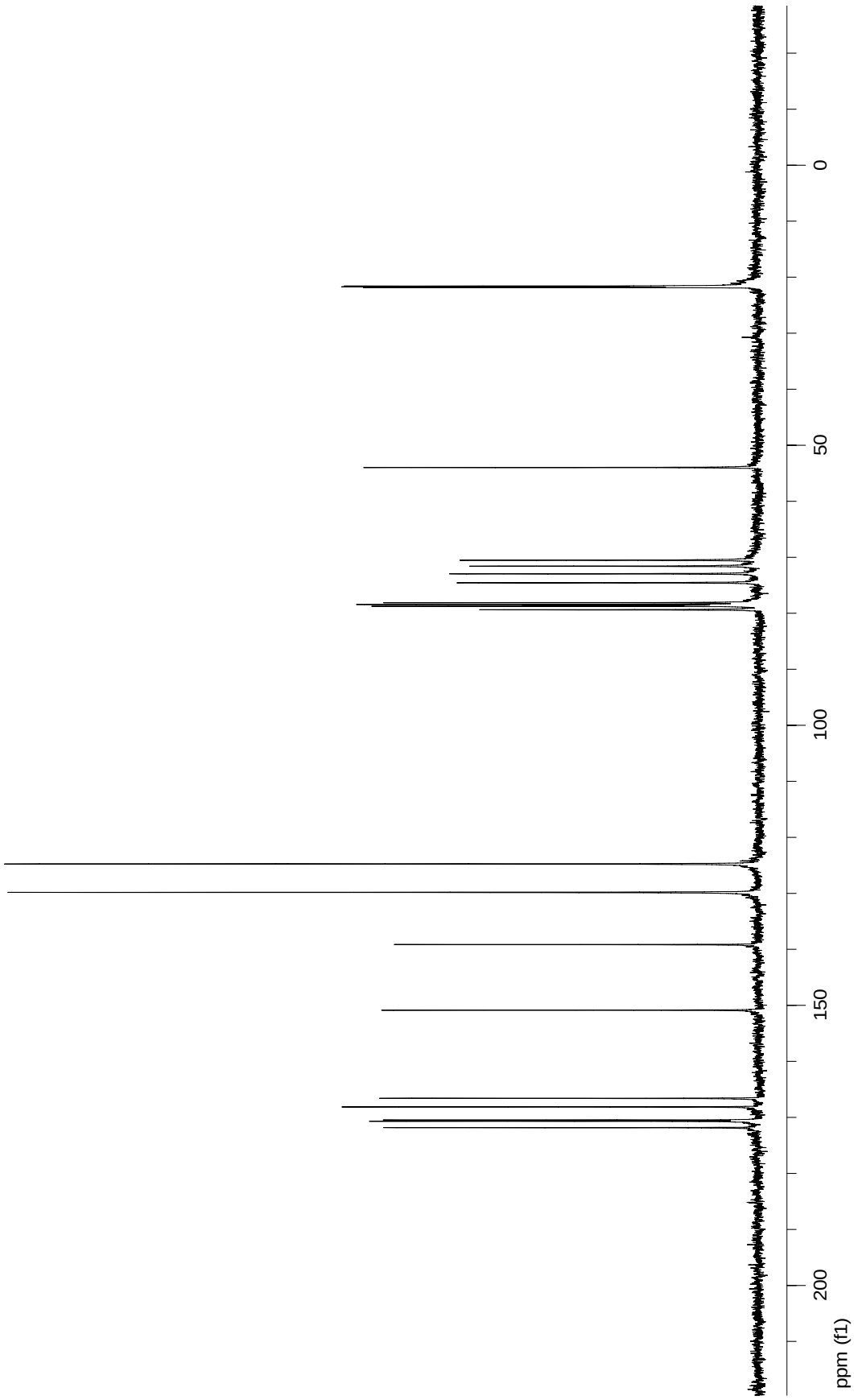

Figure 53: 100 MHz ^{13}C NMR spectrum of *p*-nitrobenzoic acid-(β-D-glucopyranuronosyl)-amide (**33**).

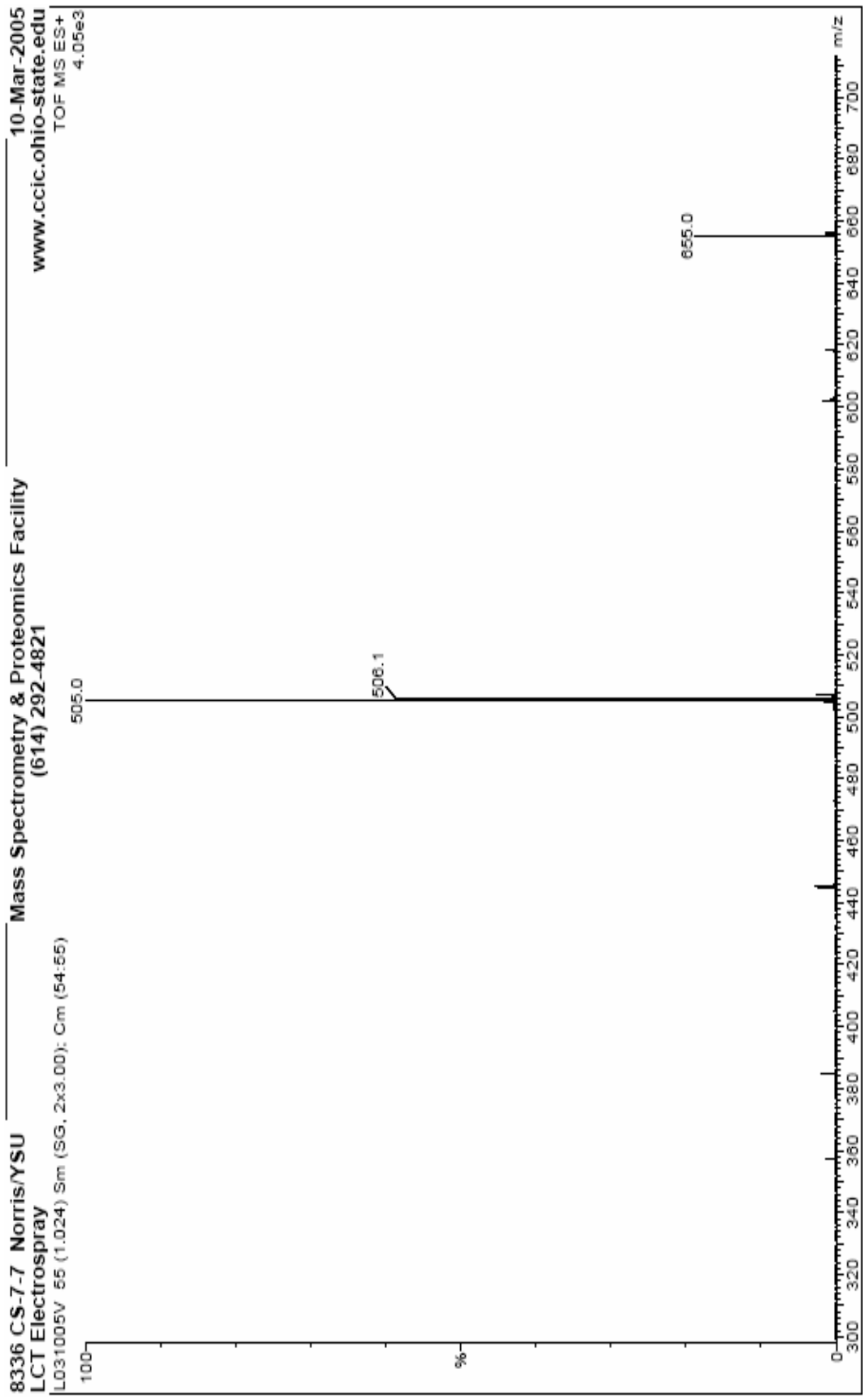

Figure 54: LC-MS spectrum of *p*-nitrobenzoic acid-(β-D-glucopyranuronosyl)-amide (**33**).

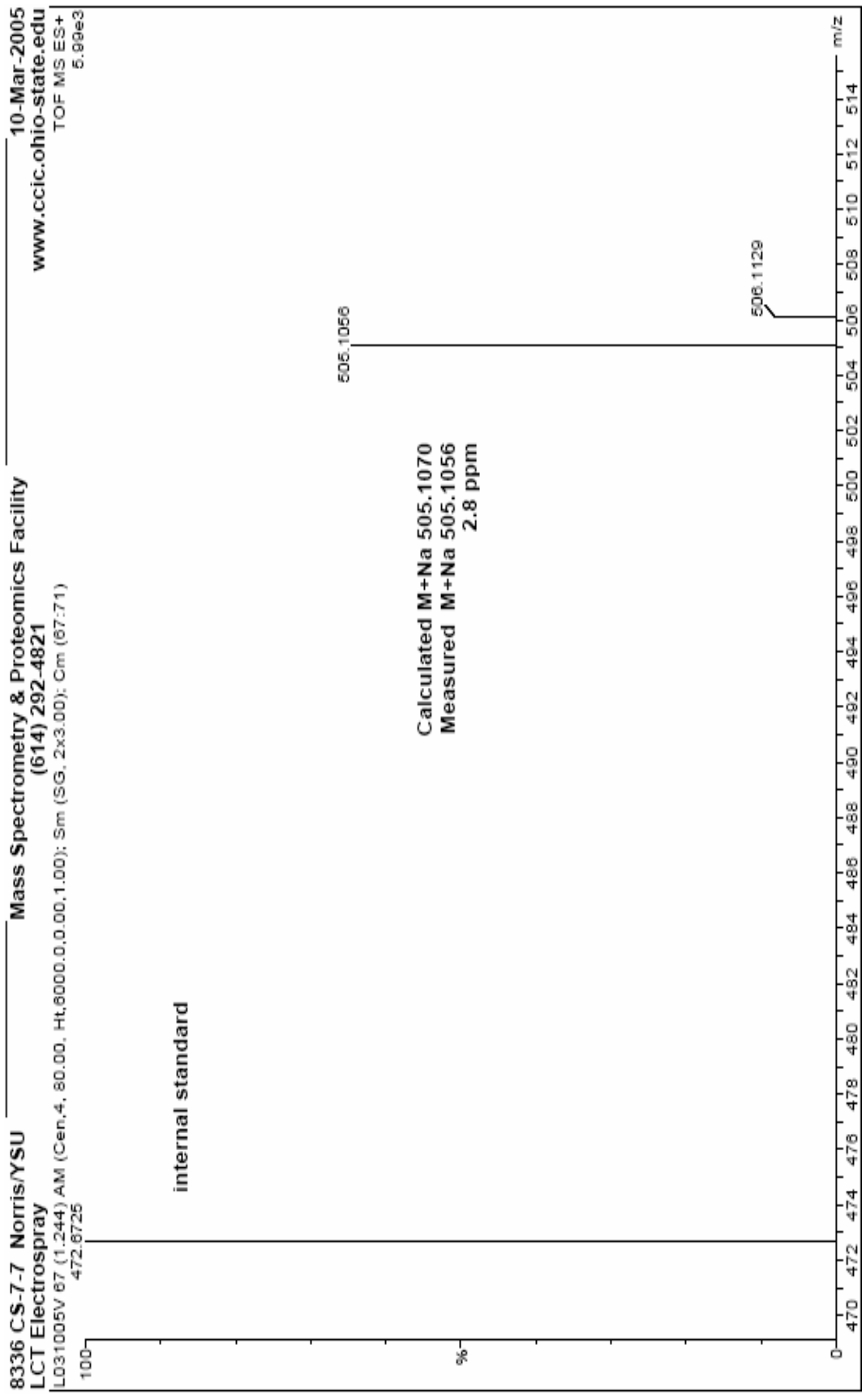

Figure 55: High Resolution TOF-MS spectrum of *p*-nitrobenzoic acid-(β-D-glucopyranuronosyl)-amide (**33**).

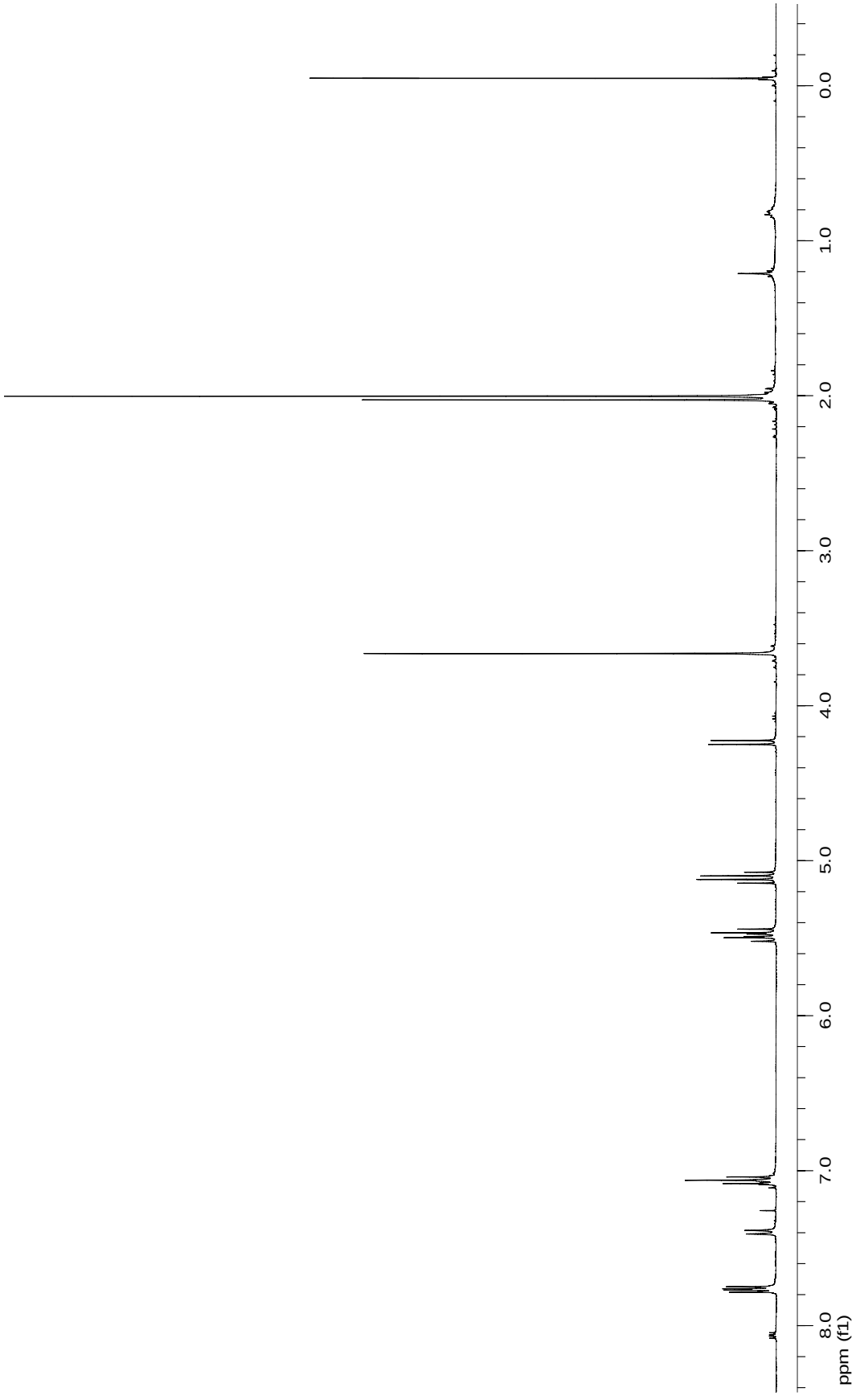

Figure 56: 400 MHz ^{1}H NMR spectrum of *p*-fluorobenzoic acid-(β-D-glucopyranuronosyl)-amide (**34**).

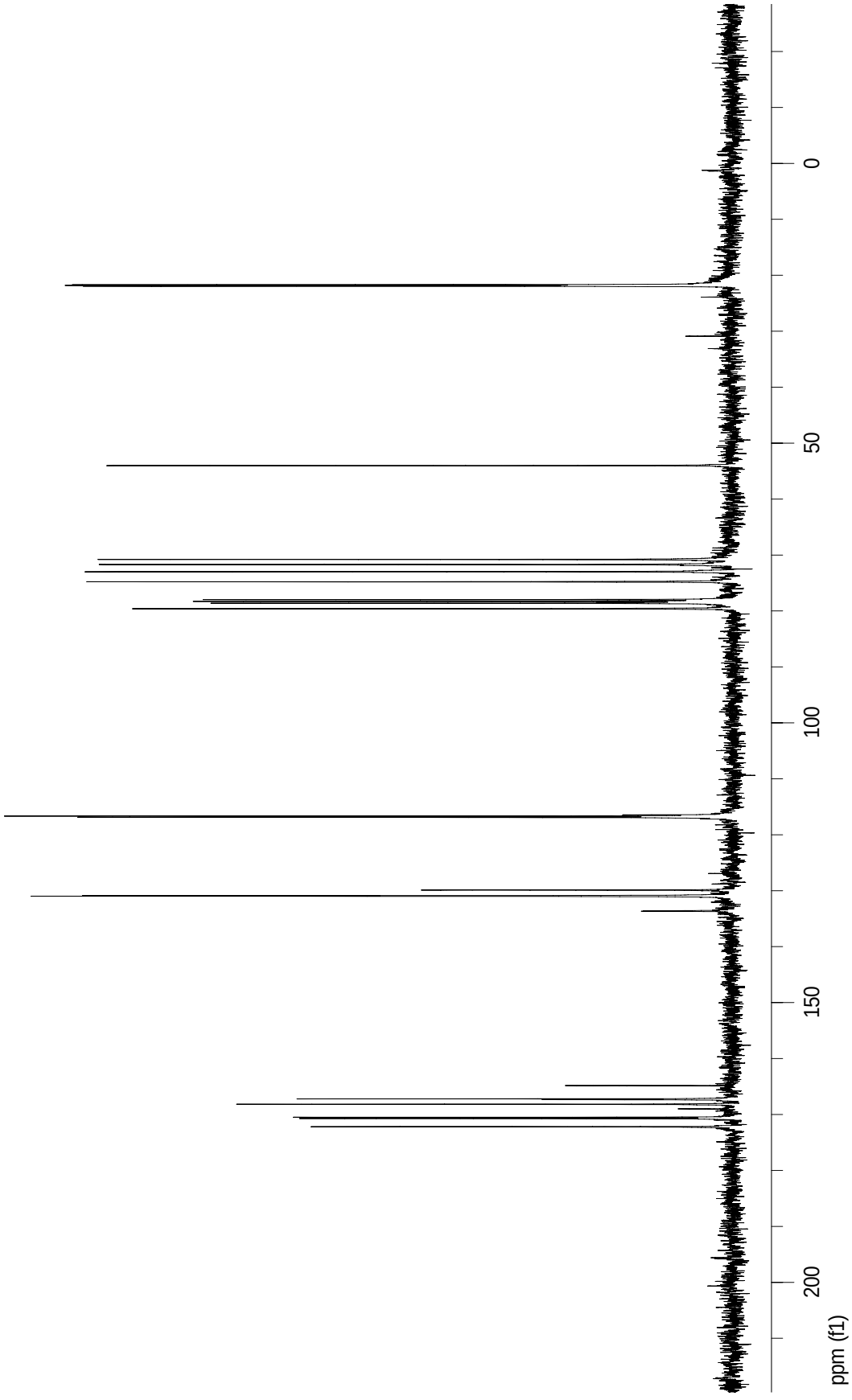

Figure 57: 100 MHz ^{13}C NMR spectrum of *p*-fluorobenzoic acid-(β-D-glucopyranuronosyl)-amide (**34**).

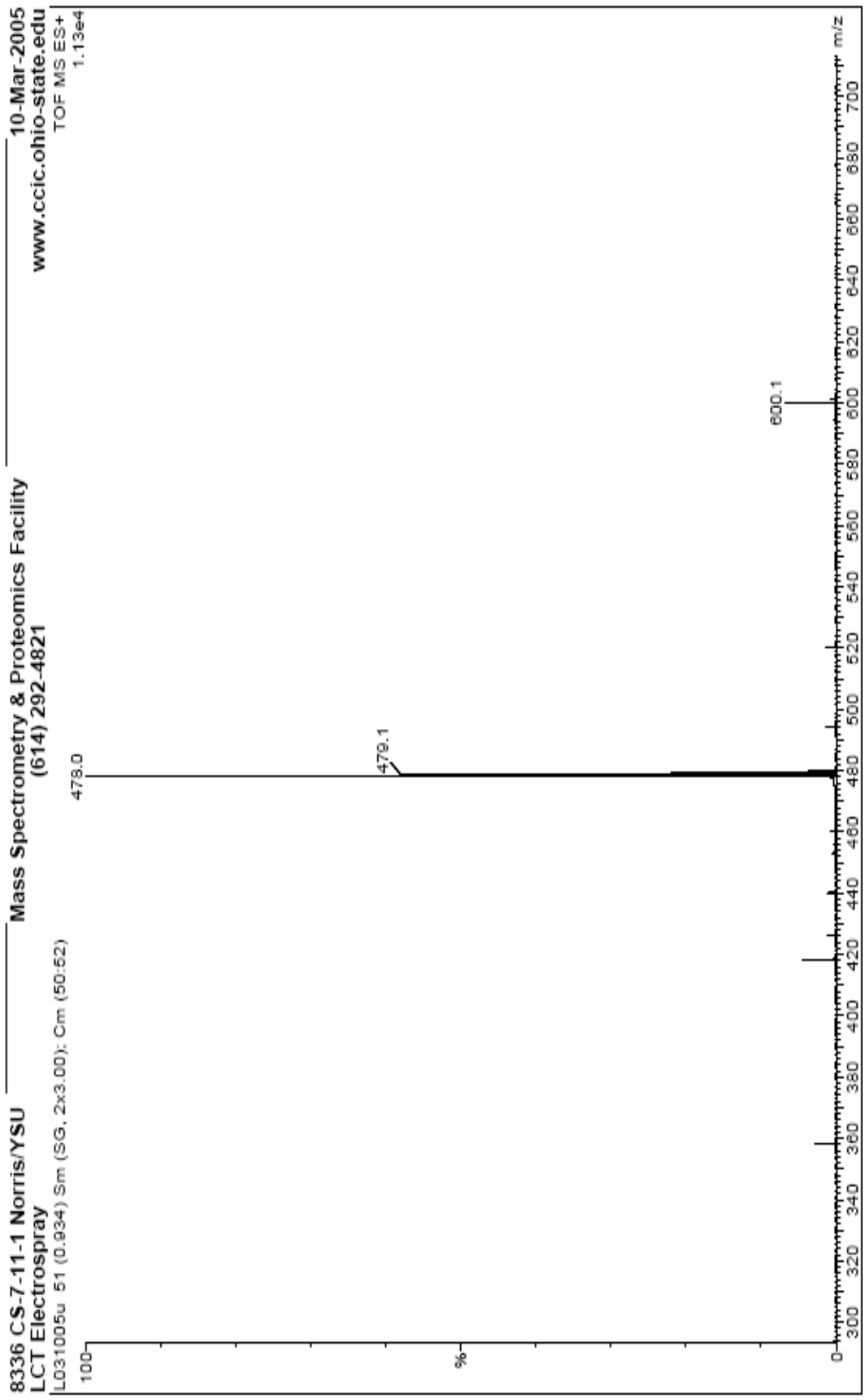

Figure 58: LC-MS spectrum of *p*-fluorobenzoic acid-(β-D-glucopyranuronosyl)-amide (**34**).

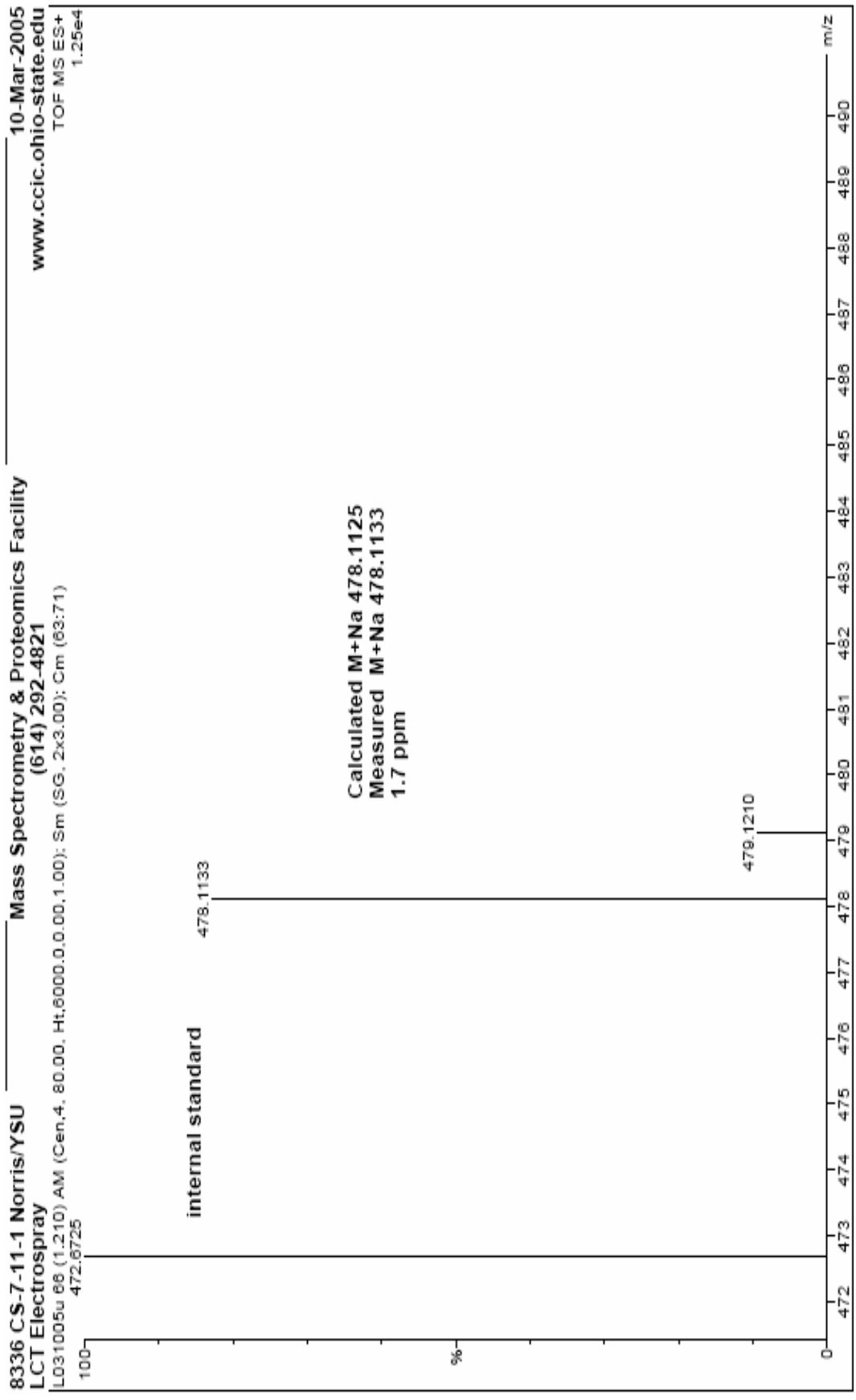

Figure 59: High Resolution TOF-MS spectrum of *p*-fluorobenzoic acid-(β-D-glucopyranuronosyl)-amide (**34**).

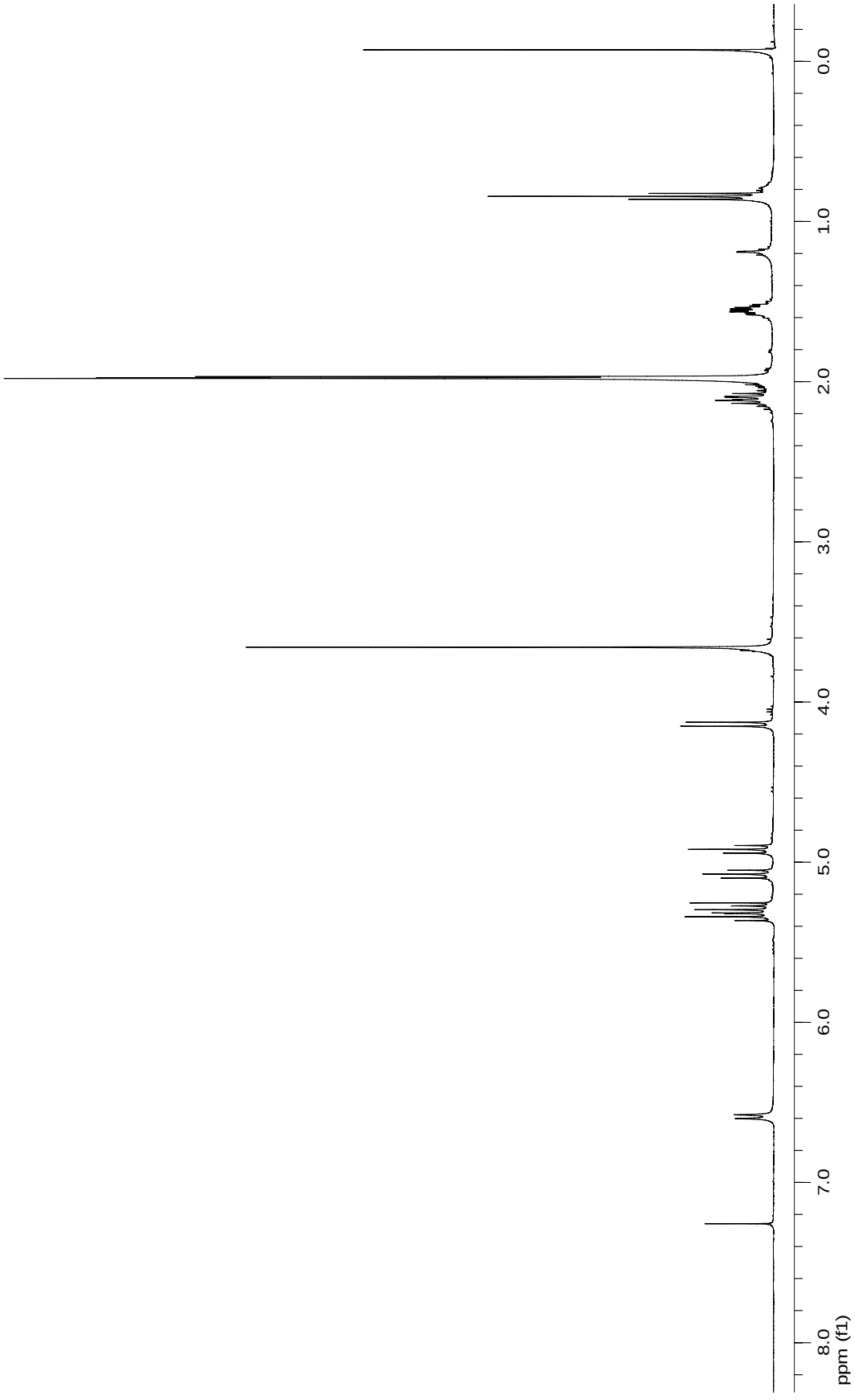

Figure 60: 400 MHz ^{1}H NMR spectrum of butyric acid-(β-D-glucopyranuronosyl)-amide (**35**).

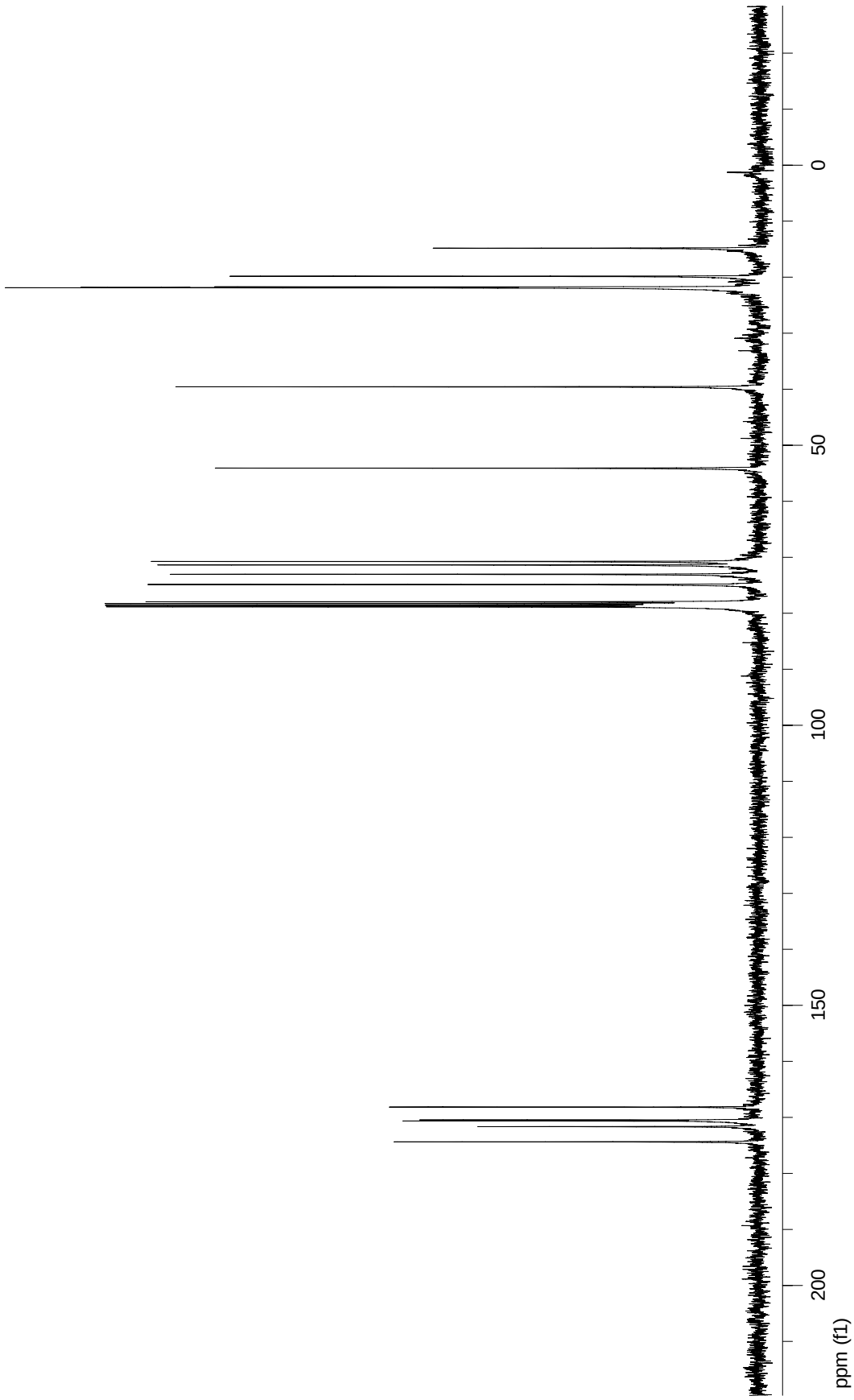

Figure 61: 100 MHz ^{13}C NMR spectrum of butyric acid-(β-D-glucopyranuronosyl)-amide (**35**).

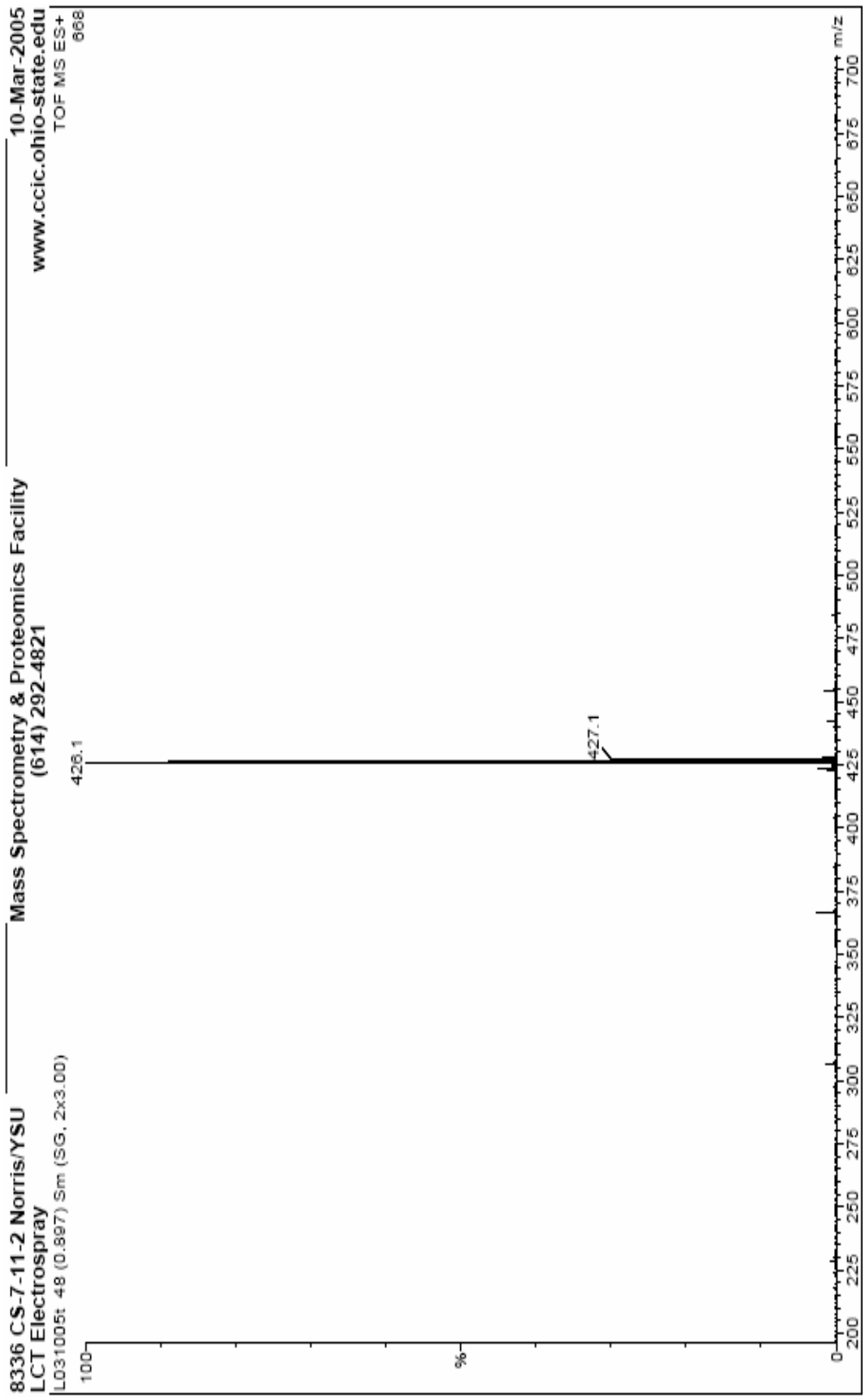

Figure 62: LC-MS spectrum of butyric acid-(β-D-glucopyranuronosyl)-amide (**35**).

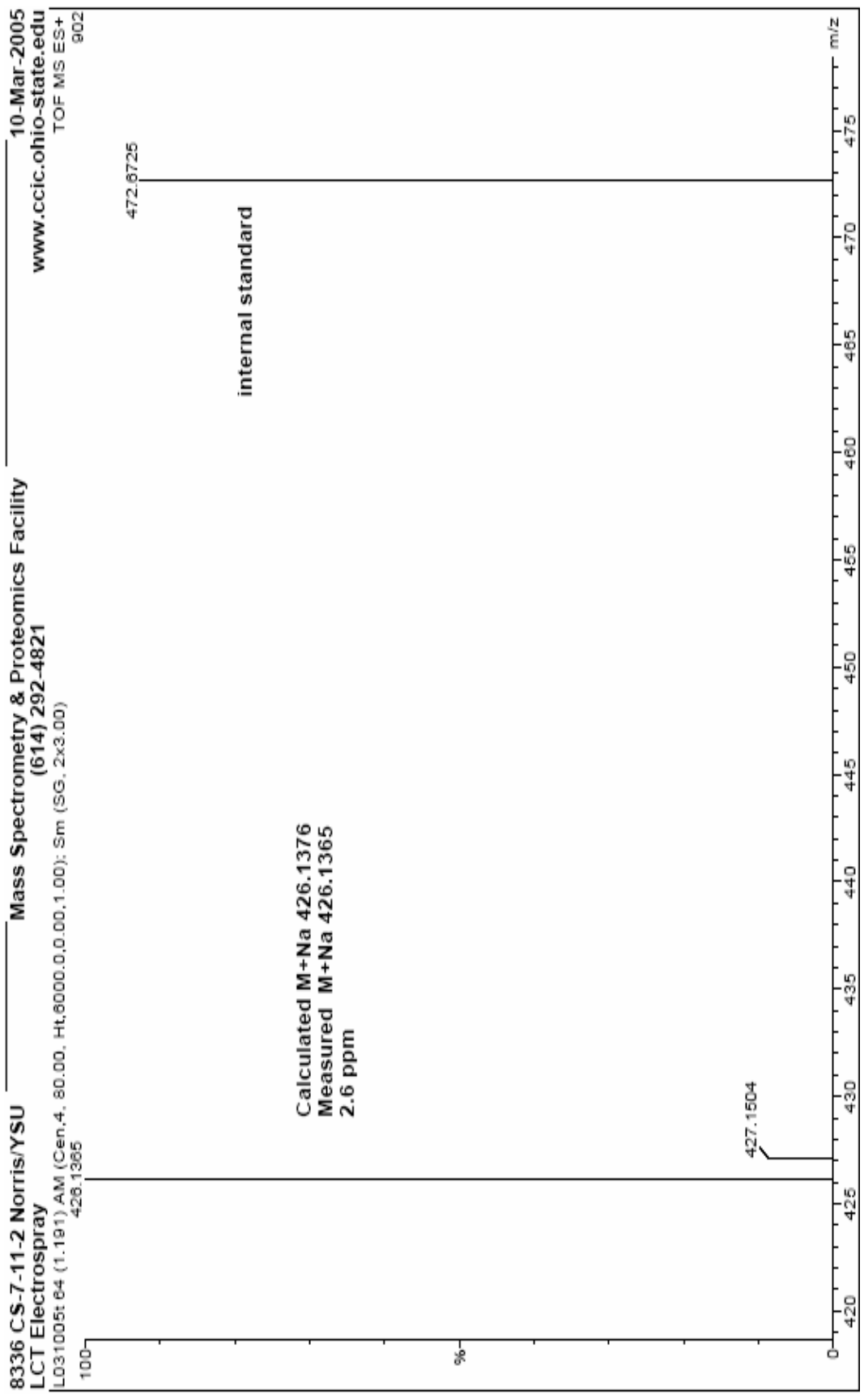

Figure 63: High Resolution TOF-MS spectrum of butyric acid-(β-D-glucopyranuronosyl)-amide (**35**).

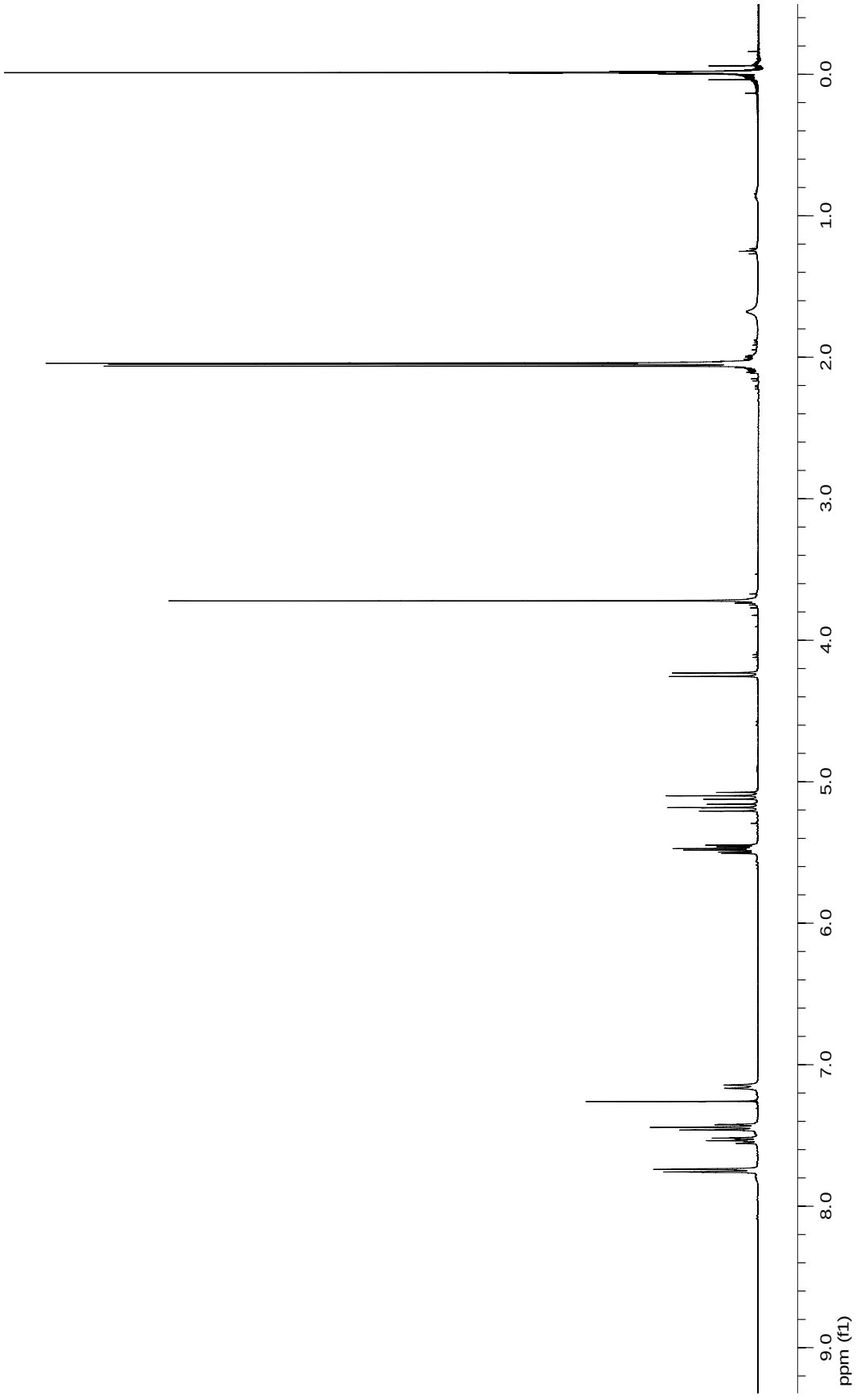

Figure 64: 400 MHz ^{1}H NMR spectrum of benzoic acid-(β-D-glucopyranuronosyl)-amide (**36**).

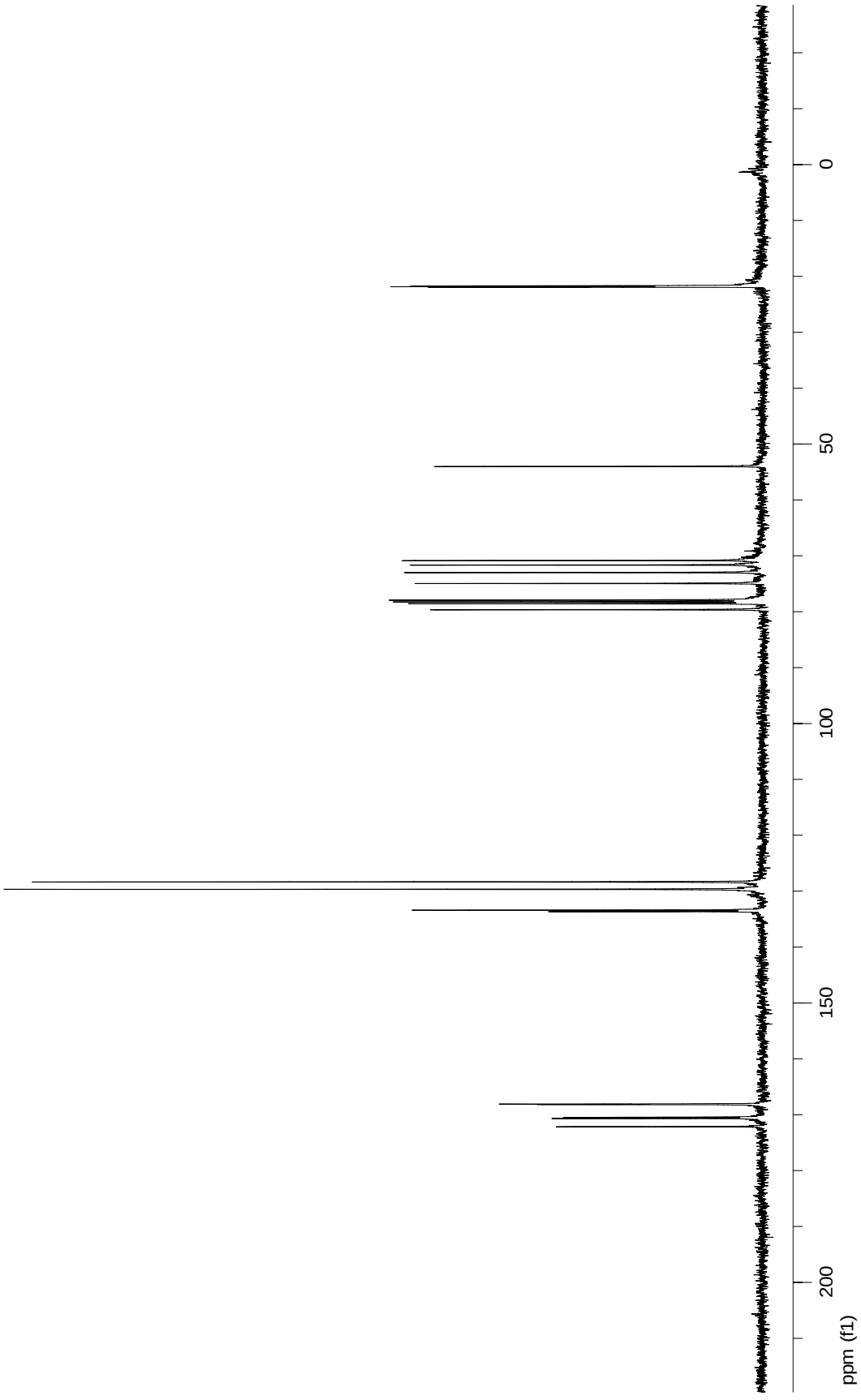

Figure 65: 100 MHz ^{13}C NMR spectrum of benzoic acid-(β-D-glucopyranuronosyl)-amide (**36**).

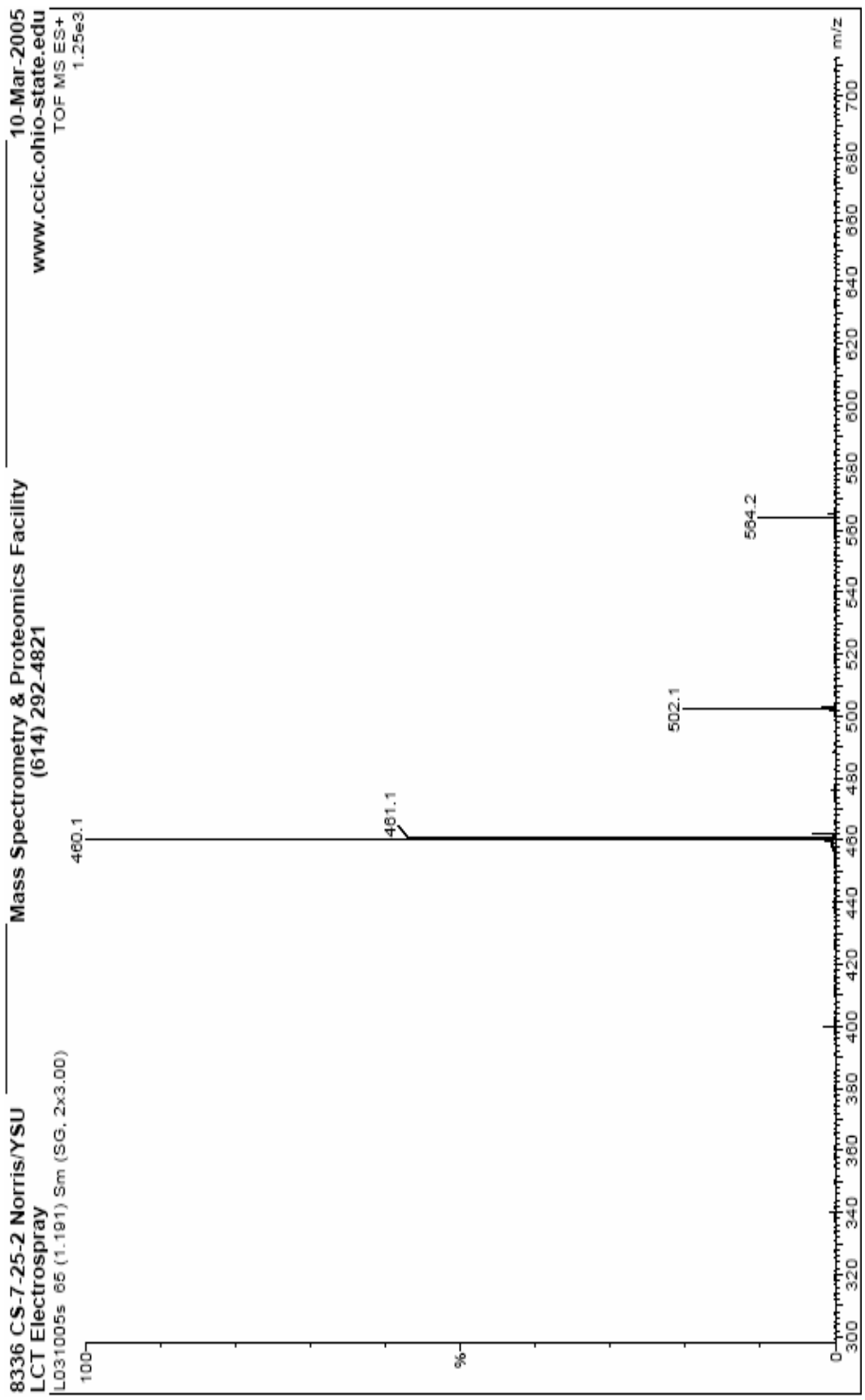

Figure 66: LC-MS spectrum of benzoic acid-(β-D-glucopyranuronosyl)-amide (**36**).

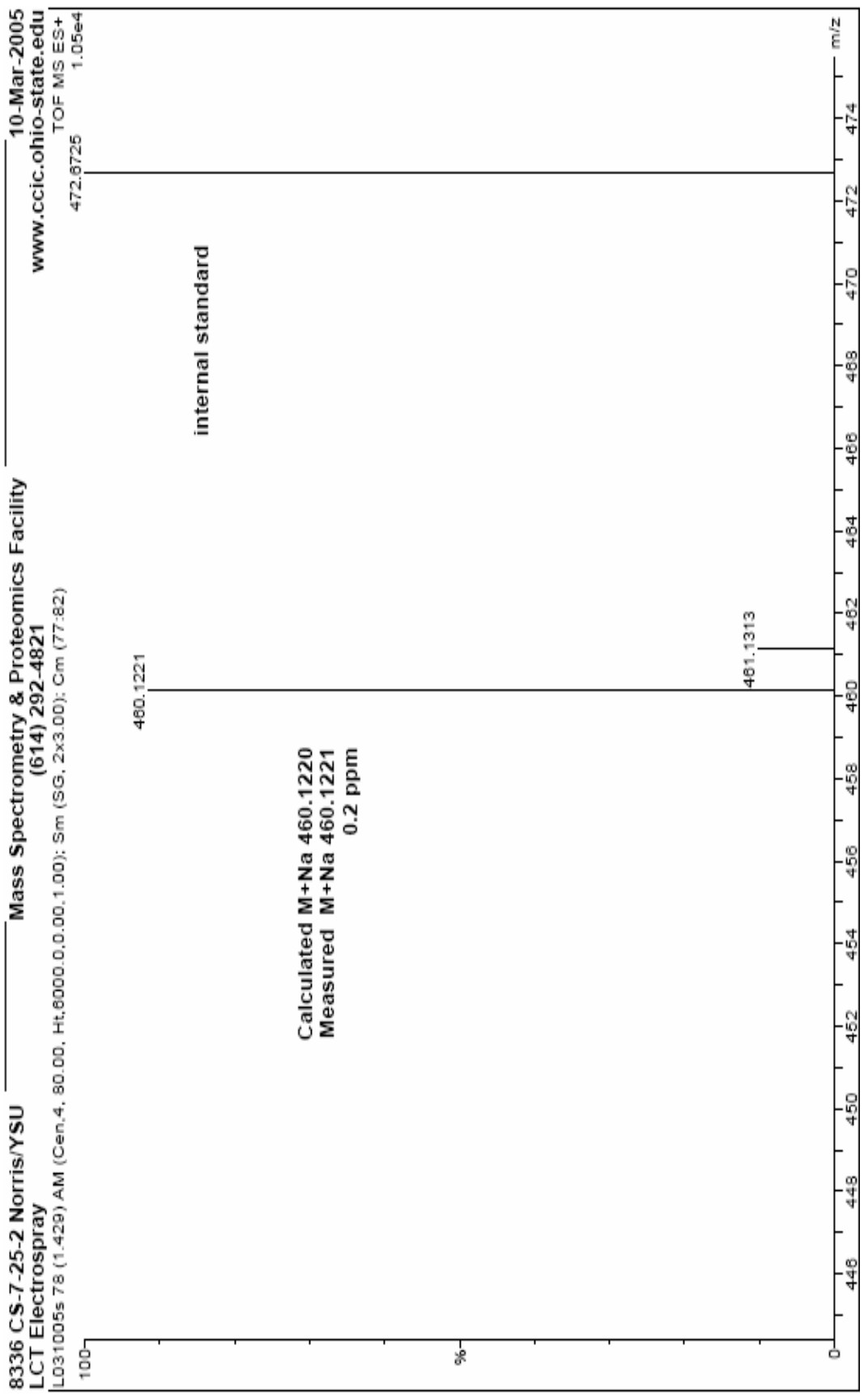

Figure 67: High Resolution TOF-MS spectrum of benzoic acid-(β-D-glucopyranuronosyl)-amide (**36**).

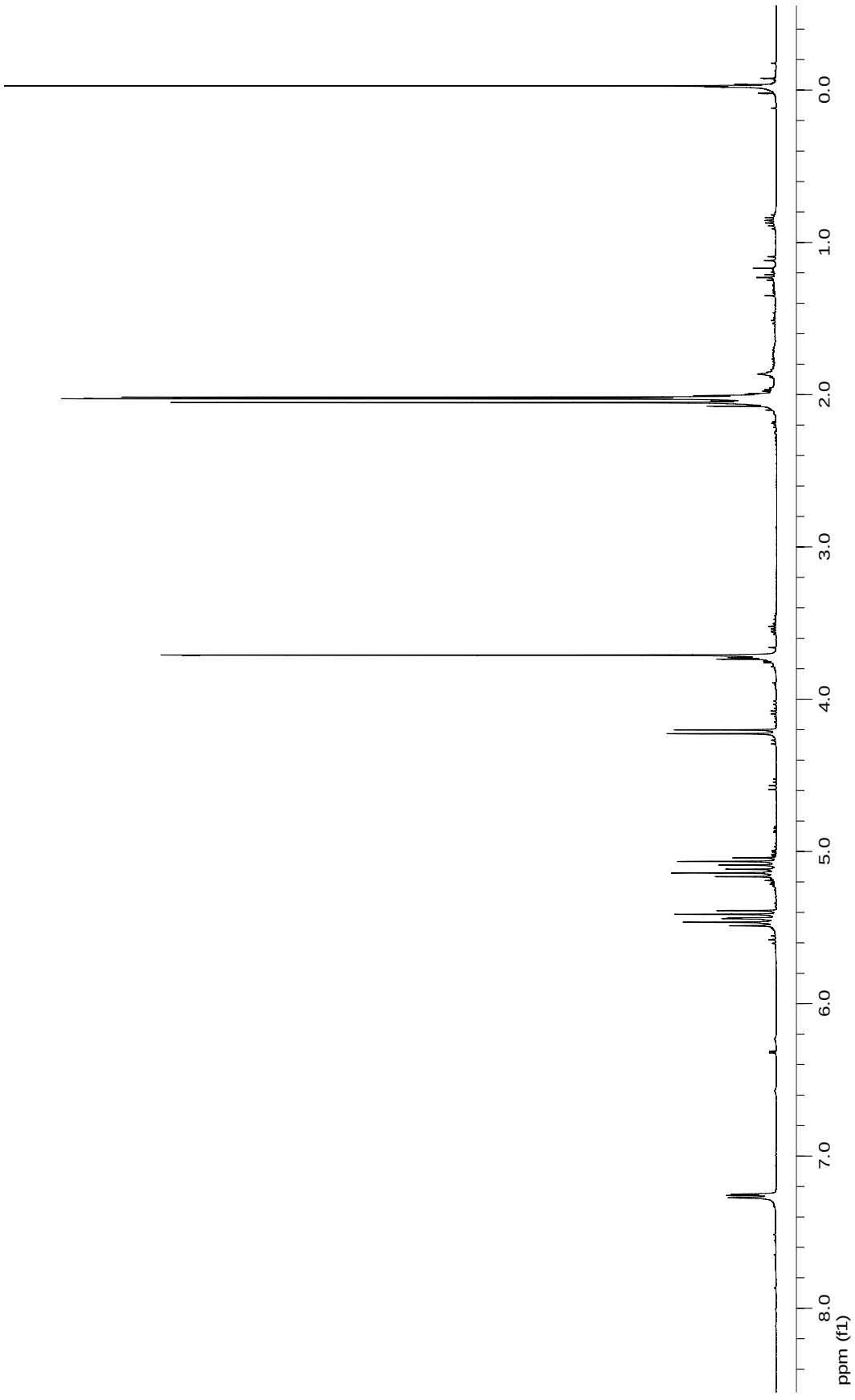

Figure 68: 400 MHz ^{1}H NMR spectrum of pentafluorobenzoic acid-(β-D-glucopyranuronosyl)-amide (**37**).

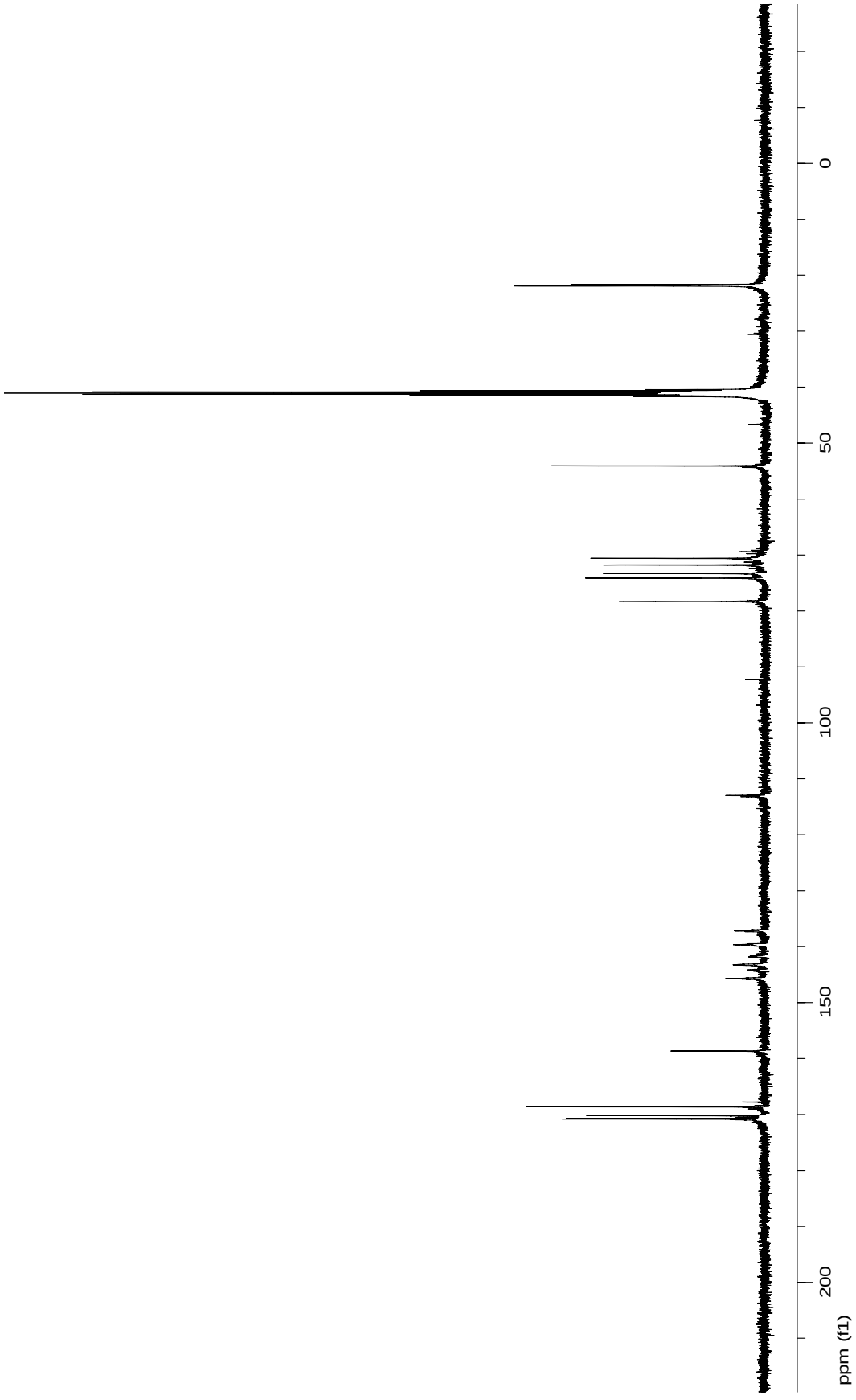

Figure 69: 100 MHz ^{13}C NMR spectrum of pentafluorobenzoic acid-(β-D-glucopyranuronosyl)-amide (**37**).

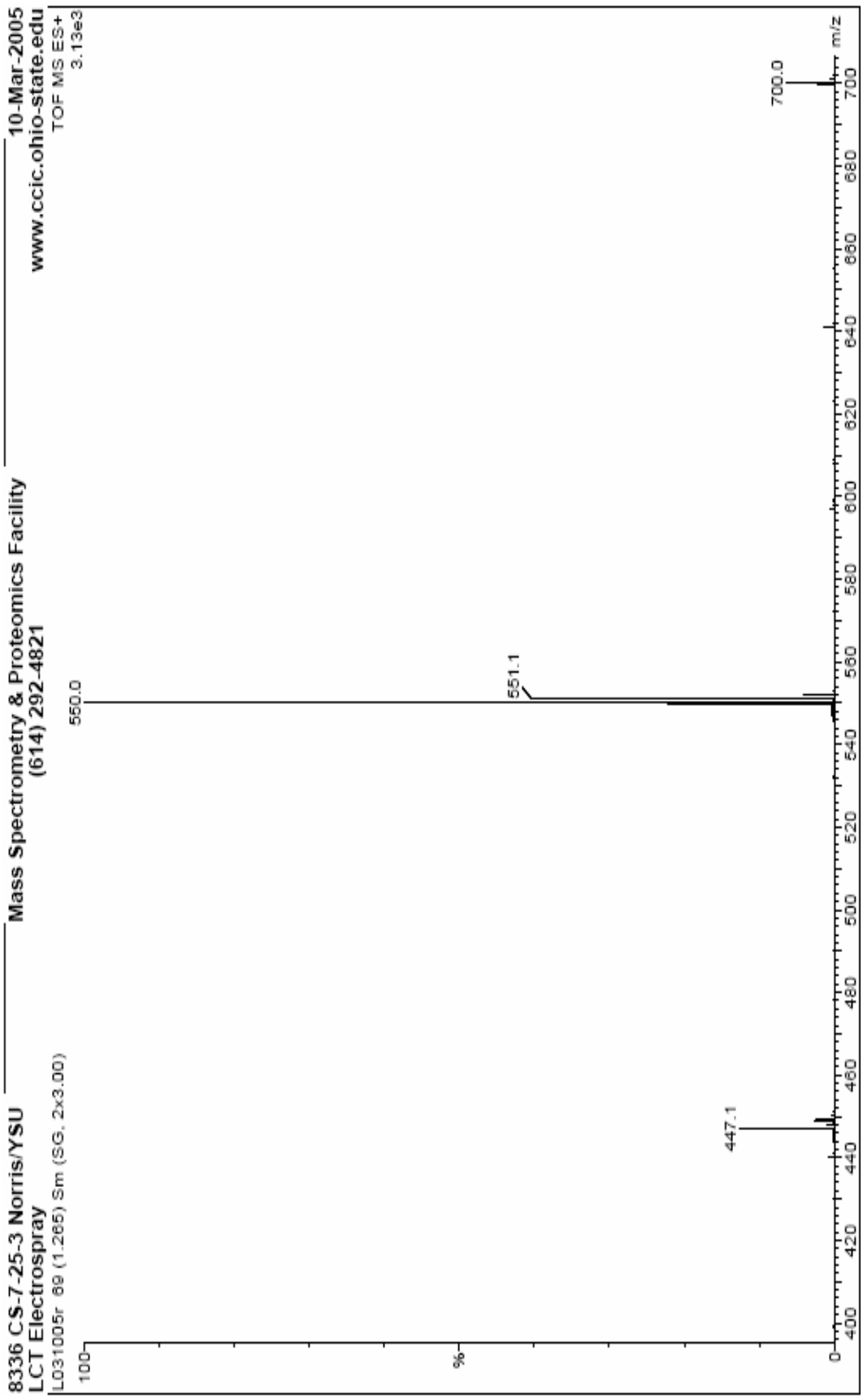

Figure 70: LC-MS spectrum of pentafluorobenzoic acid-(β-D-glucopyranuronosyl)-amide (**37**).

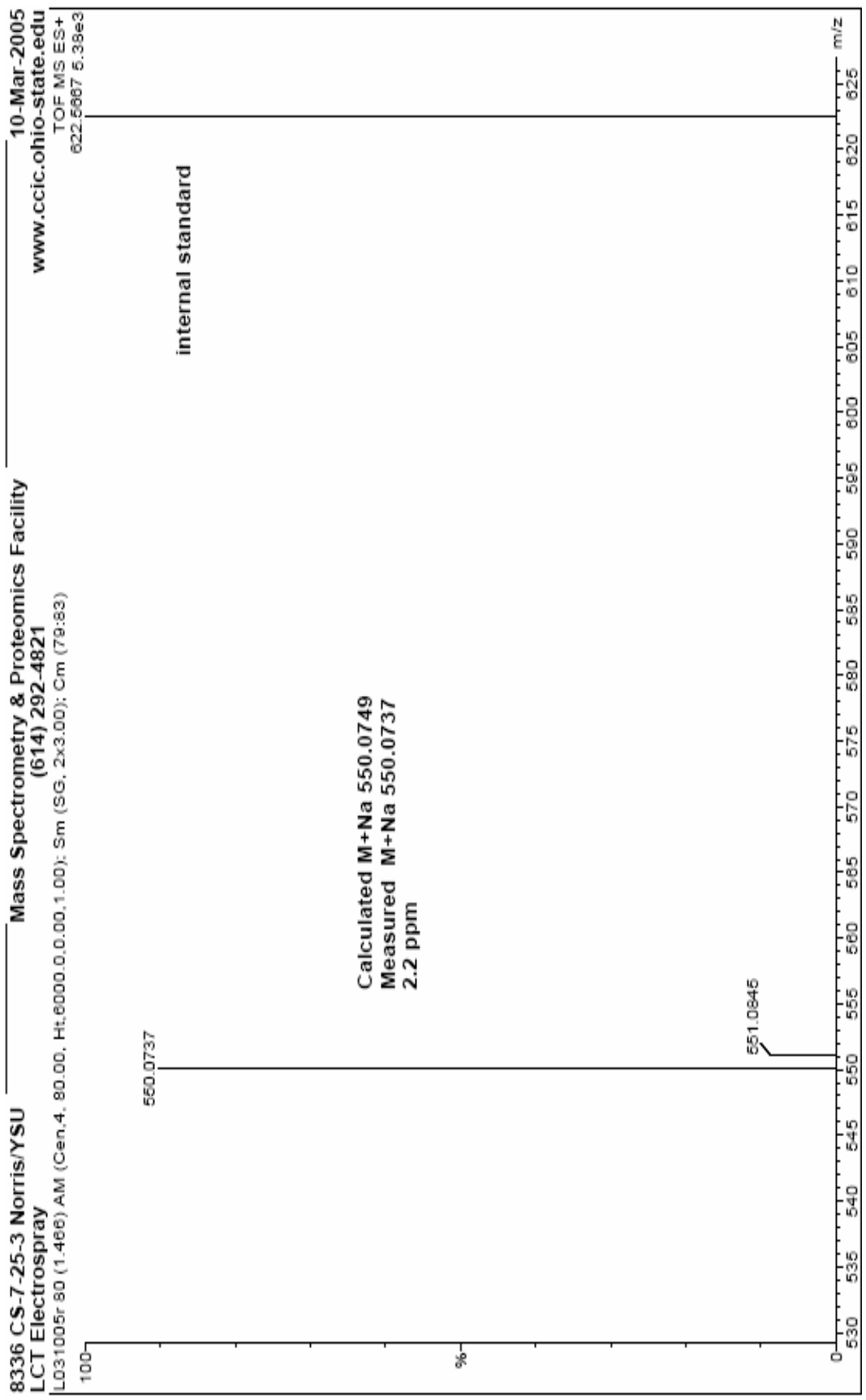

Figure 71: High Resolution TOF-MS spectrum of pentafluorobenzoic acid-(β-D-glucopyranuronosyl)-amide (**37**).

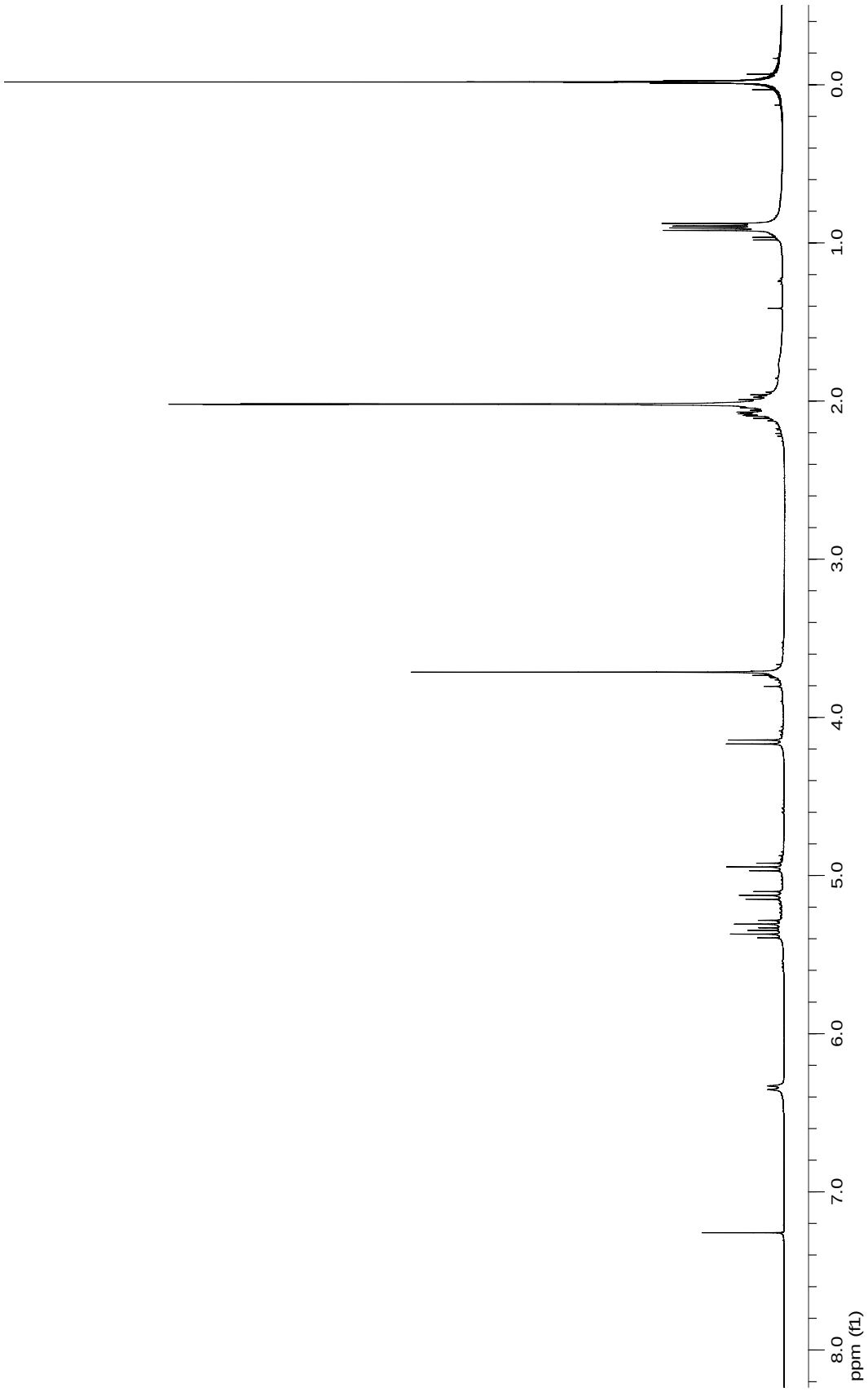

Figure 72: 400 MHz ^{1}H NMR spectrum of isovaleric acid-(β-D-glucopyranuronosyl)-amide (**38**).

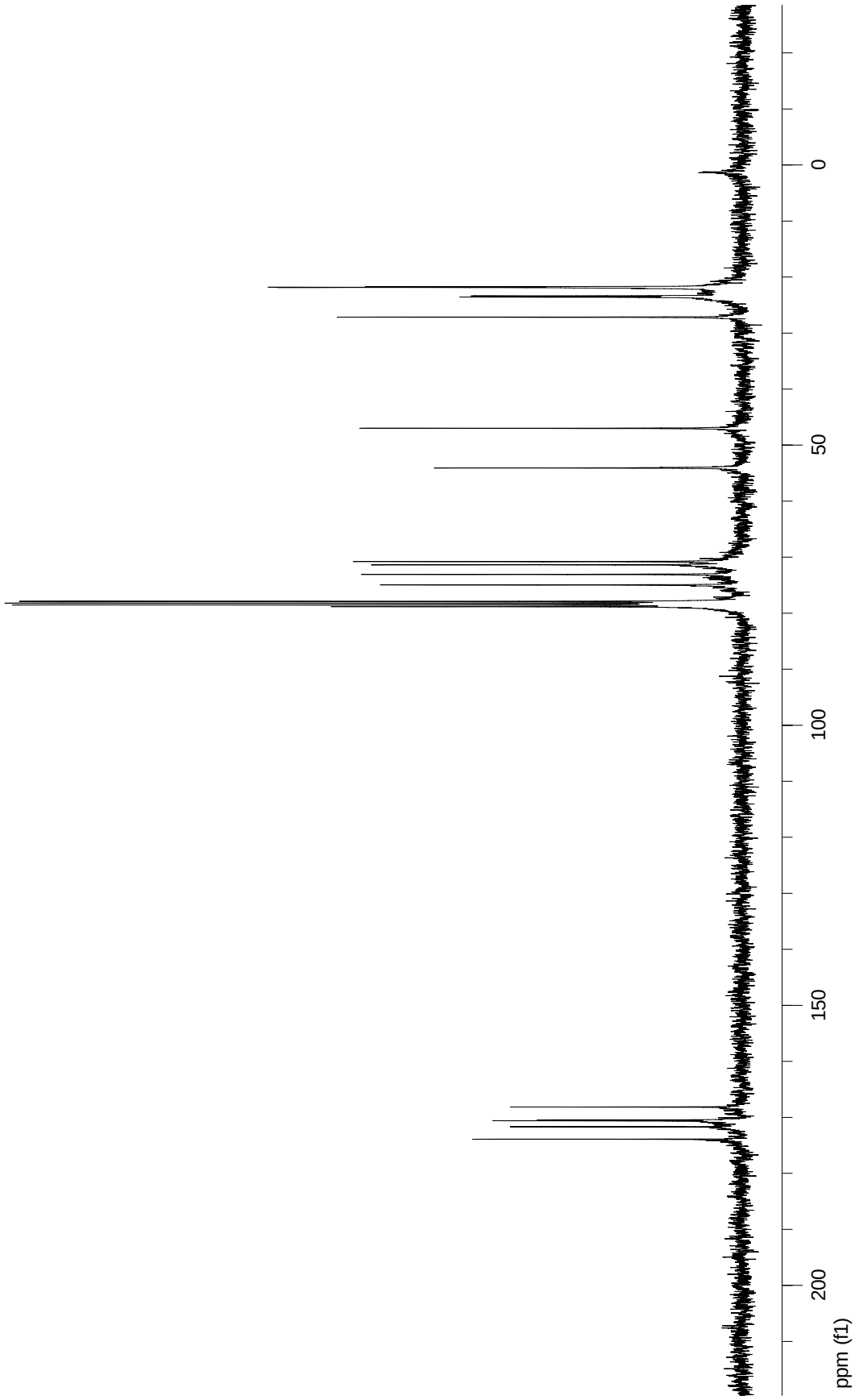

Figure 73: 100 MHz ^{13}C NMR spectrum of isovaleric acid-(β-D-glucopyranuronosyl)-amide (**38**).

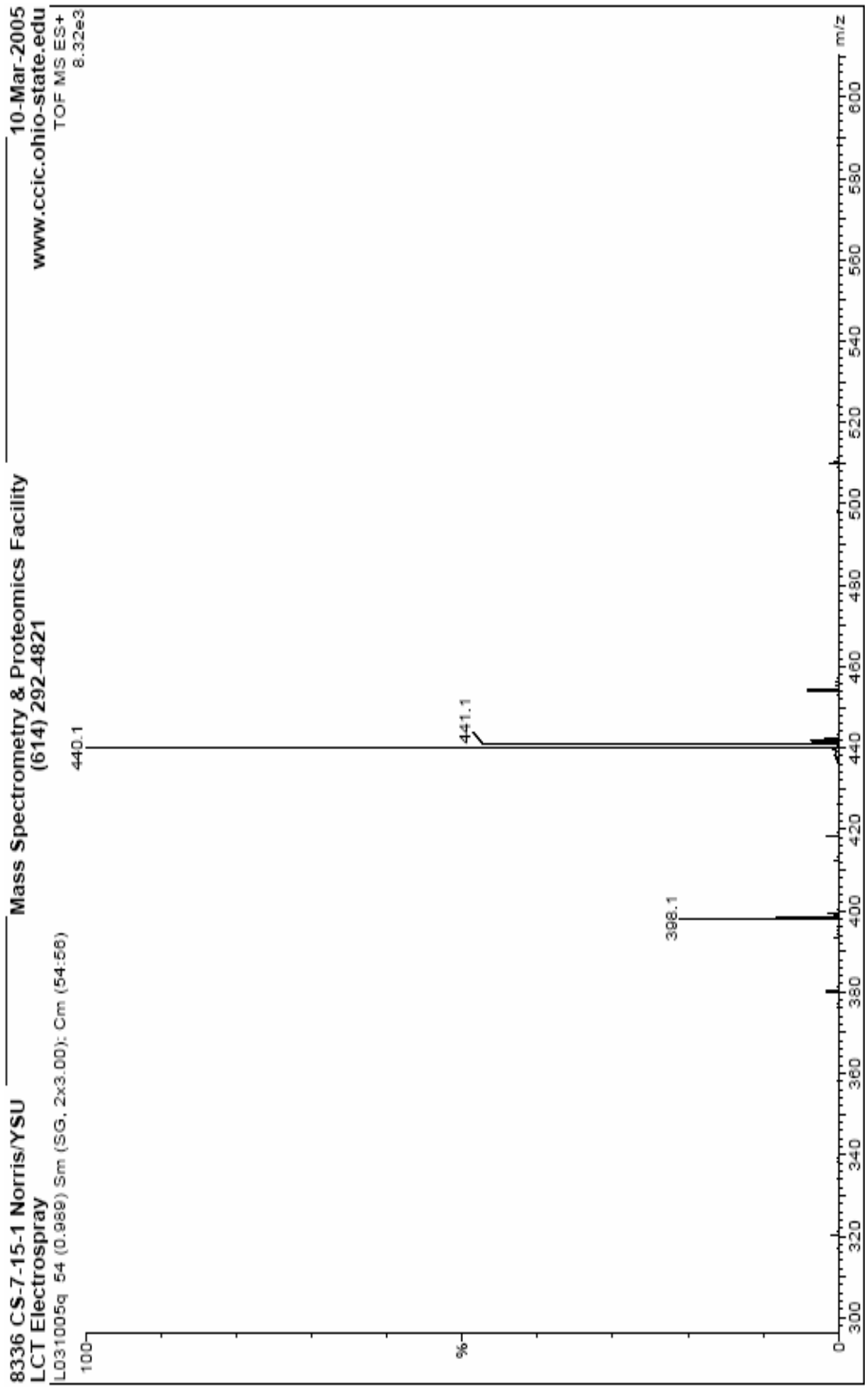

Figure 74: LC-MS spectrum of isovaleric acid-(β-D-glucopyranuronosyl)-amide (**38**).

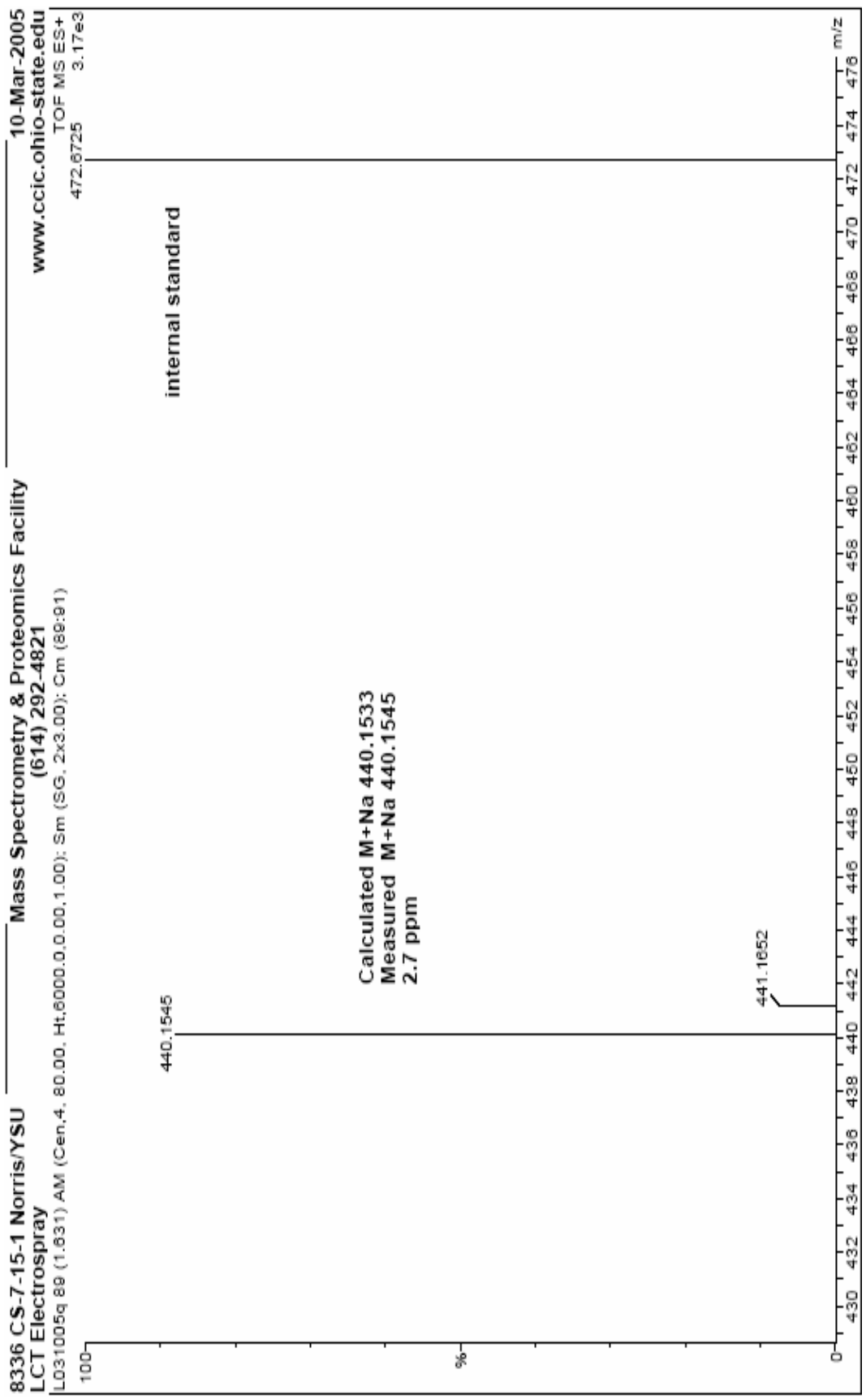

Figure 75: High Resolution TOF-MS spectrum of isovaleric acid-(β-D-glucopyranuronosyl)-amide (**38**).

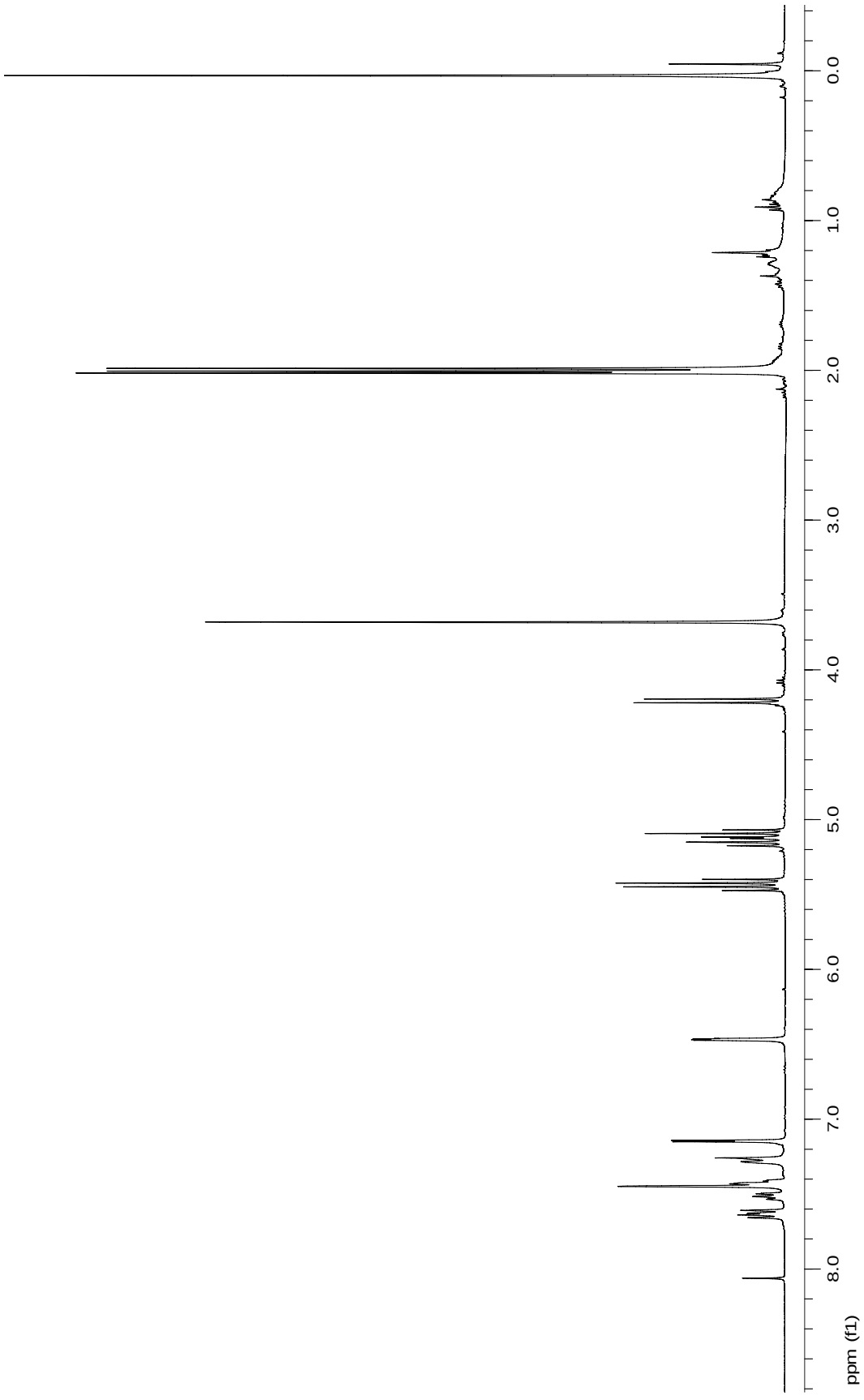

Figure 76: 400 MHz ^{1}H NMR spectrum of Furan-2-carboxylic acid-(β-D-glucopyranuronosyl)-amide (**39**).

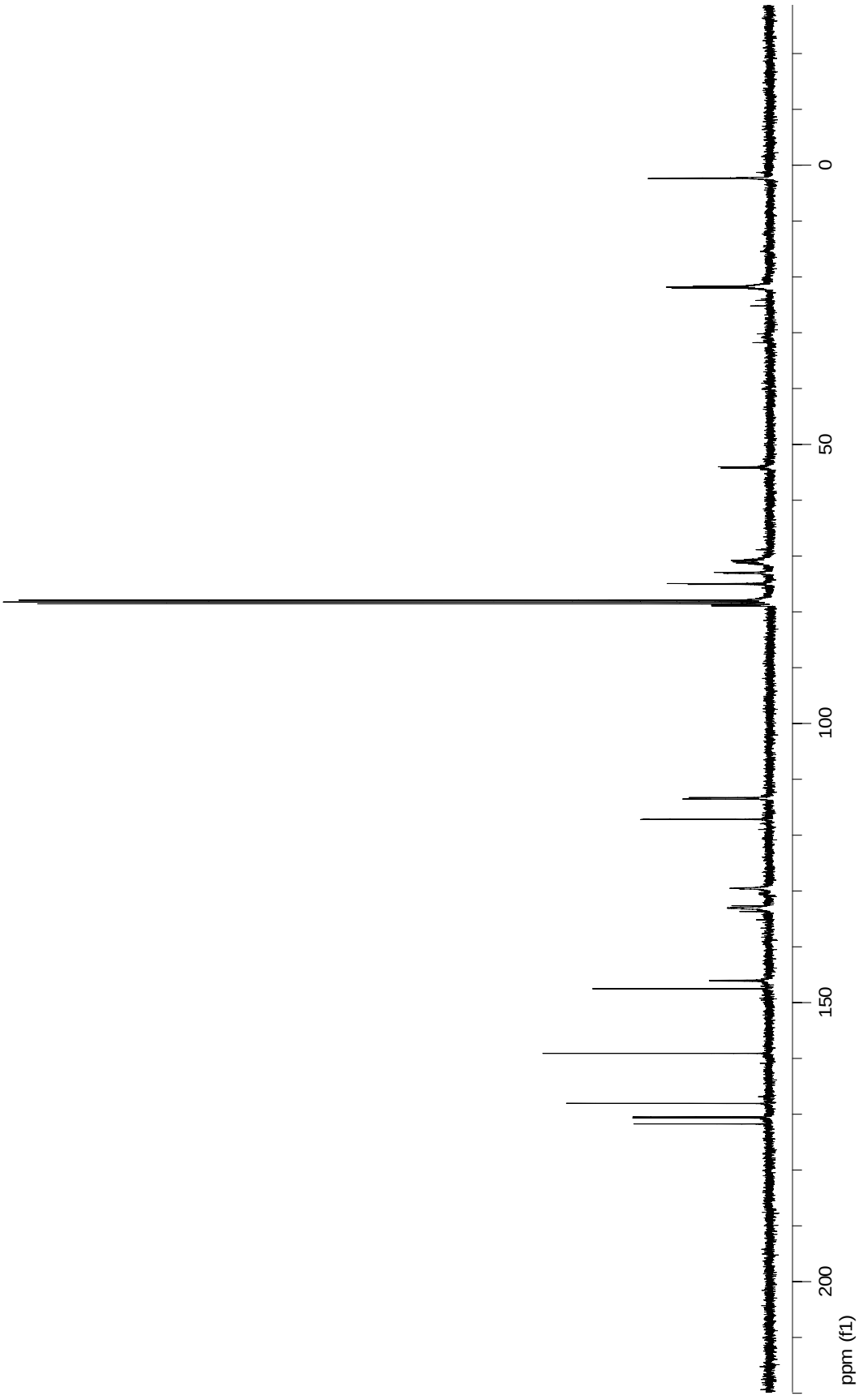

Figure 77: 100 MHz ^{13}C NMR spectrum of Furan-2-carboxylic acid-(β-D-glucopyranuronosyl)-amide (**39**).

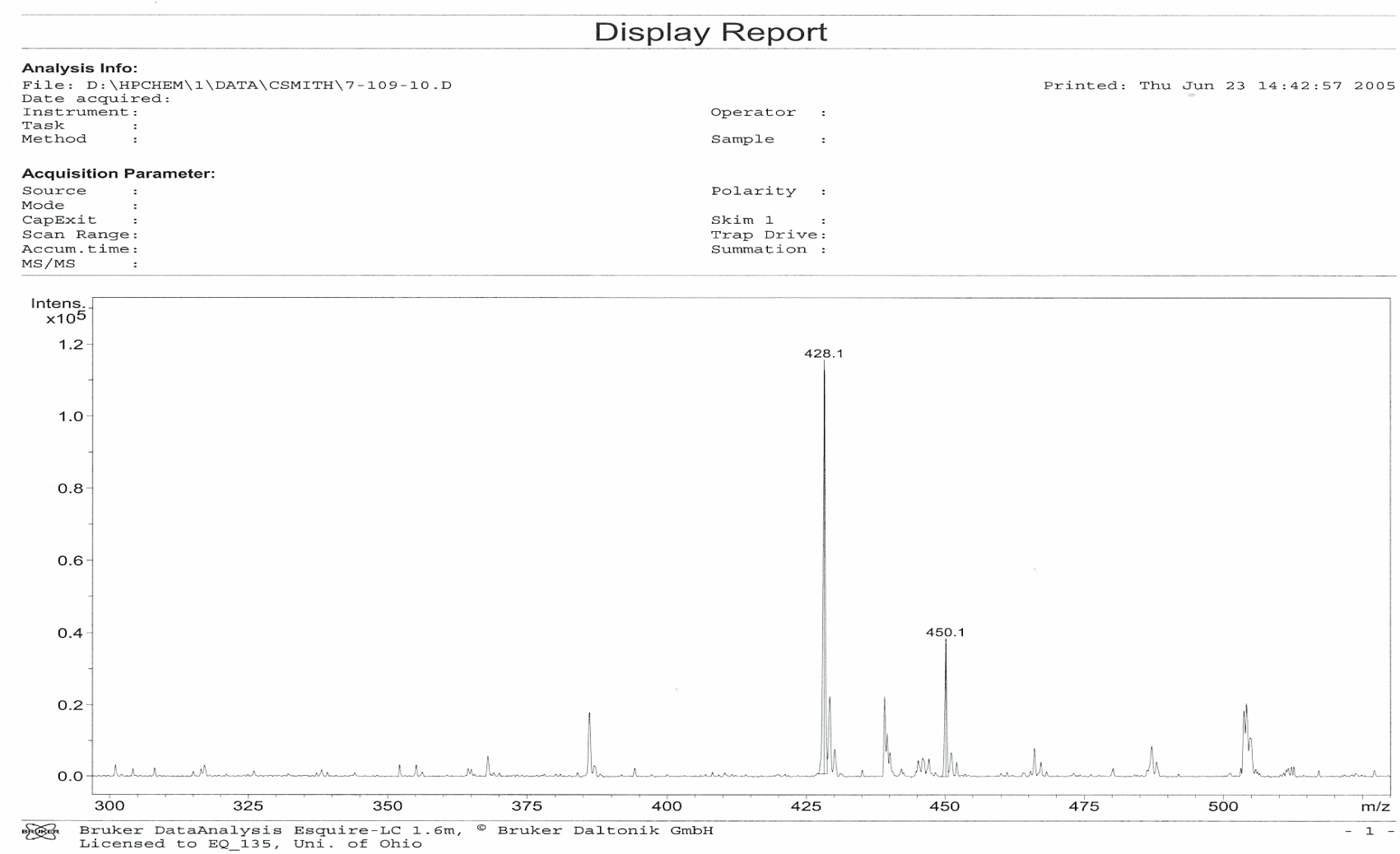

Figure 78: Mass spectrum of Furan-2-carboxylic acid-(β-D-glucopyranuronosyl)-amide (**39**).

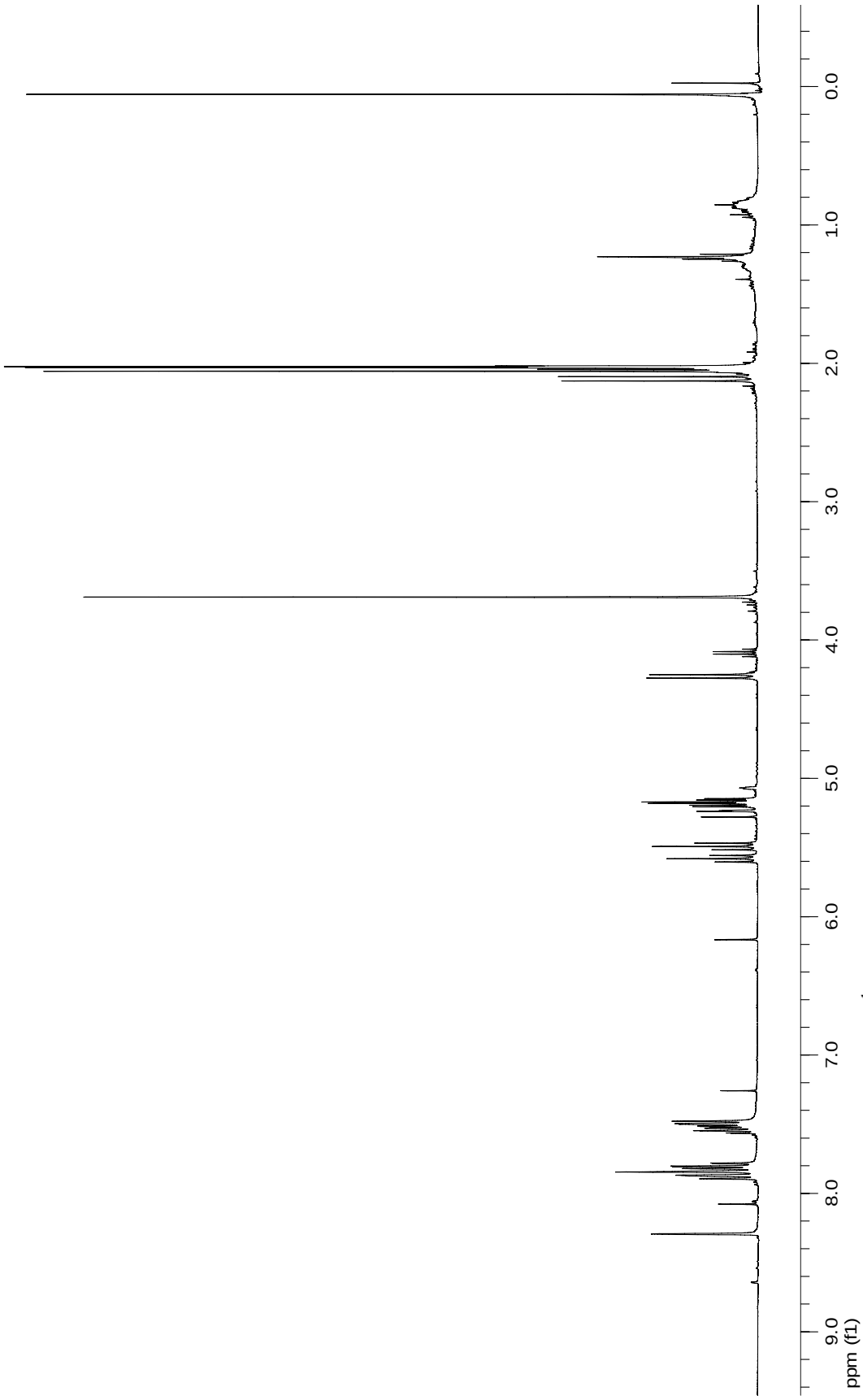

Figure 79: 400 MHz ^{1}H NMR spectrum of 2-naphthanoic acid-(β-D-glucopyranuronosyl)-amide (**40**).

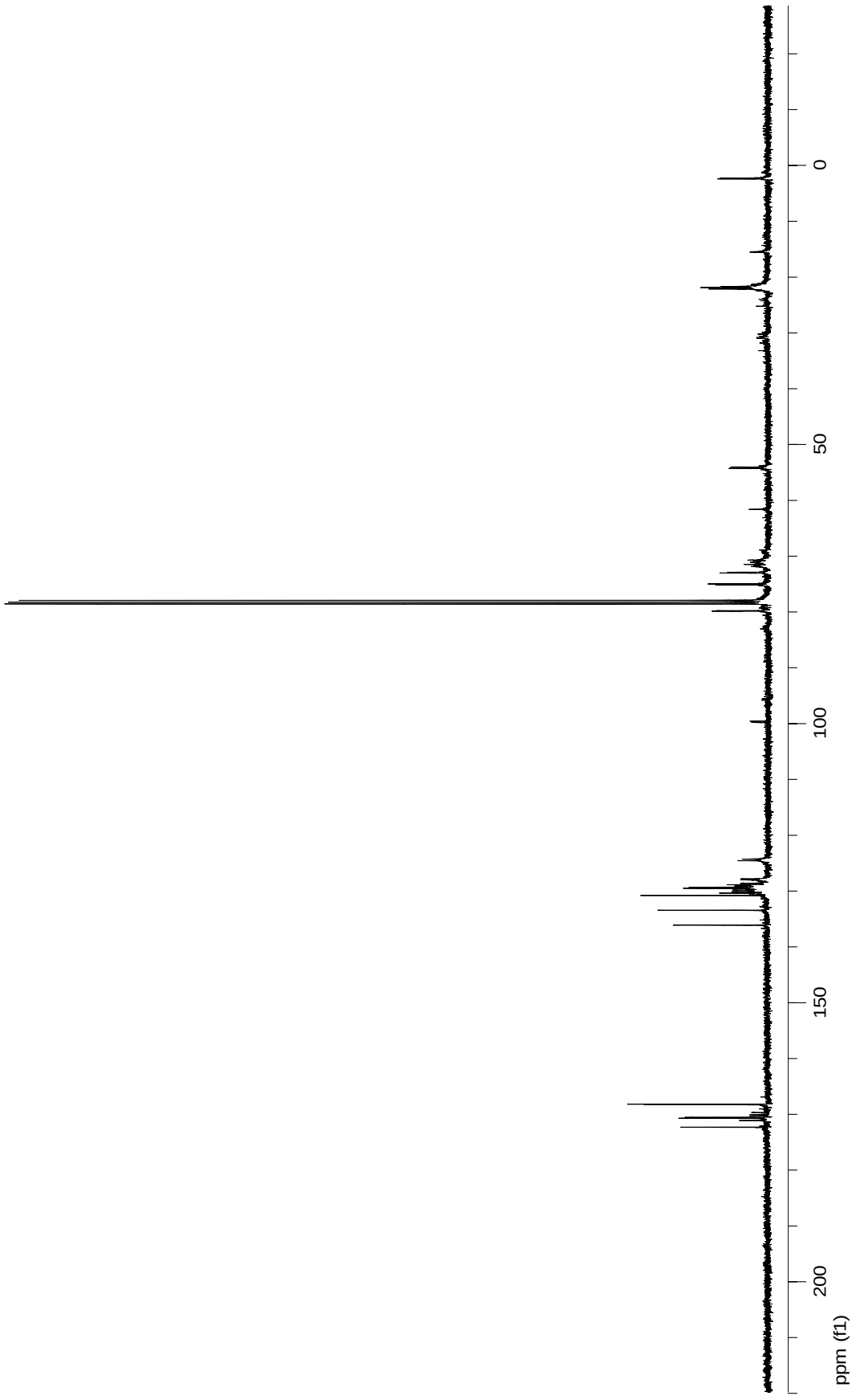

Figure 80: 100 MHz ^{13}C NMR spectrum of 2-naphthanoic acid-(β-D-glucopyranuronosyl)-amide (**40**).

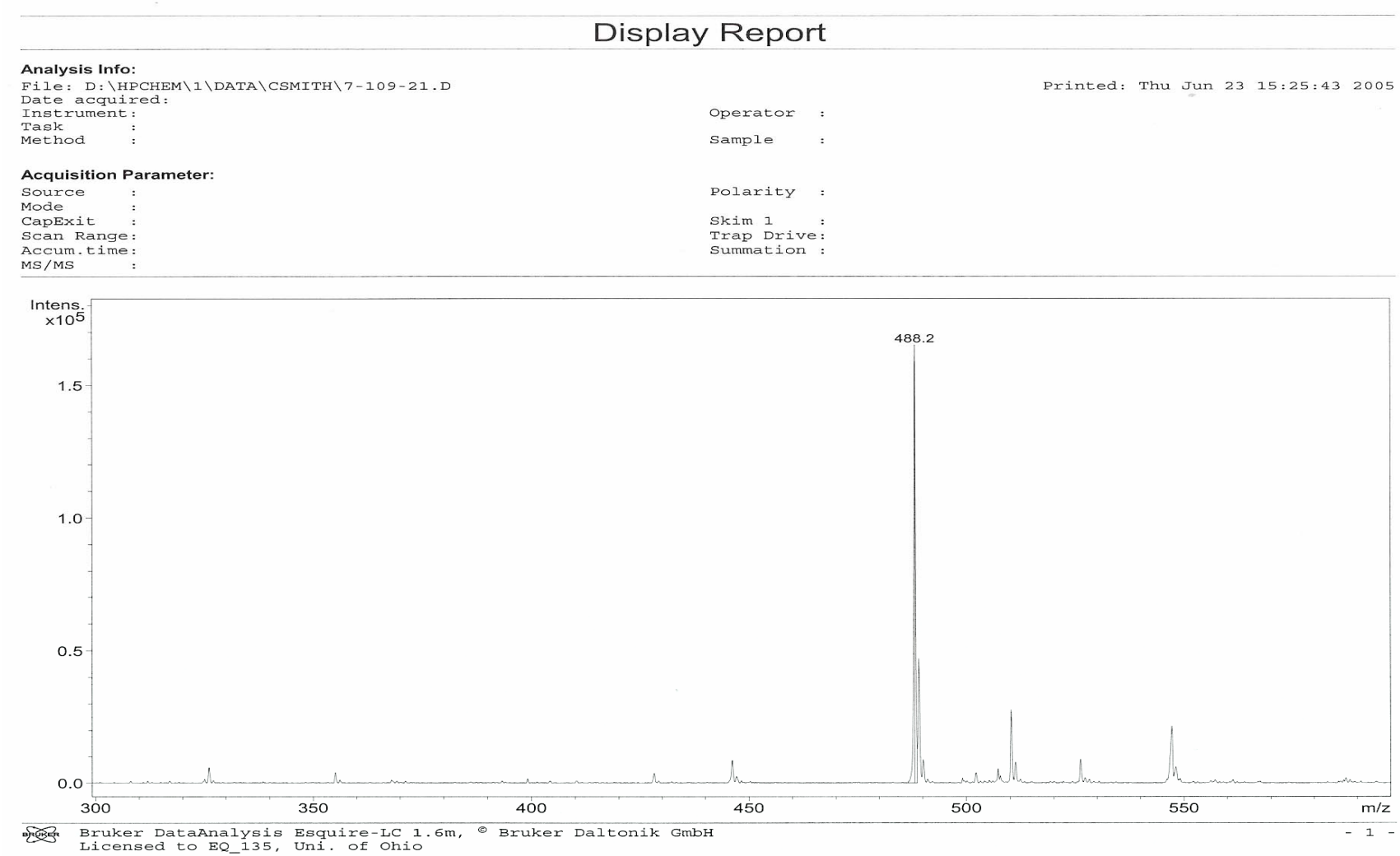

Figure 81: Mass spectrum of 2-naphthanoic acid-(β-D-glucopyranuronosyl)-amide (**40**).

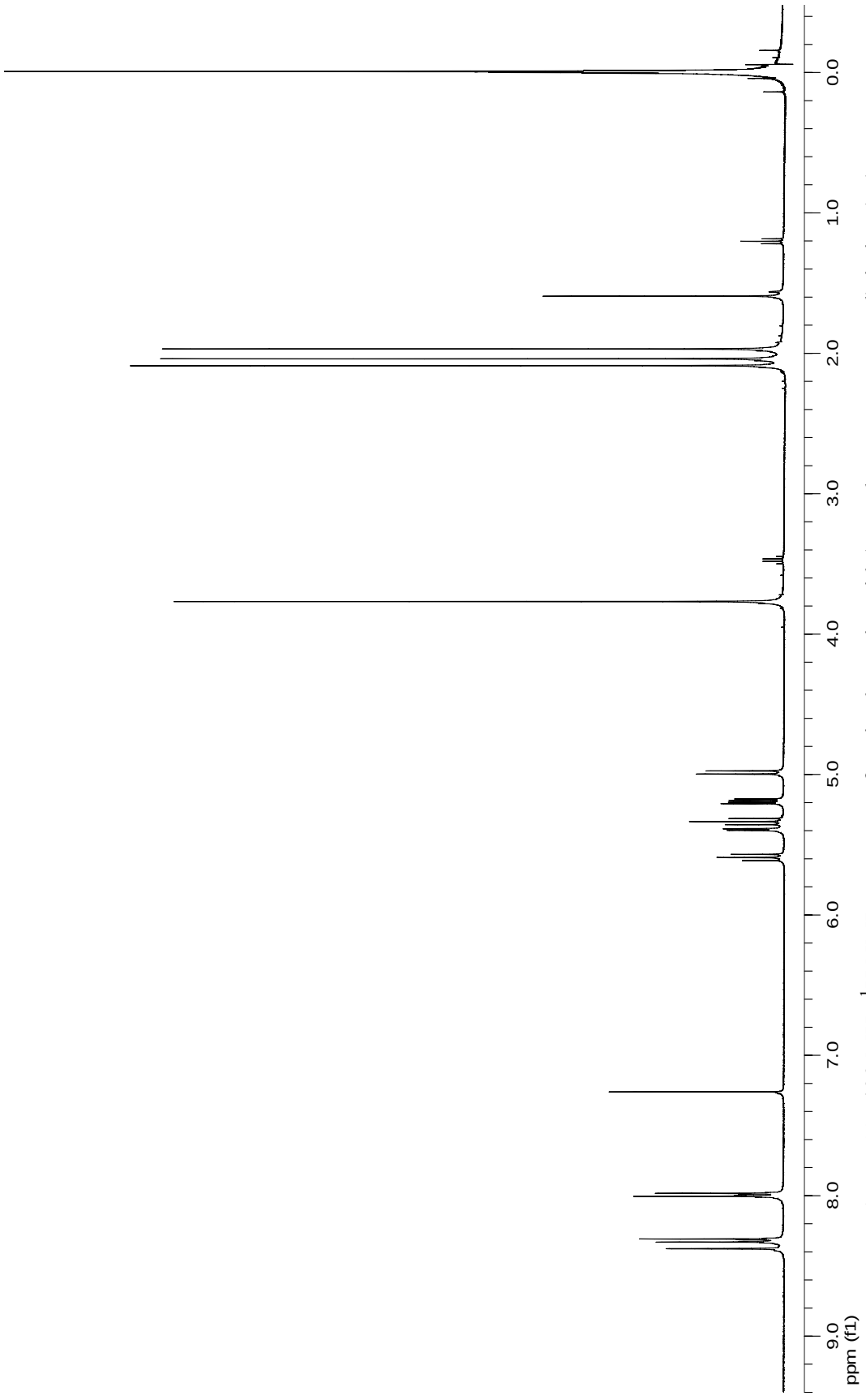

Figure 82: 400 MHz ^{1}H NMR spectrum of *p*-nitrobenzoic acid-(α-D-glucopyranuronosyl)-imine (**41**).

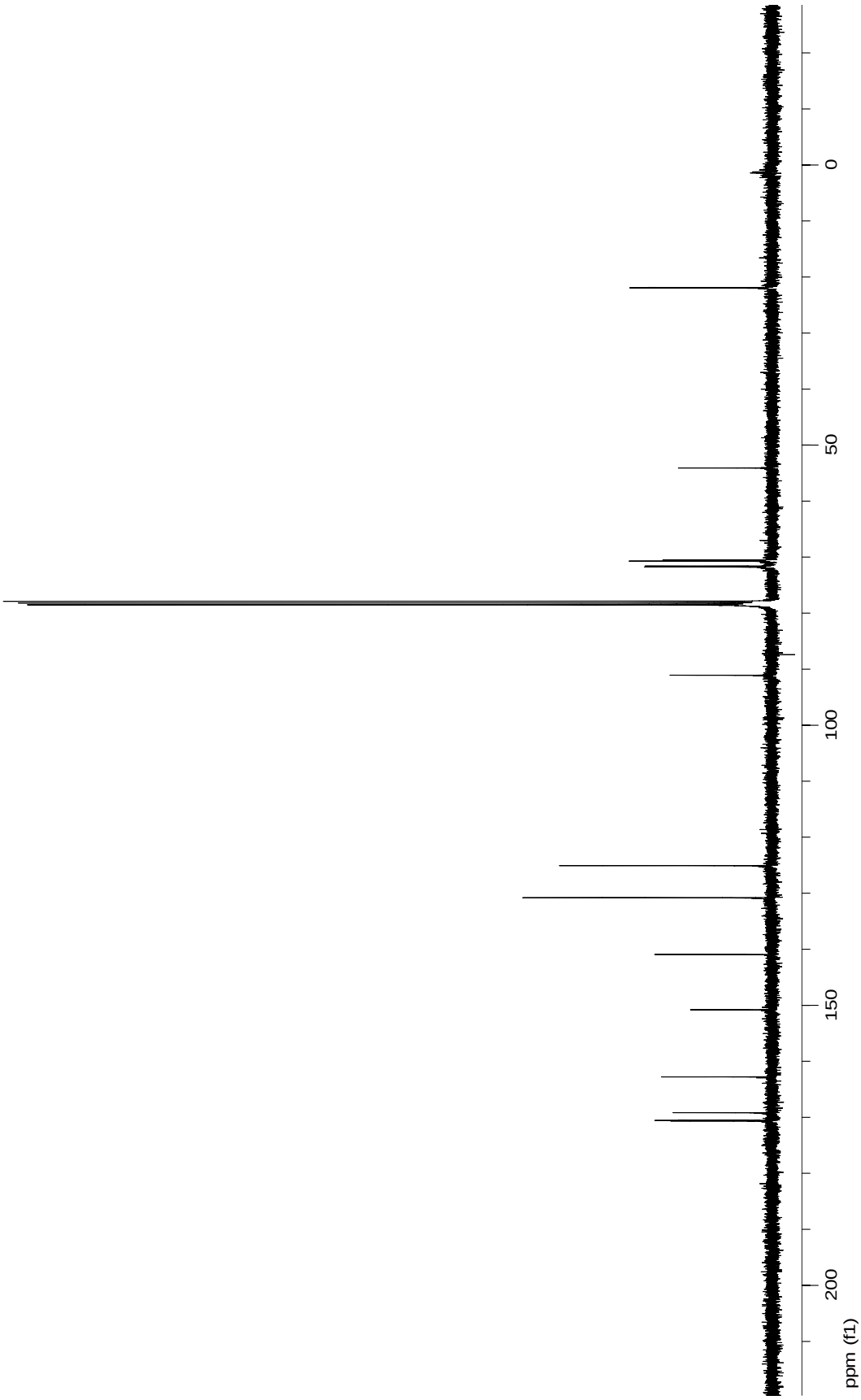

Figure 83: 100 MHz ^{13}C NMR spectrum of *p*-nitrobenzoic acid-(α-D-glucopyranuronosyl)-imine (**41**).

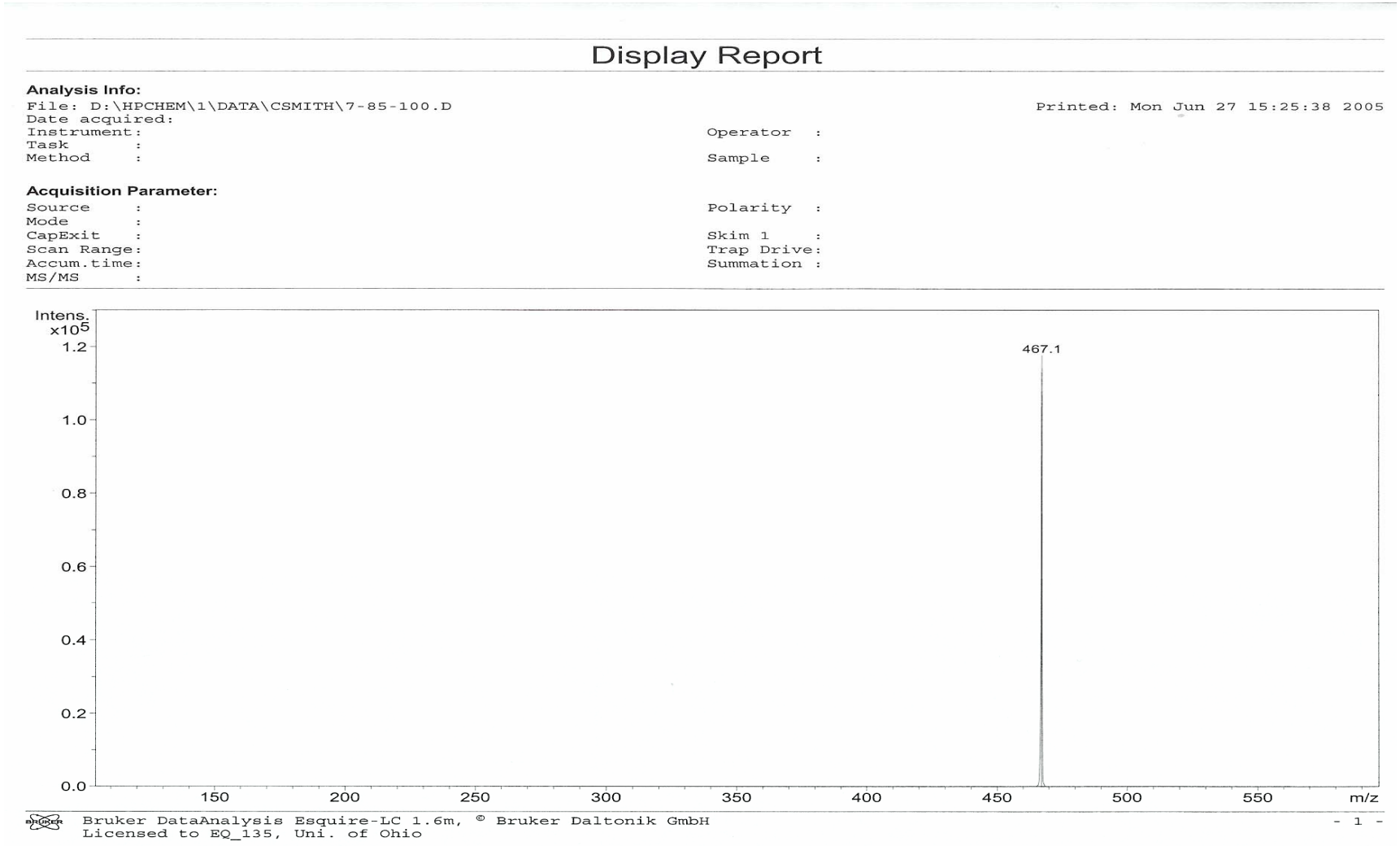

Figure 84: Mass spectrum of *p*-nitrobenzoic acid-(α-D-glucopyranuronosyl)-imine (**41**).

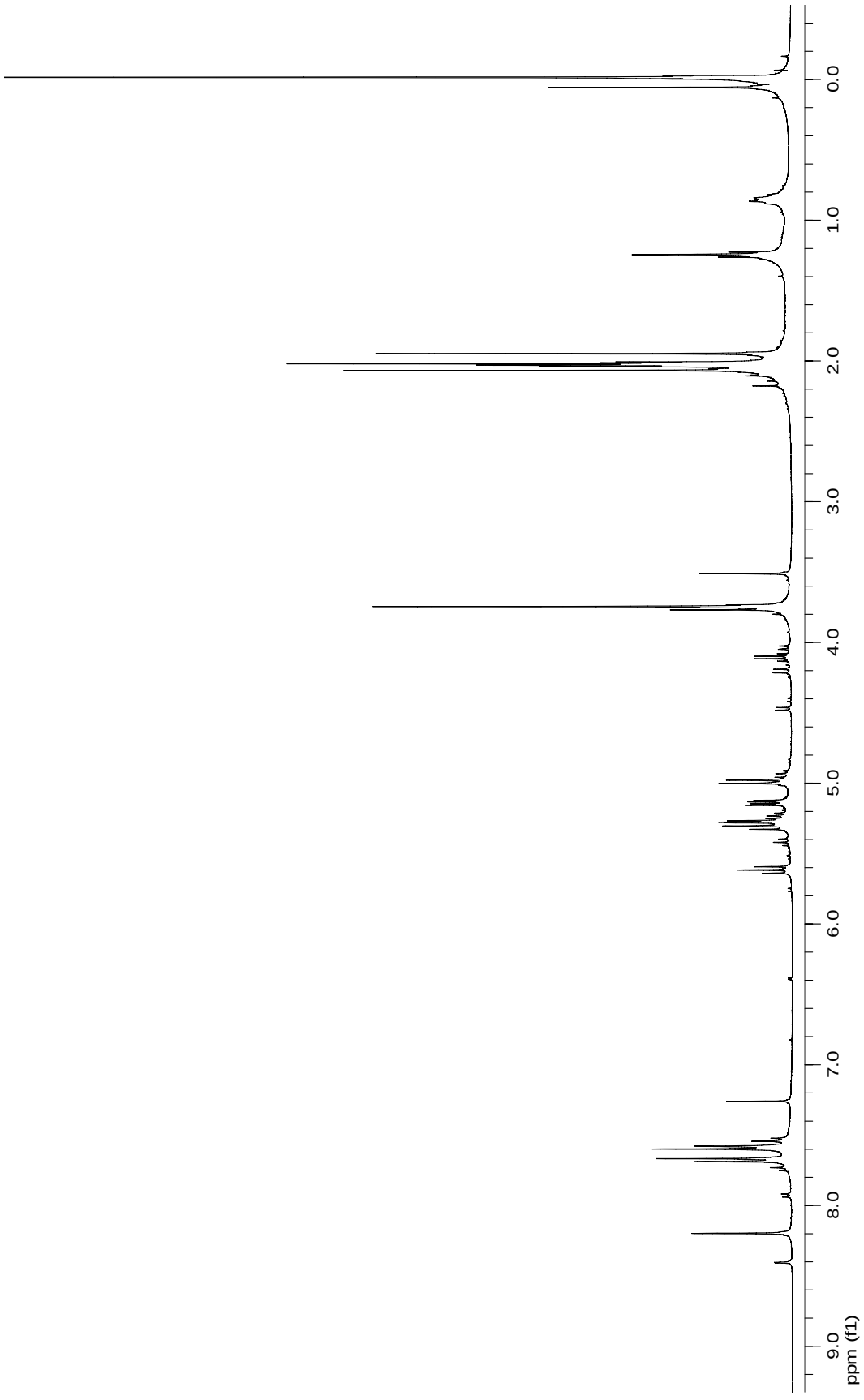

Figure 85: 400 MHz ^{1}H NMR spectrum of *p*-bromobenzoic acid-(α-D-glucopyranuronosyl)-imine (**42**).

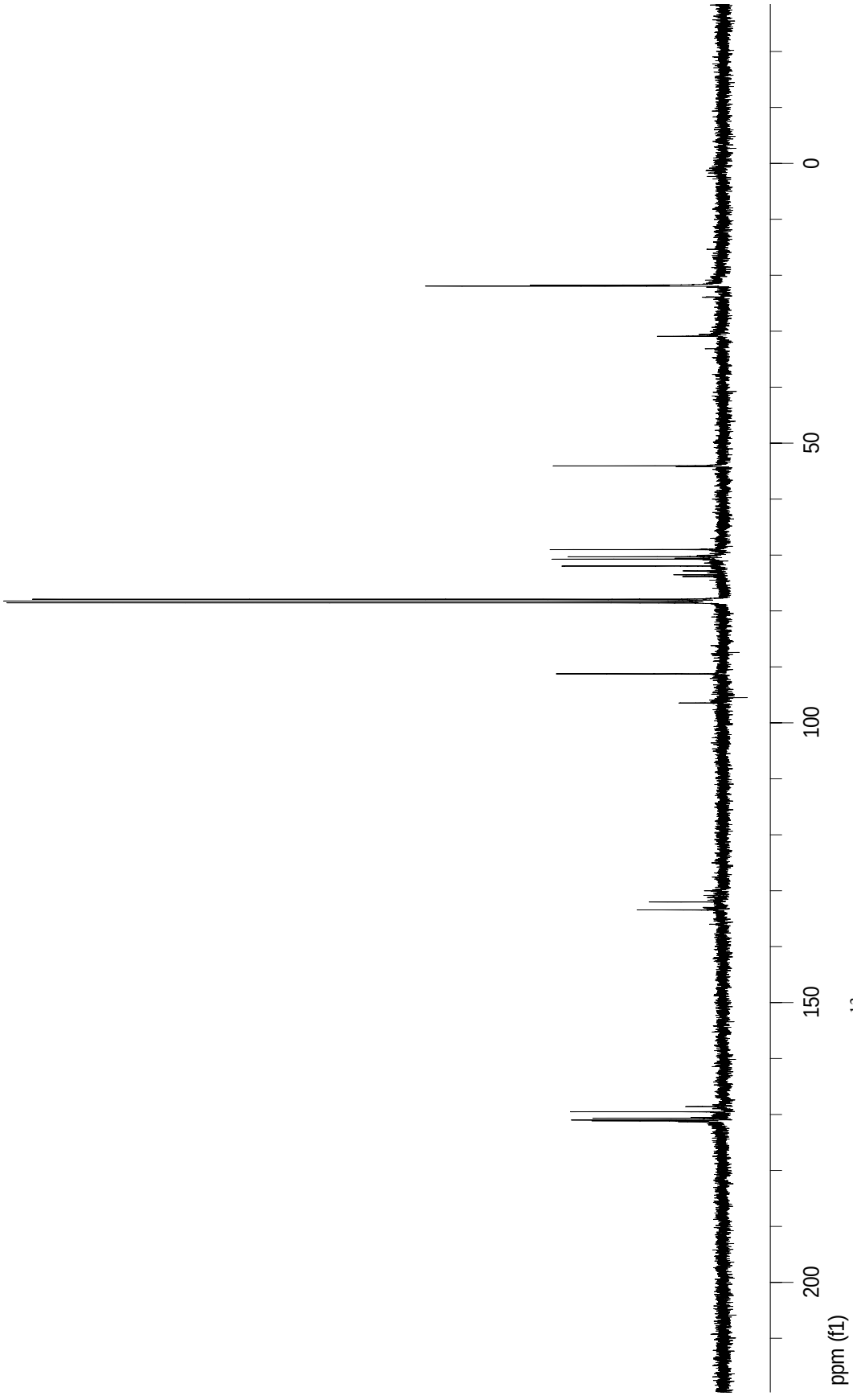

Figure 86: 100 MHz ^{13}C NMR spectrum of *p*-bromobenzoic acid-(α-D-glucopyranuronosyl)-imine (**42**).

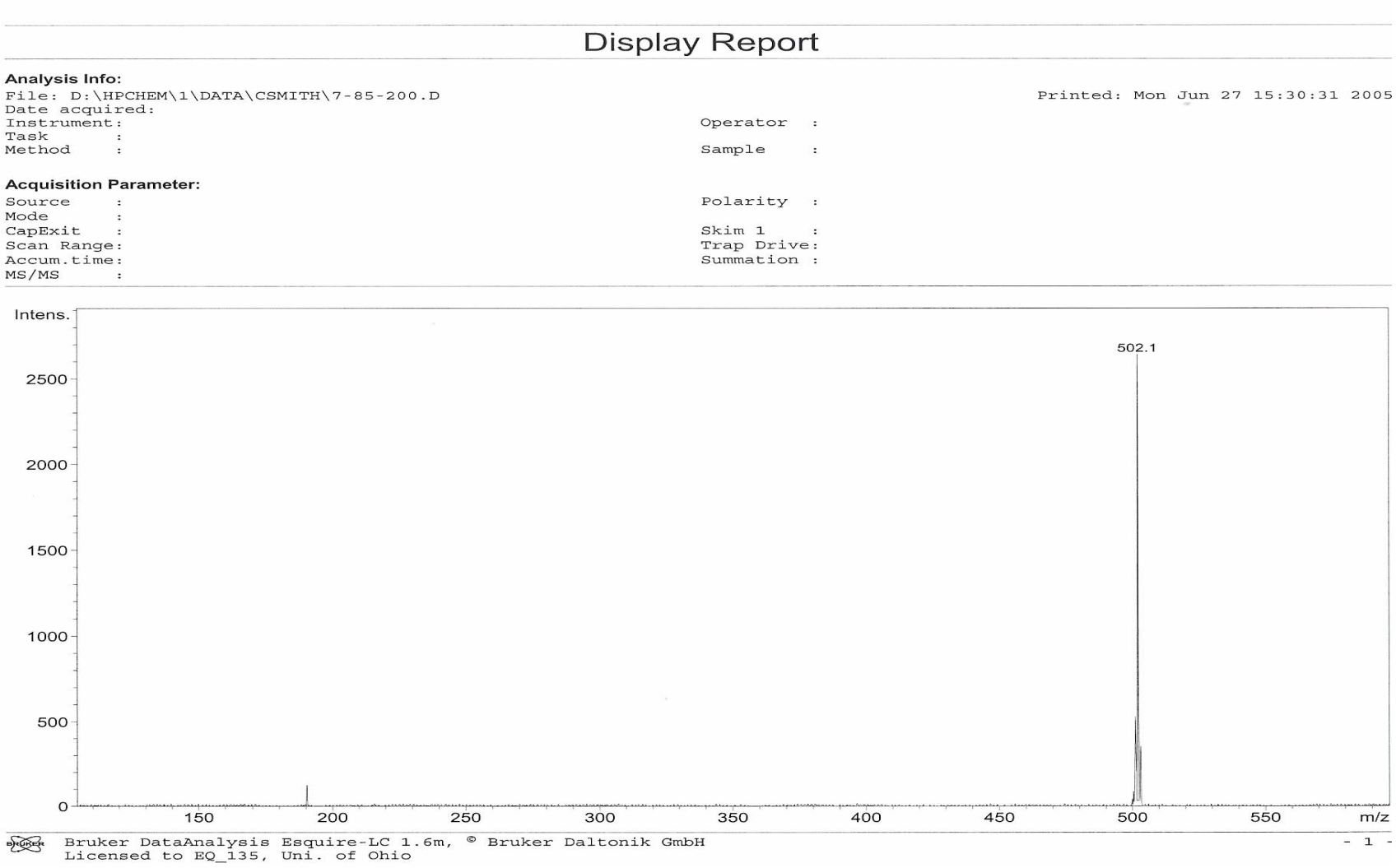

Figure 87: Mass spectrum of *p*-bromobenzoic acid-(α-D-glucopyranuronosyl)-imine (**42**).

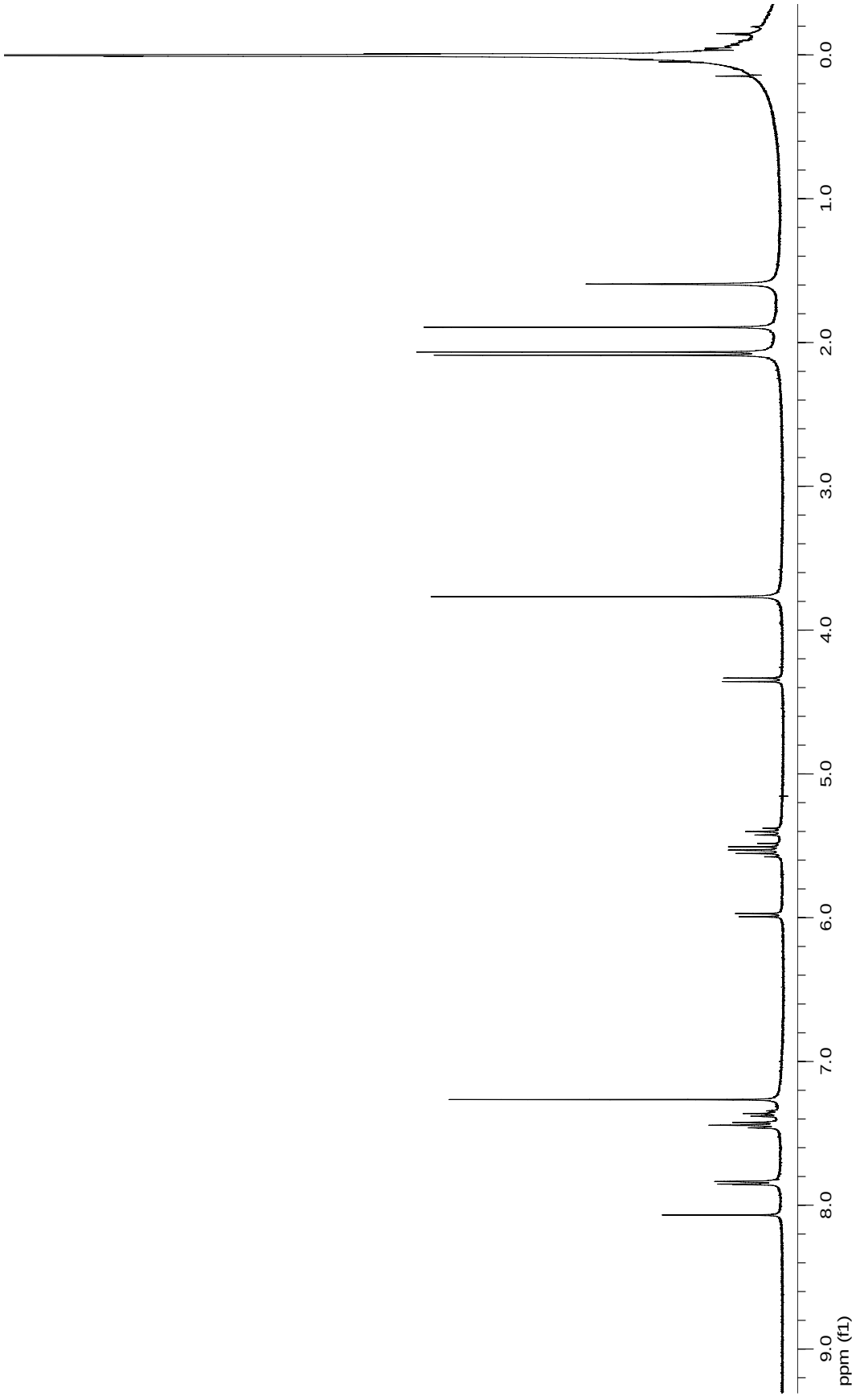

Figure 88: 400 MHz ^{1}H NMR spectrum of glucuronosyl-4-phenyl-1*H*-[1,2,3]-triazole (**43**).

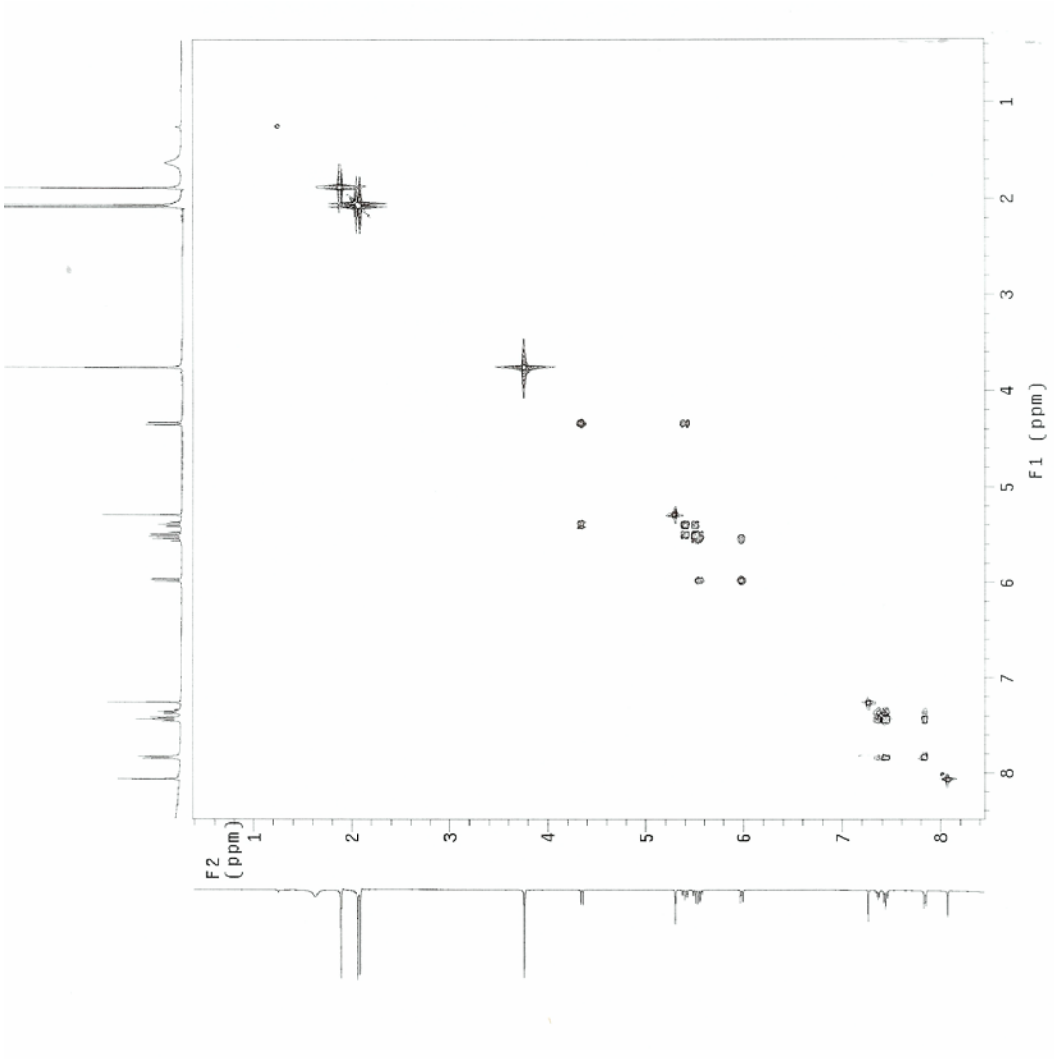

Figure 89: 400 MHz ^{1}H COSY NMR spectrum of glucuronosyl-4-phenyl-1*H*-[1,2,3]-triazole (**43**).

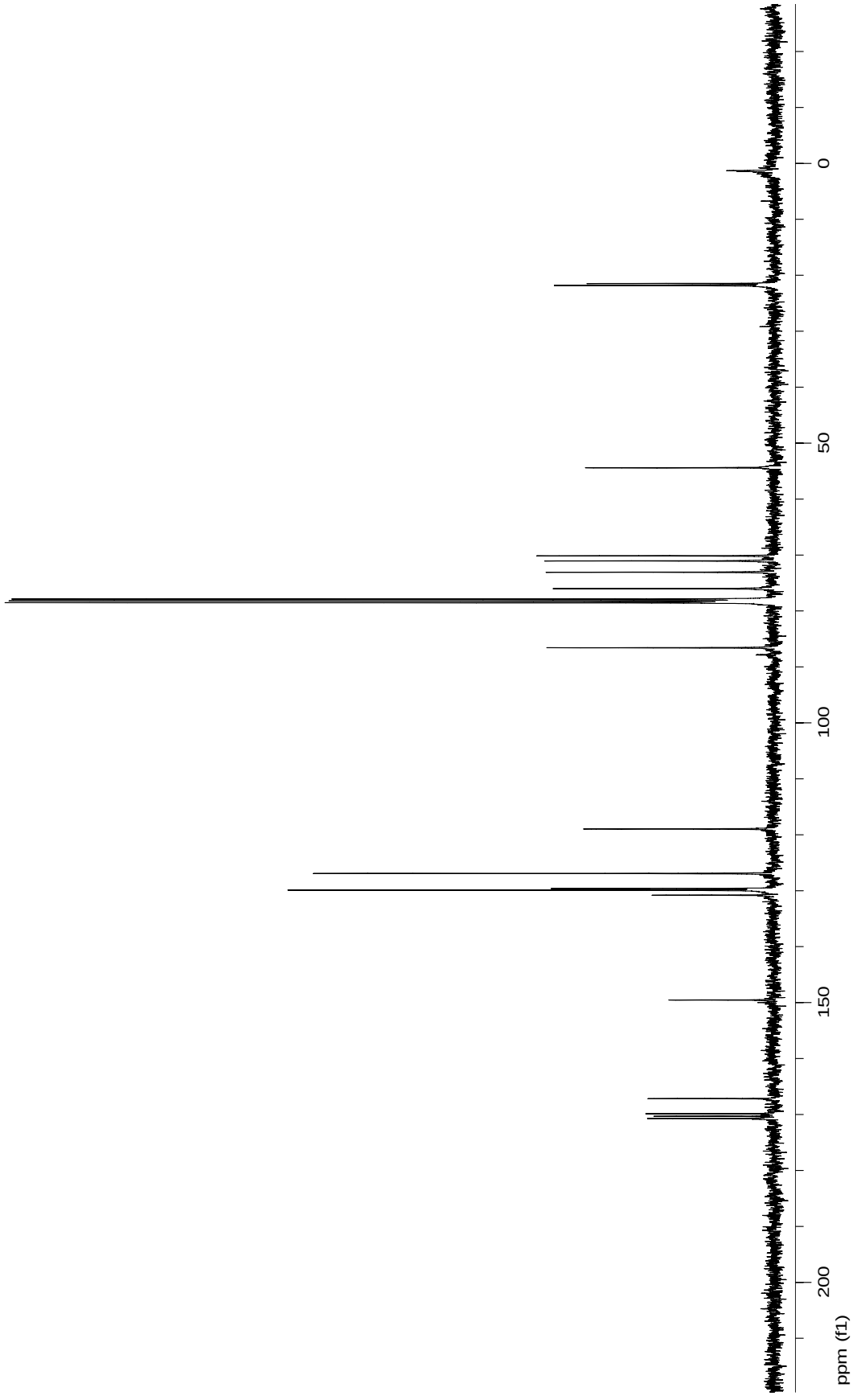

Figure 90: 100 MHz ^{13}C NMR spectrum of glucuronosyl-4-phenyl-1*H*-[1,2,3]-triazole (**43**).

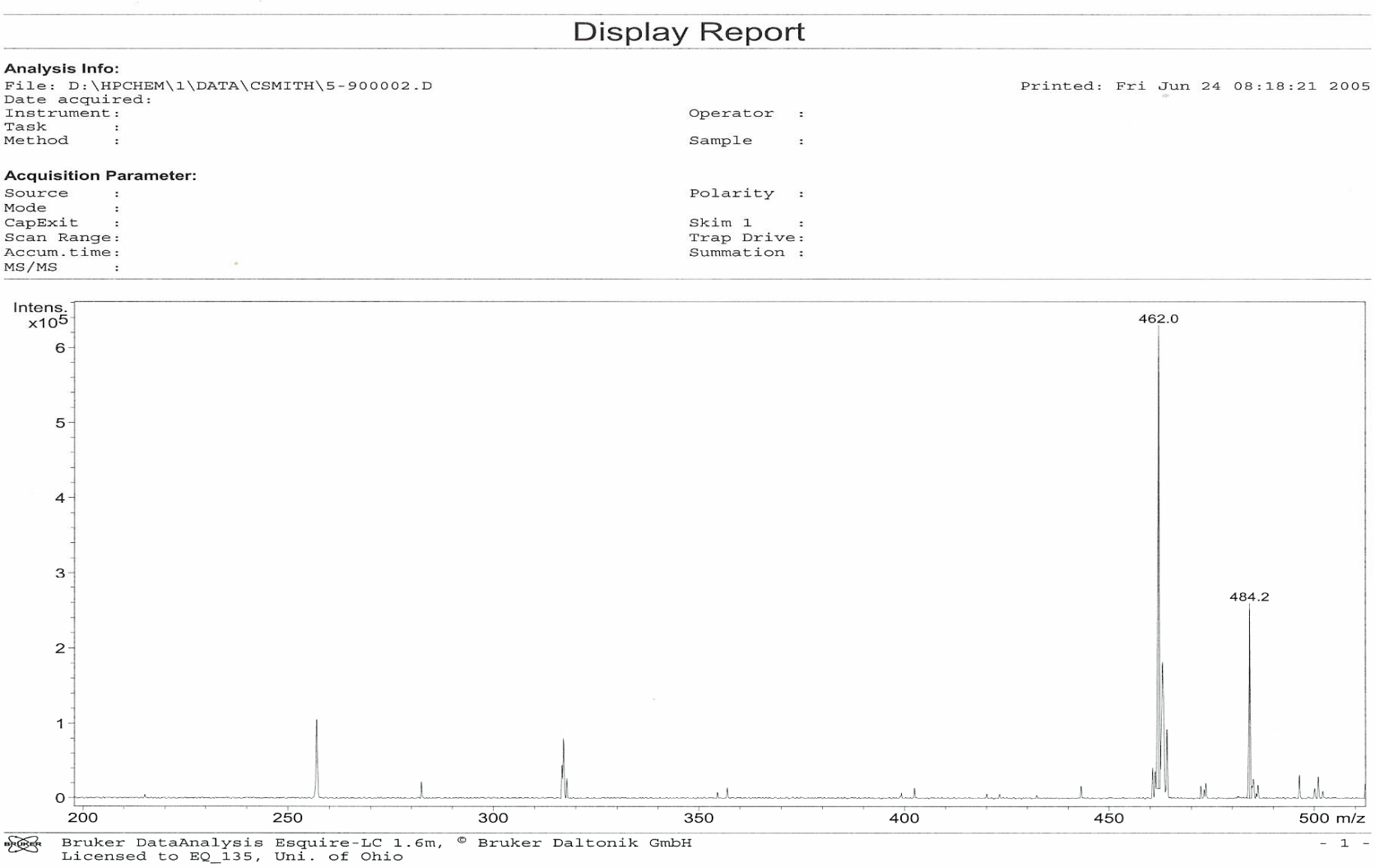

Figure 91: Mass spectrum of glucuronosyl-4-phenyl-1*H*-[1,2,3]-triazole (**43**).

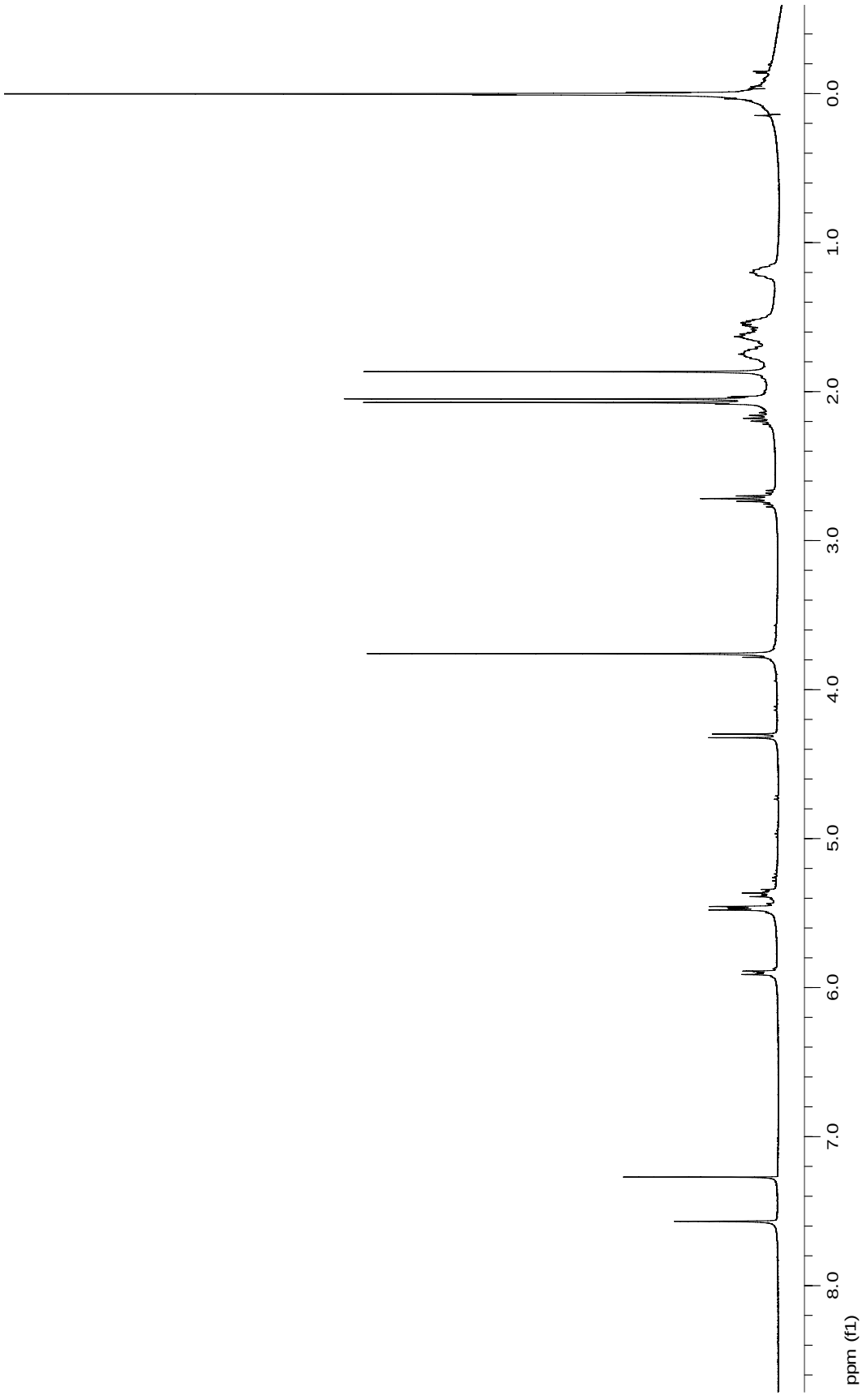

Figure 92: 400 MHz ^{1}H NMR spectrum of glucuronosyl-4-(methylcyclopentyl)-1*H*-[1,2,3]-triazole (**44**).

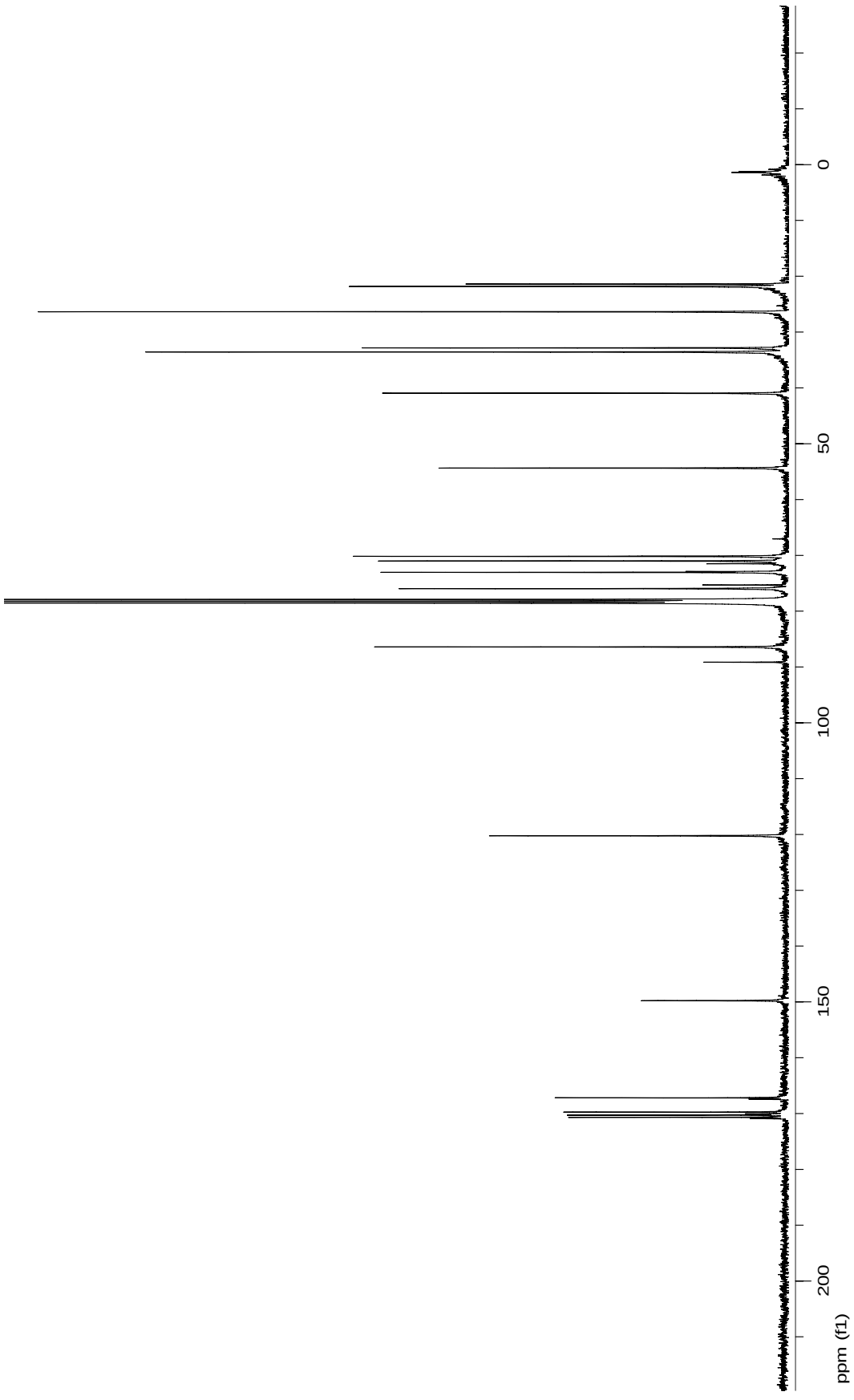

Figure 93: 100 MHz ^{13}C NMR spectrum of glucuronosyl-4-(methylcyclopentyl)-1*H*-[1,2,3]-triazole (**44**).

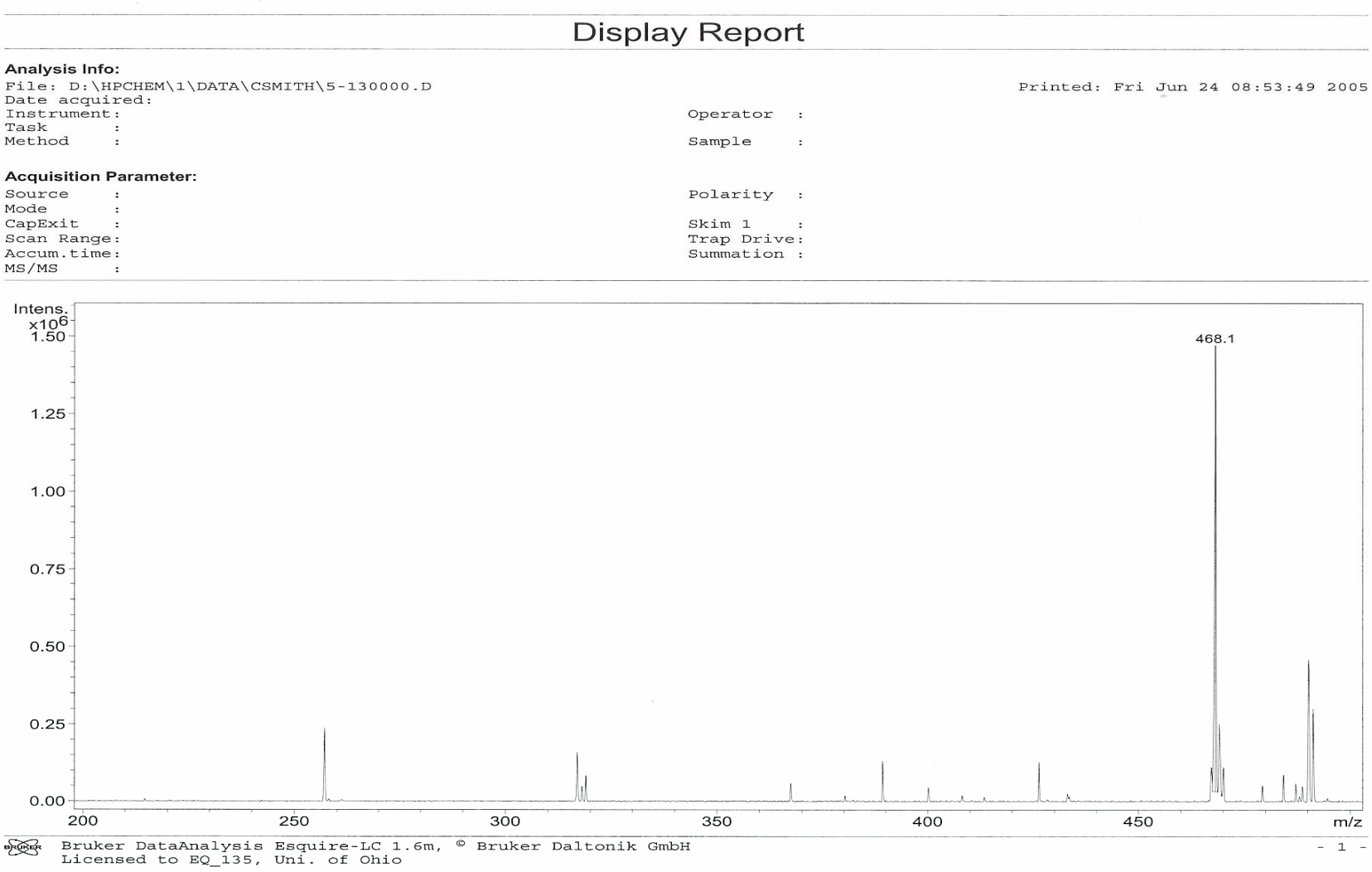

Figure 94: Mass spectrum of glucuronosyl-4-(methylcyclopentyl)-1*H*-[1,2,3]-triazole (**44**).

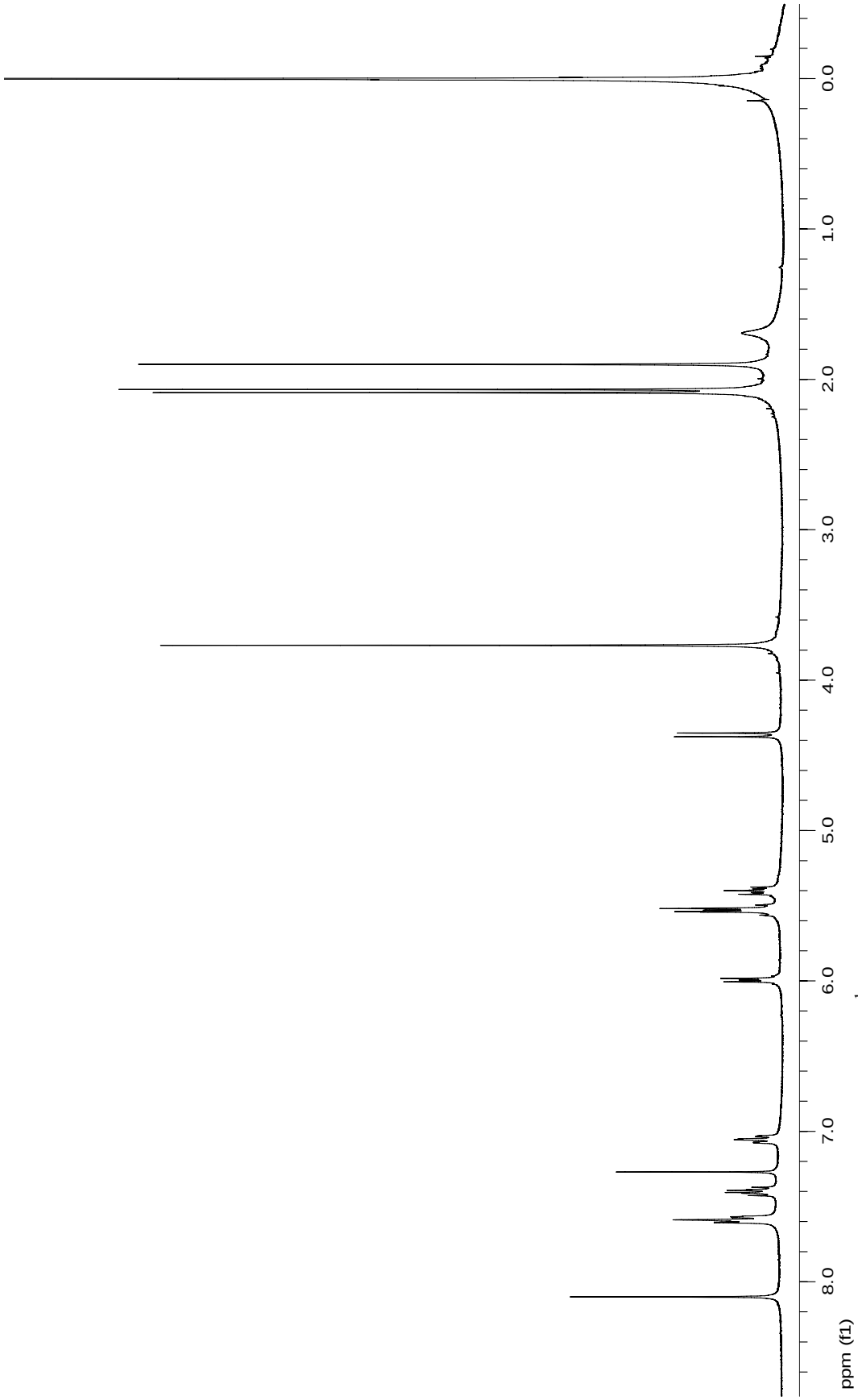

Figure 95: 400 MHz ^{1}H NMR spectrum of glucuronosyl-4-(3-fluorophenyl)-1*H*-[1,2,3]-triazole (**45**).

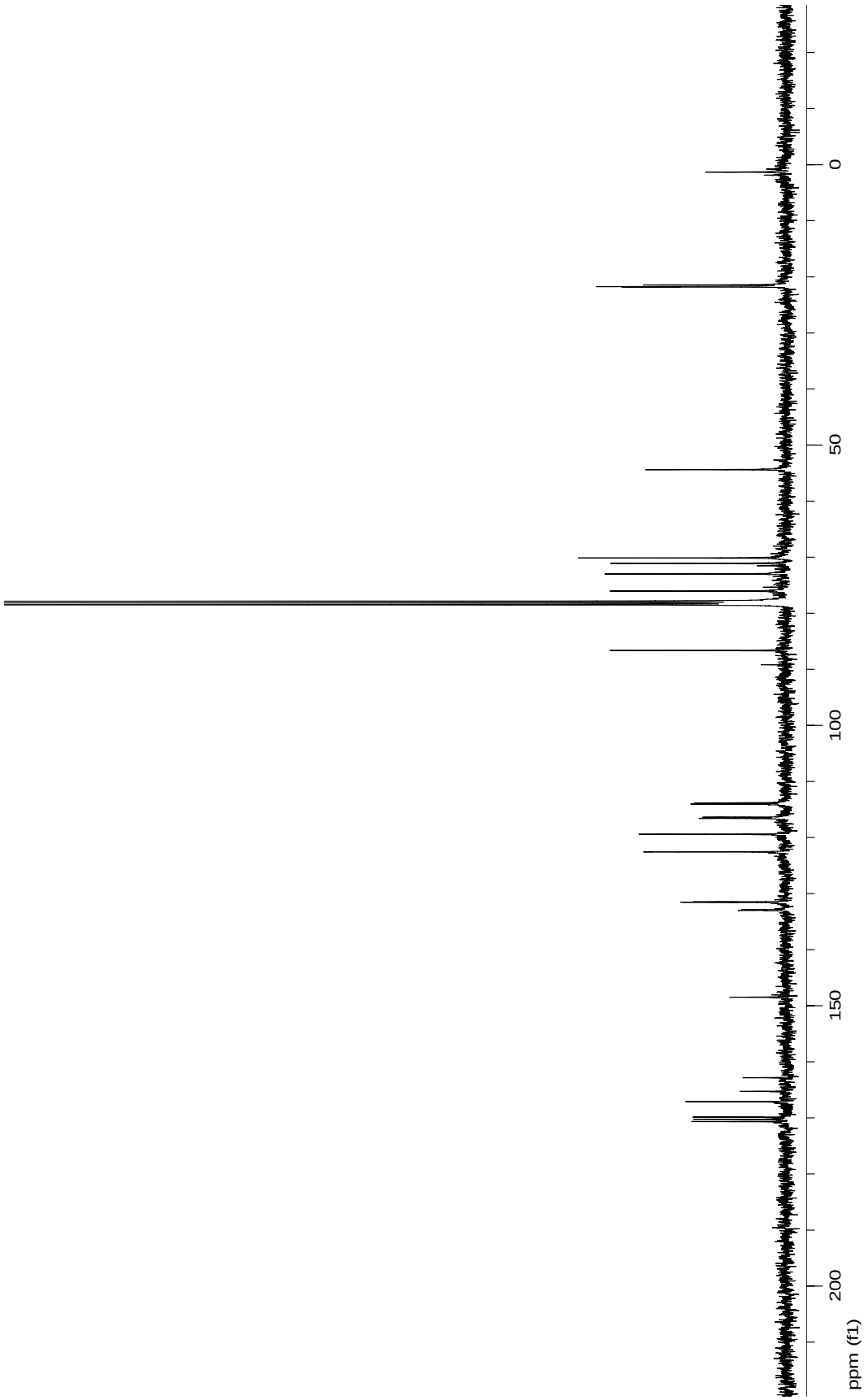

Figure 96: 100 MHz ^{13}C NMR spectrum of glucuronosyl-4-(3-fluorophenyl)-1*H*-[1,2,3]-triazole (**45**).

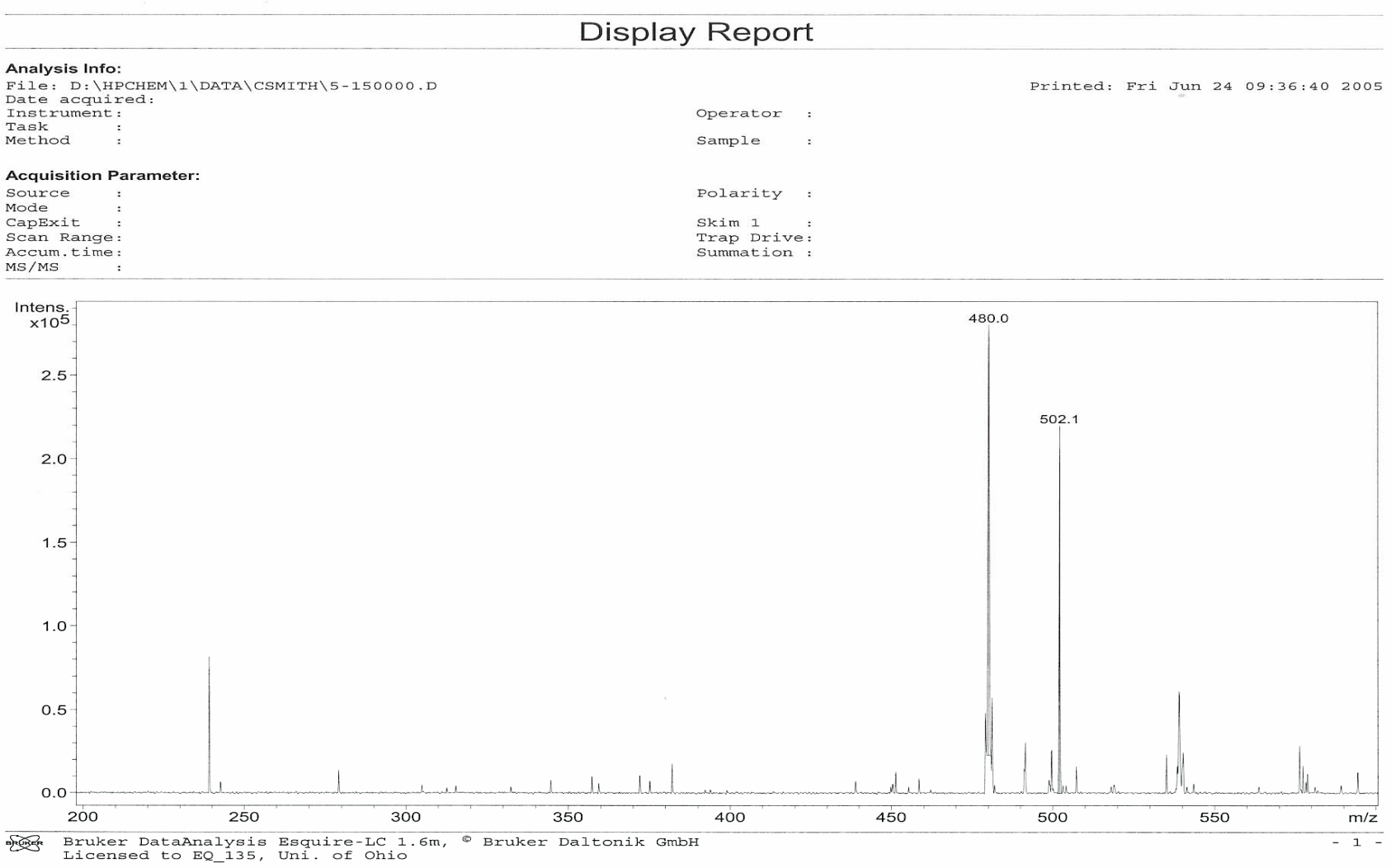

Figure 97: Mass spectrum of glucuronosyl-4-(3-fluorophenyl)-1*H*-[1,2,3]-triazole (**45**).

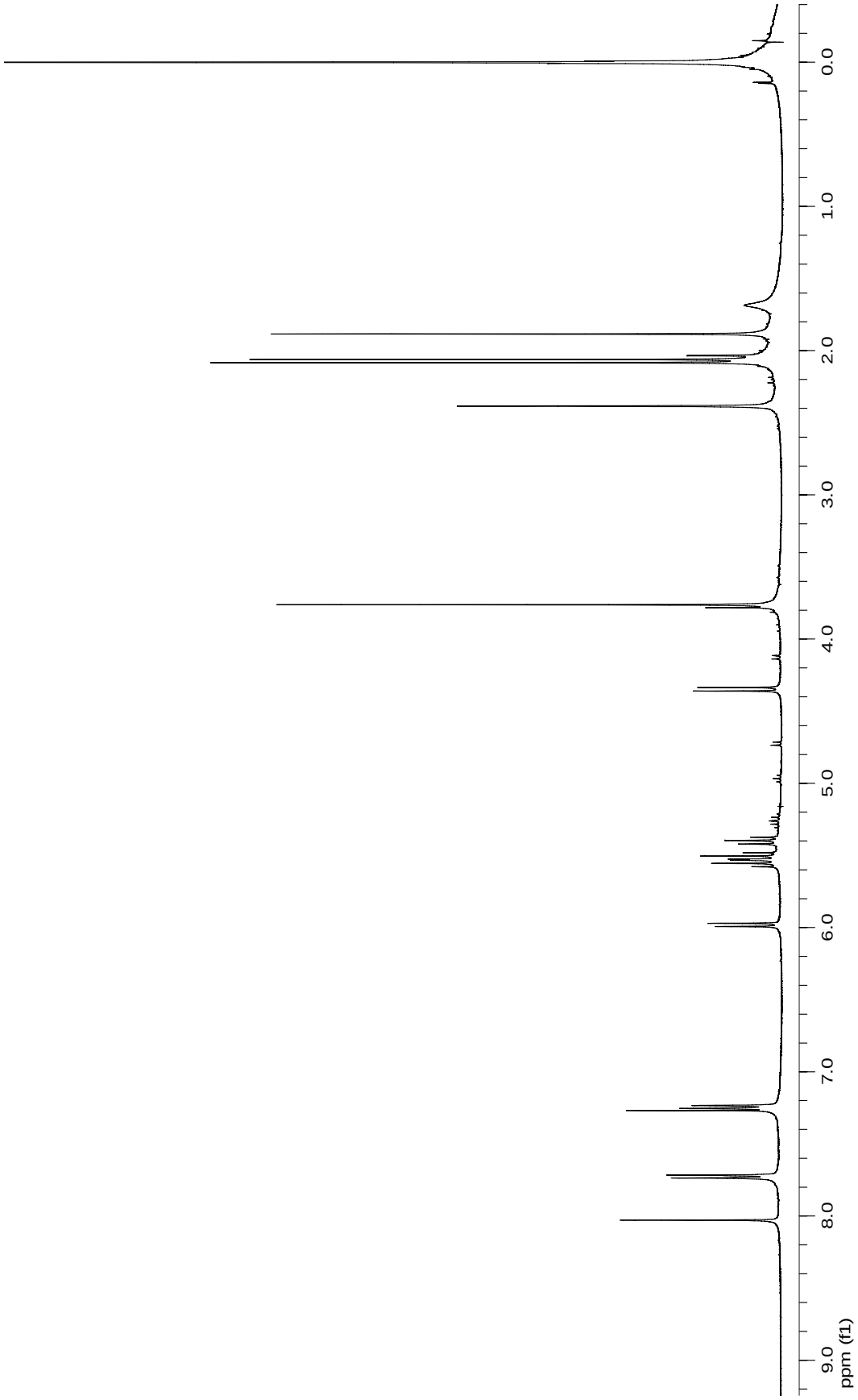

Figure 98: 400 MHz ^{1}H NMR spectrum of glucuronosyl-4-(4-methylphenyl)-1*H*-[1,2,3]-triazole (**46**).

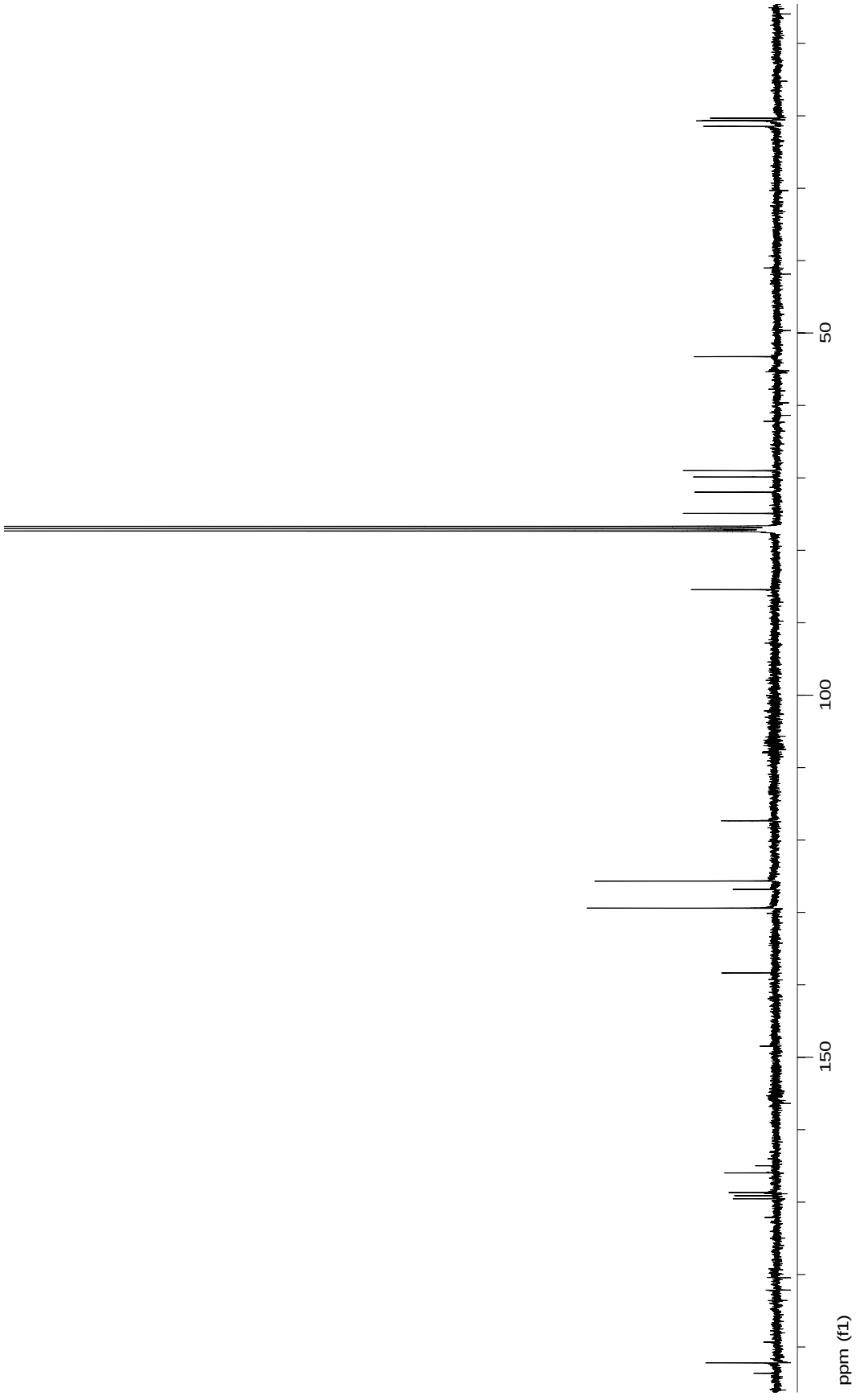

Figure 99: 100 MHz ^{13}C NMR spectrum of glucuronosyl-4-(4-methylphenyl)-1*H*-[1,2,3]-triazole (**46**).

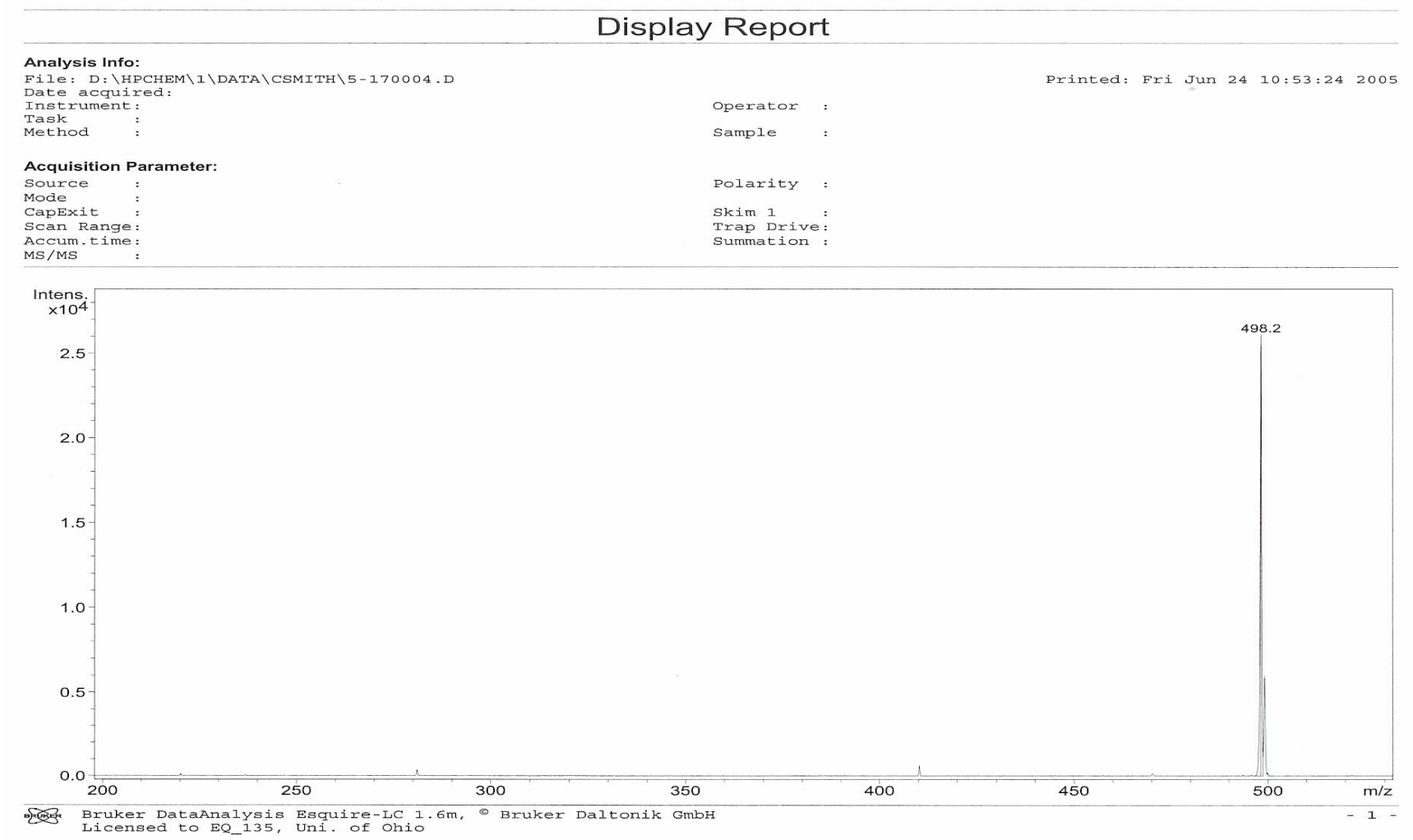

Figure 100: Mass spectrum of glucuronosyl-4-(4-methylphenyl)-1*H*-[1,2,3]-triazole (**46**).

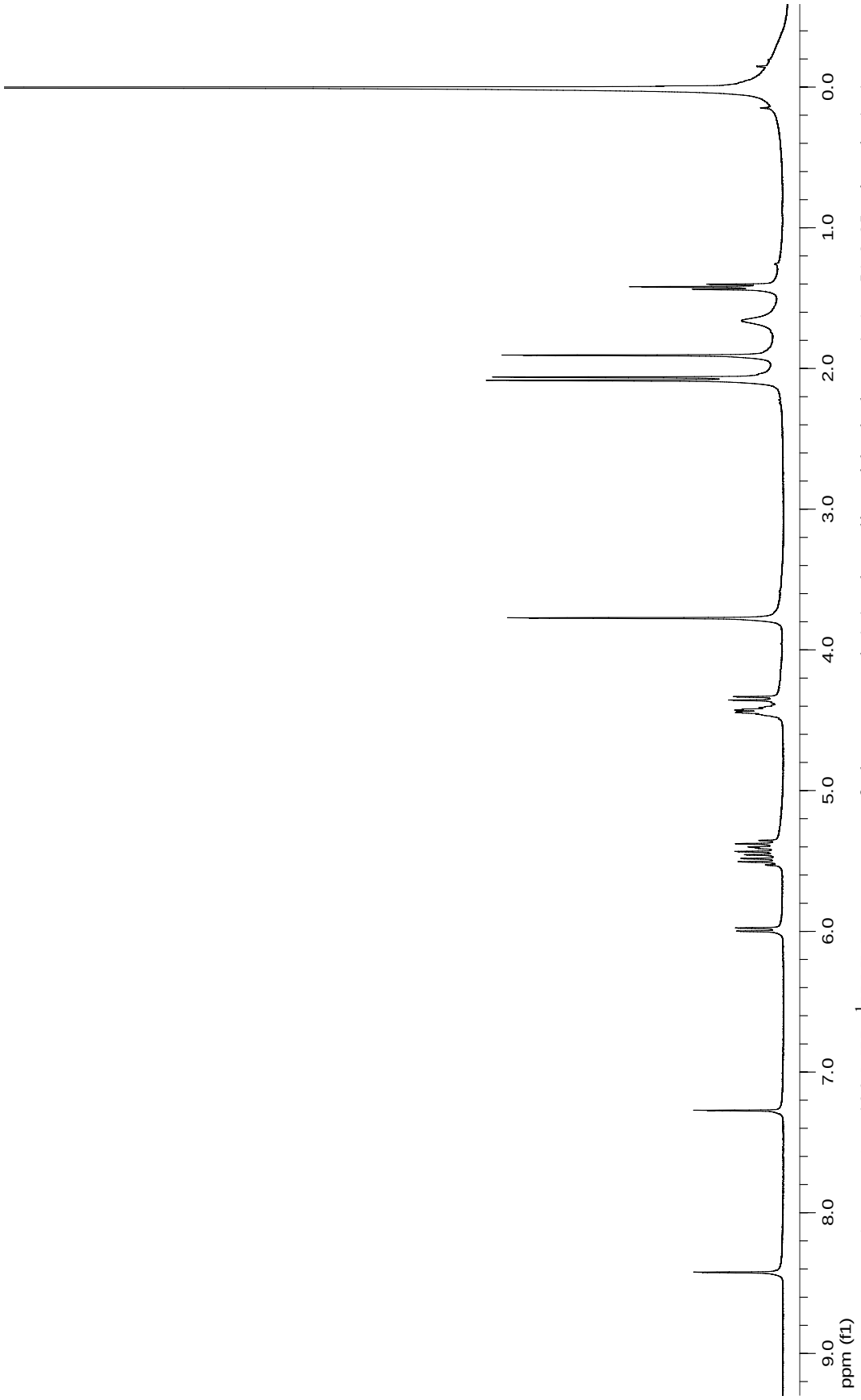

Figure 101: 400 MHz ^{1}H NMR spectrum of glucuronosyl-4-(carboxylic acid ethyl ester)-1*H*-[1,2,3]-triazole (**47**).

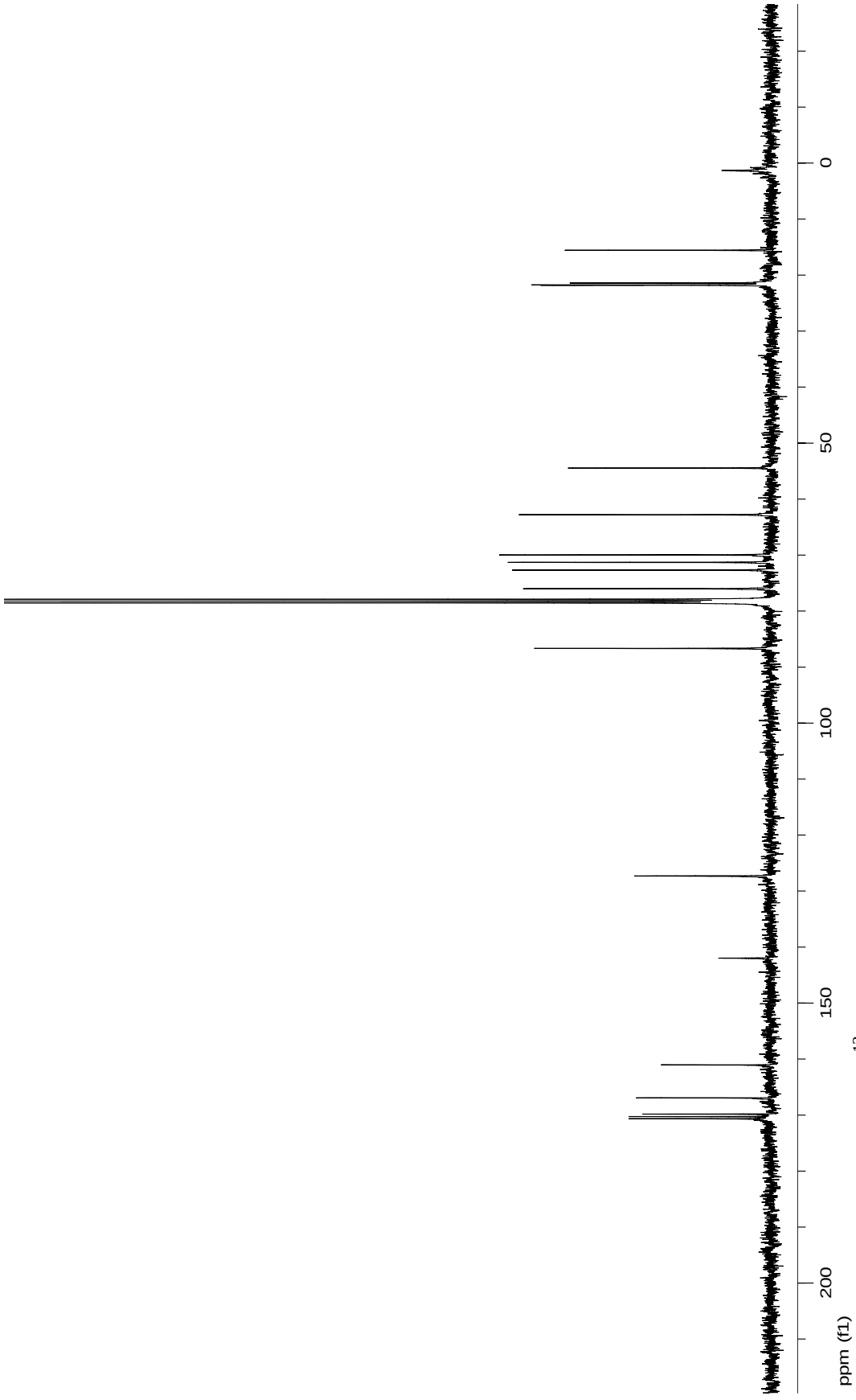

Figure 102: 100 MHz ^{13}C NMR spectrum of glucuronosyl-4-(carboxylic acid ethyl ester)-1*H*-[1,2,3]-triazole (**47**).

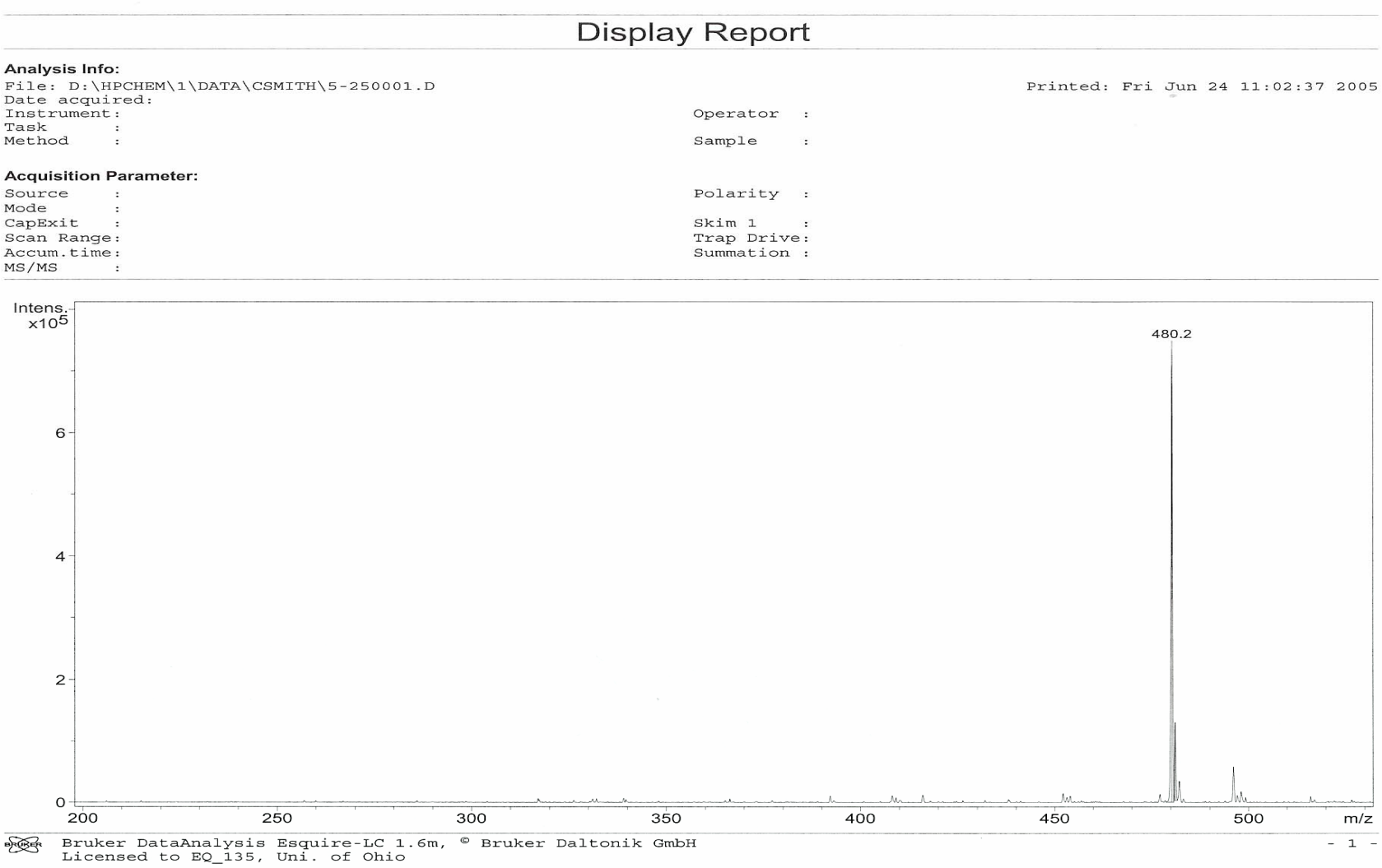

Figure 103: Mass spectrum of glucuronosyl-4-(carboxylic acid ethyl ester)-1*H*-[1,2,3]-triazole (**47**).

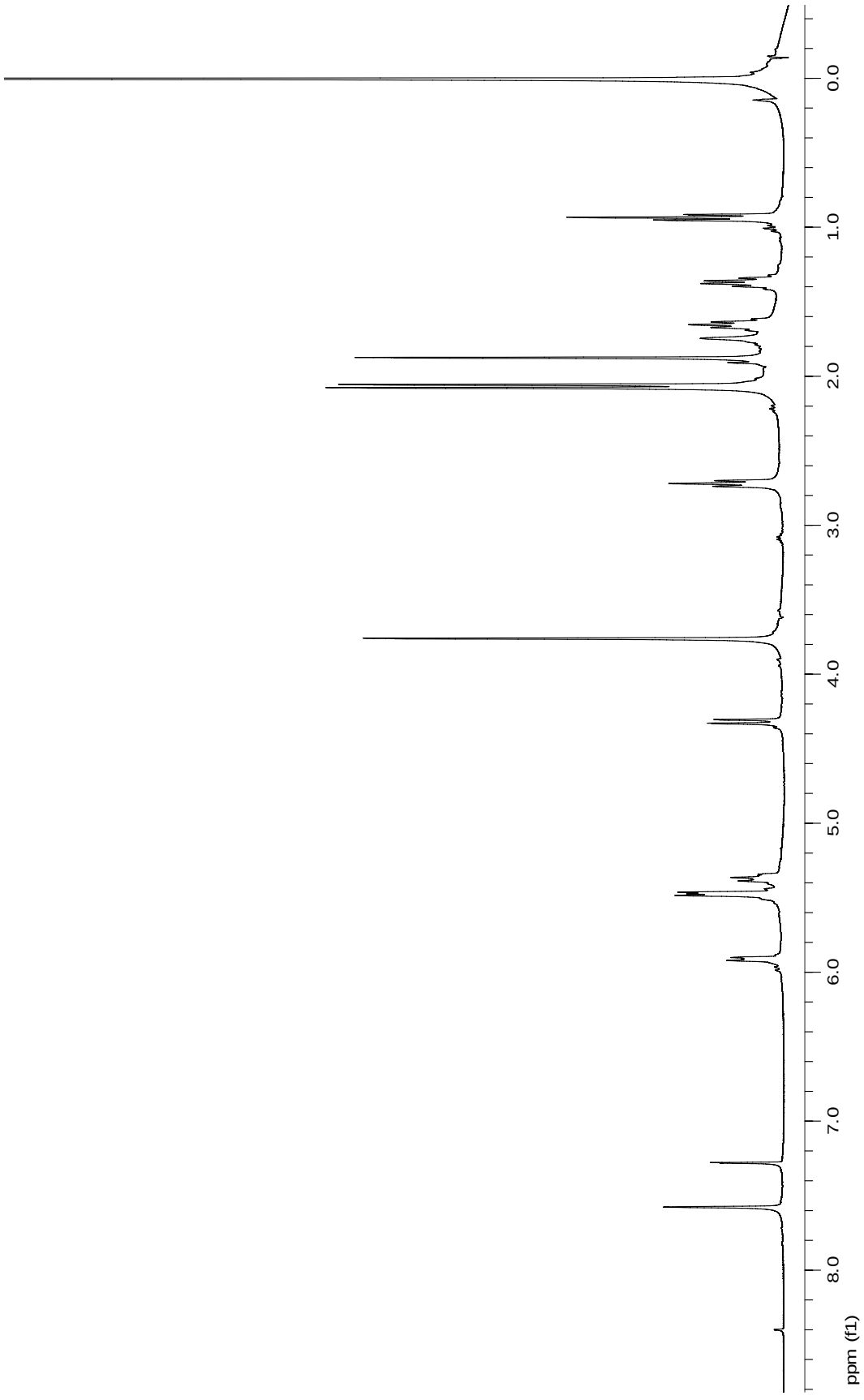

Figure 104: 400 MHz ^{1}H NMR spectrum of glucuronosyl-4-butyl-1*H*-[1,2,3]-triazole (**48**).

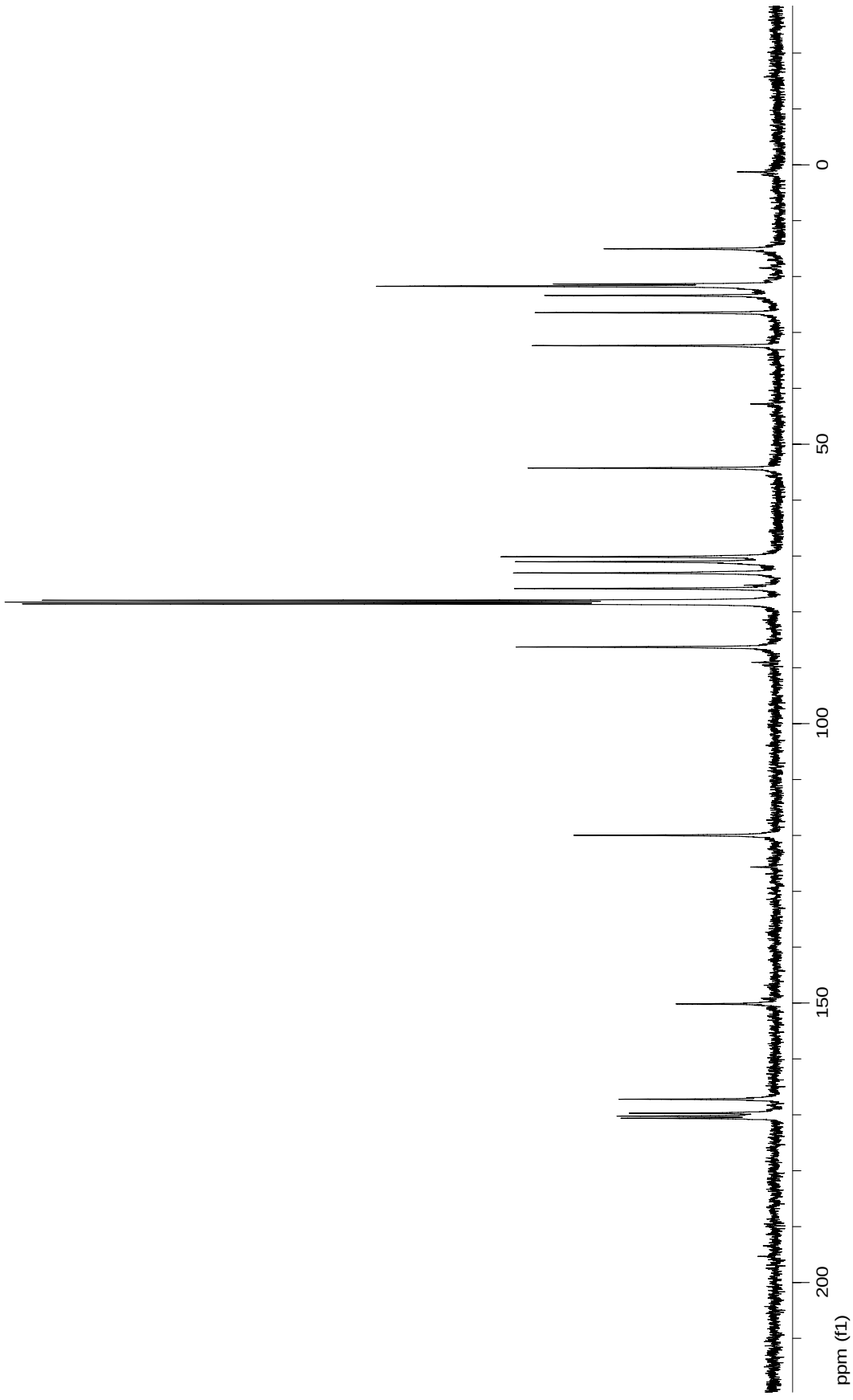

Figure 105: 100 MHz ^{13}C NMR spectrum of glucuronosyl-4-butyl-1*H*-[1,2,3]-triazole (**48**).

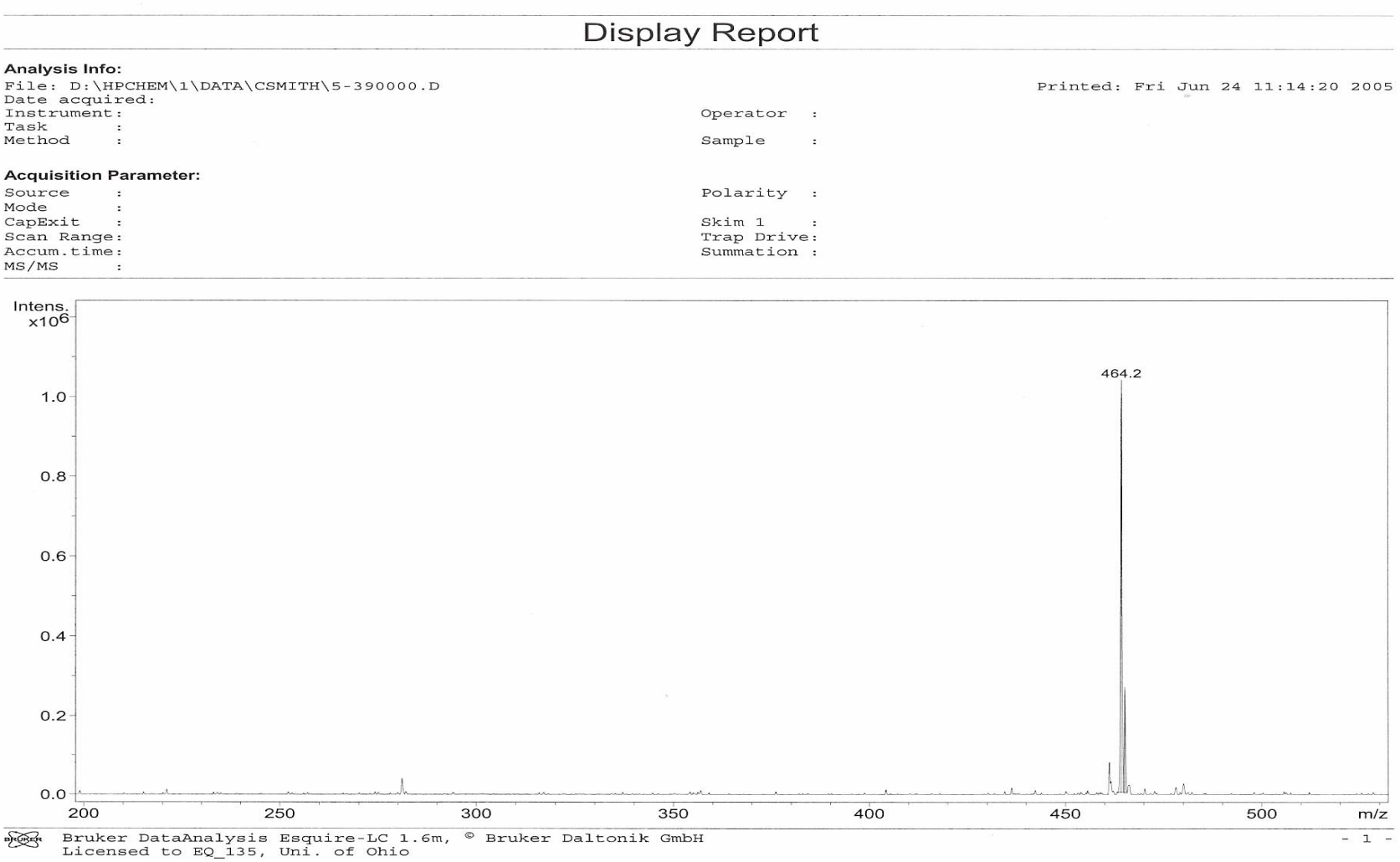

Figure 106: Mass spectrum of glucuronosyl-4-butyl-1*H*-[1,2,3]-triazole (**48**).

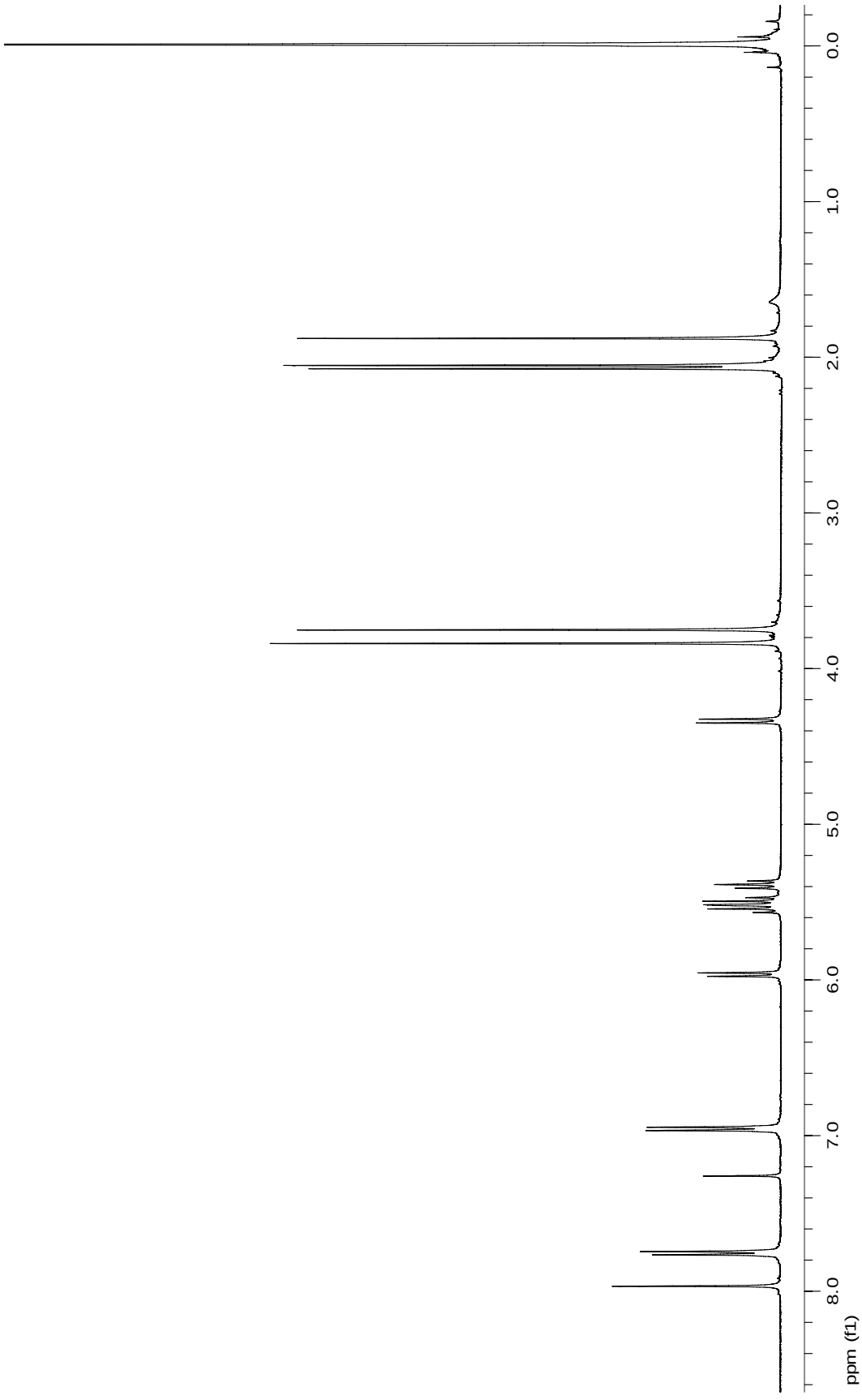

Figure 107: 400 MHz ^{1}H NMR spectrum of glucuronosyl-4-(4-methoxyphenyl)-1*H*-[1,2,3]-triazole (**49**).

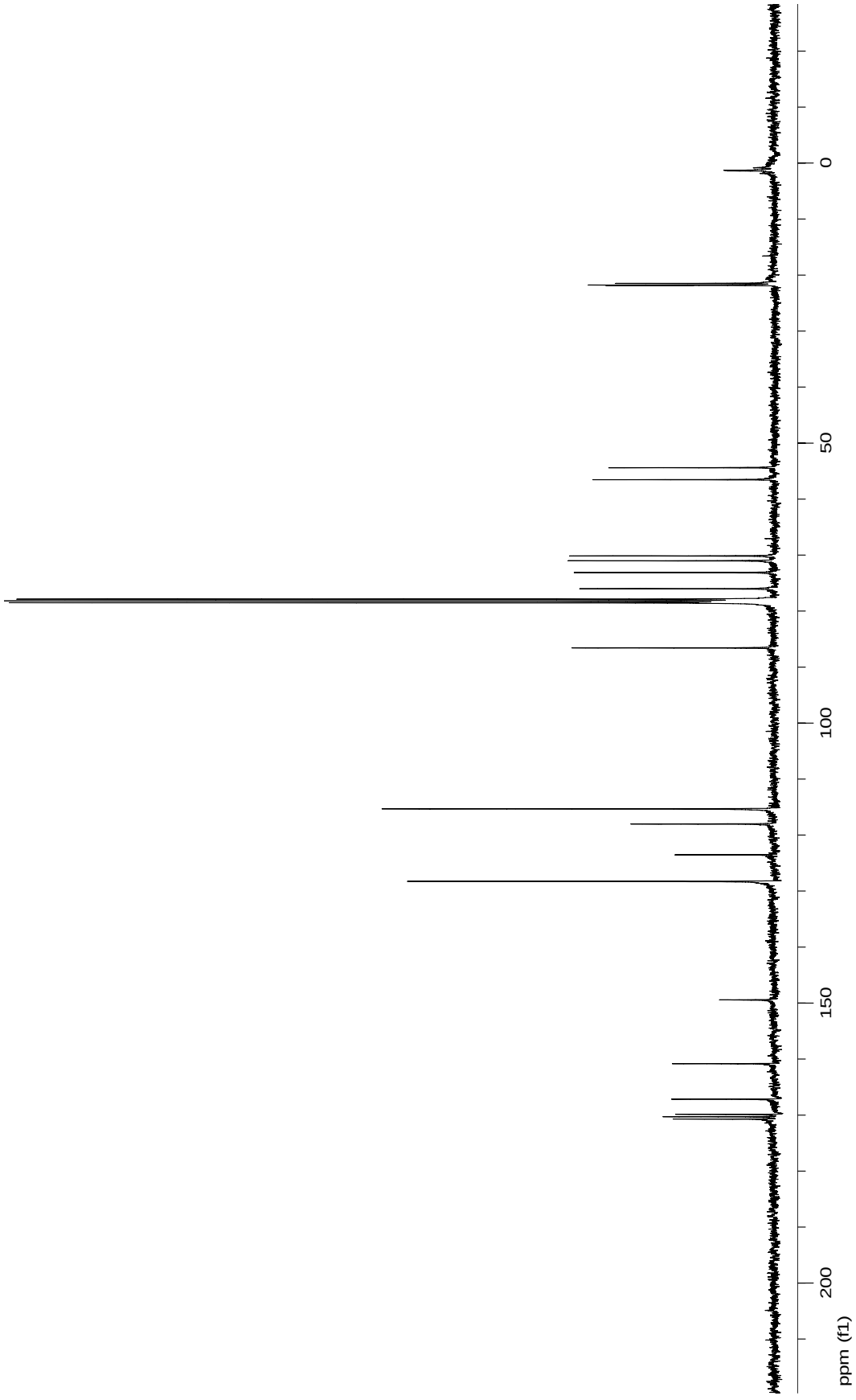

Figure 108: 100 MHz ^{13}C NMR spectrum of glucuronosyl-4-(4-methoxyphenyl)-1*H*-[1,2,3]-triazole (**49**).

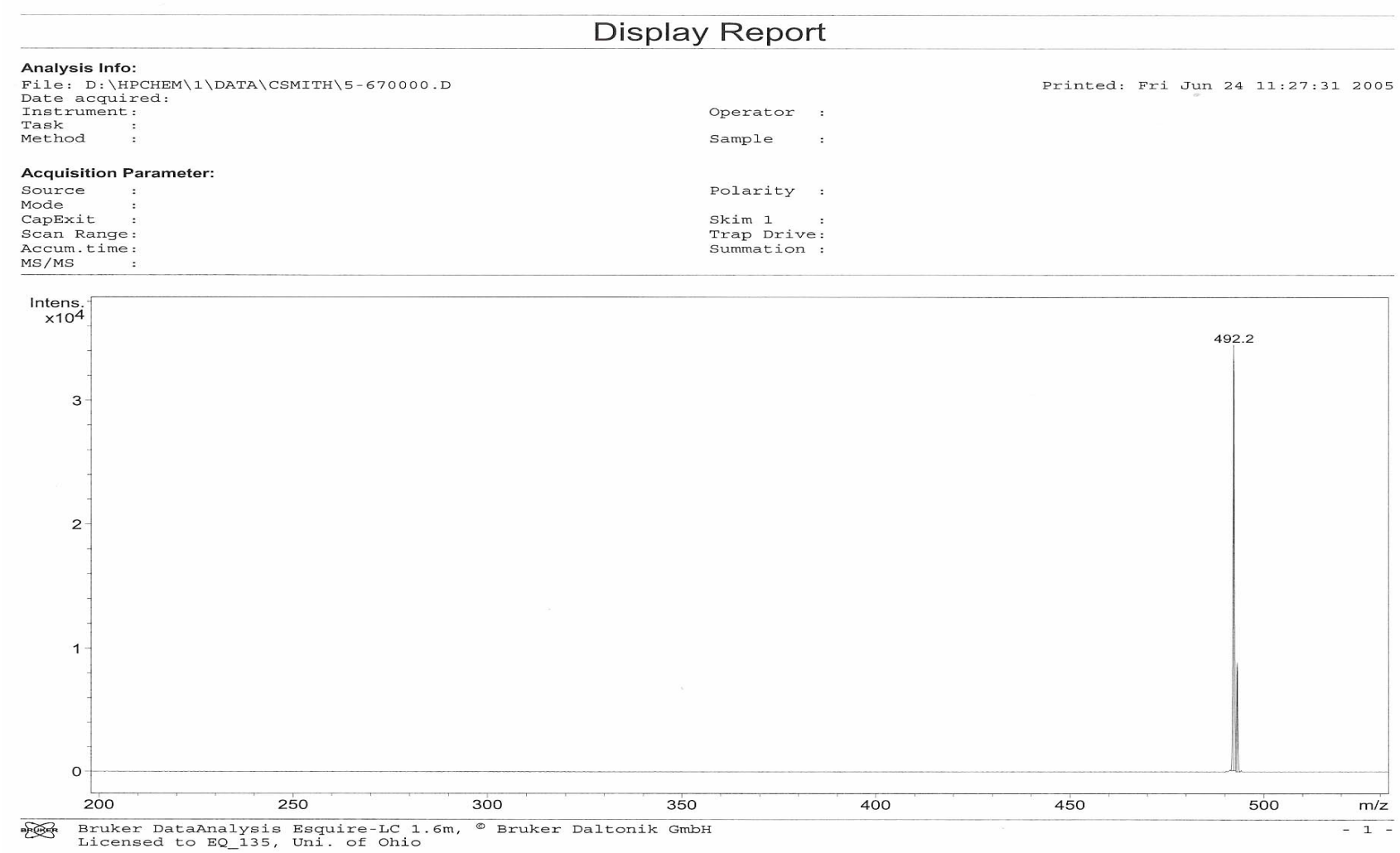

Figure 109: Mass spectrum of glucuronosyl-4-(4-methoxyphenyl)-1*H*-[1,2,3]-triazole (**49**).

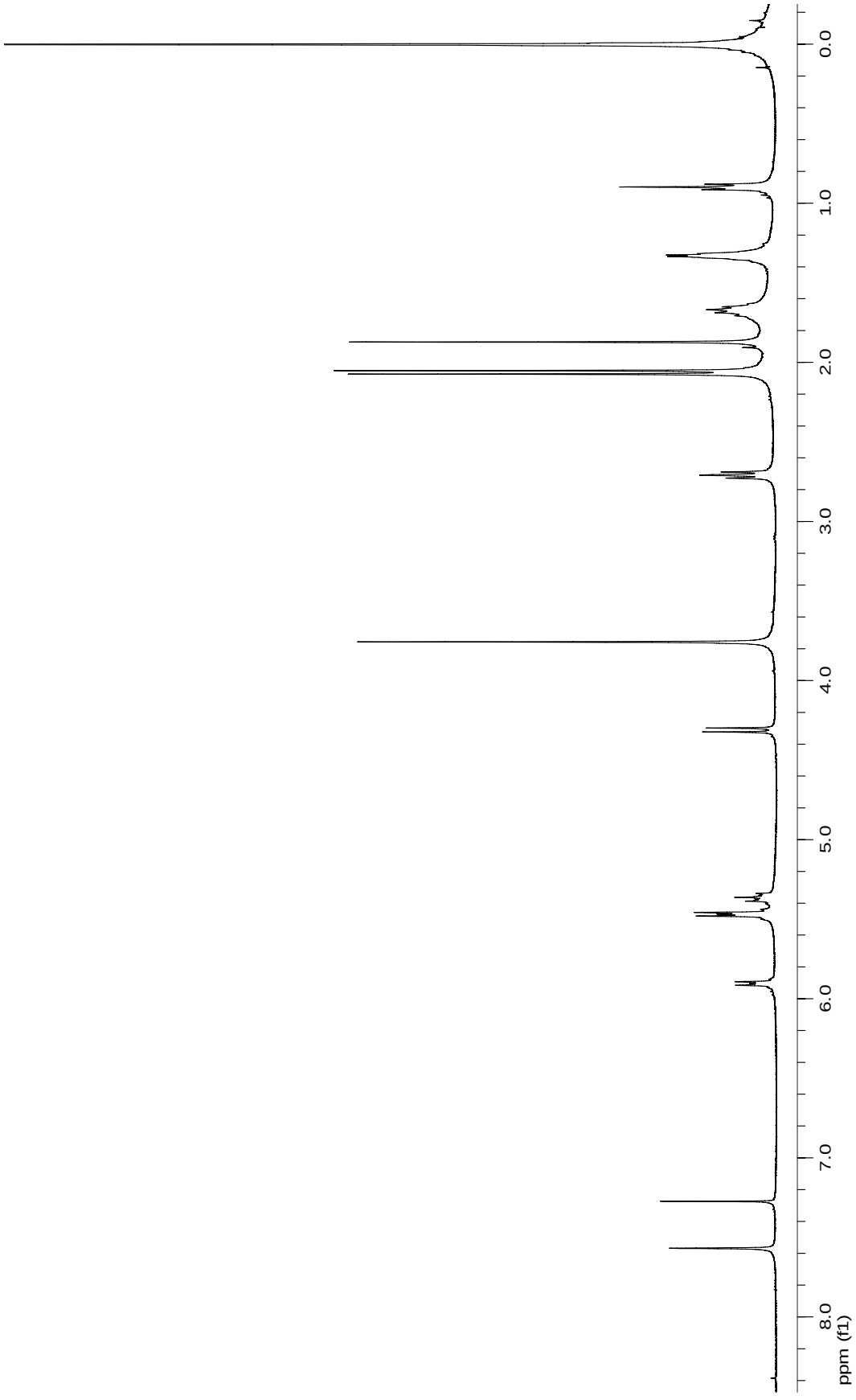

Figure 110: 400 MHz ^{1}H NMR spectrum of glucuronosyl-4-pentyl-1*H*-[1,2,3]-triazole (**50**).

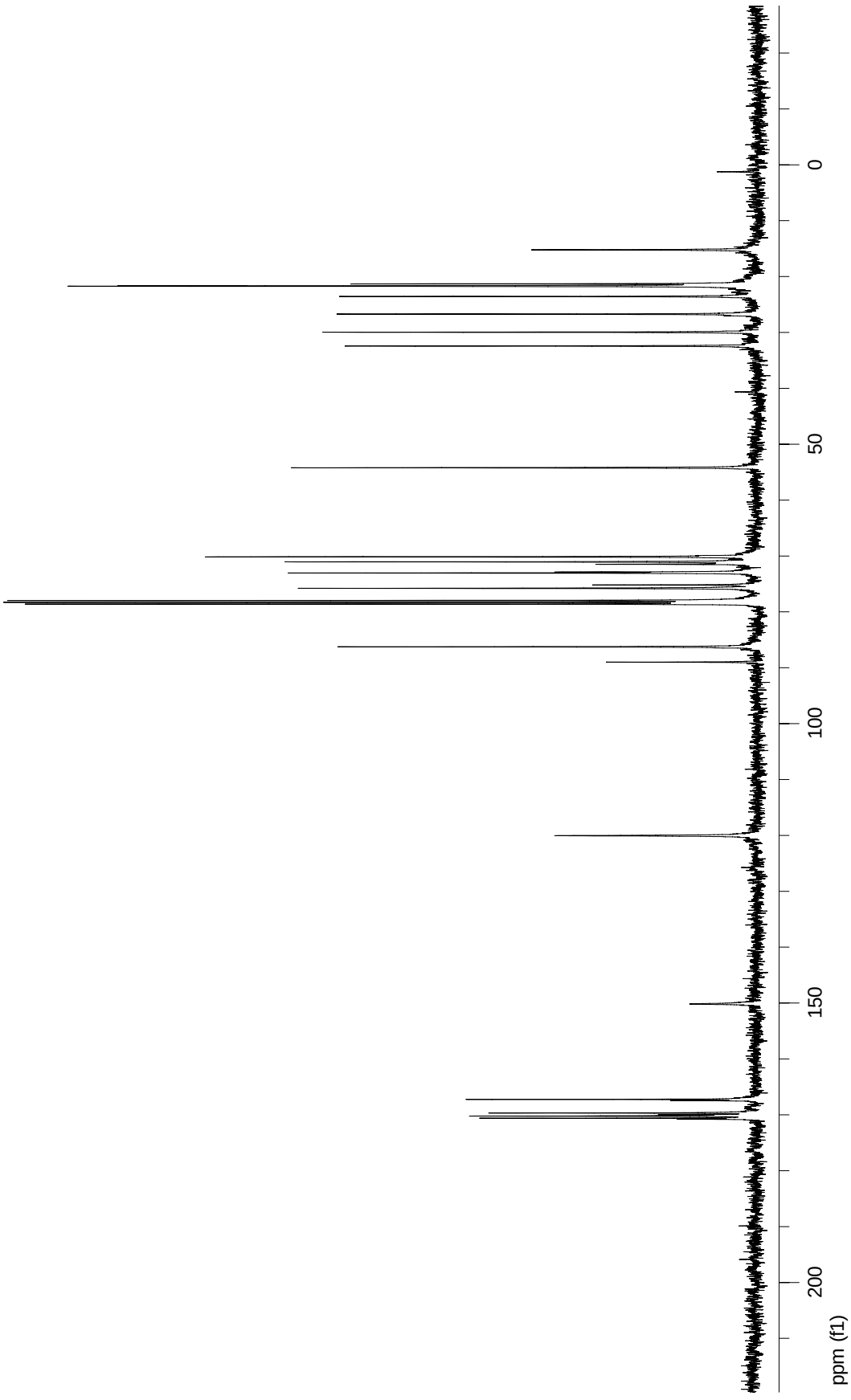

Figure 111: 100 MHz ^{13}C NMR spectrum of glucuronosyl-4-pentyl-1*H*-[1,2,3]-triazole (**50**).

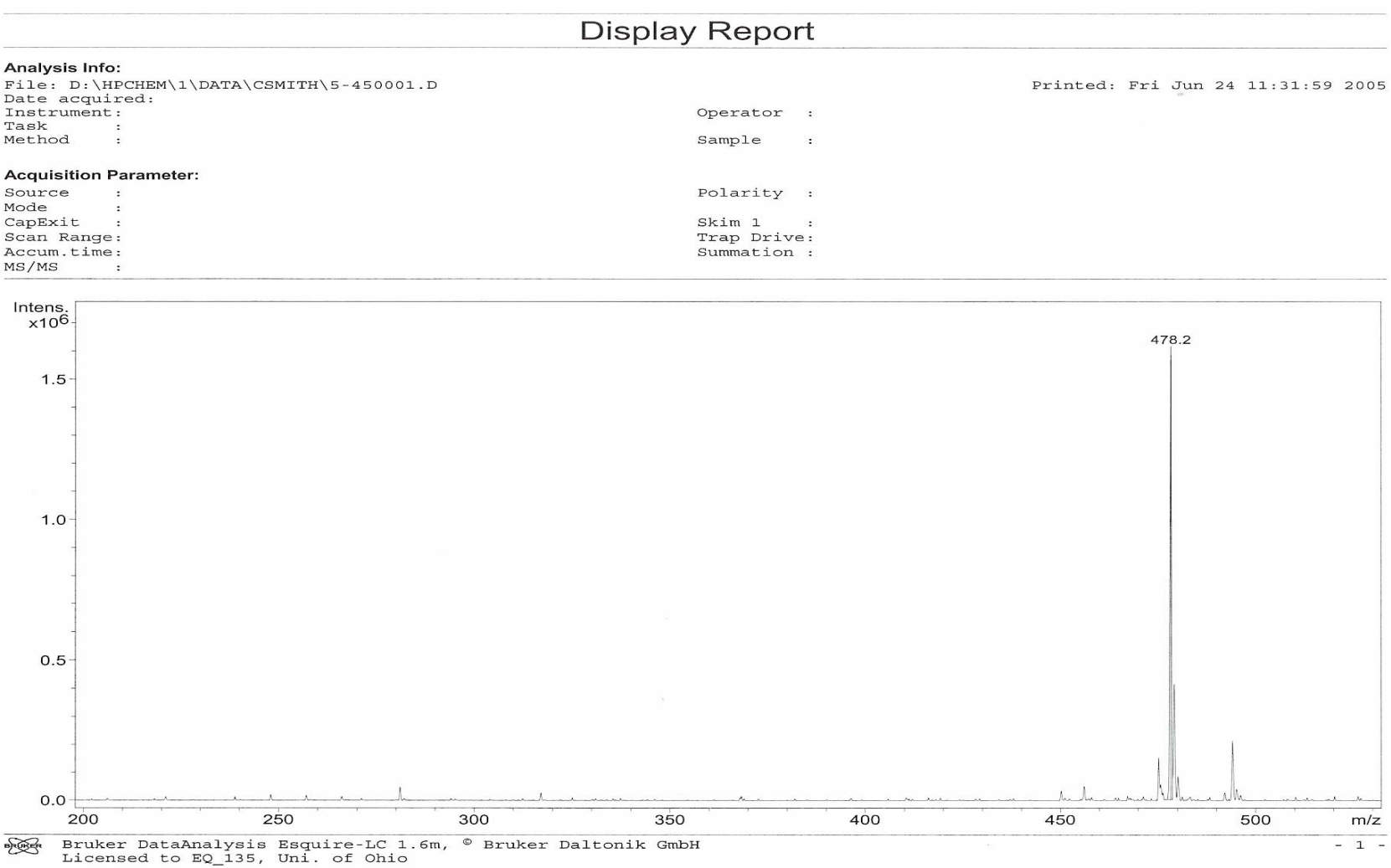

Figure 112: Mass spectrum of glucuronosyl-4-pentyl-1*H*-[1,2,3]-triazole (**50**).

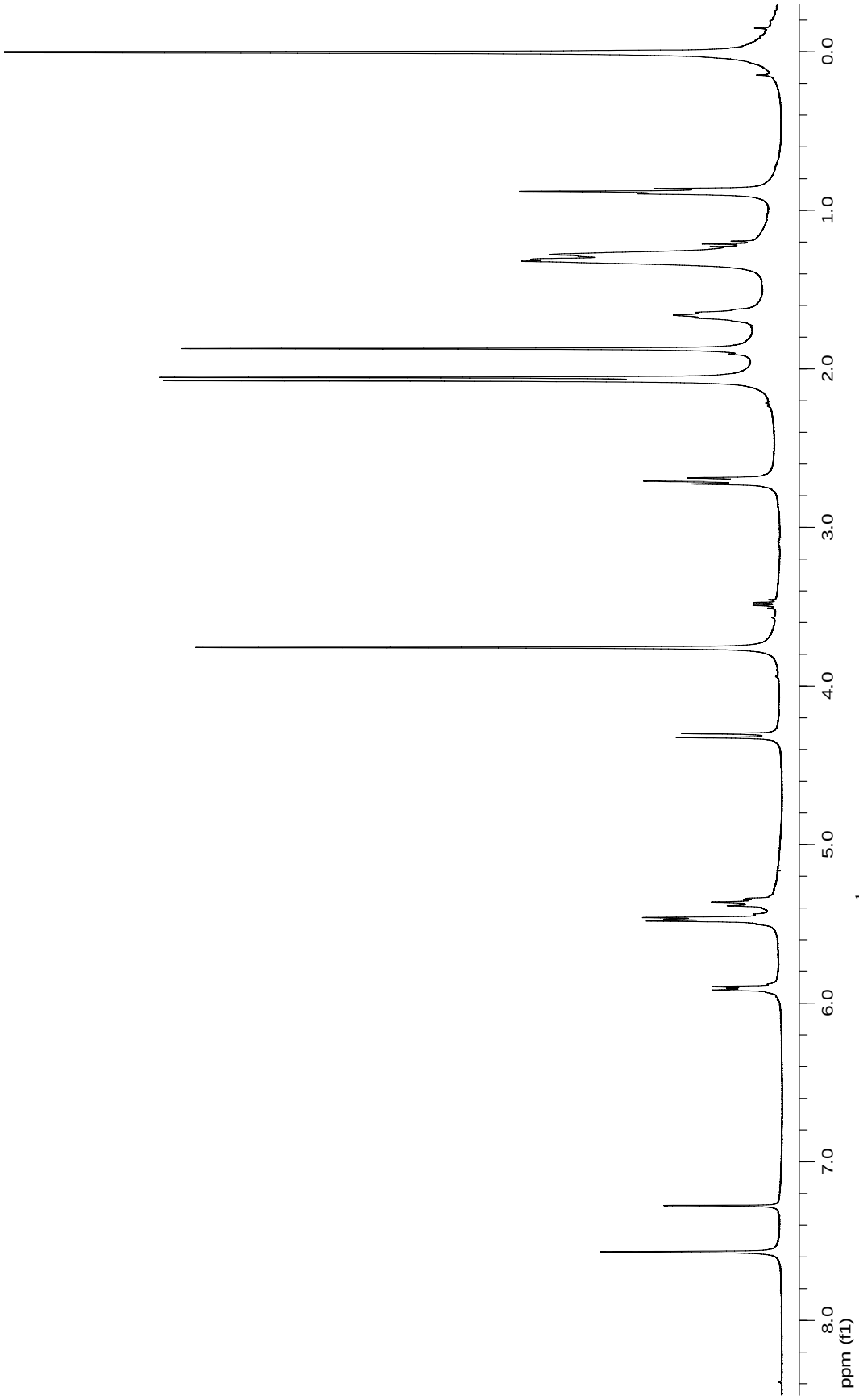

Figure 113: 400 MHz ^{1}H NMR spectrum of glucuronosyl-4-heptyl-1*H*-[1,2,3]-triazole (**51**).

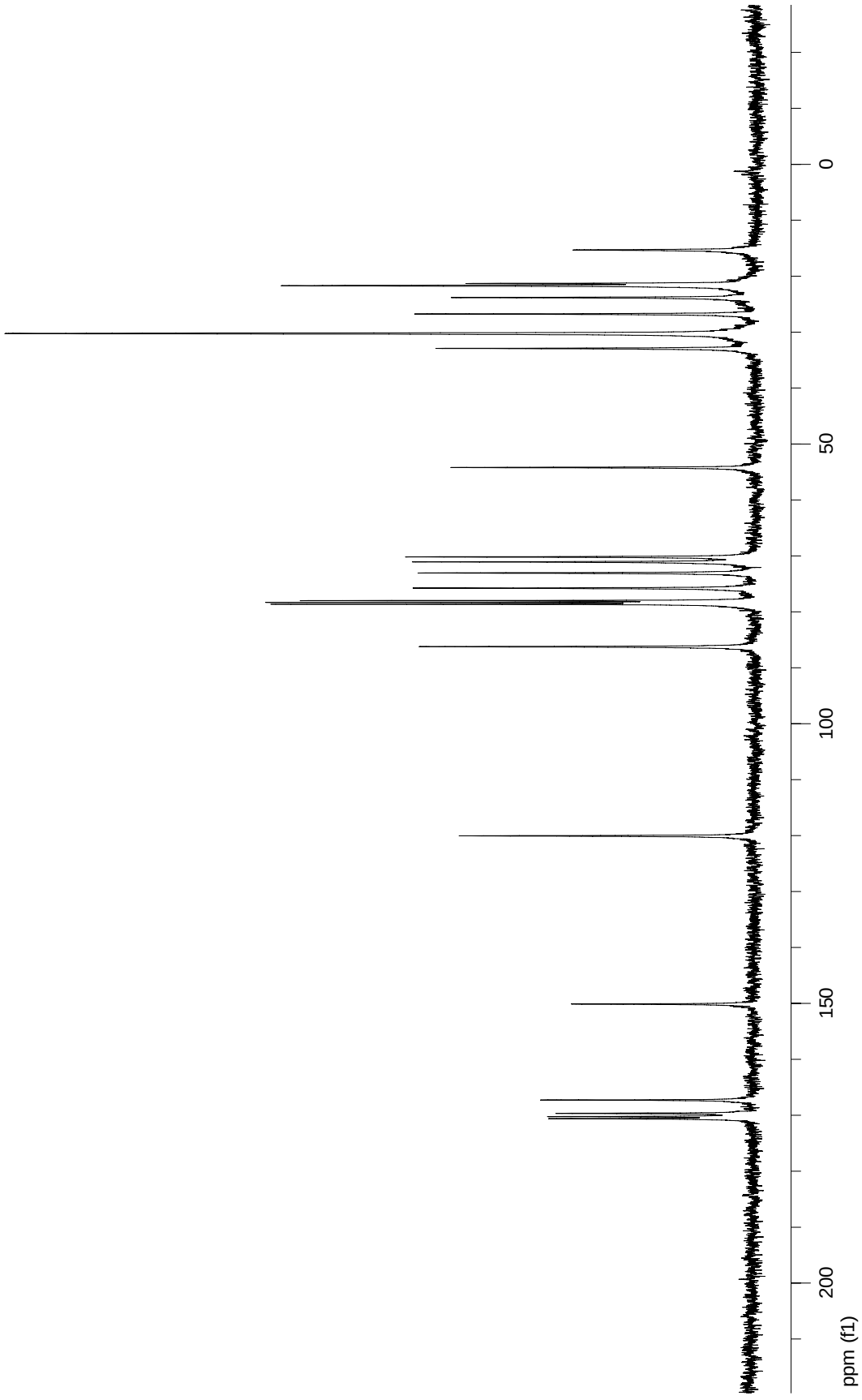

Figure 114: 100 MHz ^{13}C NMR spectrum of glucuronosyl-4-heptyl-1*H*-[1,2,3]-triazole (**51**).

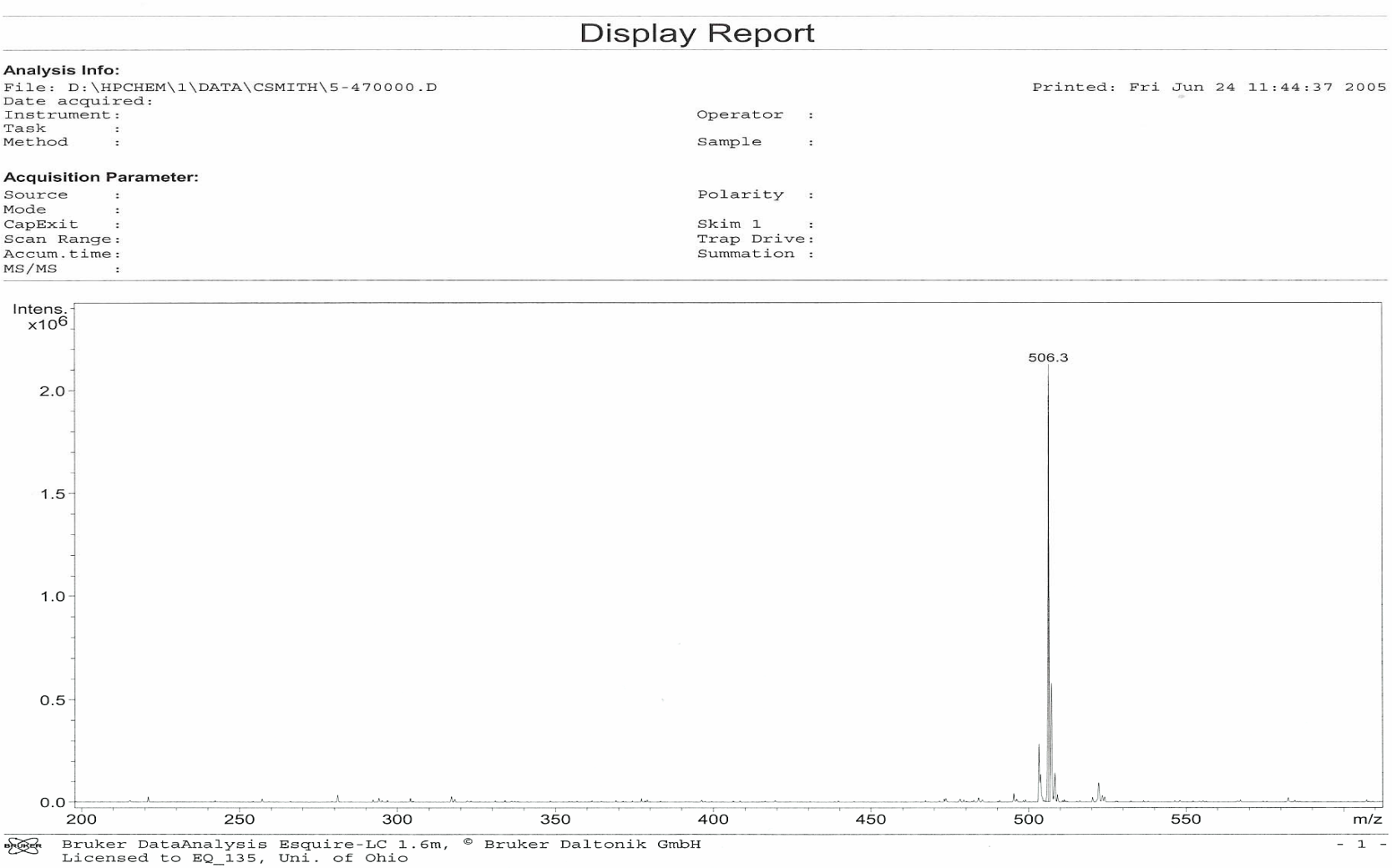

Figure 115: Mass spectrum of glucuronosyl-4-heptyl-1*H*-[1,2,3]-triazole (**51**).

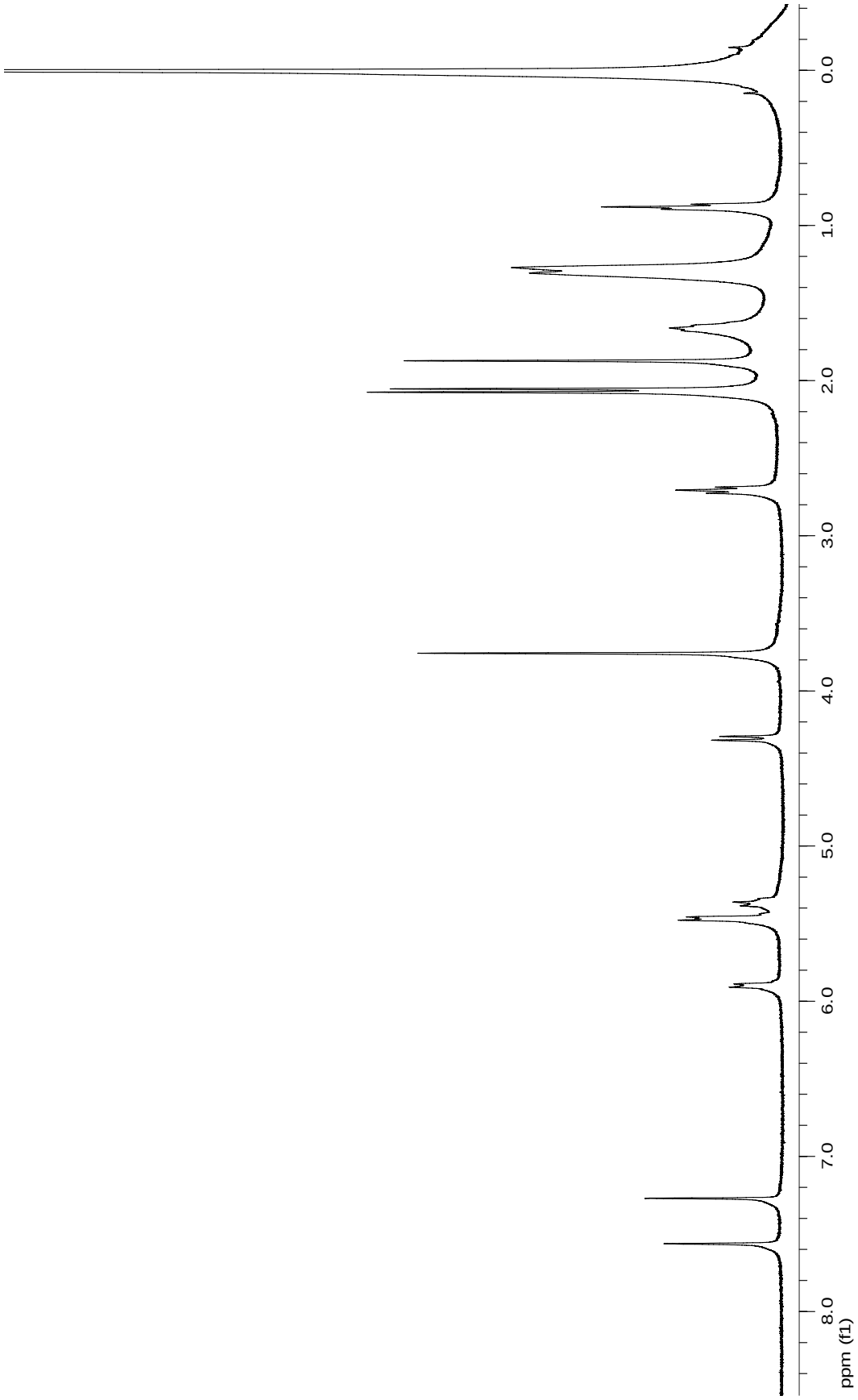

Figure 116: 400 MHz ^{1}H NMR spectrum of glucuronosyl-4-octyl-1*H*-[1,2,3]-triazole (**52**).

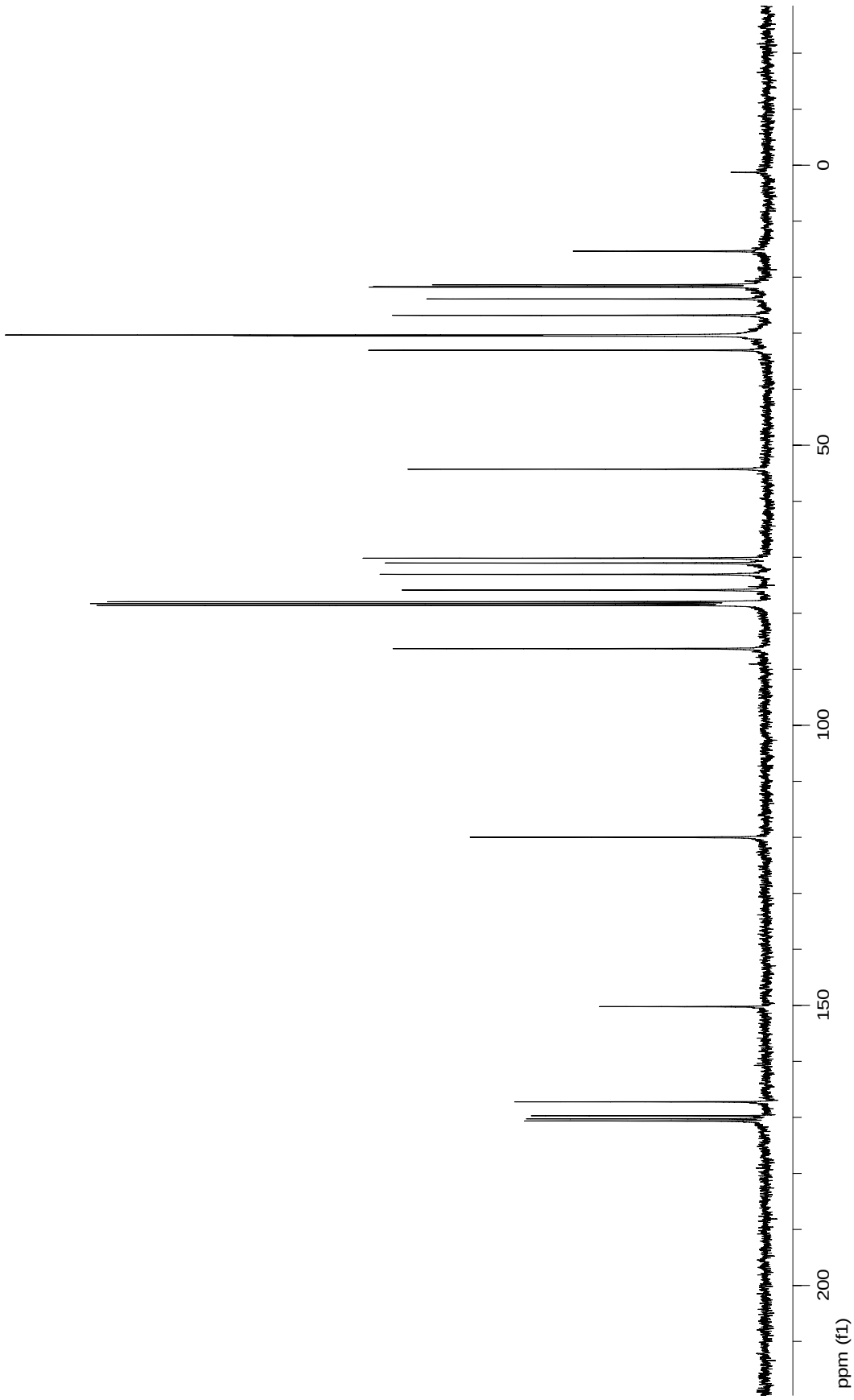

Figure 117: 100 MHz ^{13}C NMR spectrum of glucuronosyl-4-octyl-1*H*-[1,2,3]-triazole (**52**).

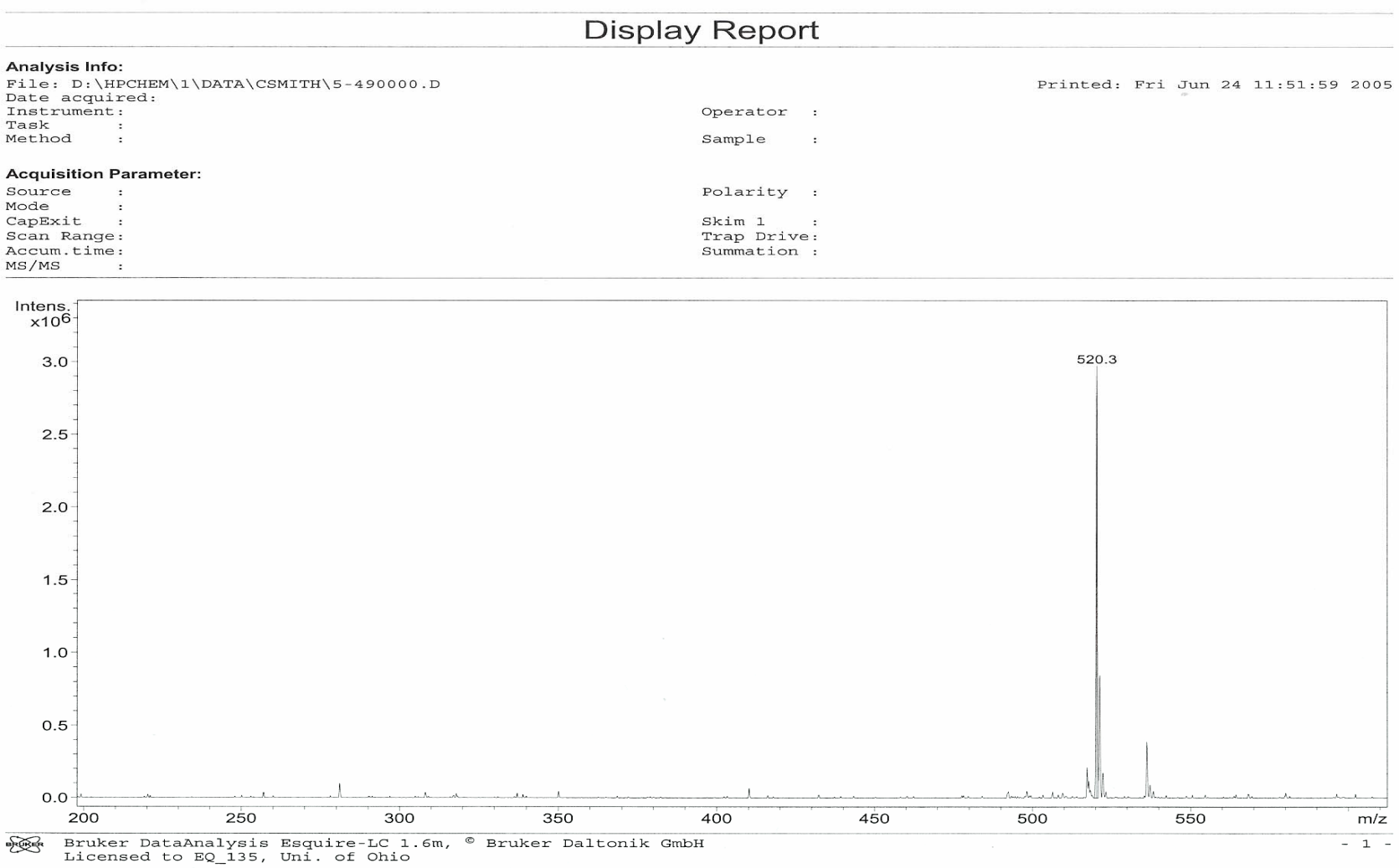

Figure 118: Mass spectrum of glucuronosyl-4-octyl-1*H*-[1,2,3]-triazole (**52**).

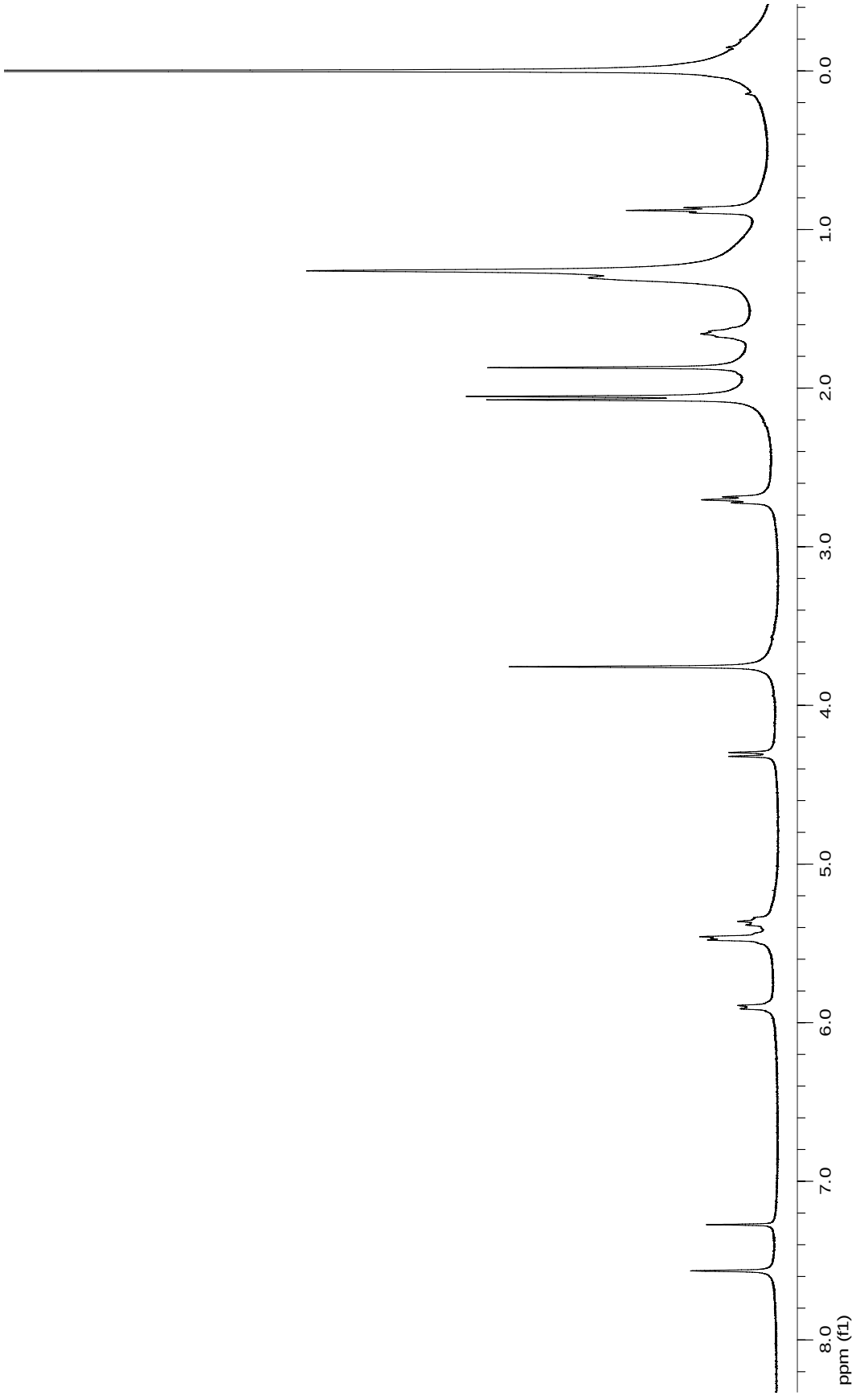

Figure 119: 400 MHz ^{1}H NMR spectrum of glucuronosyl-4-decyl-1*H*-[1,2,3]-triazole (**53**).

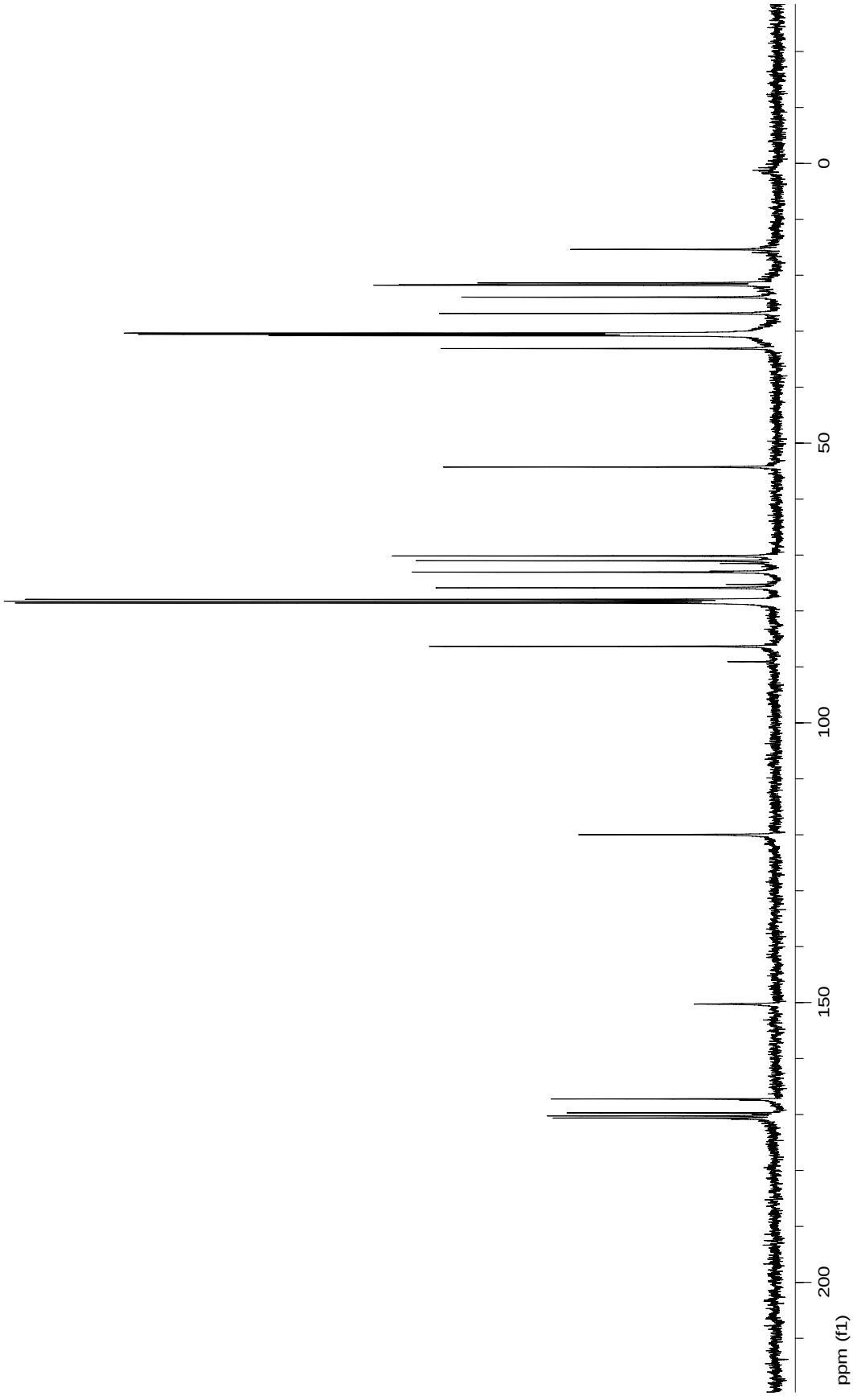

Figure 120: 100 MHz ^{13}C NMR spectrum of glucuronosyl-4-decyl-1*H*-[1,2,3]-triazole (**53**).

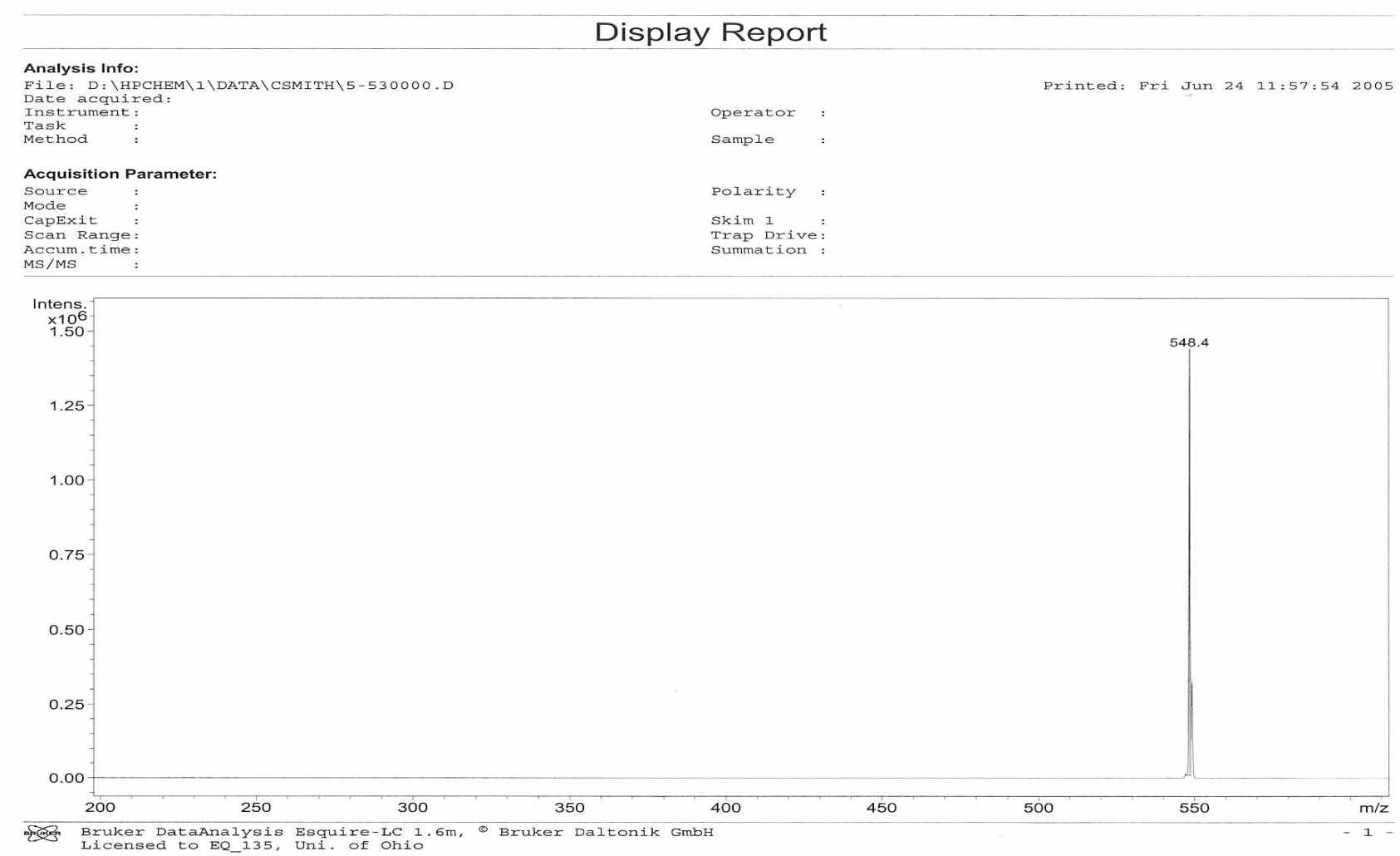

Figure 121: Mass spectrum of glucuronosyl-4-decyl-1*H*-[1,2,3]-triazole (**53**).

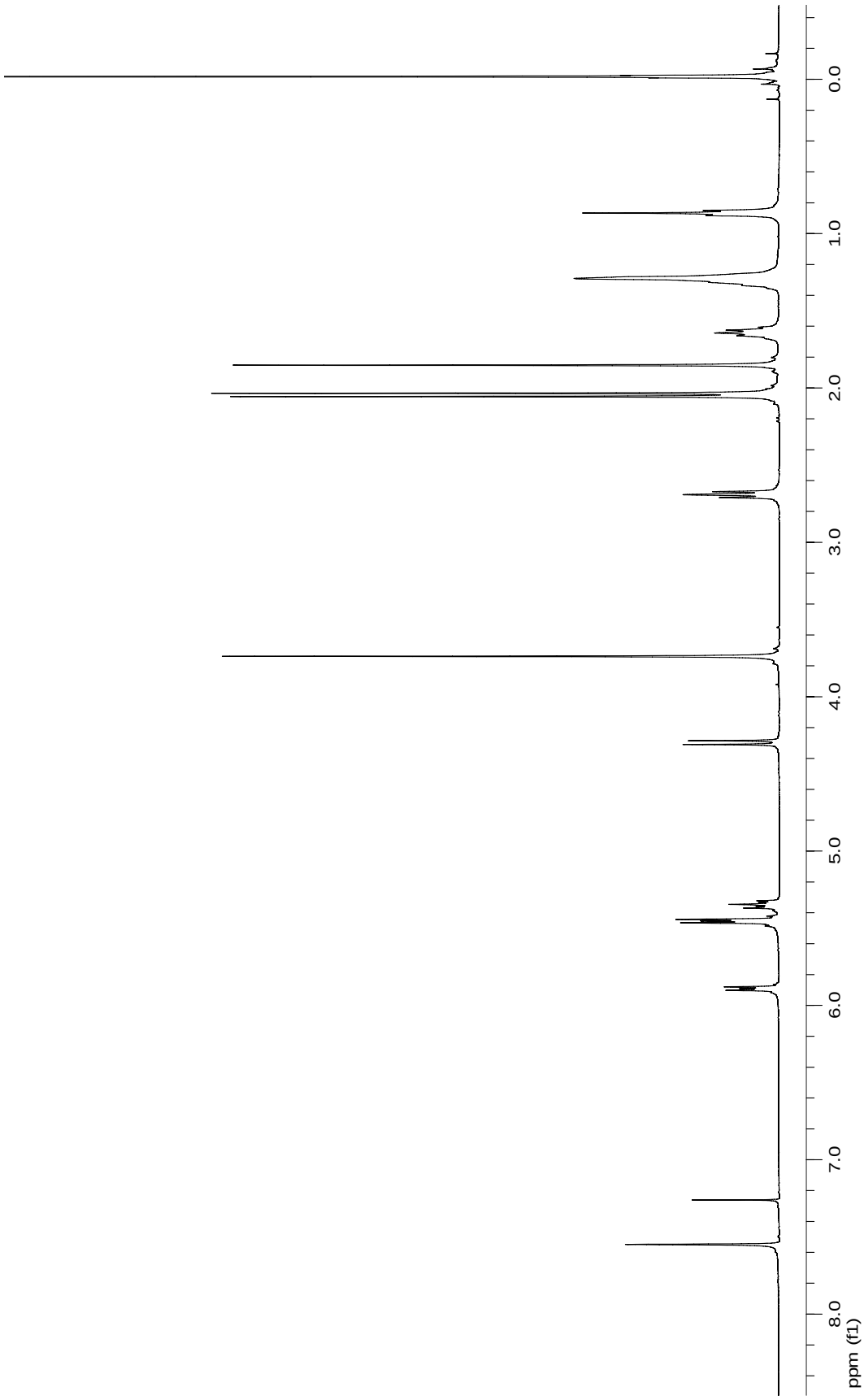

Figure 122: 400 MHz ^{1}H NMR spectrum of glucuronosyl-4-hexyl-1*H*-[1,2,3]-triazole (**54**).

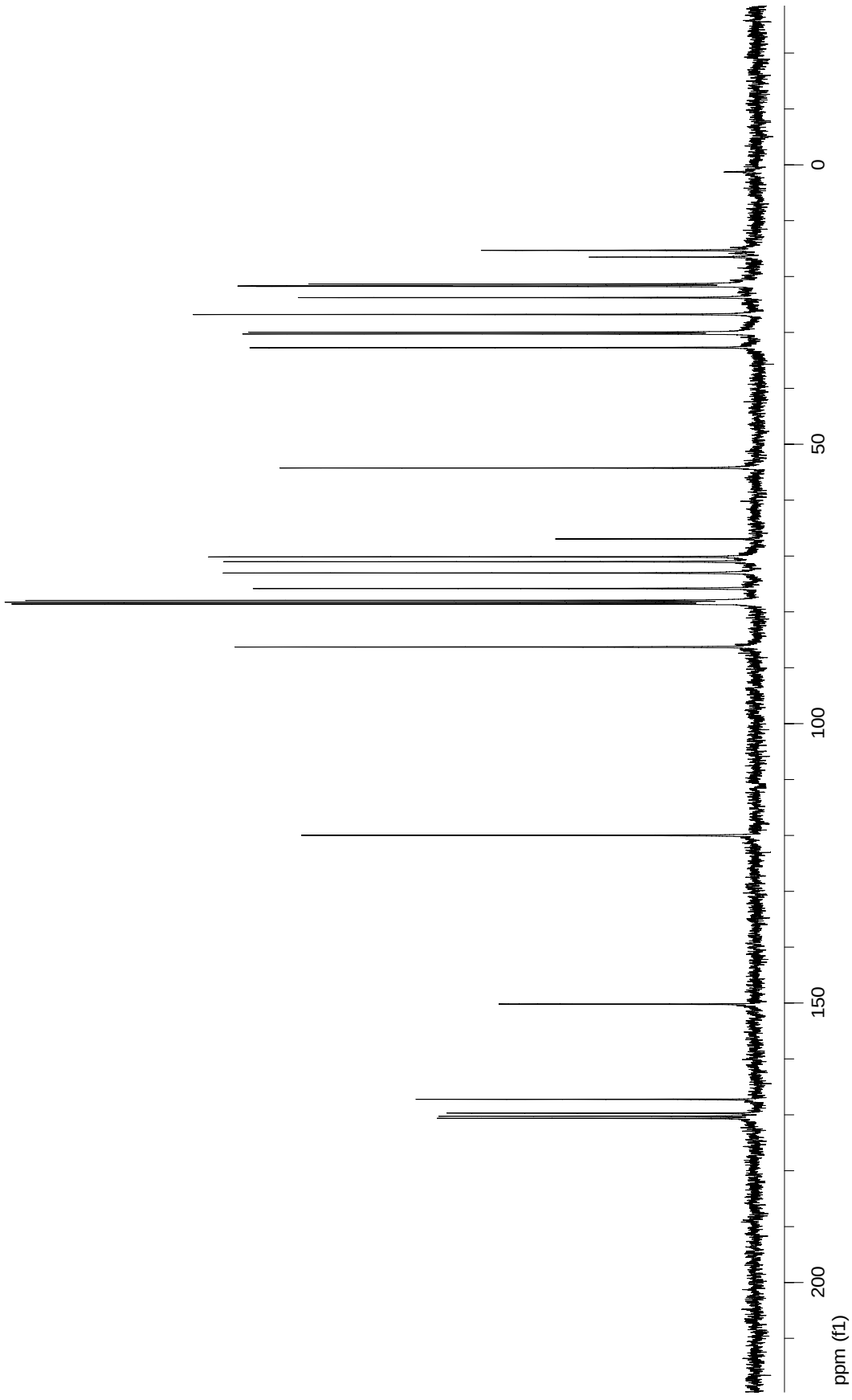

Figure 123: 100 MHz ^{13}C NMR spectrum of glucuronosyl-4-hexyl-1*H*-[1,2,3]-triazole (**54**).

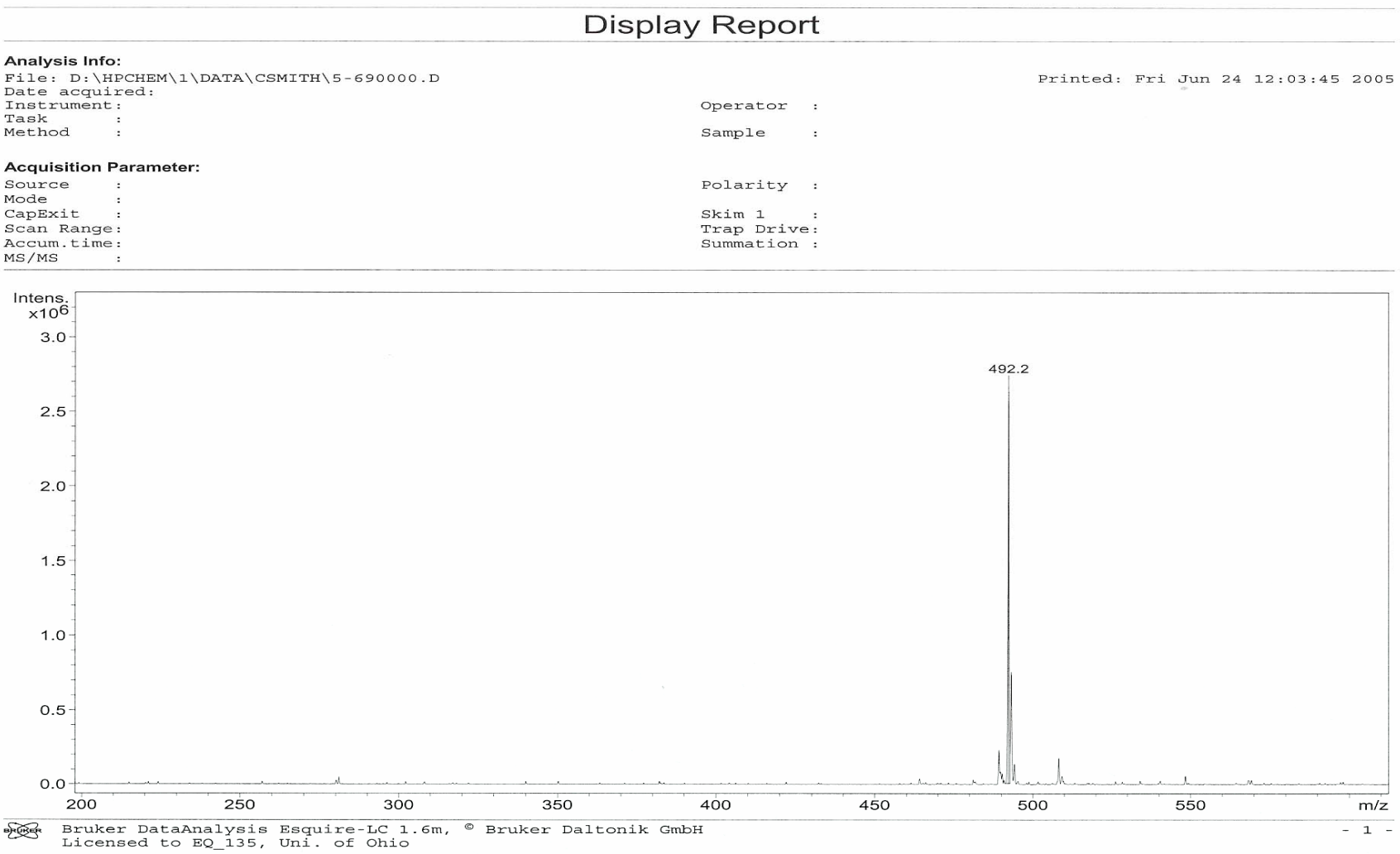

Figure 124: Mass spectrum of glucuronosyl-4-hexyl-1*H*-[1,2,3]-triazole (**54**).

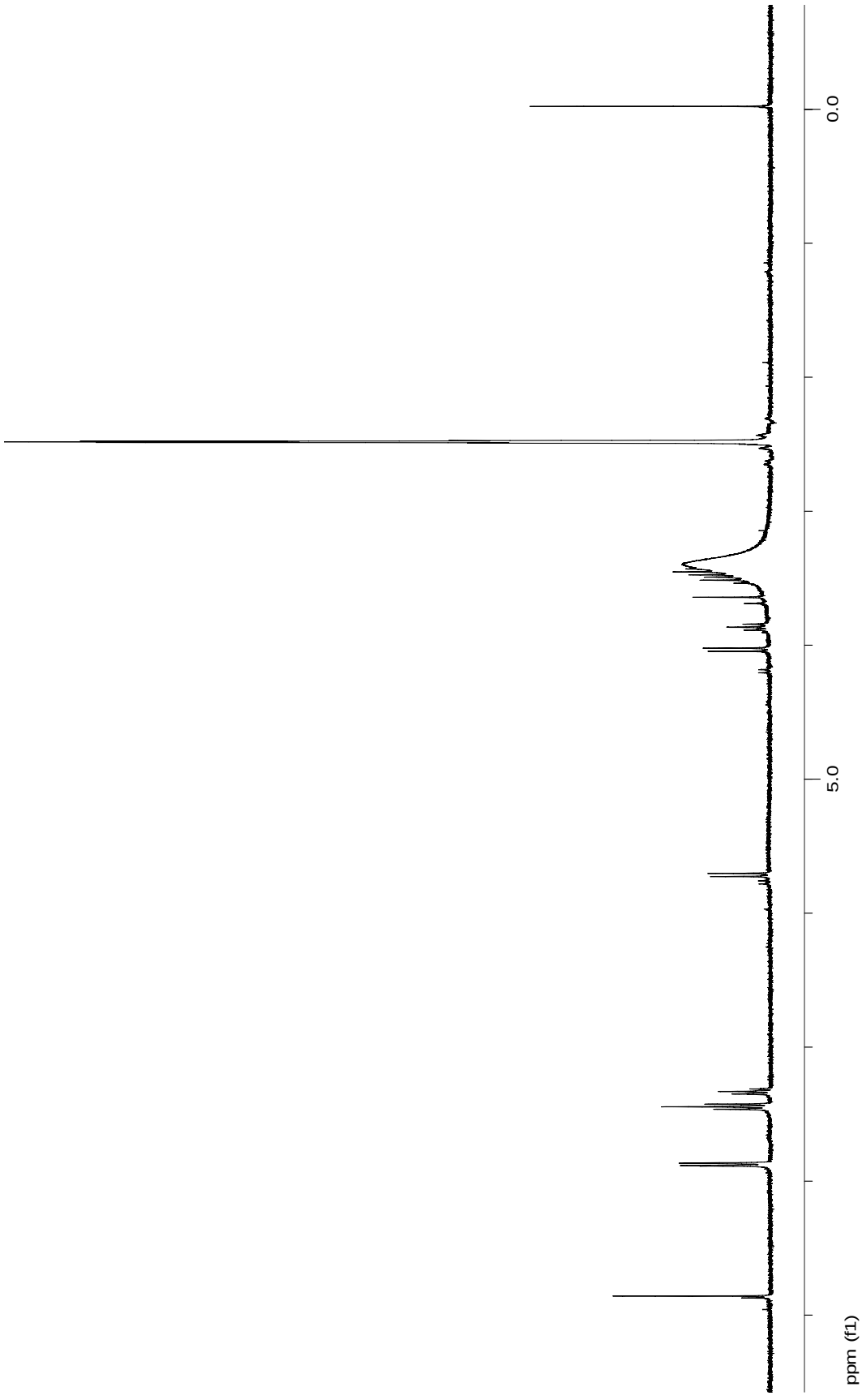

Figure 125: 400 MHz ^{1}H NMR spectrum of glucuronosyl-4-phenyl-1*H*-[1,2,3]-triazole (**55**).

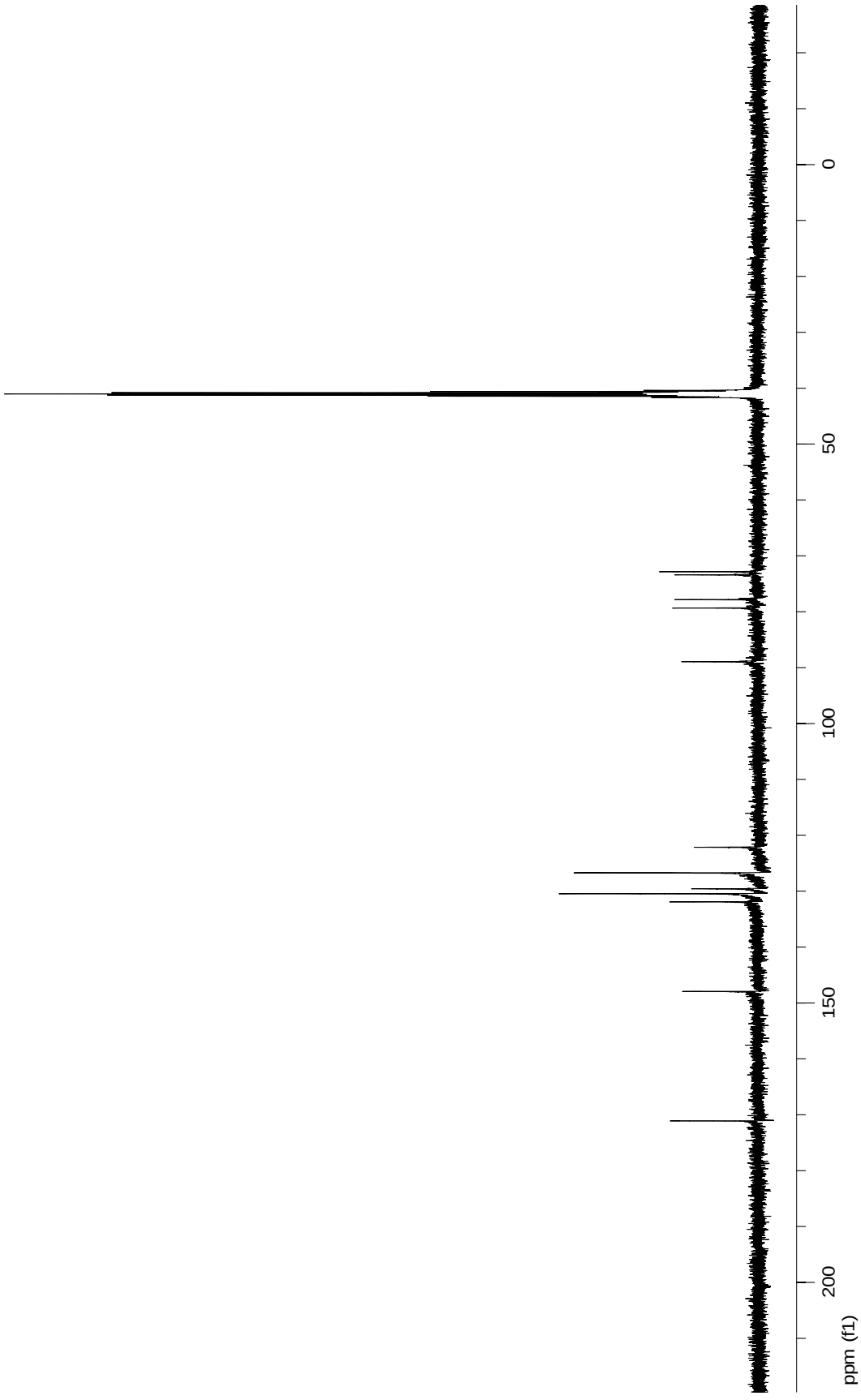

Figure 126: 100 MHz ^{13}C NMR spectrum of glucuronosyl-4-phenyl-1*H*-[1,2,3]-triazole (**55**).

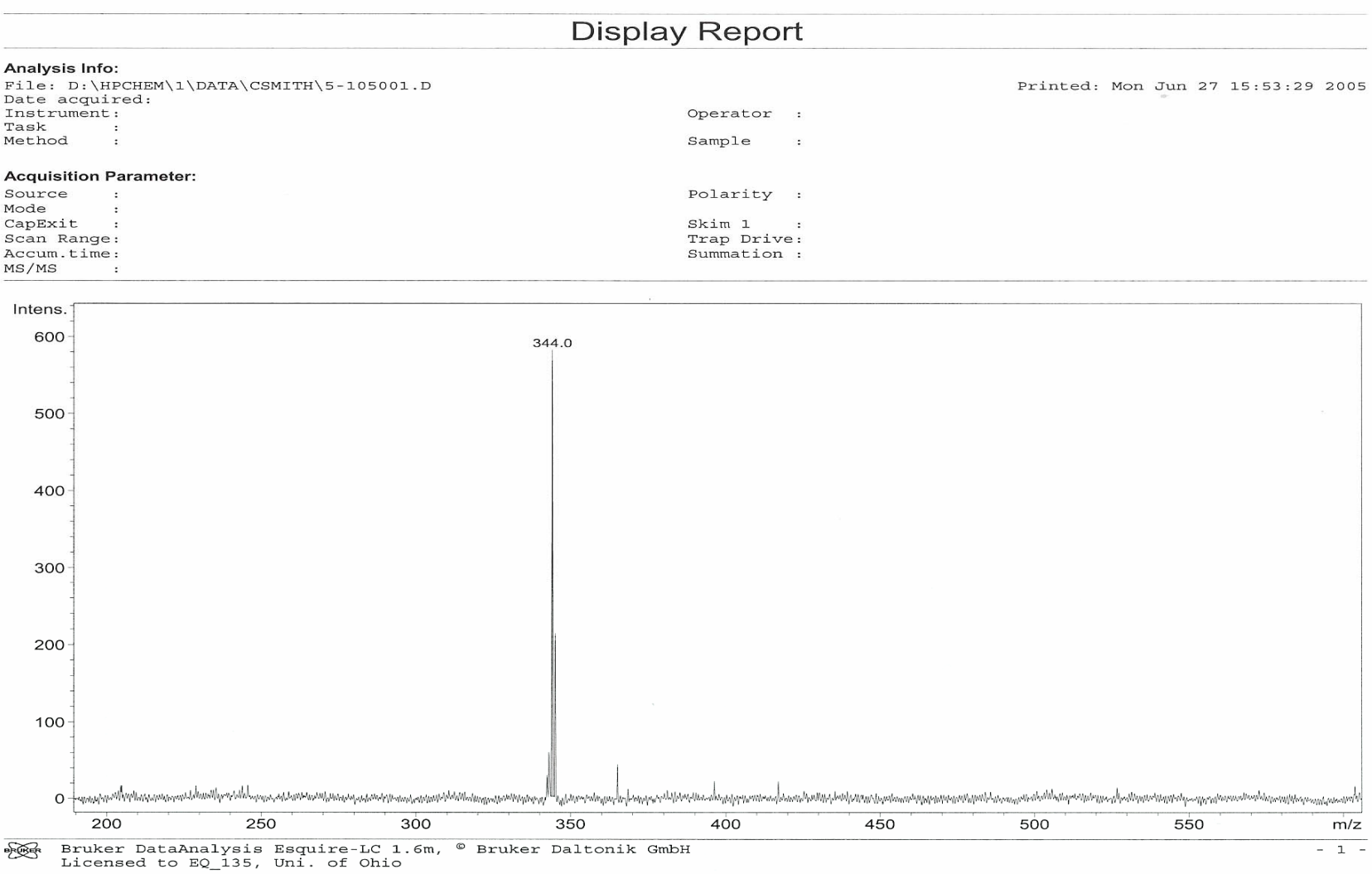

Figure 127: Mass spectrum of glucuronosyl-4-phenyl-1*H*-[1,2,3]-triazole (**55**).

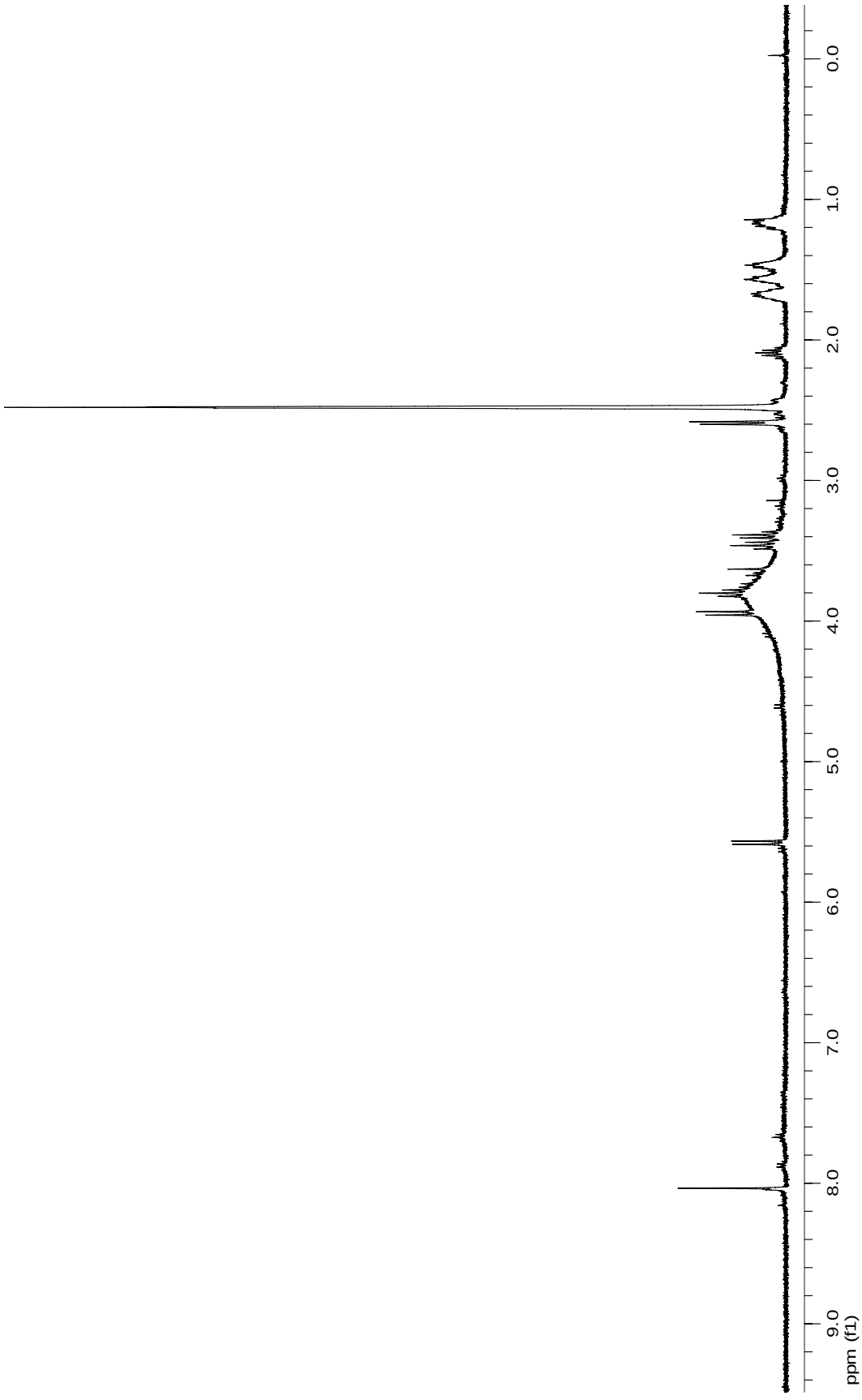

Figure 128: 400 MHz ^{1}H NMR spectrum of glucuronosyl-4-(methylcyclopentyl)-1*H*-[1,2,3]-triazole (**56**).

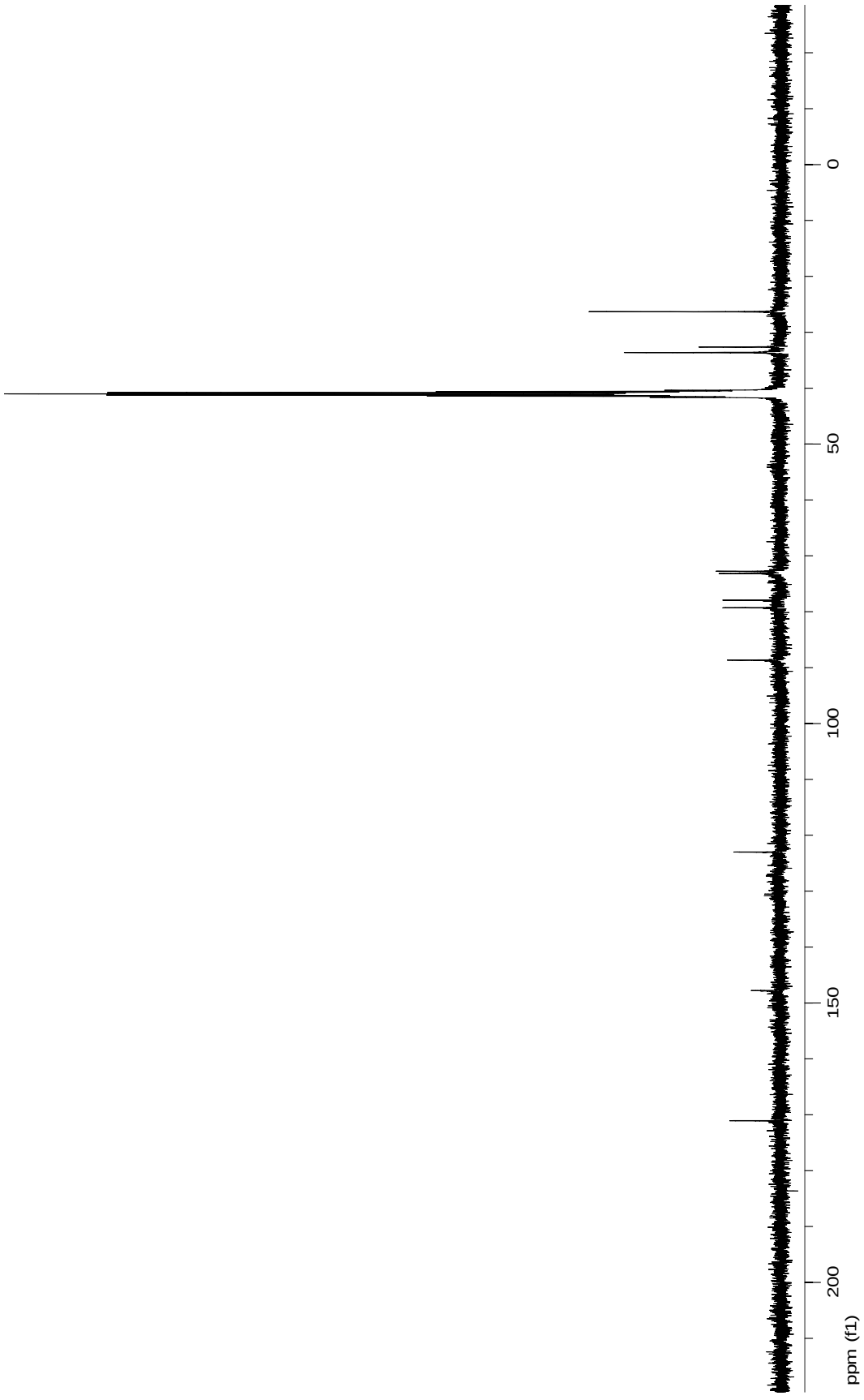

Figure 129: 100 MHz ^{13}C NMR spectrum of glucuronosyl-4-(methylcyclopentyl)-1*H*-[1,2,3]-triazole (**56**).

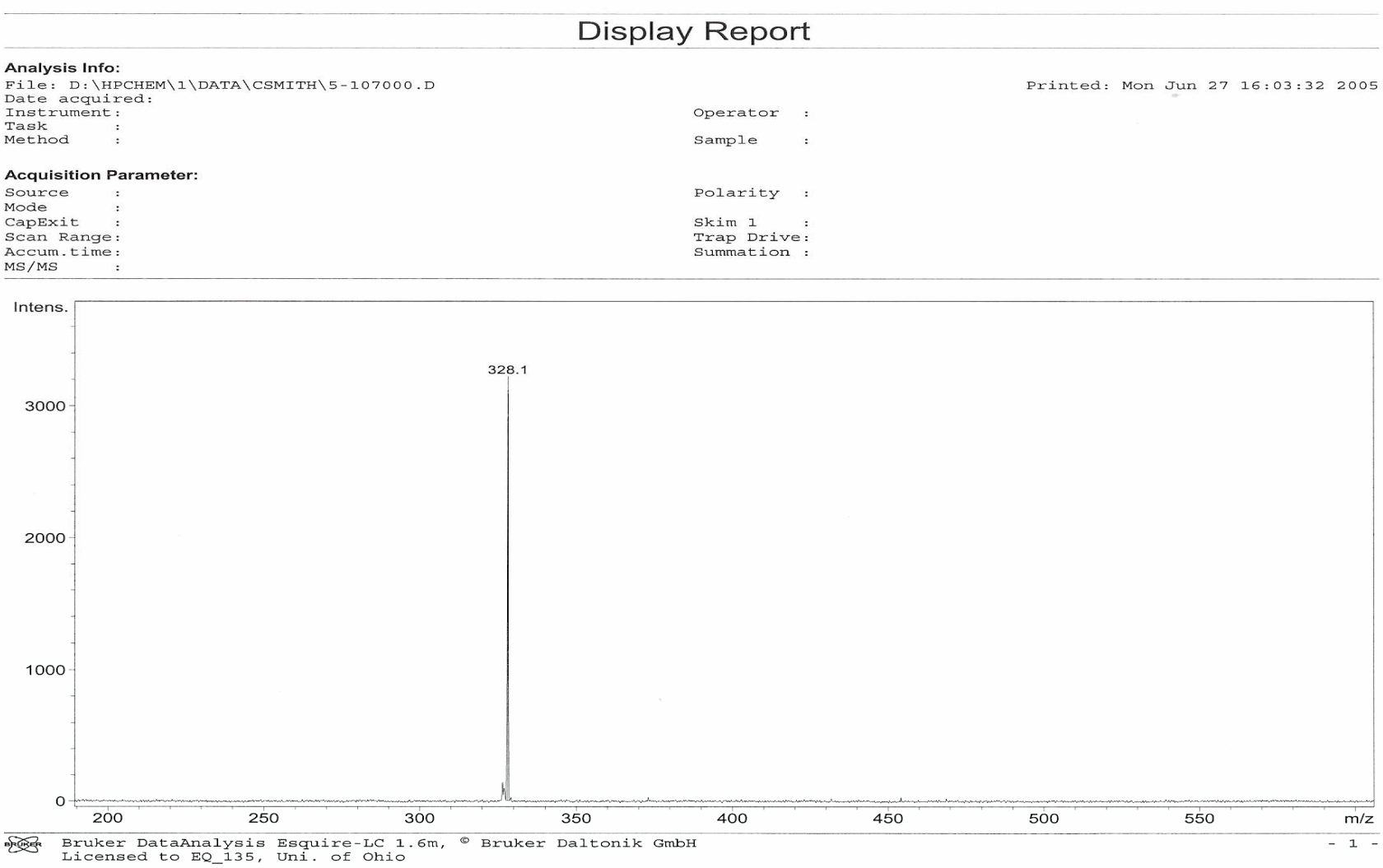

Figure 130: Mass spectrum of glucuronosyl-4-(methylcyclopentyl)-1*H*-[1,2,3]-triazole (**56**).

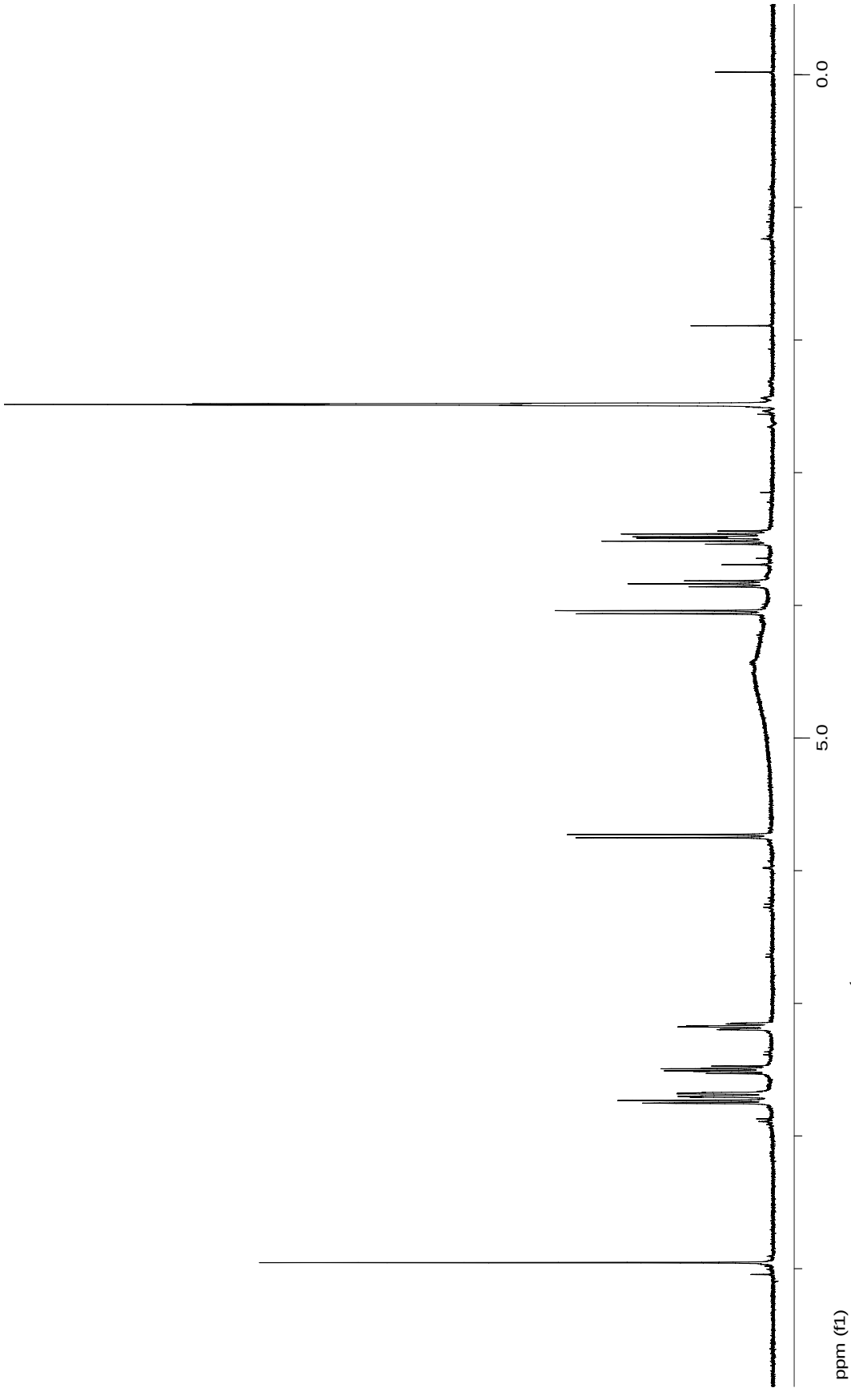

Figure 131: 400 MHz ^{1}H NMR spectrum of glucuronosyl-4-(3-fluorophenyl)-1*H*-[1,2,3]-triazole (**57**).

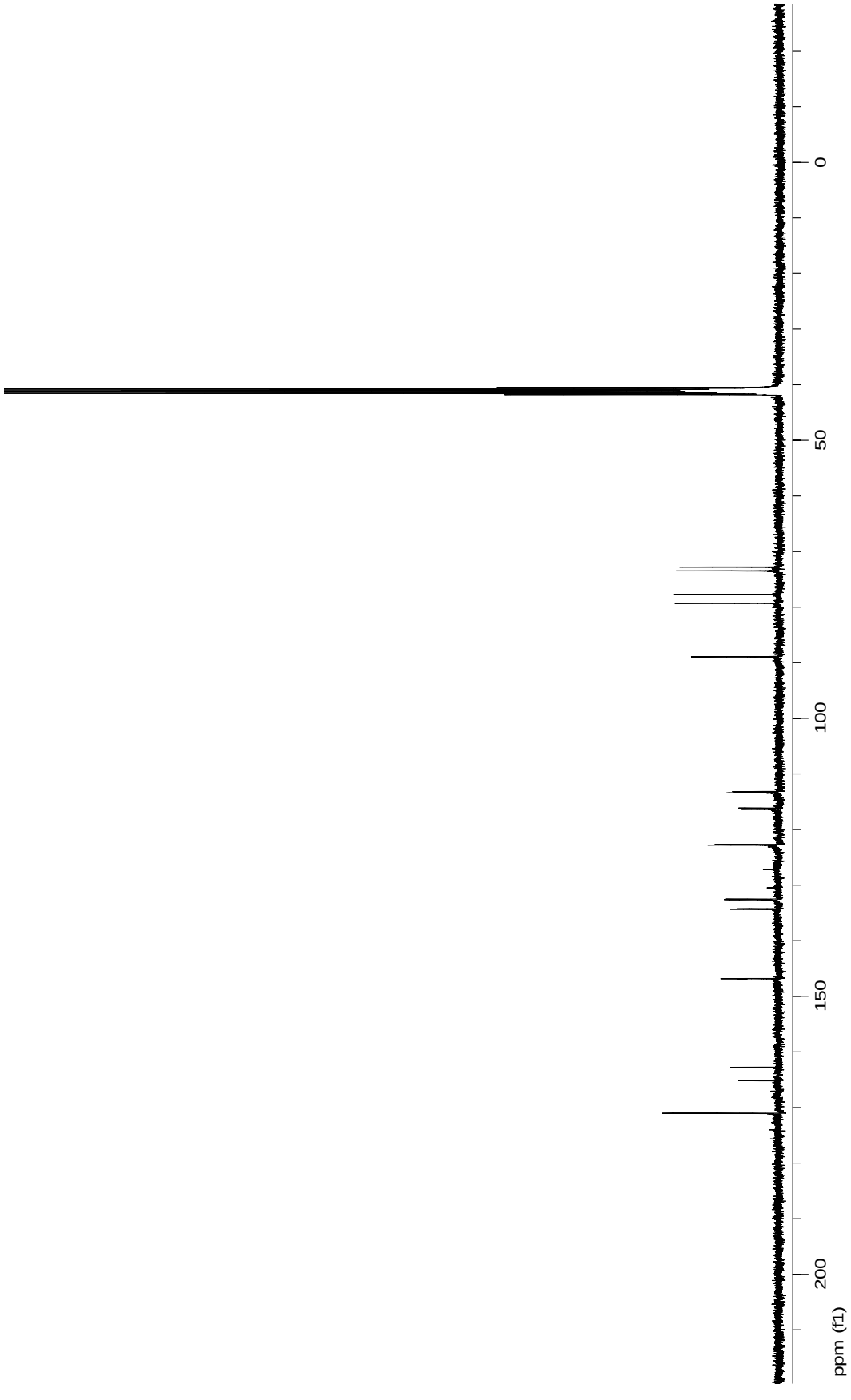

Figure 132: 100 MHz ^{13}C NMR spectrum of glucuronosyl-4-(3-fluorophenyl)-1*H*-[1,2,3]-triazole (**57**).

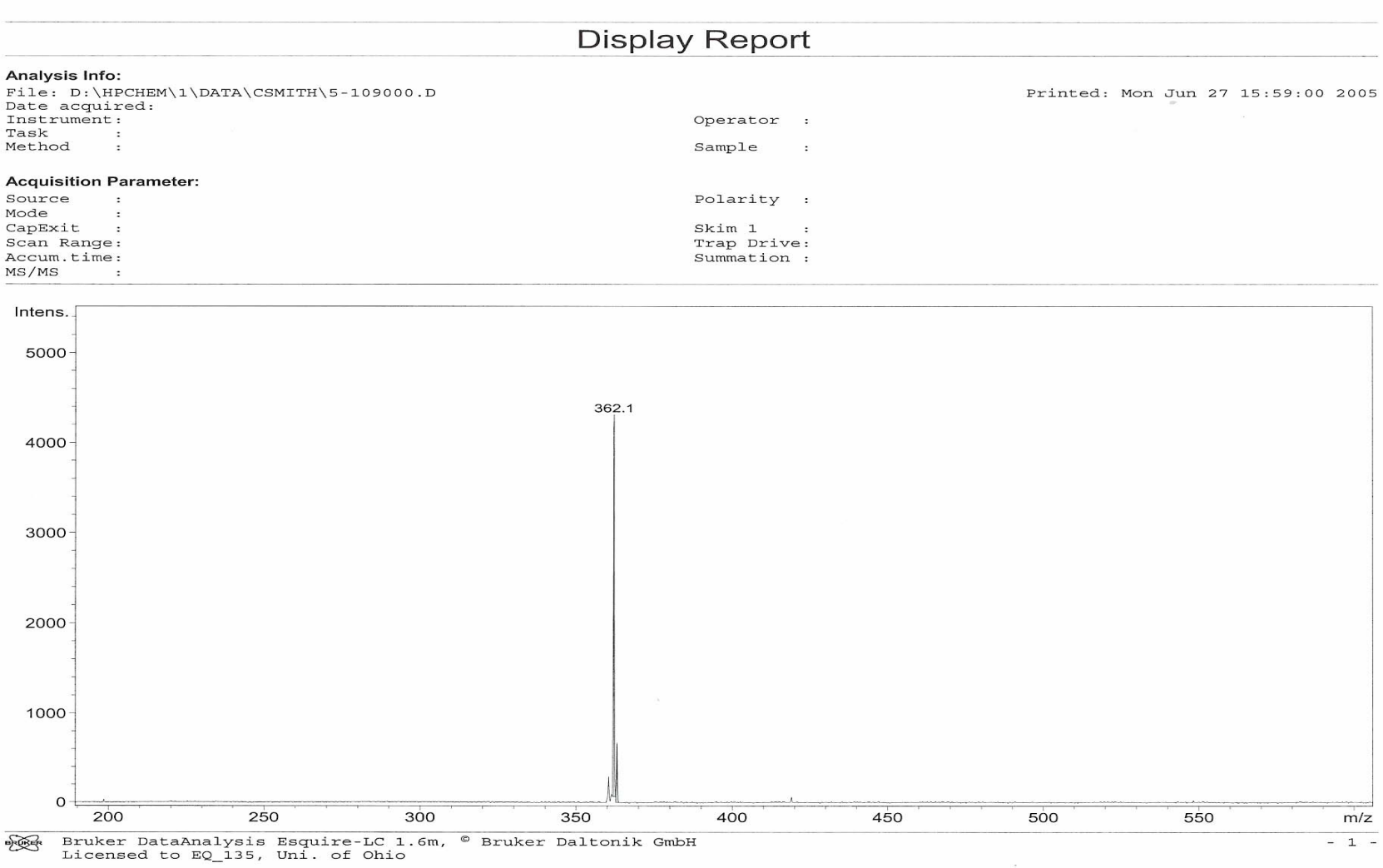

Figure 133: Mass spectrum of glucuronosyl-4-(3-fluorophenyl)-1*H*-[1,2,3]-triazole (**57**).

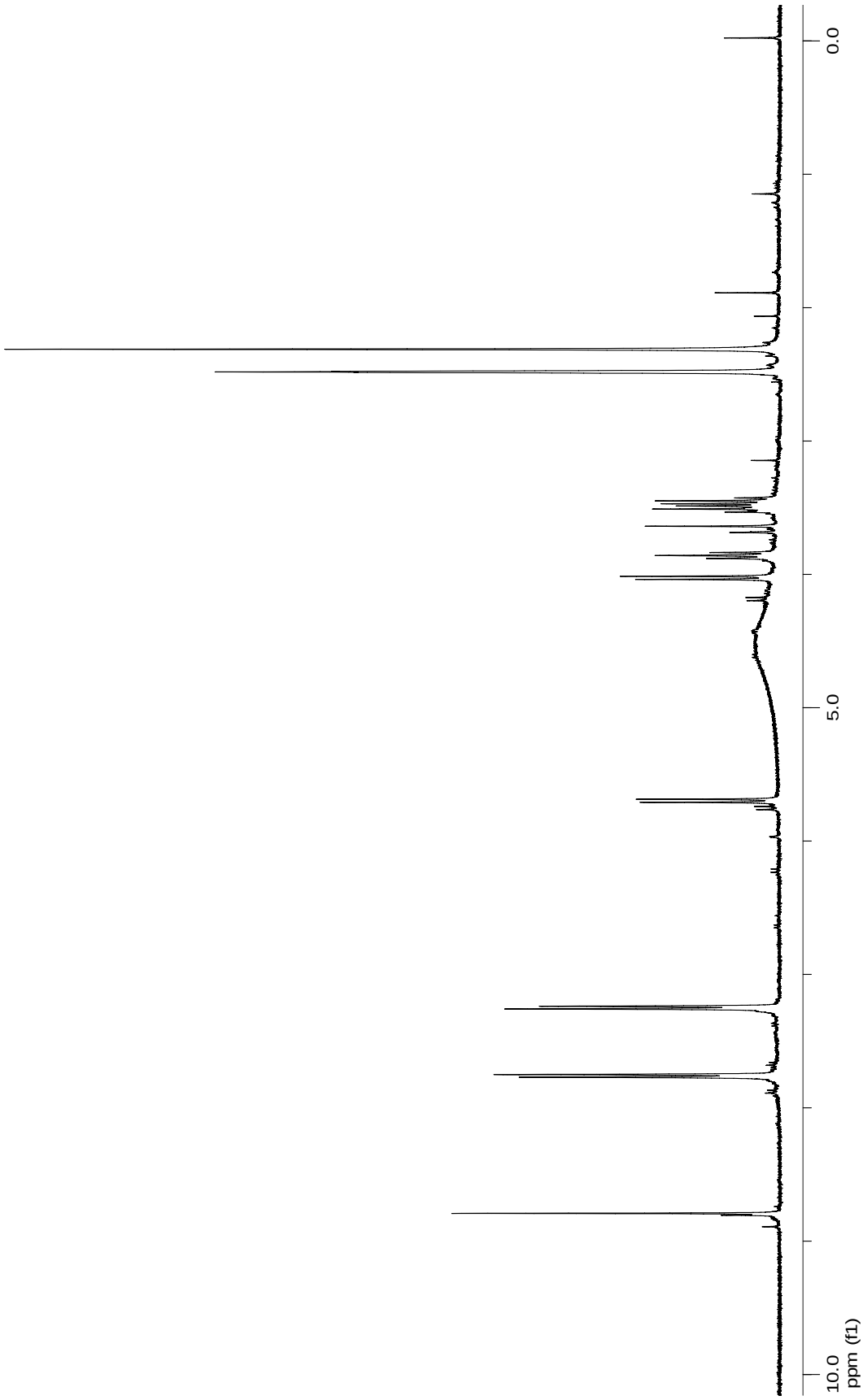

Figure 134: 400 MHz ^{1}H NMR spectrum of glucuronosyl-4-(4-methylphenyl)-1*H*-[1,2,3]-triazole (**58**).

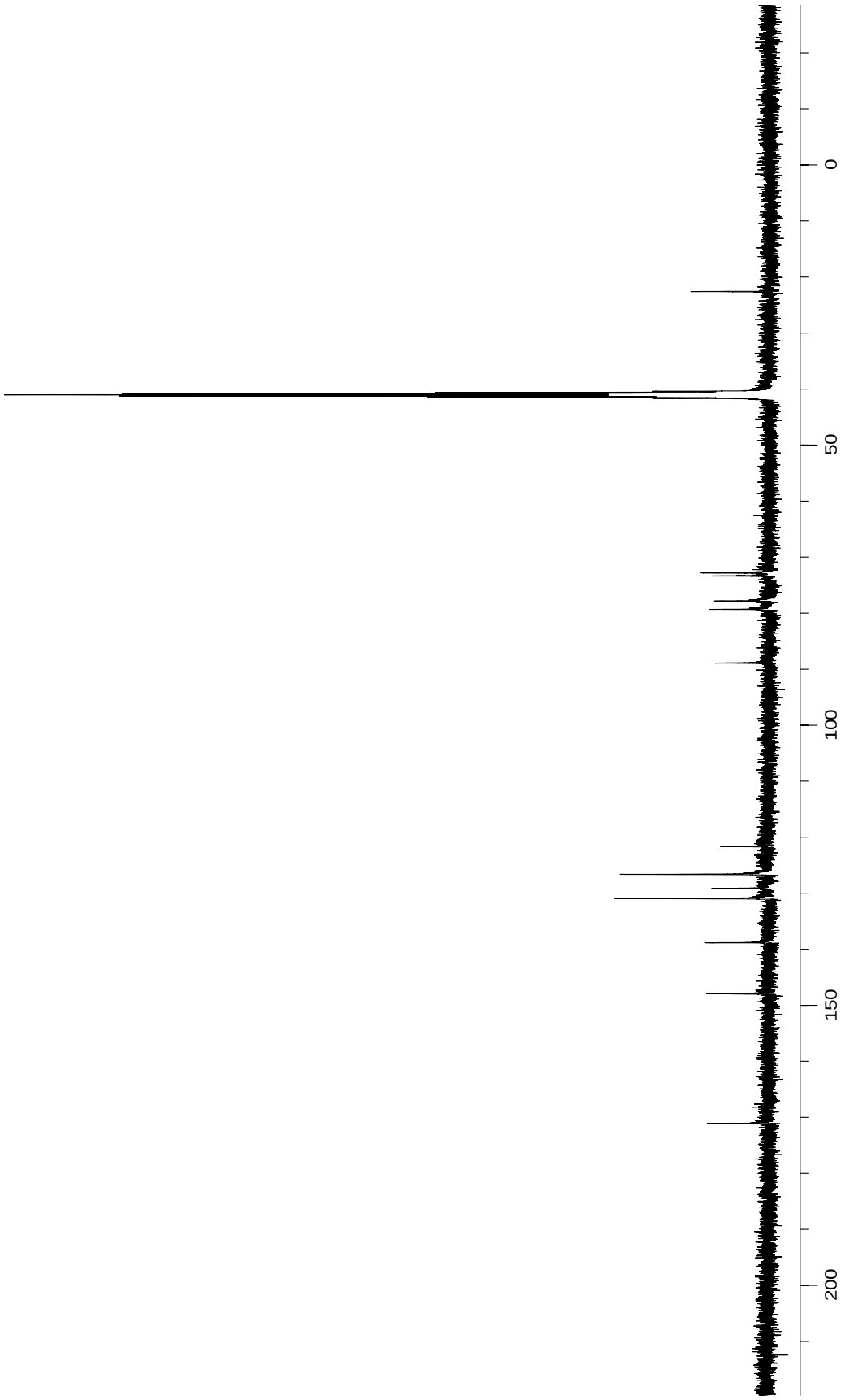

Figure 135: 100 MHz ^{13}C NMR spectrum of glucuronosyl-4-(4-methylphenyl)-1*H*-[1,2,3]-triazole (**58**).

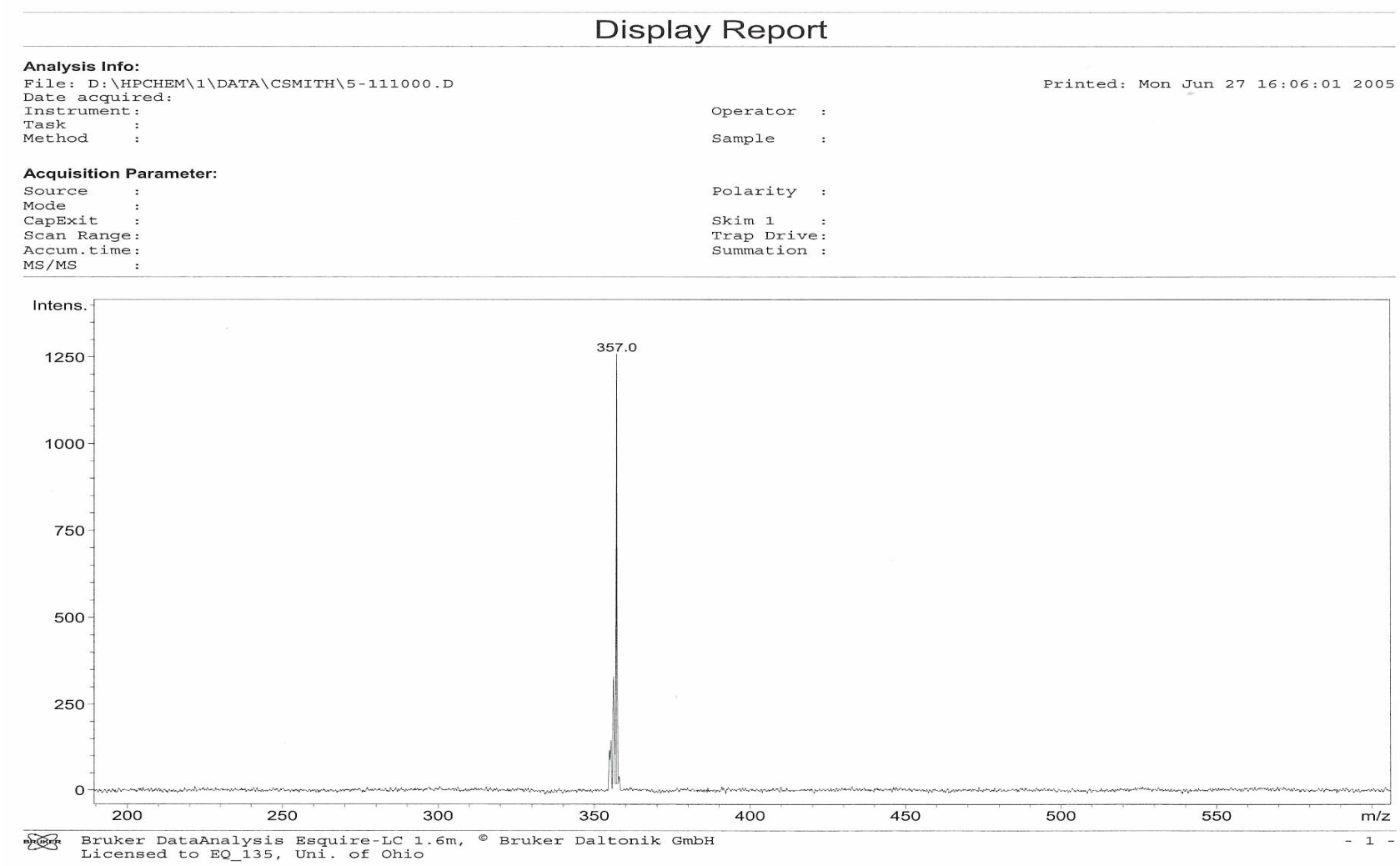

Figure 136: Mass spectrum of glucuronosyl-4-(4-methylphenyl)-1*H*-[1,2,3]-triazole (**58**).

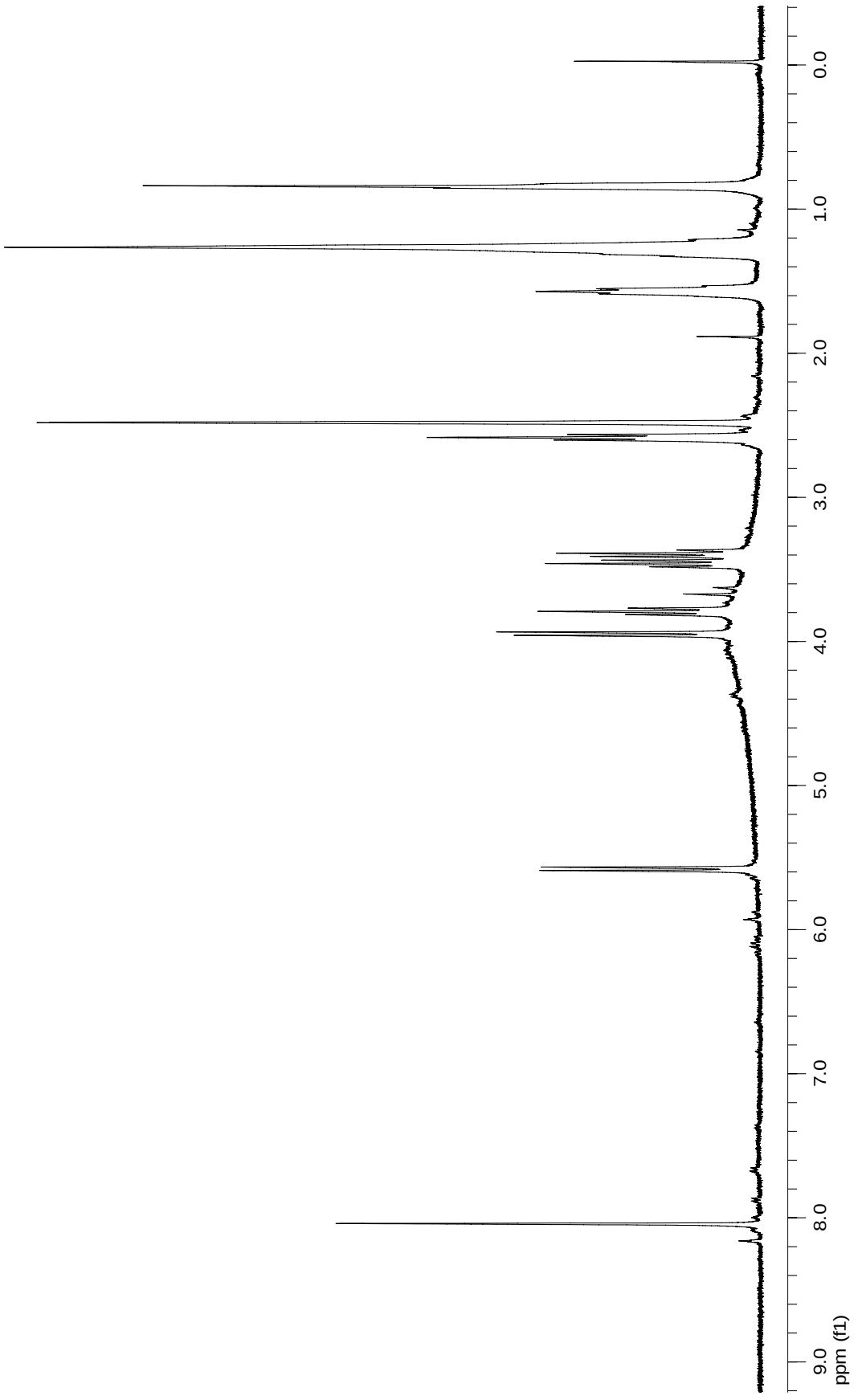

Figure 137: 400 MHz ^{1}H NMR spectrum of glucuronosyl-4-hexyl-1*H*-[1,2,3]-triazole (**59**).

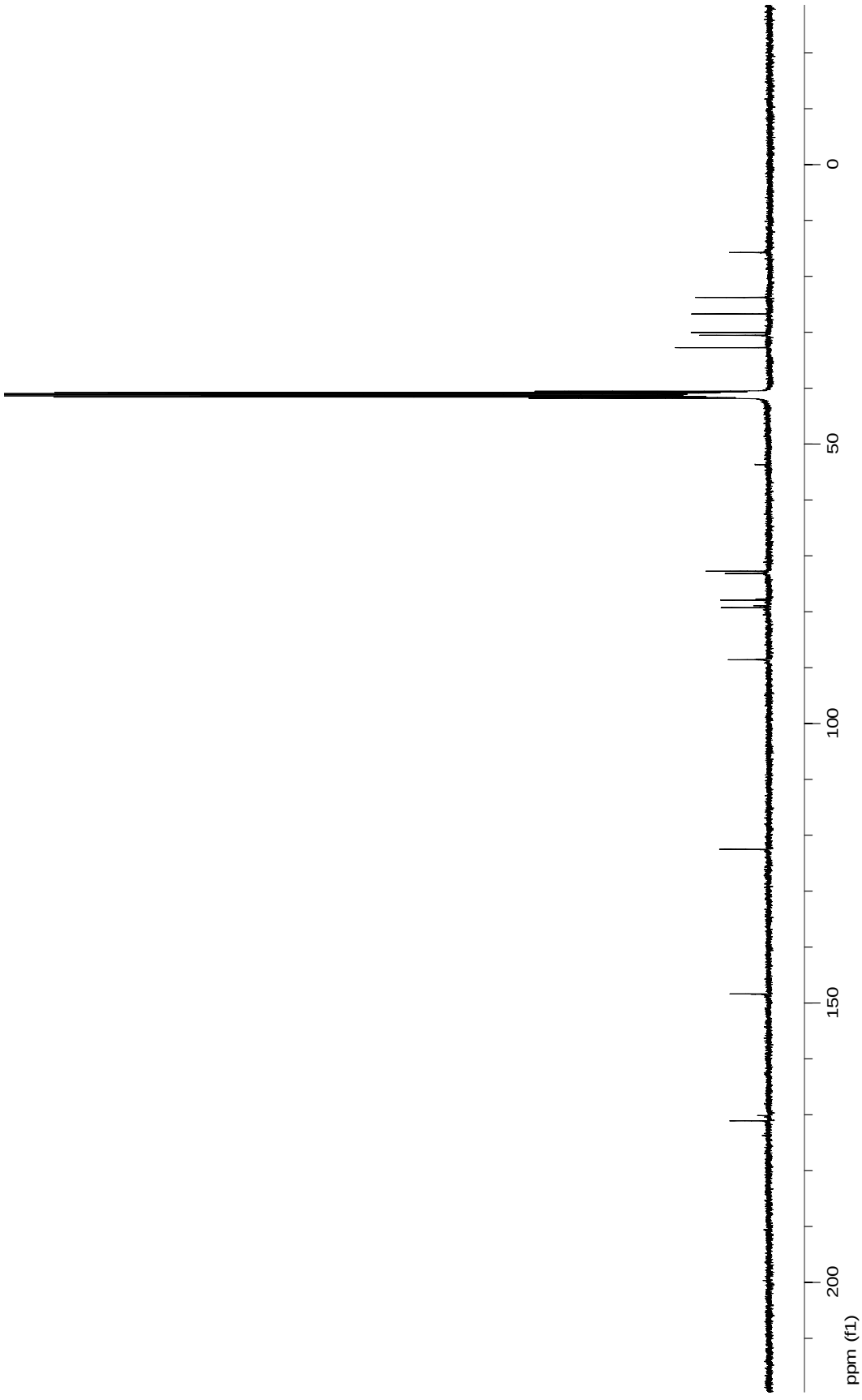

Figure 138: 100 MHz ^{13}C NMR spectrum of glucuronosyl-4-hexyl-1*H*-[1,2,3]-triazole (**59**).

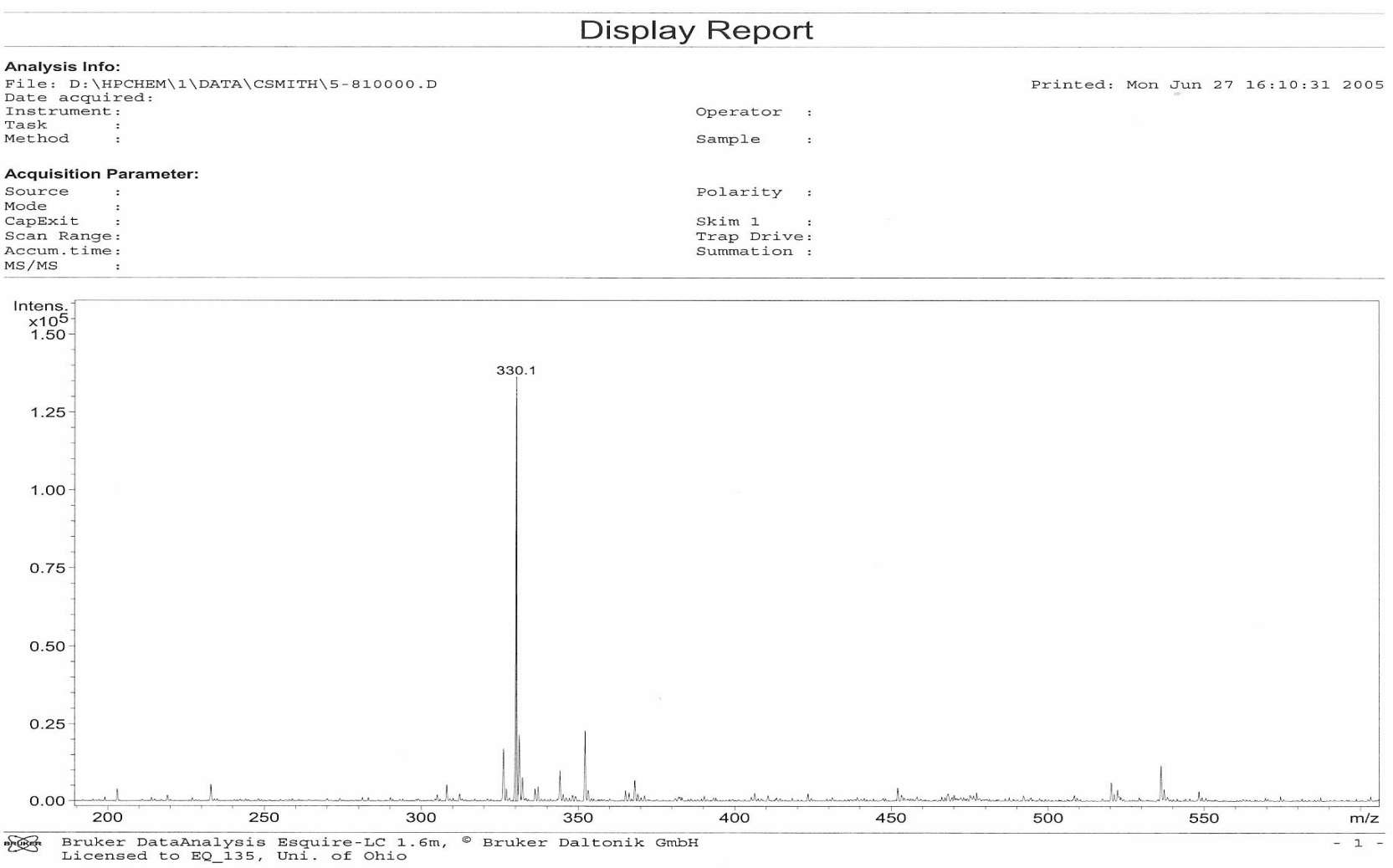

Figure 139: Mass spectrum of glucuronosyl-4-hexyl-1*H*-[1,2,3]-triazole (**59**).

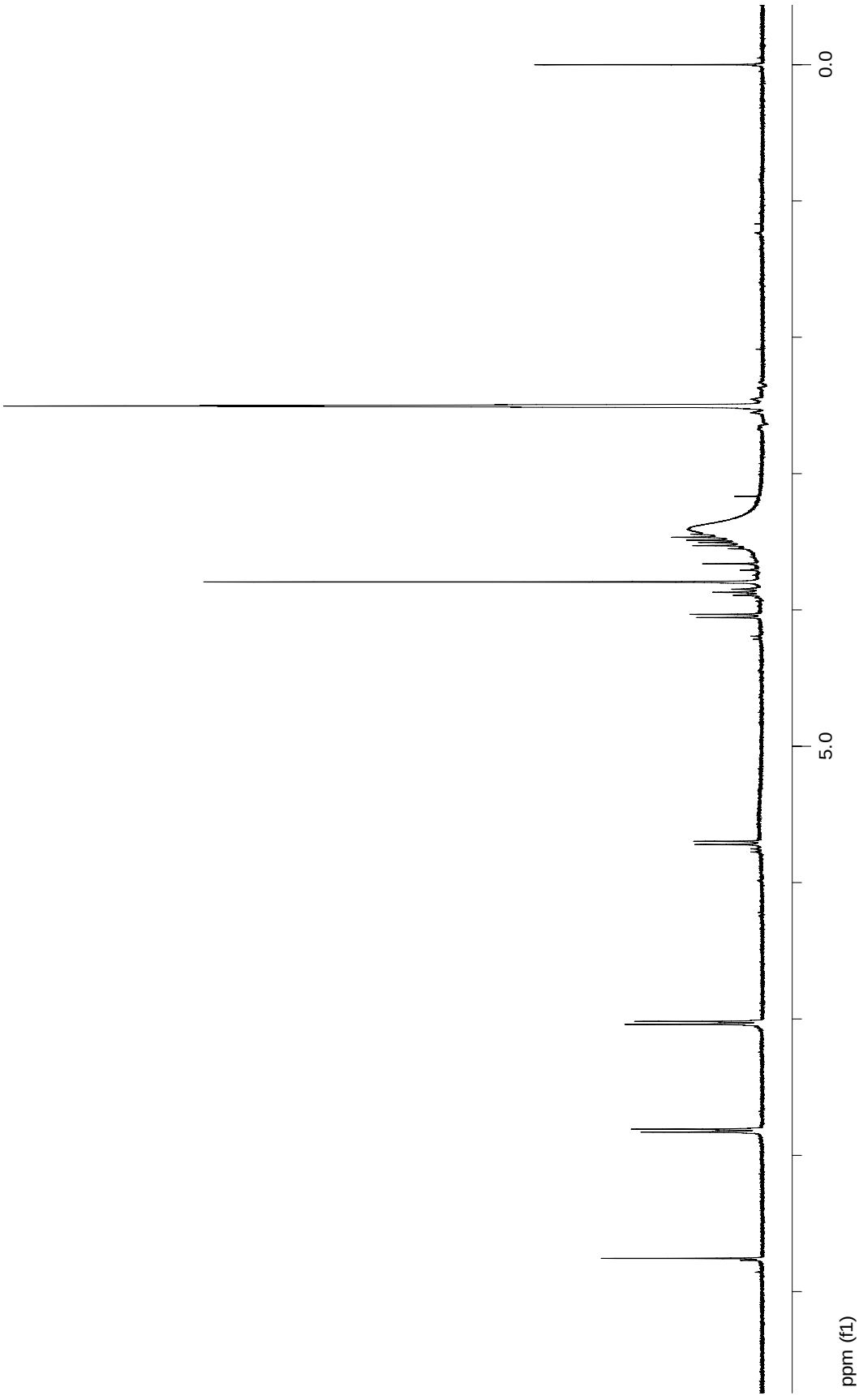

Figure 140: 400 MHz ^{1}H NMR spectrum of glucuronosyl-4-(4-methoxyphenyl)-1*H*-[1,2,3]-triazole (**60**).

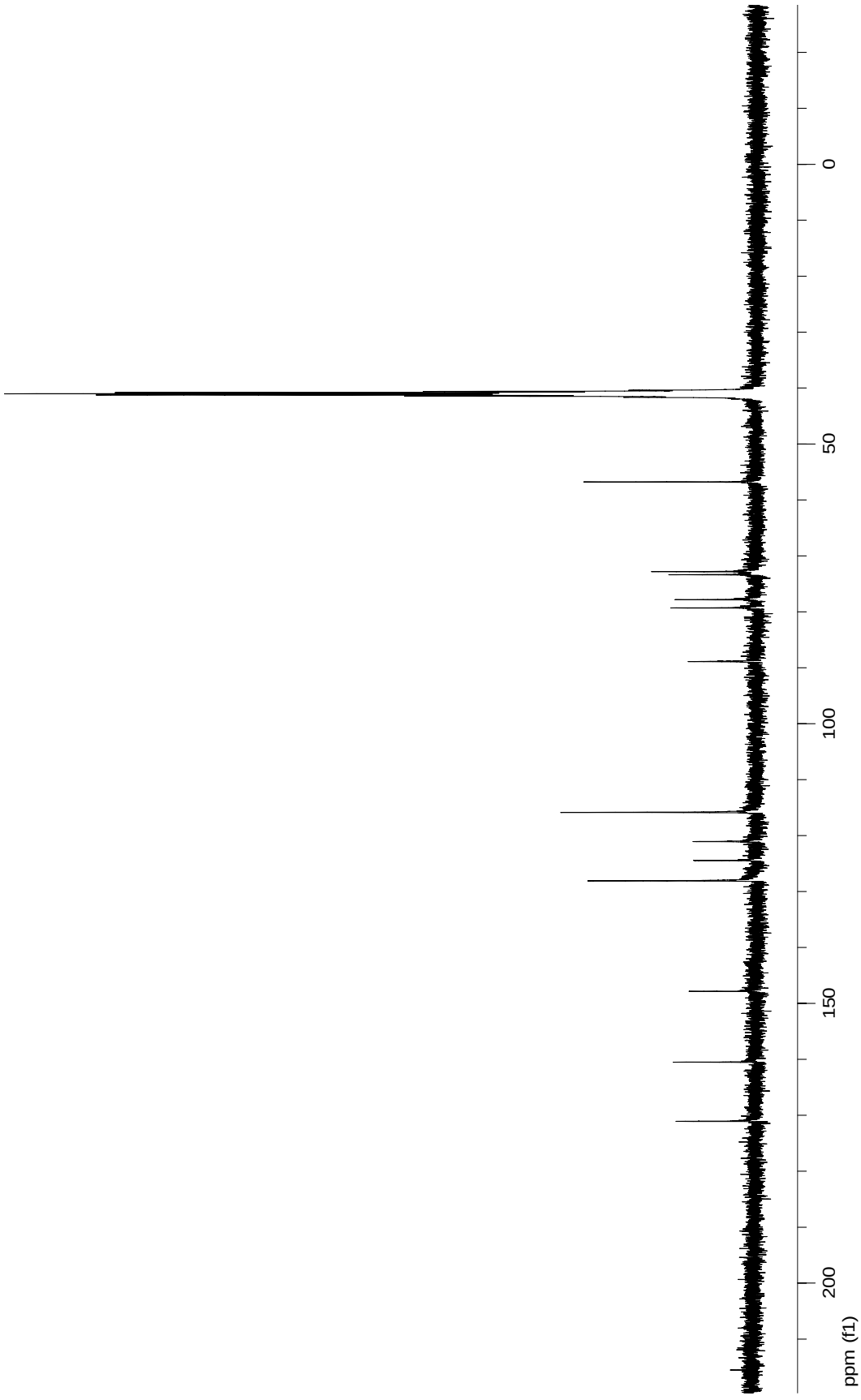

Figure 141: 100 MHz ^{13}C NMR spectrum of glucuronosyl-4-(4-methoxyphenyl)-1*H*-[1,2,3]-triazole (**60**).

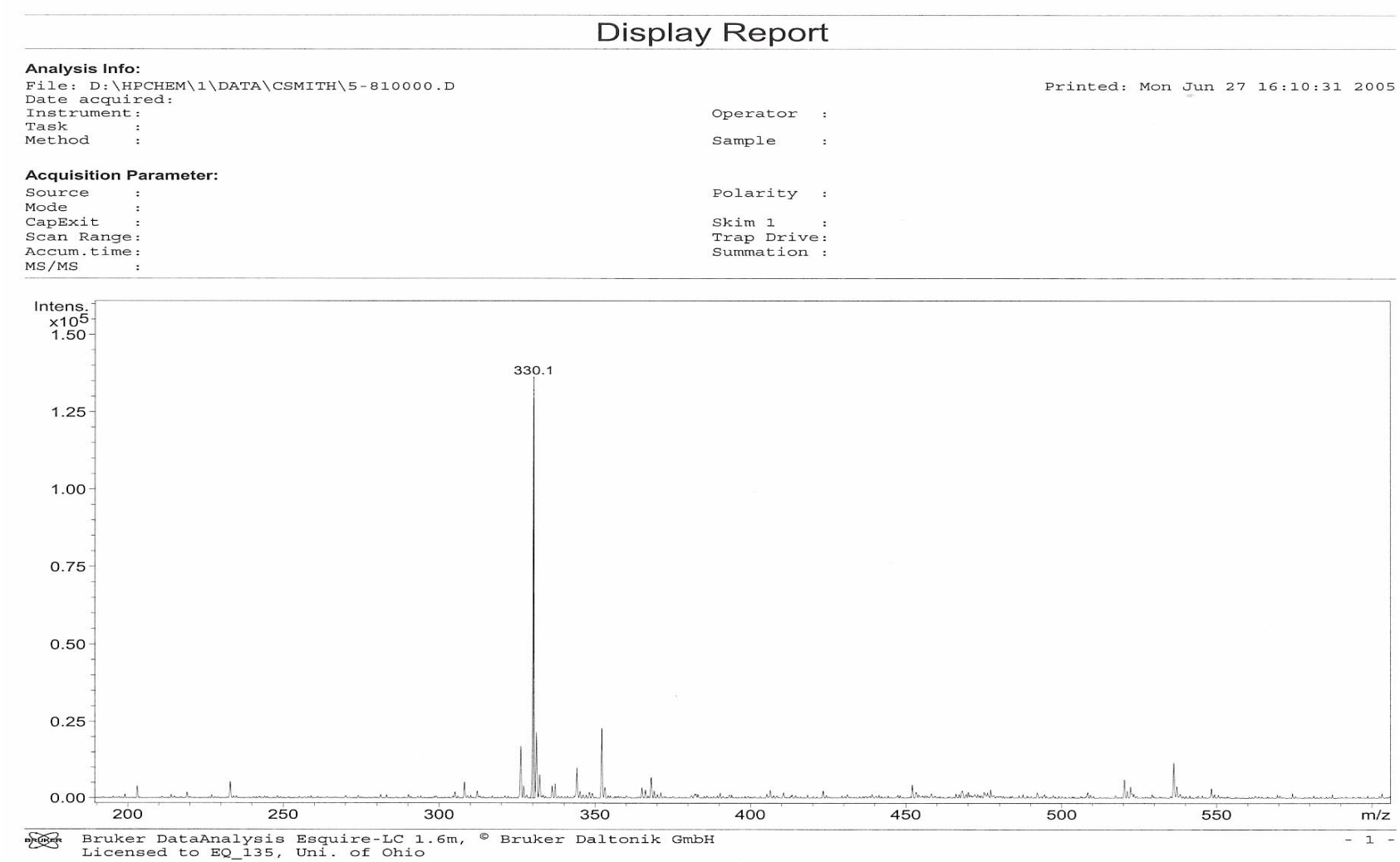

Figure 142: Mass spectrum of glucuronosyl-4-(4-methoxyphenyl)-1*H*-[1,2,3]-triazole (**60**).

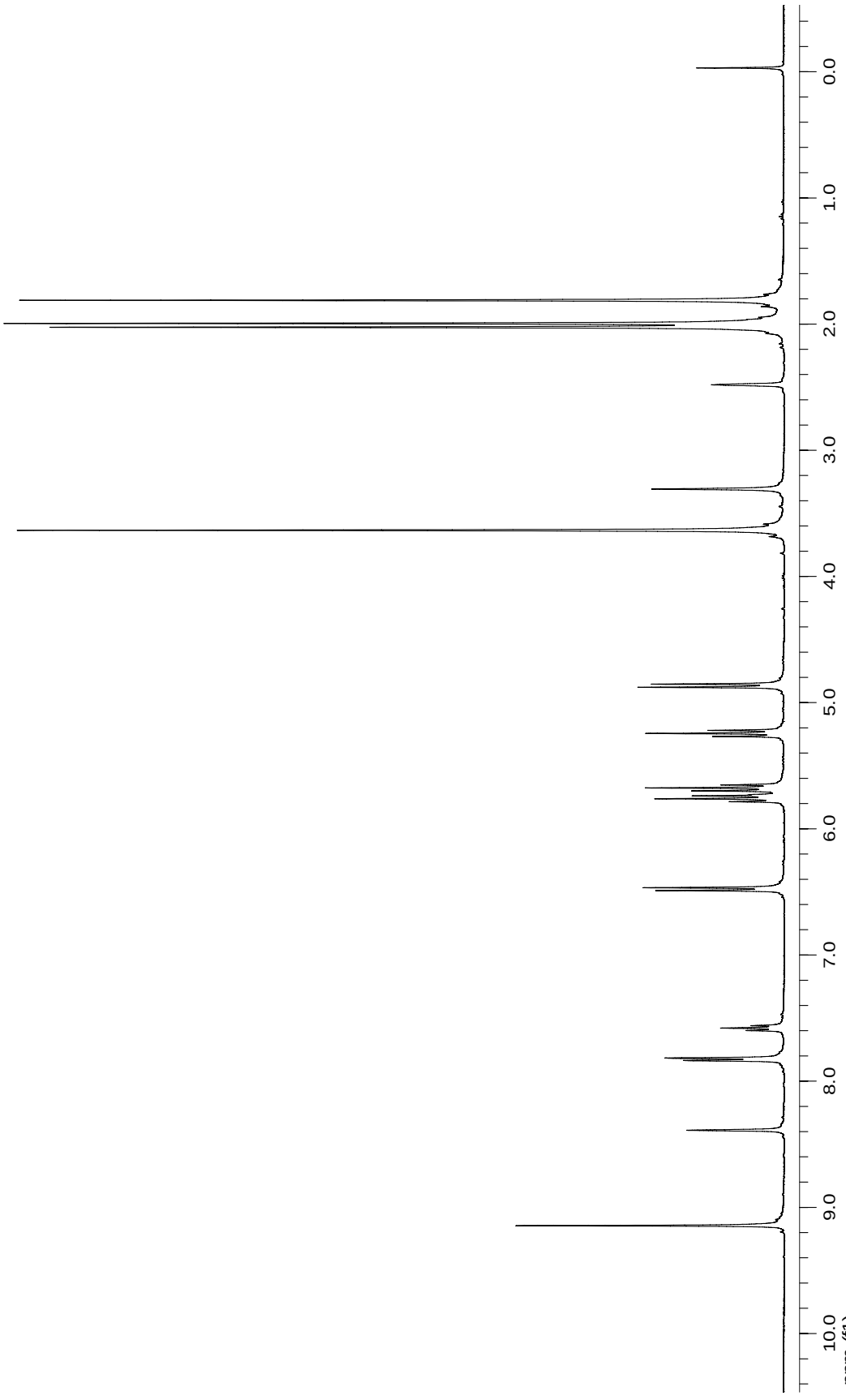

Figure 143: 400 MHz ^{1}H NMR spectrum of phenyl 1,3-bis[methyl 2,3,4-tri-*O*-acetyl-β-D-glucuronosyl-1H-[1,2,3]-triazole] (**61**).

Display Report

Analysis Info:

File: D:\HPCHEM\1\DATA\CSMITH\7-27-105.D
Printed: Fri Jul 01 10:27:49 2005
Date acquired:
Instrument:
Operator :
Task :
Method :
Sample :

Acquisition Parameter:

Source :
Polarity :
Mode :
CapExit :
Skim 1 :
Scan Range:
Trap Drive:
Accum.time:
Summation :
MS/MS :

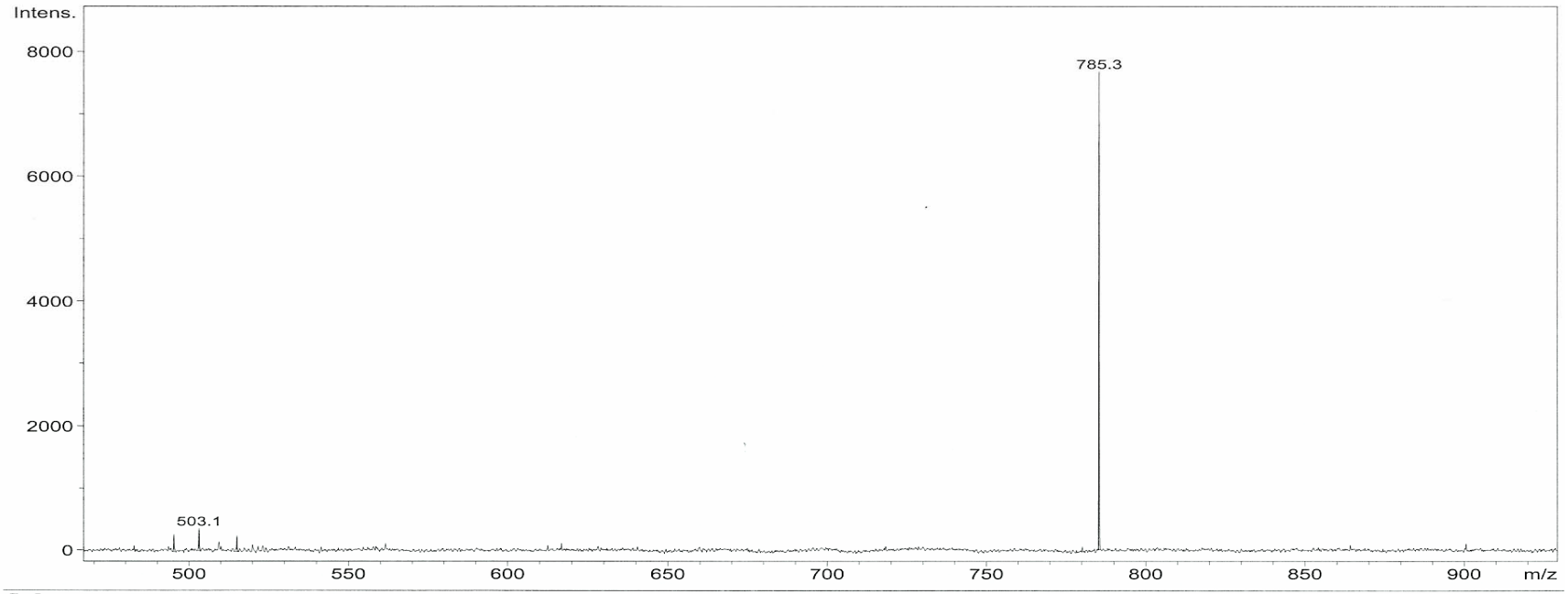

Bruker DataAnalysis Esquire-LC 1.6m, © Bruker Daltonik GmbH
Licensed to EQ_135, Uni. of Ohio
- 1 -

Figure 144: Mass spectrum of phenyl 1,3-bis[methyl 2,3,4-tri-*O*-acetyl-β-D-glucuronosyl-1H-[1,2,3]-triazole] (**61**).

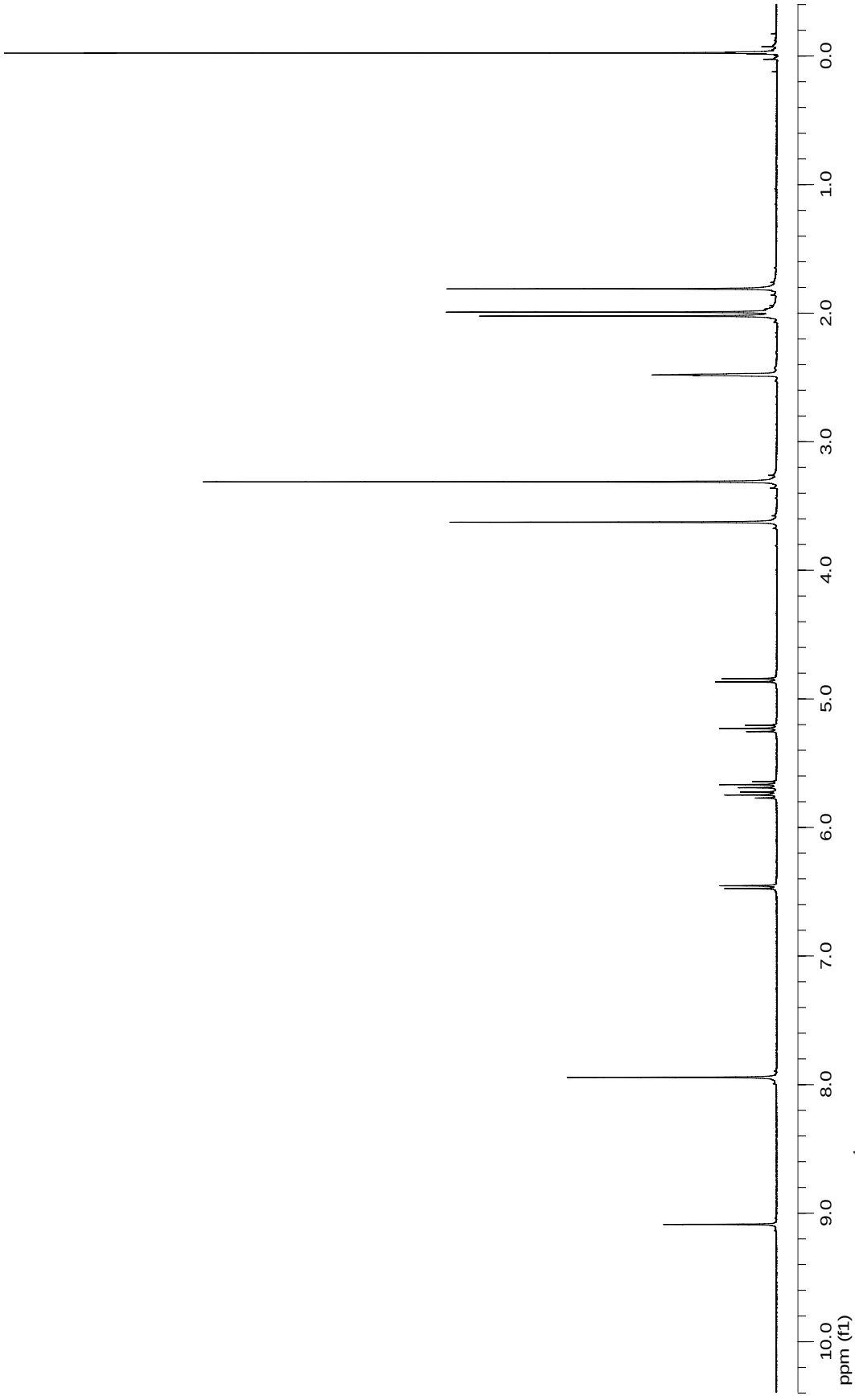

Figure 145: 400 MHz ^{1}H NMR spectrum of phenyl 1,4-bis[methyl 2,3,4-tri-*O*-acetyl-β-D-glucuronosyl-1H-[1,2,3]-triazole] (**62**).

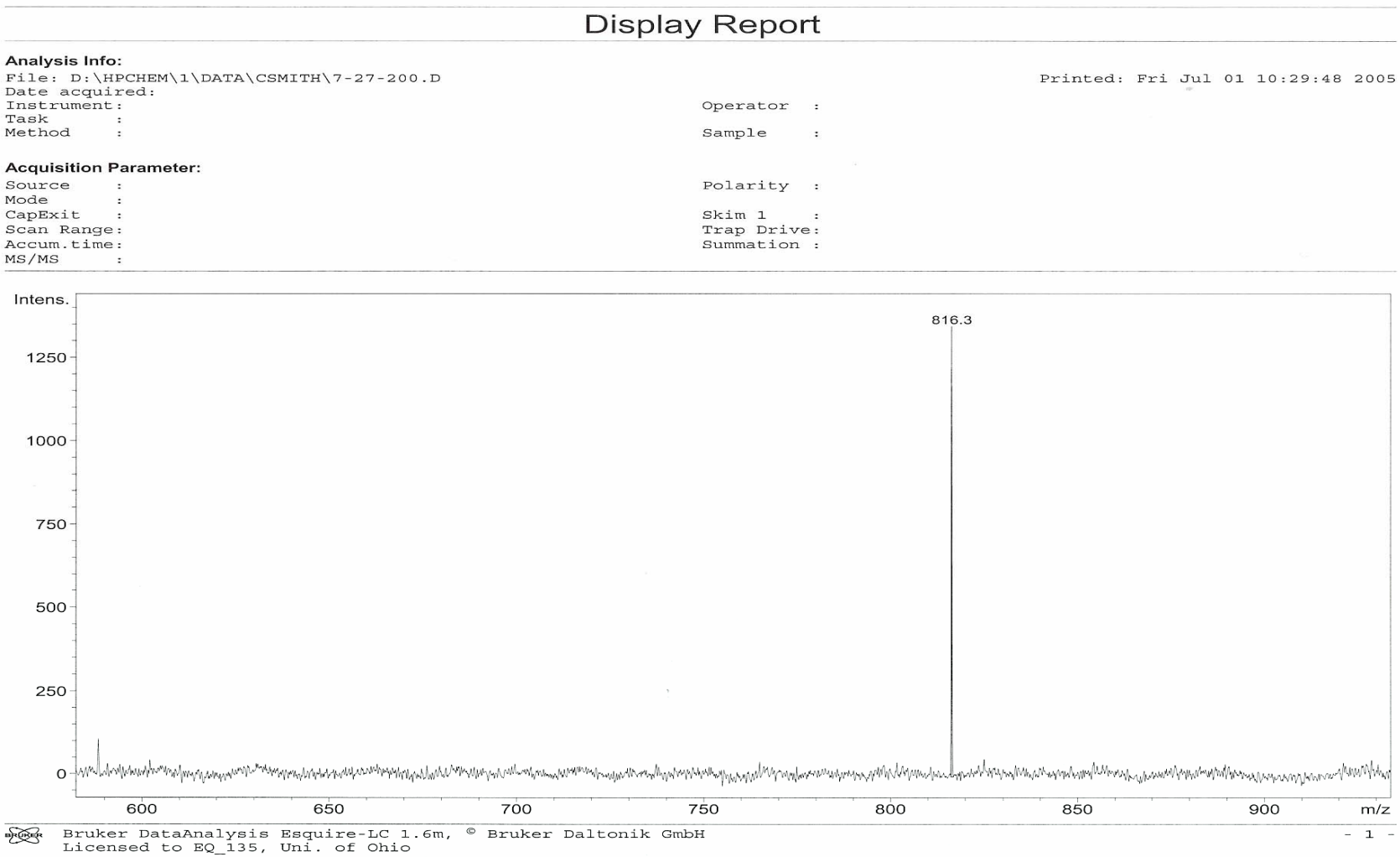

Figure 146: Mass spectrum of phenyl 1,4-bis[methyl 2,3,4-tri-*O*-acetyl-β-D-glucuronosyl-1H-[1,2,3]-triazole] (**62**).

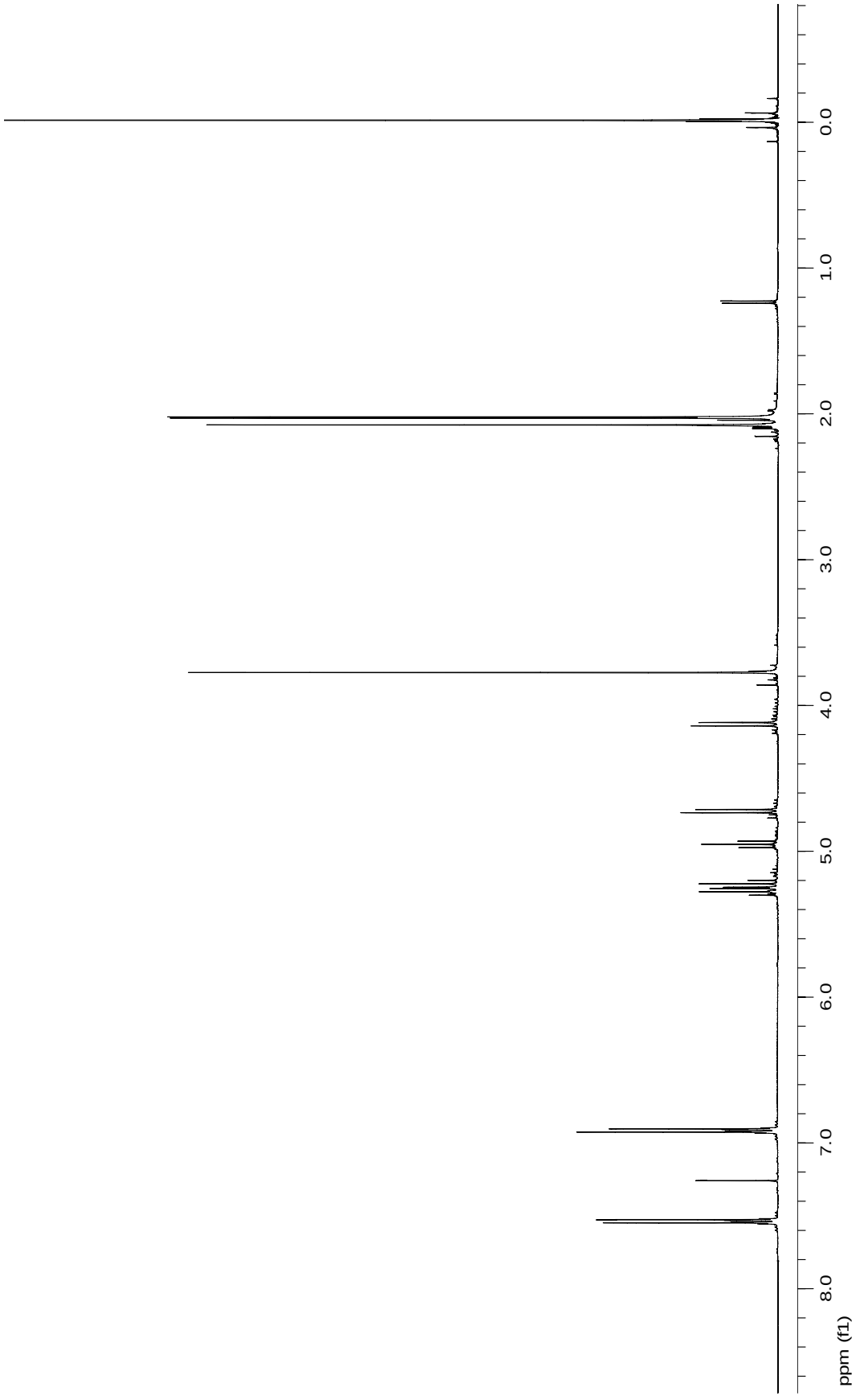

Figure 147: 400 MHz ^{1}H NMR spectrum of glucuronosyl-4-(4-hydroxyphenyl)-[1,2,3,5]-tetrazole (**63**).

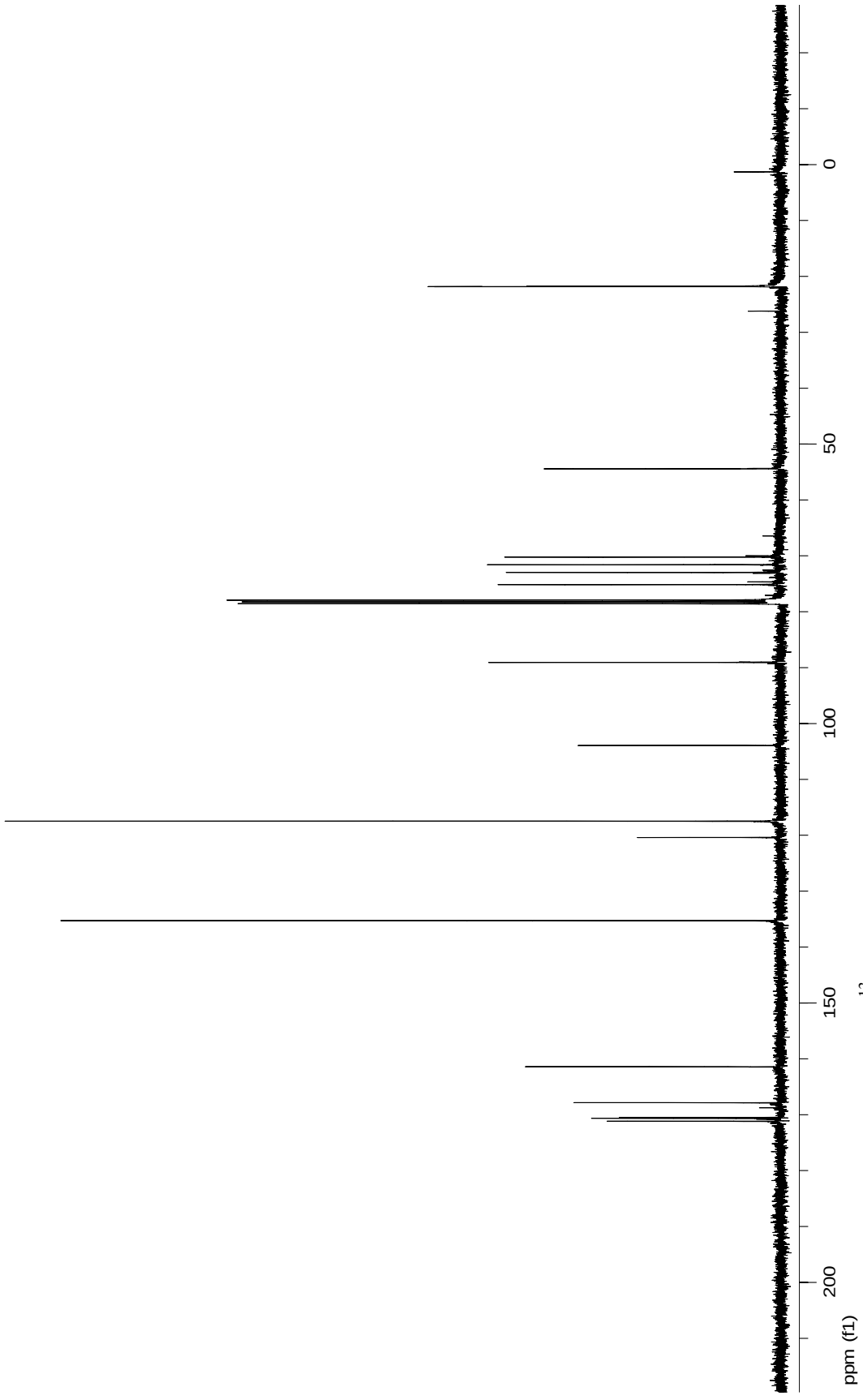

Figure 148: 100 MHz ^{13}C NMR spectrum of glucuronosyl-4-(4-hydroxyphenyl)-[1,2,3,5]-tetrazole (**63**).

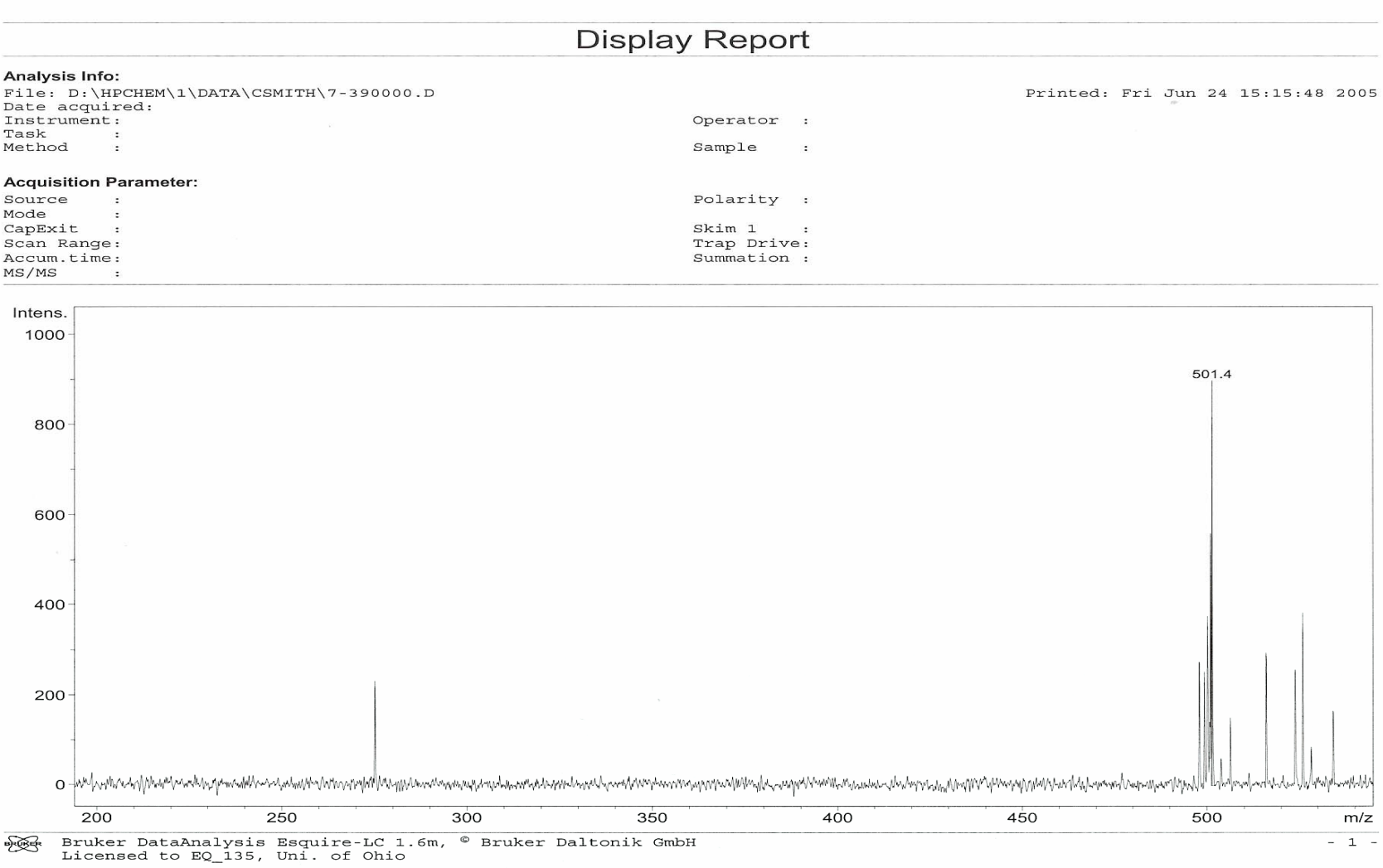

Figure 149: Mass spectrum of glucuronosyl-4-(4-hydroxyphenyl)-[1,2,3,5]-tetrazole (**63**).

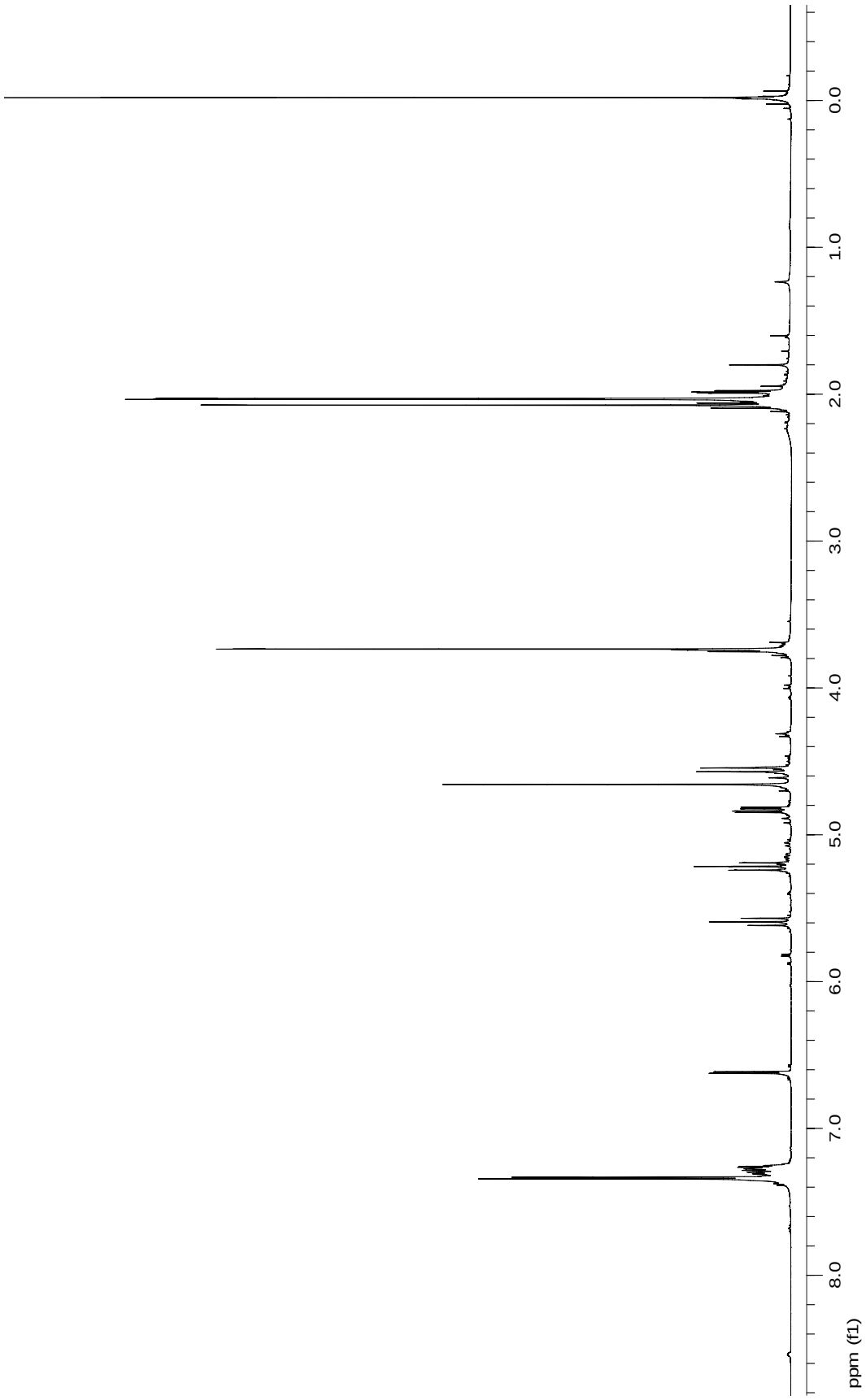

Figure 150: 400 MHz ^{1}H NMR spectrum of benzyl-(β-D-glucopyranosyl) uronate (**64**).

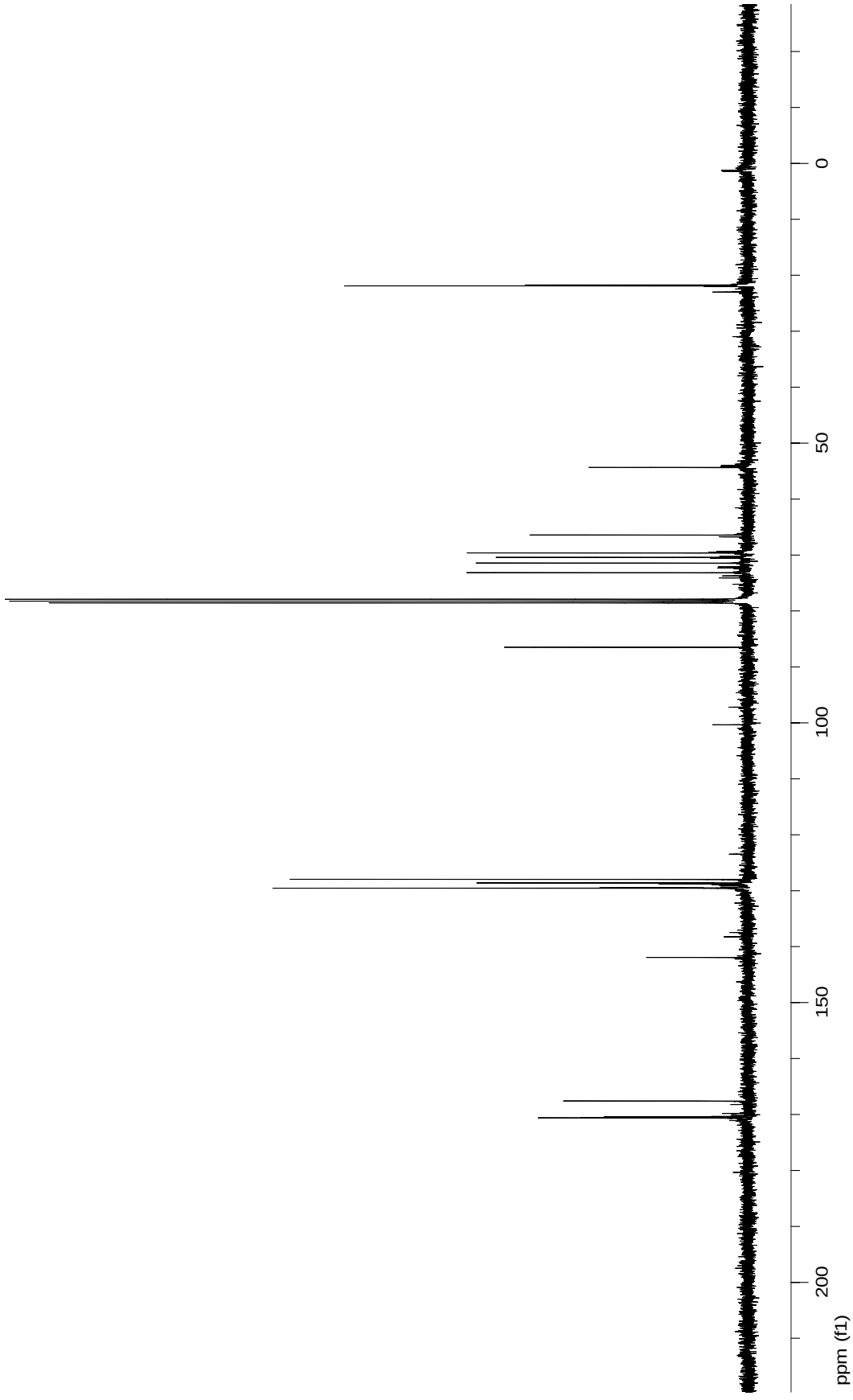

Figure 151: 100 MHz ^{13}C NMR spectrum of benzyl-(β-D-glucopyranosyl) uronate (**64**).

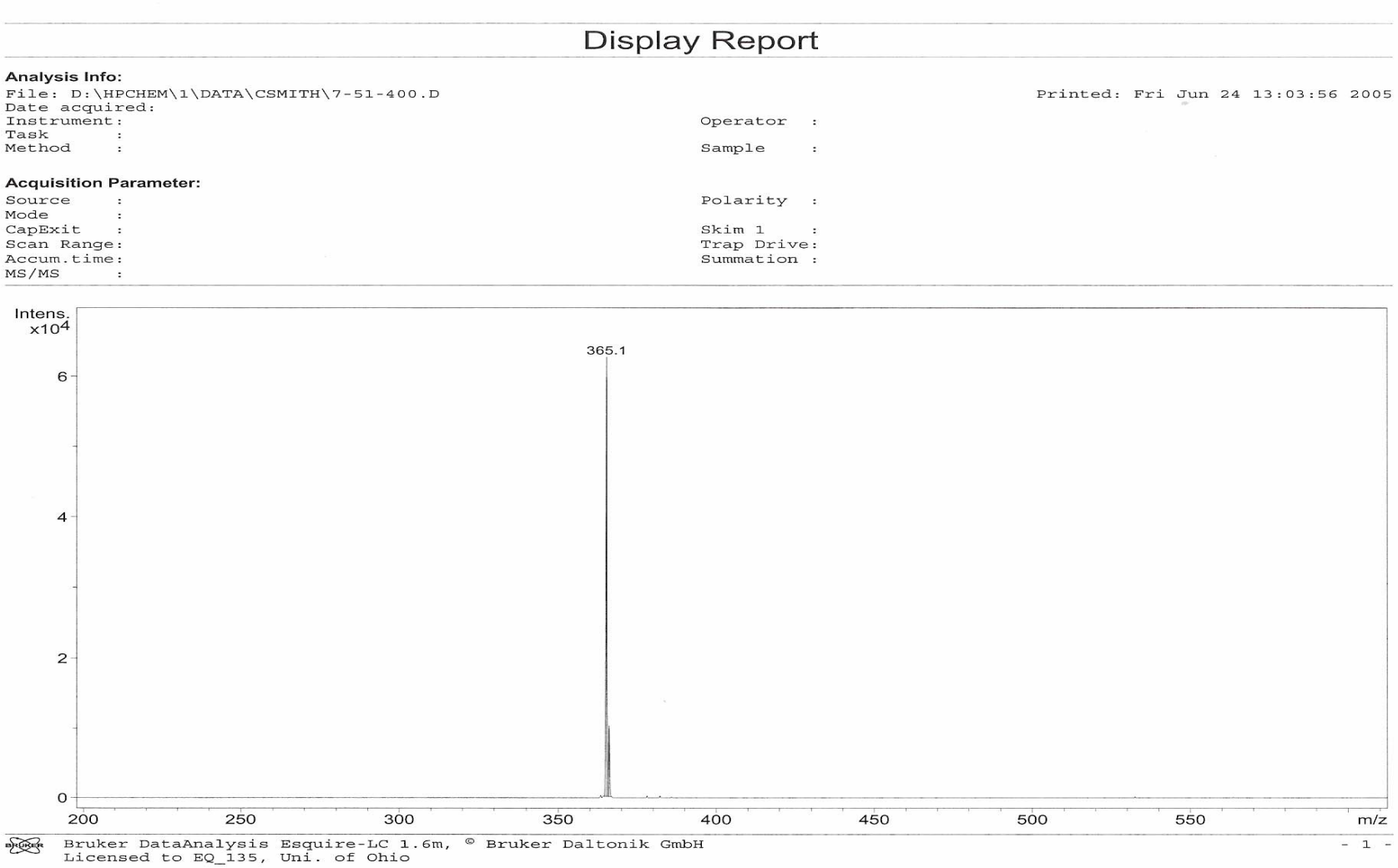

Figure 152: Mass spectrum of benzyl-(β-D-glucopyranosyl) uronate (**64**).

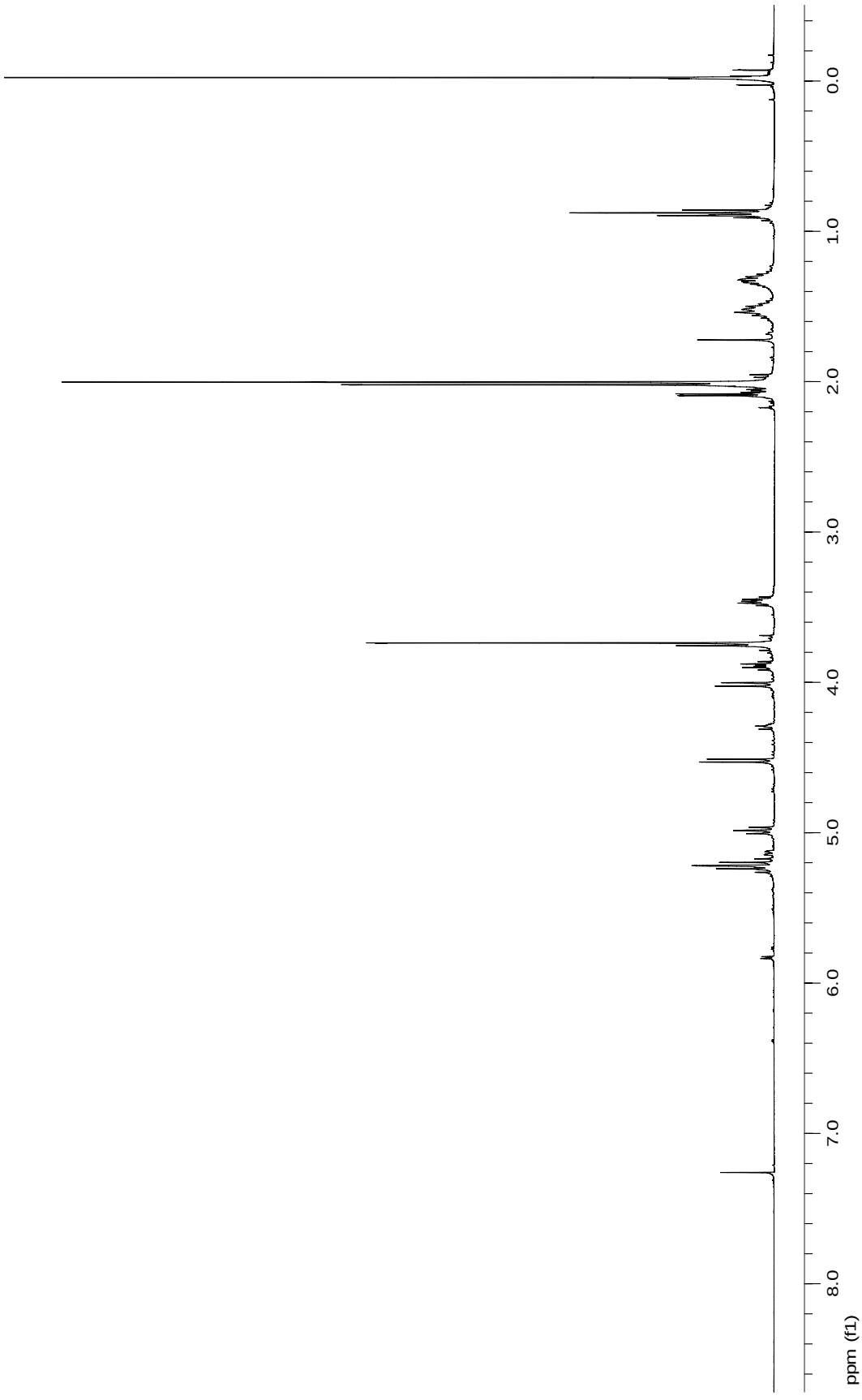

Figure 153: 400 MHz ^{1}H NMR spectrum of *n*-butyl-(β-D-glucopyranosyl) uronate (**65**).

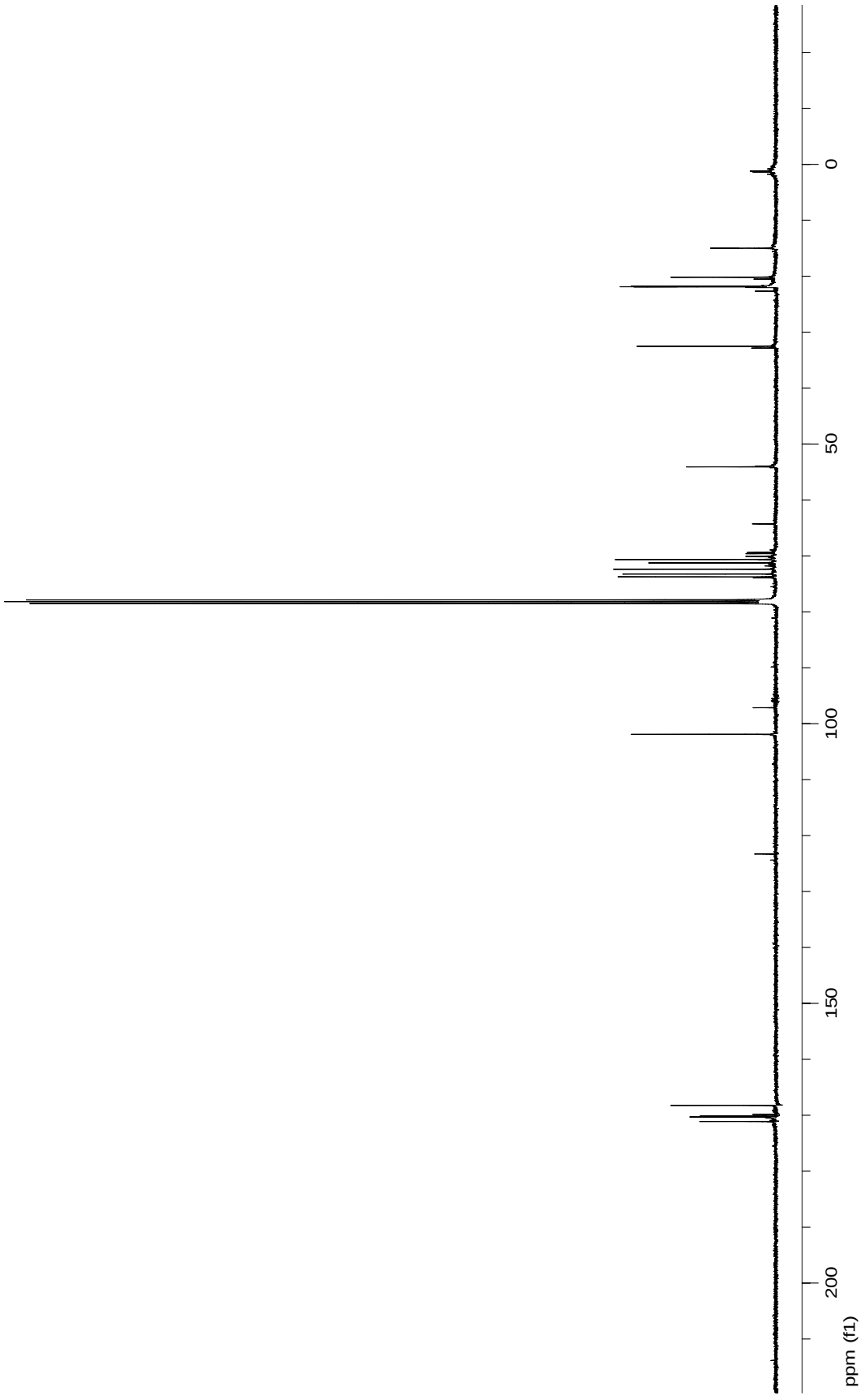

Figure 154: 100 MHz ^{13}C NMR spectrum of *n*-butyl-(β-D-glucopyranosyl) uronate (**65**).

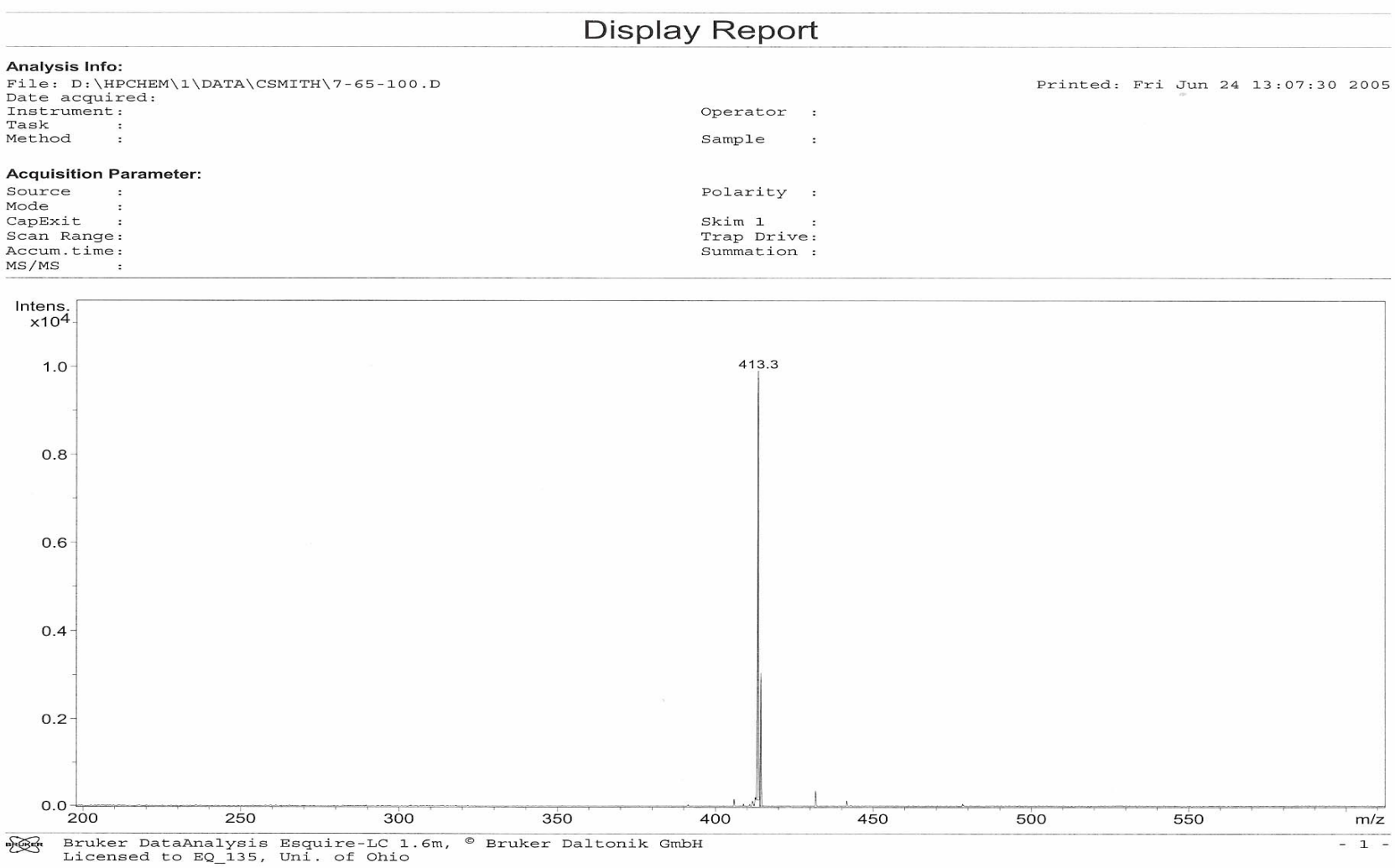

Figure 155: Mass spectrum of *n*-butyl-(β-D-glucopyranosyl) uronate (**65**).

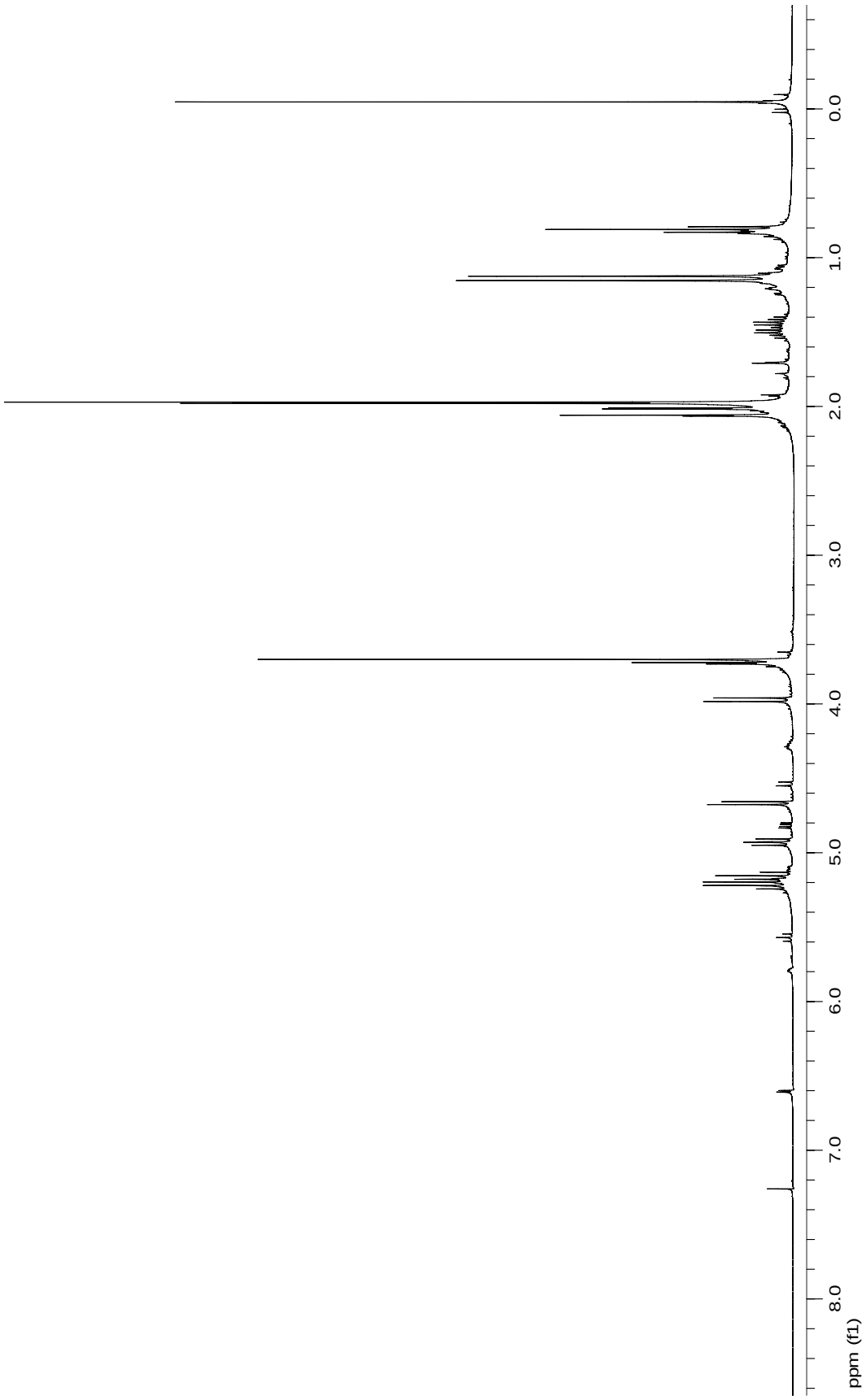

Figure 156: 400 MHz ^{1}H NMR spectrum of *t*-amyl-(β-D-glucopyranosyl) uronate (**66**).

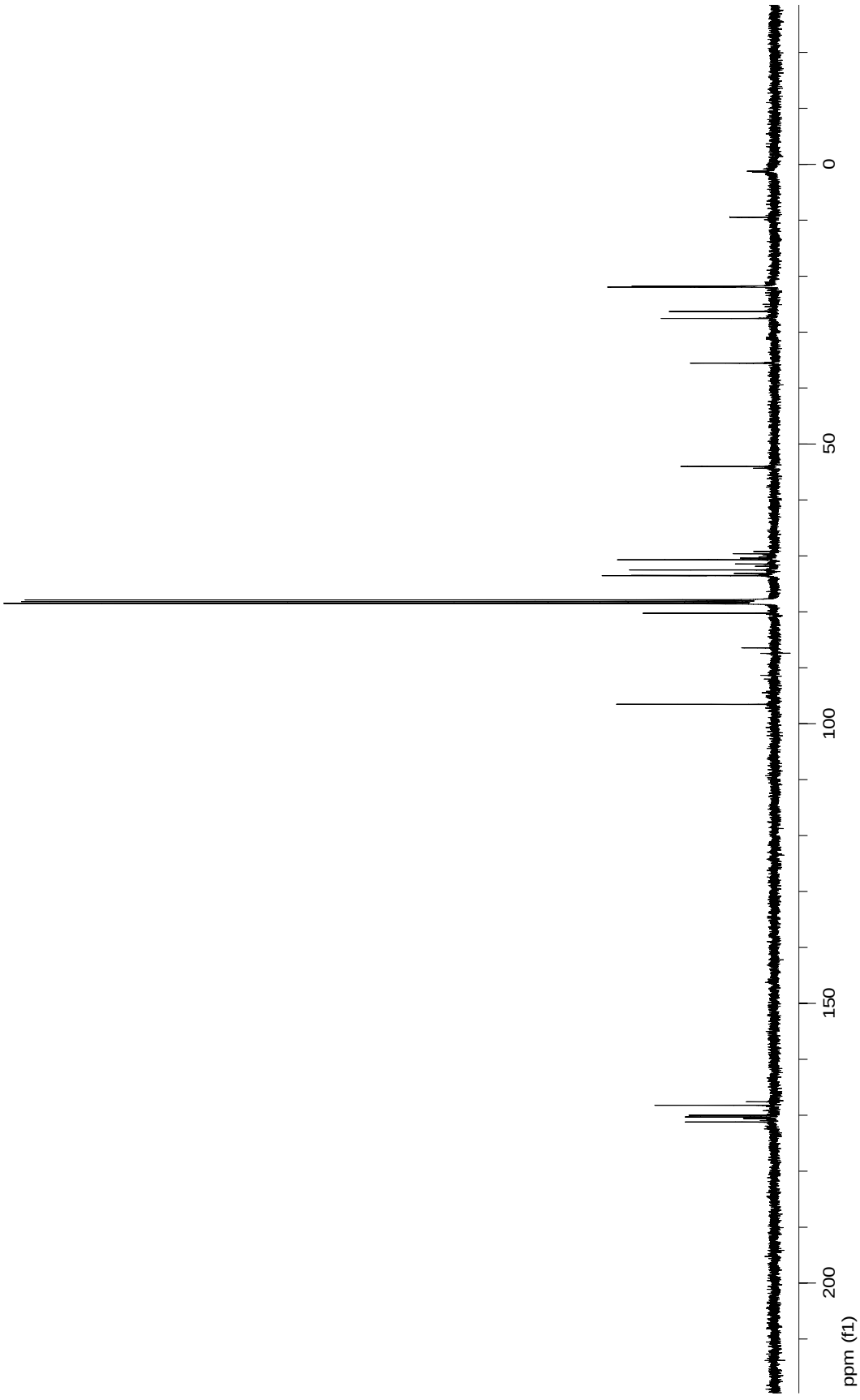

Figure 157: 100 MHz ^{13}C NMR spectrum of *t*-amyl-(β-D-glucopyranosyl) uronate (**66**).

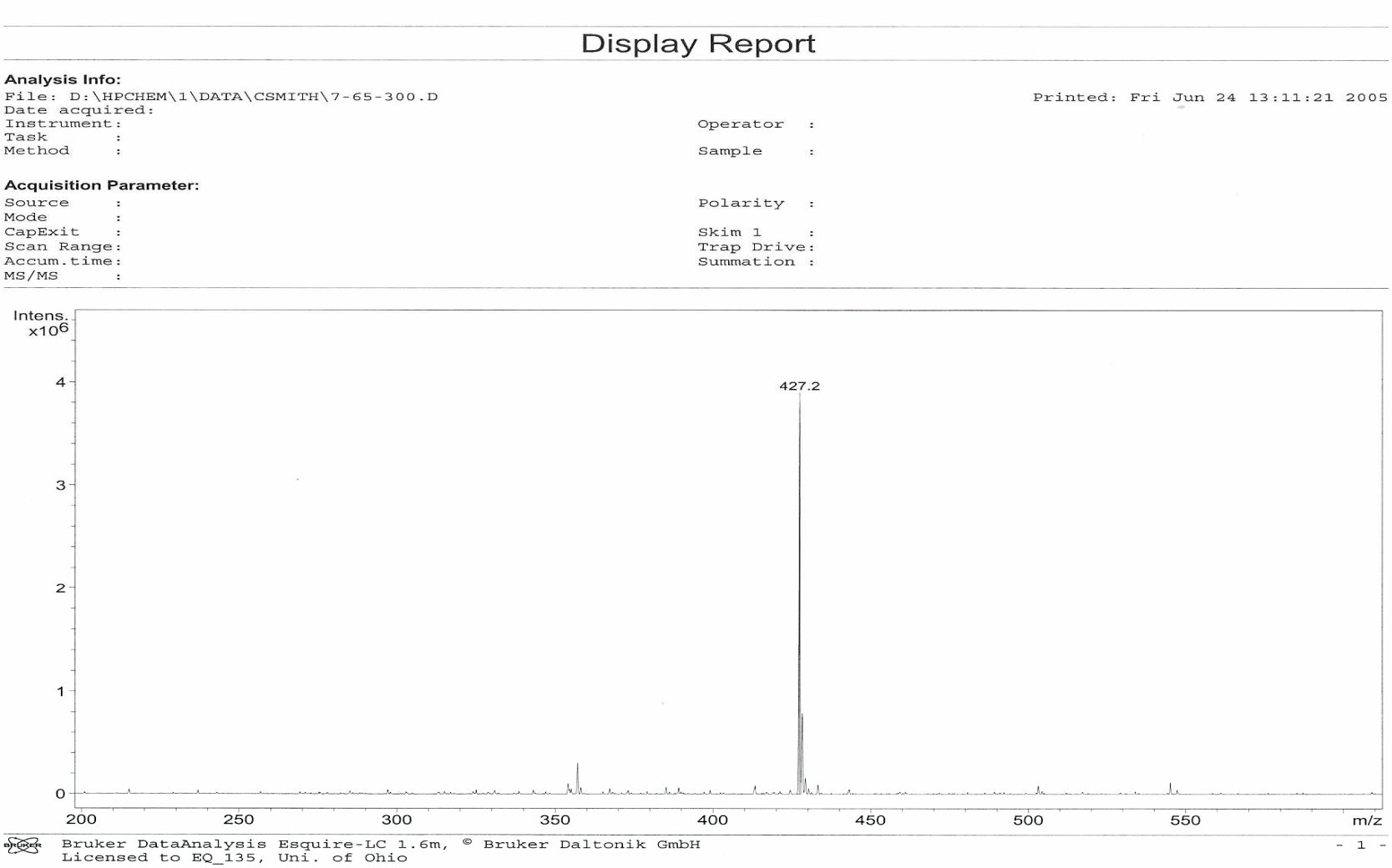

Figure 158: Mass spectrum of *t*-amyl-(β-D-glucopyranosyl) uronate (**66**).

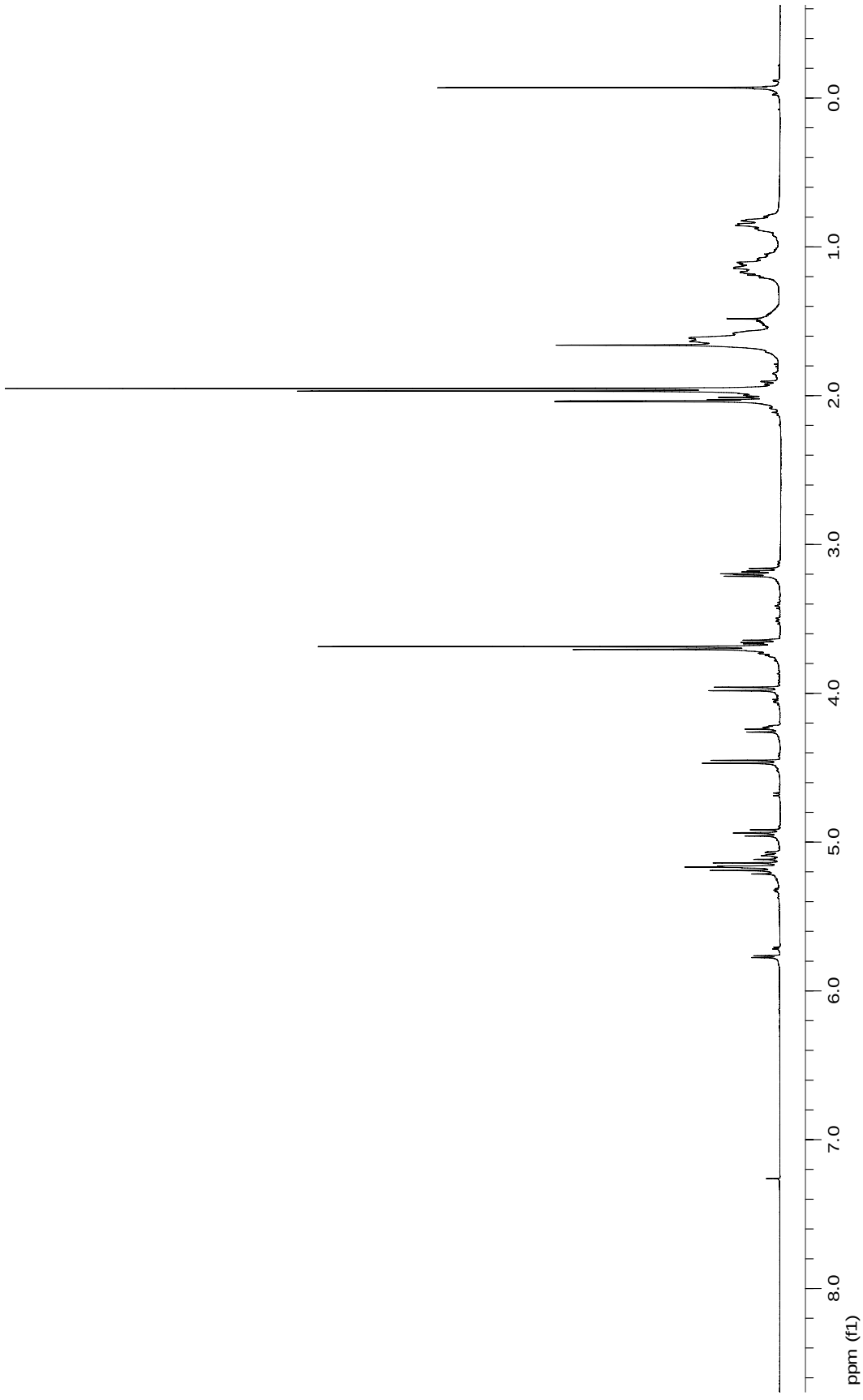

Figure 159: 400 MHz ^{1}H NMR spectrum of cyclohexyl-(β-D-glucopyranosyl) uronate (**67**).

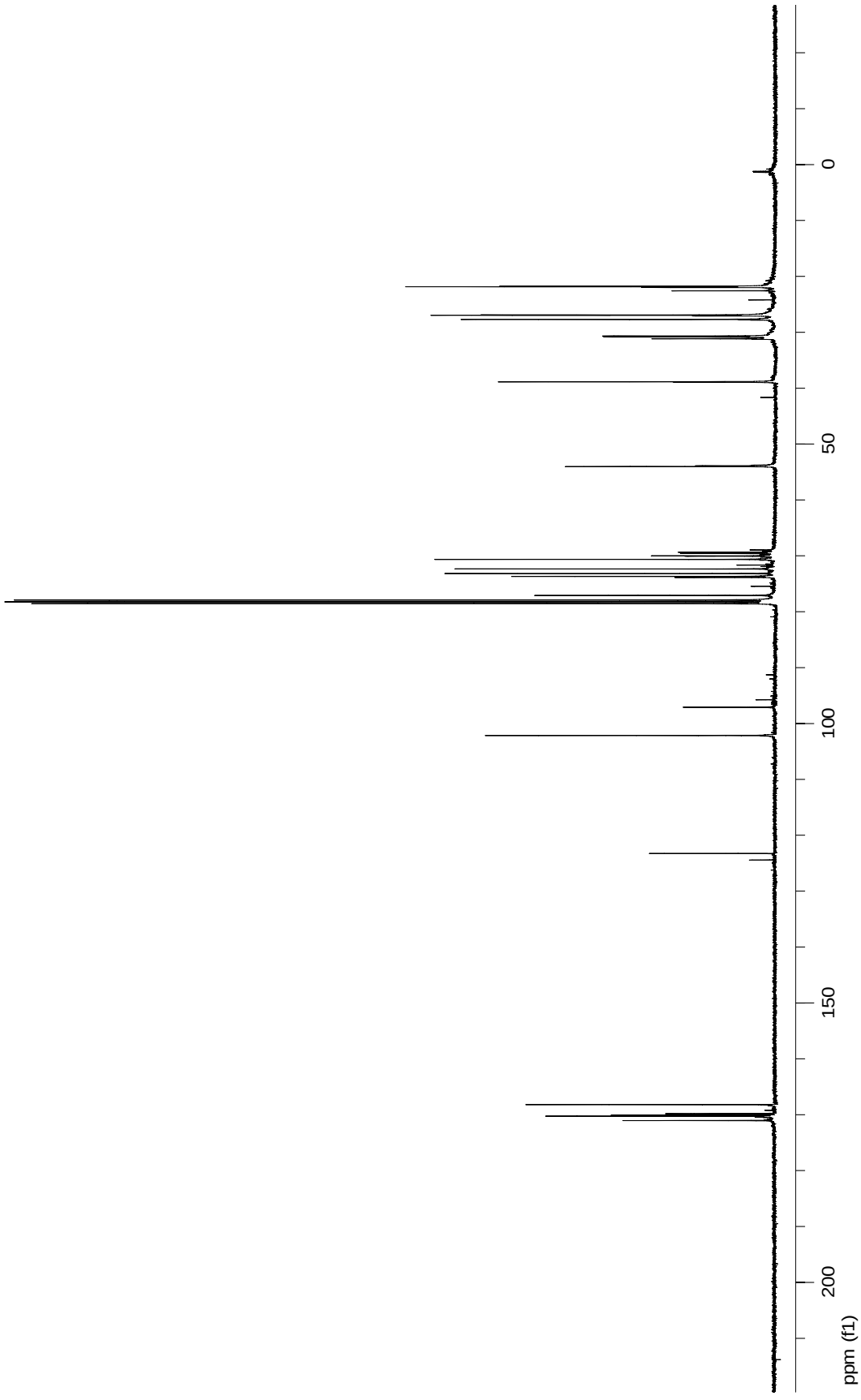

Figure 160: 100 MHz ^{13}C NMR spectrum of cyclohexyl-(β-D-glucopyranosyl) uronate (**67**).

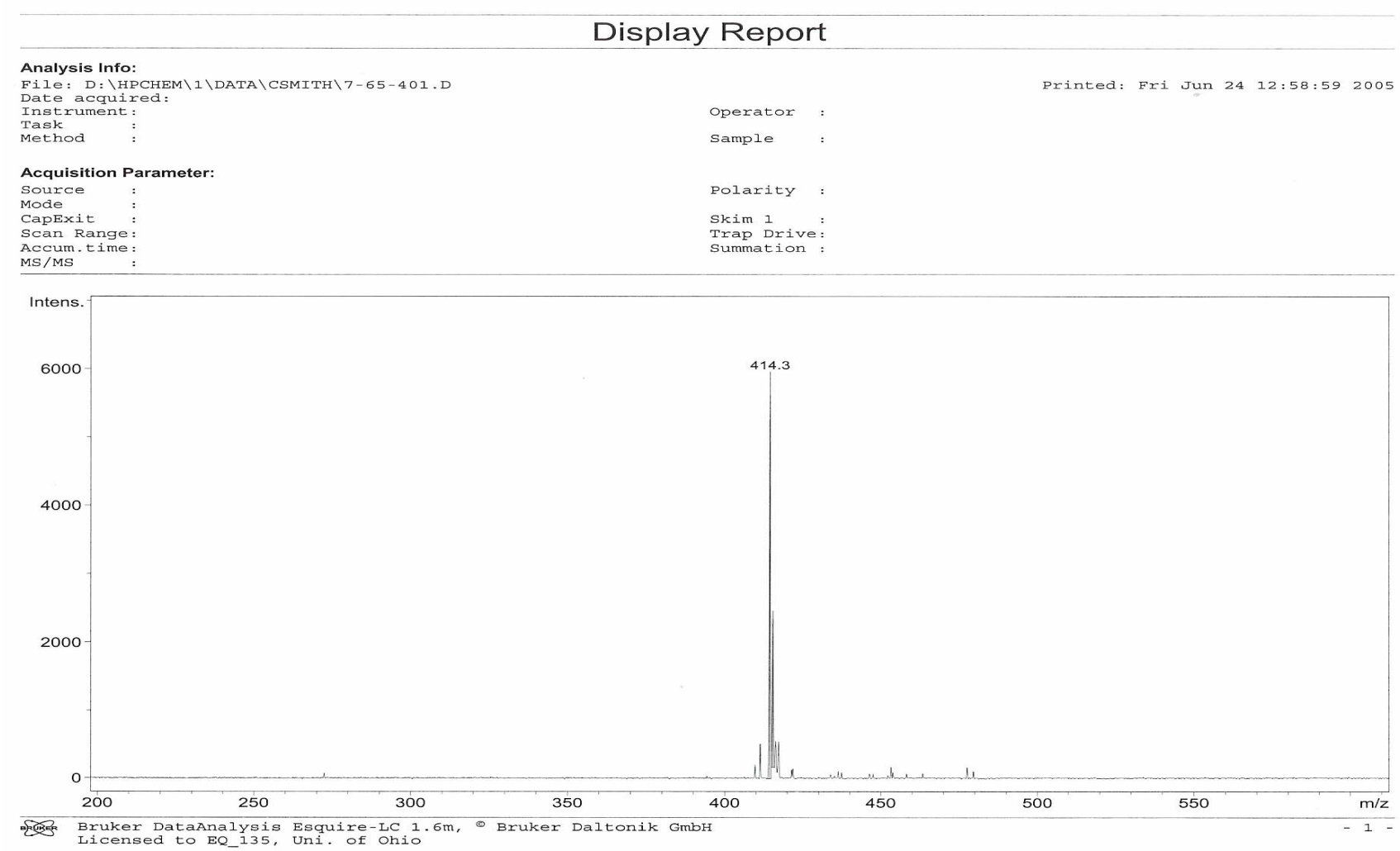

Figure 161: Mass spectrum of cyclohexyl-(β-D-glucopyranosyl) uronate (**67**).

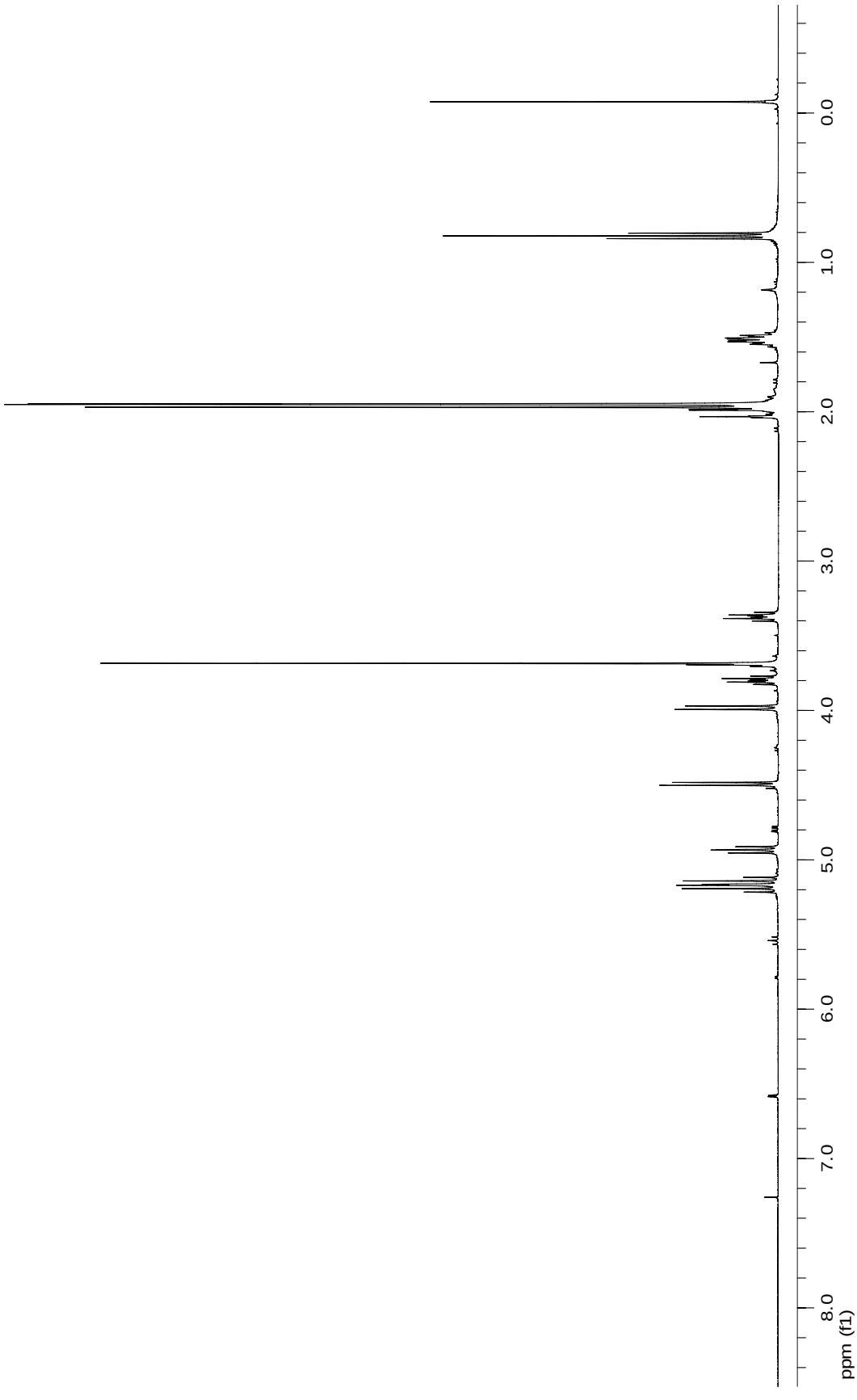

Figure 162: 400 MHz ^{1}H NMR spectrum of *n*-propyl-(β-D-glucopyranosyl) uronate (**68**).

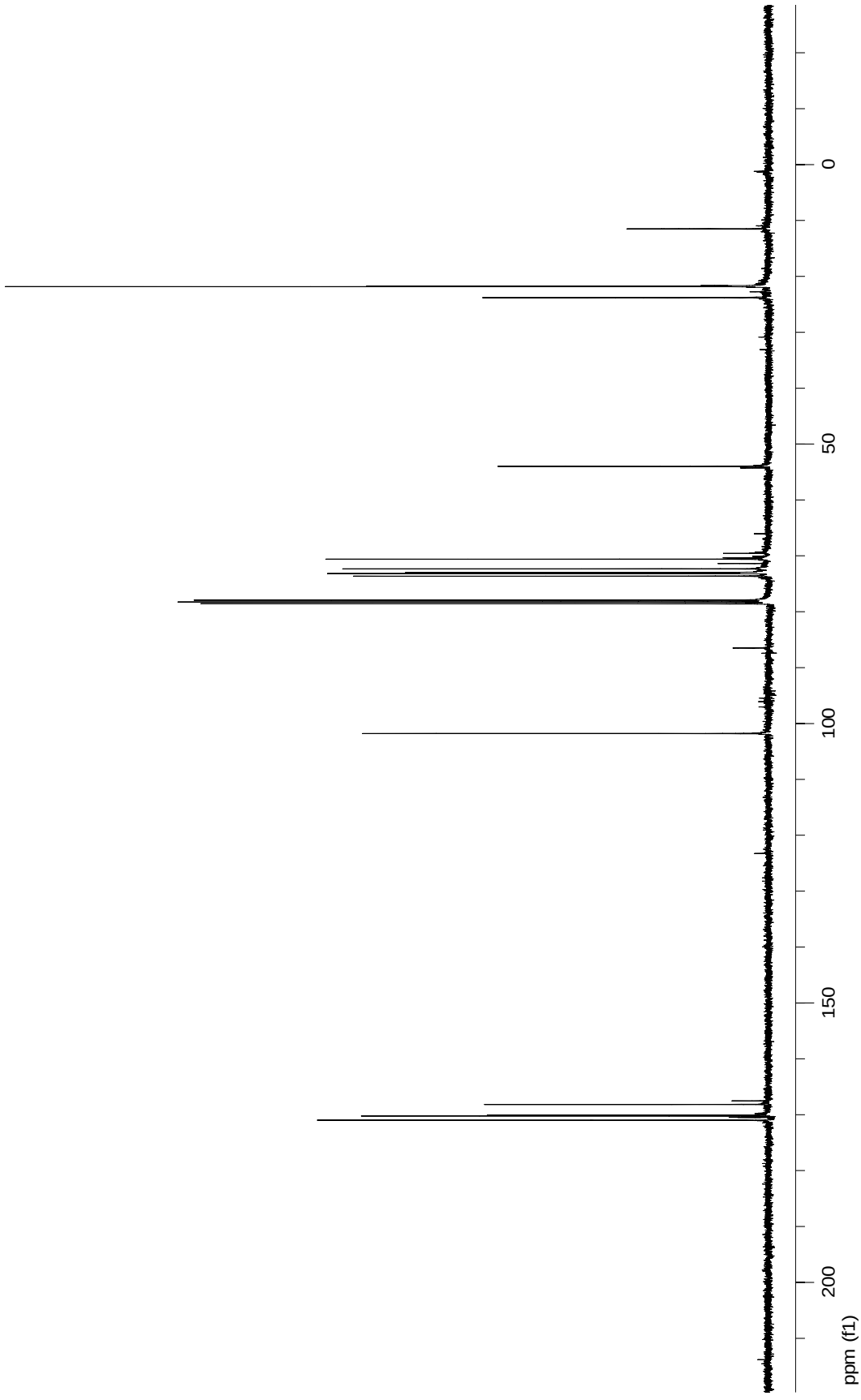

Figure 163: 100 MHz ^{13}C NMR spectrum of *n*-propyl-(β-D-glucopyranosyl) uronate (**68**).

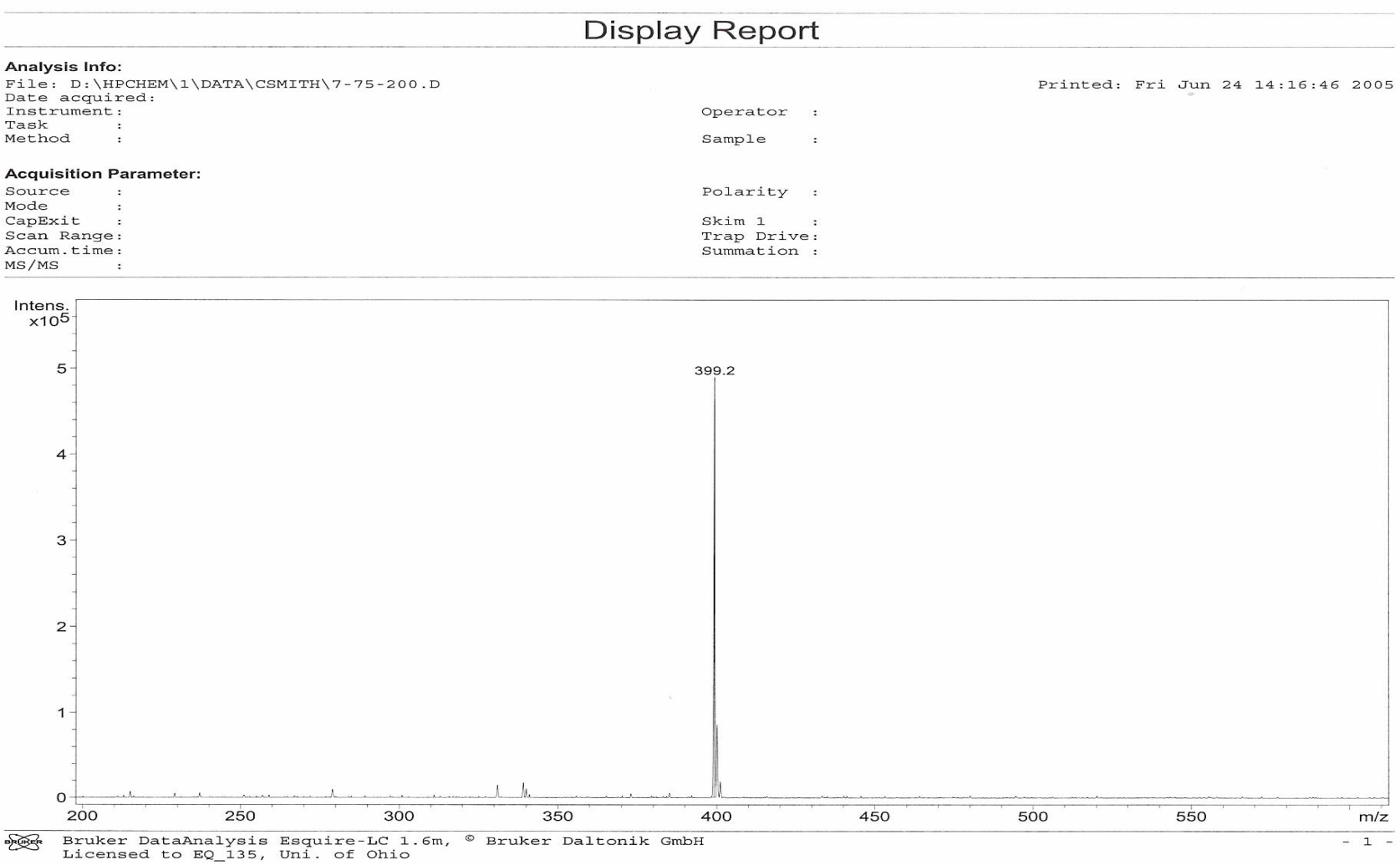

Figure 164: Mass spectrum of *n*-propyl-(β-D-glucopyranosyl) uronate (**68**).

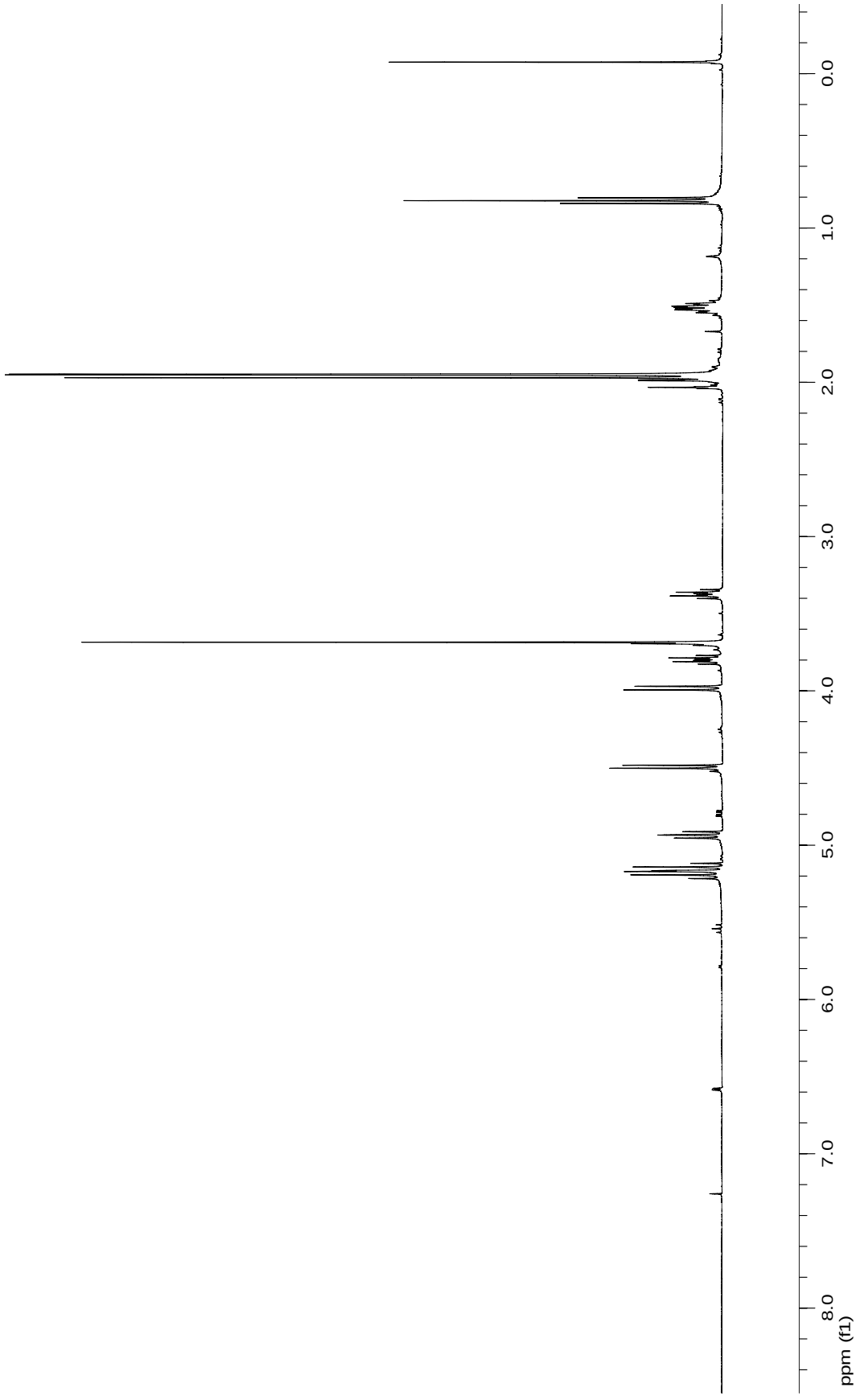

Figure 165: 400 MHz ^{1}H NMR spectrum of ethyl-(β-D-glucopyranosyl) uronate (**69**).

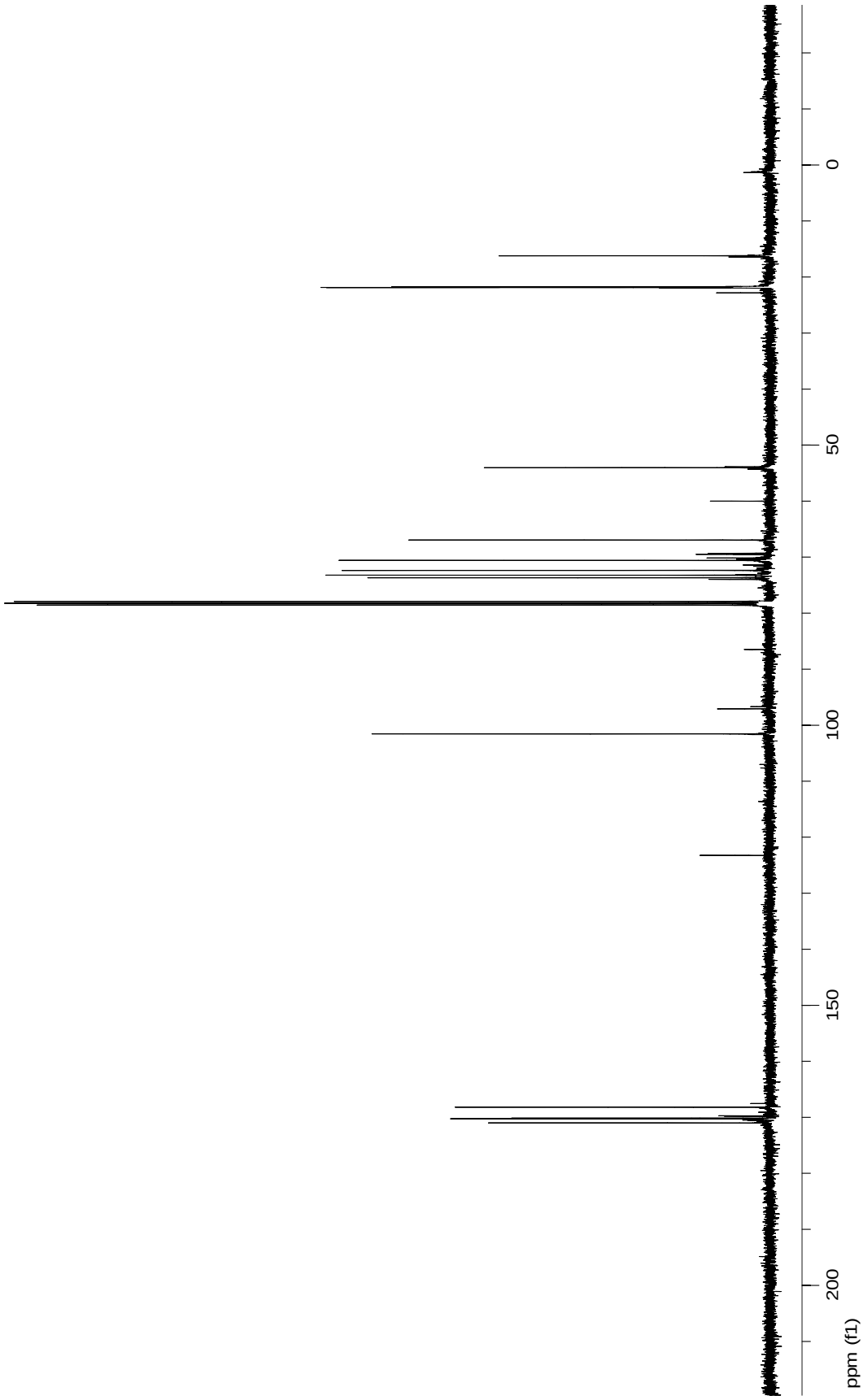

Figure 166: 100 MHz ^{13}C NMR spectrum of ethyl-(β-D-glucopyranosyl) uronate (**69**).

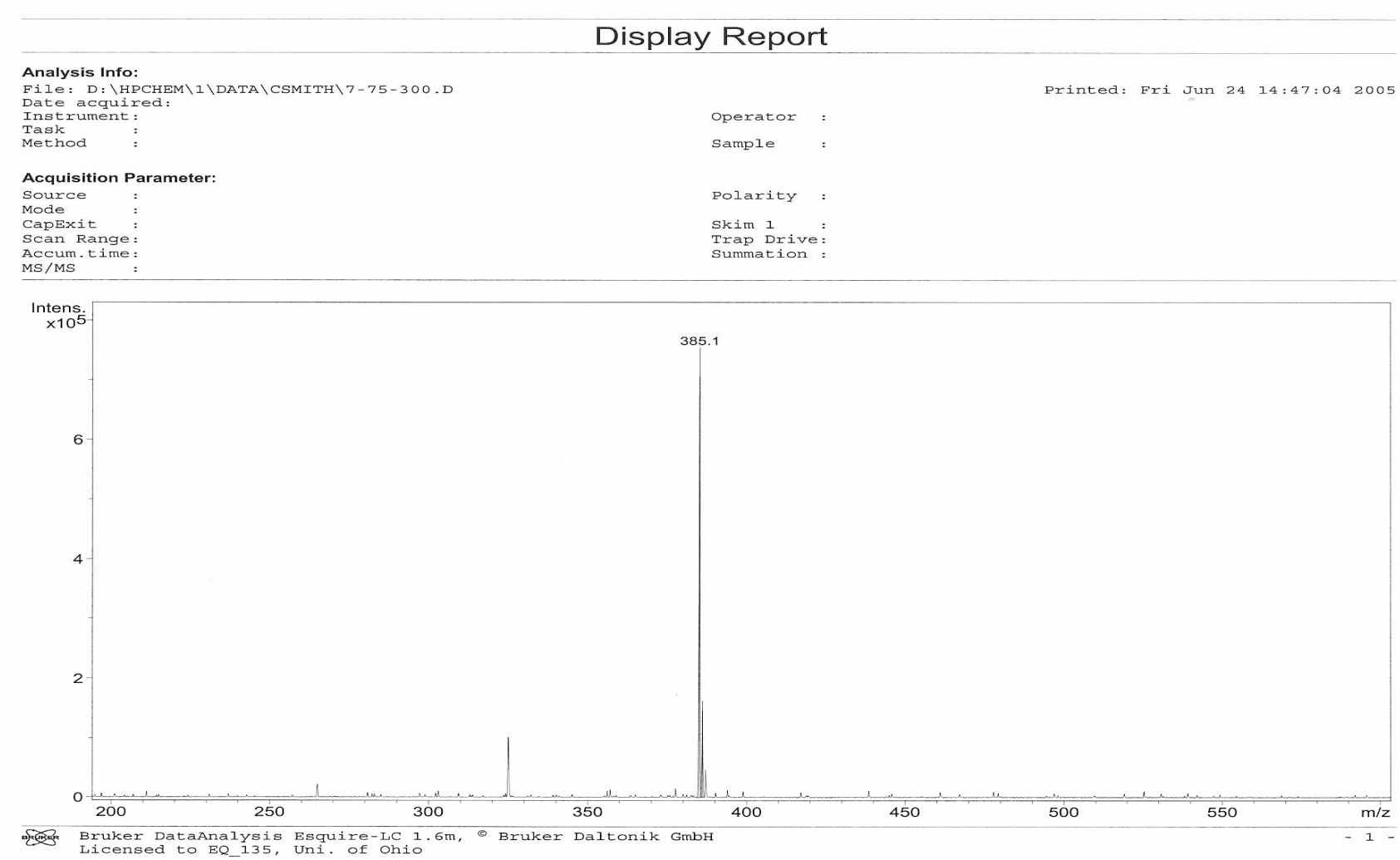

Figure 167: Mass spectrum of ethyl-(β-D-glucopyranosyl) uronate (**69**).

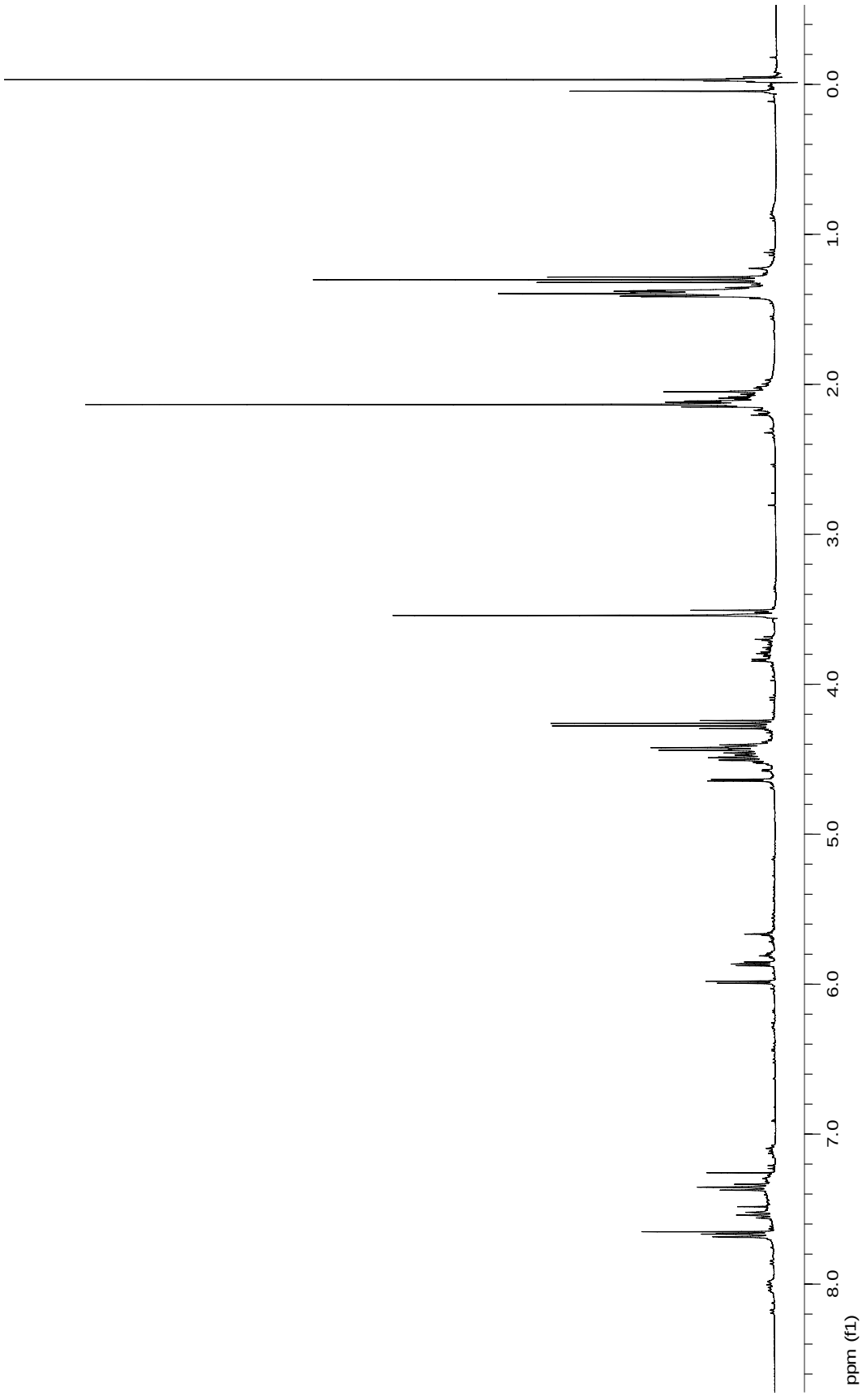

Figure 168: 400 MHz ^{1}H NMR spectrum of methyl D-fructuronate-*O*-benzoyloxime triazole **(70).**

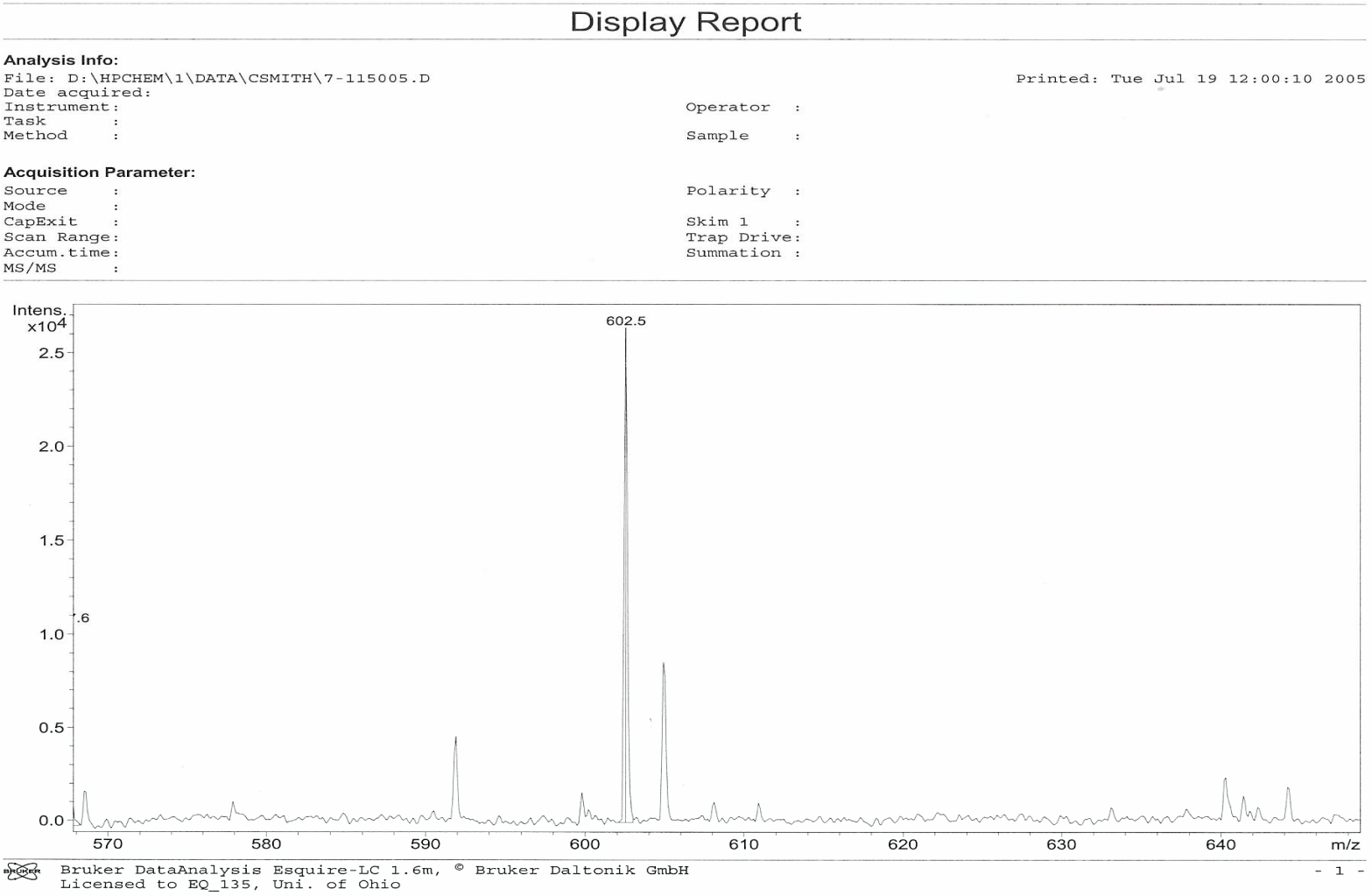

Figure 169: Mass spectrum of methyl D-fructuronate-*O*-benzoyloxime triazole **(70).**

Appendix B

X-ray Crystallography

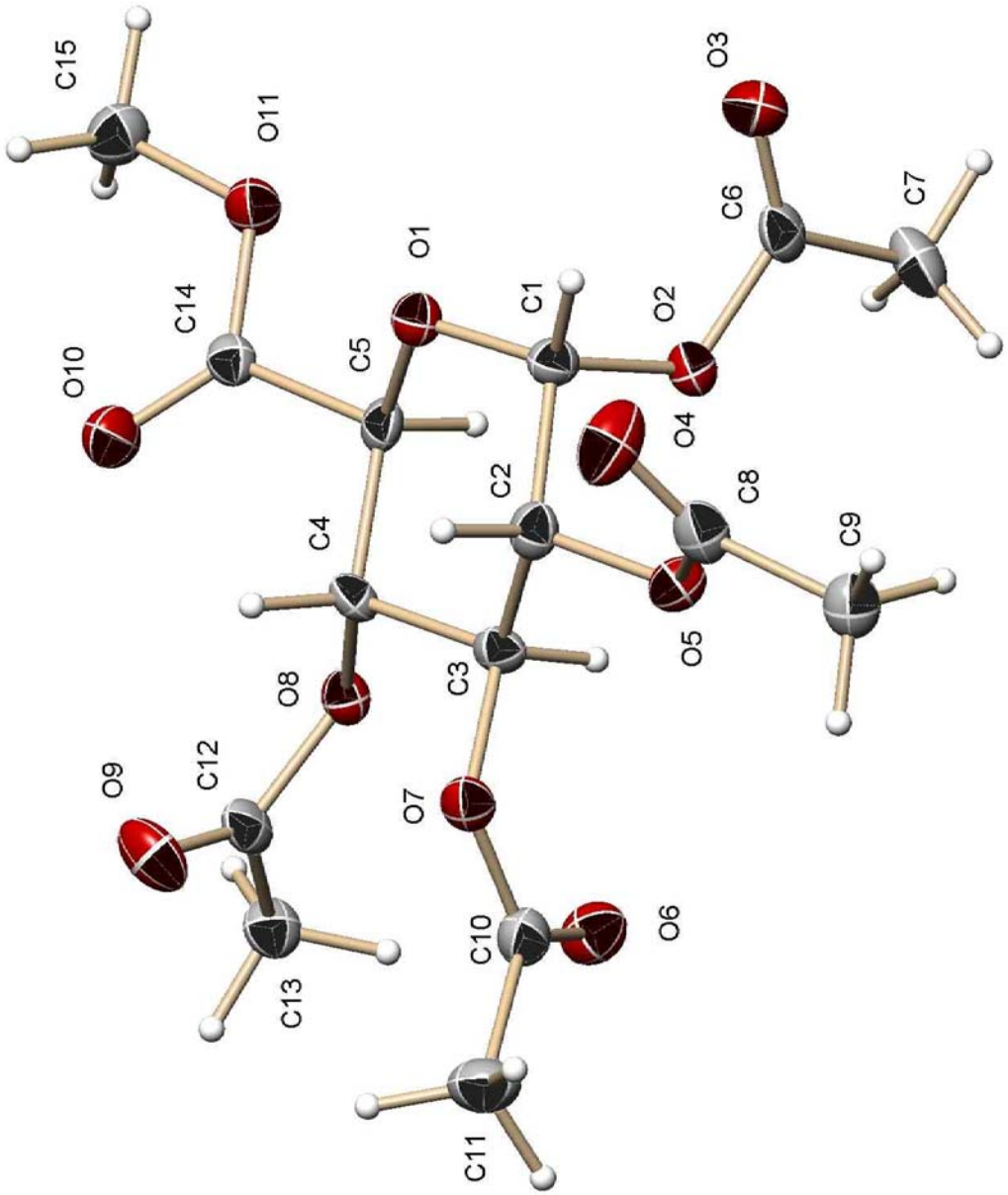

Figure 170: X-ray crystal structure of methyl 1,2,3,4-tetra-*O*-acetyl-α-D-glucopyranuroate (**2*α***).

Table 1. Crystal data and structure refinement for 05SD011m:

Identification code:	05SD011m
Empirical formula:	$C_{15}H_{20}O_{11}$
Formula weight:	376.31
Temperature:	100(2) K
Wavelength:	0.71073 Å
Crystal system:	Monoclinic
Space group:	$P2_1$
Unit cell dimensions:	a = 12.7912(18) Å, α = 90°
	b = 7.9478(11) Å, β = 99.391(2)°
	c = 26.494(4) Å, γ = 90°
Volume, *Z*:	2657.4(6) $Å^3$, 6
Density (calculated):	1.411 Mg/m^3
Absorption coefficient:	0.122 mm^{-1}
F(000):	1188
Crystal size:	0.52 × 0.43 × 0.16 mm
Theta range for data collection:	0.78 to 26.37°
Limiting indices:	$-15 \leq h \leq 15$, $-9 \leq k \leq 9$, $-33 \leq l \leq 33$
Reflections collected:	23091
Independent reflections:	5839 (*R*(int) = 0.0661)
Completeness to $\theta = 26.37°$:	100.0 %

Absorption correction:	multi-scan
Max. and min. transmission:	0.98 and 0.6344
Refinement method:	Full-matrix least-squares on F^2
Data / restraints / parameters:	5839 / 1 / 718
Goodness-of-fit on F^2:	1.210
Final R indices [$I>2\sigma(I)$]:	R1 = 0.0735, wR2 = 0.1783
R indices (all data):	R1 = 0.0785, wR2 = 0.1816
Largest diff. peak and hole:	0.697 and -0.365 e × $Å^{-3}$

Table 2. Atomic coordinates [$\times 10^4$] and equivalent isotropic displacement parameters [$Å^2 \times 10^3$] for 05SD011m. U(eq) is defined as one third of the trace of the orthogonalized U_{ij} tensor.

	x	y	z	U(eq)
O(50)	-224(4)	1793(8)	3436(2)	62(2)
O(1)	8441(3)	5469(5)	681(1)	21(1)
O(5)	10403(3)	3780(5)	1718(1)	22(1)
O(2)	10104(3)	4294(5)	677(1)	20(1)
O(7)	8703(3)	1672(5)	1757(1)	21(1)
O(10)	6000(3)	3934(6)	286(2)	30(1)
O(11)	6959(3)	5480(5)	-179(1)	24(1)
O(8)	7366(3)	1234(5)	747(1)	20(1)
C(3)	8836(4)	2540(7)	1293(2)	20(1)
O(6)	9013(3)	-821(5)	1405(2)	30(1)
O(3)	10739(3)	6667(6)	368(2)	32(1)
C(14)	6835(4)	4442(7)	203(2)	19(1)
C(6)	10704(4)	5173(8)	386(2)	22(1)
C(2)	9382(4)	4188(7)	1444(2)	21(1)
C(4)	7756(4)	2828(7)	963(2)	17(1)
O(9)	6299(3)	905(6)	1338(1)	33(1)
C(5)	7906(4)	3950(7)	512(2)	19(1)
C(8)	10893(4)	4985(8)	2043(2)	25(1)
O(4)	10508(3)	6320(6)	2083(2)	37(1)
C(1)	9451(4)	5234(7)	968(2)	19(1)
C(12)	6686(4)	363(7)	987(2)	22(1)
C(9)	11926(4)	4339(8)	2322(2)	26(1)
C(15)	5990(4)	5997(8)	-501(2)	29(1)
C(10)	8829(4)	-21(8)	1763(2)	25(1)
C(7)	11301(4)	3975(8)	102(2)	31(1)
C(13)	6492(4)	-1351(7)	754(2)	25(1)
C(11)	8691(5)	-718(8)	2273(2)	34(1)
O(21)	4804(3)	9485(5)	2763(1)	23(1)
O(24)	2802(3)	9020(5)	1620(1)	24(1)
O(22)	3031(3)	8666(5)	2661(1)	23(1)
O(26)	4405(3)	6797(5)	1422(1)	21(1)
O(23)	2672(4)	10870(6)	3127(2)	37(1)
O(27)	2819(3)	5490(5)	1242(1)	27(1)
C(22)	3834(4)	9011(7)	1921(2)	22(1)
O(28)	5481(3)	5288(5)	2351(1)	23(1)
C(25)	5179(4)	7800(7)	2814(2)	22(1)
O(30)	6789(3)	9149(6)	3132(2)	34(1)
C(24)	5270(4)	7037(7)	2284(2)	21(1)
C(23)	4221(4)	7216(7)	1928(2)	22(1)

C(30)	3615(4)	5964(7)	1115(2)	22(1)
C(21)	3809(4)	9645(7)	2468(2)	20(1)
O(31)	6577(4)	6538(6)	3391(2)	44(1)
C(26)	2486(4)	9455(7)	2999(2)	21(1)
C(28)	2435(4)	10512(8)	1421(2)	26(1)
C(34)	6256(4)	7763(8)	3154(2)	27(1)
C(32)	6468(4)	4729(8)	2306(2)	26(1)
O(25)	2926(4)	11778(6)	1497(2)	40(1)
O(29)	7143(3)	5594(6)	2196(2)	44(1)
C(33)	6566(5)	2889(8)	2435(2)	31(1)
C(29)	1383(5)	10275(10)	1092(2)	38(2)
C(27)	1701(4)	8307(8)	3168(2)	26(1)
C(31)	3929(5)	5755(9)	596(2)	34(1)
O(42)	3559(3)	3499(5)	4105(1)	23(1)
O(46)	2166(3)	995(5)	5226(1)	26(1)
O(41)	1800(3)	4428(5)	4049(1)	23(1)
O(48)	993(3)	101(5)	4265(1)	24(1)
O(44)	3837(3)	3332(6)	5124(1)	32(1)
C(45)	1390(4)	2792(7)	3916(2)	22(1)
C(44)	1262(4)	1800(7)	4401(2)	22(1)
O(51)	179(3)	4465(6)	3358(2)	37(1)
C(41)	2801(4)	4405(7)	4345(2)	24(1)
C(42)	2780(4)	3500(8)	4858(2)	25(1)
C(54)	342(4)	2945(8)	3542(2)	25(1)
O(49)	-437(3)	167(6)	4658(2)	39(1)
C(46)	3983(4)	4327(8)	3734(2)	24(1)
O(43)	3703(3)	5693(6)	3592(2)	37(1)
C(52)	141(4)	-591(8)	4425(2)	22(1)
C(43)	2331(5)	1751(8)	4753(2)	27(1)
C(53)	55(5)	-2407(8)	4283(2)	31(1)
O(45)	3541(4)	5196(7)	5713(2)	50(1)
C(47)	4803(5)	3272(8)	3548(2)	31(1)
C(51)	2155(5)	-1277(9)	5786(2)	33(1)
O(47)	2939(6)	-1425(8)	5022(2)	79(2)
C(48)	4127(4)	4298(8)	5543(2)	26(1)
C(49)	5258(5)	4002(10)	5765(2)	40(2)
C(50)	2493(5)	-613(10)	5311(2)	42(2)
C(55)	-790(5)	4660(9)	2994(2)	40(2)
C(35)	7824(5)	9181(11)	3448(2)	43(2)

Table 3. Bond lengths [Å] and angles [deg] for 05SD011m.

O(50)-C(54)	1.173(8)
O(1)-C(1)	1.399(6)
O(1)-C(5)	1.424(6)
O(5)-C(8)	1.370(7)
O(5)-C(2)	1.424(6)
O(2)-C(6)	1.365(6)
O(2)-C(1)	1.436(6)
O(7)-C(10)	1.356(7)
O(7)-C(3)	1.443(6)
O(10)-C(14)	1.195(6)
O(11)-C(14)	1.336(6)
O(11)-C(15)	1.445(6)
O(8)-C(12)	1.348(6)
O(8)-C(4)	1.445(6)
C(3)-C(2)	1.508(8)
C(3)-C(4)	1.528(7)
C(3)-H(3)	1
O(6)-C(10)	1.197(7)
O(3)-C(6)	1.190(7)
C(14)-C(5)	1.528(7)
C(6)-C(7)	1.497(8)
C(2)-C(1)	1.526(7)
C(2)-H(2)	1
C(4)-C(5)	1.528(7)
C(4)-H(4)	1
O(9)-C(12)	1.204(7)
C(5)-H(5)	1
C(8)-O(4)	1.183(7)
C(8)-C(9)	1.495(7)
C(1)-H(1)	1
C(12)-C(13)	1.499(8)
C(9)-H(9A)	0.98
C(9)-H(9B)	0.98
C(9)-H(9C)	0.98
C(15)-H(15A)	0.98
C(15)-H(15B)	0.98
C(15)-H(15C)	0.98
C(7)-H(7B)	0.98
C(7)-H(7C)	0.98
C(13)-H(13B)	0.98
C(13)-H(13C)	0.98
C(11)-H(11A)	0.98
C(11)-H(11B)	0.98
C(11)-H(11C)	0.98

O(21)-C(21)	1.387(6)
O(21)-C(25)	1.421(7)
O(24)-C(28)	1.350(7)
O(24)-C(22)	1.426(6)
O(22)-C(26)	1.372(6)
O(22)-C(21)	1.423(6)
O(26)-C(30)	1.362(6)
O(26)-C(23)	1.439(6)
O(23)-C(26)	1.188(7)
O(27)-C(30)	1.509(8)
C(22)-C(21)	1.541(7)
C(22)-H(22)	1
O(28)-C(32)	1.362(7)
O(28)-C(24)	1.517(7)
C(25)-C(24)	1.552(7)
C(25)-H(25)	1.301(8)
O(30)-C(35)	1.447(7)
C(24)-C(23)	1.516(7)
C(24)-H(24)	1
C(23)-H(23)	1
C(30)-C(31)	1.501(7)
C(21)-H(21)	1
O(31)-C(34)	1.194(8)
C(26)-C(27)	1.480(8)
C(28)-O(25)	1.186(8)
C(28)-C(29)	1.491(8)
C(32)-O(29)	1.177(7)
C(32)-C(33)	1.502(9)
C(33)-H(33A)	0.98
C(33)-H(33B)	0.98
C(33)-H(33C)	0.98
C(29)-H(29A)	0.98
C(29)-H(29B)	0.98
C(29)-H(29C)	0.98
C(27)-H(27A)	0.98
C(27)-H(27B)	0.98
C(27)-H(27C)	0.98
C(31)-H(31A)	0.98
C(31)-H(31B)	0.98
C(31)-H(31C)	0.98
O(42)-C(46)	1.367(6)
O(42)-C(41)	1.438(6)
O(46)-C(50)	1.352(8)
O(46)-C(43)	1.436(6)
O(41)-C(41)	1.388(6)
O(41)-C(45)	1.425(7)

O(48)-C(52)	1.349(6)
O(48)-C(44)	1.425(7)
O(44)-C(48)	1.352(7)
O(44)-C(42)	1.425(6)
C(45)-C(54)	1.536(7)
C(45)-C(44)	1.538(7)
C(45)-H(45)	1
C(44)-C(43)	1.525(8)
C(44)-H(44)	1
O(51)-C(54)	1.307(8)
O(51)-C(55)	1.449(7)
C(41)-C(42)	1.541(7)
C(41)-H(41)	1
C(42)-C(43)	1.513(9)
C(42)-H(42)	1
O(49)-C(52)	1.200(7)
C(46)-O(43)	1.185(7)
C(46)-C(47)	1.488(8)
C(52)-C(53)	1.491(9)
C(43)-H(43)	1
C(53)-H(53A)	0.98
C(53)-H(53B)	0.98
C(53)-H(53C)	0.98
O(45)-C(48)	1.176(7)
C(47)-H(47A)	0.98
C(47)-H(47B)	0.98
C(47)-H(47C)	0.98
C(51)-C(50)	1.492(8)
C(51)-H(51A)	0.98
C(51)-H(51B)	0.98
C(51)-H(51C)	0.98
O(47)-C(50)	1.212(8)
C(48)-C(49)	1.488(8)
C(49)-H(49A)	0.98
C(49)-H(49B)	0.98
C(49)-H(49C)	0.98
C(55)-H(55A)	0.98
C(55)-H(55B)	0.98
C(55)-H(55C)	0.98
C(35)-H(35A)	0.98
C(35)-H(35B)	0.98
C(35)-H(35C)	0.98
C(1)-O(1)-C(5)	114.3(4)
C(8)-O(5)-C(2)	116.7(4)
C(6)-O(2)-C(1)	117.9(4)
C(10)-O(7)-C(3)	117.0(4)

C(14)-O(11)-C(15)	115.2(4)
C(12)-O(8)-C(4)	118.2(4)
O(7)-C(3)-C(2)	107.6(4)
O(7)-C(3)-C(4)	109.8(4)
C(2)-C(3)-C(4)	111.0(4)
O(7)-C(3)-H(3)	109.5
C(2)-C(3)-H(3)	109.5
C(4)-C(3)-H(3)	109.5
O(10)-C(14)-O(11)	124.6(5)
O(10)-C(14)-C(5)	124.4(5)
O(11)-C(14)-C(5)	110.9(4)
O(3)-C(6)-O(2)	124.2(5)
O(3)-C(6)-C(7)	126.1(5)
O(2)-C(6)-C(7)	109.8(5)
O(5)-C(2)-C(3)	106.5(4)
O(5)-C(2)-C(1)	111.9(4)
C(3)-C(2)-C(1)	109.9(4)
O(5)-C(2)-H(2)	109.5
C(3)-C(2)-H(2)	109.5
C(1)-C(2)-H(2)	109.5
O(8)-C(4)-C(5)	106.4(4)
O(8)-C(4)-C(3)	108.4(4)
C(5)-C(4)-C(3)	108.6(4)
O(8)-C(4)-H(4)	111.1
C(5)-C(4)-H(4)	111.1
C(3)-C(4)-H(4)	111.1
O(1)-C(5)-C(14)	107.2(4)
O(1)-C(5)-C(4)	111.3(4)
C(14)-C(5)-C(4)	110.6(4)
O(1)-C(5)-H(5)	109.3
C(14)-C(5)-H(5)	109.3
C(4)-C(5)-H(5)	109.3
O(4)-C(8)-O(5)	122.0(5)
O(4)-C(8)-C(9)	127.7(5)
O(5)-C(8)-C(9)	110.3(5)
O(1)-C(1)-O(2)	110.1(4)
O(1)-C(1)-C(2)	110.4(4)
O(2)-C(1)-C(2)	106.1(4)
O(1)-C(1)-H(1)	110
O(2)-C(1)-H(1)	110
C(2)-C(1)-H(1)	110
O(9)-C(12)-O(8)	123.9(5)
O(9)-C(12)-C(13)	125.6(5)
O(8)-C(12)-C(13)	110.5(4)
C(8)-C(9)-H(9A)	109.5
C(8)-C(9)-H(9B)	109.5

H(9A)-C(9)-H(9B)	109.5
C(8)-C(9)-H(9C)	109.5
H(9A)-C(9)-H(9C)	109.5
H(9B)-C(9)-H(9C)	109.5
O(11)-C(15)-H(15A)	109.5
O(11)-C(15)-H(15B)	109.5
H(15A)-C(15)-H(15B)	109.5
O(11)-C(15)-H(15C)	109.5
H(15A)-C(15)-H(15C)	109.5
H(15B)-C(15)-H(15C)	109.5
O(6)-C(10)-O(7)	123.8(5)
O(6)-C(10)-C(11)	125.9(6)
O(7)-C(10)-C(11)	110.3(5)
C(6)-C(7)-H(7A)	109.5
C(6)-C(7)-H(7B)	109.5
H(7A)-C(7)-H(7B)	109.5
C(6)-C(7)-H(7C)	109.5
H(7A)-C(7)-H(7C)	109.5
H(7B)-C(7)-H(7C)	109.5
C(12)-C(13)-H(13A)	109.5
C(12)-C(13)-H(13B)	109.5
H(13A)-C(13)-H(13B)	109.5
C(12)-C(13)-H(13C)	109.5
H(13A)-C(13)-H(13C)	109.5
H(13B)-C(13)-H(13C)	109.5
C(10)-C(11)-H(11A)	109.5
C(10)-C(11)-H(11B)	109.5
H(11A)-C(11)-H(11B)	109.5
C(10)-C(11)-H(11C)	109.5
H(11A)-C(11)-H(11C)	109.5
H(11B)-C(11)-H(11C)	109.5
C(21)-O(21)-C(25)	113.9(4)
C(28)-O(24)-C(22)	117.0(4)
C(26)-O(22)-C(21)	116.3(4)
C(30)-O(26)-C(23)	116.8(4)
O(24)-C(22)-C(23)	106.5(4)
O(24)-C(22)-C(21)	111.4(4)
C(23)-C(22)-C(21)	110.7(4)
O(24)-C(22)-H(22)	109.4
C(23)-C(22)-H(22)	109.4
C(21)-C(22)-H(22)	109.4
C(32)-O(28)-C(24)	117.9(4)
O(21)-C(25)-C(34)	109.5(4)
O(21)-C(25)-C(24)	110.8(4)
C(34)-C(25)-C(24)	109.6(4)
O(21)-C(25)-H(25)	109

C(34)-C(25)-H(25)	109
C(24)-C(25)-H(25)	109
C(34)-O(30)-C(35)	115.1(5)
O(28)-C(24)-C(23)	107.5(4)
O(28)-C(24)-C(25)	108.0(4)
C(23)-C(24)-C(25)	109.7(4)
O(28)-C(24)-H(24)	110.5
C(23)-C(24)-H(24)	110.5
C(25)-C(24)-H(24)	110.5
O(26)-C(23)-C(22)	108.0(4)
O(26)-C(23)-C(24)	107.1(4)
C(22)-C(23)-C(24)	110.6(4)
O(26)-C(23)-H(23)	110.3
C(22)-C(23)-H(23)	110.3
C(24)-C(23)-H(23)	110.3
O(27)-C(30)-O(26)	124.9(5)
O(27)-C(30)-C(31)	126.6(5)
O(26)-C(30)-C(31)	108.5(4)
O(21)-C(21)-O(22)	112.2(4)
O(21)-C(21)-C(22)	110.0(4)
O(22)-C(21)-C(22)	106.5(4)
O(22)-C(21)-C(22)	106.5(4)
O(21)-C(21)-H(21)	109.4
O(22)-C(21)-H(21)	109.4
C(22)-C(21)-H(21)	109.4
O(23)-C(26)-O(22)	121.3(5)
O(23)-C(26)-C(27)	127.7(5)
O(22)-C(26)-C(27)	110.9(5)
O(25)-C(28)-O(24)	122.5(5)
O(25)-C(28)-C(29)	127.5(6)
O(24)-C(28)-C(29)	109.9(5)
O(31)-C(34)-O(30)	125.2(5)
O(31)-C(34)-C(25)	121.8(5)
O(30)-C(34)-C(25)	112.8(5)
O(29)-C(32)-O(28)	124.0(6)
O(29)-C(32)-C(33)	126.0(6)
O(28)-C(32)-C(33)	110.0(5)
C(32)-C(33)-H(33A)	109.5
C(32)-C(33)-H(33B)	109.5
H(33A)-C(33)-H(33B)	109.5
C(32)-C(33)-H(33C)	109.5
H(33A)-C(33)-H(33C)	109.5
H(33B)-C(33)-H(33C)	109.5
C(28)-C(29)-H(29A)	109.5
C(28)-C(29)-H(29B)	109.5
H(29A)-C(29)-H(29B)	109.5

C(28)-C(29)-H(29C)	109.5
H(29A)-C(29)-H(29C)	109.5
H(29B)-C(29)-H(29C)	109.5
C(26)-C(27)-H(27A)	109.5
C(26)-C(27)-H(27B)	109.5
H(27A)-C(27)-H(27B)	109.5
C(26)-C(27)-H(27C)	109.5
H(27A)-C(27)-H(27C)	109.5
H(27B)-C(27)-H(27C)	109.5
C(30)-C(31)-H(31A)	109.5
C(30)-C(31)-H(31B)	109.5
H(31A)-C(31)-H(31B)	109.5
C(30)-C(31)-H(31C)	109.5
H(31A)-C(31)-H(31C)	109.5
H(31B)-C(31)-H(31C)	109.5
C(46)-O(42)-C(41)	116.9(4)
C(50)-O(46)-C(43)	117.0(4)
C(41)-O(41)-C(45)	113.3(4)
C(52)-O(48)-C(44)	118.8(4)
C(48)-O(44)-C(42)	117.7(4)
O(41)-C(45)-C(54)	109.5(4)
O(41)-C(45)-C(44)	110.3(4)
C(54)-C(45)-C(44)	112.2(4)
O(41)-C(45)-H(45)	108.2
C(54)-C(45)-H(45)	108.2
C(44)-C(45)-H(45)	108.2
O(48)-C(44)-C(43)	106.6(4)
O(48)-C(44)-C(45)	109.2(4)
C(43)-C(44)-C(45)	108.5(4)
O(48)-C(44)-H(44)	110.8
C(43)-C(44)-H(44)	110.8
C(45)-C(44)-H(44)	110.8
C(54)-O(51)-C(55)	114.5(5)
O(41)-C(41)-O(42)	112.5(4)
O(41)-C(41)-C(42)	111.0(4)
O(42)-C(41)-C(42)	105.4(4)
O(41)-C(41)-H(41)	109.3
O(42)-C(41)-H(41)	109.3
C(42)-C(41)-H(41)	109.3
O(44)-C(42)-C(43)	107.8(5)
O(44)-C(42)-C(41)	109.2(4)
C(43)-C(42)-C(41)	109.1(4)
O(44)-C(42)-H(42)	110.2
C(43)-C(42)-H(42)	110.2
C(41)-C(42)-H(42)	110.2
O(50)-C(54)-O(51)	125.3(5)

O(50)-C(54)-C(45)	122.2(6)
O(51)-C(54)-C(45)	112.6(5)
O(43)-C(46)-O(42)	122.3(5)
O(43)-C(46)-C(47)	127.2(5)
O(42)-C(46)-C(47)	110.5(5)
O(49)-C(52)-O(48)	123.7(5)
O(49)-C(52)-C(53)	126.1(5)
O(48)-C(52)-C(53)	110.2(5)
O(46)-C(43)-C(42)	109.2(4)
O(46)-C(43)-C(44)	107.5(4)
C(42)-C(43)-C(44)	111.4(5)
O(46)-C(43)-H(43)	109.6
C(42)-C(43)-H(43)	109.6
C(44)-C(43)-H(43)	109.6
C(52)-C(53)-H(53A)	109.5
C(52)-C(53)-H(53B)	109.5
H(53A)-C(53)-H(53B)	109.5
C(52)-C(53)-H(53C)	109.5
H(53A)-C(53)-H(53C)	109.5
H(53B)-C(53)-H(53C)	109.5
C(46)-C(47)-H(47A)	109.5
C(46)-C(47)-H(47B)	109.5
H(47A)-C(47)-H(47B)	109.5
C(46)-C(47)-H(47C)	109.5
H(47A)-C(47)-H(47C)	109.5
H(47B)-C(47)-H(47C)	109.5
C(50)-C(51)-H(51A)	109.5
C(50)-C(51)-H(51B)	109.5
H(51A)-C(51)-H(51B)	109.5
C(50)-C(51)-H(51C)	109.5
H(51A)-C(51)-H(51C)	109.5
H(51B)-C(51)-H(51C)	109.5
O(45)-C(48)-O(44)	123.6(5)
O(45)-C(48)-C(49)	125.7(5)
O(44)-C(48)-C(49)	110.7(5)
C(48)-C(49)-H(49A)	109.5
C(48)-C(49)-H(49B)	109.5
H(49A)-C(49)-H(49B)	109.5
C(48)-C(49)-H(49C)	109.5
H(49A)-C(49)-H(49C)	109.5
H(49B)-C(49)-H(49C)	109.5
O(47)-C(50)-O(46)	124.3(6)
O(47)-C(50)-C(51)	125.1(7)
O(46)-C(50)-C(51)	110.5(5)
O(51)-C(55)-H(55A)	109.5
O(51)-C(55)-H(55B)	109.5

H(55A)-C(55)-H(55B)	109.5
O(51)-C(55)-H(55C)	109.5
H(55A)-C(55)-H(55C)	109.5
H(55B)-C(55)-H(55C)	109.5
O(30)-C(35)-H(35A)	109.5
O(30)-C(35)-H(35B)	109.5
H(35A)-C(35)-H(35B)	109.5
O(30)-C(35)-H(35C)	109.5
H(35A)-C(35)-H(35C)	109.5
H(35B)-C(35)-H(35C)	109.5

Table 4. Anisotropic displacement parameters [$Å^2 \times 10^3$] for 05SD011m. The anisotropic displacement factor exponent takes the form: $-2\pi2 [(h a^*)^2 U11 + ... + 2 h k a^* b^* U12]$

	U11	U22	U33	U23	U13	U12
O(50)	57(3)	51(3)	65(3)	20(3)	-32(3)	-28(3)
O(1)	20(2)	21(2)	21(2)	-1(2)	4(1)	1(2)
O(5)	24(2)	22(2)	18(2)	0(1)	-1(1)	1(2)
O(2)	18(2)	24(2)	20(2)	-1(2)	4(1)	-1(2)
O(7)	22(2)	27(2)	16(2)	2(2)	4(1)	1(2)
O(10)	22(2)	36(2)	31(2)	7(2)	0(2)	0(2)
O(11)	22(2)	31(2)	19(2)	4(2)	4(1)	1(2)
O(8)	18(2)	24(2)	18(2)	-1(1)	3(1)	0(2)
C(3)	25(3)	19(3)	17(2)	1(2)	9(2)	1(2)
O(6)	35(2)	27(2)	27(2)	-1(2)	5(2)	4(2)
O(3)	33(2)	31(2)	33(2)	8(2)	9(2)	1(2)
C(14)	18(2)	18(2)	21(2)	-2(2)	3(2)	-2(2)
C(6)	13(2)	32(3)	21(2)	1(2)	0(2)	-3(2)
C(2)	20(2)	24(3)	19(2)	-2(2)	5(2)	4(2)
C(4)	15(2)	21(3)	16(2)	0(2)	3(2)	-5(2)
O(9)	36(2)	41(2)	26(2)	-9(2)	16(2)	-10(2)
C(5)	16(2)	20(3)	22(2)	-1(2)	5(2)	5(2)
C(8)	22(3)	36(3)	17(2)	0(2)	3(2)	-2(2)
O(4)	31(2)	36(3)	38(2)	-14(2)	-11(2)	5(2)
C(1)	19(2)	18(3)	20(2)	1(2)	3(2)	-1(2)
C(12)	13(2)	29(3)	22(2)	4(2)	-1(2)	-5(2)
C(9)	24(3)	34(3)	20(2)	-2(2)	3(2)	2(3)
C(15)	27(3)	32(3)	26(3)	3(2)	1(2)	2(3)
C(10)	21(3)	29(3)	25(3)	3(2)	4(2)	2(2)
C(7)	24(3)	37(3)	34(3)	-5(3)	14(2)	-7(3)
C(13)	21(3)	25(3)	27(3)	-3(2)	2(2)	-5(2)
C(11)	41(3)	30(3)	31(3)	9(3)	9(2)	1(3)
O(21)	29(2)	21(2)	19(2)	-2(2)	7(1)	-6(2)
O(24)	26(2)	25(2)	21(2)	-2(2)	4(1)	6(2)
O(22)	25(2)	25(2)	21(2)	-3(2)	8(1)	3(2)
O(26)	18(2)	29(2)	16(2)	-4(2)	5(1)	-1(2)
O(23)	49(3)	34(3)	33(2)	-13(2)	21(2)	-7(2)
O(27)	31(2)	27(2)	23(2)	2(2)	2(2)	-8(2)
C(22)	26(3)	25(3)	15(2)	-1(2)	5(2)	-6(2)
O(28)	17(2)	26(2)	25(2)	-1(2)	3(1)	-2(2)
C(25)	24(3)	28(3)	15(2)	-3(2)	7(2)	-8(2)
O(30)	32(2)	39(3)	28(2)	-1(2)	-1(2)	-7(2)
C(24)	18(2)	27(3)	17(2)	-2(2)	4(2)	0(2)
C(23)	24(3)	27(3)	16(2)	0(2)	8(2)	-10(2)

C(30)	23(3)	19(3)	22(2)	5(2)	2(2)	-1(2)
C(21)	22(2)	20(3)	20(2)	-1(2)	8(2)	-4(2)
O(31)	44(3)	40(3)	44(3)	13(2)	-11(2)	-5(2)
C(26)	18(2)	28(3)	17(2)	-2(2)	1(2)	1(2)
C(28)	32(3)	27(3)	22(2)	0(2)	14(2)	9(3)
C(34)	31(3)	29(3)	21(2)	-3(2)	7(2)	-2(3)
C(32)	21(3)	36(3)	18(2)	-2(2)	-3(2)	-2(2)
O(25)	48(3)	29(2)	45(3)	5(2)	15(2)	7(2)
O(29)	28(2)	37(3)	68(3)	12(2)	15(2)	3(2)
C(33)	35(3)	28(3)	33(3)	-4(3)	9(2)	8(3)
C(29)	34(3)	48(4)	34(3)	4(3)	11(2)	24(3)
C(27)	26(3)	34(3)	20(2)	-8(2)	7(2)	6(2)
C(31)	38(3)	43(4)	23(3)	-11(3)	6(2)	-8(3)
O(42)	19(2)	25(2)	26(2)	-1(2)	8(1)	-4(2)
O(46)	25(2)	37(2)	16(2)	2(2)	7(1)	3(2)
O(41)	21(2)	24(2)	25(2)	-1(2)	5(1)	-2(2)
O(48)	28(2)	24(2)	23(2)	-2(2)	12(2)	-2(2)
O(44)	26(2)	43(3)	24(2)	-9(2)	-2(2)	6(2)
C(45)	20(2)	27(3)	20(2)	1(2)	7(2)	4(2)
C(44)	21(3)	25(3)	21(2)	1(2)	8(2)	2(2)
O(51)	38(2)	32(2)	37(2)	0(2)	-8(2)	1(2)
C(41)	28(3)	23(3)	22(2)	-3(2)	8(2)	-3(2)
C(42)	18(2)	36(3)	22(2)	-2(2)	6(2)	6(2)
C(54)	27(3)	31(3)	18(2)	0(2)	5(2)	-5(3)
O(49)	34(2)	45(3)	44(2)	-14(2)	19(2)	-13(2)
C(46)	26(3)	26(3)	22(2)	0(2)	8(2)	-7(2)
O(43)	44(2)	34(3)	36(2)	9(2)	15(2)	7(2)
C(52)	18(2)	32(3)	14(2)	1(2)	3(2)	-1(2)
C(43)	38(3)	31(3)	16(2)	1(2)	18(2)	6(3)
C(53)	36(3)	29(3)	29(3)	3(2)	10(2)	-1(3)
O(45)	38(2)	60(3)	46(3)	-28(3)	-4(2)	11(3)
C(47)	29(3)	38(3)	30(3)	3(3)	13(2)	-8(3)
C(51)	39(3)	38(3)	24(3)	4(2)	10(2)	7(3)
O(47)	27(6)	58(4)	70(4)	29(3)	67(4)	48(4)
C(48)	26(3)	28(3)	24(2)	-3(2)	7(2)	-7(2)
C(49)	41(3)	55(4)	23(3)	-3(3)	3(2)	3(3)
C(50)	46(4)	50(4)	38(3)	14(3)	23(3)	20(3)
C(55)	36(3)	46(4)	32(3)	2(3)	-9(3)	2(3)
C(35)	36(3)	55(5)	33(3)	-4(3)	-2(3)	-9(3)

Table 5. Hydrogen coordinates ($\times 10^4$) and isotropic displacement parameters ($Å^2 \times 10^3$) for 05mz062m.

	x	y	z	U(eq)
H(11A)	371	6127	-4102	64
H(11B)	100	6198	-2059	64
H(11C)	510	5302	-1762	64
H(7)	1015	4601	4549	28
H(5)	1166	5362	201	23
H(6A)	1721	4749	4023	26
H(6B)	1629	3571	1981	26
H(9A)	1491	546	4397	45
H(9B)	1784	623	6655	45
H(9C)	1847	1747	4597	45
H(8A)	484	2125	4998	63
H(8B)	221	1888	2654	63
H(8C)	309	3582	3608	63
H(12A)	496	9994	-1705	65
H(12B)	91	9065	-1828	65
H(12C)	331	9171	-4003	65
H(4)	1786	5602	-1116	25
H(3)	1674	7945	-2581	26
H(2)	1183	9610	-1000	28
H(1)	1031	8995	2459	25
H(14A)	2730	7265	-6	42
H(14B)	2608	8929	-966	42
H(14C)	2380	7441	-1974	42
H(15A)	2187	8862	4373	47
H(15B)	2490	9804	3011	47
H(15C)	2606	8138	3987	47

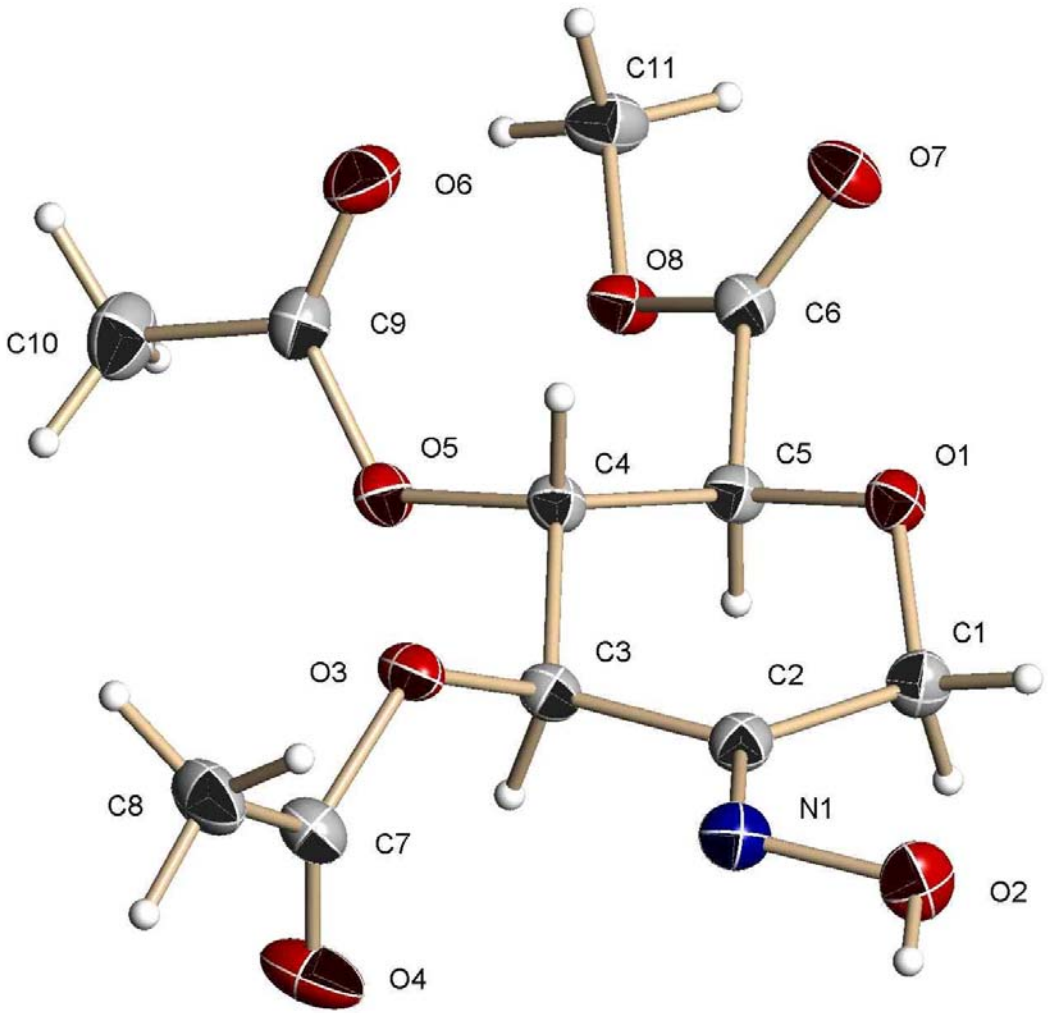

Figure 171: X-ray crystal structure of the oxime of methyl 3,4-di-*O*-acetyl-1,5-anhydro-D-fructuronate (**28**).

Table 1. Crystal data and structure refinement for 05mz063m:

Identification code:	05mz063m
Empirical formula:	$C_{11}H_{15}N_1O_8$
Formula weight:	289.24
Temperature:	100(2) K
Wavelength:	0.71073 Å
Crystal system:	Monoclinic
Space group:	$P2_1$
Unit cell dimensions:	a = 5.139(2) Å, α = 90°
	b = 10.592(4) Å, β = 95.203(7)°
	c = 11.885(5) Å, γ = 90°
Volume, *Z*:	644.2(5) $Å^3$, 2
Density (calculated):	1.491 Mg/m^3
Absorption coefficient:	0.129 mm^{-1}
F(000):	304
Crystal size:	0.53 × 0.27 × 0.20 mm
Theta range for data collection:	1.72 to 30.45°
Limiting indices:	$-7 \le h \le 7$, $-14 \le k \le 14$, $-16 \le l \le 16$
Reflections collected:	7454
Independent reflections:	2033 (*R*(int) = 0.0293)
Completeness to $\theta = 30.45°$:	99.2 %

Absorption correction:	multi-scan
Max. and min. transmission:	0.98 and 0.7981
Refinement method:	Full-matrix least-squares on F^2
Data / restraints / parameters:	2033 / 1 / 185
Goodness-of-fit on F^2:	1.099
Final R indices [$I>2\sigma(I)$]:	R1 = 0.0378, wR2 = 0.0952
R indices (all data):	R1 = 0.0386, wR2 = 0.0959
Largest diff. peak and hole:	0.337 and -0.203 e × $Å^{-3}$

Table 2. Atomic coordinates [$\times 10^4$] and equivalent isotropic displacement parameters [$Å^2 \times 10^3$] for 05mz063m. U(eq) is defined as one third of the trace of the orthogonalized U_{ij} tensor.

	x	y	z	U(eq)
C(1)	2115(3)	4230(2)	-64(1)	22(1)
C(2)	3184(3)	3112(2)	616(1)	19(1)
C(3)	1966(3)	2794(2)	1692(1)	19(1)
C(4)	1133(3)	3969(2)	2288(1)	18(1)
C(5)	-343(3)	4860(2)	1436(1)	18(1)
C(6)	-1201(3)	6046(2)	2012(1)	19(1)
C(7)	3975(3)	901(2)	2406(2)	24(1)
C(8)	6386(4)	431(2)	3064(2)	30(1)
C(9)	-303(3)	4153(2)	4124(1)	23(1)
C(10)	-2110(4)	3596(2)	4910(2)	32(1)
C(11)	-4117(3)	6849(2)	3244(2)	26(1)
N(1)	4983(3)	2369(2)	356(1)	23(1)
O(1)	1429(2)	5239(1)	659(1)	20(1)
O(2)	5945(3)	2710(1)	-664(1)	28(1)
O(3)	3851(2)	2177(1)	2465(1)	21(1)
O(4)	2337(3)	270(2)	1897(2)	39(1)
O(5)	-484(2)	3531(1)	3132(1)	21(1)
O(6)	1122(3)	5042(2)	4328(1)	30(1)
O(7)	-102(2)	7043(1)	1985(1)	24(1)
O(8)	-3284(2)	5810(1)	2573(1)	21(1)

Table 3. Bond lengths [Å] and angles [deg] for 05mz063m.

C(1)-O(1)	1.435(2)
C(1)-C(2)	1.509(2)
C(1)-H(1A)	0.99
C(1)-H(1B)	0.99
C(2)-N(1)	1.273(2)
C(2)-C(3)	1.512(2)
C(3)-O(3)	1.431(2)
C(3)-C(4)	1.513(2)
C(3)-H(3)	1
C(4)-O(5)	1.4368(19)
C(4)-C(5)	1.533(2)
C(4)-H(4)	1
C(5)-O(1)	1.4132(18)
C(5)-C(6)	1.515(2)
C(5)-H(5)	1
C(6)-O(7)	1.199(2)
C(6)-O(8)	1.3349(19)
C(7)-O(4)	1.195(2)
C(7)-O(3)	1.355(2)
C(7)-C(8)	1.489(3)
C(8)-H(8A)	0.98
C(8)-H(8B)	0.98
C(8)-H(8C)	0.98
C(9)-O(6)	1.204(2)
C(9)-O(5)	1.347(2)
C(9)-C(10)	1.496(2)
C(10)-H(10A)	0.98
C(10)-H(10B)	0.98
C(10)-H(10C)	0.98
C(11)-O(8)	1.446(2)
C(11)-H(11A)	0.98
C(11)-H(11B)	0.98
C(11)-H(11C)	0.98
N(1)-O(2)	1.397(2)
O(2)-H(2)	0.84
O(1)-C(1)-C(2)	111.19(13)
O(1)-C(1)-H(1A)	109.4
C(2)-C(1)-H(1A)	109.4
O(1)-C(1)-H(1B)	109.4
C(2)-C(1)-H(1B)	109.4
H(1A)-C(1)-H(1B)	108
N(1)-C(2)-C(1)	126.34(15)
N(1)-C(2)-C(3)	115.63(15)
C(1)-C(2)-C(3)	117.98(14)

O(3)-C(3)-C(2)	109.70(13)
O(3)-C(3)-C(4)	106.19(13)
C(2)-C(3)-C(4)	111.65(13)
O(3)-C(3)-H(3)	109.7
C(2)-C(3)-H(3)	109.7
C(4)-C(3)-H(3)	109.7
O(5)-C(4)-C(3)	105.52(12)
O(5)-C(4)-C(5)	112.12(13)
C(3)-C(4)-C(5)	109.97(13)
O(5)-C(4)-H(4)	109.7
C(3)-C(4)-H(4)	109.7
C(5)-C(4)-H(4)	109.7
O(1)-C(5)-C(6)	106.88(13)
O(1)-C(5)-C(4)	107.27(12)
C(6)-C(5)-C(4)	111.06(13)
O(1)-C(5)-H(5)	110.5
C(6)-C(5)-H(5)	110.5
C(4)-C(5)-H(5)	110.5
O(7)-C(6)-O(8)	125.37(15)
O(7)-C(6)-C(5)	124.13(14)
O(8)-C(6)-C(5)	110.47(13)
O(4)-C(7)-O(3)	123.33(17)
O(4)-C(7)-C(8)	126.36(17)
O(3)-C(7)-C(8)	110.31(15)
C(7)-C(8)-H(8A)	109.5
C(7)-C(8)-H(8B)	109.5
H(8A)-C(8)-H(8B)	109.5
C(7)-C(8)-H(8C)	109.5
H(8A)-C(8)-H(8C)	109.5
H(8B)-C(8)-H(8C)	109.5
O(6)-C(9)-O(5)	123.45(16)
O(6)-C(9)-C(10)	125.69(17)
O(5)-C(9)-C(10)	110.86(16)
C(9)-C(10)-H(10A)	109.5
C(9)-C(10)-H(10B)	109.5
H(10A)-C(10)-H(10B)	109.5
C(9)-C(10)-H(10C)	109.5
H(10A)-C(10)-H(10C)	109.5
H(10B)-C(10)-H(10C)	109.5
O(8)-C(11)-H(11A)	109.5
O(8)-C(11)-H(11B)	109.5
H(11A)-C(11)-H(11B)	109.5
O(8)-C(11)-H(11C)	109.5
H(11A)-C(11)-H(11C)	109.5
H(11B)-C(11)-H(11C)	109.5
C(2)-N(1)-O(2)	111.88(14)

C(5)-O(1)-C(1)	112.78(13)
N(1)-O(2)-H(2)	109.5
C(7)-O(3)-C(3)	117.05(13)
C(9)-O(5)-C(4)	117.08(13)
C(6)-O(8)-C(11)	115.08(13)

Table 4. Anisotropic displacement parameters [$Å^2 \times 10^3$] for 05mz063m. The anisotropic displacement factor exponent takes the form: $-2\pi 2 [(h\ a^*)^2\ U11 + ... + 2\ h\ k\ a^*\ b^*\ U12]$

	U11	U22	U33	U23	U13	U12
C(1)	24(1)	23(1)	20(1)	0(1)	4(1)	4(1)
C(2)	17(1)	23(1)	18(1)	-1(1)	1(1)	-2(1)
C(3)	16(1)	18(1)	22(1)	0(1)	1(1)	-2(1)
C(4)	17(1)	19(1)	18(1)	0(1)	4(1)	-3(1)
C(5)	14(1)	20(1)	20(1)	0(1)	3(1)	-2(1)
C(6)	16(1)	21(1)	21(1)	0(1)	2(1)	0(1)
C(7)	25(1)	19(1)	28(1)	1(1)	2(1)	-1(1)
C(8)	32(1)	22(1)	33(1)	6(1)	-5(1)	1(1)
C(9)	22(1)	29(1)	19(1)	2(1)	3(1)	0(1)
C(10)	29(1)	44(1)	25(1)	3(1)	9(1)	-5(1)
C(11)	24(1)	25(1)	30(1)	-9(1)	8(1)	-1(1)
N(1)	20(1)	26(1)	24(1)	-1(1)	3(1)	0(1)
O(1)	21(1)	21(1)	20(1)	0(1)	7(1)	-1(1)
O(2)	26(1)	31(1)	29(1)	1(1)	11(1)	5(1)
O(3)	24(1)	17(1)	22(1)	0(1)	-3(1)	0(1)
O(4)	32(1)	22(1)	59(1)	-7(1)	-8(1)	-3(1)
O(5)	22(1)	22(1)	20(1)	1(1)	6(1)	-5(1)
O(6)	31(1)	37(1)	22(1)	-6(1)	4(1)	-9(1)
O(7)	20(1)	19(1)	35(1)	0(1)	6(1)	-3(1)
O(8)	18(1)	20(1)	25(1)	-4(1)	7(1)	-2(1)

Table 5. Hydrogen coordinates ($\times 10^4$) and isotropic displacement parameters ($Å^2 \times 10^3$) for 05mz063m.

	x	y	z	U(eq)
H(1A)	3442	4532	-555	27
H(1B)	549	3968	-555	27
H(3)	424	2228	1516	22
H(4)	2707	4407	2659	21
H(5)	-1883	4421	1036	21
H(8A)	6298	621	3867	44
H(8B)	7917	847	2796	44
H(8C)	6528	-483	2962	44
H(10A)	-1691	3938	5671	48
H(10B)	-1905	2677	4927	48
H(10C)	-3919	3810	4646	48
H(11A)	-2628	7159	3740	39
H(11B)	-5493	6559	3702	39
H(11C)	-4795	7531	2743	39
H(2)	6972	2148	-856	42

Table 6. Hydrogen bonds for 05mz063m [Å and deg].

D-H...A	d(D-H)	d(H...A)	d(D...A)	<(DHA)
O(2)-H(2): O(7)#1	0.8	2.2	2.8522(19)	136
O(2)-H(2): O(1)#1	0.8	2.2	2.944(2)	150

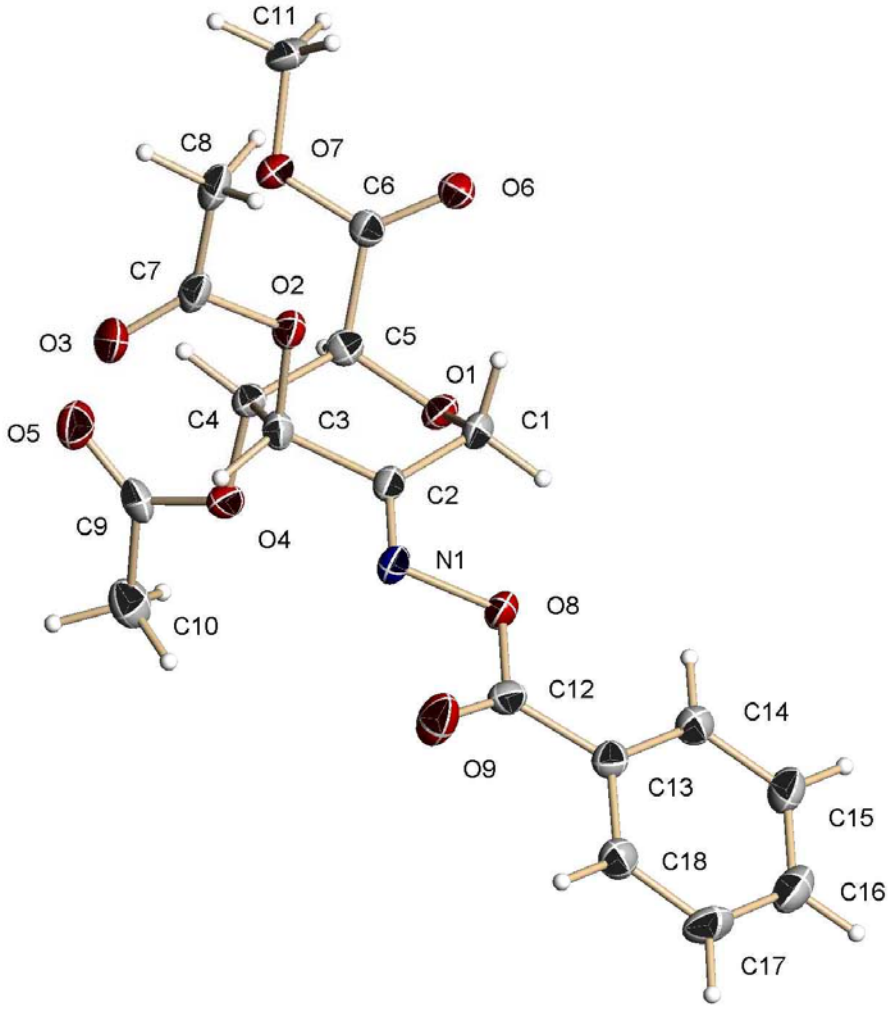

Figure 172: X-ray crystal structure of *O*-benzoyloxime of methyl 3,4-di-*O*-acetyl-1,5-anhydro-D-fructuronate (**29**).

Table 1. Crystal data and structure refinement for 05mz092m:

Identification code:	05mz092m
Empirical formula:	$C_{18}H_{19}NO_9$
Formula weight:	393.34
Temperature:	100(2) K
Wavelength:	0.71073 Å
Crystal system:	Monoclinic
Space group:	$P2_1$
Unit cell dimensions:	a = 8.2791(8) Å, α = 90°
	b = 8.6916(8) Å, β = 97.087(2)°
	c = 12.9621(12) Å, γ = 90°
Volume, *Z*:	925.61(15) $Å^3$, 2
Density (calculated):	1.411 Mg/m^3
Absorption coefficient:	0.115 mm^{-1}
F(000):	412
Crystal size:	0.45 × 0.32 × 0.20 mm
Theta range for data collection:	1.58 to 27.48°
Limiting indices:	$-10 \leq h \leq 10$, $-11 \leq k \leq 11$, $-16 \leq l \leq 16$
Reflections collected:	8741
Independent reflections:	2258 (*R*(int) = 0.0416)
Completeness to $\theta = 27.48°$:	100.0 %

Absorption correction:	multi-scan
Max. and min. transmission:	0.98 and 0.6962
Refinement method:	Full-matrix least-squares on F^2
Data / restraints / parameters:	2258 / 1 / 256
Goodness-of-fit on F^2:	1.321
Final R indices [$I>2\sigma(I)$]:	R1 = 0.0558, wR2 = 0.1313
R indices (all data):	R1 = 0.0563, wR2 = 0.1315
Largest diff. peak and hole:	0.323 and -0.231 e × Å^{-3}

Table 2. Atomic coordinates [$\times 10^4$] and equivalent isotropic displacement parameters [$Å^2 \times 10^3$] for 05mz092m. U(eq) is defined as one third of the trace of the orthogonalized U_{ij} tensor.

	x	y	z	U(eq)
O(8)	7789(3)	10253(3)	1423(2)	25(1)
O(7)	12221(3)	7667(4)	5642(2)	27(1)
O(1)	8730(3)	7368(3)	3707(2)	23(1)
O(6)	9640(3)	8420(3)	5690(2)	23(1)
O(2)	11989(3)	9964(3)	3753(2)	23(1)
O(4)	11248(3)	6151(3)	2629(2)	27(1)
O(3)	14528(3)	9725(5)	3334(2)	42(1)
N(1)	9485(3)	9910(4)	1705(2)	23(1)
O(9)	8625(4)	11471(4)	37(2)	40(1)
C(5)	10315(4)	7031(4)	4195(3)	22(1)
C(6)	10666(4)	7822(4)	5249(3)	21(1)
C(13)	5785(4)	11034(4)	69(3)	23(1)
C(16)	2567(5)	11101(5)	-823(4)	35(1)
C(4)	11590(4)	7261(4)	3455(3)	22(1)
O(5)	13411(3)	4758(4)	3300(2)	33(1)
C(2)	9712(4)	9278(4)	2590(3)	21(1)
C(12)	7553(5)	10989(5)	468(3)	25(1)
C(3)	11460(4)	8857(4)	2952(3)	23(1)
C(17)	3793(5)	11507(5)	-1407(3)	34(1)
C(7)	13630(4)	10292(5)	3873(3)	25(1)
C(1)	8506(4)	8918(4)	3339(3)	23(1)
C(18)	5398(5)	11509(5)	-951(3)	28(1)
C(14)	4548(5)	10592(5)	642(3)	27(1)
C(11)	12657(5)	8280(6)	6684(3)	31(1)
C(9)	12225(4)	4883(5)	2673(3)	26(1)
C(15)	2938(5)	10640(5)	195(3)	33(1)
C(8)	14042(4)	11411(5)	4728(3)	28(1)
C(10)	11629(5)	3733(5)	1867(4)	35(1)

Table 3. Bond lengths [Å] and angles [deg] for 05mz092m.

O(8)-C(12)	1.385(5)
O(8)-N(1)	1.438(4)
O(7)-C(6)	1.332(4)
O(7)-C(11)	1.456(5)
O(1)-C(5)	1.415(4)
O(1)-C(1)	1.434(5)
O(6)-C(6)	1.199(4)
O(2)-C(7)	1.378(4)
O(2)-C(3)	1.443(5)
O(4)-C(9)	1.364(5)
O(4)-C(4)	1.444(4)
O(3)-C(7)	1.188(5)
N(1)-C(2)	1.265(5)
O(9)-C(12)	1.183(5)
C(5)-C(4)	1.524(5)
C(5)-C(6)	1.525(5)
C(5)-H(5)	1
C(13)-C(18)	1.384(5)
C(13)-C(14)	1.392(5)
C(13)-C(12)	1.492(5)
C(16)-C(15)	1.377(6)
C(16)-C(17)	1.385(7)
C(16)-H(16)	0.95
C(4)-C(3)	1.531(5)
C(4)-H(4)	1
O(5)-C(9)	1.200(5)
C(2)-C(1)	1.509(5)
C(2)-C(3)	1.510(5)
C(3)-H(3)	1
C(17)-C(18)	1.386(6)
C(17)-H(17)	0.95
C(7)-C(8)	1.483(6)
C(1)-H(1A)	0.99
C(1)-H(1B)	0.99
C(18)-H(18)	0.95
C(14)-C(15)	1.387(5)
C(14)-H(14)	0.95
C(11)-H(11A)	0.98
C(11)-H(11B)	0.98
C(11)-H(11C)	0.98
C(9)-C(10)	1.486(6)
C(15)-H(15)	0.95
C(8)-H(8A)	0.98
C(8)-H(8B)	0.98

C(8)-H(8C)	0.98
C(10)-H(10A)	0.98
C(10)-H(10B)	0.98
C(10)-H(10C)	0.98
C(12)-O(8)-N(1)	110.4(3)
C(6)-O(7)-C(11)	115.8(3)
C(5)-O(1)-C(1)	114.7(3)
C(7)-O(2)-C(3)	115.2(3)
C(9)-O(4)-C(4)	116.6(3)
C(2)-N(1)-O(8)	110.6(3)
O(1)-C(5)-C(4)	111.6(3)
O(1)-C(5)-C(6)	111.8(3)
C(4)-C(5)-C(6)	115.7(3)
O(1)-C(5)-H(5)	105.6
C(4)-C(5)-H(5)	105.6
C(6)-C(5)-H(5)	105.6
O(6)-C(6)-O(7)	124.7(3)
O(6)-C(6)-C(5)	123.7(3)
O(7)-C(6)-C(5)	111.4(3)
C(18)-C(13)-C(14)	119.6(3)
C(18)-C(13)-C(12)	116.2(3)
C(14)-C(13)-C(12)	124.2(3)
C(15)-C(16)-C(17)	120.4(4)
C(15)-C(16)-H(16)	119.8
C(17)-C(16)-H(16)	119.8
O(4)-C(4)-C(5)	106.9(3)
O(4)-C(4)-C(3)	107.0(3)
C(5)-C(4)-C(3)	111.7(3)
O(4)-C(4)-H(4)	110.4
C(5)-C(4)-H(4)	110.4
C(3)-C(4)-H(4)	110.4
N(1)-C(2)-C(1)	129.6(3)
N(1)-C(2)-C(3)	114.6(3)
C(1)-C(2)-C(3)	115.8(3)
O(9)-C(12)-O(8)	123.7(3)
O(9)-C(12)-C(13)	126.0(3)
O(8)-C(12)-C(13)	110.3(3)
O(2)-C(3)-C(2)	104.9(3)
O(2)-C(3)-C(4)	107.4(3)
C(2)-C(3)-C(4)	111.4(3)
O(2)-C(3)-H(3)	111
C(2)-C(3)-H(3)	111
C(4)-C(3)-H(3)	111
C(16)-C(17)-C(18)	119.7(4)
C(16)-C(17)-H(17)	120.1
C(18)-C(17)-H(17)	120.1

O(3)-C(7)-O(2)	121.9(4)
O(3)-C(7)-C(8)	127.5(3)
O(2)-C(7)-C(8)	110.6(3)
O(1)-C(1)-C(2)	109.9(3)
O(1)-C(1)-H(1A)	109.7
C(2)-C(1)-H(1A)	109.7
O(1)-C(1)-H(1B)	109.7
C(2)-C(1)-H(1B)	109.7
H(1A)-C(1)-H(1B)	108.2
C(13)-C(18)-C(17)	120.3(4)
C(13)-C(18)-H(18)	119.9
C(17)-C(18)-H(18)	119.9
C(15)-C(14)-C(13)	120.0(4)
C(15)-C(14)-H(14)	120
C(13)-C(14)-H(14)	120
O(7)-C(11)-H(11A)	109.5
O(7)-C(11)-H(11B)	109.5
H(11A)-C(11)-H(11B)	109.5
O(7)-C(11)-H(11C)	109.5
H(11A)-C(11)-H(11C)	109.5
H(11B)-C(11)-H(11C)	109.5
O(5)-C(9)-O(4)	122.2(4)
O(5)-C(9)-C(10)	126.0(4)
O(4)-C(9)-C(10)	111.7(3)
C(16)-C(15)-C(14)	119.9(4)
C(16)-C(15)-H(15)	120
C(14)-C(15)-H(15)	120
C(7)-C(8)-H(8A)	109.5
C(7)-C(8)-H(8B)	109.5
H(8A)-C(8)-H(8B)	109.5
C(7)-C(8)-H(8C)	109.5
H(8A)-C(8)-H(8C)	109.5
H(8B)-C(8)-H(8C)	109.5
C(9)-C(10)-H(10A)	109.5
C(9)-C(10)-H(10B)	109.5
H(10A)-C(10)-H(10B)	109.5
C(9)-C(10)-H(10C)	109.5
H(10A)-C(10)-H(10C)	109.5
H(10B)-C(10)-H(10C)	109.5

Table 4. Anisotropic displacement parameters [$Å^2 \times 10^3$] for 05mz092m. The anisotropic displacement factor exponent takes the form: $-2\pi^2 [(h\,a^*)^2 U11 + ... + 2\,h\,k\,a^*\,b^*\,U12]$

	U11	U22	U33	U23	U13	U12
O(8)	17(1)	33(2)	24(1)	2(1)	0(1)	3(1)
O(7)	21(1)	36(2)	23(1)	-3(1)	-3(1)	4(1)
O(1)	18(1)	26(1)	22(1)	1(1)	-2(1)	0(1)
O(6)	21(1)	25(1)	22(1)	-2(1)	3(1)	-3(1)
O(2)	17(1)	27(1)	25(1)	1(1)	3(1)	0(1)
O(4)	26(1)	31(2)	22(1)	-4(1)	-2(1)	8(1)
O(3)	17(1)	73(2)	36(2)	-9(2)	4(1)	3(2)
N(1)	17(1)	26(2)	26(2)	1(1)	-1(1)	4(1)
O(9)	25(1)	57(2)	38(2)	17(2)	5(1)	1(2)
C(5)	23(2)	21(2)	22(2)	2(1)	2(1)	0(1)
C(6)	21(2)	22(2)	21(2)	3(1)	4(1)	0(1)
C(13)	23(2)	23(2)	24(2)	-1(2)	1(1)	4(2)
C(16)	24(2)	35(2)	44(2)	-6(2)	-7(2)	3(2)
C(4)	20(2)	24(2)	22(2)	-4(2)	-1(1)	3(1)
O(5)	26(1)	32(2)	41(2)	-3(1)	2(1)	8(1)
C(2)	17(2)	21(2)	24(2)	-4(1)	0(1)	2(1)
C(12)	26(2)	28(2)	19(2)	-1(2)	-1(1)	5(2)
C(3)	17(2)	27(2)	25(2)	0(2)	6(1)	2(1)
C(17)	41(2)	34(2)	24(2)	5(2)	-9(2)	7(2)
C(7)	14(2)	33(2)	26(2)	6(2)	2(1)	-1(2)
C(1)	17(2)	27(2)	23(2)	1(2)	0(1)	5(1)
C(18)	27(2)	31(2)	26(2)	3(2)	3(2)	4(2)
C(14)	25(2)	32(2)	25(2)	2(2)	3(1)	3(2)
C(11)	25(2)	44(2)	21(2)	-3(2)	-6(1)	-2(2)
C(9)	23(2)	27(2)	29(2)	1(2)	13(1)	2(2)
C(15)	20(2)	40(2)	38(2)	-4(2)	1(2)	-1(2)
C(8)	14(2)	35(2)	35(2)	7(2)	1(1)	0(2)
C(10)	37(2)	31(2)	39(2)	-2(2)	10(2)	8(2)

Table 5. Hydrogen coordinates ($\times 10^4$) and isotropic displacement parameters ($Å^2 \times 10^3$) for 05mz092m.

	x	y	z	U(eq)
H(5)	10316	5903	4347	26
H(16)	1463	11140	-1127	42
H(4)	12707	7096	3828	26
H(3)	12140	8923	2368	27
H(17)	3535	11784	-2118	41
H(1A)	8661	9640	3933	27
H(1B)	7384	9048	2985	27
H(18)	6235	11837	-1340	33
H(14)	4807	10256	1341	33
H(11A)	12099	7691	7179	46
H(11B)	12327	9362	6700	46
H(11C)	13837	8201	6875	46
H(15)	2092	10356	591	39
H(8A)	15225	11440	4916	42
H(8B)	13521	11098	5334	42
H(8C)	13652	12436	4500	42
H(10A)	10980	2951	2172	53
H(10B)	12560	3240	1602	53
H(10C)	10955	4248	1294	53

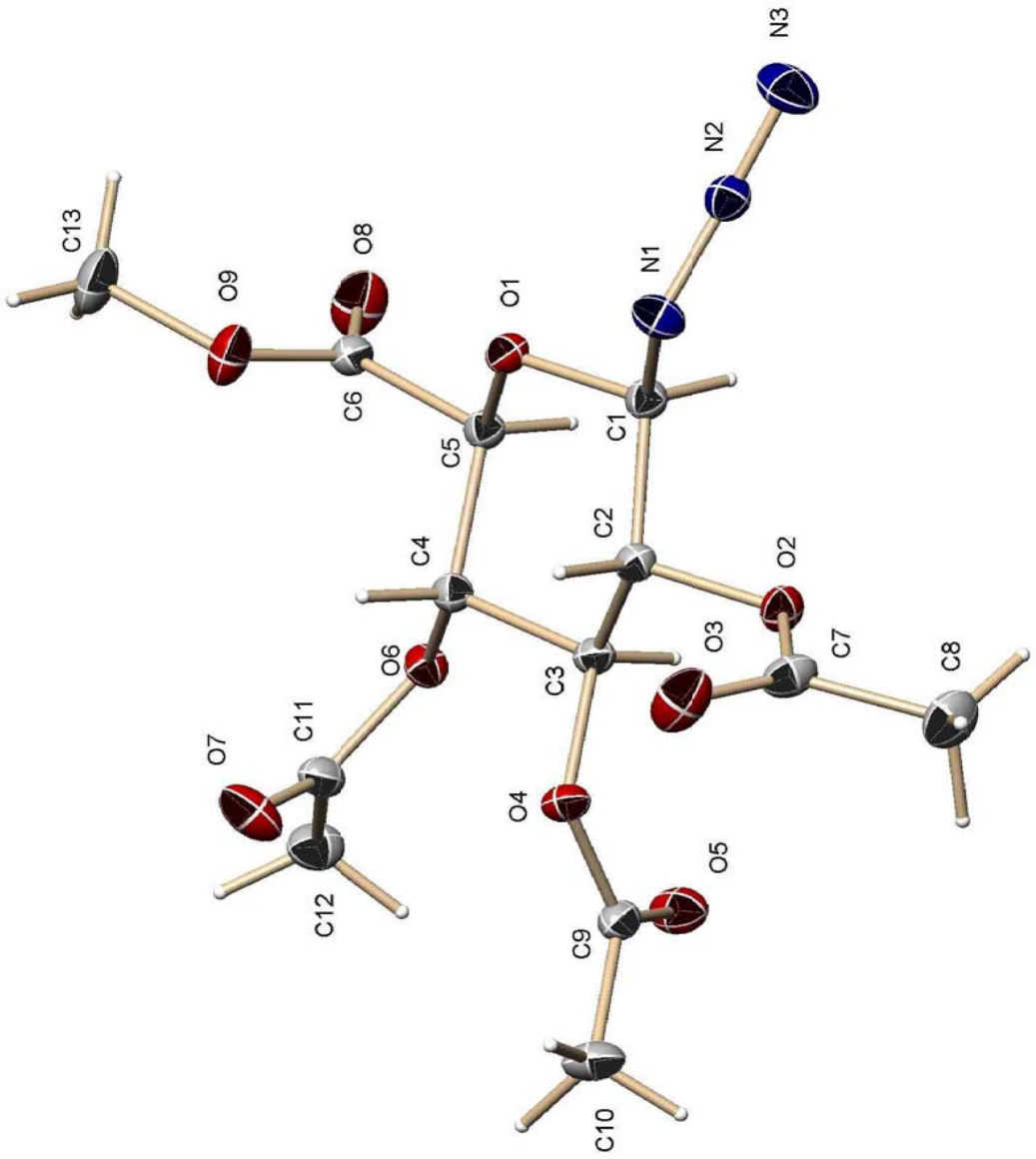

Figure 173: X-ray crystal structure of methyl 3,4,5-tri-*O*-acetyl-β-D-glucopyranosyl azide (**32**).

Table 1. Crystal data and structure refinement for 04mz131m:

Identification code:	04mz131m
Empirical formula:	$C_{13}H_{17}N_3O_9$
Formula weight:	359.30
Temperature:	100(2) K
Wavelength:	0.71073 Å
Crystal system:	Orthorhombic
Space group:	$P2_12_12_1$
Unit cell dimensions:	a = 7.3201(8) Å, α = 90°
	b = 13.9189(14) Å, β = 90°
	c = 15.8356(16) Å, γ = 90°
Volume, *Z*:	1613.5(3) $Å^3$, 4
Density (calculated):	1.479 Mg/m^3
Absorption coefficient:	0.127 mm^{-1}
F(000):	752
Crystal size:	0.59 × 0.54 × 0.46 mm
Theta range for data collection:	1.95 to 28.28°
Limiting indices:	$-9 \le h \le 9$, $-18 \le k \le 18$, $-21 \le l \le 21$
Reflections collected:	16714
Independent reflections:	2290 (*R*(int) = 0.0202)
Completeness to $\theta = 28.28°$:	100.0 %

Absorption correction:	multi-scan
Max. and min. transmission:	0.94 and 0.7804
Refinement method:	Full-matrix least-squares on F^2
Data / restraints / parameters:	2290 / 0 / 277
Goodness-of-fit on F^2:	1.078
Final R indices [$I>2\sigma(I)$]:	R1 = 0.0309, wR2 = 0.0793
R indices (all data):	R1 = 0.0312, wR2 = 0.0795
Largest diff. peak and hole:	0.325 and -0.190 e × $Å^{-3}$

Table 2. Atomic coordinates [$\times 10^4$] and equivalent isotropic displacement parameters [$Å^2 \times 10^3$] for 04mz131m. U(eq) is defined as one third of the trace of the orthogonalized U_{ij} tensor.

	x	y	z	U(eq)
C(1)	-1831(2)	5220(1)	1276(1)	15(1)
C(2)	-123(2)	5736(1)	1589(1)	14(1)
C(3)	1042(2)	6085(1)	852(1)	14(1)
C(4)	1405(2)	5256(1)	243(1)	14(1)
C(5)	-447(2)	4839(1)	-20(1)	14(1)
C(6)	-254(2)	4015(1)	-648(1)	16(1)
C(7)	-51(2)	6665(1)	2860(1)	20(1)
C(8)	-764(3)	7568(1)	3250(1)	26(1)
C(9)	3465(2)	7248(1)	926(1)	17(1)
C(10)	5071(3)	7540(1)	1453(1)	24(1)
C(11)	4117(2)	5518(1)	-564(1)	19(1)
C(12)	4788(3)	5970(1)	-1362(1)	24(1)
C(13)	860(3)	2440(1)	-829(1)	30(1)
N(1)	-2677(2)	4768(1)	2009(1)	19(1)
N(2)	-4360(2)	4670(1)	1969(1)	18(1)
N(3)	-5866(2)	4528(1)	2032(1)	28(1)
O(1)	-1312(2)	4464(1)	719(1)	15(1)
O(2)	-709(2)	6564(1)	2058(1)	17(1)
O(3)	996(2)	6116(1)	3179(1)	30(1)
O(4)	2718(2)	6427(1)	1227(1)	17(1)
O(5)	2895(2)	7674(1)	321(1)	24(1)
O(6)	2265(2)	5605(1)	-511(1)	16(1)
O(7)	5025(2)	5150(1)	-23(1)	28(1)
O(8)	-864(2)	4030(1)	-1349(1)	29(1)
O(9)	657(2)	3288(1)	-305(1)	23(1)

Table 3. Bond lengths [Å] and angles [deg] for 04mz131m.

C(1)-O(1)	1.4258(18)
C(1)-N(1)	1.4582(19)
C(1)-C(2)	1.524(2)
C(1)-H(1)	0.98(2)
C(2)-O(2)	1.4370(18)
C(2)-C(3)	1.525(2)
C(2)-H(2)	0.95(2)
C(3)-O(4)	1.4437(17)
C(3)-C(4)	1.527(2)
C(3)-H(3)	0.94(2)
C(4)-O(6)	1.4340(17)
C(4)-C(5)	1.532(2)
C(4)-H(4)	0.97(2)
C(5)-O(1)	1.4287(17)
C(5)-C(6)	1.525(2)
C(5)-H(5)	0.94(2)
C(6)-O(8)	1.196(2)
C(6)-O(9)	1.3281(19)
C(7)-O(3)	1.194(2)
C(7)-O(2)	1.3661(19)
C(7)-C(8)	1.495(2)
C(8)-H(8A)	0.97(3)
C(8)-H(8B)	0.96(3)
C(8)-H(8C)	0.90(3)
C(9)-O(5)	1.201(2)
C(9)-O(4)	1.3544(18)
C(9)-C(10)	1.499(2)
C(10)-H(10A)	0.90(3)
C(10)-H(10B)	0.91(3)
C(10)-H(10C)	0.99(3)
C(11)-O(7)	1.200(2)
C(11)-O(6)	1.3637(18)
C(11)-C(12)	1.494(2)
C(12)-H(12A)	0.94(3)
C(12)-H(12B)	0.96(3)
C(12)-H(12C)	0.96(3)
C(13)-O(9)	1.451(2)
C(13)-H(13A)	0.93(3)

C(13)-H(13B)	0.95(3)
C(13)-H(13C)	0.95(3)
N(1)-N(2)	1.2412(19)
N(2)-N(3)	1.124(2)
O(1)-C(1)-N(1)	106.66(12)
O(1)-C(1)-C(2)	109.27(12)
N(1)-C(1)-C(2)	107.08(12)
O(1)-C(1)-H(1)	109.3(12)
N(1)-C(1)-H(1)	112.7(12)
C(2)-C(1)-H(1)	111.7(12)
O(2)-C(2)-C(1)	107.47(12)
O(2)-C(2)-C(3)	107.90(12)
C(1)-C(2)-C(3)	111.12(12)
O(2)-C(2)-H(2)	111.9(12)
C(1)-C(2)-H(2)	107.9(12)
C(3)-C(2)-H(2)	110.6(12)
O(4)-C(3)-C(2)	105.33(11)
O(4)-C(3)-C(4)	111.20(12)
C(2)-C(3)-C(4)	109.85(12)
O(4)-C(3)-H(3)	110.2(12)
C(2)-C(3)-H(3)	111.6(13)
C(4)-C(3)-H(3)	108.6(13)
O(6)-C(4)-C(3)	110.16(12)
O(6)-C(4)-C(5)	106.94(11)
C(3)-C(4)-C(5)	107.69(11)
O(6)-C(4)-H(4)	111.7(12)
C(3)-C(4)-H(4)	112.3(12)
C(5)-C(4)-H(4)	107.8(11)
O(1)-C(5)-C(6)	107.48(11)
O(1)-C(5)-C(4)	107.95(11)
C(6)-C(5)-C(4)	112.35(12)
O(1)-C(5)-H(5)	111.5(13)
C(6)-C(5)-H(5)	108.3(12)
C(4)-C(5)-H(5)	109.3(12)
O(8)-C(6)-O(9)	125.51(15)
O(8)-C(6)-C(5)	123.87(14)
O(9)-C(6)-C(5)	110.61(13)
O(3)-C(7)-O(2)	123.62(15)
O(3)-C(7)-C(8)	126.00(15)
O(2)-C(7)-C(8)	110.33(14)
C(7)-C(8)-H(8A)	106.4(16)

C(7)-C(8)-H(8B)	111.7(16)
H(8A)-C(8)-H(8B)	110(2)
C(7)-C(8)-H(8C)	108.3(17)
H(8A)-C(8)-H(8C)	106(2)
H(8B)-C(8)-H(8C)	114(2)
O(5)-C(9)-O(4)	123.92(15)
O(5)-C(9)-C(10)	125.66(15)
O(4)-C(9)-C(10)	110.42(14)
C(9)-C(10)-H(10A)	109.1(17)
C(9)-C(10)-H(10B)	112.5(17)
H(10A)-C(10)-H(10B)	115(2)
C(9)-C(10)-H(10C)	109.2(15)
H(10A)-C(10)-H(10C)	103(2)
H(10B)-C(10)-H(10C)	107(2)
O(7)-C(11)-O(6)	122.98(15)
O(7)-C(11)-C(12)	126.99(16)
O(6)-C(11)-C(12)	110.00(14)
C(11)-C(12)-H(12A)	107.5(16)
C(11)-C(12)-H(12B)	110.8(15)
H(12A)-C(12)-H(12B)	108(2)
C(11)-C(12)-H(12C)	104.5(16)
H(12A)-C(12)-H(12C)	116(2)
H(12B)-C(12)-H(12C)	110(2)
O(9)-C(13)-H(13A)	111.0(18)
O(9)-C(13)-H(13B)	107.1(17)
H(13A)-C(13)-H(13B)	113(3)
O(9)-C(13)-H(13C)	109.5(17)
H(13A)-C(13)-H(13C)	108(2)
H(13B)-C(13)-H(13C)	109(2)
N(2)-N(1)-C(1)	115.43(14)
N(3)-N(2)-N(1)	171.21(18)
C(1)-O(1)-C(5)	110.82(11)
C(7)-O(2)-C(2)	117.27(12)
C(9)-O(4)-C(3)	118.39(12)
C(11)-O(6)-C(4)	117.26(12)
C(6)-O(9)-C(13)	115.89(14)

Table 4. Anisotropic displacement parameters [$Å^2 \times 10^3$] for 04mz131m. The anisotropic displacement factor exponent takes the form: $-2\pi2 [(h a^*)^2 U11 + ... + 2 h k a^* b^* U12]$

	U11	U22	U33	U23	U13	U12
C(1)	16(1)	14(1)	15(1)	0(1)	1(1)	0(1)
C(2)	15(1)	13(1)	14(1)	-1(1)	0(1)	-1(1)
C(3)	14(1)	13(1)	15(1)	0(1)	-1(1)	-1(1)
C(4)	14(1)	14(1)	14(1)	0(1)	0(1)	0(1)
C(5)	14(1)	14(1)	14(1)	0(1)	-1(1)	0(1)
C(6)	16(1)	15(1)	18(1)	-1(1)	0(1)	-1(1)
C(7)	25(1)	19(1)	15(1)	-3(1)	0(1)	-6(1)
C(8)	34(1)	24(1)	21(1)	-8(1)	1(1)	0(1)
C(9)	17(1)	15(1)	20(1)	-3(1)	3(1)	-2(1)
C(10)	23(1)	24(1)	27(1)	-1(1)	-5(1)	-9(1)
C(11)	15(1)	21(1)	19(1)	-5(1)	2(1)	-3(1)
C(12)	23(1)	28(1)	21(1)	-3(1)	6(1)	-6(1)
C(13)	40(1)	19(1)	31(1)	-9(1)	-1(1)	8(1)
N(1)	15(1)	25(1)	17(1)	2(1)	2(1)	-2(1)
N(2)	20(1)	16(1)	18(1)	2(1)	1(1)	0(1)
N(3)	18(1)	32(1)	33(1)	10(1)	3(1)	-2(1)
O(1)	17(1)	14(1)	15(1)	-1(1)	2(1)	-2(1)
O(2)	20(1)	17(1)	15(1)	-4(1)	0(1)	1(1)
O(3)	44(1)	24(1)	23(1)	-2(1)	-13(1)	2(1)
O(4)	17(1)	16(1)	18(1)	0(1)	-3(1)	-4(1)
O(5)	24(1)	22(1)	27(1)	6(1)	-1(1)	-5(1)
O(6)	15(1)	17(1)	14(1)	1(1)	2(1)	0(1)
O(7)	17(1)	45(1)	22(1)	1(1)	-2(1)	2(1)
O(8)	39(1)	29(1)	20(1)	-6(1)	-11(1)	6(1)
O(9)	33(1)	17(1)	20(1)	-4(1)	-4(1)	7(1)

Table 5. Hydrogen coordinates ($\times 10^4$) and isotropic displacement parameters ($Å^2 \times 10^3$) for 04mz131m.

	x	y	z	U(eq)
H(1)	-2660(30)	5657(15)	982(13)	18
H(2)	550(30)	5299(15)	1930(13)	17
H(3)	470(30)	6581(15)	555(13)	17
H(4)	2110(30)	4742(14)	503(13)	17
H(5)	-1150(30)	5325(15)	-273(13)	17
H(8A)	130(40)	8070(20)	3130(17)	40
H(8B)	-1930(40)	7742(19)	3023(18)	40
H(8C)	-760(40)	7494(18)	3813(19)	40
H(10A)	4970(40)	8170(20)	1584(16)	37
H(10B)	5250(40)	7140(19)	1899(17)	37
H(10C)	6190(40)	7517(18)	1103(17)	37
H(12A)	5920(40)	5687(19)	-1493(16)	36
H(12B)	3960(40)	5839(18)	-1822(15)	36
H(12C)	4810(40)	6646(18)	-1242(17)	36
H(13A)	1270(40)	2600(20)	-1366(18)	45
H(13B)	1670(40)	2010(20)	-541(18)	45
H(13C)	-290(40)	2130(20)	-889(16)	45

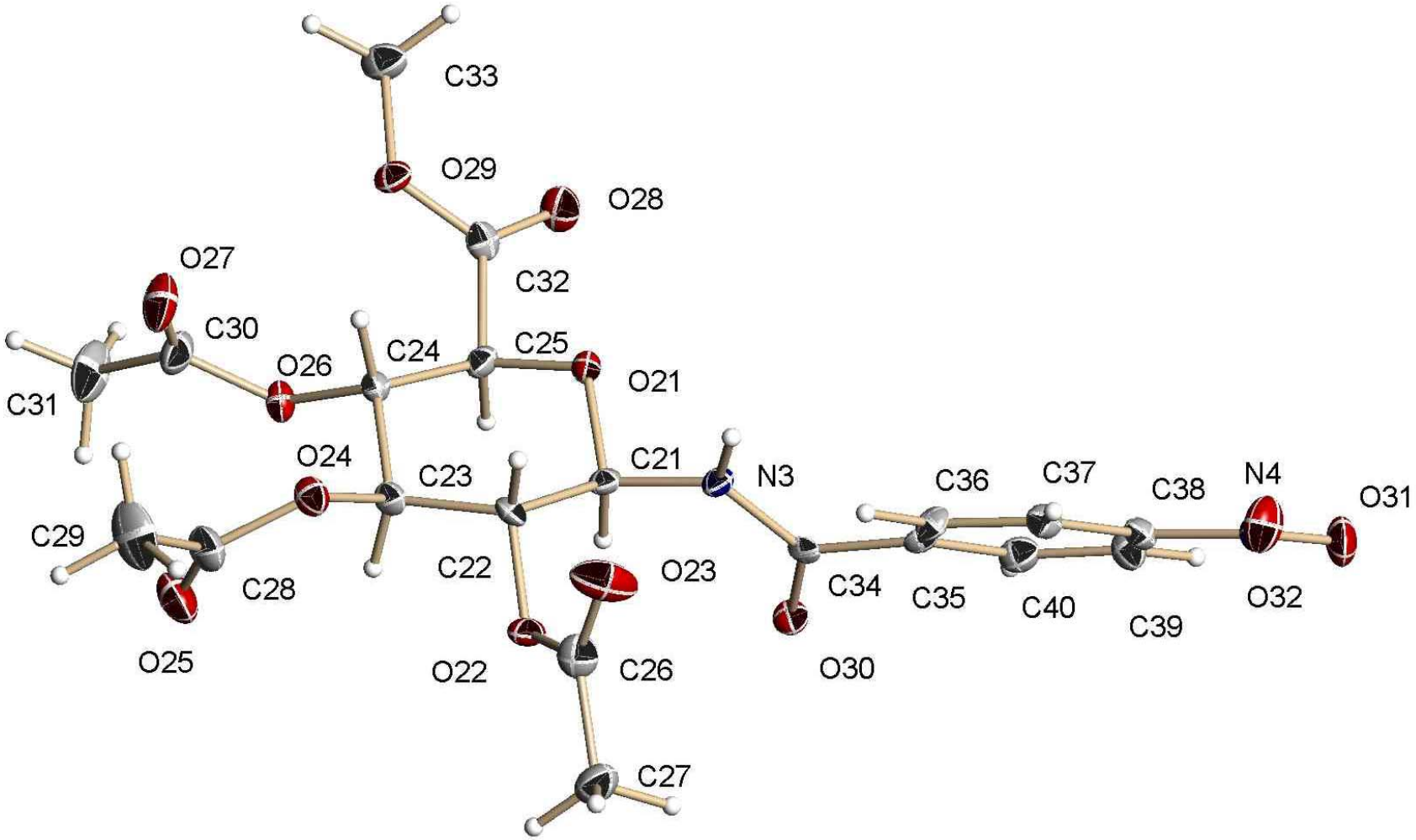

Figure 174: X-ray crystal structure of *p*-Nitrobenzoic acid-(methyl 2,3,4-tri-*O*-acetyl-β-D-glucopyranuronosyl)-amide (**33**).

Table 1. Crystal data and structure refinement for 05mz056m:

Identification code:	05mz056m
Empirical formula:	$C_{21}H_{24}Cl_2N_2O_{12}$
Moiety frormula:	$C_{20}H_{24}N_2O_{12}$
Formula weight:	567.32
Temperature:	100(2) K
Wavelength:	0.71073 Å
Crystal system:	Triclinic
Space group:	P1
Unit cell dimensions:	a = 8.899(2) Å, α = 82.056(4)°
	b = 9.367(2) Å, β = 84.507(4)°
	c = 15.511(4) Å, γ = 89.937(4)°
Volume, *Z*:	1274.5(5) $Å^3$, 2
Density (calculated):	1.478 Mg/m^3
Absorption coefficient:	0.320 mm^{-1}
F(000):	588
Crystal size:	0.47 × 0.40 × 0.29 mm
Theta range for data collection:	1.33 to 26.37°
Limiting indices:	$-11 \leq h \leq 11$, $-11 \leq k \leq 11$, $-19 \leq l \leq 19$
Reflections collected:	9751
Independent reflections:	8888 (*R*(int) = 0.0489)

Completeness to θ = 26.37°:	97.1 %
Absorption correction:	multi-scan
Max. and min. transmission:	0.91 and 0.2351
Refinement method:	Full-matrix least-squares on F^2
Data / restraints / parameters:	8888 / 93 / 707
Goodness-of-fit on F^2:	1.128
Final *R* indices [$I>2\sigma(I)$]:	R1 = 0.0885, wR2 = 0.2340
R indices (all data):	R1 = 0.0894, wR2 = 0.2354
Largest diff. peak and hole:	1.888 and -0.649 e × Å^{-3}

Table 2. Atomic coordinates [$\times 10^4$] and equivalent isotropic displacement parameters [$Å^2 \times 10^3$] for 05mz056m. U(eq) is defined as one third of the trace of the orthogonalized U_{ij} tensor.

	x	y	z	U(eq)
O(21)	2168(4)	3254(3)	5037(2)	14(1)
O(1)	7373(4)	-1236(3)	3936(2)	15(1)
O(4)	6888(4)	590(4)	1452(2)	21(1)
O(2)	5245(4)	1735(4)	2877(2)	16(1)
N(1)	6491(5)	790(4)	4515(3)	17(1)
O(9)	9197(4)	-3701(4)	2959(2)	19(1)
O(22)	-272(4)	287(4)	6111(2)	18(1)
O(26)	902(4)	4738(4)	7017(2)	17(1)
O(29)	3666(4)	5741(4)	5991(2)	18(1)
O(30)	-606(4)	1742(4)	3752(2)	17(1)
O(10)	4168(4)	298(3)	5228(2)	17(1)
O(12)	5856(5)	3994(4)	8547(3)	29(1)
N(2)	6389(5)	4399(4)	7807(3)	22(1)
O(6)	6808(4)	-2694(4)	1949(2)	18(1)
O(24)	1033(4)	1443(4)	7526(2)	19(1)
N(3)	1491(4)	1235(4)	4469(3)	15(1)
C(38)	2119(5)	-1432(5)	1848(3)	16(1)
O(8)	8185(5)	-4147(4)	4348(2)	24(1)
C(4)	7328(5)	-1600(5)	2422(3)	14(1)
C(18)	6223(5)	3483(5)	7124(3)	18(1)
O(28)	3086(5)	6174(4)	4599(3)	25(1)
C(36)	2003(5)	-1031(5)	3347(3)	15(1)
O(31)	2304(5)	-1908(5)	419(3)	28(1)
C(22)	970(5)	1284(5)	6034(3)	16(1)
C(40)	856(6)	638(5)	2282(3)	20(1)
C(24)	1629(5)	3651(5)	6551(3)	13(1)
C(21)	1051(5)	2136(5)	5123(3)	14(1)
N(4)	2569(5)	-2332(5)	1170(3)	21(1)
C(35)	1203(5)	215(4)	3142(3)	13(1)
O(5)	5250(5)	-496(5)	718(3)	29(1)
C(15)	5770(5)	1829(5)	5840(3)	14(1)
O(27)	2462(5)	4256(5)	8082(3)	32(1)
O(11)	7107(5)	5553(4)	7579(3)	30(1)
O(32)	3208(5)	-3469(4)	1389(3)	30(1)

C(14)	5413(5)	914(5)	5156(3)	13(1)
O(25)	-884(5)	2428(5)	8291(3)	33(1)
C(34)	621(5)	1119(4)	3817(3)	12(1)
C(20)	6654(5)	3083(5)	5631(3)	15(1)
O(7)	8716(5)	-2131(5)	873(3)	33(1)
C(2)	6472(5)	729(5)	2948(3)	14(1)
O(3)	6805(5)	3579(4)	2987(4)	45(1)
C(19)	6874(5)	3924(5)	6272(3)	17(1)
C(1)	6266(5)	-119(5)	3862(3)	14(1)
C(5)	7124(5)	-2280(5)	3382(3)	16(1)
C(33)	4759(6)	6923(6)	5816(4)	24(1)
C(16)	5117(5)	1410(5)	6695(3)	18(1)
C(17)	5363(6)	2231(5)	7345(3)	19(1)
C(23)	659(5)	2285(5)	6723(3)	16(1)
C(3)	6357(5)	-249(5)	2256(3)	15(1)
C(39)	1330(6)	-172(5)	1635(3)	19(1)
C(9)	6217(6)	377(6)	717(3)	24(1)
C(32)	2895(5)	5517(5)	5336(3)	17(1)
C(25)	1729(5)	4311(5)	5588(3)	16(1)
C(6)	8234(5)	-3497(5)	3629(3)	18(1)
C(11)	7634(6)	-2902(5)	1195(3)	21(1)
C(28)	174(7)	1631(6)	8267(4)	27(1)
C(26)	37(6)	-1119(6)	6043(4)	23(1)
C(13)	10218(6)	-4895(6)	3123(4)	23(1)
C(30)	1451(6)	4945(6)	7778(4)	24(1)
C(7)	5582(6)	3143(5)	2926(3)	21(1)
C(27)	-1373(7)	-1969(6)	6060(4)	27(1)
C(8)	4163(7)	4020(7)	2954(4)	31(1)
O(23)	1302(5)	-1562(4)	5970(4)	38(1)
C(31)	627(8)	6132(7)	8150(4)	36(1)
C(10)	6883(10)	1380(8)	-54(4)	41(2)
C(37)	2461(5)	-1894(5)	2697(3)	17(1)
C(29)	750(10)	703(8)	9042(4)	42(2)
C(12)	7039(8)	-4159(7)	845(4)	34(1)
C(50A)	5596(9)	7815(11)	8847(6)	39(2)
Cl(1A)	7194(3)	8832(4)	8343(3)	51(1)
Cl(2A)	4089(4)	7999(4)	8178(3)	48(1)
C(50B)	5720(30)	7500(60)	9040(30)	39(2)
Cl(1B)	7480(20)	8250(30)	8604(12)	68(6)
Cl(2B)	4240(20)	8190(20)	8449(17)	57(5)
C(51A)	2561(8)	4233(8)	140(4)	34(2)

Cl(3A)	3625(3)	3033(3)	824(2)	49(1)
Cl(4A)	615(4)	3992(5)	488(2)	76(1)
C(51B)	1800(40)	4200(50)	140(30)	34(2)
Cl(4B)	140(20)	3210(40)	595(19)	76(1)
Cl(3B)	3430(20)	3370(30)	540(18)	49(1)

Table 3. Bond lengths [Å] and angles [deg] for 05mz056m.

O(21)-C(25)	1.426(5)
O(21)-C(21)	1.428(5)
O(1)-C(5)	1.419(5)
O(1)-C(1)	1.437(5)
O(4)-C(9)	1.374(6)
O(4)-C(3)	1.420(6)
O(2)-C(7)	1.367(6)
O(2)-C(2)	1.444(5)
N(1)-C(14)	1.332(6)
N(1)-C(1)	1.437(6)
N(1)-H(1B)	0.88
O(9)-C(6)	1.317(6)
O(9)-C(13)	1.450(5)
O(22)-C(26)	1.362(6)
O(22)-C(22)	1.433(5)
O(26)-C(30)	1.357(6)
O(26)-C(24)	1.446(5)
O(29)-C(32)	1.318(6)
O(29)-C(33)	1.455(6)
O(30)-C(34)	1.243(6)
O(10)-C(14)	1.237(6)
O(12)-N(2)	1.208(6)
N(2)-O(11)	1.246(6)
N(2)-C(18)	1.471(6)
O(6)-C(11)	1.357(6)
O(6)-C(4)	1.442(5)
O(24)-C(28)	1.350(7)
O(24)-C(23)	1.446(5)
N(3)-C(34)	1.348(6)
N(3)-C(21)	1.433(6)
N(3)-H(3B)	0.88
C(38)-C(39)	1.389(7)
C(38)-C(37)	1.391(7)
C(38)-N(4)	1.463(6)
O(8)-C(6)	1.192(6)
C(4)-C(5)	1.531(6)
C(4)-C(3)	1.537(6)
C(4)-H(4)	1
C(18)-C(17)	1.386(7)

C(18)-C(19)	1.398(7)
O(28)-C(32)	1.218(6)
C(36)-C(35)	1.381(6)
C(36)-C(37)	1.407(7)
C(36)-H(36)	0.95
O(31)-N(4)	1.222(6)
C(22)-C(21)	1.519(6)
C(22)-C(23)	1.523(6)
C(22)-H(22)	1
C(40)-C(39)	1.375(7)
C(40)-C(35)	1.402(7)
C(40)-H(40)	0.95
C(24)-C(23)	1.522(6)
C(24)-C(25)	1.529(6)
C(24)-H(24)	1
C(21)-H(21)	1
N(4)-O(32)	1.228(6)
C(35)-C(34)	1.490(6)
O(5)-C(9)	1.188(7)
C(15)-C(20)	1.397(6)
C(15)-C(16)	1.400(7)
C(15)-C(14)	1.509(6)
O(27)-C(30)	1.201(7)
O(25)-C(28)	1.201(8)
C(20)-C(19)	1.380(7)
C(20)-H(20)	0.95
O(7)-C(11)	1.228(7)
C(2)-C(3)	1.514(6)
C(2)-C(1)	1.521(6)
C(2)-H(2)	1
O(3)-C(7)	1.180(7)
C(19)-H(19)	0.95
C(1)-H(1)	1
C(5)-C(6)	1.540(6)
C(5)-H(5)	1
C(33)-H(33A)	0.98
C(33)-H(33B)	0.98
C(33)-H(33C)	0.98
C(16)-C(17)	1.384(7)
C(16)-H(16)	0.95
C(17)-H(17)	0.95

C(23)-H(23)	1
C(3)-H(3)	1
C(39)-H(39)	0.95
C(9)-C(10)	1.489(9)
C(32)-C(25)	1.520(6)
C(25)-H(25)	1
C(11)-C(12)	1.482(8)
C(28)-C(29)	1.514(8)
C(26)-O(23)	1.200(7)
C(26)-C(27)	1.483(7)
C(13)-H(13A)	0.98
C(13)-H(13B)	0.98
C(13)-H(13C)	0.98
C(30)-C(31)	1.484(7)
C(7)-C(8)	1.507(7)
C(27)-H(27A)	0.98
C(27)-H(27B)	0.98
C(27)-H(27C)	0.98
C(8)-H(8A)	0.98
C(8)-H(8B)	0.98
C(8)-H(8C)	0.98
C(31)-H(31A)	0.98
C(31)-H(31B)	0.98
C(31)-H(31C)	0.98
C(10)-H(10A)	0.98
C(10)-H(10B)	0.98
C(10)-H(10C)	0.98
C(37)-H(37)	0.95
C(29)-H(29A)	0.98
C(29)-H(29B)	0.98
C(29)-H(29C)	0.98
C(12)-H(12A)	0.98
C(12)-H(12B)	0.98
C(12)-H(12C)	0.98
C(50A)-Cl(2A)	1.767(8)
C(50A)-Cl(1A)	1.767(9)
C(50A)-H(50A)	0.99
C(50A)-H(50B)	0.99
C(50B)-Cl(2B)	1.746(18)
C(50B)-Cl(1B)	1.748(18)
C(50B)-H(50C)	0.99

C(50B)-H(50D)	0.99
C(51A)-Cl(4A)	1.768(8)
C(51A)-Cl(3A)	1.774(7)
C(51A)-H(51A)	0.99
C(51A)-H(51B)	0.99
C(51B)-Cl(3B)	1.770(17)
C(51B)-Cl(4B)	1.773(18)
C(51B)-H(51C)	0.99
C(51B)-H(51D)	0.99
C(25)-O(21)-C(21)	110.9(3)
C(5)-O(1)-C(1)	111.0(3)
C(9)-O(4)-C(3)	117.9(4)
C(7)-O(2)-C(2)	116.6(4)
C(14)-N(1)-C(1)	120.5(4)
C(14)-N(1)-H(1B)	119.7
C(1)-N(1)-H(1B)	119.7
C(6)-O(9)-C(13)	115.1(4)
C(26)-O(22)-C(22)	118.2(4)
C(30)-O(26)-C(24)	116.7(4)
C(32)-O(29)-C(33)	116.3(4)
O(12)-N(2)-O(11)	124.1(4)
O(12)-N(2)-C(18)	119.2(4)
O(11)-N(2)-C(18)	116.7(4)
C(11)-O(6)-C(4)	117.5(4)
C(28)-O(24)-C(23)	117.1(4)
C(34)-N(3)-C(21)	120.7(4)
C(34)-N(3)-H(3B)	119.7
C(21)-N(3)-H(3B)	119.7
C(39)-C(38)-C(37)	122.0(4)
C(39)-C(38)-N(4)	119.5(4)
C(37)-C(38)-N(4)	118.5(4)
O(6)-C(4)-C(5)	104.6(4)
O(6)-C(4)-C(3)	109.2(3)
C(5)-C(4)-C(3)	111.7(4)
O(6)-C(4)-H(4)	110.4
C(5)-C(4)-H(4)	110.4
C(3)-C(4)-H(4)	110.4
C(17)-C(18)-C(19)	122.3(4)
C(17)-C(18)-N(2)	118.1(4)
C(19)-C(18)-N(2)	119.6(4)
C(35)-C(36)-C(37)	120.4(4)

C(35)-C(36)-H(36)	119.8
C(37)-C(36)-H(36)	119.8
O(22)-C(22)-C(21)	107.4(4)
O(22)-C(22)-C(23)	108.2(4)
C(21)-C(22)-C(23)	110.3(4)
O(22)-C(22)-H(22)	110.3
C(21)-C(22)-H(22)	110.3
C(23)-C(22)-H(22)	110.3
C(39)-C(40)-C(35)	120.2(4)
C(39)-C(40)-H(40)	119.9
C(35)-C(40)-H(40)	119.9
O(26)-C(24)-C(23)	109.0(4)
O(26)-C(24)-C(25)	104.6(3)
C(23)-C(24)-C(25)	111.6(4)
O(26)-C(24)-H(24)	110.5
C(23)-C(24)-H(24)	110.5
C(25)-C(24)-H(24)	110.5
O(21)-C(21)-N(3)	106.8(4)
O(21)-C(21)-C(22)	110.0(3)
N(3)-C(21)-C(22)	111.0(4)
O(21)-C(21)-H(21)	109.6
N(3)-C(21)-H(21)	109.6
C(22)-C(21)-H(21)	109.6
O(31)-N(4)-O(32)	123.8(4)
O(31)-N(4)-C(38)	118.5(4)
O(32)-N(4)-C(38)	117.7(4)
C(36)-C(35)-C(40)	120.1(4)
C(36)-C(35)-C(34)	122.3(4)
C(40)-C(35)-C(34)	117.5(4)
C(20)-C(15)-C(16)	120.7(4)
C(20)-C(15)-C(14)	122.0(4)
C(16)-C(15)-C(14)	117.2(4)
O(10)-C(14)-N(1)	123.7(4)
O(10)-C(14)-C(15)	119.1(4)
N(1)-C(14)-C(15)	117.2(4)
O(30)-C(34)-N(3)	123.2(4)
O(30)-C(34)-C(35)	119.8(4)
N(3)-C(34)-C(35)	117.0(4)
C(19)-C(20)-C(15)	119.6(4)
C(19)-C(20)-H(20)	120.2
C(15)-C(20)-H(20)	120.2

O(2)-C(2)-C(3)	107.2(3)
O(2)-C(2)-C(1)	107.3(4)
C(3)-C(2)-C(1)	111.2(4)
O(2)-C(2)-H(2)	110.4
C(3)-C(2)-H(2)	110.4
C(1)-C(2)-H(2)	110.4
C(20)-C(19)-C(18)	118.8(4)
C(20)-C(19)-H(19)	120.6
C(18)-C(19)-H(19)	120.6
O(1)-C(1)-N(1)	107.2(3)
O(1)-C(1)-C(2)	109.4(4)
N(1)-C(1)-C(2)	111.1(4)
O(1)-C(1)-H(1)	109.7
N(1)-C(1)-H(1)	109.7
C(2)-C(1)-H(1)	109.7
O(1)-C(5)-C(4)	110.4(4)
O(1)-C(5)-C(6)	104.8(3)
C(4)-C(5)-C(6)	114.7(4)
O(1)-C(5)-H(5)	108.9
C(4)-C(5)-H(5)	108.9
C(6)-C(5)-H(5)	108.9
O(29)-C(33)-H(33A)	109.5
O(29)-C(33)-H(33B)	109.5
H(33A)-C(33)-H(33B)	109.5
O(29)-C(33)-H(33C)	109.5
H(33A)-C(33)-H(33C)	109.5
H(33B)-C(33)-H(33C)	109.5
C(17)-C(16)-C(15)	119.9(4)
C(17)-C(16)-H(16)	120
C(15)-C(16)-H(16)	120
C(16)-C(17)-C(18)	118.6(5)
C(16)-C(17)-H(17)	120.7
C(18)-C(17)-H(17)	120.7
O(24)-C(23)-C(24)	108.9(4)
O(24)-C(23)-C(22)	104.4(4)
C(24)-C(23)-C(22)	113.5(4)
O(24)-C(23)-H(23)	110
C(24)-C(23)-H(23)	110
C(22)-C(23)-H(23)	110
O(4)-C(3)-C(2)	105.5(4)
O(4)-C(3)-C(4)	110.2(4)

C(2)-C(3)-C(4)	111.6(3)
O(4)-C(3)-H(3)	109.8
C(2)-C(3)-H(3)	109.8
C(4)-C(3)-H(3)	109.8
C(40)-C(39)-C(38)	119.3(4)
C(40)-C(39)-H(39)	120.4
C(38)-C(39)-H(39)	120.4
O(5)-C(9)-O(4)	123.4(5)
O(5)-C(9)-C(10)	126.4(5)
O(4)-C(9)-C(10)	110.3(5)
O(28)-C(32)-O(29)	125.0(4)
O(28)-C(32)-C(25)	122.3(4)
O(29)-C(32)-C(25)	112.7(4)
O(21)-C(25)-C(32)	104.9(4)
O(21)-C(25)-C(24)	110.6(4)
C(32)-C(25)-C(24)	114.4(4)
O(21)-C(25)-H(25)	108.9
C(32)-C(25)-H(25)	108.9
C(24)-C(25)-H(25)	108.9
O(8)-C(6)-O(9)	126.2(5)
O(8)-C(6)-C(5)	122.1(5)
O(9)-C(6)-C(5)	111.8(4)
O(7)-C(11)-O(6)	122.9(5)
O(7)-C(11)-C(12)	126.7(5)
O(6)-C(11)-C(12)	110.4(5)
O(25)-C(28)-O(24)	123.9(5)
O(25)-C(28)-C(29)	126.2(5)
O(24)-C(28)-C(29)	109.9(5)
O(23)-C(26)-O(22)	122.5(5)
O(23)-C(26)-C(27)	126.5(5)
O(22)-C(26)-C(27)	111.0(5)
O(9)-C(13)-H(13A)	109.5
O(9)-C(13)-H(13B)	109.5
H(13A)-C(13)-H(13B)	109.5
O(9)-C(13)-H(13C)	109.5
H(13A)-C(13)-H(13C)	109.5
H(13B)-C(13)-H(13C)	109.5
O(27)-C(30)-O(26)	123.6(5)
O(27)-C(30)-C(31)	126.7(5)
O(26)-C(30)-C(31)	109.8(5)
O(3)-C(7)-O(2)	124.2(5)

O(3)-C(7)-C(8)	125.3(5)
O(2)-C(7)-C(8)	110.3(5)
C(26)-C(27)-H(27A)	109.5
C(26)-C(27)-H(27B)	109.5
H(27A)-C(27)-H(27B)	109.5
C(26)-C(27)-H(27C)	109.5
H(27A)-C(27)-H(27C)	109.5
H(27B)-C(27)-H(27C)	109.5
C(7)-C(8)-H(8A)	109.5
C(7)-C(8)-H(8B)	109.5
H(8A)-C(8)-H(8B)	109.5
C(7)-C(8)-H(8C)	109.5
H(8A)-C(8)-H(8C)	109.5
H(8B)-C(8)-H(8C)	109.5
C(30)-C(31)-H(31A)	109.5
C(30)-C(31)-H(31B)	109.5
H(31A)-C(31)-H(31B)	109.5
C(30)-C(31)-H(31C)	109.5
H(31A)-C(31)-H(31C)	109.5
H(31B)-C(31)-H(31C)	109.5
C(9)-C(10)-H(10A)	109.5
C(9)-C(10)-H(10B)	109.5
H(10A)-C(10)-H(10B)	109.5
C(9)-C(10)-H(10C)	109.5
H(10A)-C(10)-H(10C)	109.5
H(10B)-C(10)-H(10C)	109.5
C(38)-C(37)-C(36)	118.0(4)
C(38)-C(37)-H(37)	121
C(36)-C(37)-H(37)	121
C(28)-C(29)-H(29A)	109.5
C(28)-C(29)-H(29B)	109.5
H(29A)-C(29)-H(29B)	109.5
C(28)-C(29)-H(29C)	109.5
H(29A)-C(29)-H(29C)	109.5
H(29B)-C(29)-H(29C)	109.5
C(11)-C(12)-H(12A)	109.5
C(11)-C(12)-H(12B)	109.5
H(12A)-C(12)-H(12B)	109.5
C(11)-C(12)-H(12C)	109.5
H(12A)-C(12)-H(12C)	109.5
H(12B)-C(12)-H(12C)	109.5

Cl(2A)-C(50A)-Cl(1A)	111.1(5)
Cl(2A)-C(50A)-H(50A)	109.4
Cl(1A)-C(50A)-H(50A)	109.4
Cl(2A)-C(50A)-H(50B)	109.4
Cl(1A)-C(50A)-H(50B)	109.4
H(50A)-C(50A)-H(50B)	108
Cl(2B)-C(50B)-Cl(1B)	112.9(16)
Cl(2B)-C(50B)-H(50C)	109
Cl(1B)-C(50B)-H(50C)	109
Cl(2B)-C(50B)-H(50D)	109
Cl(1B)-C(50B)-H(50D)	109
H(50C)-C(50B)-H(50D)	107.8
Cl(4A)-C(51A)-Cl(3A)	109.7(4)
Cl(4A)-C(51A)-H(51A)	109.7
Cl(3A)-C(51A)-H(51A)	109.7
Cl(4A)-C(51A)-H(51B)	109.7
Cl(3A)-C(51A)-H(51B)	109.7
H(51A)-C(51A)-H(51B)	108.2
Cl(3B)-C(51B)-Cl(4B)	111.1(15)
Cl(3B)-C(51B)-H(51C)	109.4
Cl(4B)-C(51B)-H(51C)	109.4
Cl(3B)-C(51B)-H(51D)	109.4
Cl(4B)-C(51B)-H(51D)	109.4
H(51C)-C(51B)-H(51D)	108

Table 4. Anisotropic displacement parameters [$Å^2 \times 10^3$] for 05mz056m. The anisotropic displacement factor exponent takes the form: $-2\pi^2 [(h\,a^*)^2 U11 + ... + 2\,h\,k\,a^*\,b^*\,U12]$

	U11	U22	U33	U23	U13	U12
O(21)	16(1)	15(2)	13(2)	-3(1)	-1(1)	-1(1)
O(1)	14(1)	15(2)	18(2)	-4(1)	-6(1)	5(1)
O(4)	28(2)	19(2)	14(2)	3(1)	0(1)	3(1)
O(2)	13(1)	20(2)	18(2)	-5(1)	-7(1)	6(1)
N(1)	15(2)	19(2)	19(2)	-7(2)	-4(2)	0(1)
O(9)	16(2)	21(2)	20(2)	-2(1)	-1(1)	3(1)
O(22)	11(1)	22(2)	23(2)	-6(1)	0(1)	-2(1)
O(26)	21(2)	19(2)	13(2)	-3(1)	-2(1)	6(1)
O(29)	15(2)	20(2)	19(2)	-2(1)	-6(1)	-1(1)
O(30)	15(2)	19(2)	17(2)	-2(1)	-4(1)	3(1)
O(10)	14(1)	16(2)	20(2)	-3(1)	-1(1)	0(1)
O(12)	31(2)	28(2)	27(2)	-8(2)	5(2)	1(2)
N(2)	25(2)	17(2)	26(2)	-7(2)	-12(2)	6(2)
O(6)	21(2)	18(2)	16(2)	-7(1)	-4(1)	0(1)
O(24)	19(2)	23(2)	16(2)	-1(1)	-2(1)	3(1)
N(3)	12(2)	17(2)	17(2)	-6(2)	-4(2)	1(1)
C(38)	15(2)	16(2)	15(2)	-1(2)	2(2)	-1(2)
O(8)	33(2)	21(2)	16(2)	6(1)	-1(2)	3(2)
C(4)	14(2)	18(2)	12(2)	-6(2)	-4(2)	2(2)
C(18)	18(2)	17(2)	18(2)	-4(2)	-2(2)	6(2)
O(28)	35(2)	19(2)	20(2)	1(1)	-2(2)	-3(2)
C(36)	15(2)	16(2)	15(2)	-2(2)	-8(2)	2(2)
O(31)	33(2)	37(2)	14(2)	-7(2)	-2(2)	1(2)
C(22)	12(2)	20(2)	14(2)	-3(2)	4(2)	-1(2)
C(40)	20(2)	18(2)	22(2)	1(2)	-4(2)	-2(2)
C(24)	14(2)	13(2)	12(2)	-2(2)	0(2)	0(2)
C(21)	10(2)	16(2)	16(2)	-3(2)	-3(2)	-1(2)
N(4)	21(2)	22(2)	19(2)	-6(2)	1(2)	-3(2)
C(35)	13(2)	10(2)	16(2)	-3(2)	-2(2)	-5(2)
O(5)	31(2)	38(2)	23(2)	-13(2)	-11(2)	2(2)
C(15)	14(2)	14(2)	14(2)	-4(2)	-3(2)	5(2)
O(27)	40(2)	40(2)	20(2)	-11(2)	-12(2)	13(2)
O(11)	41(2)	23(2)	27(2)	-10(2)	-2(2)	-8(2)
O(32)	41(2)	25(2)	27(2)	-10(2)	-7(2)	9(2)

C(14)	11(2)	14(2)	13(2)	1(2)	-3(2)	2(2)
O(25)	31(2)	45(2)	20(2)	-2(2)	5(2)	4(2)
C(34)	13(2)	9(2)	10(2)	5(2)	1(2)	-3(2)
C(20)	13(2)	14(2)	18(2)	-1(2)	-3(2)	4(2)
O(7)	29(2)	33(2)	37(2)	-13(2)	7(2)	-8(2)
C(2)	10(2)	17(2)	14(2)	-4(2)	-6(2)	6(2)
O(3)	28(2)	18(2)	91(4)	2(2)	-20(2)	-4(2)
C(19)	17(2)	15(2)	20(2)	-3(2)	-3(2)	4(2)
C(1)	10(2)	20(2)	13(2)	-3(2)	-3(2)	1(2)
C(5)	19(2)	13(2)	14(2)	-1(2)	-4(2)	-1(2)
C(33)	25(2)	21(2)	24(3)	5(2)	-5(2)	-6(2)
C(16)	19(2)	15(2)	20(2)	3(2)	-6(2)	-2(2)
C(17)	20(2)	20(2)	17(2)	-1(2)	0(2)	2(2)
C(23)	17(2)	17(2)	13(2)	1(2)	0(2)	-2(2)
C(3)	15(2)	19(2)	10(2)	-5(2)	0(2)	-3(2)
C(39)	21(2)	22(2)	15(2)	0(2)	-2(2)	3(2)
C(9)	32(3)	22(2)	18(2)	-6(2)	-4(2)	8(2)
C(32)	21(2)	13(2)	17(2)	-3(2)	0(2)	4(2)
C(25)	14(2)	19(2)	17(2)	-6(2)	-4(2)	1(2)
C(6)	14(2)	16(2)	25(2)	-4(2)	-1(2)	-4(2)
C(11)	26(2)	23(2)	13(2)	-3(2)	-4(2)	2(2)
C(28)	30(3)	33(3)	14(2)	1(2)	2(2)	-3(2)
C(26)	28(3)	19(2)	22(2)	1(2)	-3(2)	1(2)
C(13)	17(2)	20(2)	31(3)	2(2)	0(2)	10(2)
C(30)	27(2)	25(2)	23(3)	-13(2)	-5(2)	1(2)
C(7)	26(2)	20(2)	18(2)	-1(2)	-5(2)	5(2)
C(27)	30(3)	25(2)	27(3)	-3(2)	-6(2)	-8(2)
C(8)	38(3)	31(3)	23(3)	-5(2)	-3(2)	14(2)
O(23)	26(2)	17(2)	67(3)	-2(2)	8(2)	-1(2)
C(31)	46(3)	32(3)	36(3)	-23(3)	-10(3)	16(3)
C(10)	59(4)	43(4)	19(3)	4(3)	-2(3)	-3(3)
C(37)	16(2)	15(2)	18(2)	-2(2)	-1(2)	1(2)
C(29)	61(4)	41(4)	18(3)	11(2)	0(3)	13(3)
C(12)	43(3)	32(3)	30(3)	-14(2)	-1(3)	3(3)
C(50A)	60(4)	35(4)	24(4)	-5(3)	-15(3)	13(3)
Cl(1A)	46(1)	47(2)	70(2)	-32(2)	-22(1)	8(1)
Cl(2A)	52(2)	56(2)	34(2)	-5(1)	-2(1)	-10(1)
C(50B)	60(4)	35(4)	24(4)	-5(3)	-15(3)	13(3)
Cl(1B)	59(8)	80(10)	66(8)	4(7)	-21(6)	-25(7)
Cl(2B)	49(7)	83(8)	40(8)	-22(6)	6(6)	-22(6)
C(51A)	46(4)	38(3)	18(3)	-7(2)	0(3)	-4(3)

Cl(3A)	49(1)	44(1)	52(1)	4(1)	-2(1)	11(1)
Cl(4A)	52(2)	94(3)	78(2)	14(2)	-23(1)	20(2)
C(51B)	46(4)	38(3)	18(3)	-7(2)	0(3)	-4(3)
Cl(4B)	52(2)	94(3)	78(2)	14(2)	-23(1)	20(2)
Cl(3B)	49(1)	44(1)	52(1)	4(1)	-2(1)	11(1)

Table 5. Hydrogen coordinates ($\times 10^4$) and isotropic displacement parameters ($Å^2 \times 10^3$) for 05mz056m.

	x	y	z	U(eq)
H(1B)	7349	1267	4490	20
H(3B)	2338	752	4495	18
H(4)	8416	-1361	2236	17
H(36)	2246	-1307	3929	18
H(22)	1932	755	6121	19
H(40)	292	1487	2146	24
H(24)	2661	3448	6739	15
H(21)	45	2567	5017	16
H(20)	7102	3355	5051	18
H(2)	7464	1255	2852	16
H(19)	7458	4789	6138	21
H(1)	5229	-557	3973	17
H(5)	6068	-2666	3523	19
H(33A)	5556	6711	5372	36
H(33B)	5206	7041	6356	36
H(33C)	4253	7814	5603	36
H(16)	4505	562	6828	22
H(17)	4950	1942	7931	23
H(23)	-435	2540	6774	19
H(3)	5279	-539	2242	17
H(39)	1120	127	1048	23
H(25)	716	4688	5449	19
H(13A)	10814	-4738	3602	35
H(13B)	10896	-4958	2594	35
H(13C)	9634	-5794	3284	35
H(27A)	-1673	-1919	5465	40
H(27B)	-2176	-1574	6432	40
H(27C)	-1202	-2976	6294	40
H(8A)	3747	4009	3564	46
H(8B)	3420	3606	2629	46
H(8C)	4398	5016	2689	46
H(31A)	988	6241	8716	54
H(31B)	-456	5906	8233	54
H(31C)	807	7032	7749	54
H(10A)	6085	1976	-305	62

H(10B)	7359	822	-493	62
H(10C)	7642	2001	131	62
H(37)	2989	-2766	2835	20
H(29A)	102	821	9574	62
H(29B)	1786	996	9105	62
H(29C)	734	-310	8948	62
H(12A)	7422	-4125	229	51
H(12B)	5933	-4134	896	51
H(12C)	7367	-5051	1179	51
H(50A)	5868	6786	8964	47
H(50B)	5271	8146	9415	47
H(50C)	5759	6444	9045	47
H(50D)	5524	7692	9651	47
H(51A)	2869	5240	167	41
H(51B)	2757	4045	-473	41
H(51C)	1877	4265	-504	41
H(51D)	1727	5195	292	41

Table 6. Hydrogen bonds for 05mz056m [Å and deg].

D-H...A	d(D-H)	d(H...A)	d(D...A)	<(DHA)
N(3)-H(3B): O(10)	0.9	2.1	2.842(5)	144
N(1)-H(1B): O(30)#1	0.9	2.1	2.828(5)	144

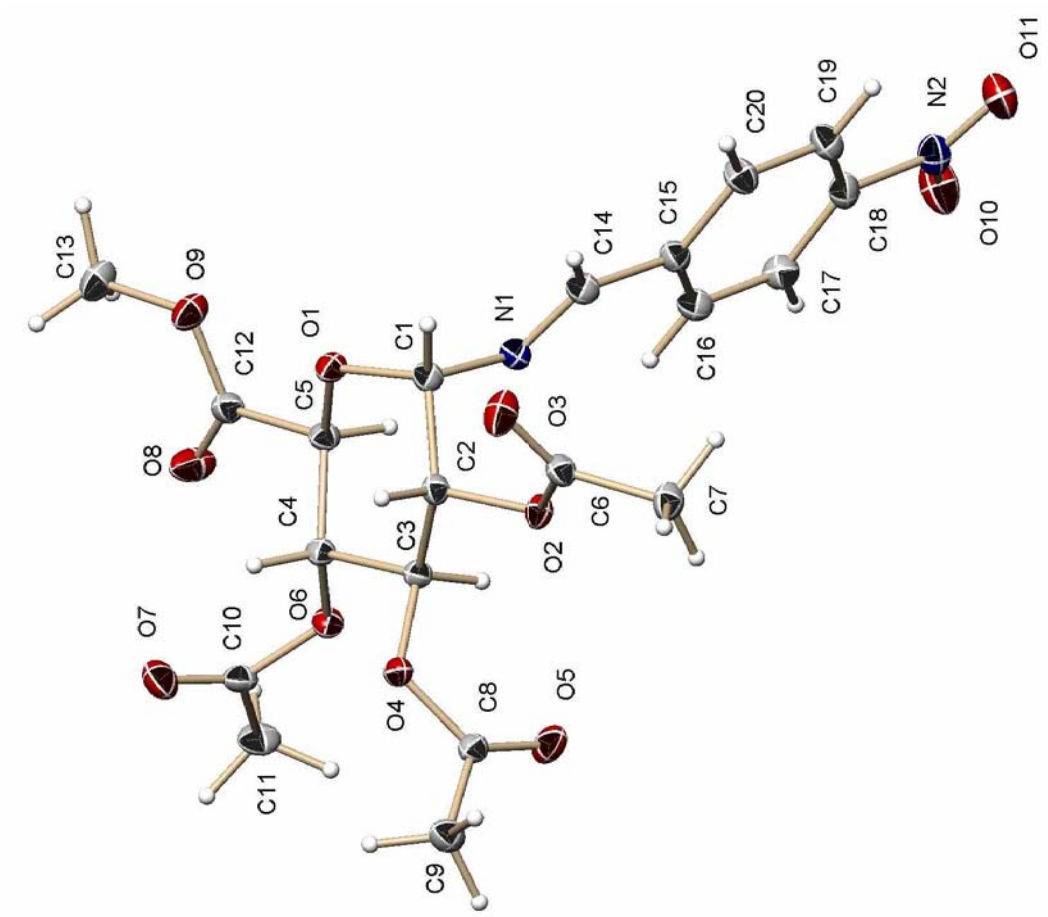

Figure 175: Mass spectrum of *p*-nitrobenzoic acid-(α-D-glucopyranuronosyl)-imine (**41**).

Table 1. Crystal data and structure refinement for 05mz050m:

Identification code:	05mz050m
Empirical formula:	$C_{20}H_{22}N_2O_{11}$
Formula weight:	466.40
Temperature:	100(2) K
Wavelength:	0.71073 Å
Crystal system:	Monoclinic
Space group:	C2
Unit cell dimensions:	a = 21.5913(11) Å, α = 90°
	b = 5.4411(3) Å, β = 117.5780(10)°
	c = 20.6250(10) Å, γ = 90°
Volume, *Z*:	2147.73(19) $Å^3$, 4
Density (calculated):	1.442 Mg/m^3
Absorption coefficient:	0.119 mm^{-1}
F(000):	976
Crystal size:	0.58 × 0.20 × 0.077 mm
Theta range for data collection:	1.11 to 30.36°
Limiting indices:	$-30 \leq h \leq 30$, $-7 \leq k \leq 7$, $-29 \leq l \leq 29$
Reflections collected:	12709
Independent reflections:	3566 (*R*(int) = 0.0192)
Completeness to $\theta = 30.36°$:	100.0 %

Absorption correction:	multi-scan
Max. and min. transmission:	1 and 0.8882
Refinement method:	Full-matrix least-squares on F^2
Data / restraints / parameters:	3566 / 1 / 302
Goodness-of-fit on F^2:	1.032
Final *R* indices [$I>2\sigma(I)$]:	R1 = 0.0330, wR2 = 0.0848
R indices (all data):	R1 = 0.0345, wR2 = 0.0864
Largest diff. peak and hole:	0.369 and -0.159 e × $Å^{-3}$

Table 2. Atomic coordinates [$\times 10^4$] and equivalent isotropic displacement parameters [$Å^2 \times 10^3$] for 05mz050m. U(eq) is defined as one third of the trace of the orthogonalized U_{ij} tensor.

	x	y	z	U(eq)
N(1)	5833(1)	9394(2)	7222(1)	18(1)
O(9)	4142(1)	14884(2)	6515(1)	23(1)
O(1)	5267(1)	12811(2)	7398(1)	17(1)
O(4)	5509(1)	8995(2)	9180(1)	16(1)
O(6)	4161(1)	8966(2)	7892(1)	17(1)
O(2)	6577(1)	8663(2)	8747(1)	17(1)
O(5)	5602(1)	4871(2)	9184(1)	25(1)
O(7)	3666(1)	11715(2)	8332(1)	27(1)
C(16)	5790(1)	5416(3)	6294(1)	20(1)
C(1)	5894(1)	11406(3)	7704(1)	16(1)
O(8)	3452(1)	12429(3)	6768(1)	31(1)
C(6)	7238(1)	9529(3)	9035(1)	17(1)
O(3)	7367(1)	11674(2)	9021(1)	27(1)
N(2)	6302(1)	1771(3)	5091(1)	24(1)
C(3)	5391(1)	9170(3)	8434(1)	15(1)
O(11)	6824(1)	1520(3)	5006(1)	30(1)
C(9)	5864(1)	6992(3)	10303(1)	21(1)
O(10)	5769(1)	541(3)	4767(1)	35(1)
C(4)	4722(1)	10628(3)	8015(1)	15(1)
C(15)	6325(1)	7163(3)	6568(1)	18(1)
C(5)	4665(1)	11423(3)	7273(1)	16(1)
C(2)	6024(1)	10469(3)	8458(1)	15(1)
C(8)	5642(1)	6759(3)	9500(1)	16(1)
C(18)	6316(1)	3644(3)	5611(1)	20(1)
C(19)	6857(1)	5331(3)	5880(1)	21(1)
C(14)	6333(1)	9107(3)	7068(1)	18(1)
C(11)	3081(1)	7902(3)	7815(1)	24(1)
C(17)	5784(1)	3630(3)	5812(1)	21(1)
C(10)	3651(1)	9777(3)	8048(1)	18(1)
C(20)	6857(1)	7104(3)	6363(1)	21(1)
C(7)	7764(1)	7516(3)	9341(1)	21(1)
C(12)	4017(1)	12964(3)	6834(1)	18(1)
C(13)	3537(1)	16397(3)	6084(1)	25(1)

Table 3. Bond lengths [Å] and angles [deg] for 05mz050m.

N(1)-C(14)	1.2673(17)
N(1)-C(1)	1.4429(18)
O(9)-C(12)	1.3285(18)
O(9)-C(13)	1.4495(17)
O(1)-C(5)	1.4206(15)
O(1)-C(1)	1.4219(16)
O(4)-C(8)	1.3500(17)
O(4)-C(3)	1.4423(15)
O(6)-C(10)	1.3562(16)
O(6)-C(4)	1.4372(15)
O(2)-C(6)	1.3503(15)
O(2)-C(2)	1.4453(16)
O(5)-C(8)	1.1978(18)
O(7)-C(10)	1.200(2)
C(16)-C(17)	1.385(2)
C(16)-C(15)	1.3976(19)
C(16)-H(16)	0.95
C(1)-C(2)	1.5343(18)
C(1)-H(1)	1
O(8)-C(12)	1.1981(17)
C(6)-O(3)	1.2032(19)
C(6)-C(7)	1.4913(19)
N(2)-O(11)	1.2254(17)
N(2)-O(10)	1.2280(18)
N(2)-C(18)	1.4700(19)
C(3)-C(4)	1.5184(18)
C(3)-C(2)	1.5195(17)
C(3)-H(3)	1
C(9)-C(8)	1.5015(17)
C(9)-H(9A)	0.98
C(9)-H(9B)	0.98
C(9)-H(9C)	0.98
C(4)-C(5)	1.5395(17)
C(4)-H(4)	1
C(15)-C(20)	1.3957(17)
C(15)-C(14)	1.472(2)
C(5)-C(12)	1.5195(19)
C(5)-H(5)	1

C(2)-H(2)	1
C(18)-C(19)	1.384(2)
C(18)-C(17)	1.3904(19)
C(19)-C(20)	1.387(2)
C(19)-H(19)	0.95
C(14)-H(14)	0.95
C(11)-C(10)	1.496(2)
C(11)-H(11A)	0.98
C(11)-H(11B)	0.98
C(11)-H(11C)	0.98
C(17)-H(17)	0.95
C(20)-H(20)	0.95
C(7)-H(7A)	0.98
C(7)-H(7B)	0.98
C(7)-H(7C)	0.98
C(13)-H(13A)	0.98
C(13)-H(13B)	0.98
C(13)-H(13C)	0.98
C(14)-N(1)-C(1)	116.73(12)
C(12)-O(9)-C(13)	114.64(11)
C(5)-O(1)-C(1)	113.43(10)
C(8)-O(4)-C(3)	118.26(10)
C(10)-O(6)-C(4)	117.67(11)
C(6)-O(2)-C(2)	116.52(11)
C(17)-C(16)-C(15)	119.95(12)
C(17)-C(16)-H(16)	120
C(15)-C(16)-H(16)	120
O(1)-C(1)-N(1)	109.76(10)
O(1)-C(1)-C(2)	108.61(10)
N(1)-C(1)-C(2)	111.19(11)
O(1)-C(1)-H(1)	109.1
N(1)-C(1)-H(1)	109.1
C(2)-C(1)-H(1)	109.1
O(3)-C(6)-O(2)	122.49(13)
O(3)-C(6)-C(7)	125.66(13)
O(2)-C(6)-C(7)	111.83(12)
O(11)-N(2)-O(10)	123.65(14)
O(11)-N(2)-C(18)	118.22(13)
O(10)-N(2)-C(18)	118.13(12)
O(4)-C(3)-C(4)	107.03(10)
O(4)-C(3)-C(2)	106.50(10)

C(4)-C(3)-C(2)	112.34(11)
O(4)-C(3)-H(3)	110.3
C(4)-C(3)-H(3)	110.3
C(2)-C(3)-H(3)	110.3
C(8)-C(9)-H(9A)	109.5
C(8)-C(9)-H(9B)	109.5
H(9A)-C(9)-H(9B)	109.5
C(8)-C(9)-H(9C)	109.5
H(9A)-C(9)-H(9C)	109.5
H(9B)-C(9)-H(9C)	109.5
O(6)-C(4)-C(3)	105.87(11)
O(6)-C(4)-C(5)	109.18(10)
C(3)-C(4)-C(5)	109.24(10)
O(6)-C(4)-H(4)	110.8
C(3)-C(4)-H(4)	110.8
C(5)-C(4)-H(4)	110.8
C(20)-C(15)-C(16)	120.27(13)
C(20)-C(15)-C(14)	118.97(13)
C(16)-C(15)-C(14)	120.76(12)
O(1)-C(5)-C(12)	109.14(11)
O(1)-C(5)-C(4)	108.92(10)
C(12)-C(5)-C(4)	112.03(10)
O(1)-C(5)-H(5)	108.9
C(12)-C(5)-H(5)	108.9
C(4)-C(5)-H(5)	108.9
O(2)-C(2)-C(3)	104.86(11)
O(2)-C(2)-C(1)	111.91(10)
C(3)-C(2)-C(1)	112.41(10)
O(2)-C(2)-H(2)	109.2
C(3)-C(2)-H(2)	109.2
C(1)-C(2)-H(2)	109.2
O(5)-C(8)-O(4)	124.18(11)
O(5)-C(8)-C(9)	125.32(13)
O(4)-C(8)-C(9)	110.48(12)
C(19)-C(18)-C(17)	123.02(13)
C(19)-C(18)-N(2)	118.66(12)
C(17)-C(18)-N(2)	118.32(13)
C(18)-C(19)-C(20)	117.94(12)
C(18)-C(19)-H(19)	121
C(20)-C(19)-H(19)	121
N(1)-C(14)-C(15)	121.94(13)

N(1)-C(14)-H(14)	119
C(15)-C(14)-H(14)	119
C(10)-C(11)-H(11A)	109.5
C(10)-C(11)-H(11B)	109.5
H(11A)-C(11)-H(11B)	109.5
C(10)-C(11)-H(11C)	109.5
H(11A)-C(11)-H(11C)	109.5
H(11B)-C(11)-H(11C)	109.5
C(16)-C(17)-C(18)	118.35(13)
C(16)-C(17)-H(17)	120.8
C(18)-C(17)-H(17)	120.8
O(7)-C(10)-O(6)	124.06(13)
O(7)-C(10)-C(11)	126.08(13)
O(6)-C(10)-C(11)	109.86(13)
C(19)-C(20)-C(15)	120.46(13)
C(19)-C(20)-H(20)	119.8
C(15)-C(20)-H(20)	119.8
C(6)-C(7)-H(7A)	109.5
C(6)-C(7)-H(7B)	109.5
H(7A)-C(7)-H(7B)	109.5
C(6)-C(7)-H(7C)	109.5
H(7A)-C(7)-H(7C)	109.5
H(7B)-C(7)-H(7C)	109.5
O(8)-C(12)-O(9)	124.47(14)
O(8)-C(12)-C(5)	122.77(14)
O(9)-C(12)-C(5)	112.72(11)
O(9)-C(13)-H(13A)	109.5
O(9)-C(13)-H(13B)	109.5
H(13A)-C(13)-H(13B)	109.5
O(9)-C(13)-H(13C)	109.5
H(13A)-C(13)-H(13C)	109.5
H(13B)-C(13)-H(13C)	109.5

Table 4. Anisotropic displacement parameters [$Å^2 \times 10^3$] for 05mz050m. The anisotropic displacement factor exponent takes the form: $-2\pi^2 [(h\ a^*)^2\ U11 + ... + 2\ h\ k\ a^*\ b^*\ U12]$

	U11	U22	U33	U23	U13	U12
N(1)	18(1)	20(1)	18(1)	0(1)	9(1)	0(1)
O(9)	17(1)	21(1)	29(1)	7(1)	8(1)	2(1)
O(1)	14(1)	17(1)	22(1)	3(1)	9(1)	0(1)
O(4)	20(1)	14(1)	16(1)	0(1)	10(1)	1(1)
O(6)	14(1)	16(1)	22(1)	1(1)	10(1)	-2(1)
O(2)	14(1)	14(1)	21(1)	0(1)	7(1)	0(1)
O(5)	37(1)	14(1)	23(1)	0(1)	13(1)	1(1)
O(7)	27(1)	26(1)	37(1)	-4(1)	22(1)	-1(1)
C(16)	19(1)	22(1)	20(1)	0(1)	10(1)	-2(1)
C(1)	14(1)	17(1)	19(1)	0(1)	8(1)	-1(1)
O(8)	17(1)	42(1)	35(1)	19(1)	13(1)	5(1)
C(6)	15(1)	18(1)	19(1)	-1(1)	9(1)	0(1)
O(3)	18(1)	18(1)	43(1)	1(1)	12(1)	-1(1)
N(2)	24(1)	23(1)	21(1)	-3(1)	8(1)	4(1)
C(3)	15(1)	15(1)	15(1)	1(1)	7(1)	0(1)
O(11)	29(1)	31(1)	33(1)	-7(1)	18(1)	3(1)
C(9)	19(1)	26(1)	17(1)	2(1)	8(1)	2(1)
O(10)	26(1)	36(1)	39(1)	-18(1)	12(1)	-4(1)
C(4)	14(1)	15(1)	18(1)	1(1)	9(1)	-1(1)
C(15)	17(1)	19(1)	17(1)	0(1)	8(1)	2(1)
C(5)	13(1)	18(1)	17(1)	2(1)	8(1)	-1(1)
C(2)	14(1)	14(1)	17(1)	-1(1)	7(1)	0(1)
C(8)	15(1)	17(1)	18(1)	2(1)	8(1)	1(1)
C(18)	21(1)	19(1)	17(1)	-1(1)	7(1)	4(1)
C(19)	17(1)	26(1)	22(1)	-2(1)	10(1)	2(1)
C(14)	17(1)	20(1)	19(1)	0(1)	9(1)	-1(1)
C(11)	17(1)	29(1)	26(1)	3(1)	11(1)	-5(1)
C(17)	21(1)	21(1)	20(1)	-1(1)	8(1)	-3(1)
C(10)	17(1)	22(1)	18(1)	5(1)	9(1)	0(1)
C(20)	17(1)	23(1)	23(1)	-3(1)	10(1)	-2(1)
C(7)	16(1)	18(1)	28(1)	0(1)	9(1)	2(1)
C(12)	18(1)	20(1)	17(1)	2(1)	9(1)	1(1)
C(13)	22(1)	22(1)	26(1)	7(1)	6(1)	5(1)

Table 5. Hydrogen coordinates ($\times 10^4$) and isotropic displacement parameters ($Å^2 \times 10^3$) for 05mz046m.

	x	y	z	U(eq)
H(16)	5431	5453	6438	24
H(1)	6292	12483	7763	19
H(3)	5342	7493	8217	18
H(9A)	6369	7278	10568	31
H(9B)	5750	5475	10480	31
H(9C)	5618	8377	10385	31
H(4)	4711	12090	8304	18
H(5)	4646	9921	6985	19
H(2)	6152	11888	8804	18
H(19)	7217	5276	5738	25
H(14)	6724	10179	7282	22
H(11A)	2787	7995	7284	35
H(11B)	2795	8223	8062	35
H(11C)	3287	6257	7947	35
H(17)	5424	2426	5624	25
H(20)	7222	8287	6556	25
H(7A)	8120	7969	9833	31
H(7B)	7985	7260	9025	31
H(7C)	7531	5998	9365	31
H(13A)	3399	17284	6410	38
H(13B)	3150	15350	5753	38
H(13C)	3652	17579	5797	38

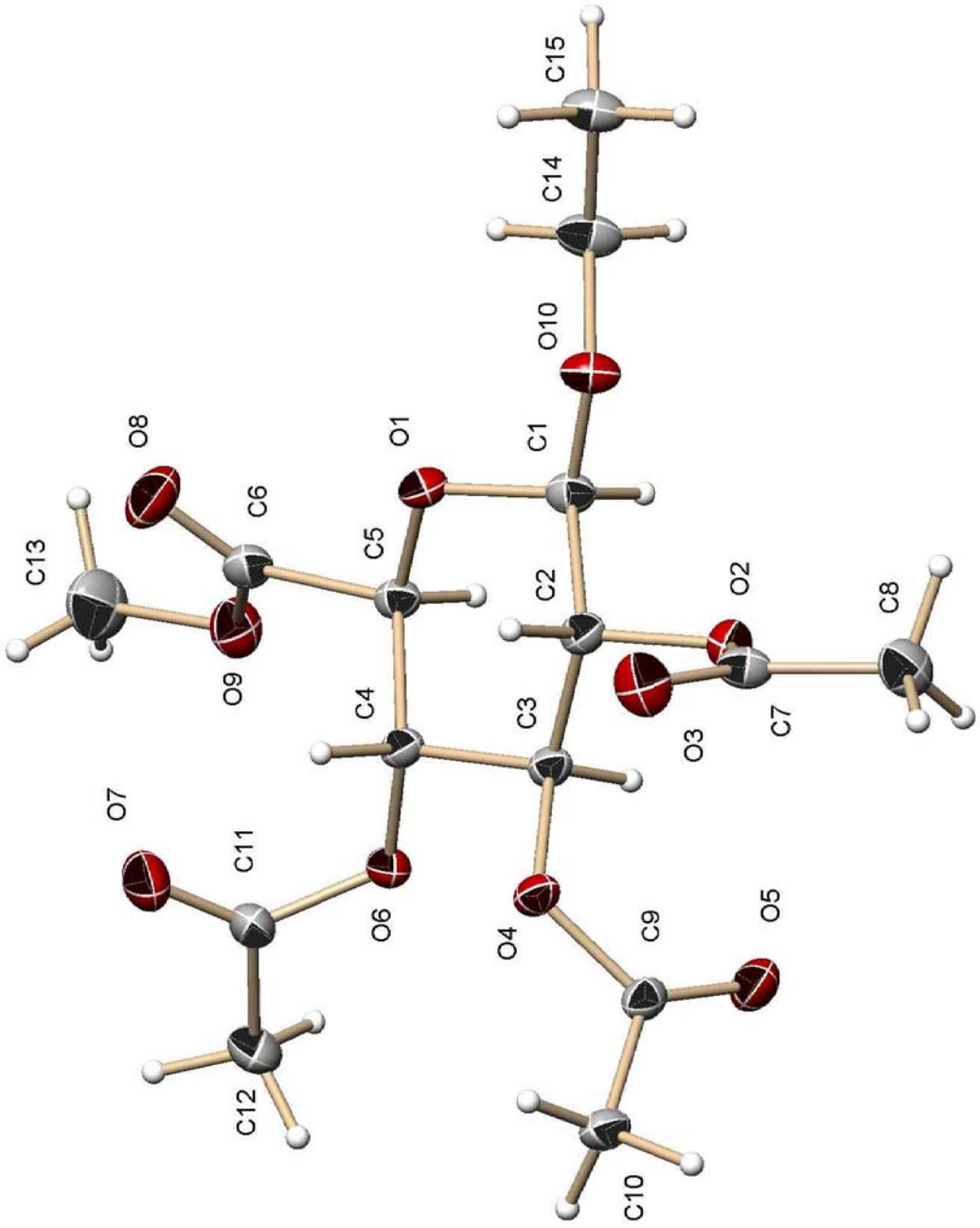

Figure 176: X-ray crystal structure of ethyl-(β-D-glucopyranosyl) uronate (**69**).

Table 1. Crystal data and structure refinement for 05mz060m:

Identification code:	05mz060m
Empirical formula:	$C_{15}H_{22}O_{10}$
Formula weight:	362.33
Temperature:	100(2) K
Wavelength:	0.71073 Å
Crystal system:	Orthorhombic
Space group:	$P2_12_12_1$
Unit cell dimensions:	a = 7.3382(3) Å, α = 90°
	b = 14.2727(7) Å, β = 90°
	c = 17.1263(8) Å, γ = 90°
Volume, *Z*:	1793.74(14) $Å^3$, 4
Density (calculated):	1.342 Mg/m^3
Absorption coefficient:	0.114 mm^{-1}
F(000):	768
Crystal size:	0.55 × 0.39 × 0.32 mm
Theta range for data collection:	1.86 to 28.28°
Limiting indices:	$-9 \le h \le 9$, $-19 \le k \le 19$, $-22 \le l \le 22$
Reflections collected:	18674
Independent reflections:	2547 (*R*(int) = 0.0208)
Completeness to $\theta = 28.28°$:	100.0 %
Absorption correction:	multi-scan

Max. and min. transmission:	0.96 and 0.9116
Refinement method:	Full-matrix least-squares on F^2
Data / restraints / parameters:	2547 / 0 / 231
Goodness-of-fit on F^2:	1.076
Final *R* indices [$I>2\sigma(I)$]:	R1 = 0.0345, wR2 = 0.0901
R indices (all data):	R1 = 0.0349, wR2 = 0.0905
Largest diff. peak and hole:	0.318 and -0.250 e × $Å^{-3}$

Table 2. Atomic coordinates [$\times 10^4$] and equivalent isotropic displacement parameters [$Å^2 \times 10^3$] for 05mz060m. U(eq) is defined as one third of the trace of the orthogonalized U_{ij} tensor.

	x	y	z	U(eq)
C(1)	5555(2)	5134(1)	9470(1)	18(1)
C(2)	3798(2)	4586(1)	9335(1)	17(1)
C(3)	4259(2)	3628(1)	8993(1)	16(1)
C(4)	5421(2)	3741(1)	8265(1)	17(1)
C(5)	7079(2)	4359(1)	8450(1)	17(1)
C(6)	8202(2)	4580(1)	7727(1)	21(1)
C(7)	1101(2)	4710(1)	10108(1)	20(1)
C(8)	393(2)	4588(1)	10925(1)	27(1)
C(9)	1996(2)	2428(1)	9153(1)	19(1)
C(10)	356(2)	2011(1)	8765(1)	22(1)
C(11)	6082(3)	2647(1)	7257(1)	24(1)
C(12)	6658(3)	1659(1)	7104(1)	31(1)
C(13)	10544(3)	4024(2)	6915(1)	40(1)
C(14)	6732(2)	6563(1)	9917(1)	25(1)
C(15)	6140(2)	7549(1)	10110(1)	25(1)
O(1)	6421(2)	5228(1)	8729(1)	18(1)
O(2)	2895(2)	4460(1)	10072(1)	19(1)
O(3)	249(2)	4991(1)	9562(1)	29(1)
O(4)	2599(2)	3181(1)	8743(1)	19(1)
O(5)	2710(2)	2148(1)	9741(1)	27(1)
O(6)	5987(2)	2816(1)	8037(1)	19(1)
O(7)	5739(2)	3226(1)	6773(1)	35(1)
O(8)	8019(2)	5269(1)	7334(1)	36(1)
O(9)	9393(2)	3895(1)	7589(1)	27(1)
O(10)	5122(2)	6021(1)	9733(1)	21(1)

Table 3. Bond lengths [Å] and angles [deg] for 05mz060m.

C(1)-O(10)	1.3811(19)
C(1)-O(1)	1.4267(19)
C(1)-C(2)	1.525(2)
C(1)-H(1)	1
C(2)-O(2)	1.4362(18)
C(2)-C(3)	1.526(2)
C(2)-H(2)	1
C(3)-O(4)	1.4396(18)
C(3)-C(4)	1.519(2)
C(3)-H(3)	1
C(4)-O(6)	1.4384(18)
C(4)-C(5)	1.535(2)
C(4)-H(4)	1
C(5)-O(1)	1.4145(18)
C(5)-C(6)	1.521(2)
C(5)-H(5)	1
C(6)-O(8)	1.198(2)
C(6)-O(9)	1.333(2)
C(7)-O(3)	1.194(2)
C(7)-O(2)	1.3653(19)
C(7)-C(8)	1.502(2)
C(8)-H(8A)	0.98
C(8)-H(8B)	0.98
C(8)-H(8C)	0.98
C(9)-O(5)	1.203(2)
C(9)-O(4)	1.3573(19)
C(9)-C(10)	1.498(2)
C(10)-H(10A)	0.98
C(10)-H(10B)	0.98
C(10)-H(10C)	0.98
C(11)-O(7)	1.197(2)
C(11)-O(6)	1.3604(19)
C(11)-C(12)	1.496(2)
C(12)-H(12A)	0.98
C(12)-H(12B)	0.98
C(12)-H(12C)	0.98
C(13)-O(9)	1.442(2)
C(13)-H(13A)	0.98

C(13)-H(13B)	0.98
C(13)-H(13C)	0.98
C(14)-O(10)	1.4473(19)
C(14)-C(15)	1.509(2)
C(14)-H(14A)	0.99
C(14)-H(14B)	0.99
C(15)-H(15A)	0.98
C(15)-H(15B)	0.98
C(15)-H(15C)	0.98
O(10)-C(1)-O(1)	107.83(12)
O(10)-C(1)-C(2)	108.98(13)
O(1)-C(1)-C(2)	106.85(12)
O(10)-C(1)-H(1)	111
O(1)-C(1)-H(1)	111
C(2)-C(1)-H(1)	111
O(2)-C(2)-C(1)	108.74(12)
O(2)-C(2)-C(3)	109.14(12)
C(1)-C(2)-C(3)	109.31(12)
O(2)-C(2)-H(2)	109.9
C(1)-C(2)-H(2)	109.9
C(3)-C(2)-H(2)	109.9
O(4)-C(3)-C(4)	106.20(12)
O(4)-C(3)-C(2)	108.89(12)
C(4)-C(3)-C(2)	110.13(12)
O(4)-C(3)-H(3)	110.5
C(4)-C(3)-H(3)	110.5
C(2)-C(3)-H(3)	110.5
O(6)-C(4)-C(3)	106.62(11)
O(6)-C(4)-C(5)	110.75(13)
C(3)-C(4)-C(5)	109.67(12)
O(6)-C(4)-H(4)	109.9
C(3)-C(4)-H(4)	109.9
C(5)-C(4)-H(4)	109.9
O(1)-C(5)-C(6)	106.11(12)
O(1)-C(5)-C(4)	107.63(12)
C(6)-C(5)-C(4)	112.36(12)
O(1)-C(5)-H(5)	110.2
C(6)-C(5)-H(5)	110.2
C(4)-C(5)-H(5)	110.2
O(8)-C(6)-O(9)	125.14(16)
O(8)-C(6)-C(5)	124.52(16)

O(9)-C(6)-C(5)	110.33(13)
O(3)-C(7)-O(2)	123.81(16)
O(3)-C(7)-C(8)	125.98(15)
O(2)-C(7)-C(8)	110.21(14)
C(7)-C(8)-H(8A)	109.5
C(7)-C(8)-H(8B)	109.5
H(8A)-C(8)-H(8B)	109.5
C(7)-C(8)-H(8C)	109.5
H(8A)-C(8)-H(8C)	109.5
H(8B)-C(8)-H(8C)	109.5
O(5)-C(9)-O(4)	123.66(15)
O(5)-C(9)-C(10)	126.04(15)
O(4)-C(9)-C(10)	110.30(13)
C(9)-C(10)-H(10A)	109.5
C(9)-C(10)-H(10B)	109.5
H(10A)-C(10)-H(10B)	109.5
C(9)-C(10)-H(10C)	109.5
H(10A)-C(10)-H(10C)	109.5
H(10B)-C(10)-H(10C)	109.5
O(7)-C(11)-O(6)	123.24(16)
O(7)-C(11)-C(12)	126.11(16)
O(6)-C(11)-C(12)	110.66(14)
C(11)-C(12)-H(12A)	109.5
C(11)-C(12)-H(12B)	109.5
H(12A)-C(12)-H(12B)	109.5
C(11)-C(12)-H(12C)	109.5
H(12A)-C(12)-H(12C)	109.5
H(12B)-C(12)-H(12C)	109.5
O(9)-C(13)-H(13A)	109.5
O(9)-C(13)-H(13B)	109.5
H(13A)-C(13)-H(13B)	109.5
O(9)-C(13)-H(13C)	109.5
H(13A)-C(13)-H(13C)	109.5
H(13B)-C(13)-H(13C)	109.5
O(10)-C(14)-C(15)	108.11(14)
O(10)-C(14)-H(14A)	110.1
C(15)-C(14)-H(14A)	110.1
O(10)-C(14)-H(14B)	110.1
C(15)-C(14)-H(14B)	110.1
H(14A)-C(14)-H(14B)	108.4
C(14)-C(15)-H(15A)	109.5

C(14)-C(15)-H(15B)	109.5
H(15A)-C(15)-H(15B)	109.5
C(14)-C(15)-H(15C)	109.5
H(15A)-C(15)-H(15C)	109.5
H(15B)-C(15)-H(15C)	109.5
C(5)-O(1)-C(1)	111.71(11)
C(7)-O(2)-C(2)	116.89(13)
C(9)-O(4)-C(3)	118.22(12)
C(11)-O(6)-C(4)	116.31(12)
C(6)-O(9)-C(13)	115.61(16)
C(1)-O(10)-C(14)	111.91(12)

Table 4. Anisotropic displacement parameters [$Å^2 \times 10^3$] for 05mz060m. The anisotropic displacement factor exponent takes the form: $-2\pi2 [(h a^*)^2 U11 + ... + 2 h k a^* b^* U12]$

	U11	U22	U33	U23	U13	U12
C(1)	16(1)	17(1)	21(1)	-1(1)	-2(1)	-1(1)
C(2)	16(1)	17(1)	19(1)	2(1)	-2(1)	-1(1)
C(3)	15(1)	16(1)	18(1)	2(1)	-2(1)	-2(1)
C(4)	17(1)	15(1)	18(1)	2(1)	-2(1)	-2(1)
C(5)	16(1)	15(1)	19(1)	0(1)	-3(1)	-1(1)
C(6)	20(1)	23(1)	22(1)	-1(1)	0(1)	-6(1)
C(7)	15(1)	18(1)	26(1)	-4(1)	-1(1)	0(1)
C(8)	22(1)	35(1)	25(1)	-4(1)	4(1)	-1(1)
C(9)	20(1)	16(1)	20(1)	-1(1)	5(1)	-1(1)
C(10)	23(1)	19(1)	24(1)	-1(1)	2(1)	-6(1)
C(11)	30(1)	24(1)	18(1)	-2(1)	-2(1)	-8(1)
C(12)	47(1)	23(1)	23(1)	-7(1)	1(1)	-5(1)
C(13)	36(1)	51(1)	34(1)	-6(1)	16(1)	-5(1)
C(14)	16(1)	23(1)	35(1)	-8(1)	-1(1)	-2(1)
C(15)	22(1)	21(1)	34(1)	-7(1)	-4(1)	-1(1)
O(1)	18(1)	14(1)	22(1)	1(1)	1(1)	-1(1)
O(2)	16(1)	21(1)	19(1)	3(1)	0(1)	1(1)
O(3)	19(1)	38(1)	29(1)	0(1)	-4(1)	5(1)
O(4)	18(1)	18(1)	20(1)	3(1)	-3(1)	-5(1)
O(5)	30(1)	27(1)	25(1)	8(1)	-3(1)	-7(1)
O(6)	25(1)	15(1)	17(1)	-1(1)	-1(1)	-2(1)
O(7)	57(1)	30(1)	20(1)	1(1)	-4(1)	-1(1)
O(8)	47(1)	26(1)	34(1)	9(1)	11(1)	-3(1)
O(9)	23(1)	33(1)	24(1)	-1(1)	5(1)	1(1)
O(10)	16(1)	17(1)	30(1)	-5(1)	-2(1)	0(1)

Table 5. Hydrogen coordinates ($\times 10^4$) and isotropic displacement parameters ($Å^2 \times 10^3$) for 05mz060m.

	x	y	z	U(eq)
H(1)	6365	4803	9850	21
H(2)	2988	4938	8969	20
H(3)	4903	3232	9388	20
H(4)	4684	4033	7838	20
H(5)	7859	4052	8855	20
H(8A)	731	5134	11240	41
H(8B)	922	4022	11155	41
H(8C)	-938	4529	10911	41
H(10A)	720	1454	8469	33
H(10B)	-185	2472	8411	33
H(10C)	-539	1833	9163	33
H(12A)	5630	1236	7202	46
H(12B)	7670	1494	7451	46
H(12C)	7050	1597	6560	46
H(13A)	9790	4042	6443	61
H(13B)	11409	3503	6878	61
H(13C)	11214	4615	6965	61
H(14A)	7574	6569	9465	30
H(14B)	7375	6283	10368	30
H(15A)	5499	7819	9661	38
H(15B)	7213	7931	10231	38
H(15C)	5324	7538	10562	38